

Enclosure 3 to E-25322

Replacement and New Pages for NUHOMS® HD UFSAR, Revision 1
(Non-Proprietary version)

Non-Proprietary Version



NUHOMS[®] HD
Horizontal Modular Storage System
For Irradiated Nuclear Fuel

UPDATED FINAL SAFETY ANALYSIS REPORT

Revision 1

7135 MINSTREL WAY, COLUMBIA, MARYLAND 21045

Rev. 1, 9/07

REVISION LOG SHEET

FSAR Revision	Date	Record of Changes/FCNs
0	2/23/07	None
1	10/2/07	FCNs 721030-004 Rev. 0, 008 Rev. 1, 009 Rev. 1, 010 Rev. 1, 012 Rev. 1, 016 Rev. 1, 037 Rev. 0, 054 Rev. 0, 056 Rev. 0, 057 Rev. 0, 058 Rev. 2, 060 Rev. 1, 064 Rev. 1, 081 Rev. 1, 082 Rev. 0, 084 Rev. 0, 085 Rev. 0, 087 Rev. 0, 089 Rev. 1, 105 Rev. 0, 107 Rev. 0, 108 Rev. 1, 109 Rev. 0, 116 Rev. 0, 117 Rev. 0, 119 Rev. 0, 121 Rev. 0, 122 Rev. 0, 123 Rev. 0, 124 Rev. 0, 126 Rev. 1

LIST OF EFFECTIVE PAGES (Non-proprietary Version)

Page Number/ Description	Revision	Date
-----------------------------	----------	------

Cover page	1	9/07
Revision Log Sheet	1	9/07
LOEP-1	1	9/07
LOEP-2	1	9/07
LOEP-3	1	9/07
LOEP-4	1	9/07
LOEP-5	1	9/07
LOEP-6	1	9/07
LOEP-7	1	9/07
LOEP-8	1	9/07
LOEP-9	1	9/07
LOEP-10	1	9/07
LOEP-11	1	9/07
LOEP-12	1	9/07
LOEP-13	1	9/07
LOEP-14	1	9/07
LOEP-15	1	9/07
LOEP-16	1	9/07
LOEP-17	1	9/07
LOEP-18	1	9/07
i	0	1/07
ii	0	1/07
iii	1	9/07
iv	1	9/07
v	0	1/07
vi	0	1/07
vii	0	1/07
viii	0	1/07
ix	1	9/07
1-i	0	1/07
1-ii	0	1/07
1-1	1	9/07
1-2	1	9/07
1-3	0	1/07
1-4	1	9/07
1-5	1	9/07
1-6	0	1/07
1-7	0	1/07
1-8	0	1/07
1-9	0	1/07
1-10	0	1/07
1-11	0	1/07
1-12	0	1/07
1-13	0	1/07

Page Number/ Description	Revision	Date
-----------------------------	----------	------

1-14	0	1/07
1-15	1	9/07
Table 1-1	1	9/07
Figure 1-1	1	9/07
Figure 1-2	0	1/07
Figure 1-3	0	1/07
Figure 1-4	1	9/07
Figure 1-5	0	1/07
Figure 1-6	0	1/07
Figure 1-7	0	1/07
Figure 1-8	0	1/07
Figure 1-9	1	9/07
Figure 1-10	1	9/07
Figure 1-11	1	9/07
Drawing No 10494-72-1	2	not shown
Drawing No 10494-72-2	2	not shown
Drawing No 10494-72-3	2	not shown
Drawing No 10494-72-4 Sh1	2	not shown
Drawing No 10494-72-4 Sh2	2	not shown
Drawing No 10494-72-5	2	not shown
Drawing No 10494-72-6	2	not shown
Drawing No 10494-72-7	2	not shown
Drawing No 10494-72-8	2	not shown
Drawing No 10494-72-9	2	not shown
Drawing No 10494-72-10	2	not shown
Drawing No 10494-72-11	2	not shown
Drawing No 10494-72-12	2	not shown
Drawing No 10494-72-15	2	not shown
Drawing No 10494-72-16	2	not shown
Drawing No 10494-72-17	2	not shown
Drawing No 10494-72-18	1	not shown
Drawing No 10494-72-19	2	not shown
Drawing No 10494-72-20	2	not shown
Drawing No 10494-72-21	2	not shown
Drawing No 10494-72-100	2	not shown
Drawing No 10494-72-101 Sh1	1	not shown
Drawing No 10494-72-101 Sh2	1	not shown
Drawing No 10494-72-102	1	not shown
Drawing No 10494-72-103 Sh1	1	not shown
Drawing No 10494-72-103 Sh2	1	not shown
Drawing No 10494-72-104	2	not shown
Drawing No 10494-72-105	1	not shown
Drawing No 10494-72-106	1	not shown
Drawing No 10494-72-107	1	not shown

LIST OF EFFECTIVE PAGES (Non-proprietary Version)

Page Number/ Description	Revision	Date
-----------------------------	----------	------

Drawing No 10494-72-108	2	not shown
Drawing No 10494-72-109	1	not shown
Drawing No 10494-72-110	0	not shown
Drawing No 10494-72-30	1	not shown
2-i	0	1/07
2-ii	0	1/07
2-1	1	9/07
2-2	0	1/07
2-3	0	1/07
2-4	0	1/07
2-5	0	1/07
2-6	0	1/07
2-7	0	1/07
2-8	0	1/07
2-9	0	1/07
2-10	0	1/07
2-11	0	1/07
2-12	0	1/07
2-13	0	1/07
2-14	0	1/07
2-15	0	1/07
2-16	0	1/07
2-17	0	1/07
2-18	0	1/07
2-19	0	1/07
2-20	1	9/07
2-21	1	9/07
Table 2-1	1	9/07
Table 2-2	0	1/07
Table 2-2 concluded	0	1/07
Table 2-3 & 2-4	0	1/07
Table 2-5	1	9/07
Figure 2-1	0	1/07
Figure 2-2	0	1/07
3-i	0	1/07
3-ii	0	1/07
3-iii	0	1/07
3-iv	0	1/07
3-1	1	9/07
3-2	1	9/07
3-3	0	1/07
3-4	1	9/07
3-5	1	9/07
3-6	1	9/07

Page Number/ Description	Revision	Date
-----------------------------	----------	------

3-7	1	9/07
3-8	0	1/07
3-9	1	9/07
3-9a	0	1/07
3-10	0	1/07
3-11	0	1/07
3-12	0	1/07
3-13	1	9/07
3-14	0	1/07
3-15	0	1/07
3-16	0	1/07
3-17	1	9/07
3-18	0	1/07
3-19	0	1/07
3-20	0	1/07
3-21	0	1/07
3-22	0	1/07
3-23	0	1/07
3-24	1	9/07
3-25	0	1/07
3-26	0	1/07
3-27	0	1/07
3-28	0	1/07
3-29	0	1/07
3-30	0	1/07
3-31	0	1/07
3-32	0	1/07
3-33	0	1/07
3-34	1	9/07
3-35	0	1/07
3-36	0	1/07
3-37	0	1/07
3-38	0	1/07
3-39	0	1/07
3-40	0	1/07
3-41	0	1/07
3-42	1	9/07
3-43	1	9/07
3-44	1	9/07
3-45	0	1/07
3-46	0	1/07
3-47	0	1/07
3-48	0	1/07
3-49	0	1/07

LIST OF EFFECTIVE PAGES (Non-proprietary Version)

Page Number/ Description	Revision	Date
-----------------------------	----------	------

3-50	0	1/07
3-51	0	1/07
3-52	0	1/07
3-53	0	1/07
3-54	1	9/07
3-55	1	9/07
3-56	1	9/07
3-57	0	1/07
3-58	1	9/07
3-59	0	1/07
3-60	1	9/07
Table 3-1	0	1/07
Table 3-2	0	1/07
Table 3-2 continued	0	1/07
Table 3-3	1	9/07
Table 3-4	0	1/07
Table 3-5	0	1/07
Table 3-6	0	1/07
Table 3-7	0	1/07
Table 3-7A	0	1/07
Table 3-7B	0	1/07
Table 3-8	0	1/07
Table 3-9	0	1/07
Table 3-10	0	1/07
Table 3-11	1	9/07
Table 3-12	0	1/07
Table 3-13	0	1/07
Table 3-14	0	1/07
Table 3-15	0	1/07
Figure 3-1	0	1/07
Figure 3-2	0	1/07
Figure 3-3	0	1/07
Figure 3-4	0	1/07
Figure 3-5	0	1/07
Figure 3-6	0	1/07
Figure 3-7	0	1/07
3.9.1-i	1	9/07
3.9.1-ii	1	9/07
3.9.1-iii	1	9/07
3.9.1-iv	1	9/07
3.9.1-v	1	9/07
3.9.1-vi	1	9/07
3.9.1-1	0	1/07
3.9.1-2	1	9/07

Page Number/ Description	Revision	Date
-----------------------------	----------	------

3.9.1-3	1	9/07
3.9.1-4	0	1/07
3.9.1-5	0	1/07
3.9.1-6	0	1/07
3.9.1-7	1	9/07
3.9.1-8	1	9/07
3.9.1-9	0	1/07
3.9.1-10	0	1/07
3.9.1-11	1	9/07
3.9.1-12	0	1/07
3.9.1-13	1	9/07
3.9.1-14	1	9/07
3.9.1-15	0	1/07
3.9.1-16	1	9/07
3.9.1-17	0	1/07
3.9.1-18	1	9/07
3.9.1-19	0	1/07
3.9.1-20	0	1/07
3.9.1-21	0	1/07
3.9.1-22	0	1/07
3.9.1-23	1	9/07
3.9.1-24	1	9/07
3.9.1-25	1	9/07
3.9.1-26	1	9/07
3.9.1-27	1	9/07
3.9.1-28	1	9/07
3.9.1-29	0	1/07
3.9.1-30	0	1/07
3.9.1-31	0	1/07
3.9.1-32	0	1/07
3.9.1-33	0	1/07
3.9.1-34	0	1/07
3.9.1-35	0	1/07
3.9.1-36	0	1/07
3.9.1-37	0	1/07
3.9.1-38	0	1/07
3.9.1-39	0	1/07
3.9.1-40	0	1/07
3.9.1-41	0	1/07
3.9.1-42	0	1/07
3.9.1-43	1	9/07
3.9.1-44	1	9/07
3.9.1-45	0	1/07
3.9.1-46	0	1/07

LIST OF EFFECTIVE PAGES (Non-proprietary Version)

Page Number/ Description	Revision	Date
-----------------------------	----------	------

3.9.1-47	0	1/07
3.9.1-48	0	1/07
3.9.1-49	0	1/07
3.9.1-50	0	1/07
3.9.1-51	0	1/07
3.9.1-52	0	1/07
3.9.1-53	0	1/07
3.9.1-54	0	1/07
3.9.1-55	0	1/07
3.9.1-56	0	1/07
3.9.1-56a	0	1/07
3.9.1-56b	0	1/07
3.9.1-56c	0	1/07
3.9.1-57	0	1/07
3.9.1-58	1	9/07
3.9.1-59	0	1/07
3.9.1-60	0	1/07
3.9.1-61	0	1/07
3.9.1-62	0	1/07
3.9.1-63	0	1/07
3.9.1-64	0	1/07
3.9.1-65	0	1/07
3.9.1-66	0	1/07
3.9.1-67	0	1/07
3.9.1-68	0	1/07
3.9.1-69	1	9/07
3.9.1-70	0	1/07
3.9.1-71	0	1/07
3.9.1-72	0	1/07
3.9.1-73	0	1/07
3.9.1-74	0	1/07
3.9.1-75	0	1/07
3.9.1-76	0	1/07
3.9.1-77	0	1/07
3.9.1-78	0	1/07
3.9.1-79	0	1/07
3.9.1-80	0	1/07
3.9.1-81	0	1/07
3.9.1-82	0	1/07
3.9.1-83	0	1/07
3.9.1-84	0	1/07
3.9.1-85	1	9/07
3.9.1-86	1	9/07
3.9.1-87	1	9/07

Page Number/ Description	Revision	Date
-----------------------------	----------	------

3.9.1-88	1	9/07
3.9.1-89	1	9/07
Table 3.9.1-1	0	1/07
Table 3.9.1-2	0	1/07
Table 3.9.1-3	1	9/07
Table 3.9.1-4(a)	1	9/07
Table 3.9.1-4(b)	1	9/07
Table 3.9.1-5	1	9/07
Table 3.9.1-6	0	1/07
Table 3.9.1-7	0	1/07
Table 3.9.1-8	0	1/07
Table 3.9.1-9	0	1/07
Table 3.9.1-10	0	1/07
Table 3.9.1-11	0	1/07
Table 3.9.1-12	1	9/07
Table 3.9.1-13	0	1/07
Table 3.9.1-14	0	1/07
Table 3.9.1-15	0	1/07
Table 3.9.1-16	1	9/07
Table 3.9.1-17	0	1/07
Table 3.9.1-18	0	1/07
Table 3.9.1-19	0	1/07
Table 3.9.1-20	1	9/07
Table 3.9.1-21	1	9/07
Table 3.9.1-22	0	1/07
Table 3.9.1-23	0	1/07
Table 3.9.1-24	1	9/07
Table 3.9.1-25	1	9/07
Table 3.9.1-26	1	9/07
Table 3.9.1-27	1	9/07
Table 3.9.1-28	0	1/07
Table 3.9.1-29	0	1/07
Table 3.9.1-30	0	1/07
Table 3.9.1-31	0	1/07
Table 3.9.1-32	0	1/07
Table 3.9.1-33	0	1/07
Table 3.9.1-34	0	1/07
Table 3.9.1-35	0	1/07
Figure 3.9.1-1	1	9/07
Figure 3.9.1-2	1	9/07
Figure 3.9.1-3	1	9/07
Figure 3.9.1-4	1	9/07
Figure 3.9.1-5	1	9/07
Figure 3.9.1-6	1	9/07

LIST OF EFFECTIVE PAGES (Non-proprietary Version)

Page Number/ Description	Revision	Date
-----------------------------	----------	------

Figure 3.9.1-7	1	9/07
Figure 3.9.1-8	1	9/07
Figure 3.9.1-9	1	9/07
Figure 3.9.1-10	1	9/07
Figure 3.9.1-11	0	1/07
Figure 3.9.1-12	0	1/07
Figure 3.9.1-13	1	9/07
Figure 3.9.1-14	1	9/07
Figure 3.9.1-15	0	1/07
Figure 3.9.1-16	0	1/07
Figure 3.9.1-17	0	1/07
Figure 3.9.1-18	0	1/07
Figure 3.9.1-19	0	1/07
Figure 3.9.1-20	0	1/07
Figure 3.9.1-21	0	1/07
Figure 3.9.1-22	1	9/07
Figure 3.9.1-23	0	1/07
Figure 3.9.1-24	1	9/07
Figure 3.9.1-25	1	9/07
Figure 3.9.1-26	1	9/07
Figure 3.9.1-27	0	1/07
Figure 3.9.1-28	0	1/07
Figure 3.9.1-29	0	1/07
Figure 3.9.1-30	0	1/07
Figure 3.9.1-31	0	1/07
Figure 3.9.1-32	0	1/07
3.9.2-i	0	1/07
3.9.2-ii	1	9/07
3.9.2-iii	0	1/07
3.9.2-1	0	1/07
3.9.2-2	0	1/07
3.9.2-3	0	1/07
3.9.2-4	0	1/07
3.9.2-5	1	9/07
3.9.2-6	1	9/07
3.9.2-7	0	1/07
3.9.2-8	0	1/07
3.9.2-9	0	1/07
3.9.2-10	0	1/07
3.9.2-11	0	1/07
3.9.2-12	0	1/07
3.9.2-13	0	1/07
3.9.2-14	0	1/07
3.9.2-15	0	1/07

Page Number/ Description	Revision	Date
-----------------------------	----------	------

3.9.2-16	0	1/07
3.9.2-17	0	1/07
3.9.2-18	0	1/07
3.9.2-19	0	1/07
3.9.2-20	0	1/07
3.9.2-21	0	1/07
3.9.2-22	0	1/07
3.9.2-23	0	1/07
3.9.2-24	0	1/07
3.9.2-25	0	1/07
3.9.2-26	0	1/07
3.9.2-27	0	1/07
3.9.2-28	0	1/07
3.9.2-29	0	1/07
3.9.2-30	0	1/07
3.9.2-31	0	1/07
3.9.2-32	0	1/07
3.9.2-33	1	9/07
3.9.2-34	0	1/07
3.9.2-35	1	9/07
3.9.2-36	1	9/07
3.9.2-37	1	9/07
3.9.2-38	0	1/07
3.9.2-39	0	1/07
3.9.2-40	0	1/07
3.9.2-41	1	9/07
Table 3.9.2-1	0	1/07
Table 3.9.2-1 continued	0	1/07
Table 3.9.2-1 concluded	1	9/07
Table 3.9.2-2	0	1/07
Table 3.9.2-3	0	1/07
Table 3.9.2-4	1	9/07
Table 3.9.2-5	0	1/07
Table 3.9.2-6	0	1/07
Table 3.9.2-7	1	9/07
Table 3.9.2-8	1	9/07
Figure 3.9.2-1	0	1/07
Figure 3.9.2-2	0	1/07
Figure 3.9.2-3	0	1/07
Figures 3.9.2-3A & B	0	1/07
Figure 3.9.2-3 C & D	0	1/07
Figure 3.9.2-3E	0	1/07
Figure 3.9.2-4	0	1/07
Figure 3.9.2-5	0	1/07

LIST OF EFFECTIVE PAGES (Non-proprietary Version)

Page Number/ Description	Revision	Date
-----------------------------	----------	------

Figure 3.9.2-6	0	1/07
Figure 3.9.2-7	0	1/07
Figure 3.9.2-8	0	1/07
Figure 3.9.2-9	0	1/07
Figure 3.9.2-10	0	1/07
Figure 3.9.2-11	0	1/07
Figure 3.9.2-12	0	1/07
Figure 3.9.2-13	0	1/07
Figure 3.9.2-14	1	9/07
Figure 3.9.2-15	1	9/07
Figure 3.9.2-16	1	9/07
Figure 3.9.2-17	0	1/07
Figure 3.9.2-18	0	1/07
Figure 3.9.2-19	0	1/07
Figure 3.9.2-20	0	1/07
Figure 3.9.2-21	0	1/07
Figure 3.9.2-22	0	1/07
Figure 3.9.2-23	0	1/07
3.9.3-i	1	9/07
3.9.3-ii	0	1/07
3.9.3-1	0	1/07
3.9.3-2	0	1/07
3.9.3-3	0	1/07
3.9.3-4	0	1/07
3.9.3-5	0	1/07
3.9.3-6	0	1/07
3.9.3-7	0	1/07
3.9.3-8	0	1/07
3.9.3-9	0	1/07
3.9.3-10	0	1/07
3.9.3-11	0	1/07
3.9.3-12	0	1/07
3.9.3-13	0	1/07
3.9.3-14	0	1/07
3.9.3-15	0	1/07
3.9.3-16	0	1/07
3.9.3-17	0	1/07
3.9.3-18	0	1/07
3.9.3-19	0	1/07
3.9.3-20	0	1/07
3.9.3-21	0	1/07
3.9.3-22	0	1/07
3.9.3-23	0	1/07
3.9.3-24	0	1/07

Page Number/ Description	Revision	Date
-----------------------------	----------	------

3.9.3-25	0	1/07
3.9.3-26	0	1/07
3.9.3-27	0	1/07
3.9.3-28	0	1/07
3.9.3-29	1	9/07
3.9.3-30	0	1/07
3.9.3-31	0	1/07
3.9.3-32	0	1/07
3.9.3-33	1	9/07
Table 3.9.3-1	0	1/07
Table 3.9.3-2	0	1/07
Table 3.9.3-3	0	1/07
Table 3.9.3-4	0	1/07
Table 3.9.3-5	0	1/07
Figure 3.9.3-1	0	1/07
Figure 3.9.3-2	0	1/07
Figure 3.9.3-3	0	1/07
3.9.4-i	0	1/07
3.9.4-ii	0	1/07
3.9.4-1	0	1/07
3.9.4-2	0	1/07
3.9.4-3	0	1/07
3.9.4-4	0	1/07
3.9.4-5	0	1/07
3.9.4-6	0	1/07
3.9.4-7	0	1/07
3.9.4-8	0	1/07
3.9.4-9	0	1/07
3.9.4-10	0	1/07
3.9.4-11	0	1/07
3.9.4-12	0	1/07
3.9.4-13	1	9/07
Figure 3.9.4-1	0	1/07
Figure 3.9.4-2	0	1/07
Figure 3.9.4-3	0	1/07
Figure 3.9.4-4	0	1/07
Figure 3.9.4-5	0	1/07
Figure 3.9.4-6	0	1/07
Figure 3.9.4-7	0	1/07
Figure 3.9.4-8	0	1/07
Figure 3.9.4-9	0	1/07
Figure 3.9.4-10	0	1/07
Figure 3.9.4-11	0	1/07
Figure 3.9.4-12	0	1/07

LIST OF EFFECTIVE PAGES (Non-proprietary Version)

Page Number/ Description	Revision	Date
-----------------------------	----------	------

Figure 3.9.4-13	0	1/07
Figure 3.9.4-14	0	1/07
Figure 3.9.4-15	0	1/07
Figure 3.9.4-16	0	1/07
Figure 3.9.4-17	0	1/07
3.9.5-i	0	1/07
3.9.5-1	0	1/07
3.9.5-2	0	1/07
3.9.5-3	0	1/07
3.9.5-4	0	1/07
3.9.5-5	0	1/07
3.9.5-6	0	1/07
3.9.5-7	1	9/07
3.9.5-8	1	9/07
3.9.5-9	0	1/07
3.9.5-10	0	1/07
3.9.5-11	1	9/07
3.9.5-12	1	9/07
3.9.5-13	0	1/07
3.9.5-14	1	9/07
Table 3.9.5-1	1	9/07
Figure 3.9.5-1	0	1/07
Figure 3.9.5-2	0	1/07
Figure 3.9.5-3	0	1/07
3.9.6-i	0	1/07
3.9.6-ii	1	9/07
3.9.6-1	0	1/07
3.9.6-2	0	1/07
3.9.6-3	0	1/07
3.9.6-4	0	1/07
3.9.6-5	0	1/07
3.9.6-6	0	1/07
3.9.6-7	0	1/07
3.9.6-8	1	9/07
Table 3.9.6-1	0	1/07
Figure 3.9.6-1	0	1/07
Figure 3.9.6-2	0	1/07
Figure 3.9.6-3	0	1/07
Figure 3.9.6-4	0	1/07
Figure 3.9.6-5	0	1/07
Figure 3.9.6-6	0	1/07
Figure 3.9.6-7	0	1/07
Figure 3.9.6-8	0	1/07
Figure 3.9.6-9	0	1/07

Page Number/ Description	Revision	Date
-----------------------------	----------	------

Figure 3.9.6-10	0	1/07
Figure 3.9.6-11	0	1/07
3.9.7-i	0	1/07
3.9.7-ii	1	9/07
3.9.7-1	0	1/07
3.9.7-2	0	1/07
3.9.7-3	0	1/07
3.9.7-4	0	1/07
3.9.7-5	0	1/07
3.9.7-6	0	1/07
3.9.7-7	0	1/07
3.9.7-8	0	1/07
3.9.7-9	0	1/07
3.9.7-10	0	1/07
Table 3.9.7-1	0	1/07
Table 3.9.7-2	0	1/07
Table 3.9.7-3	0	1/07
Table 3.9.7-4	0	1/07
Figure 3.9.7-1	0	1/07
Figure 3.9.7-2	0	1/07
Figure 3.9.7-3	0	1/07
Figure 3.9.7-4	1	9/07
Figure 3.9.7-5	1	9/07
Figure 3.9.7-6	0	1/07
3.9.8-i	1	9/07
3.9.8-ii	1	9/07
3.9.8-1	0	1/07
3.9.8-2	0	1/07
3.9.8-3	0	1/07
3.9.8-4	0	1/07
3.9.8-5	0	1/07
3.9.8-6	0	1/07
3.9.8-7	0	1/07
3.9.8-8	0	1/07
3.9.8-9	0	1/07
3.9.8-10	0	1/07
3.9.8-11	0	1/07
3.9.8-12	0	1/07
3.9.8-13	0	1/07
3.9.8-14	0	1/07
3.9.8-15	0	1/07
3.9.8-16	0	1/07
3.9.8-17	0	1/07
3.9.8-18	0	1/07

LIST OF EFFECTIVE PAGES (Non-proprietary Version)

Page Number/ Description	Revision	Date
-----------------------------	----------	------

3.9.8-19	1	9/07
3.9.8-20	0	1/07
3.9.8-21	1	9/07
3.9.8-22	0	1/07
3.9.8-23	0	1/07
3.9.8-24	0	1/07
3.9.8-25	0	1/07
3.9.8-26	0	1/07
3.9.8-27	0	1/07
3.9.8-28	0	1/07
3.9.8-29	1	9/07
3.9.8-30	0	1/07
Table 3.9.8-1	0	1/07
Table 3.9.8-2	0	1/07
Table 3.9.8-3	0	1/07
Table 3.9.8-4	0	1/07
Table 3.9.8-5	0	1/07
Table 3.9.8-6	0	1/07
Table 3.9.8-7	0	1/07
Table 3.9.8-8	0	1/07
Table 3.9.8-9	0	1/07
Table 3.9.8-9 concluded	1	9/07
Table 3.9.8-10	0	1/07
Table 3.9.8-10 concluded	1	9/07
Figure 3.9.8-1	0	1/07
Figure 3.9.8-2	0	1/07
Figure 3.9.8-3	0	1/07
Figure 3.9.8-4	0	1/07
Figure 3.9.8-5	0	1/07
3.9.9-i	0	1/07
3.9.9-ii	1	9/07
3.9.9-iii	0	1/07
3.9.9-1	1	9/07
3.9.9-2	1	9/07
3.9.9-3	1	9/07
3.9.9-4	0	1/07
3.9.9-5	1	9/07
3.9.9-6	0	1/07
3.9.9-7	0	1/07
3.9.9-8	0	1/07
3.9.9-9	0	1/07
3.9.9-10	0	1/07
3.9.9-11	0	1/07
3.9.9-12	0	1/07

Page Number/ Description	Revision	Date
-----------------------------	----------	------

3.9.9-13	1	9/07
3.9.9-14	1	9/07
3.9.9-15	0	1/07
3.9.9-16	1	9/07
3.9.9-17	0	1/07
3.9.9-18	0	1/07
3.9.9-19	0	1/07
3.9.9-20	0	1/07
3.9.9-21	0	1/07
3.9.9-22	0	1/07
3.9.9-23	1	9/07
3.9.9-24	0	1/07
3.9.9-25	0	1/07
3.9.9-26	0	1/07
3.9.9-27	0	1/07
3.9.9-28	1	9/07
3.9.9-29	1	9/07
Table 3.9.9-1	0	1/07
Table 3.9.9-2	0	1/07
Table 3.9.9-3	0	1/07
Table 3.9.9-4	0	1/07
Table 3.9.9-5	0	1/07
Table 3.9.9-6	0	1/07
Table 3.9.9-7	0	1/07
Table 3.9.9-8	0	1/07
Table 3.9.9-9	0	1/07
Table 3.9.9-10	0	1/07
Table 3.9.9-11	1	9/07
Table 3.9.9-12	0	1/07
Table 3.9.9-13	0	1/07
Table 3.9.9-14	0	1/07
Table 3.9.9-15	0	1/07
Table 3.9.9-16	1	9/07
Figure 3.9.9-1	0	1/07
Figure 3.9.9-2	0	1/07
Figure 3.9.9-3	0	1/07
Figure 3.9.9-4	0	1/07
Figure 3.9.9-5	0	1/07
Figure 3.9.9-6	1	9/07
3.9.10-i	0	1/07
3.9.10-ii	0	1/07
3.9.10-1	0	1/07
3.9.10-2	0	1/07
3.9.10-3	0	1/07

LIST OF EFFECTIVE PAGES (Non-proprietary Version)

Page Number/ Description	Revision	Date
-----------------------------	----------	------

3.9.10-4	0	1/07
3.9.10-5	0	1/07
3.9.10-6	0	1/07
3.9.10-7	0	1/07
3.9.10-8	0	1/07
3.9.10-9	0	1/07
3.9.10-10	1	9/07
3.9.10-11	1	9/07
3.9.10-12	1	9/07
3.9.10-13	1	9/07
3.9.10-14	1	9/07
3.9.10-15	1	9/07
3.9.10-16	1	9/07
Figure 3.9.10-1	0	1/07
Figure 3.9.10-2	0	1/07
Figure 3.9.10-3	0	1/07
Figure 3.9.10-4	0	1/07
Figure 3.9.10-5	0	1/07
Figure 3.9.10-6	0	1/07
Figure 3.9.10-7	0	1/07
Figure 3.9.10-8	0	1/07
Figure 3.9.10-9	0	1/07
Figure 3.9.10-10	0	1/07
Figure 3.9.10-11	0	1/07
Figure 3.9.10-12	0	1/07
Figure 3.9.10-13	0	1/07
Figure 3.9.10-14	0	1/07
Figure 3.9.10-15	0	1/07
Figure 3.9.10-16	0	1/07
Figure 3.9.10-17	0	1/07
Figure 3.9.10-18	0	1/07
Figure 3.9.10-19	0	1/07
Figure 3.9.10-20	0	1/07
Figure 3.9.10-21	0	1/07
Figure 3.9.10-22	0	1/07
Figure 3.9.10-23	0	1/07
3.9.11-i	1	9/07
3.9.11-1	0	1/07
3.9.11-2	0	1/07
3.9.11-3	0	1/07
3.9.11-4	0	1/07
3.9.11-5	1	9/07
3.9.11-6	1	9/07
3.9.11-7	1	9/07

Page Number/ Description	Revision	Date
-----------------------------	----------	------

Figure 3.9.11-1	1	9/07
Figure 3.9.11-2	1	9/07
Figure 3.9.11-3	1	9/07
Figure 3.9.11-4	0	1/07
Figure 3.9.11-5	0	1/07
Figure 3.9.11-6	0	1/07
Figure 3.9.11-7	0	1/07
Figure 3.9.11-8	1	9/07
Figure 3.9.11-9	0	1/07
Figure 3.9.11-10	1	9/07
4-i	1	9/07
4-ii	0	1/07
4-iii	1	9/07
4-iv	1	9/07
4-v	1	9/07
4-1	1	9/07
4-2	0	1/07
4-3	0	1/07
4-4	0	1/07
4-5	1	9/07
4-6	1	9/07
4-7	0	1/07
4-8	0	1/07
4-9	0	1/07
4-10	0	1/07
4-11	0	1/07
4-12	0	1/07
4-13	1	9/07
4-14	1	9/07
4-15	1	9/07
4-16	1	9/07
4-17	1	9/07
4-18	1	9/07
4-19	1	9/07
4-20	1	9/07
4-21	1	9/07
4-22	1	9/07
4-22A	1	9/07
4-23	0	1/07
4-24	0	1/07
4-25	0	1/07
4-26	0	1/07
4-27	1	9/07
4-28	1	9/07

LIST OF EFFECTIVE PAGES (Non-proprietary Version)

Page Number/ Description	Revision	Date
-----------------------------	----------	------

4-29	0	1/07
4-30	0	1/07
4-31	0	1/07
4-32	0	1/07
4-33	0	1/07
4-34	0	1/07
4-35	0	1/07
4-36	1	9/07
4-37	1	9/07
4-38	1	9/07
4-39	1	9/07
4-40	0	1/07
4-41	0	1/07
4-42	0	1/07
4-43	0	1/07
4-44	0	1/07
4-45	0	1/07
4-46	0	1/07
4-47	0	1/07
4-48	0	1/07
4-49	0	1/07
4-50	0	1/07
4-51	0	1/07
4-52	0	1/07
4-53	0	1/07
4-54	0	1/07
4-55	0	1/07
4-56	0	1/07
4-57	0	1/07
4-58	0	1/07
4-59	1	9/07
4-60	0	1/07
4-61	0	1/07
4-62	0	1/07
4-63	0	1/07
4-64	0	1/07
4-65	0	1/07
4-66	0	1/07
4-67	1	9/07
4-68	0	1/07
4-69	1	9/07
4-70	0	1/07
4-71	0	1/07
4-72	0	1/07

Page Number/ Description	Revision	Date
-----------------------------	----------	------

4-73	1	9/07
4-74	1	9/07
4-75	0	1/07
Table 4-1	1	9/07
Table 4-2	1	9/07
Tables 4-3 & 4-4	1	9/07
Tables 4-5 & 4-6	1	9/07
Table 4-7	0	1/07
Tables 4-8 & 4-9	0	1/07
Table 4-10	1	9/07
Table 4-11	0	1/07
Table 4-11 concluded	1	9/07
Table 4-12	0	1/07
Table 4-13	0	1/07
Table 4-13 continued	0	1/07
Table 4-13 continued	0	1/07
Table 4-13 concluded	1	9/07
Table 4-14	0	1/07
Table 4-14 continued	0	1/07
Table 4-14 concluded	1	9/07
Table 4-15	0	1/07
Table 4-15 concluded	1	9/07
Table 4-16	0	1/07
Table 4-17	0	1/07
Table 4-17 concluded	1	9/07
Table 4-18	0	1/07
Table 4-19	0	1/07
Table 4-20	1	9/07
Table 4-21	1	9/07
Table 4-21 continued	1	9/07
Table 4-21 continued	1	9/07
Table 4-21 concluded	1	9/07
Table 4-22	0	1/07
Table 4-23	0	1/07
Table 4-24	0	1/07
Table 4-25	0	1/07
Table 4-26	0	1/07
Table 4-27	0	1/07
Table 4-28	0	1/07
Figure 4-1	0	1/07
Figure 4-2	0	1/07
Figure 4-3	0	1/07
Figure 4-4	0	1/07
Figure 4-5	0	1/07

LIST OF EFFECTIVE PAGES (Non-proprietary Version)

Page Number/ Description	Revision	Date
-----------------------------	----------	------

Figure 4-6	1	9/07
Figure 4-7	0	1/07
Figure 4-8	1	9/07
Figure 4-9	1	9/07
Figure 4-9 continued	1	9/07
Figure 4-10	1	9/07
Figure 4-10 continued	1	9/07
Figure 4-11	0	1/07
Figure 4-12	0	1/07
Figure 4-13	0	1/07
Figure 4-14	1	9/07
Figure 4-15	0	1/07
Figure 4-15 concluded	1	9/07
Figure 4-16	0	1/07
Figure 4-17	0	1/07
Figure 4-18	0	1/07
Figure 4-19	0	1/07
Figure 4-20	0	1/07
Figure 4-21	0	1/07
Figure 4-22	1	9/07
Figure 4-23	1	9/07
Figure 4-24	0	1/07
Figure 4-25	0	1/07
Figure 4-26	0	1/07
Figure 4-27	0	1/07
Figure 4-28	0	1/07
Figure 4-29	0	1/07
Figure 4-30	1	9/07
Figure 4-30 continued	1	9/07
Figure 4-31	1	9/07
Figure 4-32	0	1/07
Figure 4-33	0	1/07
Figure 4-34	0	1/07
Figure 4-35	0	1/07
Figure 4-36	0	1/07
Figure 4-37	0	1/07
Figure 4-38	0	1/07
Figure 4-39	0	1/07
Figure 4-40	0	1/07
Figure 4-41	0	1/07
Figure 4-42	0	1/07
Figure 4-43	0	1/07
Figure 4-44	1	9/07
Figure 4-45	1	9/07

Page Number/ Description	Revision	Date
-----------------------------	----------	------

Figure 4-46	0	1/07
Figure 4-47	0	1/07
Figure 4-48	0	1/07
Figure 4-49	0	1/07
Figure 4-50	0	1/07
Figure 4-51	0	1/07
Appendix 4.16.1	0	1/07
Appendix 4.16.2	0	1/07
5-i	0	1/07
5-ii	1	9/07
5-iii	0	1/07
5-iv	0	1/07
5-1	1	9/07
5-2	0	1/07
5-3	0	1/07
5-4	0	1/07
5-5	0	1/07
5-6	0	1/07
5-7	0	1/07
5-8	1	9/07
5-9	0	1/07
5-10	0	1/07
5-11	0	1/07
5-12	0	1/07
5-13	0	1/07
5-14	0	1/07
5-15	0	1/07
5-16	0	1/07
5-17	1	9/07
Table 5-1	0	1/07
Table 5-2	0	1/07
Table 5-3	0	1/07
Tables 5-4 & 5-5	0	1/07
Tables 5-6 & 5-7	0	1/07
Table 5-8	0	1/07
Table 5-9	1	9/07
Table 5-10	0	1/07
Tables 5-11 & 5-12	0	1/07
Table 5-13	0	1/07
Table 5-14	0	1/07
Table 5-15	0	1/07
Table 5-16	0	1/07
Tables 5-17 & 5-18	1	9/07
Table 5-19	0	1/07

LIST OF EFFECTIVE PAGES (Non-proprietary Version)

Page Number/ Description	Revision	Date
-----------------------------	----------	------

Table 5-20	0	1/07
Table 5-21	0	1/07
Table 5-22	0	1/07
Table 5-23	0	1/07
Figure 5-1	0	1/07
Figure 5-2	0	1/07
Figure 5-3	0	1/07
Figure 5-4	0	1/07
Figure 5-5	0	1/07
Figure 5-6	0	1/07
Figure 5-7	0	1/07
Figure 5-8	0	1/07
Figure 5-9	0	1/07
Figure 5-10	0	1/07
Figure 5-11	0	1/07
Figure 5-12	0	1/07
Figure 5-13	0	1/07
Figure 5-14	0	1/07
Figure 5-15	0	1/07
Figure 5-16	0	1/07
Figure 5-17	0	1/07
Figure 5-18	0	1/07
6-i	0	1/07
6-ii	1	9/07
6-iii	0	1/07
6-1	1	9/07
6-2	1	9/07
6-3	1	9/07
6-4	0	1/07
6-5	0	1/07
6-6	0	1/07
6-7	0	1/07
6-8	1	9/07
6-9	1	9/07
6-10	0	1/07
6-11	0	1/07
6-12	1	9/07
6-13	0	1/07
6-14	0	1/07
6-15	1	9/07
6-16	0	1/07
6-17	0	1/07
6-18	0	1/07
6-19	0	1/07

Page Number/ Description	Revision	Date
-----------------------------	----------	------

6-20	0	1/07
6-21	0	1/07
6-22	0	1/07
6-23	0	1/07
6-24	0	1/07
6-25	1	9/07
6-26	0	1/07
6-27	0	1/07
Table 6-1	0	1/07
Table 6-2	0	1/07
Tables 6-3 & 6-4	1	9/07
Tables 6-5 & 6-6	0	1/07
Table 6-7	0	1/07
Table 6-8	0	1/07
Table 6-9	0	1/07
Table 6-10	0	1/07
Table 6-10 concluded	1	9/07
Tables 6-11	0	1/07
Table 6-12 & 6-13	0	1/07
Table 6-14	0	1/07
Table 6-15	0	1/07
Table 6-15 concluded	1	9/07
Table 6-16	0	1/07
Table 6-16 continued	0	1/07
Table 6-16 concluded	1	9/07
Table 6-17	0	1/07
Table 6-17 concluded	1	9/07
Table 6-18	0	1/07
Table 6-18 continued	0	1/07
Table 6-18 continued	0	1/07
Table 6-18 concluded & 6-19	1	9/07
Table 6-20	0	1/07
Table 6-20 continued	0	1/07
Table 6-20 concluded	1	9/07
Table 6-21	0	1/07
Table 6-21 continued	0	1/07
Table 6-21 continued	0	1/07
Table 6-21 concluded & 6-22	1	9/07
Table 6-22 continued	0	1/07
Table 6-22 concluded	1	9/07
Table 6-23	0	1/07
Tables 6-24 & 6-25	0	1/07

LIST OF EFFECTIVE PAGES (Non-proprietary Version)

Page Number/ Description	Revision	Date
Table 6-26	0	1/07
Table 6-26 continued	0	1/07
Table 6-26 concluded	1	9/07
Table 6-27	0	1/07
Table 6-27 continued	0	1/07
Table 6-27 continued	0	1/07
Table 6-27 concluded	1	9/07
Table 6-28	0	1/07
Table 6-29	0	1/07
Table 6-30	0	1/07
Table 6-30 continued	0	1/07
Table 6-30 concluded	0	1/07
Table 6-31	0	1/07
Table 6-32	0	1/07
Table 6-33	0	1/07
Table 6-33 concluded	1	9/07
Table 6-34	0	1/07
Table 6-34 continued	0	1/07
Table 6-34 concluded	1	9/07
Figure 6-1	0	1/07
Figure 6-2	0	1/07
Figure 6-3	0	1/07
Figure 6-4	0	1/07
Figure 6-5	0	1/07
Figure 6-6	0	1/07
Figure 6-7	0	1/07
Figure 6-8	0	1/07
Figure 6-9	0	1/07
Figure 6-10	0	1/07
Figure 6-11	0	1/07
Figure 6-12	0	1/07
Figure 6-13	0	1/07
Figure 6-14	0	1/07
Figure 6-15	0	1/07
Figure 6-16	0	1/07
Figure 6-17	0	1/07
Figure 6-18	0	1/07
Figure 6-19	0	1/07
7-i	1	9/07
7-1	1	9/07
7-2	0	1/07
7-3	0	1/07
7-4	0	1/07
7-5	0	1/07

Page Number/ Description	Revision	Date
Figure 7-1	1	9/07
8-i	0	1/07
8-1	1	9/07
8-2	1	9/07
8-3	1	9/07
8-4	1	9/07
8-5	1	9/07
8-6	1	9/07
8-7	1	9/07
8-8	1	9/07
8-9	1	9/07
8-10	1	9/07
8-11	0	1/07
8-12	1	9/07
8-13	1	9/07
8-14	1	9/07
8-15	1	9/07
Table 8-1	0	1/07
Figure 8-1	0	1/07
Figure 8-1 concluded	0	1/07
9-i	0	1/07
9-1	1	9/07
9-2	1	9/07
9-3	0	1/07
9-4	0	1/07
9-5	1	9/07
9-6	1	9/07
9-7	0	1/07
9-8	0	1/07
9-9	0	1/07
9-10	0	1/07
9-11	0	1/07
9-12	0	1/07
9-13	0	1/07
9-14	1	9/07
Table 9-1	0	1/07
Table 9-2	0	1/07
Table 9-3	0	1/07
10-i	1	9/07
10-ii	0	1/07
10-1	1	9/07
10-2	1	9/07
10-3	0	1/07
10-4	0	1/07

LIST OF EFFECTIVE PAGES (Non-proprietary Version)

Page Number/ Description	Revision	Date
10-5	0	1/07
10-6	0	1/07
10-7	0	1/07
10-8	0	1/07
10-9	0	1/07
10-10	0	1/07
Table 10-1	0	1/07
Table 10-1 concluded	0	1/07
Table 10-2	0	1/07
Table 10-3	0	1/07
Table 10-4	0	1/07
Table 10-5	0	1/07
Table 10-6	0	1/07
Table 10-7	0	1/07
Figure 10-1	0	1/07
11-i	0	1/07
11-1	1	9/07
11-2	0	1/07
11-3	1	9/07
11-4	1	9/07
11-5	0	1/07
11-6	0	1/07
11-7	0	1/07
11-8	0	1/07
11-9	0	1/07
11-10	0	1/07
11-11	0	1/07
11-12	0	1/07
11-13	0	1/07
11-14	0	1/07
11-15	0	1/07
11-16	0	1/07
11-17	0	1/07
11-18	0	1/07
11-19	0	1/07
11-20	0	1/07
11-21	0	1/07
11-22	0	1/07
11-23	0	1/07
11-24	0	1/07
11-25	0	1/07
11-26	0	1/07
11-27	0	1/07
11-28	0	1/07

Page Number/ Description	Revision	Date
Figure 11-1 (withheld)	not shown	not shown
12-1	0	1/07
B12-i	0	1/07
B12-1	0	1/07
B12-2	0	1/07
B12-3	0	1/07
B12-4	0	1/07
B12-5	0	1/07
B12-6	0	1/07
B12-7	0	1/07
B12-8	0	1/07
B12-9	0	1/07
B12-10	0	1/07
B12-11	0	1/07
B12-12	0	1/07
B12-13	0	1/07
B12-14	0	1/07
13-i	0	1/07
13-1	0	1/07
13-2	0	1/07
13-3	0	1/07
13-4	0	1/07
13-5	0	1/07
13-6	0	1/07
13-7	0	1/07
13-8	0	1/07
13-9	0	1/07
13-10	0	1/07
Table 13-1	0	1/07
Figure 13-1	0	1/07
14-i	0	1/07
14-1	0	1/07
14-2	0	1/07
14-3	0	1/07
14-4	0	1/07
Appendix A Cover	1	9/07
A.1-i	1	9/07
A.1-1	1	9/07
A.1-2	1	9/07
A.1-3	1	9/07
A.1-4	1	9/07
A.1-5	1	9/07
A.1-6	1	9/07
A.1-7	1	9/07

LIST OF EFFECTIVE PAGES (Non-proprietary Version)

Page Number/ Description	Revision	Date
-----------------------------	----------	------

A.1-8	1	9/07
A.1-9	1	9/07
A.1-10	1	9/07
A.1-11	1	9/07
10494-72-2001-SAR sh1	0	Not shown
10494-72-2001-SAR sh2	0	Not shown
10494-72-2001-SAR sh3	0	Not shown
10494-72-2002-SAR sh1	0	Not shown
10494-72-2002-SAR sh2	0	Not shown
10494-72-2003-SAR sh1	0	Not shown
10494-72-2003-SAR sh2	0	Not shown
10494-72-2003-SAR sh3	0	Not shown
10494-72-2003-SAR sh4	0	Not shown
10494-72-2003-SAR sh5	0	Not shown
10494-72-2004-SAR sh1	0	Not shown
10494-72-2004-SAR sh2	0	Not shown
10494-72-2004-SAR sh3	0	Not shown
10494-72-2005-SAR sh1	0	Not shown
10494-72-2005-SAR sh2	0	Not shown
10494-72-2005-SAR sh3	0	Not shown
10494-72-2005-SAR sh4	0	Not shown
10494-72-2005-SAR sh5	0	Not shown
10494-72-9001-SAR sh1	0	Not shown
10494-72-9001-SAR sh2	0	Not shown
10494-72-9001-SAR sh3	0	Not shown
10494-72-9002-SAR sh1	0	Not shown
10494-72-9002-SAR sh2	0	Not shown
10494-72-9002-SAR sh3	0	Not shown
10494-72-9003-SAR sh1	0	Not shown
10494-72-9003-SAR sh2	0	Not shown
10494-72-9003-SAR sh3	0	Not shown
A.2-1	1	9/07
A.3-i	1	9/07
A.3-1	1	9/07
A.3-2	1	9/07
A.3-3	1	9/07
A.3-4	1	9/07
A.3-5	1	9/07
A.3-6	1	9/07
A.3-7	1	9/07
A.3-8	1	9/07
A.3-9	1	9/07
A.3-10	1	9/07
A.3-11	1	9/07

Page Number/ Description	Revision	Date
-----------------------------	----------	------

A.3-12	1	9/07
A.3-13	1	9/07
A.3-14	1	9/07
A.3-15	1	9/07
A.3-16	1	9/07
A.3-17	1	9/07
A.3-18	1	9/07
A.3-19	1	9/07
A.3-20	1	9/07
A.3-21	1	9/07
A.3-22	1	9/07
A.3-23	1	9/07
A.3-24	1	9/07
A.3-25	1	9/07
A.3.9.1-i	1	9/07
A.3.9.1-ii	1	9/07
A.3.9.1-iii	1	9/07
A.3.9.1-1	1	9/07
A.3.9.1-2	1	9/07
A.3.9.1-3	1	9/07
A.3.9.1-4	1	9/07
A.3.9.1-5	1	9/07
A.3.9.1-6	1	9/07
A.3.9.1-7	1	9/07
A.3.9.1-8	1	9/07
A.3.9.1-9	1	9/07
A.3.9.1-10	1	9/07
A.3.9.1-11	1	9/07
A.3.9.1-12	1	9/07
A.3.9.1-13	1	9/07
A.3.9.1-14	1	9/07
A.3.9.1-15	1	9/07
A.3.9.1-16	1	9/07
A.3.9.1-17	1	9/07
A.3.9.1-18	1	9/07
A.3.9.1-19	1	9/07
A.3.9.1-20	1	9/07
A.3.9.1-21	1	9/07
A.3.9.1-22	1	9/07
A.3.9.1-23	1	9/07
A.3.9.1-24	1	9/07
A.3.9.1-25	1	9/07
A.3.9.1-26	1	9/07
A.3.9.1-27	1	9/07

LIST OF EFFECTIVE PAGES (Non-proprietary Version)

Page Number/ Description	Revision	Date
-----------------------------	----------	------

A.3.9.1-28	1	9/07
A.3.9.1-29	1	9/07
A.3.9.1-30	1	9/07
A.3.9.1-31	1	9/07
A.3.9.1-32	1	9/07
A.3.9.1-33	1	9/07
A.3.9.1-34	1	9/07
A.3.9.1-35	1	9/07
A.3.9.1-36	1	9/07
A.3.9.1-37	1	9/07
A.3.9.1-38	1	9/07
A.3.9.1-39	1	9/07
A.3.9.1-40	1	9/07
A.3.9.1-41	1	9/07
A.3.9.1-42	1	9/07
A.3.9.1-43	1	9/07
A.3.9.1-44	1	9/07
A.3.9.1-45	1	9/07
A.3.9.1-46	1	9/07
A.3.9.1-47	1	9/07
A.3.9.2-i	1	9/07
A.3.9.2-ii	1	9/07
A.3.9.2-iii	1	9/07
A.3.9.2-1	1	9/07
A.3.9.2-2	1	9/07
A.3.9.2-3	1	9/07
A.3.9.2-4	1	9/07
A.3.9.2-5	1	9/07
A.3.9.2-6	1	9/07
A.3.9.2-7	1	9/07
A.3.9.2-8	1	9/07
A.3.9.2-9	1	9/07
A.3.9.2-10	1	9/07
A.3.9.2-11	1	9/07
A.3.9.2-12	1	9/07
A.3.9.2-13	1	9/07
A.3.9.2-14	1	9/07
A.3.9.2-15	1	9/07
A.3.9.2-16	1	9/07
A.3.9.2-17	1	9/07
A.3.9.2-18	1	9/07
A.3.9.2-19	1	9/07
A.3.9.2-20	1	9/07
A.3.9.2-21	1	9/07

Page Number/ Description	Revision	Date
-----------------------------	----------	------

A.3.9.2-22	1	9/07
A.3.9.2-23	1	9/07
A.3.9.2-24	1	9/07
A.3.9.2-25	1	9/07
A.3.9.2-26	1	9/07
A.3.9.2-27	1	9/07
A.3.9.2-28	1	9/07
A.3.9.2-29	1	9/07
A.3.9.2-30	1	9/07
A.3.9.2-31	1	9/07
A.3.9.2-32	1	9/07
A.3.9.2-33	1	9/07
A.3.9.2-34	1	9/07
A.3.9.2-35	1	9/07
A.3.9.2-36	1	9/07
A.3.9.2-37	1	9/07
A.3.9.2-38	1	9/07
A.3.9.2-39	1	9/07
A.3.9.2-40	1	9/07
A.3.9.2-41	1	9/07
A.3.9.2-42	1	9/07
A.3.9.2-43	1	9/07
A.3.9.2-44	1	9/07
A.3.9.2-45	1	9/07
A.3.9.2-46	1	9/07
A.3.9.2-47	1	9/07
A.3.9.2-48	1	9/07
A.3.9.2-49	1	9/07
A.3.9.2-50	1	9/07
A.3.9.2-51	1	9/07
A.3.9.2-52	1	9/07
A.3.9.2-53	1	9/07
A.3.9.2-54	1	9/07
A.3.9.2-55	1	9/07
A.3.9.2-56	1	9/07
A.3.9.2-57	1	9/07
A.3.9.2-58	1	9/07
A.3.9.2-59	1	9/07
A.3.9.2-60	1	9/07
A.3.9.2-61	1	9/07
A.3.9.2-62	1	9/07
A.3.9.2-63	1	9/07
A.3.9.2-64	1	9/07
A.3.9.2-65	1	9/07

LIST OF EFFECTIVE PAGES (Non-proprietary Version)

Page Number/ Description	Revision	Date
-----------------------------	----------	------

A.3.9.2-66	1	9/07
A.3.9.2-67	1	9/07
A.3.9.2-68	1	9/07
A.3.9.2-69	1	9/07
A.3.9.2-70	1	9/07
A.3.9.3-i	1	9/07
A.3.9.3-ii	1	9/07
A.3.9.3-1	1	9/07
A.3.9.3-2	1	9/07
A.3.9.3-3	1	9/07
A.3.9.3-4	1	9/07
A.3.9.3-5	1	9/07
A.3.9.3-6	1	9/07
A.3.9.3-7	1	9/07
A.3.9.3-8	1	9/07
A.3.9.3-9	1	9/07
A.3.9.3-10	1	9/07
A.3.9.3-11	1	9/07
A.3.9.3-12	1	9/07
A.3.9.3-13	1	9/07
A.3.9.3-14	1	9/07
A.3.9.3-15	1	9/07
A.3.9.3-16	1	9/07
A.3.9.3-17	1	9/07
A.3.9.3-18	1	9/07
A.3.9.3-19	1	9/07
A.3.9.3-20	1	9/07
A.3.9.3-21	1	9/07
A.3.9.3-22	1	9/07
A.3.9.3-23	1	9/07
A.3.9.3-24	1	9/07
A.3.9.3-25	1	9/07
A.3.9.3-26	1	9/07
A.3.9.3-27	1	9/07
A.3.9.3-28	1	9/07
A.3.9.3-29	1	9/07
A.3.9.3-30	1	9/07
A.3.9.3-31	1	9/07
A.3.9.3-32	1	9/07
A.3.9.3-33	1	9/07
A.3.9.3-34	1	9/07
A.3.9.3-35	1	9/07
A.3.9.3-36	1	9/07
A.3.9.3-37	1	9/07

Page Number/ Description	Revision	Date
-----------------------------	----------	------

A.3.9.3-38	1	9/07
A.3.9.3-39	1	9/07
A.3.9.4-1	1	9/07
A.3.9.5-i	1	9/07
A.3.9.5-1	1	9/07
A.3.9.5-2	1	9/07
A.3.9.5-3	1	9/07
A.3.9.5-4	1	9/07
A.3.9.5-5	1	9/07
A.3.9.5-6	1	9/07
A.3.9.5-7	1	9/07
A.3.9.5-8	1	9/07
A.3.9.5-9	1	9/07
A.3.9.5-10	1	9/07
A.3.9.5-11	1	9/07
A.3.9.5-12	1	9/07
A.3.9.5-13	1	9/07
A.3.9.5-14	1	9/07
A.3.9.6-i	1	9/07
A.3.9.6-ii	1	9/07
A.3.9.6-1	1	9/07
A.3.9.6-2	1	9/07
A.3.9.6-3	1	9/07
A.3.9.6-4	1	9/07
A.3.9.6-5	1	9/07
A.3.9.6-6	1	9/07
A.3.9.6-7	1	9/07
A.3.9.6-8	1	9/07
A.3.9.6-9	1	9/07
A.3.9.6-10	1	9/07
A.3.9.6-11	1	9/07
A.3.9.6-12	1	9/07
A.3.9.6-13	1	9/07
A.3.9.6-14	1	9/07
A.3.9.6-15	1	9/07
A.3.9.6-16	1	9/07
A.3.9.6-17	1	9/07
A.3.9.6-18	1	9/07
A.3.9.6-19	1	9/07
A.3.9.6-20	1	9/07
A.3.9.6-21	1	9/07
A.3.9.6-22	1	9/07
A.3.9.7-1	1	9/07
A.3.9.8-1	1	9/07

LIST OF EFFECTIVE PAGES (Non-proprietary Version)

Page Number/ Description	Revision	Date
-----------------------------	----------	------

A.3.9.9-1	1	9/07
A.3.9.10-1	1	9/07
A.3.9.11-i	1	9/07
A.3.9.11-1	1	9/07
A.3.9.11-2	1	9/07
A.3.9.11-3	1	9/07
A.3.9.11-4	1	9/07
A.3.9.11-5	1	9/07
A.4-i	1	9/07
A.4-1	1	9/07
A.4-2	1	9/07
A.4-3	1	9/07
A.5-i	1	9/07
A.5-1	1	9/07
A.5-2	1	9/07
A.5-3	1	9/07
A.6-1	1	9/07
A.7-i	1	9/07
A.7-1	1	9/07
A.7-2	1	9/07
A.7-3	1	9/07
A.7-4	1	9/07
A.7-5	1	9/07
A.7-6	1	9/07
A.8-i	1	9/07
A.8-1	1	9/07
A.8-2	1	9/07
A.8-3	1	9/07
A.8-4	1	9/07
A.8-5	1	9/07
A.8-6	1	9/07
A.8-7	1	9/07
A.8-8	1	9/07
A.8-9	1	9/07
A.8-10	1	9/07
A.8-11	1	9/07
A.8-12	1	9/07
A.8-13	1	9/07
A.9-1	1	9/07
A.10-i	1	9/07
A.10-1	1	9/07
A.10-2	1	9/07
A.10-3	1	9/07
A.11-i	1	9/07

Page Number/ Description	Revision	Date
-----------------------------	----------	------

A.11-1	1	9/07
A.11-2	1	9/07
A.11-3	1	9/07
A.11-4	1	9/07
A.11-5	1	9/07
A.11-6	1	9/07
A.11-7	1	9/07
A.11-8	1	9/07
A.11-9	1	9/07
A.11-10	1	9/07
A.12-1	1	9/07
A.13-1	1	9/07
A.14-1	1	9/07

3.7.3	OS187H Transfer Cask Off-Normal and Accident Conditions Structural Analysis	3-50
3.8	References.....	3-54
3.9	Appendices.....	3-57
3.9.1	32PTH DSC (Canister and Basket) structural Analysis	3.9.1-1
3.9.2	OS187H Transfer Cask Body Structural Analysis.....	3.9.2-1
3.9.3	OS187H Transfer Cask Top Cover and RAM Access Cover Bolts Analyses	3.9.3-1
3.9.4	OS187H Transfer Cask Lead Slump and Inner Shell Buckling Analyses	3.9.4-1
3.9.5	OS187H Transfer Cask Trunnion Analysis	3.9.5-1
3.9.6	OS187H Transfer Cask Shield Panel Structural Analysis	3.9.6-1
3.9.7	OS187H Transfer Cask Impact Analysis.....	3.9.7-1
3.9.8	Damaged Fuel Cladding Structural Evaluation	3.9.8-1
3.9.9	HSM-H Structural Analysis.....	3.9.9-1
3.9.10	OS187H Transfer Cask Dynamic Impact Analysis.....	3.9.10-1
3.9.11	32PTH DSC Dynamic Impact Analysis.....	3.9.11-1
3.10	ASME Code Alternatives	3-58
4.	THERMAL EVALUATION.....	4-1
4.1	Discussion.....	4-1
4.2	Summary of Thermal Properties of Materials.....	4-3
4.3	Thermal Evaluation for Normal and Off-Normal Conditions	4-9
4.3.1	Thermal Models for Normal and Off-Normal Conditions.....	4-9
4.3.2	Maximum Temperatures for Normal and Off-Normal Conditions.....	4-20
4.3.3	Minimum Temperatures for Normal and Off-Normal Conditions	4-21
4.3.4	Maximum Internal Pressures for Normal and Off-Normal Conditions.	4-21
4.3.5	Maximum Thermal Stresses for Normal and Off-Normal Conditions..	4-21
4.3.6	Evaluation of Thermal Performance for Normal and Off-Normal Conditions.....	4-21
4.4	Thermal Evaluation for Accident Conditions	4-22A
4.4.1	Thermal Models for Accident Conditions	4-22A
4.4.2	Maximum Temperatures for Accident Conditions	4-27
4.4.3	Maximum Internal Pressures for Accident Conditions.....	4-28
4.4.4	Maximum Thermal Stresses for Accident Conditions.....	4-28
4.4.5	Evaluation of Thermal Performance for Accident Conditions	4-28
4.5	Thermal Evaluation for Loading and Unloading Conditions.....	4-29
4.5.1	Vacuum Drying.....	4-29

4.5.2	Reflooding.....	4-34
4.6	Maximum Internal Pressure.....	4-36
4.6.1	Average Gas Temperature	4-36
4.6.2	Amount of Initial Helium Backfill.....	4-37
4.6.3	Free Gas within Fuel Assemblies / BPRA	4-38
4.6.4	Total Amount of Gases within DSC	4-38
4.6.5	Maximum DSC Internal Pressures.....	4-39
4.6.6	Maximum Pressure in Annulus.....	4-39
4.7	Axial Decay Heat Profile	4-40
4.8	Effective Fuel Properties	4-43
4.8.1	Discussion.....	4-43
4.8.2	Summary of Material Properties.....	4-43
4.8.3	Effective Fuel Conductivity	4-45
4.8.4	Effective Fuel Density and Specific Heat.....	4-46
4.8.5	Conclusion	4-47
4.9	Effective Conductivity of Fluids in the Transfer Cask.....	4-48
4.9.1	Effective Conductivity in the Shielding Panel.....	4-48
4.9.2	Effective Water Conductivity in Annulus between TC and DSC.....	4-50
4.10	Justification of the Assumed Hot Gap Sizes.....	4-52
4.10.1	Radial Gap between Basket Rails and DSC shell.....	4-52
4.10.2	Radial Gap between Lead and the Cask Structural Shell	4-53
4.11	Heat Transfer Coefficients	4-55
4.11.1	Total heat Transfer Coefficient to Ambient.....	4-55
4.11.2	Free Convection Coefficients	4-55
4.12	Effective Conductivity of Air in Closed Cavity of HSM-H.....	4-63
4.13	Thermal-Hydraulic Equations for the HSM-H.....	4-65
4.14	Thermal Evaluation of DSC Containing Damaged Fuel.....	4-68
4.14.1	Normal / Off-Normal Conditions	4-68
4.14.2	Accident Conditions.....	4-68
4.14.3	Effective Properties of Damaged Fuel.....	4-70
4.14.4	Evaluation of DSC Thermal Performance with Damaged Fuel.....	4-71
4.15	References.....	4-73
4.16	Appendices.....	4-75
5.	SHIELDING EVALUATION.....	5-1

13.4	Conditions of Approval Records	13-9
13.5	Supplemental Information	13-10
13.5.1	References.....	13-10
14.	DECOMMISSIONING	14-1
14.1	Decommissioning Considerations.....	14-1
14.2	Supplemental Information	14-4
14.2.1	References.....	14-4
APPENDIX A 32PTH Type 1 DSC and OS187H Type 1 TC.....		A.1-1

1. GENERAL INFORMATION

This Safety Analysis Report (SAR) describes the design and forms the licensing basis for 10CFR 72[1], Subpart L certification of the NUHOMS® HD dry spent fuel storage system. The NUHOMS® HD System provides for the horizontal storage of high burnup spent Pressurized Water Reactor (PWR) fuel assemblies in a dry shielded canister (DSC) that is placed in a Horizontal Storage Module (HSM-H) utilizing an OS187H transfer cask. The NUHOMS® HD System is designed to be installed in an Independent Spent Fuel Storage Installation (ISFSI) at power reactor sites under the provision of a general license in accordance with 10CFR 72, Subpart K. This system has been specifically optimized for high thermal loads, limited space, and needs for superior radiation shielding performance.

The QA program applicable to this design satisfies the requirements of 10CFR 72, Subpart G and is described in Chapter 13. The format of this SAR follows the guidance of NRC Regulatory Guide 3.61[2]. To facilitate NRC review of this application, this SAR has been prepared in compliance with the information and methods defined in NUREG-1536 [3], "Standard Review Plan for Dry Cask Storage Systems" and the associated Interim Staff Guidance (ISGs).

The NUHOMS® HD System is an improved version of the Standardized NUHOMS® System described in Certificate of Compliance (C of C) 72-1004 [4]. The 32PTH DSC included in this application is similar to the 24PTH DSC previously included in the license for the Standardized NUHOMS® System [5]. The HSM-H is virtually identical to the HSM-H in the 24PTH amendment. The OS187H transfer cask (TC) is very similar to the previously licensed OS197 transfer cask but with a slightly larger diameter and closures containing seals.

The NUHOMS® HD System has been designed for enhanced heat rejection capabilities, and to permit storage of Non Fuel Assembly Hardware (NFAH) with the fuel and/or damaged spent fuel assemblies. Protection afforded to the public is equivalent to or has been increased relative to standardized HSM designs [5] by substantially reducing radiation dose rates. Details of the system design, analyses, operation, and margins are provided in the remainder of this SAR.

The NUHOMS® HD system also includes a longer DSC and a corresponding TC, designated the 32PTH Type 1 DSC and OS187H Type 1 TC, respectively. A detailed description of the 32PTH Type 1 DSC and OS187H Type 1 TC are provided in Appendix A. The 32PTH Type 1 DSC is stored in an HSM-H with a slightly increased support rail length. The design details of these additional HD system components are provided in the drawings shown in Section A.1.5.

1.1 Introduction

The type of fuel to be stored in the NUHOMS® HD System is Light Water Reactor (LWR) fuel of the PWR type. The NUHOMS® HD System accommodates up to 32 PWR fuel assemblies with zircaloy, (zirlo, M5) cladding, uranium dioxide (UO₂), and Non-Fuel Assembly Hardware (NFAH). Provisions have been made, as discussed in Chapter 2, for storage of up to sixteen damaged fuel assemblies in the 32PTH DSC. The physical and radiological characteristics of these payloads are provided in Chapter 2.

The NUHOMS® HD System consists of the following components as shown in Figure 1-1, Figure 1-2, and Figure 1-6:

- A Horizontal Storage Module (HSM-H) that provides spent fuel decay heat removal, physical and radiological protection for the 32PTH DSC. The HSM-H consists primarily of thick concrete walls, a steel support structure for the 32PTH DSC, and a thick concrete door. Each HSM-H includes provisions for thermal monitoring instrumentation. The HSM-H is virtually identical to the HSM-H for the NUHOMS® 24PTH DSC included in UFSAR Revision 9 [5].
- A Dry Shielded Canister (32PTH DSC) that provides confinement, an inert environment, structural support, and criticality control for 32 PWR fuel assemblies. The 32PTH DSC shell is a welded stainless steel pressure vessel that includes thick shield plugs at either end to maintain occupational exposures ALARA. The 32PTH DSC basket consists of stainless steel square tubes and support strips for structural support, and geometry control; and aluminum/borated aluminum for heat transfer and criticality control. The 32PTH DSC is very similar to the 24PTH DSC.
- The OS187H TC provides shielding and protection from potential hazards during the DSC closure operations and transfer to the HSM-H. It also provides a helium environment around the DSC during transfer operations. It is very similar to the previously licensed OS197 transfer cask for the Standardized NUHOMS® System.
- HSM-Hs are arranged in arrays to minimize space and maximize self-shielding. The 32PTH DSC is longitudinally restrained to prevent movement during seismic events. Arrays are fully expandable to permit modular expansion in support of operating power plants.
- The HSM-H provides the bulk of the radiation shielding for the 32PTH DSC. The HSM-Hs can be arranged in either a single-row or a back-to-back arrangement. Thick concrete supplemental shield walls are used at either end of an HSM-H array and along the back wall of single-row arrays to minimize radiation dose rates both onsite and offsite.

Approval of the NUHOMS® HD System components described above is sought under the provisions of 10CFR 72, Subpart L for use under the general license provisions of 10CFR 72, Subpart K. The components are intended for storage on a reinforced concrete pad at a nuclear power plant. In addition to these components, the system requires use of an onsite transfer cask,

1.2 General Description of the NUHOMS® HD System

The NUHOMS® HD System provides for the horizontal, dry storage of canisterized Spent Fuel Assemblies (SFAs) in a concrete HSM-H. The storage system components consist of a reinforced concrete HSM-H and a stainless steel 32PTH DSC confinement vessel which holds the SFAs. The general arrangement of the NUHOMS® HD System components is shown in Figure 1-3 and Figure 1-4. The confinement boundary is defined in Section 7.1 of Chapter 7 and is shown in Figure 7-1. This SAR addresses the design and analysis of the storage system components, including the 32PTH DSC, the OS187H TC, and the HSM-H, which are important to safety in accordance with 10CFR 72.

In addition to these storage system components, the NUHOMS® HD System also utilizes transfer equipment to move the 32PTH DSCs from the plant's fuel/reactor building, where they are loaded with SFAs and readied for storage, to the HSM-Hs where they are stored. This transfer system consists of a transfer cask, a lifting yoke, a hydraulic ram system, a prime mover for towing, a transfer trailer, a cask support skid, and a skid positioning system. This transfer system interfaces with the existing plant fuel pool, the cask handling crane, the site infrastructure (i.e. roadways and topography) and other site specific conditions and procedural requirements. Auxiliary equipment such as a cask/canister annulus seal, a vacuum drying system and a welding system are also used to facilitate canister loading, draining, drying, inerting, and sealing operations. Similar transfer system and auxiliary equipment have been previously licensed under C of C 72-1004 [5].

During dry storage of the spent fuel, no active systems are required for the removal and dissipation of the decay heat from the fuel. The NUHOMS® HD System is designed to transfer the decay heat from the fuel to the canister and from the canister to the surrounding air by conduction, radiation and natural convection.

Each canister is identified by a Model Number, XXX-32PTH-YYY-Z, where XXX identifies the site for which the 32PTH DSC was fabricated, Z designates the basket type, and YYY is a sequential number corresponding to a specific canister. The basket types are described in SAR drawing no. 10494-72-10.

The NUHOMS® HD System components do not include receptacles, valves, sampling ports, impact limiters, protrusions, or pressure relief systems.

The alternate DSC design and the alternate TC design, designated the 32PTH Type 1 DSC and the OS187H Type 1 TC, respectively, as well as the modifications required for the HSM-H to accommodate the 32PTH Type 1 DSC, are discussed in detail in Appendix A.

1.2.1 NUHOMS® HD System Characteristics

1.2.1.1 Dry Shielded Canister (32PTH DSC)

The key design parameters of the 32PTH DSC are listed in Table 1-1. The cylindrical shell, the inner top cover/shield plug¹ (including vent and siphon cover plates), and shell bottom form the pressure retaining confinement boundary for the spent fuel. The inner top cover/shield plug¹ and shell bottom provide shielding for the 32PTH DSC so that occupational doses at the ends are minimized during drying, sealing, handling, and transfer operations.

¹ See Chapter 1 drawings for option 2 and option 3 designs and Chapter 7 for confinement boundary definitions.

The cylindrical shell and inner bottom cover plate confinement boundary welds are fully compliant to Subsection NB of the ASME Code and are made during fabrication. The confinement boundary weld between the shell and the inner top cover/shield plug¹ (including siphon/vent cover welds) and structural attachment weld between the shell and the outer top cover plate are in accordance with Alternatives to the ASME code as described in Section 3.10.

Both siphon and vent covers are welded after drying operations are complete. There are no credible accidents which could breach the confinement boundary of the 32PTH DSC as documented in Chapters 3 and 11.

The 32PTH DSC is designed for a maximum heat load of 34.8 kW. The internal basket assembly contains a storage position for each fuel assembly. The criticality analysis credits the fixed borated neutron absorbing material placed between the fuel assemblies. The analysis takes credit for soluble boron during loading operations. Sub-criticality during wet loading, drying, sealing, transfer, and storage operations is maintained through the geometric separation of the fuel assemblies by the basket assembly, the boron loading of the pool water, and the neutron absorbing capability of the 32PTH DSC materials, as applicable. Based on poison material and boron loading, several basket types are provided, as shown on drawing 10494-72-10 and described in Chapter 6.

Structural support for the PWR fuel is provided by the basket fuel compartments and support strips. The support strips are located periodically over the full length of the basket with allowance provided for thermal growth. Stainless steel transition rails are provided at the basket periphery for support and heat transfer.

Dimensions of the 32PTH DSC components described in the text and provided in figures and tables of this SAR are nominal dimensions for general system description purposes. Actual design dimensions are contained in the drawings in Section 1.5.2 of this SAR. For a discussion of the contents authorized to be stored in this DSC, see Section 2.1.1 of this SAR.

1.2.1.2 Horizontal Storage Module (HSM-H)

Each HSM-H provides a self-contained modular structure for storage of spent fuel canisterized in a 32PTH DSC. The HSM-H is constructed from reinforced concrete and structural steel. The thick concrete roof and walls provide substantial neutron and gamma shielding. Contact doses for the HSM-H are designed to be ALARA. The key design parameters of the HSM-H are listed in Table 1-1.

The nominal thickness of the HSM-H roof is four feet for biological shielding. Separate shield walls at the end of a module row in conjunction with the module wall, provide a minimum thickness of four feet for shielding. Similarly, an additional shield wall is used at the rear of the module if the ISFSI is configured as single module arrays. Sufficient shielding is provided by thick concrete side walls between HSM-Hs in an array to minimize doses in adjacent HSMs during loading and retrieval operations.

¹ See Chapter 1 drawings for option 2 and option 3 designs and Chapter 7 for confinement boundary definitions.

1.5 Supplemental Data

1.5.1 References

1. Title 10, Code of Federal Regulations, Part 72, "Licensing Requirements for the Storage of Spent Fuel in an Independent Spent Fuel Storage Installation."
2. U.S. Nuclear Regulatory Commission, Regulatory Guide 3.61, Standard Format and Content for a Topical Safety Analysis Report for a Spent Fuel Dry Storage Cask, February 1989.
3. U.S. Nuclear Regulatory Commission, "Standard Review Plan for Dry Cask Storage Systems," NUREG 1536, U.S. NRC, January 1997.
4. NRC Certificate of Compliance 72-1004, NUHOMS® General License Spent Fuel Storage System, Amendment No. 8, December, 2005.
5. Updated Final Safety Analysis Report, Standardized NUHOMS® Horizontal Modular Storage System for Irradiated Nuclear Fuel, Revision 9, February 2006, USNRC Docket No. 72-1004.
6. Title 10, Code of Federal Regulations, Part 50, "Domestic Licensing of Production and Utilization Facilities."

1.5.2 Drawings

- 32PTH DSC: 10494-72-(1 to 12) (PROPRIETARY)
- OS187H: 10494-72-(15 to 21) (PROPRIETARY)
- HSM-H: 10494-72-(100 to 110) (PROPRIETARY)
- Damaged Fuel End Caps: 10494-72-30 (PROPRIETARY)

Drawings for the 32PTH Type 1 DSC and OS187H Type 1 TC are shown in Appendix A, Section A.1.5.2.

Table 1-1
Key Design Parameters of the NUHOMS® HD System Components

Dry Shielded Canister (32PTH DSC)^(a)	
Overall Length (in)	185.75 (max)
Outside Diameter (in)	69.75
Cavity Length (in)	164.5 (min)
Shell Thickness (in)	0.5
Design Weight of Loaded 32PTH DSC (lbs.)	108,800
Materials of Construction	Stainless Steel Shell Assembly and Internals, Carbon Steel and/or Stainless Steel Shield Plugs, Aluminum
Neutron Absorbing Material	Boral™, borated aluminum, metal matrix composite (MMC) as specified in Chapter 9
Internal Atmosphere	Helium

Horizontal Storage Module (HSM-H):	
Overall length (without back shield wall)	20'-8"
Overall width (without end shield walls)	9'-8"
Overall height	18' 6"
Total Weight not including 32PTH DSC (lbs.)	306,000
Materials of Construction	Reinforced Concrete and Structural Steel
Heat Removal	Conduction, Convection, and Radiation

On-Site Transfer Cask (OS187H)^(b)	
Overall Length (in)	197.1
Outside Diameter (in)	92.2
Cavity Length (in)	186.6
Lead Thickness (in)	3.60 (nom)
Gross Weight (including 32PTH DSC) (tons)	114.5
Materials of Construction	Stainless Steel Shell Assemblies and closures with lead shielding
Internal Atmosphere	Helium

^(a) See appendix A for 32 PTH Type 1 DSC.

^(b) See appendix A for OS187H Type 1 TC.

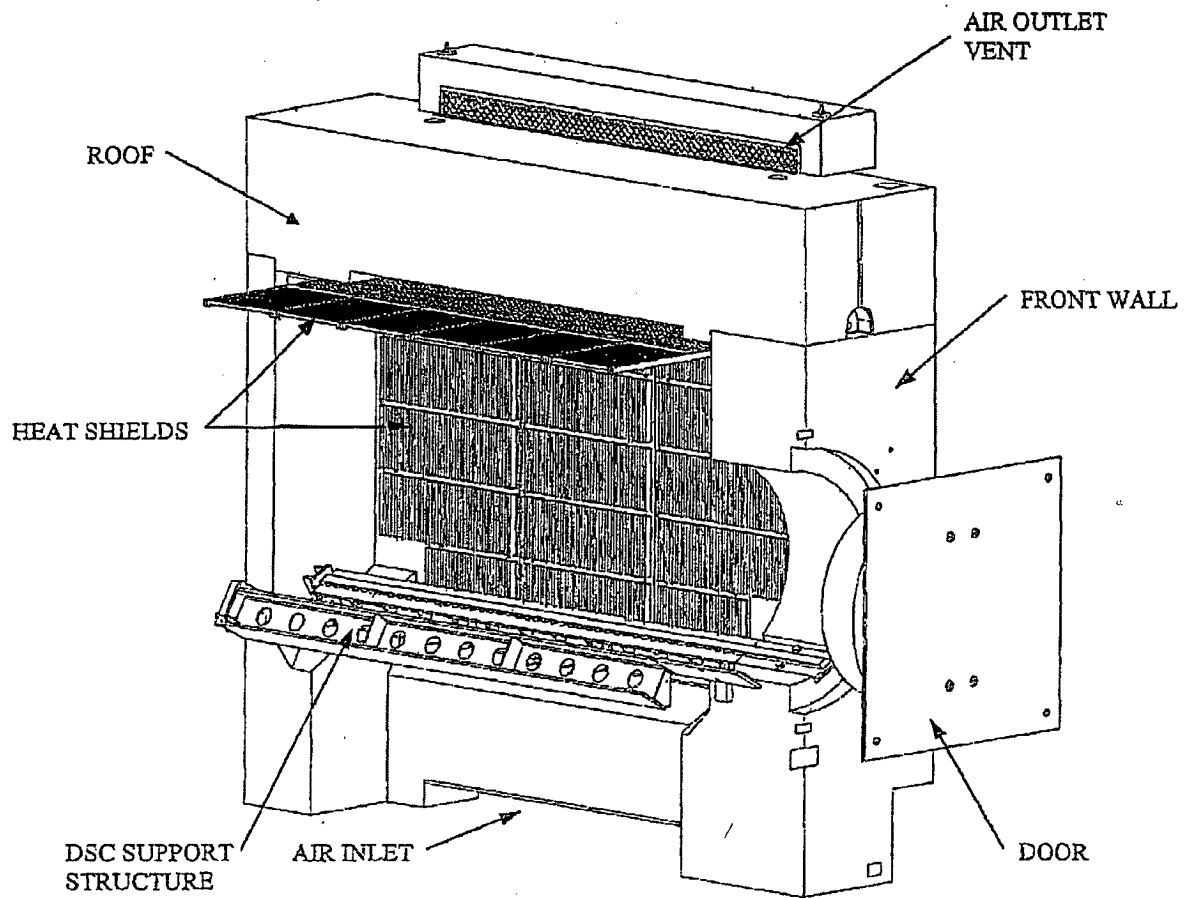


Figure 1-1
NUHOMS® HD System Horizontal Storage Module (HSM-H)

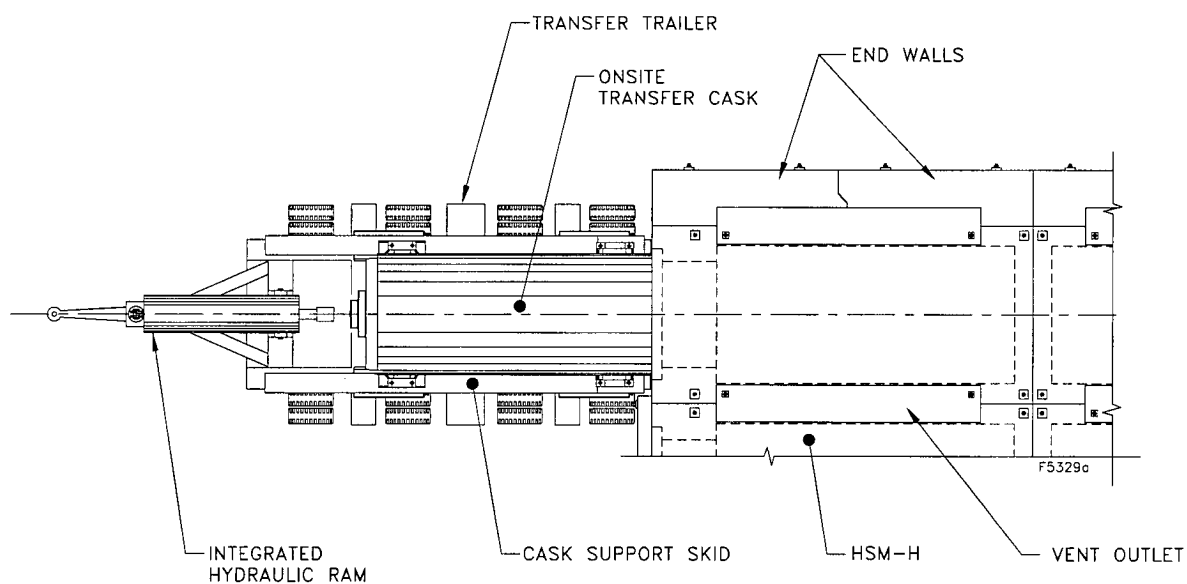


Figure 1-4
NUHOMS® HD System Components, Structures, and
Transfer Equipment – Plan View (Typical)

Figure Withheld Under 10 CFR 2.390

Figure 1-9
Typical Double Module Row HSM-H ISFSI Layout


Figure Withheld Under 10 CFR 2.390

Figure 1-10
Typical Single Module Row HSM-H ISFSI Layout


Figure Withheld Under 10 CFR 2.390

Figure 1-11
Typical Combined Single and Double Module Row HSM-H ISFSI Layout

PROPRIETARY AND
SECURITY RELATED INFORMATION
WITHHELD UNDER 10 CFR 2.390

<p>UNLESS OTHERWISE SPECIFIED ALL DIMENSIONS ARE IN INCHES & DEGREES.</p> <p>TOLERANCES ALL DIMENSIONS ARE NOMINAL UNLESS A SPECIFIC TOLERANCE IS INDICATED WITH THE DRAWING DIMENSION</p> <p>THIS DRAWING AND ANY INFORMATION RELATED TO IT CONTAINS INFORMATION THAT IS PROPRIETARY TO TRANSNUCLEAR INC. THIS INFORMATION IS FURNISHED IN CONFIDENCE TO SUPPLY THE REQUIRED ENGINEERING DATA FOR JOBS PURSUING TO WORK BEING DONE BY TRANSNUCLEAR.</p>	 TRANSNUCLEAR AN AREVA COMPANY			
	SAFETY ANALYSIS REPORT NUHOMS®32PTH TRANSPORTABLE CANISTER FOR PWR FUEL PARTS LIST			
	DRAWING NO. 10494-72-1	SCALE NONE	SHEET 1 OF 1	REVISION 2

PROPRIETARY AND
SECURITY RELATED INFORMATION
WITHHELD UNDER 10 CFR 2.390

<p>UNLESS OTHERWISE SPECIFIED ALL DIMENSIONS ARE IN INCHES & DEGREES.</p> <p>TOLERANCES ALL DIMENSIONS ARE NOMINAL, UNLESS A SPECIFIC TOLERANCE IS INDICATED WITH THE DRAWING DIMENSION</p> <p>THIS DRAWING AND ANY INFORMATION RELATED TO IT CONTAINS INFORMATION THAT IS PROPRIETARY TO TRANSCORPORATE INC. THIS INFORMATION IS FURNISHED IN CONFIDENCE TO SUPPLY THE REQUIRED ENGINEERING DATA FOR JOBS PERTAINING TO WORK BEING DONE BY TRANSCORPORATE.</p>	 TRANSCORPORATE AN AREVA COMPANY			
	SAFETY ANALYSIS REPORT NUHOMS-32PTH TRANSPORTABLE CANISTER FOR PWR FUEL MAIN ASSEMBLY			
	DRAWING NO. 10494-72-2	SCALE NONE	SHEET 1 OF 1	REVISION 2

PROPRIETARY AND SECURITY RELATED INFORMATION WITHHELD UNDER 10 CFR 2.390

<p>UNLESS OTHERWISE SPECIFIED ALL DIMENSIONS ARE IN INCHES & DEGREES.</p>	<p>A TRANSNUCLEAR AN AREVA COMPANY</p>								
<p>TOLERANCES ALL DIMENSIONS ARE NOMINAL, UNLESS A SPECIFIC TOLERANCE IS INDICATED WITH THE DRAWING DIMENSION</p>									
<p>THIS DRAWING AND ANY INFORMATION RELATED TO IT CONTAINS INFORMATION THAT IS PROPRIETARY TO TRANSNUCLEAR INC. THIS INFORMATION IS FURNISHED IN CONFIDENCE TO SUPPLY THE REQUIRED ENGINEERING DATA FOR JOBS PERTAINING TO WORK BEING DONE BY TRANSNUCLEAR.</p>	<p>SAFETY ANALYSIS REPORT NUHOMS* 32PTH TRANSPORTABLE CANISTER FOR PWR FUEL SIPHON PIPE DETAILS</p> <table border="1"> <tr> <td>DRAWING NO.</td> <td>SCALE</td> <td>SHEET</td> <td>REVISION</td> </tr> <tr> <td>10494-72-3</td> <td>NONE</td> <td>1 OF 1</td> <td>2</td> </tr> </table>	DRAWING NO.	SCALE	SHEET	REVISION	10494-72-3	NONE	1 OF 1	2
DRAWING NO.	SCALE	SHEET	REVISION						
10494-72-3	NONE	1 OF 1	2						


PROPRIETARY AND SECURITY RELATED INFORMATION WITHHELD UNDER 10 CFR 2.390

<p>UNLESS OTHERWISE SPECIFIED ALL DIMENSIONS ARE IN INCHES & DEGREES.</p>	<p>A TRANSNUCLEAR AN AREVA COMPANY</p>								
<p>TOLERANCES ALL DIMENSIONS ARE NOMINAL, UNLESS A SPECIFIC TOLERANCE IS INDICATED WITH THE DRAWING DIMENSION</p>									
<p>THIS DRAWING AND ANY INFORMATION RELATED TO IT CONTAINS INFORMATION THAT IS PROPRIETARY TO TRANSNUCLEAR INC. THIS INFORMATION IS FURNISHED IN CONFIDENCE TO SUPPLY THE REQUIRED ENGINEERING DATA FOR JOBS PERTAINING TO WORK BEING DONE BY TRANSNUCLEAR.</p>	<p>SAFETY ANALYSIS REPORT NUHOMS* 32PTH TRANSPORTABLE CANISTER FOR PWR FUEL INNER TOP COVER DETAILS</p> <table border="1"> <tr> <td>DRAWING NO.</td> <td>10494-72-4</td> <td>SCALE</td> <td>NONE</td> <td>SHEET</td> <td>1 OF 2</td> <td>REVISION</td> <td>2</td> </tr> </table>	DRAWING NO.	10494-72-4	SCALE	NONE	SHEET	1 OF 2	REVISION	2
DRAWING NO.	10494-72-4	SCALE	NONE	SHEET	1 OF 2	REVISION	2		


PROPRIETARY AND SECURITY RELATED INFORMATION WITHHELD UNDER 10 CFR 2.390

<p>UNLESS OTHERWISE SPECIFIED ALL DIMENSIONS ARE IN INCHES & DECIMALS.</p>	<p>A TRANSNUCLEAR AN AREVA COMPANY</p>
<p>TOLERANCES ALL DIMENSIONS ARE NOMINAL, UNLESS A SPECIFIC TOLERANCE IS INDICATED WITH THE DRAWING DIMENSION</p>	
<p>THIS DRAWING AND ANY INFORMATION RELATED TO IT CONTAINS INFORMATION THAT IS PROPRIETARY TO TRANSNUCLEAR INC. THIS INFORMATION IS FURNISHED IN CONFIDENCE TO SUPPLY THE REQUIRED ENGINEERING DATA FOR JOBS PERFORMED TO WORK BEING DONE BY TRANSNUCLEAR.</p>	
<p>SAFETY ANALYSIS REPORT NUHOM*32PTH TRANSPORTABLE CANISTER FOR PWR FULE OUTER TOP COVER DETAILS</p>	<p>DRAWING NO. 10494-72-4 SCALE NONE SHEET 2 OF 2 REVISION 2</p>


PROPRIETARY AND
SECURITY RELATED INFORMATION
WITHHELD UNDER 10 CFR 2.390

UNLESS OTHERWISE SPECIFIED ALL DIMENSIONS ARE IN INCHES & DEGREES		 TRANSNUCLEAR AN AREVA COMPANY	
TOLERANCES ALL DIMENSIONS ARE NOMINAL UNLESS A SPECIFIC TOLERANCE IS INDICATED WITH THE DRAWING DIMENSION			
THIS DRAWING AND ANY INFORMATION RELATED TO IT CONTAINS INFORMATION THAT IS PROPRIETARY TO TRANSNUCLEAR INC. THIS INFORMATION IS FURNISHED IN CONFIDENCE TO SUPPLY THE REQUIRED DIMENSIONS DATA FOR JOBS PERTAINING TO WORK BEING DONE BY TRANSNUCLEAR		SAFETY ANALYSIS REPORT NUHOMS [®] 32PTH TRANSPORTABLE CANISTER FOR PWR FUEL SHELL ASSEMBLY	
DRAWING NO. 10494-72-5		SCALE NONE	SHEET 1 OF 1 REVISION 2

PROPRIETARY AND
SECURITY RELATED INFORMATION
WITHHELD UNDER 10 CFR 2.390

UNLESS OTHERWISE SPECIFIED ALL DIMENSIONS ARE IN INCHES & DEGREES.		 TRANSNUCLEAR AN AREVA COMPANY	
TOLERANCES ALL DIMENSIONS ARE NOMINAL UNLESS A SPECIFIC TOLERANCE IS INDICATED WITH THE DRAWING DIMENSION			
<small>THIS DRAWING AND ANY INFORMATION RELATED TO IT CONTAINS INFORMATION THAT IS PROPRIETARY TO TRANSNUCLEAR INC. THIS INFORMATION IS FURNISHED IN CONFORMANCE TO SUPPLY THE REQUIRED ENGINEERING DATA FOR JOBS PERTAINING TO WORK BEING DONE BY TRANSNUCLEAR.</small>		SAFETY ANALYSIS REPORT NUHOMS 32PTH TRANSPORTABLE CANISTER FOR PWR FUEL SHELL BOTTOM DETAILS	
		10494-72-0	SCALE NONE


PROPRIETARY AND
SECURITY RELATED INFORMATION
WITHHELD UNDER 10 CFR 2.390

UNLESS OTHERWISE SPECIFIED ALL DIMENSIONS ARE IN INCHES & DEGREES.		 TRANSNUCLEAR AN AREVA COMPANY	
TOLERANCES ALL DIMENSIONS ARE NOMINAL UNLESS A SPECIFIC TOLERANCE IS INDICATED WITH THE DIMENSION			
THIS DRAWING AND ANY INFORMATION RELATED TO IT CONTAINS INFORMATION THAT IS PROPRIETARY TO TRANSNUCLEAR INC. THIS INFORMATION IS FURNISHED IN CONFIDENCE TO SUPPLY THE REQUIRED DIMENSION DATA FOR JOBS PERTAINING TO WORK BEING DONE BY TRANSNUCLEAR.		SAFETY ANALYSIS REPORT NUHOMS' 32PTH TRANSPORTABLE CANISTER FOR PWR FUEL GRAPPLE RING DETAILS	
DRAWING NO. 10494-72-7		SCALE NONE	SHEET 1 OF 1
			REVISION 2


PROPRIETARY AND
SECURITY RELATED INFORMATION
WITHHELD UNDER 10 CFR 2.390

<p>UNLESS OTHERWISE SPECIFIED ALL DIMENSIONS ARE IN INCHES & DEGREES.</p>	<p>A TRANSNUCLEAR AN AREVA COMPANY</p>								
<p>TOLERANCES ALL DIMENSIONS ARE NOMINAL, UNLESS A SPECIFIC TOLERANCE IS INDICATED WITH THE DRAWING DIMENSION</p>									
<p>THIS DRAWING AND ANY INFORMATION RELATED TO IT CONTAINS INFORMATION THAT IS PROPRIETARY TO TRANSNUCLEAR AND THIS INFORMATION IS FURNISHED IN CONFIDENCE TO SUPPLY THE REQUIRED ENGINEERING DATA FOR JOBS PERTAINING TO WORK BEING DONE BY TRANSNUCLEAR.</p>	<p>SAFETY ANALYSIS REPORT NUHOMS 32PTH TRANSPORTABLE CANISTER FOR PWR FUEL BASKET ASSEMBLY</p> <table border="1"> <tr> <td>DRAWING NO.</td> <td>10494-72-8</td> <td>SCALE</td> <td>NONE</td> <td>SHEET</td> <td>1 OF 1</td> <td>REVISION</td> <td>2</td> </tr> </table>	DRAWING NO.	10494-72-8	SCALE	NONE	SHEET	1 OF 1	REVISION	2
DRAWING NO.	10494-72-8	SCALE	NONE	SHEET	1 OF 1	REVISION	2		


PROPRIETARY AND
SECURITY RELATED INFORMATION
WITHHELD UNDER 10 CFR 2.390

UNLESS OTHERWISE SPECIFIED ALL DIMENSIONS ARE IN INCHES & DEGREES.	 TRANSNUCLEAR AN AREVA COMPANY	
TOLERANCES ALL DIMENSIONS ARE NOMINAL UNLESS A SPECIFIC TOLERANCE IS INDICATED WITH THE DRAWING DIMENSION	SAFETY ANALYSIS REPORT NUHOMS [®] 32 PTH	
THIS DRAWING AND ANY INFORMATION RELATED TO IT, CONTAINS INFORMATION THAT IS PROPRIETARY TO TRANSNUCLEAR INC. THIS INFORMATION IS FURNISHED IN CONFIDENCE TO SUPPLY THE REQUIRED ENGINEERING DATA FOR JOBS PERTAINING TO WORK BEING DONE BY TRANSNUCLEAR.	TRANSPORTABLE CANISTER FOR PWR FUEL BASKET ASSEMBLY DETAILS	
FIGURE NO. 10494-72-9	SCALE NONE	REVISION 1 OF 1
		2


PROPRIETARY AND
SECURITY RELATED INFORMATION
WITHHELD UNDER 10 CFR 2.390

UNLESS OTHERWISE SPECIFIED ALL DIMENSIONS ARE IN INCHES & DEGREES.	 TRANSNUCLEAR AN AREVA COMPANY		
TOLERANCES ALL DIMENSIONS ARE NOMINAL, UNLESS A SPECIFIC TOLERANCE IS INDICATED WITH THE DRAWING DIMENSION			
THIS DRAWING AND ANY INFORMATION RELATED TO IT CONTAINS INFORMATION THAT IS PROPRIETARY TO TRANSNUCLEAR INC. THIS INFORMATION IS FURNISHED IN CONFIDENCE TO SUPPLY THE REQUIRED ENGINEERING DATA FOR JOBS PURSUING TO WORK BEING DONE BY TRANSNUCLEAR.	SAFETY ANALYSIS REPORT NUHOMS*32PTH TRANSPORTABLE CANISTER FOR PWR FUEL BASKET ASSEMBLY DETAILS		
DRAWING NO. 10494-72-10	SCALE NONE	SHEET 1 OF 1	REVISION 2

PROPRIETARY AND
SECURITY RELATED INFORMATION
WITHHELD UNDER 10 CFR 2.390

UNLESS OTHERWISE SPECIFIED ALL DIMENSIONS ARE IN INCHES & DEGREES.	 TRANSNUCLEAR AN AREVA COMPANY		
TOLERANCES ALL DIMENSIONS ARE NOMINAL UNLESS A SPECIFIC TOLERANCE IS INDICATED WITH THE DRAWING DIMENSION			
THIS DRAWING AND ANY INFORMATION RELATED TO IT CONTAINS INFORMATION THAT IS PROPRIETARY TO TRANSNUCLEAR INC. THIS INFORMATION IS FURNISHED IN CONFIDENCE TO SUPPLY THE REQUIRED ENGINEERING DATA FOR JOBS PERTAINING TO WORK BEING DONE BY TRANSNUCLEAR.	SAFETY ANALYSIS REPORT NUHOMS*32PTH TRANSPORTABLE CANISTER FOR PWR FUEL BASKET RAIL A180		
10494-72-11	SCALE NONE	SHEET 1 OF 1	REVISION 2

PROPRIETARY AND
SECURITY RELATED INFORMATION
WITHHELD UNDER 10 CFR 2.390

UNLESS OTHERWISE SPECIFIED ALL DIMENSIONS ARE IN INCHES & DEGREES.	 TRANSNUCLEAR AN AREVA COMPANY	SAFETY ANALYSIS REPORT		
		NUHOMS* 32PTH		
TOLERANCES ALL DIMENSIONS ARE NOMINAL, UNLESS A SPECIFIC TOLERANCE IS INDICATED WITH THE DRAWING DIMENSION	TRANSPORTABLE CANISTER FOR PWR FUEL BASKET RAIL A90			
THIS DRAWING AND ANY INFORMATION RELATED TO IT CONTAINS INFORMATION THAT IS PROPRIETARY TO TRANSNUCLEAR INC. THIS INFORMATION IS FURNISHED IN CONFIDENCE TO SUPPLY THE REQUIRED ENGINEERING DATA FOR JOBS PURSUING TO WORK BEING DONE BY TRANSNUCLEAR.	DRAWING NO. 10494-72-12	SCALE NONE	SHEET 1 OF 1	REVISION 2

PROPRIETARY AND SECURITY RELATED INFORMATION WITHHELD UNDER 10 CFR 2.390

<p>UNLESS OTHERWISE SPECIFIED ALL DIMENSIONS ARE IN INCHES & DEGREES.</p>	<p>A TRANSNUCLEAR AN AREVA COMPANY</p>								
<p>TOLERANCES ALL DIMENSIONS ARE NOMINAL UNLESS A SPECIFIC TOLERANCE IS INDICATED WITH THE DRAWING DIMENSION</p>									
<p>THIS DRAWING AND ANY INFORMATION RELATED TO IT CONTAINS INFORMATION THAT IS PROPRIETARY TO TRANSNUCLEAR INC. THIS INFORMATION IS FURNISHED IN CONFIDENCE TO SUPPLY THE REQUIRED ENGINEERING DATA FOR JOBS PERSONNEL TO WORK BEING DONE BY TRANSNUCLEAR.</p>	<p>SAFETY ANALYSIS REPORT NUHOMS' OS187H ONSITE TRANSFER CASK PARTS LIST</p> <table border="1"> <tr> <td>DRAWING NO.</td> <td>10494-72-15</td> <td>SCALE</td> <td>NONE</td> <td>SHEET</td> <td>1 OF 1</td> <td>REVISION</td> <td>2</td> </tr> </table>	DRAWING NO.	10494-72-15	SCALE	NONE	SHEET	1 OF 1	REVISION	2
DRAWING NO.	10494-72-15	SCALE	NONE	SHEET	1 OF 1	REVISION	2		

PROPRIETARY AND SECURITY RELATED INFORMATION WITHHELD UNDER 10 CFR 2.390

<p>UNLESS OTHERWISE SPECIFIED ALL DIMENSIONS ARE IN INCHES & DEGREES.</p>	<p>A TRANSNUCLEAR AN AREVA COMPANY</p>								
<p>TOLERANCES ALL DIMENSIONS ARE NOMINAL UNLESS A SPECIFIC TOLERANCE IS INDICATED WITH THE DRAWING DIMENSION</p>									
<p>THIS DRAWING AND ANY INFORMATION RELATED TO IT, CONTAINING INFORMATION THAT IS PROPRIETARY TO TRANSNUCLEAR INC. THIS INFORMATION IS FURNISHED IN CONFIDENCE TO SUPPLY THE REQUIRED ENGINEERING DATA FOR JOBS PERTAINING TO WORK BEING DONE BY TRANSNUCLEAR.</p>	<p>SAFETY ANALYSIS REPORT NUHOMS[®] OS187H ONSITE TRANSFER CASK MAIN ASSEMBLY</p> <table border="1"> <tr> <td>DRAWING NO.</td> <td>10494-72-16</td> <td>SCALE</td> <td>NONE</td> <td>SHEET</td> <td>1 OF 1</td> <td>REVISION</td> <td>2</td> </tr> </table>	DRAWING NO.	10494-72-16	SCALE	NONE	SHEET	1 OF 1	REVISION	2
DRAWING NO.	10494-72-16	SCALE	NONE	SHEET	1 OF 1	REVISION	2		

PROPRIETARY AND SECURITY RELATED INFORMATION WITHHELD UNDER 10 CFR 2.390

<p>UNLESS OTHERWISE SPECIFIED ALL DIMENSIONS ARE IN INCHES & DEGREES.</p>	<p>A TRANSNUCLEAR AN AREVA COMPANY</p>								
<p>TOLERANCES ALL DIMENSIONS ARE NOMINAL, UNLESS A SPECIFIC TOLERANCE IS INDICATED WITH THE DRAWING DIMENSION</p>									
<p>THIS DRAWING AND ANY INFORMATION RELATED TO IT CONTAINS INFORMATION THAT IS PROPRIETARY TO TRANSNUCLEAR INC. THIS INFORMATION IS FURNISHED IN CONFIDENCE TO SUPPLY THE REQUIRED ENGINEERING DATA FOR JOBS PERTAINING TO WORK BEING DONE BY TRANSNUCLEAR.</p>	<p>SAFETY ANALYSIS REPORT NUHOMS[®] OS187H ONSITE TRANSFER CASK TOP COVER ASSEMBLY</p> <table border="1"> <tr> <td>DESIGN NO.</td> <td>10494-72-17</td> <td>SCALE</td> <td>NONE</td> <td>SHEET</td> <td>1 OF 1</td> <td>REVISION</td> <td>2</td> </tr> </table>	DESIGN NO.	10494-72-17	SCALE	NONE	SHEET	1 OF 1	REVISION	2
DESIGN NO.	10494-72-17	SCALE	NONE	SHEET	1 OF 1	REVISION	2		

PROPRIETARY AND
SECURITY RELATED INFORMATION
WITHHELD UNDER 10 CFR 2.390

<p>UNLESS OTHERWISE SPECIFIED ALL DIMENSIONS ARE IN INCHES & DEGREES.</p>	<p>A TRANSNUCLEAR AN AREVA COMPANY</p>								
<p>TOLERANCES ALL DIMENSIONS ARE NOMINAL UNLESS A SPECIFIC TOLERANCE IS INDICATED WITH THE DRAWING DIMENSION</p>									
<p>THIS DRAWING AND ANY INFORMATION RELATED TO IT CONTAINS INFORMATION THAT IS PROPRIETARY TO TRANSNUCLEAR INC. THIS INFORMATION IS FURNISHED IN CONFIDENCE TO SUPPLY THE REQUIRED DIMENSIONS DATA FOR JOBS PERFORMING TO WORK BEING DONE BY TRANSNUCLEAR.</p>	<p>SAFETY ANALYSIS REPORT NUHOMS OS187H ONSITE TRANSFER CASK BOTTOM & VENT/DRAIN COVERS DETAILS</p> <table border="1"> <tr> <td>DRAWING NO.</td> <td>10494-72-1B</td> <td>SCALE</td> <td>NONE</td> <td>SHEET</td> <td>1 OF 1</td> <td>REVISION</td> <td>1</td> </tr> </table>	DRAWING NO.	10494-72-1B	SCALE	NONE	SHEET	1 OF 1	REVISION	1
DRAWING NO.	10494-72-1B	SCALE	NONE	SHEET	1 OF 1	REVISION	1		

PROPRIETARY AND
SECURITY RELATED INFORMATION
WITHHELD UNDER 10 CFR 2.390

UNLESS OTHERWISE SPECIFIED
ALL DIMENSIONS ARE IN INCHES &
DEGREES.

TOLERANCES
ALL DIMENSIONS ARE NOMINAL, UNLESS
A SPECIFIC TOLERANCE IS INDICATED
WITH THE DRAWING DIMENSION.


THIS DRAWING AND ANY INFORMATION RELATED TO IT
CONTAINS INFORMATION THAT IS PROPRIETARY TO
TRANSNUCLEAR INC. THIS INFORMATION IS FURNISHED
IN CONFIDENCE TO SUPPLY THE REQUIRED DIMENSIONS
DATA FOR JOBS PERTAINING TO WORK BEING DONE
BY TRANSNUCLEAR.

A
TRANSNUCLEAR
AN AREVA COMPANY


SAFETY ANALYSIS REPORT
NUHOMS OS187H
ONSITE TRANSFER CASK
INNER SHELL ASSEMBLY

10494-72-19	SCALE NONE	SHEET 1 OF 1	REVISION 2
-------------	---------------	-----------------	---------------


PROPRIETARY AND
SECURITY RELATED INFORMATION
WITHHELD UNDER 10 CFR 2.390

UNLESS OTHERWISE SPECIFIED ALL DIMENSIONS ARE IN INCHES & DEGREES.		 TRANSNUCLEAR AN AREVA COMPANY	
TOLERANCES ALL DIMENSIONS ARE NOMINAL UNLESS A SPECIFIC TOLERANCE IS INDICATED WITH THE DRAWING DIMENSION			
THIS DRAWING AND ANY INFORMATION RELATED TO IT CONTAINS INFORMATION THAT IS PROPRIETARY TO TRANSNUCLEAR INC. THIS INFORMATION IS FURNISHED IN CONFIDENCE TO SUPPORT THE REQUIRED ENGINEERING DATA FOR JOBS PERTAINING TO WORK BEING DONE BY TRANSNUCLEAR.		SAFETY ANALYSIS REPORT NUHOMS' OS187H ONSITE TRANSFER CASK STRUCTURAL SHELL ASSEMBLY	
DATE: 10/18/04	10484-72-20	SCALE: NONE	REVISION: 2

PROPRIETARY AND
SECURITY RELATED INFORMATION
WITHHELD UNDER 10 CFR 2.390

UNLESS OTHERWISE SPECIFIED ALL DIMENSIONS ARE IN INCHES & DEGREES.	 TRANSNUCLEAR AN AREVA COMPANY		
TOLERANCES ALL DIMENSIONS ARE NOMINAL UNLESS A SPECIFIC TOLERANCE IS INDICATED WITH THE DRAWING DIMENSION			
<small>THIS DRAWING AND ANY INFORMATION RELATED TO IT CONTAINS INFORMATION THAT IS PROPRIETARY TO TRANSNUCLEAR INC. THIS INFORMATION IS FURNISHED IN CONFIDENCE TO SUPPLY THE REQUIRED ENGINEERING DATA FOR JOBS PURSUING TO WORK BEING DONE BY TRANSNUCLEAR.</small>	<small>SAFETY ANALYSIS REPORT NUHOMS[®] OS187H ONSITE TRANSFER CASK INNER/OUTER SHELL DETAILS</small>		
<small>DRAWING NO.</small> 10494-72-21	<small>SCALE</small> NONE	<small>SHEET</small> 1 OF 1	<small>REVISION</small> 2

PROPRIETARY AND
SECURITY RELATED INFORMATION
WITHHELD UNDER 10 CFR 2.390

UNLESS OTHERWISE SPECIFIED ALL DIMENSIONS ARE IN INCHES & DEGREES.	 TRANSNUCLEAR AN AREVA COMPANY
TOLERANCES ALL DIMENSIONS ARE NOMINAL UNLESS A SPECIFIC TOLERANCE IS INDICATED WITH THE DIMENSION	
THIS DRAWING AND ANY INFORMATION RELATED TO IT CONTAINS INFORMATION THAT IS PROPRIETARY TO TRANSNUCLEAR INC. THIS INFORMATION IS FURNISHED IN CONFIDENCE TO SUPPLY THE REQUIRED DIMENSIONS DATA FOR JOBS PERTAINING TO WORK BEING DONE BY TRANSNUCLEAR.	SAFETY ANALYSIS REPORT NUHOMS' 32PTH TRANSPORTABLE CANISTER FOR PWR FUEL DAMAGED FUEL END CAPS
DRAWING NO. 10494-72-30	REVISION NONE 1 OF 1 1

PROPRIETARY AND
SECURITY RELATED INFORMATION
WITHHELD UNDER 10 CFR 2.390

UNLESS OTHERWISE SPECIFIED

ALL DIMENSIONS ARE IN INCHES &
DEGREES.

TOLERANCES

PROPRIETARY AND
SECURITY RELATED INFORMATION
WITHHELD UNDER 10 CFR 2.390

UNLESS OTHERWISE SPECIFIED

ALL DIMENSIONS ARE IN INCHES &
DEGREES.

TOLERANCES

PROPRIETARY AND
SECURITY RELATED INFORMATION
WITHHELD UNDER 10 CFR 2.390

PROPRIETARY AND
SECURITY RELATED INFORMATION
WITHHELD UNDER 10 CFR 2.390

UNLESS OTHERWISE SPECIFIED

ALL DIMENSIONS ARE IN INCHES &
DEGREES.

TOLERANCES

PROPRIETARY AND
SECURITY RELATED INFORMATION
WITHHELD UNDER 10 CFR 2.390

UNLESS OTHERWISE SPECIFIED

ALL DIMENSIONS ARE IN INCHES &
DEGREES.

TOLERANCES

PROPRIETARY AND
SECURITY RELATED INFORMATION
WITHHELD UNDER 10 CFR 2.390

PROPRIETARY AND
SECURITY RELATED INFORMATION
WITHHELD UNDER 10 CFR 2.390

UNLESS OTHERWISE SPECIFIED

ALL DIMENSIONS ARE IN INCHES &
DEGREES.

TOLERANCES

PROPRIETARY AND
SECURITY RELATED INFORMATION
WITHHELD UNDER 10 CFR 2.390

UNLESS OTHERWISE SPECIFIED

ALL DIMENSIONS ARE IN INCHES &
DEGREES.

TOLERANCES

PROPRIETARY AND
SECURITY RELATED INFORMATION
WITHHELD UNDER 10 CFR 2.390

UNLESS OTHERWISE SPECIFIED

ALL DIMENSIONS ARE IN INCHES &
DEGREES.

TOLERANCES

PROPRIETARY AND
SECURITY RELATED INFORMATION
WITHHELD UNDER 10 CFR 2.390

UNLESS OTHERWISE SPECIFIED

ALL DIMENSIONS ARE IN INCHES &
DEGREES.

TOLERANCES

PROPRIETARY AND
SECURITY RELATED INFORMATION
WITHHELD UNDER 10 CFR 2.390

UNLESS OTHERWISE SPECIFIED

ALL DIMENSIONS ARE IN INCHES &
DEGREES.

TOLERANCES

PROPRIETARY AND
SECURITY RELATED INFORMATION
WITHHELD UNDER 10 CFR 2.390

UNLESS OTHERWISE SPECIFIED

ALL DIMENSIONS ARE IN INCHES &
DEGREES.

TOLERANCES

PROPRIETARY AND
SECURITY RELATED INFORMATION
WITHHELD UNDER 10 CFR 2.390

UNLESS OTHERWISE SPECIFIED

ALL DIMENSIONS ARE IN INCHES &
DEGREES.

TOLERANCES

2. PRINCIPAL DESIGN CRITERIA

The design criteria described herein for the 32PTH DSC and the OS187H TC are also applicable to the 32PTH Type 1 DSC and the OS187H Type 1 TC discussed in Appendix A. Design criteria applicable specifically to the 32PTH Type 1 DSC and the OS187H Type 1 TC are described in Appendix A, Chapter A.2.

2.1 Spent Fuel to be Stored

The NUHOMS® HD System components have currently been designed for the storage of 32 intact and or up to 16 damaged with remaining intact, Westinghouse 15x15 (WE 15x15 and WES 15x15), Westinghouse 17x17 (WE 17x17, WEV 17x17 and WEO 17x17), Framatome ANP Advanced 17x17 MK BW (MK BW 17x17), and/or Combustion Engineering 14x14 (CE 14x14) PWR fuel assemblies. Equivalent reload fuel assemblies that are enveloped by the fuel assembly design characteristics listed in Table 2-1 for a given assembly class are also acceptable. Additional payloads may be defined in future amendments to this application.

The thermal and radiological characteristics for the PWR spent fuel were generated using the SCALE computer code package [1]. The physical characteristics for the PWR fuel assembly types are shown in Table 2-1. Free volume in the 32PTH DSC cavity is addressed in Chapter 4. Specific gamma and neutron source spectra are given in Chapter 5.

Although analyses in this SAR are performed only for the design basis fuel, any other intact or damaged PWR fuel which falls within the geometric, thermal, and nuclear limits established for the design basis fuel can be stored in the 32PTH DSC.

2.1.1 Detailed Payload Description

This payload consists of 32 PWR UO₂ fuel assemblies with or without Non-Fuel Assembly Hardware (NFAH) which includes Burnable Poison Rod Assemblies, (BPRAs), Vibration Suppression Inserts (VSI) or Thimble Plug Assemblies (TPAs). CE 14x14 fuel assemblies are to be stored without NFAHs. Each 32PTH DSC can accommodate a maximum of sixteen damaged fuel assemblies, with the remaining assemblies intact. The fuel to be stored in the 32PTH DSC is limited to fuel with a maximum assembly average initial enrichment of 5.00 weight % U-235. The maximum allowable burnup is given as a function of initial fuel enrichment but does not exceed 60,000 MWd/MTU. The minimum cooling time is five years.

The 32PTH DSC may store up to 32 PWR fuel assemblies arranged in accordance with a heat load zoning configuration as shown in Figure 2-1, with a maximum decay heat of 1.5 kW per assembly and a maximum heat load of 34.8 kW per DSC, (33.8 kW per DSC for CE 14x14).

The 32PTH DSC can accommodate up to 16 damaged fuel assemblies as defined in Chapter 12. Damaged fuel assemblies shall be placed into the sixteen inner most basket fuel compartments, as shown in Figure 2-2, which contain top and bottom end caps that confine any loose material and gross fuel particles to a known, sub-critical volume during normal, off-normal and accident conditions and to facilitate handling and retrievability. Reactor records, visual/videotape records, fuel sipping, ultrasonic examination, and radio chemistry are examples of techniques utilized by utilities to identify damaged fuel.

The end caps are sized to fit inside the fuel compartment (see drawing 10494-72-30). The bottom end cap is slid into the fuel compartment before loading the fuel, utilizing a special tool.

2.6 References

1. Oak Ridge National Laboratory, RSIC Computer Code Collection, "SCALE: A Modular Code System for Performing Standardized Computer Analysis for Licensing Evaluations for Workstations and Personal Computers," NUREG/CR-0200, Revision 6, ORNL/NUREG/CSD-2/V2/R6.
2. U.S. Government, "Licensing Requirements for the Storage of Spent Fuel in an Independent Spent Fuel Storage Installation (ISFSI)," Title 10 Code of Federal Regulations, Part 72, Office of the Federal Register, Washington, D.C.
3. American Society of Mechanical Engineers, ASME Boiler and Pressure Vessel Code, Section III, Division 1, 1998 Edition through 2000 Addenda.
4. American National Standards Institute, American Nuclear Society, ANSI/ANS 57.9-1984, Design Criteria for an Independent Spent Fuel Storage Installation (Dry Storage Type).
5. American Society of Civil Engineers, ASCE 7-95, Minimum Design Loads for Buildings and Other Structures, (formerly ANSI A58.1).
6. U.S. Atomic Energy Commission, "Design Basis Tornado for Nuclear Power Plants," Regulatory Guide 1.76 (1974).
7. NUREG-0800, Standard Review Plan, Section 3.3.1, "Wind Loading" and Section 3.5.1.4 "Missiles Generated by Natural Phenomenon."
8. U.S. Government, "Reactor Site Criteria," Title 10 Code of Federal Regulations, Part 100, Office of the Federal Register, Washington, D.C.
9. U.S. Atomic Energy Commission, "Design Response Spectra for Seismic Design of Nuclear Power Plants," Regulatory Guide 1.60, Revision 1 (1973).
10. American Concrete Institute, Code Requirements for Nuclear Safety Related Concrete Structures and Commentary, ACI 349-97, and ACI 349R-97, American Concrete Institute, Detroit, Michigan.
11. American National Standards Institute, ANSI N14.6-1993, American National Standard for Special Lifting Device for Shipping Containers Weighing 10,000 lbs. or More for Nuclear Materials.
12. DELETED.
13. U.S. Government, "Packaging and Transportation of Radioactive Material," Title 10 Code of Federal Regulations, Part 71, Office of the Federal Register, Washington, D.C.

14. American Concrete Institute, "Building Code Requirements for Structural Concrete," ACI 318-95.
15. US NRC, Interim Staff Guidance -11, Rev 2, "Cladding Considerations for the Transportation and Storage of Spent Fuel," dated July 30, 2002.
16. U.S. Government, "Domestic Licensing of Production and Utilization Facilities," Title 10 Code of Federal Regulations, Part 50, Office of the Federal Register, Washington, D.C.
17. NUREG-1536, "Standard Review Plan for Dry Cask Storage Systems," 1997.

Table 2-1
Spent Fuel Assembly Physical Characteristics

Parameter	WE & WES 15x15	WE 17x17	MK BW 17x17	WEV 17x17	WEO 17x17	CE 14x14
Maximum Assembly Average Initial Enrichment, wt % U235 (max)	5.00	5.00	5.00	5.00	5.00	5.00
Clad Material	Zr-4/Zirlo	Zr-4/Zirlo	M5	Zr-4/Zirlo	Zr-4/Zirlo	Zr-4/Zirlo
No of fuel rods	204	264	264	264	264	176
No of guide/instrument tubes	21	25	25	25	25	5
Assembly Length ⁽³⁾	162.2	162.4	162.4	162.4	162.4	159.5
Max Uranium Loading (Kg)	467	467	476	467	467	385
Assembly Cross Section	8.424 x 8.424	8.426 x 8.426	8.425 x 8.425	8.426 x 8.426	8.426 x 8.426	8.25 x 8.25
Max Assembly Weight with Insert components ⁽⁴⁾ (lbs)	1528	1575	1554	1533	1533	1450 ⁽⁵⁾

- (1) Nominal values shown unless stated otherwise
- (2) All dimensions are inches
- (3) Includes allowance for irradiation growth
- (4) Weights of TPAs and VSIs are enveloped by BPRAs
- (5) Without NFAH

Table 2-5
NUHOMS® HD System Major Components and Safety Classification

Component	10CFR 72 Classification ⁽¹⁾
Dry Shielded Canister (32PTH DSC)	
Fuel compartment	Important to Safety
Poison Plate	Important to Safety
Basket Plate	Important to Safety
Basket Rail	Important to Safety
Weld Studs	Important to Safety
Shell	Important to Safety
Outer Top Cover Plate	Important to Safety
Top Shield Plug/Inner Top Cover	Important to Safety
Shell Bottom	Important to Safety
Bottom Shield Plug (alternate design)	Important to Safety
DSC Support Ring	Important to Safety
Siphon and Vent Port Cover Plates	Important to Safety
Grapple Ring and Grapple Support	Important to Safety
Weld Filler Metal	Important to Safety
Horizontal Storage Module (HSM-H)	
Reinforced Concrete	Important to Safety
32PTH DSC Support Structure	Important to Safety
Thermal Instrumentation (if used)	Not Important to Safety
ISFSI Basemat and Approach Slabs	Not Important to Safety
Transfer Equipment	
On-site OS187H	Important to Safety
Transfer Cask	
Cask Lifting Yoke	Safety Related ⁽²⁾
Transfer Trailer/Skid	Not Important to Safety
Ram Assembly	Not Important to Safety
Dry Film Lubricant	Not Important to Safety
Auxiliary Equipment	
Vacuum Drying System	Not Important to Safety
Automatic Welding System	Not Important to Safety
Transfer Cask/DSC Annulus Seal	Not Important to Safety

(1) Structures, systems and components "important to safety" are defined in 10CFR 72.3 as those features of the ISFSI whose function is (1) to maintain the conditions required to store spent fuel safely, (2) to prevent damage to the spent fuel container during handling and storage, or (3) to provide reasonable assurance that spent fuel can be received, handled, packaged, stored, and retrieved without undue risk to the health and safety of the public.

(2) Yoke and rigid or sling lifting members are classified as "Safety Related" in accordance with 10CFR 50.

3. STRUCTURAL EVALUATION

The structural evaluation described in this chapter 3.0 is applicable to the 32PTH DSC, the OS187H TC, and the HSM-H. See Appendix A, Chapter A.3 for descriptions of the structural evaluation for the 32PTH Type 1 DSC, OS187H Type 1 TC, and HSM-H changes required to accommodate the 32PTH Type 1 DSC.

3.1 Structural Design

This chapter, including its appendices, presents the structural evaluation of the NUHOMS® HD System.

The NUHOMS® HD system consists of the 32PTH DSC basket and shell assemblies, the HSM-H, and the OS187H Transfer Cask. The 32PTH DSC is a new dual purpose canister that is designed to accommodate up to 32 intact PWR fuel assemblies (or up to 16 damaged assemblies, with the remaining intact) with total heat load of up to 34.8 kw. The HSM-H is an enhanced version of the NUHOMS® Standardized HSM and incorporates design features to enable storage of the higher heat load 32PTH DSC. The OS187H is the modified version of OS197 transfer cask with a redesigned shielding panel to improve the thermal performance, shortened the cavity length and increased inside diameter to accommodate the larger diameter of 32PTH DSC.

The overall design bases for the NUHOMS® HD system are described in Chapters 1 and 2. This Chapter discusses the structural design criteria and associated design bases applicable to the 32PTH DSC, HSM-H, and OS187H transfer cask. This Chapter also describes the ability of these components to perform their design function during normal and off-normal operating conditions, as well as under postulated accident conditions and extreme natural phenomena events.

3.1.1 Discussion

The NUHOMS® HD system consists of the 32PTH DSC, a high-integrity stainless steel dry shielded canister that provides for the dry storage of spent fuel assemblies in an inert atmosphere; the HSM-H, a massive reinforced concrete storage module that houses and provides environmental protection and shielding to the 32PTH DSC; and the OS187H transfer cask, a stainless steel cask, with lead shielding, that handles and protects the 32PTH DSC during transfer to and from the HSM-H.

Multiple HSM-Hs are grouped together to form arrays in single or double rows to provide storage capacity consistent with available site space and reactor SFA discharge rates. The HSM-H is placed next to, and in contact with, adjacent module(s) to form a continuous single or double row arrays.

For purposes of the structural analyses and agreement with the criteria set forth in Regulatory Guide 3.61 [1] and NUREG 1536 [2], a single NUHOMS® HD System 32PTH DSC plus an HSM-H form the “cask” cited in [1] and [2].

The codes and standards used for the design, fabrication, and construction of the NUHOMS® HD system components, equipment, and structures are summarized in Table 3-1 and are identified throughout the SAR. Alternatives to the ASME Code [4] are provided in Section 3.10.

3.1.1.1 General Description of the 32PTH DSC

The principal characteristics of the 32PTH DSC are described in Chapter 1, Section 1.2.1. The drawings in Section 1.5 provide the principal dimensions and design parameters of the 32PTH DSC. For purposes of the structural analysis, the 32PTH DSC is divided into the 32PTH DSC shell assembly and the internal basket assembly.

A. DSC Canister (Shell) Assembly Description

The canister shell assembly and details are shown on drawings 10494-72-2 through 10494-72-7 in Chapter 1, Section 1.5. The shell assembly is a high integrity stainless steel (SA-240 Type 304 or SA-182 Type F304) welded pressure vessel that provides confinement of radioactive materials, encapsulates the fuel in an inert atmosphere (the canister is backfilled with Helium before being seal welded closed), and provides biological shielding (in axial direction).

The remaining 32PTH DSC shell assembly components include the solid stainless steel top shield plug, the grapple ring assembly, support ring, and the lifting blocks. The outer top cover, top shield plug and shell bottom provide biological shielding during fuel loading operations and storage of a loaded 32PTH DSC. The grapple ring assembly is welded to the shell bottom or outer bottom cover plate for the purpose of inserting/extracting the 32PTH DSC to and from the Horizontal Storage Module (HSM-H). The support ring, welded to the cylindrical shell, supports the top shield plug. Four lifting blocks are welded to the inside of the shell bottom and are used in conjunction with a lifting fixture to lift the unloaded 32PTH DSC into the transfer cask prior to fuel loading operations.

All primary components of the 32PTH DSC are constructed from Type 304 stainless steel. The 32PTH DSC cylindrical shell and shell bottom assembly (which includes the shell bottom and the grapple ring assembly), and the internal basket assembly, are shop-fabricated (and assembled) components. The top shield plug and outer top cover plate is installed at the plant after the spent fuel assemblies have been loaded into the 32PTH DSC internal basket.

The 32PTH DSC shell assembly is designed, fabricated, examined and tested in accordance with the requirements of Subsection NB of the ASME Code including alternatives to ASME code specified in Section 3.10. The circumferential and longitudinal shell plate weld seams are multi-layer full penetration butt welds. The butt weld joints are fully radiographed and inspected according to the requirements of NB-5000 of the ASME Boiler and Pressure Vessel Code. The full penetration inner bottom cover plate to shell weld is inspected to the same Code standards.

The 32PTH DSC top closure is designed, fabricated and inspected using alternatives to ASME code specified in Section 3.10. The outer top cover plate and inner top cover/shield plug (including option 2 or option 3 inner top cover as described in Chapter 1 drawings) are sealed by separate, redundant closure welds. The inner top cover/shield plug (including option 2 or option 3 design welds as described in Chapter 1 drawings) is welded to the 32PTH DSC shell to form the confinement boundary at the top end of the 32PTH DSC, as shown in Chapter 7, Figure 7-1.

compartment boxes, and designed to accommodate 32 PWR fuel assemblies. The sections of the stainless steel fuel compartments are fusion welded to Type 304 stainless steel structural plates, sandwiched between the box sections. The fusion welds are spaced intermittently along the box sections. Neutron poison plates, composed of a boron-aluminum alloy (or a boron carbide aluminum metal matrix composite), are sandwiched between the sections of the stainless steel walls of the adjacent box and the adjacent stainless steel plates. The Type 304 stainless steel members are the primary structural components. The neutron poison plates provide criticality control and a heat conduction path from the fuel assemblies to the canister shell. The bottom rows of plates which are 304 SST (no poison) are also sandwiched between the fuel compartment box sections, and provide structural support to the basket.

Stainless steel rails are oriented parallel to the axis of the canister and attached to the periphery of the basket to establish and maintain basket orientation and to support the basket.

The nominal open dimension of each fuel compartment cell is 8.70 inches \times 8.70 inches, which provides clearance around the fuel assemblies. The overall length of the fuel basket is 162.00 inches, which is less than the canister cavity length of the canister (164.50 inches minimum) to allow for thermal expansion, tolerances, and access to the top of the fuel assemblies.

The basket structure is open at each end. Therefore, longitudinal fuel assembly loads are applied directly on the DSC body and not on the fuel basket structure. The fuel assemblies are laterally supported by the stainless steel fuel compartments and structural plates, and the fuel basket is laterally supported by the rails and the canister shell.

The circumferential orientation of the basket, relative to the canister shell, is maintained by the four lifting blocks attached to the bottom closure assembly of the canister. The four canister lifting blocks mate with the hollow portions of the basket outer support rails, without interfering with the spent fuel assemblies. During normal transfer conditions, the DSC rests on four transfer support rails, attached to the inside surface of the NUHOMS®-OS187H Transfer Cask.

3.1.1.2 General Description of the HSM-H

The details of the HSM-H module are shown in drawings 10494-72-100 through 10494-72-110 in Chapter 1, Section 1.5. The HSM-H is a free standing reinforced concrete structure designed to provide environmental protection and radiological shielding for the 32PTH DSC. Each HSM-H provides a self contained modular structure for the storage of a 32PTH DSC containing up to 32 PWR fuel assemblies. The HSM-H provides heat rejection from the spent fuel decay heat by a combination of radiation, conduction and convection.

The HSM-H is a reinforced concrete structure consisting of two separate units: a base storage unit, where the 32PTH canister is stored, and a roof that serves to provide environmental protection and radiation shielding. The roof is attached to the base unit by four vertical ties or by four angle brackets. Three-foot thick shield walls are installed behind each HSM-H (single row array only) and at the ends of each row to provide additional environmental protection and radiological shielding.

The HSM-H module design for 32PTH canister is identical to the HSM-H design for 24PTH canister except the following modifications:

1. The module for the 32PTH canister is designed such that the center line of the loaded 32PTH canister is approximately four inches higher compared to that of the 24PTH canister.
2. The diameter of the door openings in the front and rear of the front wall are approximately four inches and two inches larger for the 32PTH canister compared to those of the 24PTH canister.
3. The transfer cask docking surface in the module for the 32PTH canister transfer cask is approximately half inch wider compared to the cask docking surface for the 24PTH canister transfer cask.
4. The diameters of the front inner circular steel plate and rear circular concrete block of the shielded door for the 32PTH canister are approximately four inches and two inches larger compared to those of the 24PTH canisters.
5. For the 32PTH design the spacers at the canister stop plate of the module will be provided similar to the 24PTH short cavity design.

The drawings in Chapter 1, Section 1.5 provide the principal dimensions and design parameters of the HSM-H. The dimension differences between the HSM-H to be used for storing the 32PTH canister and 24PTH canister are listed in the following tables. Dimensions for the 24PTH canister are detailed in the Standardized NUHOMS® UFSAR [40].

TN drawing No. 10494-72-104 (for 32PTH data)

Dimension	HSM-H	
	System Type	
	For 32PTH Canister	For 24PTH Canister
A	8' – 10"	8' – 6"
B	Ø 5' – 11 5/8"	Ø 5' – 9"
C	Ø 7' – 5"	Ø 7' – 1 1/2"

TN drawing No. 10494-72-107 (for 32PTH data)

Dimension	HSM-H	
	System Type	
	For 32PTH Canister	For 24PTH Canister
A	34.88"	33.60"

TN drawing No. 10494-72-108 (for 32PTH data)

Dimension	HSM-H	
	System Type	
	For 32PTH Canister	For 24PTH Canister
A	8' – 1 1/2"	7' – 3 3/4"
B	Ø 7' – 3"	Ø 6' – 11 1/2"
C	Ø 5' – 8 5/8"	Ø 5' – 6"
D	Ø 7' – 7 1/4"	Ø 7' – 3 3/4"
E	1' – 10 1/2"	1' – 10 1/2"

The design of the HSM-H for 32PTH DSC is the same as the HSM-H which is under NRC review as Amendment 8 to CoC 1004 for 24PTH DSC. Analyses performed for HSM-H with 24PTH DSC used bounding values to envelop both 24PTH DSC and 32PTH DSC.

3.1.1.3 General Description of the OS187H On-Site Transfer Cask

The NUHOMS®-OS187H On-Site Transfer Cask consists of a structural shell, gamma shielding material, and solid and liquid (water) neutron shield. The OS187H is the modified version of OS197 transfer cask with a redesigned shielding panel to improve the thermal performance, shortened the cavity length and increased inside diameter to accommodate the larger diameter of 32PTH DSC. The cavity between the DSC and the transfer cask contains an inert gas during transfer operations. Sets of upper and lower trunnions, welded to the structural shell of the cask that provide support, lifting, and rotation capability for the OS187H transfer cask.

The overall dimensions of the OS187H transfer cask are 197.07 inches long and 92.20 inches in diameter. The transfer cask structural shell is 82.70 inches in diameter. The transfer cask cavity is 186.60 inches long and 70.50 inches in diameter. Detailed design drawings for the OS187H Transfer Cask are provided in drawings 10494-72-15 through 10494-72-21 on Chapter 1, Section 1.5. The materials used to fabricate the transfer cask are shown in the Parts List on Drawing 10494-72-15. Where more than one material has been specified for a component, the most limiting properties are used in the analyses in the subsequent chapters of this Safety Analysis Report.

The gross weight of the loaded transfer cask is 114.3 tons including a maximum payload of 54.4 tons. Section 3.2.2 summarizes the weights of the NUHOMS®-OS187H packaging components. Trunnions, welded to the structural shell of the transfer cask, are provided for lifting and handling operations, including rotation of the packaging between the horizontal and vertical orientations. The OS187H cask transfers the DSC in the horizontal orientation, on a specially designed transfer skid, with the lid end facing the direction of travel.

The transfer cask is fabricated primarily of stainless steel. Non-stainless steel members include the cast lead shielding between the inner radial shell and the structural shell, the o-ring seals, the resin and water neutron shield material and the carbon steel closure bolts. The lead is poured into

the annulus in a molten state using a carefully controlled procedure. The top cover is bolted to the top flange by 24-1 1/2 in. diameter high strength bolts and sealed with O-ring. A cover plate is provided to seal the bottom hydraulic ram access penetration of the cask (by 12-1/2 in. high strength bolts with O-ring) during fuel loading and transferring the canister to the ISFSI. Drawing 10494-72-15 provides the part list for the NUHOMS®-OS187H transfer cask. Drawing 10494-72-16 shows the overall configuration of the NUHOMS®-OS187H transfer cask. Drawing 10494-72-17 shows the details of the transfer cask top cover. The remaining drawings (10494-72-18 through 10494-72-21) show the details of the remaining individual components that make up the transfer cask.

The following sections provide physical and functional descriptions of each major component of the transfer cask. Detail drawings showing dimensions of significance to the safety analyses, welding and NDE information, as well as a complete materials list are provided in Chapter 1, Section 1.5. Reference to these drawings is made in the following physical description sections, and in general, throughout this SAR.

A. Transfer Cask Body and Structural Components

The shell or cask body cylinder assembly is an open ended (at the top) cylindrical unit with an integral closed bottom end. This assembly consists of concentric inner shell and outer shell (both SA-240 Type 304), welded to massive closure flanges (SA-182 Type F304N) at the top and bottom ends. The inner shell is 0.50 inches thick and has a 70.50 inch inside diameter. The outer shell is the primary structural shell and is 1.5 inches to 2.0 inches thick, and has an 82.70 inch outside diameter. The annulus between the shells is filled with lead shielding. The lead gamma shield is 3.60 inch thick and is poured into the annulus in a molten state using a carefully controlled procedure.

The transfer cask bottom end assembly consists of a 2.00 inch bottom end plate and a 0.75 inch bottom neutron shield plate, that sandwich a 2.25 inch thick resin neutron shield. The RAM access penetration at the center of the bottom end assembly is used during insertion/removal operations to and from the HSM-H. The RAM access penetration is four inches thick in the radial direction and 4.25 inches thick in the axial direction. A cover plate is provided to seal the bottom hydraulic ram access penetration of the cask (by 12-1/2 in. high strength bolts with O-ring) during fuel loading and transferring the canister to the ISFSI.

The transfer cask top cover consists of a 3 inch thick structural plate constructed from SA-240, Type XM-19, and a top radial neutron shield constructed from resin encased in a 0.25 inch thick SA-240 Type 304 stainless steel shell. The top cover is fastened to the top flange of the transfer cask body with 24-1.5 inch diameter SA-540 Grade B24 Class 1 high strength steel bolts. The top closure is designed to maintain confinement of the 32PTH DSC inside the transfer cask during all normal, off normal and hypothetical accident conditions.

The transfer cask body provides additional radiation shielding and structural support for the 32PTH DSC. It also maintains an inert atmosphere (helium) in the cask cavity. Helium assists in heat removal during transfer operations and provides a non-reactive environment. To preclude air in-leakage, the cask cavity is pressurized with helium to above atmospheric pressure.

The top trunnions are constructed from SA-182 Type FXM-19 and the bottom trunnions are constructed from SA-182 Type 304. Both materials are stainless steel forgings. The top trunnions are designed fabricated and tested in accordance with ANSI N14.6 [8] as single failure proof lifting devices. Consequently they are designed with a factor of safety of six against the material yield strength and a factor of ten against the material ultimate strength.

D. Operational Features

The NUHOMS®-OS187H transfer cask is not considered to be operationally complex and is designed to be compatible with spent fuel pool loading/unloading methods. All operational features are readily apparent from inspection of the General Arrangement Drawings provided in Chapter 1, Section 1.5. The sequential steps to be followed for cask loading, testing, and unloading operations are provided in Chapter 8.

3.1.1.4 Discussion of NUHOMS® HD System Drop Analysis

All lifting of the TC loaded with the DSC must be made within the existing heavy loads requirements and procedures of the licensed nuclear power plant. The TC design has been reviewed under 10 CFR Part 72 and found to meet NUREG-0612 [5] and ANSI N14.6 [8].

The transfer cask is transported to the ISFSI in a horizontal configuration. Therefore the only credible drop accident during storage or transfer operations is a side drop. The transfer cask, canister and fuel cladding are analyzed for these credible accidents in the following sections.

In addition, a vertical or corner drop accident may be credible under 10CFR50 during loading onto trailer or during transport operations governed under 10CFR71. The transfer cask and canister have been evaluated for these postulated accidents. However, the fuel cladding integrity has not been demonstrated for these accident scenarios. An additional safety review by the user is required to demonstrate fuel cladding integrity under 10CFR50 or to demonstrate that the drop accidents are not credible.

The drop analyses of the NUHOMS® HD components are performed in the following Appendices.

Appendix 3.9.1

This appendix describes the detail analysis of the canister and basket for all the loading conditions. For the drop loads, the canister is analyzed for the 75g side and end drops. The canister end closure welds are analyzed for the 22g corner drop.

The basket is analyzed for 75g the side and end drops. The basket is not analyzed for the 22g corner drop since the 75g end drop analysis bounds the 22g corner drop.

3.2 Weights

The nominal DSC, HSM-H and OS187H Transfer Cask geometry is used to compute the weights of the NUHOMS® HD system components.

The following densities are used to compute the component weights.

NUHOMS® HD Component Material Densities

Material	Density (lb./in ³ .)	Reference
Stainless Steel	0.29	10
Aluminum	0.098	10
Water	0.0361	10
Lead	0.41	10
Resin (neutron shield) ⁽¹⁾	0.065	Table 5-17, Chapter 5

Note:

- (1) The actual resin density from Table 5-17 is 0.057 lb/in³. However, a higher density of 0.065 lb/in³ is utilized to conservatively compute higher neutron resin weight.

3.3 Mechanical Properties of Materials

3.3.1 32PTH-DSC Material Properties

The principal material of construction for the 32PTH DSC is Type 304 stainless steel. The 32PTH DSC cylindrical shell, cover plates and shield plugs are constructed from SA-240 Type 304 stainless steel for plate material and SA-182 F304 for forging material. The 32PTH DSC basket assembly fuel compartments and structural plate assemblies are also constructed from SA-240 Type 304 or equivalent stainless steel. Table 3-5 contains the ASME Code material properties for SA-240 Type 304 and SA-182 F304 stainless steel materials.

The neutron absorber plates are constructed from boron carbide/aluminum metal matrix composite material and the aluminum thermal conduction plates are constructed from B-209 (Type 1100 Aluminum). No structural credit is taken for either the neutron absorber plates or the aluminum thermal conducting plates, except for through the thickness load transmission.

3.3.1.1 Radiation Effects on 32PTH DSC Materials

Gamma radiation has no significant effect on metals. The effect of fast neutron irradiation of metals is a function of the integrated fast neutron fluence, which is on the order of 1×10^{15} neutrons/cm² inside the 32PTH DSC after 50 years. Studies on fast neutron damage in stainless steel, and low alloy steels rarely evaluate damage below 10^{17} n/cm² because it is not significant [17]. Extrapolation of the data available down to the 10^{15} range confirms that there will be no measurable neutron damage to any of the 32PTH DSC metallic components.

3.3.1.2 DSC Weld Material

Welding processes, welders and welding materials used for the welding of the 32PTH DSC meet the requirements of the appropriate ASME Section III subsections and Section IX. Non-Code welds meet the provisions of Section IX of the ASME Code or AWS D1.1 [18] or D1.6 [19]. Weld metal material properties meet the requirements of Section II of the ASME Code or associated AWS requirements.

3.3.1.3 DSC Material Brittle Fracture

Brittle fracture is not a concern for the stainless steel components, which comprises all structural components of the DSC.

If an ISFSI site is located in a coastal salt water marine atmosphere, then any load-bearing carbon steel DSC support structure rail components of any associated HSM-H shall be procured with a minimum of 0.20 percent copper content for corrosion resistance.

The sliding surface of the support rails for the DSC consists of Nitronic® 60 or equivalent stainless steel. Carbon steel embedments in the HSM-H concrete are coated to protect them from corrosion or they may be stainless steel. Other carbon steel components such as bolts, nuts, tie plates, etc., are also coated. Bird screens are stainless steel. For the side heat shield with fins, the side facing the DSC is made of anodized aluminum. The side facing the HSM-H concrete is plain aluminum surface.

Because of the coatings and the dry environment, degradation of concrete or steel parts inside the HSM-H is unlikely. Exterior parts or surfaces are also visible and accessible, and if any degradation occurs from exposure to weather, it can be corrected.

3.4.1.5 Lubricants, Sealants, and Cleaning Agents

Lubricants may be used to coat the slide rails, the threads and shoulders of bolts, o-rings, and the contact areas of the trunnions. Lubricants are generally selected from the list of materials approved for contact with the pool water at the facility where wet loading occurs.

Sealants may be used at pipe threads, e.g., at quick connect fittings.

The transfer cask and DSC are cleaned during fabrication using procedures approved by Transnuclear. After loading, exterior surfaces of the cask will be decontaminated using procedures and decontamination agents approved at the loading facility.

The cleaning agents, sealants, and lubricants have no significant effect on the cask and canister materials.

3.4.1.6 Hydrogen Generation

There is no mechanism for galvanic corrosion in the space between the DSC and the transfer cask, because both the inner shell of the TC and the outer shell of the DSC are stainless steel, and because the canister is sealed before the lid is placed on the transfer cask. Therefore, any concern for hydrogen generation applies solely inside the canister during wet loading.

Monitoring of the hydrogen concentration before and during welding operations will be performed to ensure that the hydrogen concentration does not exceed 2.4%. If the concentration exceeds 2.4%, welding operations will be suspended and the DSC will be purged with an inert gas.

Numerous NUHOMS® canisters fabricated using aluminum, neutron absorber, and stainless steel have been loaded in both borated and deionized water. Hydrogen monitoring has measured hydrogen in the range 0-2%, well below the 4% lower limit of flammability, provided that sufficient plenum space is provided between the water in the DSC and the inner top cover/shield.

3.6.1.1 32PTH DSC Fuel Basket Normal Condition Structural Evaluation

The fuel basket stress analysis is performed for normal condition loads during fuel transfer and storage. The detailed stress analysis is presented in Appendix 3.9.1, Section 3.9.1.2.3. A summary of the fuel basket load cases is provided in Appendix 3.9.1, Section 3.9.1.2.2.

The basket stress analysis is performed using a finite element method for the transfer handling, storage dead weight, and both transfer and storage thermal load cases. A 3-dimensional cross-section finite element model is utilized to evaluate the effect of transverse inertial loads on the fuel basket. The finite element model is described in detail in Appendix 3.9.1, Section 3.9.1.2.3.A (page 3.9.1-7). Analytical calculations are used for the vertical dead weight load case.

The mechanical properties of structural materials used in the basket, rail and canister are shown in the Appendix 3.9.1, Tables 3.9.1-1 and 3.9.1-2 as a function of temperature. All structural components of the fuel basket and support rails are constructed from SA-240, Type 304 stainless steel, with properties taken from AMSE B&PV Code [10].

ANSYS nonlinear elastic stress analyses are conducted for computing the elastic stresses in the fuel basket model. The nonlinearity of analysis results from the gaps in the model. In general, for each load case, the maximum total load is applied in small steps. The automatic time stepping program option "Autots" is activated. This option lets the program decide the actual size of the load-substep for a converged solution. Where shell elements are used, the shell middle surface nodal stress intensity is the membrane stress intensity and top or bottom surface stress intensity is the membrane plus bending stress intensity.

The calculated stresses in the 32PTH DSC fuel basket under normal conditions are summarized and compared with the corresponding ASME code allowable stresses for transfer load cases in Appendix 3.9.1, Table 3.9.1-3 and storage load cases in Appendix 3.9.1, Table 3.9.1-5.

The fusion weld is qualified by a pull test (shear). The required minimum test load is 17.1 kips. This load corresponds to the maximum fusion weld loads generated during a 75g hypothetical accident impact with a safety factor of 2 and a correction for material strength for room temperature testing. The maximum force generated in the fusion welds due to transfer load is 1415 lb (Appendix 3.9.1, page 3.9.1-11) and thermal load in fusion weld during transfer is 631 lb (Appendix 3.9.1, page 3.9.1-14). The combined load is 2,046 lb (2.05 kip). This combined load is much smaller than the required test load of 17.1 kips.

Based on the results of these analyses, the design of the 32PTH DSC basket is structurally adequate with respect to normal condition transfer and storage loads.

3.6.1.2 32PTH DSC Canister Shell Normal Condition Structural Evaluation

This section summarizes the evaluation of the structural adequacy of the 32PTH DSC canister under all applied normal condition loads. Detail evaluation of the stresses generated in the

stepping program option "Autots" is activated. This option lets the program decide the actual size of the load-substep for a converged solution. Where shell elements are used, the shell middle surface nodal stress intensity is the membrane stress intensity and the top or bottom surface stress intensity is the membrane plus bending stress intensity.

The calculated stresses in the 32PTH DSC fuel basket is summarized and compared with their corresponding ASME code allowable stresses. Tables 3.9.1-4a and 3.9.1-4b of Appendix 3.9.1 show these summaries for the transfer accident loads and Table 3.9.1-5 for the storage accident loads.

The maximum shear load in the fusion welds during the accident loading condition is calculated in Appendix 3.9.1 (page 3.9.1-16). The calculated maximum shear force during side drop is 7,208 lb.

The fusion weld is qualified by a pull test (shear). The minimum test load is 17.1 kips. This test load includes a safety factor of 2 and a correction for material strength for room temperature testing.

Based on the results of these analyses, the design of the 32PTH DSC basket is structurally adequate with respect to off-normal and accident conditions of transfer and storage loads.

3.7.1.1.2 32PTH DSC Fuel Basket Accident Condition Buckling Analysis

Buckling analysis of the fuel basket plates and support rails are only performed for the bounding hypothetical accident condition impact loads. The accident condition buckling evaluation is presented in detail in Appendix 3.9.1, Section 3.9.1.2.4 (page 3.9.1-26).

Only the most critical fuel basket section is analyzed in detail. The critical basket section is depicted in Appendix 3.9.1, Figure 3.9.1-11. This approach is then validated by performing a buckling evaluation for the entire fuel basket cross section for the worst case loading condition.

All structural members of the 32PTH fuel basket are constructed from SA-240 Type 304 or equivalent stainless steel. A bilinear stress-strain curve for SA-240 Type 304 stainless steel is used for the elastic-plastic buckling analysis.

The material properties used for the basket plates are taken from ASME Code, Section II, Part D [10], at 611° F. This temperature represents an average temperature for the fuel basket section analyzed and depicted in Appendix 3.9.1, Figure 3.9.1-11.

Nonlinear stress analyses are conducted in order to evaluate the plastic buckling loads for the 32PTH DSC basket plates. The three critical azimuth drop orientations analyzed are:

- i) 0° (load applied in the direction parallel to the basket plates)
- ii) 30° (load applied at 30° relative to the basket plate direction)
- iii) 45° (load applied at 45° relative to the basket plate direction)

In order to calculate the buckling load, a small three-dimensional ANSYS finite element model is constructed using SHELL43 plastic large strain shell elements. This model is shown in Appendix 3.9.1, Figure 3.9.1-12. The small model is constructed by selecting the appropriate elements and nodes from full basket cross section model as described in Appendix 3.9.1, Section 3.9.1.2.3 (page 3.9.1-7). As described in Section 3.9.1.2.3.A., the stiffness from aluminum plates is conservatively neglected but their weight is accounted for in the applied loads.

The loading on the small model are appropriately transferred from the full size basket loading. A maximum load of 200g is applied in each analysis. The ANSYS automatic time stepping option "AUTOTS" is activated. This option lets the program decide the actual size of the load sub-step for a converged solution. The program stops at the load sub-step that fails to result in a converged solution. The last load step with a converged solution is used to compute the allowable collapse load for the fuel basket grid.

The following table summarizes the input load and last converged load for all three load cases:

Basket Orientation	200g loads (psi)			Last converged Load (g)	Max. Deflection u_x (in)
	Vertical Load (lb)	Lateral Pressure (psi)	Applied Acceleration		
Vertical	239,400	0	(0, 200, 0)	107	0.005
30°	207,326	129.0	(-100, 173, 0)	84	0.1090
45°	169,281	182.4	(-141, 141, 0)	84	0.1277

As per stability criteria described in Section 3.1.2.1.2 of FSAR Chapter 3 and the Section 3.4.3.3 of SER “the load applied in the last converged load sub-step is considered to be the buckling load of the structure”, therefore the allowable buckling load for the basket is 84g.

The small finite element model technique used for the buckling analyses of the fuel basket is verified by a full basket cross section finite element analysis as well as analytical methods. Details of these verification methods are provided in Appendix 3.9.1, Section 3.9.1.2.4 (page 3.9.1-29).

Since the critical collapse load for the 32PTH DSC basket (84g for the 30° and 45° Orientations) is greater than the maximum design acceleration of 75g, the basket will not fail in buckling during the accident condition events.

3.8 References

1. NRC Regulatory Guide 3.61, Standard Format and Content for a Topical Safety Analysis Report for a Spent Fuel Dry Storage Cask, February 1989.
2. NUREG-1536, "Standard Review Plan for Dry Cask Storage Systems - Final Report," U.S. Nuclear Regulatory Commission, Office of Nuclear Material Safety and Safeguards, January 1997.
3. Title 10, Code of Federal Regulations, Part 72, "Licensing Requirements for the Storage of Spent Fuel in an Independent Spent Fuel Storage Installation."
4. American Society of Mechanical Engineers, Boiler & Pressure Vessel Code, Section III, 1998 through 2000 Addenda.
5. NUREG-0612, "Control of Heavy Loads at Nuclear Power Plants," July 1980.
6. American National Standards Institute, ANSI N14.5-1997, Leakage Tests on Packages for Shipment of Radioactive Materials.
7. American Society of Mechanical Engineers, ASME Boiler and Pressure Vessel Code, Section III, Subsection NC, 1998 through 2000 addenda.
8. American National Standards Institute, ANSI N14.6, American National Standard for Special Lifting Devices for Shipping Containers Weighing 10,000 Pounds or More for Nuclear Materials, 1993.
9. American National Standards Institute, American Nuclear Society, ANSI/ANS 57.9-1984, Design Criteria for an Independent Spent Fuel Storage Installation (Dry Storage Type).
10. American Society of Mechanical Engineers, ASME Boiler and Pressure Vessel Code, Section II, Parts A, B, C and D, 1998, through 2000 addenda.
11. DOE/ET/47912-3, Volume 3, September 1981, Nuclear Assurance Corporation, "Domestic Light Water Reactor Fuel Design Evolution".
12. American Society of Mechanical Engineers, ASME Boiler and Pressure Vessel Code, Section III, Subsection NB, 1998 through 2000 addenda.
13. ASME Boiler and Pressure Vessel Code, Section III, Division 1, Appendices, 1998, through 2000 addenda

14. American Society of Mechanical Engineers, ASME Boiler and Pressure Vessel Code, Section III, Subsection NG, 1998 through 2000 Addenda.
15. American Concrete Institute, ACI 349-97 and 349R-97, Code Requirements for Nuclear Safety Related Concrete Structures and Commentary.
16. American Institute of Steel Construction, AISC Manual of Steel Construction, Ninth Edition.
17. Regulatory Guide 1.99, "Radiation Embrittlement of Reactor Vessel Materials," Revision 2, May 1988.
18. AWS D1.1 – 1998, Structural Welding Code-Steel.
19. AWS D1.6 – 1999, Structural Welding Code-Stainless Steel.
20. H. K. Hilsdorf, J. Kropp, and H. J. Koch, "The Effects of Nuclear Radiation on the Mechanical Properties of Concrete," Paper 55-10, Douglas McHenry International Symposium on Concrete and Concrete Structures, American Concrete Institute, Detroit, MI (1978).
21. American Nuclear Society, "American National Standard Guidelines on the Nuclear Analysis and Design of Concrete Radiation Shielding for Nuclear Power Plants," ANSI/ANS-6.4-1977, American National Standards Institute, Inc., (1977).
22. "An Assessment of Stress-Strain Data Suitable for Finite Element Elastic-Plastic Analysis of Shipping Containers", NUREG/CR-0481
23. Baumeister & Marks, *Standard Handbook for Mechanical Engineers*, 7th Edition.
24. G. Wranglen, An Introduction to Corrosion and Protection of Metals, Chapman and Hall, 1985, pp. 109-112.
25. V. Brooks and Perkins , Boral Product Performance Report 624.
26. Pacific Northwest Laboratory Annual Report - FY 1979, Spent Fuel and Fuel Pool Component Integrity, May, 1980.
27. G. Wranglen, "An Introduction to Corrosion and Protection of Metals", Chapman and Hall, 1985, pp. 109-112.
28. A.J. McEvily, Jr., ed., "Atlas of Stress Corrosion and Corrosion Fatigue Curves", ASM Int'l, 1995, p. 185.

29. Baratta, et al. "Evaluation of Dimensional Stability and Corrosion Resistance of Borated Aluminum", Final Report submitted to Eagle-Picher Industries, Inc. by the Nuclear Engineering Department, Pennsylvania State University.
30. Hydrogen Generation Analysis Report for TN-68 Cask Materials, Test Report No. 61123-99N, Rev 0, Oct 23, 1998, National Technical Systems.
31. AMS-R-83485, "Rubber, Fluorocarbon, Improved Performance at Low Temperatures"
32. Harper, Charles A., ed., "Handbook of Plastics and Elastomers," McGraw-Hill, 1975
33. ANSYS Users Manual, Rev. 5.6 and 6.0, 1998
34. NUREG/CR-6007 "Stress Analysis of Closure Bolts for Shipping Casks", By Mok, Fischer, and Hsu, Lawrence Livermore National Laboratory, 1992.
35. Rashid, Nickel and James, "Structural Design of Concrete Storage Pads for Spent Fuel Casks", EPRI NP-7551, August 1991.
36. "Handbook of Concrete Engineering," Mark Fintel, September 1974
37. UCID – 21246, "Dynamic Impact Effects on Spent Fuel Assemblies," Lawrence Livermore National Laboratory, October 20, 1987.
38. K. J. Geelhood and C. E. Beyer, "PNNL Stress/Strain Correlation for Zircaloy", March 2005.
39. USNRC Spent Fuel Project Office, Interim Staff Guidance, ISG-11, Revision 3, "Cladding Considerations for the Transportation and Storage of Spent Fuel."
40. Updated Final Safety Analysis Report (UFSAR), Standardized NUHOMS® Horizontal Modular Storage System for Irradiated Nuclear Fuel, Rev. 9, Feb. 2006.

3.10 ASME Code Alternatives

The confinement boundary of the 32PTH DSC canister shell, the inner top cover/shield plug, the inner bottom cover, the siphon vent block, and the siphon/vent port cover plate are designed, fabricated and inspected in accordance with the ASME Code Subsections NB to the maximum practical extent. The basket is designed, fabricated and inspected in accordance with ASME Code Subsection NG to the maximum practical extent. Other canister components (such as outer bottom cover and shield plugs) are not governed by the ASME Code.

ASME Code Alternatives for the 32PTH DSC

Reference ASME Code Section/Article	Code Requirement	Alternatives, Justification & Compensatory Measures
NCA	All	Not compliant with NCA
NB-1100	Requirements for Code Stamping of Components	The canister shell, the inner top cover/shield plug, the inner bottom cover, and the siphon/vent port cover are designed & fabricated in accordance with the ASME Code, Section III, Subsection NB to the maximum extent practical. However, Code Stamping is not required. As Code Stamping is not required, the fabricator is not required to hold an ASME "N" or "NPT" stamp, or to be ASME Certified.
NB-2130	Material must be supplied by ASME approved material suppliers	Material is certified to meet all ASME Code criteria but is not eligible for certification or Code Stamping if a non-ASME fabricator is used. As the fabricator is not required to be ASME certified, material certification to NB-2130 is not possible. Material traceability & certification are maintained in accordance with TN's NRC approved QA program.
NB-4121	Material Certification by Certificate Holder	
NB-4243 and NB-5230	Category C weld joints in vessels and similar weld joints in other components shall be full penetration joints. These welds shall be examined by UT or RT and either PT or MT	The shell to the outer top cover weld, the shell to the inner top cover/shield plug weld (including option 2 or option 3 inner top cover as described in the SAR), and the siphon/vent cover welds, are all partial penetration welds. As an alternative to the NDE requirements of NB-5230, for Category C welds, all of these closure welds will be multi-layer welds and receive a root and final PT examination, except for the shell to the outer top cover weld. The shell to the outer top cover weld will be a multi-layer weld and receive multi-level PT examination in accordance with the guidance provided in ISG-15 for NDE. The multi-level PT examination provides reasonable assurance that flaws of interest will be identified. The PT examination is done by qualified personnel, in accordance with Section V and the acceptance standards of Section III, Subsection NB-5000. All of these welds will be designed to meet the guidance provided in ISG-15 for stress reduction factor.

ASME Code Alternatives for the 32PTH DSC Fuel Basket

Reference ASME Code Section/Article	Code Requirement	Alternatives, Justification & Compensatory Measures
NG/NF-1100	Requirement for Code Stamping of Components	The 32PTH DSC baskets are designed & fabricated in accordance with the ASME Code, Section III, Subsection NG to the maximum extent practical as described in the SAR, but Code Stamping is not required. As Code Stamping is not required, the fabricator is not required to hold an ASME N or NPT stamp or be ASME Certified.
NG/NF-2130 NG/NF-4121	Material must be supplied by ASME approved material suppliers Material Certification by Certificate Holder	Material is certified to meet all ASME Code criteria but is not eligible for certification or Code Stamping if a non-ASME fabricator is used. As the fabricator is not required to be ASME certified, material certification to NG/NF-2130 is not possible. Material traceability & certification are maintained in accordance with TN's NRC approved QA program. The poison material and aluminum plates are not used for structural analysis, but to provide criticality control and heat transfer. They are not ASME Code Class I materials. See note 1.
NG/NF-8000	Requirements for nameplates, stamping & reports per NCA-8000	The 32PTH DSC nameplates provide the information required by 10CFR71, 49CFR173, and 10CFR72 as appropriate. Code stamping is not required for the 32PTH DSC. QA Data packages are prepared in accordance with the requirements of 10CFR71, 10CFR72, and TN's approved QA program.
NCA	All	Not compliant with NCA.

Note:

1. Because Subsection NCA does not apply, the NCA-3820 requirements for accreditation or qualification of material organizations do not apply. CMTR's shall be provided using NCA-3862 for guidance.

Table 3-3
Summary of Stress Criteria for Subsection NG Components

Loadings	Stress Category (5)	Notes
Design [NG-3221]	$P_m \leq 1.0S_m$ $P_m + P_b \leq 1.5S_m$	
Level A [NG-3222]	$P_m \leq 1.0S_m$ (Note 6) $P_m + P_b \leq 1.5S_m$ (Note 6) $P_m + P_b + Q \leq 3.0S_m$ (Note 4)	
Level B [NG-3223] ⁽¹⁾	$P_m \leq 1.0S_m$ (Note 6) $P_m + P_b \leq 1.5S_m$ (Note 6) $P_m + P_b + Q \leq 3.0S_m$ (Note 4)	Note 1
Level C Elastic Analysis [NG-3224]	$P_m \leq 1.5S_m$ $P_m + P_b \leq 2.25S_m$	Notes 2 & 3
Level D Elastic Analysis [NG-3225, App. F]	$P_m \leq \min (2.4S_m, 0.7S_u)$ $P_m + P_b \leq \min (3.6S_m, 1.0S_u)$	
Level D Plastic Analysis [NG-3225, App. F]	$P_m \leq \max (0.7S_u, S_y + (S_u - S_y)/3)$ $P_m + P_b \leq 0.9S_u$	

- Notes:
1. There are no pressure loads on the basket, therefore the 10% increase permitted by NG-3223(a) for pressures exceeding the design pressure are not included.
 2. Evaluation of secondary stresses not required for Level C and D events.
 3. Criteria listed are for elastic analyses, other analysis methods permitted by NG-3224.1 are acceptable if performed in accordance with the appropriate paragraph of NG-3224.1.
 4. This limit may be exceeded provided the requirements of NG-3228.3 are satisfied, see NG-3222.2 and NG-3228.3.
 5. As appropriate, the special stress limits of NG-3227 should be applied.
 6. In accordance with NG-3222 and Note 9 of Figure NG-3221-1, the Limit Analysis provisions of NG-3228 may be used.
 7. The weld strength of each fusion weld nugget shall have a minimum capacity of 16.5 kips (70°F). The minimum capacity shall be determined by shear tests using test specimens made from production materials.

Table 3-11
Resin Material Properties

Temperature	Modulus of Elasticity⁽¹⁾ <i>E</i> (psi)	Coefficient of Thermal Expansion⁽²⁾, α (in./in.°F)	Density⁽³⁾, ρ (lb./in.³)	Poisson's Ratio⁽⁴⁾
Room Temperature	0.16×10^6	—	0.065	0.20

- (1) The modulus of elasticity utilized is lower than that of commercially available glass filled, polyester based polymers. Typical values are 0.25×10^6 psi.
- (2) The coefficient of thermal expansion for the resin material is not used in the transfer cask structural analysis. The resin material is not a structural component, and since the resin has a very low Modulus of Elasticity (relative to stainless steel) it's thermal expansion is not expected to affect the stresses in the structural components significantly.
- (3) A conservative density value of 0.065 lb/in³ is utilized to estimate a higher mass for the resin while the actual density per Table 5-17 is 0.057 lb/in³.
- (4) A Poisson's ratio of 0.20, which is closer to that of concrete (0.17) is utilized.

APPENDIX 3.9.1
32PTH DSC (CANISTER AND BASKET) STRUCTURAL ANALYSIS

TABLE OF CONTENTS

3.9.1	32PTH DSC (CANISTER AND BASKET) STRUCTURAL ANALYSIS	3.9.1-1
3.9.1.1	Introduction.....	3.9.1-1
3.9.1.2	32PTH DSC Fuel Basket Structural Evaluation.....	3.9.1-2
3.9.1.2.1	Approach.....	3.9.1-2
3.9.1.2.2	Load Conditions.....	3.9.1-5
3.9.1.2.3	Fuel Basket Stress Analysis.....	3.9.1-7
3.9.1.2.4	32PTH DSC Fuel Basket Buckling Analysis	3.9.1-26
3.9.1.3	32PTH DSC Shell Structural Evaluation	3.9.1-36
3.9.1.3.1	Approach.....	3.9.1-36
3.9.1.3.2	DSC Canister Shell Stress Analysis.....	3.9.1-36
3.9.1.3.3	DSC Shell Buckling Evaluation.....	3.9.1-61
3.9.1.3.4	Evaluation of Alternate DSC Bottom Closure Assembly Design.....	3.9.1-64
3.9.1.4	32PTH DSC and OS187H Transfer Cask Thermal Expansion Evaluation.....	3.9.1-78
3.9.1.4.1	Introduction.....	3.9.1-78
3.9.1.4.2	Approach.....	3.9.1-78
3.9.1.4.3	Mechanical Properties of Materials	3.9.1-78
3.9.1.4.4	Thermal Expansion Computation	3.9.1-79
3.9.1.4.5	Thermal Expansion Analysis Conclusions	3.9.1-88
3.9.1.5	References.....	3.9.1-89

LIST OF TABLES

- 3.9.1-1 Temperature Dependent Material Properties
- 3.9.1-2 SA-240, Type 304, Thermal Material Properties
- 3.9.1-3 Summary of Stresses in Fuel Compartments, Rails and Canister for Transfer Loads
- 3.9.1-4(a) Summary of Calculated Stresses in the Fuel Basket and Canister Shell for 75g Drop Loads
- 3.9.1-4(b) Summary of Linearized Stresses in 7/8 inch Square Bars for 75g Side Drop Load
- 3.9.1-5 Summary of Stresses in Fuel Compartments, Support Rails and Canister Shell for Storage Loads
- 3.9.1-6 Temperature Dependent Coefficients of Thermal Expansion
- 3.9.1-7 ASME Subsection NB Code Allowable Stresses for the 32PTH DSC Canister (for Transfer Loads)
- 3.9.1-8 ASME Code Allowable Stresses for the 32PTH DSC Canister for Storage Loads
- 3.9.1-9 32PTH DSC Canister Load Combinations during Transfer
- 3.9.1-10 32PTH DSC Canister Load Combinations during Lifting, Testing, and Hydraulic Loads
- 3.9.1-11 Summary of Calculated Stresses for Testing Condition Loads
- 3.9.1-12 Summary of Calculated Stress for Normal and Off-Normal Condition Transfer Loads
- 3.9.1-13 Summary of Calculated Stresses for Accident Condition Transfer Loads (Elastic Analysis)
- 3.9.1-14 Summary of Stresses for Accident Condition Transfer Loads (Elastic / Plastic Analysis)
- 3.9.1-15 Summary of Calculated Stress at the End Closure Welds for Testing Condition Loads

- 3.9.1-16 Summary of Calculated Stress at the End Closure Welds for Normal and Off-Normal Condition Transfer Loads
- 3.9.1-17 Summary of Calculated Stresses at the End Closure Welds for Accident Condition Transfer Loads (Elastic Analysis)
- 3.9.1-18 Summary of Calculated Stresses at End Closure Welds for Accident Condition Transfer Loads (Elastic/Plastic Analysis)
- 3.9.1-19 32PTH DSC Canister Load Combinations during Storage
- 3.9.1-20 Summary of Calculated Stresses for Normal and Accident Condition Loads (Canister in horizontal storage position)
- 3.9.1-21 Summary of Calculated Stresses for Normal and Accident Condition Loads (At End Closure Welds)⁽¹⁾
- 3.9.1-22 ASME Code Allowable Stresses for the Alternate Canister Bottom Assembly Design as per Subsection NF
- 3.9.1-23 ASME Code Allowable Stresses for the Weld between the Canister Shell and the Bottom Outer Cover as per Subsection NF
- 3.9.1-24 Summary of Calculated Stresses in the Alternate Canister Design for Normal Condition Loads (Subsection NB components)
- 3.9.1-25 Summary of Calculated Stresses in the Alternate Canister Design for Normal Condition Loads (Subsection NF components)
- 3.9.1-26 Summary of Calculated Stresses in the Alternate Canister Design for Normal Condition Loads (Subsection NF welds)
- 3.9.1-27 Summary of Calculated Stresses in the Alternate Canister Design at the End Closure Welds for Normal Condition Loads
- 3.9.1-28 Summary of Calculated Stresses in the Alternate Canister Design for Off-Normal Condition Loads (Subsection NB components)
- 3.9.1-29 Summary of Calculated Stresses in the Alternate Canister Design for Off-Normal Condition Loads (Subsection NF components)
- 3.9.1-30 Summary of Calculated Stresses in the Alternate Canister Design for Off-Normal Condition Loads (Subsection NF weld)
- 3.9.1-31 Summary of Calculated Stresses in the Alternate Canister Design at the End Closure Welds for Off-Normal Condition Loads

LIST OF TABLES
(continued)

- 3.9.1-32 Summary of Calculated Stresses in the Alternate Canister Design for Accident Condition Loads (Subsection NB components)
- 3.9.1-33 Summary of Calculated Stresses in the Alternate Canister Design for Accident Condition Loads (Subsection NF components)
- 3.9.1-34 Summary of Calculated Tensile Stresses Normal to the NF Weld Throat in the Alternate Canister Design for Accident Condition Loads (Subsection NF welds)
- 3.9.1-35 Summary of Calculated Stresses in the Alternate Canister Design for Accident Condition Loads (Top End Closure Welds)

LIST OF FIGURES

- 3.9.1-1 32PTH DSC Basket – 3D Cross Section Finite Element Model
- 3.9.1-2 32PTH DSC Basket Cross Section Finite Element Model – Fuel Compartments
- 3.9.1-3 32PTH DSC Basket Cross Section Finite Element Model – Center and Outer Plates
- 3.9.1-4 32PTH DSC Basket Cross Section Finite Element Model – Support Rails
- 3.9.1-5 32PTH DSC Basket Cross Section Finite Element Model – 7/8 inch Square Bars
- 3.9.1-6 32PTH DSC Basket Cross Section Finite Element Model – Canister and Gap Elements
- 3.9.1-7 32PTH DSC Basket FEM – Transfer Handling Loads Boundary Conditions
- 3.9.1-8 Fuel Compartments Finite Element Model – Thermal Analysis
- 3.9.1-9 Support Rail Finite Element Model – Thermal Analysis
- 3.9.1-10 Finite Element Model Boundary Conditions for Dead Weight Storage Load
- 3.9.1-11 32PTH DSC Basket Geometry for Buckling Evaluation
- 3.9.1-12 Finite Element Model used for Basket Fuel Compartment Buckling Evaluation
- 3.9.1-13 Deleted |
- 3.9.1-14 Deleted |
- 3.9.1-15 Fuel Basket Support Rail Cross Section Geometry
- 3.9.1-16 2-D Canister Axisymmetrical Thermal and Stress Finite Element Model
- 3.9.1-17 Top End of the 2-D Axisymmetrical Canister Model
- 3.9.1-18 Bottom End of the 2-D Axisymmetrical Canister Model

LIST OF FIGURES
(continued)

- 3.9.1-19 3-D DSC Canister Top End Assembly Finite Element Model
- 3.9.1-20 3-D DSC Canister Bottom End Assembly Finite Element Model
- 3.9.1-21 32PTH DSC Canister Finite Element Model used for Pressure Test Analysis
- 3.9.1-22 Deleted
- 3.9.1-23 2-D Axisymmetric Finite Element Model of the Alternate Canister Bottom Assembly
- 3.9.1-24 0° Drop Basket Deformation Plot
- 3.9.1-25 30° Drop Basket Deformation Plot
- 3.9.1-26 45° Drop Basket Deformation Plot
- 3.9.1-27 Canister Finite Element Model
- 3.9.1-28 Loading Condition for DSC Corner Drop
- 3.9.1-29 Boundary Condition for DSC Corner Drop
- 3.9.1-30 Maximum Stress Intensities in DSC Shell
- 3.9.1-31 Maximum Stress Intensities in DSC Outer Top Cover
- 3.9.1-32 Maximum Stress Intensities in DSC Inner Top Cover

composite bottom cover assembly is constructed to evaluate the structural adequacy of this alternate design.

3.9.1.2 32PTH DSC Fuel Basket Structural Evaluation

3.9.1.2.1 Approach

The Fuel Basket is evaluated for normal and accident condition impact and thermal loads. The basket stress analysis is performed using a finite element method for the side drop and thermal load cases and classical hand calculations for the end drop load cases. Buckling of the basket plates, when subjected to lateral impact loads, is evaluated by collapse load analysis using a finite element model to generate a relationship between displacement and applied load. A summary of the basket load cases is provided in Section 3.9.1.2.2. Stress and buckling analyses are provided in Sections 3.9.1.2.3 and 3.9.1.2.4, respectively.

A. Material Properties

The mechanical properties of structural materials used in the basket, rail and canister are shown in the Table 3.9.1-1 as a function of temperature. All structural components of the fuel basket and support rails are constructed from SA-240, Type 304 or equivalent stainless steel, with properties taken from AMSE B&PV Code [1]. The yield and ultimate strengths of the structural steel, shown in Table 3.9.1-1, are the minimum values specified in the material specifications. In general, the temperatures chosen for the evaluation of material properties for each component of the DSC bound the maximum temperatures computed in Chapter 4.

B. Design Criteria

For normal conditions, the basis for the basket allowable stress is the ASME Code, Section III, Subsection NG [2]. The primary membrane stress intensity and membrane plus bending stress intensities are limited to S_m (S_m is the code allowable stress intensity) and $1.5 S_m$, respectively, at any location in the basket for Level A (Normal Service) load combinations. The average shear stress is limited to $0.6 S_m$.

The ASME Code provides a $3S_m$ limit on primary plus secondary stress intensity for Level A conditions. This limit is specified to prevent ratcheting and distortion of a structure under primary plus secondary loads.

For accident conditions, stresses are evaluated as short duration Level D conditions as per ASME B&PV Code, Section III, Appendix F [3]. When evaluating the stainless steel basket results from the elastic analysis, the general primary membrane stress intensity in, P_m , shall not exceed $2.4S_m$ or $0.7S_u$ and membrane plus bending stress intensity ($P_m + P_b$) is limited to the smaller of $3.6S_m$ or $1.0S_u$. The average primary shear stress is limited to the smaller of $0.42S_u$ or $2(0.6S_m)$.

When evaluating the results from the non-linear elastic-plastic analysis, the general primary membrane stress intensity, P_m , shall not exceed $0.7S_u$ and the maximum stress intensity at any location (P_l or $P_m + P_b$) shall not exceed $0.9S_u$. The average primary shear stress is limited to $0.42S_u$ or $2(0.6S_m)$.

The acceptability of a component, against buckling, is described in Section 3.1.2.1.2 of Chapter 3.

For fusion welds between the stainless steel plates and the stainless steel fuel compartment are qualified by testing. The required minimum tested capacity of the weld connection (each weld) shall be 17.1 kips (at room temperature). This value is based on a margin of safety (test to design) of 2.0, corrected for temperature difference and the maximum weld load of 7208 lbs calculated from a 75g side drop (see page 3.9.1-16). This margin of safety, 2, is larger than the ASME Code-implied margin of safety for level D loads. The minimum capacity shall be determined by shear test (pull test) of individual specimen made from production material. In addition to the ASME Code requirements for weld qualification, as part of the weld qualification procedure, in order to verify proper machine setting and operation, a shear test (pull test) of test coupon from each welding machine will be performed prior to the start of each working shift.

3.9.1.2.3 Fuel Basket Stress Analysis

A. 3D Cross Section Finite Element Model Description

A three-dimensional finite element model of the basket fuel compartments, peripheral rails and canister is constructed using ANSYS [10] SHELL43 elements. The overall finite element model of the basket, peripheral rails and canister is shown in Figure 3.9.1-1. For conservatism, the strength of aluminum plates in the basket was neglected by excluding these from the finite element model. However, their weight was accounted for by increasing the basket plates and peripheral rail material densities. Because of the large number of plates in the basket and large size of the basket, certain modeling approximations were necessary. In view of continuous support of fuel compartment tubes by the peripheral rails along the entire basket length during a side drop, only a 15.0" long slice of the basket and rail was modeled. At the two cut faces of the model, symmetry boundary conditions were applied ($U_Z = ROT_X = ROT_Y = 0$). The fuel compartment tubes, structural plates, support rails, square bars, and canister shell are included in the model and are shown individually in Figures 3.9.1-2 through 3.9.1-6.

Radial gap elements (CONTAC 52) are used to simulate the interface between the basket peripheral rails and inner side of the canister and between canister outer radius and cask inner radius. Each gap element contains two nodes; one on each surface of the structure. The gap nodes specified at the inner side of cask are restrained in x, y and z directions. The gap size at each gap element is determined by the difference between the basket rails radius and the inside radius of the canister and between the canister outer radius and the inside radius of the cask. A sensitivity analysis of gap size and fusion weld effectiveness study have shown that the difference of the gaps and fusion weld effectiveness will have no significant impact to the results of the analysis. Radial gap (and link) elements are generated using a small ANSYS macro. Actual gap sizes for the gap element, at each radial location, were determined and input into the model as real constants using another small ANSYS macro. This macro accepts the drop orientation and model geometry as inputs and determines the circumferential position of each gap element. The macro then computes the appropriate real constants and applies to appropriate gap elements. At the operating temperatures, the initial gap sizes will be lower. Thus use of room temperature gap sizes is conservative. Figure 3.9.1-6 shows the locations of both sets of gap elements.

During drops on cask rails (180° side drop), the initial gaps between the canister and the cask are modified using the ANSYS macro. Two 3 inch wide and 0.12 inch thick rails are welded to the cask inside at 12° on both sides of vertical center line and another set of two rails are welded at 38° on both sides of the vertical center line. For the 180° side drop onto the rails, the initial gaps at the two inner rail locations are assumed closed. In-between these two rail locations, the initial gaps are set to 0.12 inches. On the other two rail locations, the gap statuses are initially set to open, and the gap sizes are generated by macro and decreased by the rail thickness.

The connections between the stainless steel fuel compartment tubes (with intermediate aluminum plates), between the tubes and stainless steel plates as well as between the tubes and rails are made with node couplings. The nodes of various plates are coupled together in the out-of-plane direction so that they will bend in unison under surface pressure or other lateral loading to simulate the through-the-thickness support provided by the aluminum plates. The fusion welds, connecting the fuel compartment and plates, are modeled by coupling nodes in all directions. The bolts connecting the peripheral rails with the plates are also modeled by coupling nodes (in x , y and z directions).

Material Nonlinearities

The basket fuel compartments, structural plates, peripheral rails and canister shell are constructed from SA-240, Type 304 or equivalent stainless steel. A bilinear stress-strain relationship, with kinematic hardening, was used for each component to simulate a correct nonlinear material behavior at the maximum operating temperature. The following elastic and inelastic material properties are used in the analysis:

Material Property	Basket Fuel Compartments, and Center Plates at 700° F	Peripheral Rails, Sq. Bars and Outer Plates at 550° F	Canister at 500° F
Modulus of Elasticity, E (psi)	24.8×10^6	25.6×10^6	25.8×10^6
Yield Strength, F_y (psi)	17,600	18,900	19,400
Tangent Modulus, E_t (psi)	5% of $E = 1.24 \times 10^6$	5% of $E = 1.28 \times 10^6$	5% of $E = 1.29 \times 10^6$

Since only a 15 inch length of the basket is modeled, the acceleration in axial direction is increased to account for the entire 144 inch length.

$$\text{Axial acceleration for 2g load} = 2.0g \times 144/15.0 = 19.2g$$

To simulate the axial stress due to the above acceleration, only one side of basket is restrained in z-direction.

For (2g axial + 2g Transverse + 2g Vertical) handling load, the pressures and accelerations are applied simultaneously:

Therefore the acceleration applied to the model is: accel,-2.0, 2.0, 19.2

Analysis and Results

A nonlinear elastic stress analysis was conducted for computing the elastic stresses in the basket model. The nonlinearity of analysis resulted from the gaps in the model. The total load was applied in small steps. The automatic time stepping program option "Autots" was activated. This option lets the program decide the actual size of the load-substep for a converged solution. The shell middle surface nodal stress intensity is the membrane stress intensity and top or bottom surface stress intensity is the membrane plus bending stress intensity.

Analysis of Fusion Welds for Handling Loads

The maximum fusion weld load was computed using the finite element model side drop load case (see page 3.9.1-16). The finite element model is modified by replacing the fusion weld couplings with PIPE20 elements.

A static nonlinear stress run is made and results of the run are post-processed in order to extract the axial (FX) and shear (FY and FZ) forces in the pipe elements. The maximum shear force in anyplace of the pipe elements for the 2g handling load is 1415 lbs. The thermal loads in the fusion welds are calculated in Section B.3 below (page 3.9.1-14). The maximum combined shear force due to handling load and thermal load is 2.05 kips. The fusion weld load capacity is qualified for 75g accident load by test and is 17.1 kips. The transfer loads (2g) are much smaller than the 75g load. Thus by comparison, fusion welds capacity is judged to be much higher than the combined handling and thermal loads.

In Chapter 4, the basket and rail temperatures are computed for three separate vacuum drying procedures. The table below provides the maximum basket and rail temperatures and thermal gradients for each vacuum drying procedure.

	Procedure A At 34 hours, Max. Temp (°F)	Procedure B At 32 hours, Max. Temp (°F)	Procedure C At 40 hours, Max. Temp (°F)
Basket Fuel Compartments	697	693	704
Basket Rails	531	575	579
Thermal Gradient, ΔT	166	118	125

From the above table, it is judged that 'Procedure A' case will be critical for stresses due to the highest thermal gradient and is selected for the analysis.

Thermal material properties for material (type 304 stainless steel), taken from Reference 1, are reproduced in Table 3.9.1-2.

The thermal analysis resulting temperature distributions for -20° F and 115° F ambient and vacuum drying conditions closely match the temperature distributions presented in Chapter 4.

Thermal Stress Analysis

Elastic stress analyses of the basket structure are conducted in order to compute the thermal stresses. The nodal temperature distribution from the thermal analysis results is applied to obtain the thermal stresses in the model. The resulting nodal stress intensity distribution in the basket fuel compartments reveals that the maximum thermal stress occurs during the vacuum drying load case, and is 9.86 ksi.

Thermal Stresses in Support Rails during Transfer

The temperature distribution and the thermal stresses in peripheral rails are computed using the same methodology as given above for the fuel compartments. The finite element model of the rails is taken from the full basket model described in Section 3.9.1.2.3.A and is shown in Figure 3.9.1-9.

The resulting nodal stress intensity distribution in the support rails reveals that the maximum thermal stress occurs during the vacuum drying load case, and is 18.70 ksi.

Thermal Load in Fusion Welds during Transfer

The forces in x , y and z global directions in the PIPE elements (modeling the fusion welds) for the critical vacuum dry thermal load case are tabulated for stress computation. The thermal analysis results show that the thermal loads in the fusion welds are quite small. The maximum shear force, F_{weld} , is:

$$F_{weld} = \sqrt{611^2 + 150^2} = 631 \text{ lbs.}$$

This force is combined with the force generated from 2g handling load calculated above, therefore, the total load is:

$$1,415 \text{ lb} + 631 \text{ lb} = 2,046 \text{ lb} \approx 2.05 \text{ kips}$$

This load is much smaller compared to the weld capacity of 17.1 kips from test.

B.4. Summary of Fuel Basket Stresses for Normal Condition Transfer Loads

Table 3.9.1-3 summarizes basket stress analysis results and compares them with the Code allowable stresses. For the Normal thermal condition allowable stresses, the fuel compartment temperature is taken to be 700° F uniform, the peripheral rail temperature is taken to be 600° F uniform and canister temperature is taken to be 500° F uniform. Based on the results of these analyses, the basket and rails are structurally adequate for normal transfer condition loads.

$$p_v = p_h \text{ for } 75g = 75 \times 0.875736 = 65.680 \text{ psi}$$

The inertia loads due to the basket and peripheral rail dead weights are simulated by applying the density and appropriate acceleration in the runs.

The aluminum plate weight is accounted for by increasing the densities of stainless steel basket fuel compartments, large rails and small rails, as in Section 3.9.1.2.3.B.2.

Finite Element Analysis

A nonlinear static stress analysis of the structural basket is conducted for computing the stresses for 0°, 30°, 45° and 180° (drop rails) drop orientations. The maximum load of 75g was applied in each analysis. The automatic time stepping program option "Autots" was activated. This option lets the program decide the actual size of the load-substep for a converged solution.

Displacements, Stresses and Forces at each node of model (for each converged substep load) were written in ANSYS result files. The program stops at the load substep when it fails to result in a converged solution. In all side drop cases, the program gave converged solutions up to 75g load. Results were extracted at the last load sub-step of 75g for evaluation.

Shear Load in Fusion Welds due to 75g Side Drop

The maximum fusion weld load was computed using the finite element model. The finite element model is modified by replacing the fusion weld couplings with PIPE20 elements.

A static nonlinear stress run is made and results of the run are post-processed in order to extract the axial (FX) and shear (FY and FZ) forces in the pipe elements. Reviewing the details of pipe element forces (at 'i' node and 'j' node of each pipe element) show that the axial (FX) and shear (FZ) loads are not significant.

Conservatively, the maximum shear load in a fusion weld is computed by vectorially adding the maximum FY and maximum FZ (irrespective of their locations in the finite element model) as follows.

Maximum Force, FY = 7,197 lb.

Maximum Force, FZ = 393 lb.

Maximum Shear Force = $[7,197^2 + 393^2]^{1/2} = 7,208 \text{ lb.}$

From the above, it is seen that the maximum shear load on a fusion weld is 7,208 lb. The fusion weld capacity (by test) is to match or exceed this maximum weld load.

For the fusion weld load capacity test at room temperature, it is determined to include a safety factor of 2 and a correction for material strength for room temperature testing. Therefore, the Required Minimum Fusion Weld Test Load = $7,208 \times (2) \times (F_{tu} \text{ at room temperature} / F_{tu} \text{ at } 700^\circ\text{F}) = 7,208 (2.0) (75.0 \text{ ksi} / 63.4 \text{ ksi}) = 17,054 \text{ lbs} \approx 17.1 \text{ kips}$

Weld Shear Stress for 75g = $(1297.3 \times 75) / (22 \times 0.4285) = 10,321 \text{ psi} \approx 10.3 \text{ ksi}$

Allowable Shear Stress (at 550° F) = $1.2 S_m = 0.8 \times 1.2 \times 16.95 = 16.27 \text{ ksi} > 10.3 \text{ ksi}$. |

The design is adequate.

Thermal Stresses in the Basket Fuel Compartments

A 3-dimensional finite element model of the basket is used for the thermal and stress analyses of the fuel basket. This finite element model is described in Section 3.9.1.2.3A. Due to symmetry of temperature distribution, only a ¼ model (see Figure 3.9.1-8) is used in this analysis. The rails and canister are removed from the model, as they have no effect on the fuel compartment thermal stresses. The support rails are analyzed separately.

In order to model realistic contact between the fuel compartments, the couplings are replaced by contact elements. The couplings at the fusion weld locations are replaced by pipe elements.

Two finite element analyses are required to compute the thermal stresses in the fuel basket. The first analysis is a thermal analysis that computes the temperature distribution at each node of the structural model, given the temperature distribution in the thermal model described in Chapter 4. The second finite element analysis computes the thermal stress distribution caused by the temperature distribution computed in the first analysis.

The four-node element SHELL57 (Thermal Shell) and LINK33 (Thermal Conduction Bar) are used in the thermal analysis. These elements are replaced by stress elements SHELL43 and PIPE20 in the stress analysis.

Thermal Analyses

Thermal analyses of the gross finite element model of the 32PTH DSC and fuel basket is conducted for both hot and cold normal ambient conditions as well as for the HSM blocked vent accident in Chapter 4. Steady-state thermal analyses of the detailed basket model, shown in Figure 3.9.1-8, are conducted to obtain the nodal temperatures by impressing the temperature distribution (computed in Chapter 4) as the boundary conditions for hot, cold and vent blockage cases. Thermal analyses of a gross model of NUHOMS® 32PTH Cask, DSC and Basket were conducted for hot and cold normal conditions and for HSM blocked vent accident in Chapter 4. Below are given the maximum basket and rail temperatures and thermal gradients for all cases from Chapter 4.

	115° F Ambient With Fins Max. Temp. (°F)	-20° F Ambient With Fins Max. Temp. (°F)	34 Hours After Blockage with Fins Max. Temp. (°F)
Basket Fuel Compartments	656	565	801
Basket Rails	511	418	662
Thermal Gradient, ΔT	145	147	139

Thermal material properties for material (type 304 stainless steel), taken from Reference 1, are reproduced in Table 3.9.1-2.

The thermal analysis resulting temperature distributions for each thermal load case closely match the temperature distributions presented in Chapter 4.

Thermal Stress Analyses

Elastic stress analyses of the fuel compartment structure are conducted for computing the thermal stresses in the fuel basket. The nodal temperature distribution from the above thermal analysis results are applied to obtain the thermal stresses in the model.

The resulting displacements and stresses in the model are written to ANSYS result files. The critical stresses are summarized in Table 3.9.1-5. It is seen from Table 3.9.1-5, that the maximum thermal stress intensities in fuel compartments are developed in -20° F ambient case.

Thermal Stresses in Peripheral Rails during Storage

Temperature distribution and thermal stresses in peripheral rails are computed using the same methodology as given above for the fuel compartments. The finite element model of the support rails is extracted from the model described in Section 3.9.1.2.3.A (page 3.9.1-7) and is shown in Figure 3.9.1-9.

The resulting thermal stress intensities for the 115° F, -20° F, and blocked vent cases are summarized in Table 3.9.1-5.

Fusion Welds Evaluation for Thermal Storage Loads

The forces in the X, Y and Z global directions, in the PIPE elements (modeling the fusion welds), for the critical -20° F case are post processed from the ANSYS result files.

Review of the ANSYS results files reveal that the thermal loads are quite small. The maximum shear load in a fusion weld is computed by vectorally adding the maximum FY and maximum F8 (irrespective of their location) for dead weight:

$$\text{Maximum shear force} = [282^2 + 8.4^2]^{1/2} = 282 \text{ lb.}$$

The maximum shear force in the fusion weld is for seismic + normal thermal load, 1,967 lbs.

The fusion weld load capacity, qualified by load test (for 75g horizontal drop accident) is 17.1 kips. The storage seismic and thermal loads are much smaller than the test load. Thus by comparison, fusion welds capacity is judged to be adequate for the storage loads.

C.4. Summary of Fuel Basket Stresses for Storage Loads

Table 3.9.1-5 summarizes the fuel basket stress analysis results and compares them with the code allowable stresses.

For the normal condition thermal load cases, the fuel compartment temperature is taken to be 700° F uniform, the peripheral rail temperature is taken to be 600° F uniform and the canister shell temperature is taken to be 500° F uniform. For the HSM vent blockage hypothetical accident condition the fuel compartment temperature is taken to be 800° F uniform and the peripheral rail temperature is taken to be 650° F.

Based on the results of these analyses, the basket and rails are structurally adequate for the normal and accident condition storage loads.

3.9.1.2.4 32PTH DSC Fuel Basket Buckling Analysis

This Section evaluates the 32PTH DSC basket design with respect to buckling. The basket fuel compartments and support rails are evaluated separately in the following sections.

A. Basket Fuel Compartment Buckling Analysis

A.1. Approach

Only the most critical fuel basket section is analyzed in detail here. The critical basket section is depicted in Figure 3.9.1-11. This approach is then validated by performing a buckling evaluation for the entire fuel basket cross section for the worst case loading condition.

The entire basket is 162.00 inches tall. However, the inertial load of the basket plates and fuel assemblies is conservatively assumed to be distributed over only a 144 inch length (effective fuel assembly length).

A.2. Material Properties used for Buckling Evaluation

All structural members of the 32PTH DSC fuel basket are constructed from SA-240 Type 304 or equivalent stainless steel. A bilinear stress-strain curve for SA-240 Type 304 stainless steel is used for the elastic-plastic analysis.

The material properties used for the basket plates are taken from ASME Code, Section II, Part D [1], at 611° F. This temperature represents an average temperature for the fuel basket section analyzed and depicted in Figure 3.9.1-11.

Fuel Basket Material Properties at 611° F

Stainless Steel (SA-240 Type 304)

$$E = 25.26 \times 10^6 \text{ psi [1]}$$

$$S_y = 18.31 \text{ ksi [1]}$$

$$S_u = 63.4 \text{ ksi [1]}$$

Tangent Modulus, E_T , is taken to be 5% of E ,

$$\Rightarrow E_T = 0.05 \times 25.26 \times 10^6 = 1.262 \times 10^6 \text{ psi}$$

The results of this critical basket section buckling analysis is summarized in Section 3.7.1.1.2 (Page 3-43). This result is then validated by performing a buckling evaluation for the entire fuel basket cross section as described in the following section (Section A.3).

A.3. Finite Element Buckling Analysis

Finite Element model

ANSYS 3D basket models used for stress analyses as described in Section 3.9.1.2.3 (page 3.9.1-7) are used for analyzed the buckling loads.

Material Nonlinearities

The basket fuel compartments, structural plates, peripheral rails and canister shell are constructed from SA-240, Type 304 or equivalent stainless steel. A bilinear stress-strain relationship, with kinematic hardening, was used for each component to simulate a correct nonlinear material behavior at the corresponding regions of the basket compartments.

Geometric Nonlinearities

Since the structure experiences large deformations before buckling, the large displacement option of ANSYS is used for all the analyses.

Loadings

The basket is analyzed for 0°, 30°, and 45° side drop loads. The weight of boron-aluminum alloy plate is distributed on all four sides of stainless steel boxes, and the fuel assembly weights are distributed on the top panel of the SST-ALUM-SST sandwich for the 0° side drop load orientation and proportionally distributed on the top & side panels for the 30° and 45° side drop load orientations.

Maximum load of 120g was applied in 0° drop and 100g in 30° and 45° drop analyses. The ANSYS automatic time stepping program option "Autots" was activated. This option lets the program decide the optimal size of the load-substep for a converged solution. The program will stop at the load substep which fails to result in a converged solution. The last load step with a converged solution is the buckling load for the structure.

Result

The following table summarizes the last converged load for all three load cases:

Basket Drop Orientation	Last Converged Load (g)	G load calculated From Appendix 3.9.10 LS-DYNA Analysis	G Load Used For Basket Structural Analysis	Factor of Safety
0°	102.5	63	75	1.37
30°	83.9	63	75	1.12
45°	85.6	63	75	1.14

The ANSYS displacement plots for the last converged load steps for the 0°, 30°, and 45° drop orientations are shown on Figures 3.9.1-24, 3.9.1-25, and 3.9.1-26, respectively.

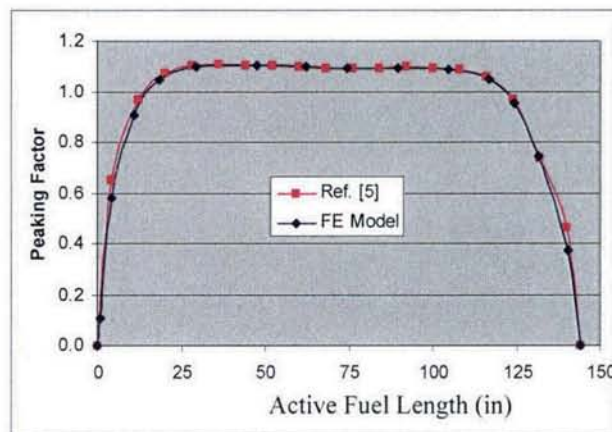
These results are conservative because the ½" aluminum plate sandwiched between the fuel compartments are not included in the model while their weights are accounted in the analyses. The ½" thick aluminum plate would provide additional safety margin if they were included in the analyses.

D.3. Canister Finite Element Analysis for Transfer Loads

All analyzed load cases in this section are identified in Tables 3.9.1-9 and 3.9.1-10 and are described in detail in the following sections.

Transfer Load Case 1: **Deadweight + 15 psig external pressure + Thermal (Vacuum Drying)**

The metal temperature profile in the canister shell is assumed to be of the same shape as that of the decay heat peaking factor reported in Chapter 4. The distribution of the decay heat along the fuel effective length for normal condition is shown in the following figure.



Three vacuum drying procedures, Procedure A, B, and C, are studied in Chapter 4. It shows that Procedure B with 12 hours after completion of vacuum drying, among all three procedures, produces the maximum metal temperature of 511° F in the canister. A steady-state thermal calculation using a 2-D canister thermal model is performed to calculate the temperature distribution throughout the canister. In this model the maximum temperature of 522° F is applied to the canister shell in locations corresponding to that between 26 inches and 125 inches of the active fuel length, where the maximum decay heat peaking factor occurs. Also an ambient temperature of 100° F is applied to the outer surfaces of the canister top and bottom plates. A steady-state thermal analysis is conducted to calculate the temperature profile in the canister. This temperature profile is then used as the thermal load for the stress analysis. The stress analysis of this load case contains two load steps. Load step 1 includes the primary loads of 1g down deadweight and an external pressure of 15 psig. Load step 2 includes these primary loads plus the secondary thermal loads from the thermal analysis.

For load step 1, the maximum stress intensity in the canister shell is 1,637 psi. The maximum stress intensity in the area of closure weld between the shell and the top shield plug is 1,341 psi., and the maximum stress intensity in the area of closure weld between the shell and the top cover plate is 410 psi.

The following load step 2 is run based on maximum temperature. Since the maximum temperature increased to 522° F, a scale factor of 1.05 $[(522-70) / (511-70) = 1.03]$ is used for the load step 2 which includes primary loads of 1g down deadweight, an external pressure of 15 psig and secondary thermal loads.

For load step 2, the maximum stress intensity in the canister shell is 18,720 psi. The maximum stress intensity in the area of closure weld between the shell and the top is 2,114 psi., and the maximum stress intensity in the area of closure weld between the shell and the top cover plate is 413psi.

Transfer Load Case 2: Handling, 2g Axial + 2g Transverse + 2g Vertical + 30 psig Int. Pressure + Thermal (115° F ambient)

The handling loads applied to the canister in the horizontal orientation are analyzed in Section 3.9.1.2.3. It is judged that under the relatively light handling loads the maximum stresses in the canister will occur in the shell section and can be obtained from the results calculated in Section 3.9.1.2.3. Therefore only the axisymmetric loads, internal pressure of 30 psig and the 115° F ambient environment loads are analyzed in this section. The calculated stress intensities from these two computations are then conservatively added for comparison with the corresponding ASME Code allowable stresses.

The maximum primary membrane stress intensity and primary membrane plus bending stress intensity in the canister shell under the handling load of 2g are calculated, in Section 3.9.1.2.3, to be 880 psi and 9,740 psi, respectively.

The stress analysis of this load case contains two load steps. Load step 1 includes the primary loads of 30 psig internal pressure. Load step 2 includes this primary load plus the secondary thermal load from the thermal analysis.

The maximum primary stress intensity in the canister was calculated to be 3,332 psi in Load Step 1 analysis. The maximum primary stress intensity in the area of closure weld between the shell and the top shield plug is calculated to be 3,134 psi. The maximum primary stress intensity in the area of closure weld between the shell and the top cover plate is calculated to be 656 psi.

The maximum primary plus secondary stress intensity in the canister is calculated to be 36,219 psi under load step 2. The maximum primary plus secondary stress intensity in the area of closure weld between the shell and the top shield plug is calculated to be 3,646 psi. The maximum primary plus secondary stress intensity in the area of closure weld between the shell and the top cover plate is calculated to be 1,292 psi.

The maximum primary stress intensities in the canister shell calculated in Section 3.9.1.2.3 are to be added to these maximum primary and primary plus secondary stress intensities calculated under this Load Case for combined load evaluation per ASME stress limits. The direct addition of stresses at the stress intensities level, in stead of at the component level, as well as the addition of the maximum stress intensities at different locations is very conservative. This enveloping technique is used to minimize the computer runs.

E. E.3. Canister Finite Element Analysis for Storage Loads

All individual load cases specified in Table 3.9.1-19 are described in details in the following sections.

Storage Load Case 1: Deadweight (1g Down)

The canister shell and fuel basket containing the fuel assemblies, resting horizontally on the rails of a HSM-H is analyzed in Section 3.9.1.2.3.C. for storage loads. The maximum primary membrane and membrane plus bending stress intensities in the canister shell due to the deadweight load are calculated to be 0.4 ksi, and 4.05 ksi, respectively (see Table 3.9.1-5).

Storage Load Case 2: Internal Pressure of 30 psig

The internal pressure of 30 psig applied on the canister is analyzed in load step1 of transfer load case 2 in Section 3.9.1.3.2.D. The maximum membrane plus bending stress intensities in the canister, calculated in Section 3.9.1.3.2.D is 3.33 ksi (see page 3.9.1-44).

Storage Load Case 3: Seismic Loads (0.65g Axial + 0.65g Transverse + 1.3g Vertical Down)

The seismic loads on the canister, containing the basket and the fuel assemblies and resting on the rails of a HSM-H, are analyzed in Section 3.9.1.2.3.C (page 3.9.1-21). The maximum primary membrane and membrane plus bending stress intensities are calculated in Section 3.9.1.2.3.C. to be 0.63 ksi, and 6.08 ksi, respectively (see Table 3.9.1-5). This specified seismic load includes a 1g deadweight load.

Storage Load Case 4: Thermal Load at -20° F Ambient

The maximum temperature in the canister for this thermal case is calculated in Chapter 4 to be 318° F. The temperatures in the canister calculated in Chapter 4 are applied to the stress model in order to compute the thermal stress intensities in the canister. The maximum secondary thermal stress intensity is calculated to be 20.60 ksi. The 20.60 ksi stress is calculated based on canister maximum temperature of 324°F. Since the revised temperature of 318° F is less than 324°F, therefore 20.60 ksi is conservatively used for load combination and compare with the allowables.

the area of closure weld between the shell and the top shield plug is calculated to be 2,112 psi. The maximum stress intensity in the area of closure weld between the shell and the top cover plate is calculated to be 420 psi.

Transfer Load Case 2: Handling 2g Axial + 2g Transverse + 2g Vertical + 30 psig Int. Pressure + Thermal (115° F ambient)

The axisymmetrical loads due to an internal pressure of 30 psig and the temperature distribution due to the 115° F ambient environment are analyzed in this load case. The calculated stress intensities for this load case are added to the stress intensities in the canister shell computed in Section 3.9.1.2.3.B for the transfer loads. This is the same procedure used in Section 3.9.1.3.2.D for the standard canister design. The combined stress intensities are evaluated against ASME code allowable stresses.

The maximum primary membrane stress intensity and primary membrane plus bending stress intensity in canister shell due to the 2g handling load, computed in Section 3.9.1.3.2.D, are 880 psi and 9,740 psi, respectively.

The maximum stress intensity in the canister due to the primary load of 30 psig internal pressure in load step 1 is calculated to be 3,831 psi and 4,067 psi in NB components and NF components respectively. The maximum stress intensity in the area of closure weld between the shell and the top shield plug is calculated to be 3,134 psi. The maximum stress intensity in the area of closure weld between the shell and the top cover plate is calculated to be 656 psi. The maximum tensile stress normal to the effective throat of the weld between the shell and the bottom outer cover plate is calculated to be 1,502 psi. These maximum stress intensities calculated in this load case are added directly to the maximum stress intensities in the shell calculated in Section 3.9.1.2.3.B for combined load evaluations. The direct addition of stresses at the stress intensities level, instead of at component level, as well as addition of maximum stress intensities at different location is a conservative enveloping approach. This enveloping technique is used to minimize the computer runs.

The maximum stress intensities in the canister due to the primary load of 30 psig internal pressure plus the secondary temperature load in load step 2 are calculated to be 35,266 psi and 4,729 psi in NB components and NF components, respectively. The maximum stress intensity in the area of closure weld between the shell and the top shield plug is calculated to be 3,646 psi. The maximum stress intensity in the area of closure weld between the shell and the top cover plate is calculated to be 1,292 psi. These calculated maximum stress intensities are to be added to the maximum shell stress intensity calculated in Section 3.9.1.2.3.B for ASME code stress evaluation as described above for load step 1.

Thermal Expansion between the O.D. of Basket and I.D. of Canister Cavity

Max. OD of cold basket =		68.370 inch	[68.53 – .16 min. gap = 68.37]					
Min. ID of cold canister cavity =		68.530 inch	[(69.75 – .12) – 2 × (.50 + .05) = 68.53]					
Event	Case	$T_{CNH}^{(2)}$ (°F)	α_{CN} (in/in-°F)	$T_{BKH}^{(3)}$ (°F)	α_{BK} (in/in-°F)	D_{CNH} (in)	D_{BKH} (in)	$D_{CNH} - D_{BKH}$ (in)
Vacuum Drying	Procedure A	210	8.940E-06	550	9.800E-06	68.616	68.692	-0.076
	Procedure A ⁽¹⁾	210	8.940E-06	390	9.460E-06	68.616	68.577	0.039
	Procedure B	360	9.340E-06	485	9.670E-06	68.716	68.644	0.071
	Procedure B	510	9.720E-06	560	9.800E-06	68.823	68.698	0.125
	Procedure C	500	9.700E-06	550	9.800E-06	68.816	68.692	0.124
Transfer (34.8 kW)	115°F Amb. Basket Type I, Conf. # 1	460	9.620E-06	640	9.880E-06	68.787	68.755	0.032
	115°F Amb. Basket Type I, Conf. # 2	460	9.620E-06	625	9.850E-06	68.787	68.744	0.043
	115°F Amb. Basket Type I, Conf. # 3	460	9.620E-06	630	9.860E-06	68.787	68.748	0.040
	115°F Amb. Basket Type I, Conf. # 4	460	9.620E-06	640	9.880E-06	68.787	68.755	0.032
	-20°F Amb. Basket Type I, Conf. # 1	390	9.460E-06	570	9.800E-06	68.737	68.705	0.032
	115°F Amb. Basket Type II, Conf. # 1	460	9.620E-06	640	9.880E-06	68.787	68.755	0.032
	115°F Amb. HSM-H w/ Finned Side Shield	400	9.500E-06	600	9.800E-06	68.745	68.725	0.020
Storage (34.8 kW)	-20°F Amb. HSM-H w/ Finned Side Shield	280	9.160E-06	505	9.710E-06	68.662	68.659	0.003
Storage Blocked Vent (34.8 kW)	34 hours after Blockage HSM-H w/ Finned Side Shield	590	9.800E-06	740	1.000E-05	68.879	68.828	0.051

Note :

- (1) Temperatures used are for 0.0" hot gap between the canister and the basket.
- (2) Canister temperatures are conservatively decreased from the values calculated in thermal analyses.
- (3) Basket temperatures are conservatively increased from the values calculated in thermal analyses.

$$D_{CNH} = 68.53 \times [1 + \alpha_{CN} \times (T_{CNH} - 70)]$$

$$D_{BKH} = 68.37 \times [1 + \alpha_{BK} \times (T_{BKH} - 70)]$$

 T_{CNH} = Temperature of hot canister α_{CN} = Thermal expansion coefficient of canister at T_{CNH} temperature T_{BKH} = Temperature of hot basket α_{BK} = Thermal expansion coefficient of basket at T_{BKH} temperature D_{CNH} = ID of hot canister at T_{CNH} temperature D_{BKH} = OD of hot basket at T_{BKH} temperature $D_{CNH} - D_{BKH}$ = diametrical clearance between the ID of the canister and the OD of the basket

C. Thermal Expansion between the Length of Basket and Canister Cavity

The maximum basket length at room temperature, $L_b = 162.120$ inches.

The minimum canister cavity length at room temperature, $L_c = 164.50$ inches.

Max. cold basket length = 162.120 inch

Min. cold canister cavity length = 164.500 inch

Event	Case	$T_{CNH}^{(1)}$ (°F)	α_{CN} (in/in-°F)	$T_{BKH}^{(2)}$ (°F)	α_{BK} (in/in-°F)	L_{CNH} (in)	L_{BKH} (in)	$L_{CNH} - L_{BKH}$ (in)
Vacuum Drying	Procedure A	210	8.940E-06	550	9.800E-06	164.706	162.883	1.823
	Procedure B	360	9.340E-06	485	9.670E-06	164.946	162.771	2.175
	Procedure B	510	9.720E-06	560	9.800E-06	165.204	162.899	2.305
	Procedure C	500	9.700E-06	550	9.800E-06	165.186	162.883	2.304
Transfer (34.8 kW)	115°F Amb. Basket Type I, Conf. # 1	460	9.620E-06	640	9.880E-06	165.117	163.033	2.084
	115°F Amb. Basket Type I, Conf. # 2	460	9.620E-06	625	9.850E-06	165.117	163.006	2.111
	115°F Amb. Basket Type I, Conf. # 3	460	9.620E-06	630	9.860E-06	165.117	163.015	2.102
	115°F Amb. Basket Type I, Conf. # 4	460	9.620E-06	640	9.880E-06	165.117	163.033	2.084
	-20°F Amb. Basket Type I, Conf. # 1	390	9.460E-06	570	9.800E-06	164.998	162.914	2.084
	115°F Amb. Basket Type II, Conf. # 1	460	9.620E-06	640	9.880E-06	165.117	163.033	2.084
Storage (34.8 kW)	115°F Amb. HSM-H w/ Finned Side Shield	400	9.500E-06	600	9.800E-06	165.016	162.962	2.054
	-20°F Amb. HSM-H w/ Finned Side Shield	280	9.160E-06	505	9.710E-06	164.816	162.805	2.012
Storage Blocked Vent (34.8 kW)	34 hours after Blockage HSM-H w/ Finned Side Shield	590	9.800E-06	740	1.000E-05	165.338	163.206	2.132

Note:

(1) Canister temperatures are conservatively decreased from the values calculated in thermal analyses.

(2) Basket temperatures are conservatively increased from the values calculated in thermal analyses.

Where,

$$L_{CNH} = 164.5 \times [1 + \alpha_{CN} \times (T_{CNH} - 70)]$$

$$L_{CNH} = 162.12 \times [1 + \alpha_{BK} \times (T_{BKH} - 70)]$$

T_{CNH} = Temperature of canister

α_{CN} = Thermal expansion coefficient of canister at T_{CNH} temperature

T_{BKH} = Average of temperatures of hot basket and basket rail

α_{BK} = Thermal expansion coefficient of basket at T_{BKH} temperature

L_{CNH} = Length of hot canister cavity at T_{CNH} temperature

L_{BKH} = Length of hot basket at T_{BKH} temperature

$L_{CNH} - L_{BKH}$ = Hot clearance between the length of the canister cavity and the length of the basket

D. Thermal Expansion between the Outer Diameter of the Canister and the Inner Diameter of the Cask Body

Max. OD of cold canister =		69.870 inch						
Min. ID of cold cask cavity =		70.350 inch						
Event	Case	$T_{CKH}^{(1)}$ (°F)	α_{CK} (in/in-°F)	$T_{CNH}^{(2)}$ (°F)	α_{CN} (in/in-°F)	D_{CKH} (in)	D_{CNH} (in)	$D_{CNH} - D_{BKH}$ (in)
Vacuum Drying	Procedure A	205	8.920E-06	230	9.020E-06	70.435	69.971	0.464
	Procedure B	190	8.870E-06	380	9.420E-06	70.425	70.074	0.351
	Procedure B	265	9.130E-06	535	9.770E-06	70.475	70.187	0.288
	Procedure C	265	9.130E-06	525	9.750E-06	70.475	70.180	0.295
Transfer (34.8 kW)	115°F Amb.	330	9.260E-06	485	9.670E-06	70.519	70.150	0.369
	-20°F Amb.	240	9.060E-06	500	9.700E-06	70.458	70.161	0.297

Note:

(1) Cask temperatures are conservatively decreased from the values calculated in thermal analyses.

(2) Canister temperatures are conservatively increased from the values calculated in thermal analyses.

Where,

$$D_{CKH} = 70.35 \times [1 + \alpha_{CK} \times (T_{CKH} - 70)]$$

$$D_{CNH} = 69.87 \times [1 + \alpha_{CN} \times (T_{CNH} - 70)]$$

T_{CKH} = Temperature of hot cask outer structural shell

α_{CK} = Thermal expansion coefficient of cask inner liner at T_{CKH} temperature

T_{CNH} = Temperature of hot canister shell

α_{CN} = Thermal expansion coefficient of canister shell at T_{CNH} temperature

D_{CKH} = ID of hot cask inner liner at T_{CKH} temperature

D_{CNH} = OD of hot canister shell at T_{CNH} temperature

$D_{CKH} - D_{CNH}$ = diametrical hot clearance between the ID of the cask inner liner and the OD of the canister shell

E. Thermal Expansion between the Length of the Canister and the Transfer Cask Cavity

Max. length of cold canister = 185.750 inch								
Min. length of cold cask cavity = 186.550 inch [186.60 – .05 = 186.55]								
Event	Case	$T_{CKH}^{(1)}$ (°F)	α_{CK} (in/in-°F)	$T_{CNH}^{(2)}$ (°F)	α_{CN} (in/in-°F)	L_{CKH} (in)	L_{CNH} (in)	$L_{CKH} - L_{CNH}$ (in)
Vacuum Drying	Procedure A	205	8.920E-06	230	9.020E-06	186.775	186.018	0.757
	Procedure B	190	8.870E-06	380	9.420E-06	186.749	186.292	0.456
	Procedure B	265	9.130E-06	535	9.770E-06	186.882	186.594	0.288
	Procedure C	265	9.130E-06	525	9.750E-06	186.882	186.574	0.308
Transfer (34.8 kW)	115°F Amb.	330	9.260E-06	485	9.670E-06	186.999	186.495	0.504
	-20°F Amb.	240	9.060E-06	500	9.700E-06	186.837	186.525	0.313

Note:

(1) Cask temperatures are conservatively decreased from the values calculated in thermal analyses.

(2) Canister temperatures are conservatively increased from the values calculated in thermal analyses.

$$L_{CKH} = 186.55 \times [1 + \alpha_{CK} \times (T_{CKH} - 70)]$$

$$L_{CNH} = 185.75 \times [1 + \alpha_{CN} \times (T_{CNH} - 70)]$$

 T_{CKH} = Temperature of hot cask structural shell α_{CK} = Thermal expansion coefficient of cask structural shell at T_{CKH} temperature T_{CNH} = Temperature of hot canister α_{CN} = Thermal expansion coefficient of canister at T_{CNH} temperature L_{CKH} = Length of hot cask cavity at T_{CKH} temperature L_{CNH} = Length of hot canister at T_{CNH} temperature $L_{CKH} - L_{CNH}$ = diametrical hot clearance between the length of the cask cavity and the length of the canister3.9.1.4.5. Thermal Expansion Analysis Conclusions

This evaluation demonstrates that adequate clearance is provided between the 32PTH DSC fuel basket and canister shell, and between the 32PTH DSC canister and the OS87H Transfer Cask to permit free thermal expansions among these components due to all specified design and service conditions.

3.9.1.5 References

1. American Society of Mechanical Engineers, ASME Boiler and Pressure Vessel Code, Section II, Part D, 1998, through 2000 addenda.
2. American Society of Mechanical Engineers, ASME Boiler and Pressure Vessel Code, Section III, Subsection NG, 1998 through 2000 addenda.
3. American Society of Mechanical Engineers, ASME Boiler and Pressure Vessel Code, Section III, Appendix F, 1998 through 2000 addenda.
4. NUREG/CR-0497-Rev 2, MATPRO-Version 11 (Revision 2), A handbook of materials properties for use in the analysis of light water reactor fuel rod behavior.
5. American Society of Mechanical Engineers, ASME Boiler and Pressure Vessel Code, Section III, Division 1, Subsection NF, 1998, through 2000 addenda.
6. Manual of Steel Construction, Ninth Edition, American Institute of Steel Construction, Inc., 1989.
7. Roark, Formulas for Stress and Strain, Sixth Edition.
8. American Society of Mechanical Engineers, ASME Boiler and Pressure Vessel Code, Section III, Division 1, Subsection NB, 1998, through 2000 addenda.
9. NUREG/CR-0481 SAND77-1872 R-7, "An Assessment of Stress-Strain Data Suitable for Finite-Element Elastic-Plastic Analysis of Shipping Containers," September 1978.
10. ANSYS User's Manual, Rev 6.0.
11. American National Standard ANSI N14.6 – 1993, "American National Standard for Radioactive Materials – Special Lifting Devices for Shipping Containers Weighing 10000 pounds (4500 kg) or More."
12. "Table speeds calculation of Strength of Threads," R. C. Boucher, Product Engineering, November 27, 1961.
13. Machinery's Handbook, 24th Edition.
14. USNRC Spent Fuel Project Office, Interim Staff Guidance – 15, "Materials Evaluation."
15. Roark, Formulas for Stress and Strain, Fourth Edition.

Table 3.9.1-3
Summary of Stresses in Fuel Compartments, Rails and Canister for Transfer Loads

Loading	Component	Service Level	Stress Classification	Loads	Stress (ksi)	Allow. Stress (ksi)
Dead Weight (Cask Vert.)	Fuel Comp. & Plates	A	P_m	1g Axial	0.16	16.0
		A	$P_m + P_b$		0.16	24.0
	Rail	A	P_m		0.16	16.4
		A	$P_m + P_b$		0.16	24.6
Handling Loads (Cask Horiz.)	Fuel Comp. & Plates	A	P_m	2g Vert. + 2g Trans. + 2g Axial	6.98	16.0
		A	$P_m + P_b$		9.98	24.0
	Rail	A	P_m		3.15	16.4
		A	$P_m + P_b$		13.8	24.6
	Canister	A	P_m		0.88	17.5
		A	$P_m + P_b$		9.74	26.25
Thermal	Fuel Comp. & Plates	A	Q	115° F Amb.	8.48	48.0
	Rail	A	Q		14.2	49.2
	Fuel Comp. & Plates	A	Q	-20° F Amb.	8.69	48.0
	Rail	A	Q		14.40	49.2
	Fuel Comp. & Plates	A	Q	Vacuum Drying (Proc. A)	9.86	48.0
	Rail	A	Q		18.50	49.2
Handling Load + Normal Thermal	Fuel Comp. & Plates	A	$P_m + P_b + Q$	Primary plus Secondary	18.70	48.0
	Rails	A	$P_m + P_b + Q$		28.20	49.2
DW + Vacuum Drying Thermal	Fuel Comp. & Plates	A	$P_m + P_b + Q$	Primary plus Secondary	10.00	48.0
	Rails	A	$P_m + P_b + Q$		18.70	49.2

Table 3.9.1-4(a)
Summary of Calculated Stresses in the Fuel Basket and Canister Shell
due to 75g Drop Loads

Drop Orientation	Component	Stress Category	Max. Stress (ksi)	Allowable Stress (ksi)
0° Side Drop	Fuel Compartment and Plates	P_m	24.5	44.38
		$P_m + P_b$	25.6	57.06
	Rails	P_m	22.0	44.38
		$P_m + P_b$	22.3	57.06
	Canister	P_m	4.61	44.38
		$P_m + P_b$	10.9	57.06
30° Side Drop	Fuel Compartment and Plates	P_m	28.3	44.38
		$P_m + P_b$	29.7	57.06
	Rails	P_m	20.6	44.38
		$P_m + P_b$	22.1	57.06
	Canister	P_m	4.81	44.38
		$P_m + P_b$	11.3	57.06
45° Side Drop	Fuel Compartment and Plates	P_m	26.4	44.38
		$P_m + P_b$	27.6	57.06
	Rails	P_m	19.8	44.38
		$P_m + P_b$	22.7	57.06
	Canister	P_m	4.53	44.38
		$P_m + P_b$	12.1	57.06
180° Side Drop (on Rails)	Fuel Compartment and Plates	P_m	25.5	44.38
		$P_m + P_b$	31.8	57.06
	Rails	P_m	13.6	44.38
		$P_m + P_b$	37.1	57.06
	Canister	P_m	13.2	44.38
		$P_m + P_b$	36.8	57.06
End Drop	Fuel Comp.	P_m	11.9	44.38

Table 3.9.1-4(b)
Summary of Linearized Stresses in 7/8 inch Square Bars for 75g Side Drop Loads

Drop Orientation	Max. Nodal Stress Intensity (ksi) ($P_m + P_b$)	Stress Category	Allowable Stress (ksi)
0° Side Drop	27.5	P_m	44.38
		$P_m + P_b$	57.06
30° Side Drop	24.7	P_m	44.38
		$P_m + P_b$	57.06
45° Side Drop	24.7	P_m	44.38
		$P_m + P_b$	57.06
180° (on rails) Side Drop	41.8	P_m	44.38
		$P_m + P_b$	57.06

All the Max. Nodal Stress Intensities ($P_m + P_b$) are below the P_m allowable.

Table 3.9.1-5
Summary of Stresses in Fuel Compartments, Support Rails and Canister Shell
for Storage Loads

Loading	Component	Service Level	Stress Classification	Applied Loads	Calculated Stress (ksi)	Allowable Stress (ksi)
Dead Weight (Cask Horiz.)	Fuel Compartment	A	P_m	1g Down	1.03	16.0
		A	$P_m + P_b$		2.93	24.0
	Rail	A	P_m		0.68	16.4
		A	$P_m + P_b$		4.37	24.6
	Canister Shell	A	P_m		0.38	17.5
		A	$P_m + P_b$		4.05	26.25
Seismic Loads (Cask Horiz.)	Fuel Compartment	A	P_m	0.65g Axial + 0.65g Trans.+ 1.30g Vertical	8.80	16.0
		A	$P_m + P_b$		9.80	24.0
	Rail	A	P_m		3.18	16.4
		A	$P_m + P_b$		12.70	24.6
	Canister Shell	A	P_m		0.63	17.5
		A	$P_m + P_b$		6.08	26.25
Thermal	Fuel Compartment	A	Q	115° F Amb. (with fins)	7.98	48.0
	Rail	A	Q		13.5	49.2
	Fuel Compartment	A	Q	-20° F Amb. (with fins)	8.38	48.0
	Rail	A	Q		13.7	49.2
	Fuel Compartment	A	Q	HSM Vent Blockage	7.04	45.6
	Rail	A	Q		8.68	48.6
Seismic Load + Normal Thermal	Fuel Compartment	A	$P_m + P_b + Q$	Primary plus Secondary	18.18	48.0
	Rails	A	$P_m + P_b + Q$		26.4	49.2
DW + Vent Blockage Thermal	Fuel Compartment	A	$P_m + P_b + Q$	Primary plus Secondary	9.97	45.6
	Rails	A	$P_m + P_b + Q$		13.05	48.6

Table 3.9.1-12
Summary of Calculated Stress for Normal and Off-Normal Condition Transfer Loads

Load Case	Combination Of Loads	Canister Orientation	Stress Intensity Limits (NB-3220) ⁽¹⁾		
			$P_m < S_m$ ($S_m = 17,500$ psi)	$P_L + P_b < 1.5 S_m$ ($1.5 S_m = 26,250$ psi)	$P_L + P_b + Q < 3 S_m$ ($3 S_m = 52,500$ psi)
1	1g down + 15 psig Ext. Press. + Vac. Dry Thermal	Vertical	1,637	1,637	19,574 ⁽²⁾
2	Handling 2g + 30 psig Int. Press. + Thermal (115° F)	Horizontal	880 + 3,332 = 4,212	9,740 + 3,332 = 13,072	9,740 + 36,219 = 45,959
3	Handling 2g's + 15 psig Ext. Press. + Thermal (-20° F)	Horizontal	880 + 1,666 = 2,546	9,740 + 1,666 = 11,406	9,740 + 35,001 = 44,741
19	30 psig Int. Press. + 80 kip push + Thermal (115° F)	Horizontal	7,238	7,238	34,916
20	30 psig Int. Press. + 60 kip pull + Thermal (115° F)	Horizontal	11,484	11,484	36,753
21	30 psig Int. Press. + 80 kip push + Thermal (115° F)	Horizontal	7,238	7,238	34,916
22	30 psig Int. Press. + 80 kip pull + Thermal (115° F)	Horizontal	5,249	13,790	36,931

Notes:

- Design stress intensity, S_m is taken at 500° F of material SA-240 Gr.304 and SA-182 F304.
- A scale factor of 1.05 is used, $19,574 = 1,637 + (18,720 - 1,637) \times 1.05$

Table 3.9.1-16
Summary of Calculated Stress at the End Closure Welds
for Normal and Off-Normal Condition Transfer Loads

Load Case	Combination Of Loads	Canister Orientation	Stress Intensity Limits (NB-3220) ⁽¹⁾		
			$P_m < 0.8S_m$ ($0.8S_m = 14,000$ psi)	$P_L + P_b < 0.8(1.5 S_m)$ ($1.2S_m = 21,000$ psi)	$P_L + P_b + Q < 0.8(3 S_m)$ ($2.4 S_m = 42,000$ psi)
1	1g down + 15 psig Ext. Press. + Vac. Dry Thermal	Vertical	1,341	1,341	2153 ⁽²⁾
2	Handling 2g's + 30 psig Int. Press. + Thermal (115° F)	Horizontal	880 + 3,134 = 4,014	9,740 + 3,134 = 12,874	9,740 + 4,160 = 13,900
3	Handling 2g's + 15 psig Ext. Press. + Thermal (-20° F)	Horizontal	880 + 1,234 = 2,114	9,740 + 1,234 = 10,974	9,740 + 2,318 = 12,058
19	30 psig Int. Press.+80 kip push + Thermal (115° F)	Horizontal	3,123	3,123	3,602
20	30 psig Int. Press. + 60 kip pull + Thermal (115° F)	Horizontal	3,134	3,134	3,646
21	30 psig Int. Press.+80 kip push + Thermal (115° F)	Horizontal	3,123	3,123	3,602
22	30 psig Int. Press.+ 80 kip pull + Thermal (115° F)	Horizontal	3,134	3,134	3,646

Notes:

- Design stress intensity, S_m is taken at 500° F of material SA-240 Gr.304 and SA-182 F304.
- A scale factor of 1.05 is used, $2153 = 1341 + (2114 - 1341) \times 1.05$

Table 3.9.1-20
Summary of Calculated Stresses for Normal and Accident Condition Loads ⁽¹⁾
(Canister in horizontal storage position)

Load Case	Applied Loads	Stress Intensity Limits			
		$P_m < S_m$ ($S_m = 18.1$ ksi)	$P_L + P_b < 1.5S_m$ ($1.5S_m =$ 27.15 ksi)	Q	$P_L + P_b + Q < 3S_m$ ($3S_m = 54.3$ ksi)
1	Deadweight (1g down) ⁽²⁾	0.4	4.05	---	---
2	30 psig Internal Pressure	3.33	3.33	---	---
3	Seismic (.65g Axial + .65g Trans. + 1.3g Vertical Down) ⁽³⁾	0.63	6.08	---	---
4	Thermal (-20° F)	---	---	20.60	---
5	Thermal (115° F)	---	---	18.48	---
6	Thermal (Blocked Vent)	---	---	15.50	---
7	Accident 70 psig Internal Pressure	7.77	7.77	---	---
8	Accident Flood (Enveloped by ext. pressure of 30 psig)	3.33	3.33	---	---
3 + 4	30 psig Internal Pressure + Seismic + Thermal (-20° F)	$3.33 + 0.63$ $= 3.96$	$3.33 + 6.08$ $= 9.41$	20.60	$3.33 + 6.08 +$ $20.60 = 30.01$
3 + 5	30 psig Internal Pressure + Seismic + Thermal (115° F)	$3.33 + 0.63$ $= 3.96$	$3.33 + 6.08$ $= 9.41$	18.48	$3.33 + 6.08 +$ $18.48 = 27.89$
1 + 6 + 7	Deadweight + 70 psig Int. Pressure + Thermal (Blocked Vent) ⁽⁴⁾	$0.4 + 7.77$ $= 8.17$	$4.05 + 7.77$ $= 11.82$	15.50	$4.05 + 7.77 +$ $15.50 = 27.32^{(5)}$
1 + 8	Deadweight + Flood (30 psig ext. pressure)	$0.4 + 3.33$ $= 3.73$	$4.05 + 3.33$ $= 7.38$	---	---

Notes:

1. Accident loads are conservatively treated as Normal loads since the allowable stress intensities for accident loads are higher than those for normal loads as indicated in Table 3.9.1-8.
2. The maximum stress intensities are obtained from Table 3.9.1-5.
3. Seismic load includes 1g down Deadweight. The maximum stress intensities are obtained from Table 3.9.1-5.
4. Seismic event is assumed not to occur with accident event of blocked vent.
5. For blocked vent accident condition, $3S_m = 49.2$ ksi (600°F)

Table 3.9.1-21
Summary of Calculated Stresses for Normal and Accident Conditions of Storage Loads
(At End Closure Welds)⁽¹⁾

Load Case	Combination of Loads	Stress Intensity Limits			
		$P_m < 0.7S_m$ [$0.7S_m = 12.67 \text{ ksi}$]	$P_L + P_b < 0.7 (1.5S_m)$ [$0.7 (1.5S_m) = 19.0 \text{ ksi}$]	Q	$P_L + P_b + Q < 0.7(3S_m)$ [$0.7 (3S_m) = 38.0 \text{ ksi}$]
1	Deadweight (1g down) ⁽²⁾	0.4	4.05	---	---
2	30 psig Internal Pressure	3.33	3.33	---	---
3	Seismic (.65g Axial + .65g Trans. + 1.3g Vertical Down) ⁽³⁾	0.63	6.08	---	---
4	Thermal (-20° F)	---	---	20.60	---
5	Thermal (115° F)	---	---	18.48	---
6	Thermal (Blocked Vent)	---	---	15.5	---
7	Accident 70 psig Internal Pressure	7.77	7.77	---	---
8	Accident Flood (Enveloped by ext. pressure of 30 psig)	3.33	3.33	---	---
3 + 4	30 psig Internal Pressure + Seismic + Thermal (-20° F)	$3.33 + 0.63 = 3.96$	$3.33 + 6.08 = 9.41$	20.60	$3.33 + 6.08 + 20.60 = 30.01$
3 + 5	30 psig Internal Pressure + Seismic + Thermal (115° F)	$3.33 + 0.63 = 3.96$	$3.33 + 6.08 = 9.41$	18.48	$3.33 + 6.08 + 18.48 = 27.89$
1 + 6 + 7	Deadweight + 70 psig Internal Pressure + Thermal (Blocked Vent) ⁽⁴⁾	$0.4 + 7.77 = 8.17$	$4.05 + 7.77 = 11.82$	15.50	$4.05 + 7.77 + 15.50 = 27.32^{(5)}$
1 + 8	Deadweight + Flood (30 ext. pressure)	$0.4 + 3.33 = 3.73$	$4.05 + 3.33 = 7.38$	---	---

Notes:

1. Accident loads are conservatively treated as normal condition loads since the allowable stress intensities for accident loads are higher than those for normal loads as indicated in Table 3.9.1-8.
2. The maximum stress intensities are obtained from Table 3.9.1-5.
3. Seismic load includes 1g down Deadweight. The maximum stress intensities are obtained from Table 3.9.1-5.
4. Seismic event is assumed not to occur with accident event of blocked vent
5. For blocked vent accident condition, $0.7 (3 S_m) = 34.44 \text{ ksi}$ (600°F)

Table 3.9.1-24
Summary of Calculated Stresses in the Alternate Canister Design
for Normal Condition Loads (Subsection NB components)

Load Case	Combination of Loads	Canister Orientation	Stress Intensity Limits (NB-3222) ⁽¹⁾		
			$P_m < S_m$ ($S_m =$ 17,500 psi)	$P_L + P_b < 1.5 S_m$ ($1.5 S_m =$ 26,250 psi)	$P_L + P_b + Q < 3 S_m$ ($3 S_m =$ 52,500 psi)
1	1g down + 15 psig Ext. Press. + Vac. Dry Thermal	Vertical	1,657	1,657	14,668
2	Handling 2g + 30 psig Int. Press. + Thermal (115° F)	Horizontal	880 + 3,831 = 4,711 ⁽²⁾	9,740 + 3,831 = 13,571 ⁽²⁾	9,740 + 35,266 = 45,006 ⁽²⁾
3	Handling 2g + 15 psig Ext. Press. + Thermal (-20° F)	Horizontal	880 + 1,772 = 2,652 ⁽²⁾	9,740 + 1,772 = 11,512 ⁽²⁾	9,740 + 27,619 = 37,359 ⁽²⁾
19	30 psig Int. Press. + 80 kip push + Thermal (115° F)	Horizontal	7,238	7,238	33,189
20	30 psig Int. Press. + 60 kip pull + Thermal (115° F)	Horizontal	4,115	4,115	35,029

Notes:

1. Design stress intensity, S_m is taken at 500° F of material SA-240 Gr.304 and SA-182 F304; see Table 3.9.1-97 for allowable stresses.
2. Maximum stress intensity in the canister due to pressure and thermal loads from this evaluation are conservatively added to the maximum stress intensity due to the 2g transfer load from Table 3.9.1-3.

Table 3.9.1-25
Summary of Calculated Stresses in the Alternate Canister Design
for Normal Condition Loads (Subsection NF components)

Load Case	Combination Of Loads	Canister Orientation	Stress Intensity Limits (NF-3221.2) ⁽¹⁾		
			$P_m < S_m$ ($S_m = 17,500$ psi)	$P_m + P_b < 1.5 S_m$ ($1.5 S_m = 26,250$ psi)	$P_m + P_b + Q < 2 S_y$ ($2 S_y = 38,800$ psi)
1	1g down + 15 psig Ext. Press. + Vac. Dry Thermal	Vertical	331	331	6,369
2	Handling 2g's + 30 psig Int. Press. + Thermal (115 °F)	Horizontal	$880 + 4,067$ $= 4,947^{(2)}$	$9,740 + 4,067$ $= 13,807^{(2)}$	$9,740 + 4,729$ $= 14,469^{(2)}$
3	Handling 2g's + 15 psig Ext. Press. + Thermal (-20 °F)	Horizontal	$880 + 540$ $= 1,420^{(2)}$	$9,740 + 540$ $= 10,280^{(2)}$	$9,740 + 12,448$ $= 22,188^{(2)}$
19	30 psig Int. Press. + 80 kip push + Thermal (115 °F)	Horizontal	2,499	2,499	6,394
20	30 psig Int. Press. + 60 kip pull + Thermal (115 °F)	Horizontal	$10,410^{(3)}$	$24,790^{(3)}$	30,340

Notes:

1. Design stress intensity (S_m) and yield stress (S_y) are taken at 500° F for all materials, see Table 3.9.1-22 for allowable stresses.
2. Maximum stress intensity in the canister due to pressure and thermal loads from this evaluation are conservatively added to the maximum stress intensity due to the 2g transfer load from Table 3.9.1-3.
3. Linearized stress intensities through the thickness of the component plates.

Table 3.9.1-26
Summary of Calculated Stresses in the Alternate Canister Design
for Normal Condition Loads (Subsection NF welds)

Load Case	Combination of Loads	Canister Orientation	Stress Intensity Limits ⁽¹⁾ (NF-3226.2)
			$S_x < 0.3 S_u$ ($0.3 S_u = 19,020$ psi)
1	1g down + 15 psig Ext. Press. + Vac. Dry Thermal	Vertical	0
2	Handling 2g + 30 psig Int. Press. + Thermal (115° F)	Horizontal	9,740 + 1,502 = 11,242 ⁽²⁾
3	Handling 2g's + 15 psig Ext. Press. + Thermal (-20° F)	Horizontal	9,740 + 23 = 9,763 ⁽²⁾
19	30 psig Int. Press. + 80 kip push + Thermal (115° F)	Horizontal	152
20	30 psig Int. Press. + 60 kip pull + Thermal (115° F)	Horizontal	12,498

Notes:

1. Tensile strength, S_u , is taken at 500° F for material SA-240 Gr.304, see Table 3.9.1-23 for allowable stresses.
2. Maximum stress intensity in the canister due to pressure and thermal loads from this evaluation are conservatively added to the maximum stress intensity due to the 2g transfer load from Table 3.9.1-3.

Table 3.9.1-27
Summary of Calculated Stresses in the Alternate Canister Design
at the End Closure Welds for Normal Condition Loads

Load Case	Combination of Loads	Canister Orientation	Stress Intensity Limits ⁽¹⁾ (NB-3222)		
			$P_m < 0.8S_m$ ($0.8S_m = 14,000$ psi)	$P_L + P_b < 0.8(1.5 S_m)$ ($1.2S_m = 21,000$ psi)	$P_L + P_b + Q < 0.8(3 S_m)$ ($2.4 S_m = 42,000$ psi)
1	1g down + 15 psig Ext. Press. + Vac. Dry Thermal	Vertical	1,341	1,341	2,112
2	Handling 2g + 30 psig Int. Press. + Thermal (115° F)	Horizontal	$880 + 3,134 = 4,014^{(2)}$	$9,740 + 3,134 = 12,874^{(2)}$	$9,740 + 3,646 = 13,386^{(2)}$
3	Handling 2g + 15 psig Ext. Press. + Thermal (-20° F)	Horizontal	$880 + 1,232 = 2,112^{(2)}$	$9,740 + 1,232 = 10,972^{(2)}$	$9,740 + 2,247 = 11,987^{(2)}$
19	30 psig Int. Press. + 80 kip push + Thermal (115° F)	Horizontal	3,123	3,123	3,602
20	30 psig Int. Press. + 80 kip pull + Thermal (115° F)	Horizontal	3,110	3,110	3,660

Notes:

1. Design stress intensity, S_m is taken at 500° F for material SA-240 Gr.304; see Table 3.9.1-7 for allowable stresses.
2. Maximum stress intensity in the canister due to pressure and thermal loads from this evaluation are conservatively added to the maximum stress intensity due to the 2g transfer load from Table 3.9.1-3.

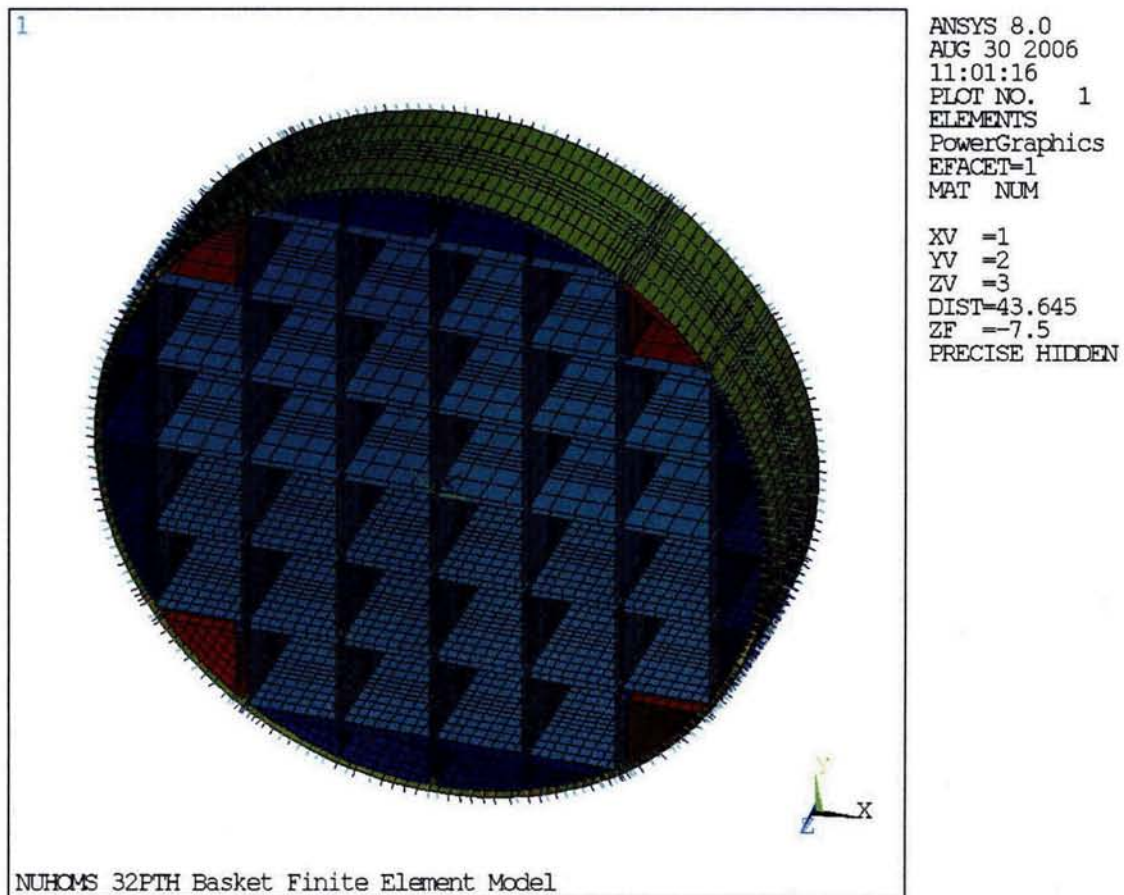


Figure 3.9.1-1

32PTH DSC Basket – 3D Cross Section Finite Element Model

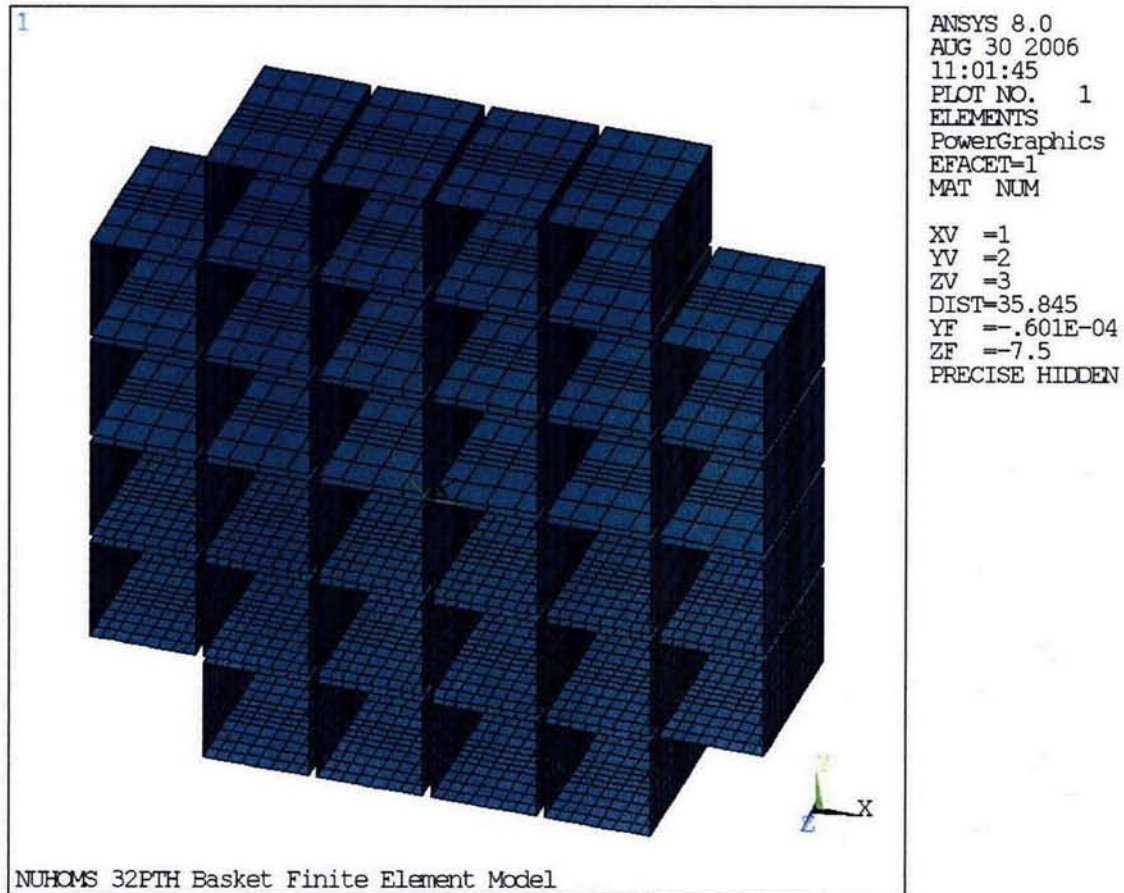


Figure 3.9.1-2
32PTH DSC Basket Cross Section Finite Element Model – Fuel Compartments

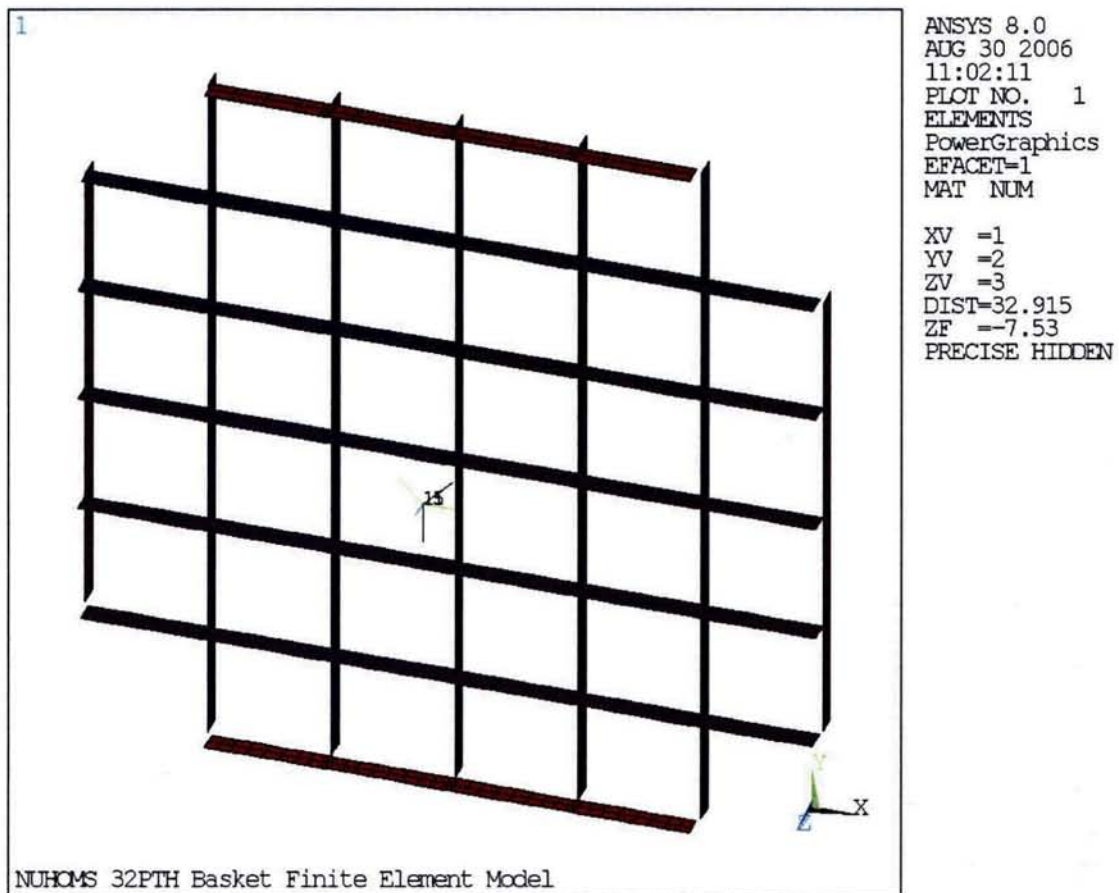


Figure 3.9.1-3
32PTH DSC Basket Cross Section Finite Element Model – Center and Outer Plates

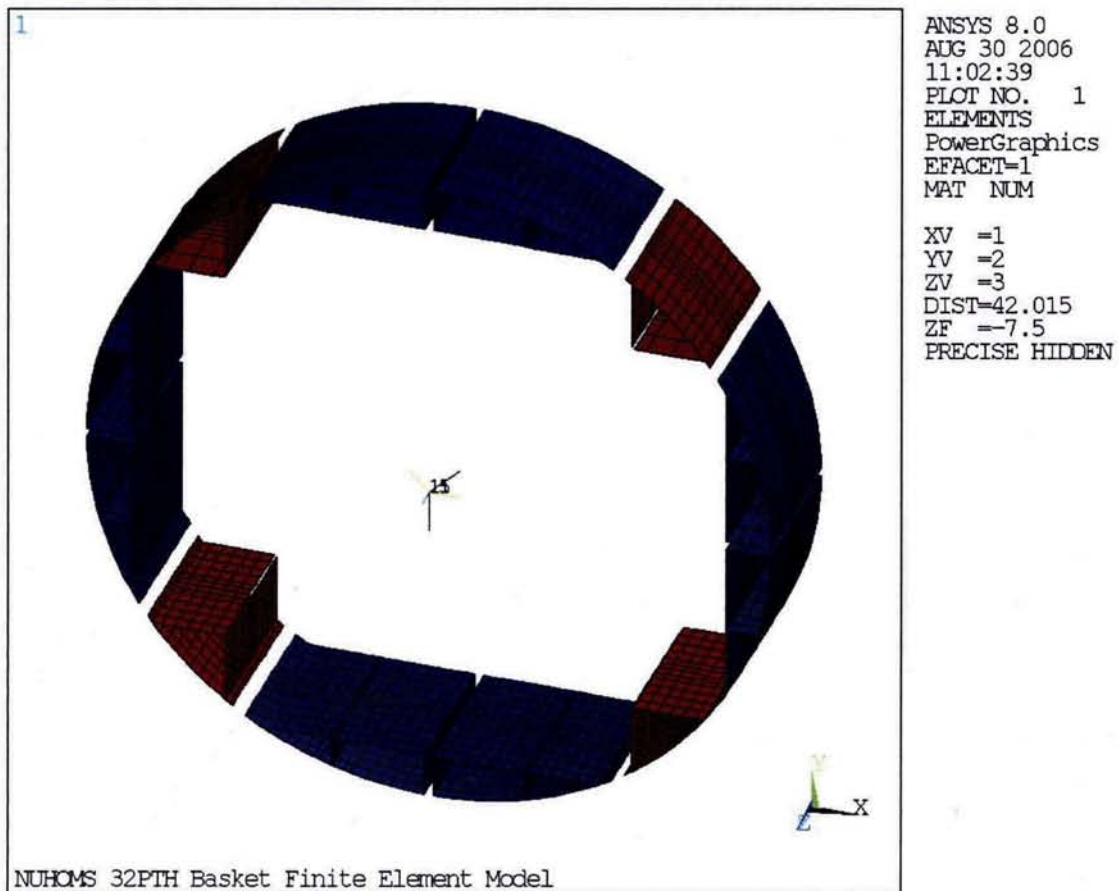


Figure 3.9.1-4
32PTH DSC Basket Cross Section Finite Element Model – Support Rails

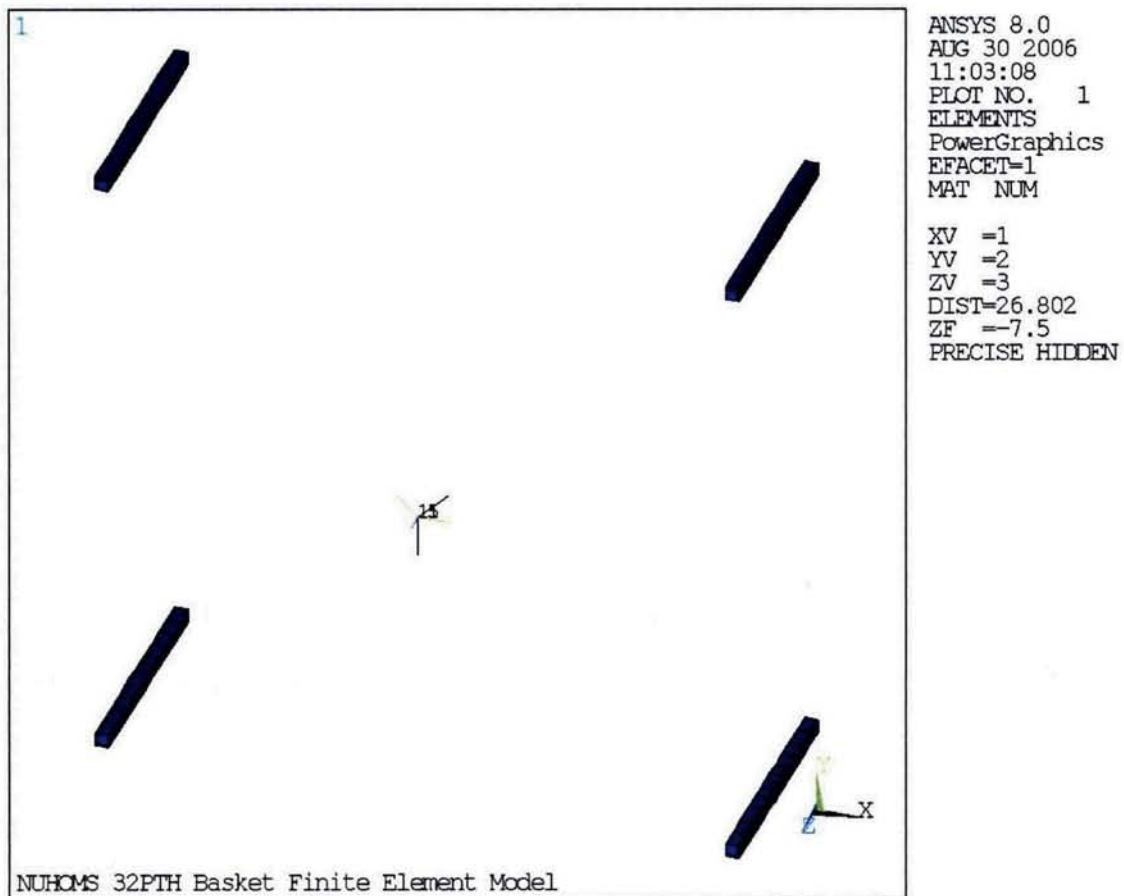


Figure 3.9.1-5
32PTH DSC Basket Cross Section Finite Element Model – 7/8 inch Square Bars

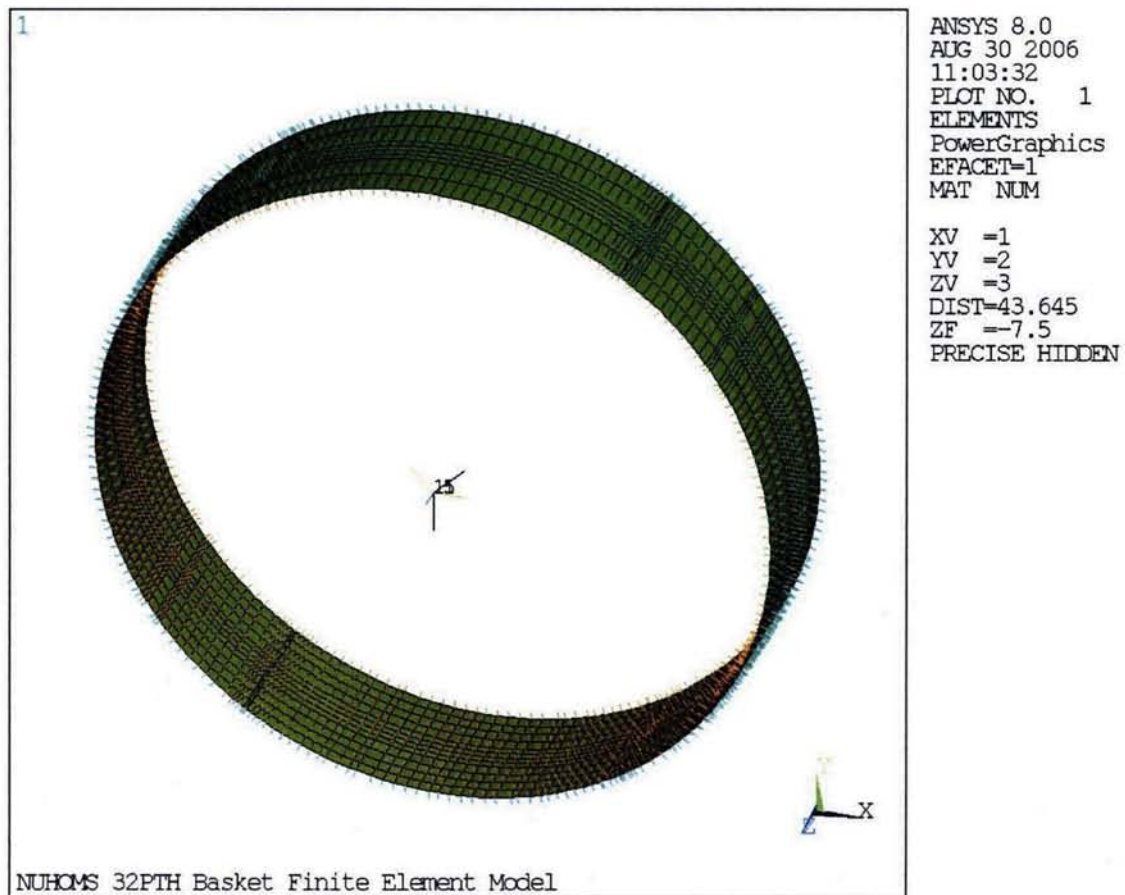


Figure 3.9.1-6
32PTH DSC Basket Cross Section Finite Element Model –
Canister and Gap Elements

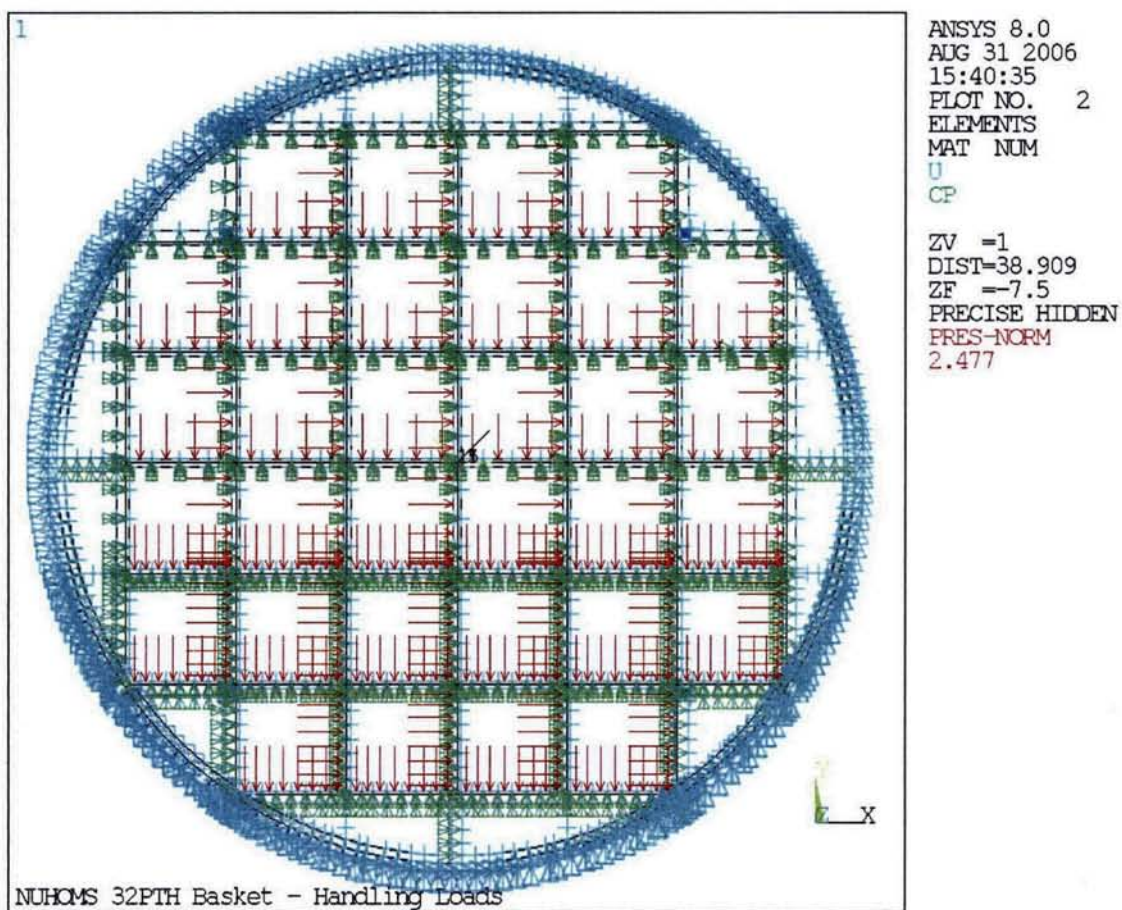


Figure 3.9.1-7
32PTH DSC Basket FEM – Transfer Handling Loads Boundary Conditions

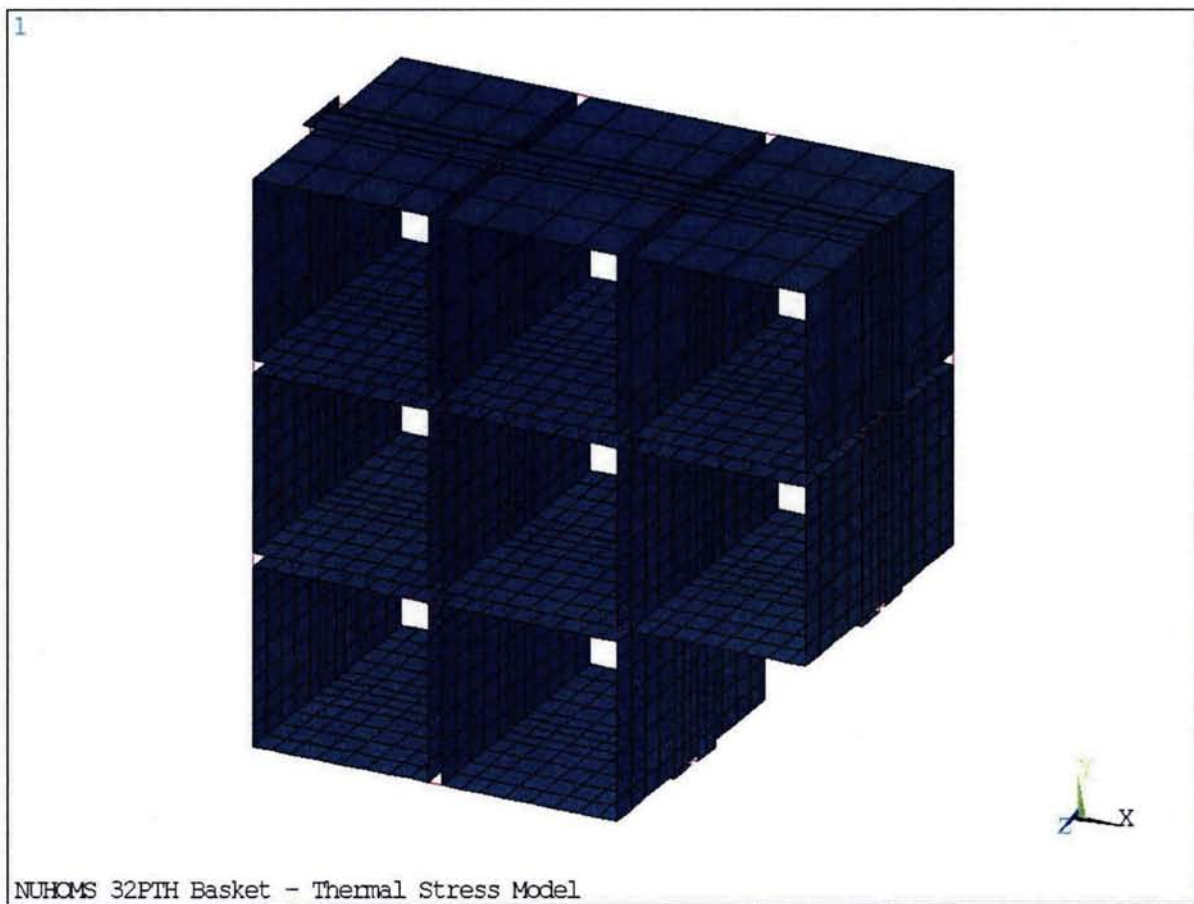


Figure 3.9.1-8
Fuel Compartments Finite Element Model – Thermal Analysis

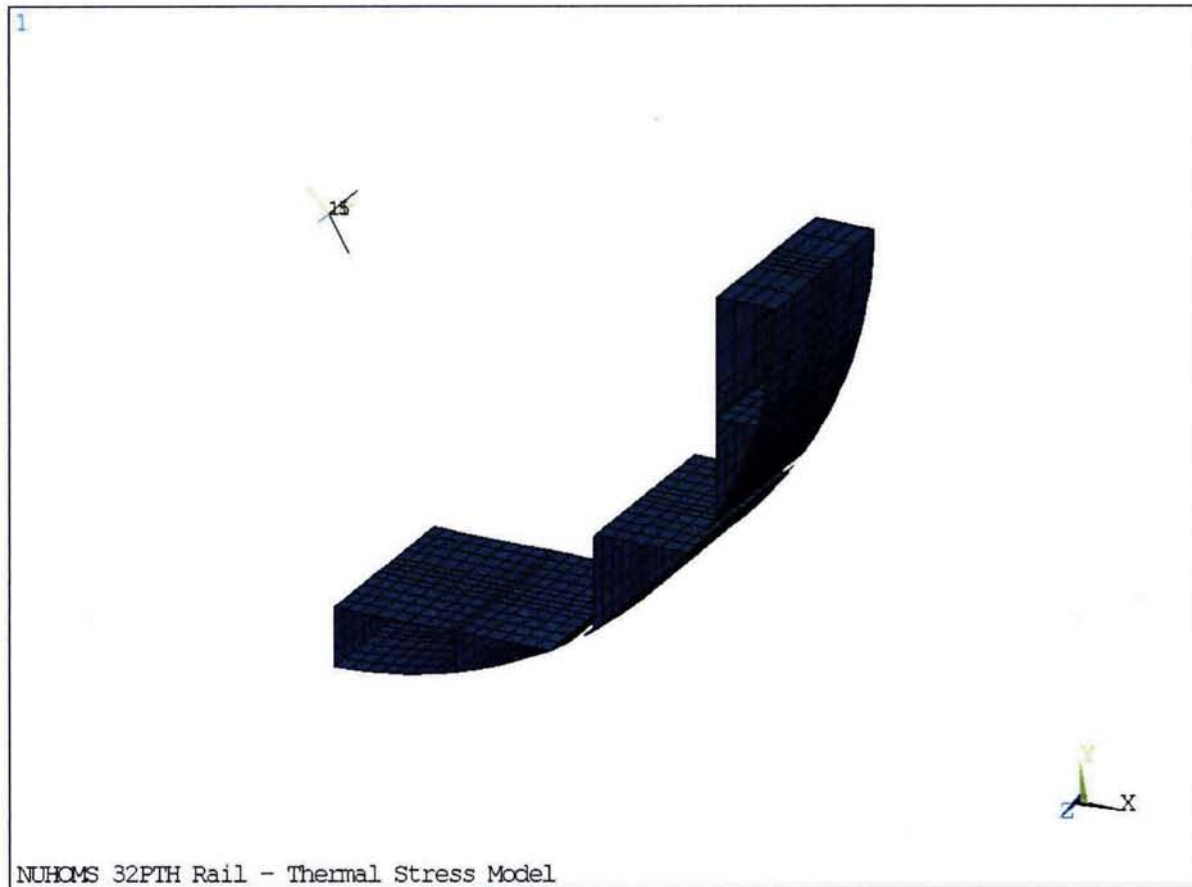


Figure 3.9.1-9
Support Rail Finite Element Model – Thermal Analysis

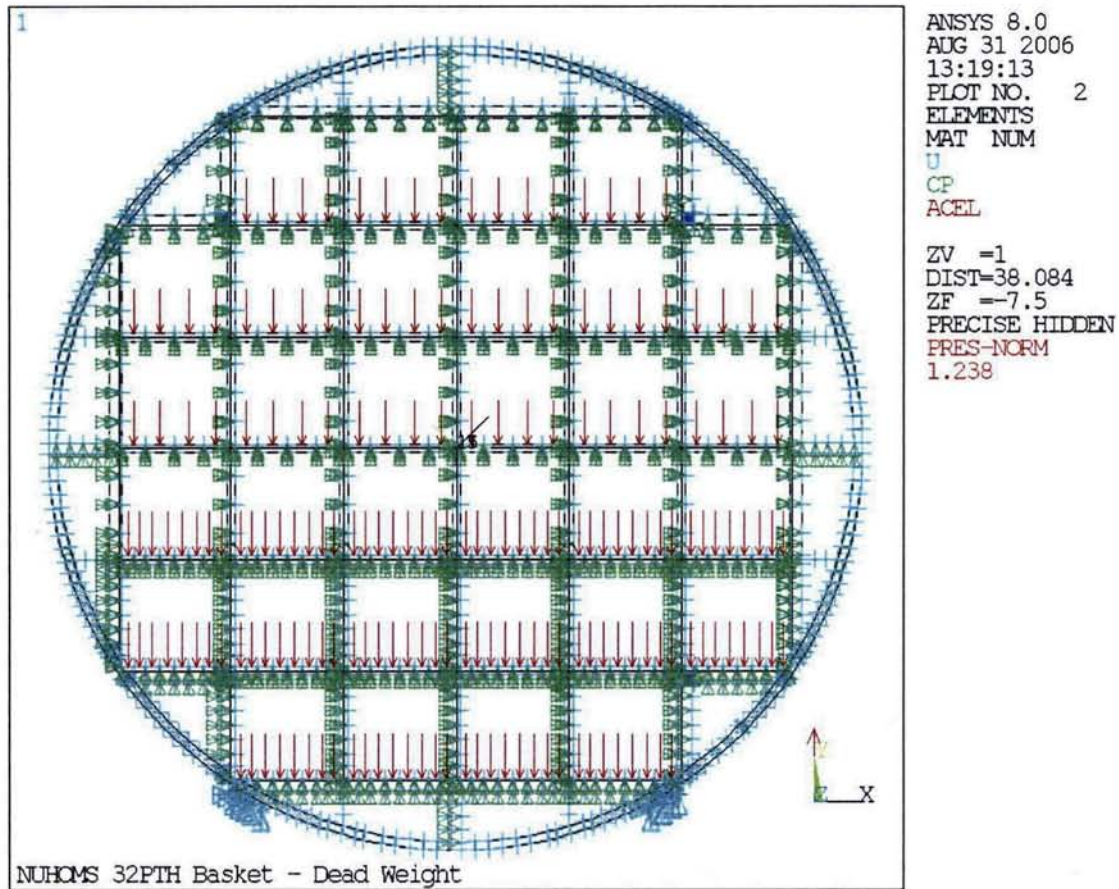


Figure 3.9.1-10
Finite Element Model Boundary Conditions for Dead Weight Storage Load

Figure Deleted in its Entirety

Figure 3.9.1-13

Figure Deleted in its Entirety

Figure 3.9.1-14

Figure Deleted in its Entirety

Figure 3.9.1-22

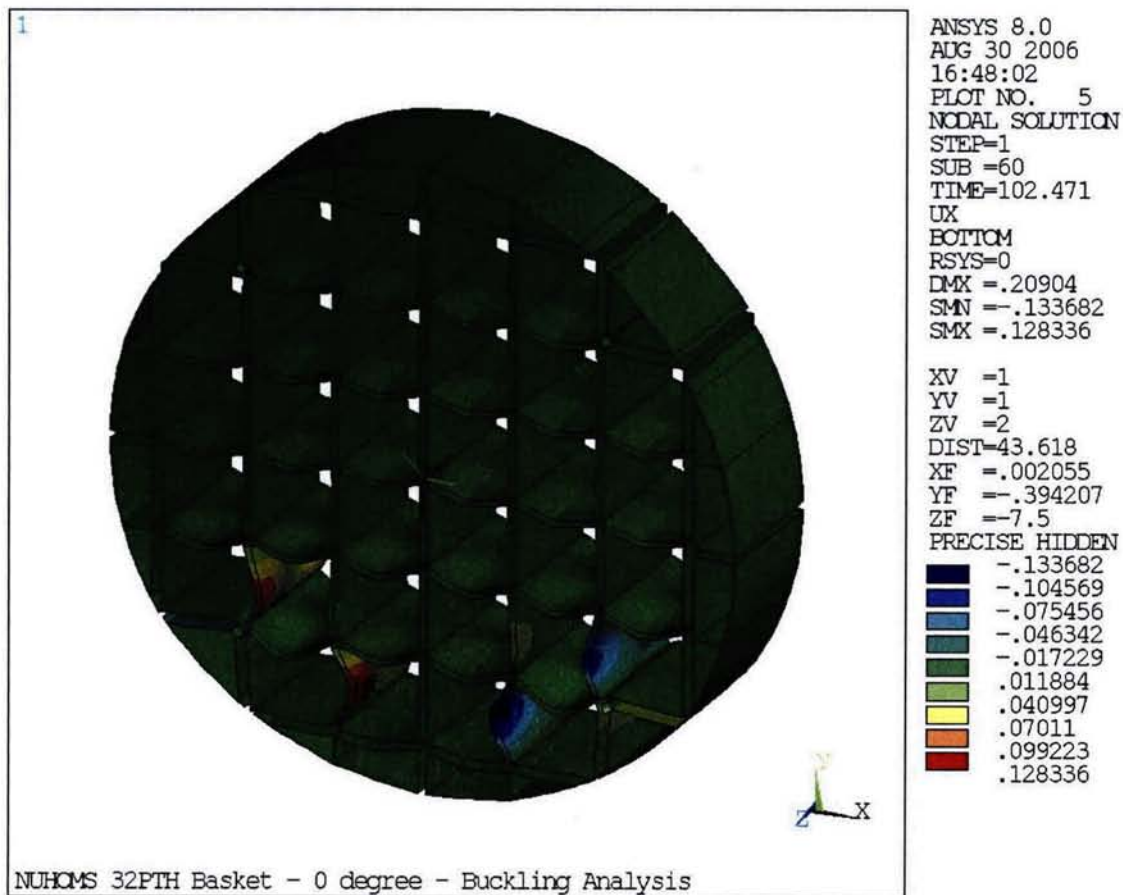


Figure 3.9.1-24
0° Drop Basket Deformation Plot

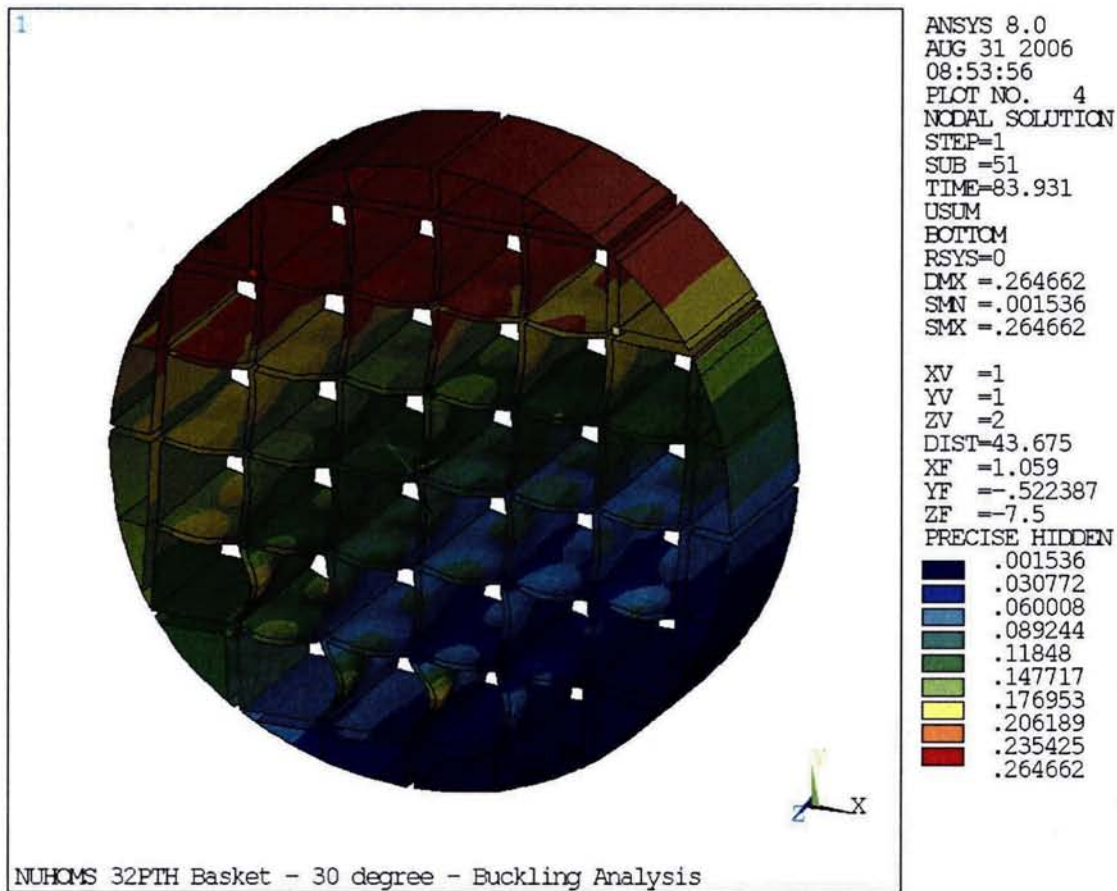


Figure 3.9.1-25
30° Drop Basket Deformation Plot

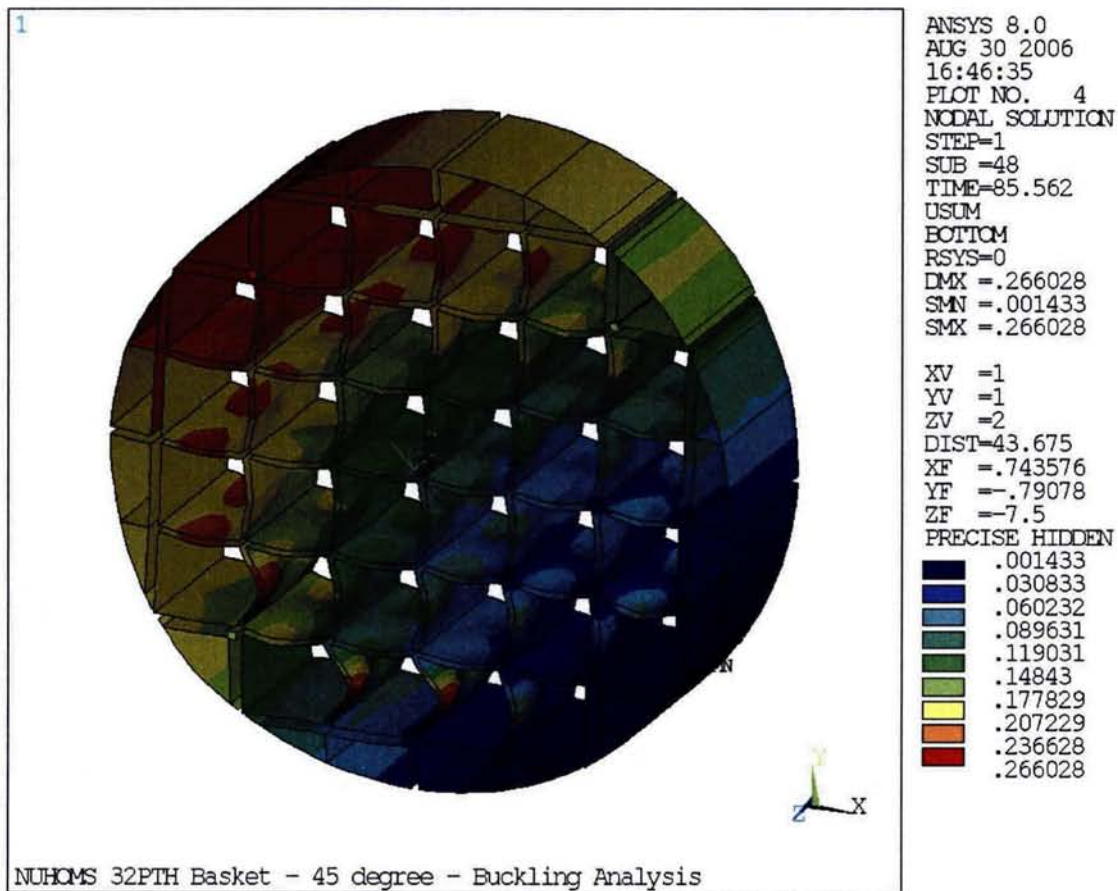


Figure 3.9.1-26
45° Drop Basket Deformation Plot

LIST OF FIGURES

3.9.2-1	NUHOMS®-OS187H Transfer Cask Key Components and Dimensions	
3.9.2-2	2-Dimensional Finite Element Model, Element Plot	
3.9.2-3	3-Dimensional Finite Element Model, Element Plot	
3.9.2-3A	Cask Top Cover/Flange/Bolt Model	
3.9.2-3B	Cask Bottom Ram Access/Cover/Bolt Model	
3.9.2-3C	Cask Top Cover/Flange CONTAC52 Element Representation	
3.9.2-3D	Cask Shell/Lead CONTAC52 Element Representation	
3.9.2-3E	Cask Bottom Access/Shell/Flange/Lead CONTAC52 Element Representation	
3.9.2-4	115°F Ambient Temperature Distribution	
3.9.2-5	-20°F Ambient Temperature Distribution	
3.9.2-6	6g Lifting Boundary Conditions	
3.9.2-7	30 psi Internal Pressure Boundary Conditions	
3.9.2-8	Transfer Loads Boundary Conditions	
3.9.2-9	75g Bottom End Drop Boundary Conditions	
3.9.2-10	75g Top End Drop Boundary Conditions	
3.9.2-11	75g Side Drop Boundary Conditions	
3.9.2-12	Local Trunnion Stress Computation Sheet	
3.9.2-13	3-D Model of Transfer Cask	
3.9.2-14	Canister/Cask Top Cover/Flange CONTAC52 Element Representation	
3.9.2-15	Canister/Cask Shell/Lead CONTAC52 Element Representation	
3.9.2-16	Canister/Cask Bottom Access/Shell/Flange/Lead CONTAC52 Element Representation	
3.9.2-17	Transfer Cask Inner Shell & Rails	

3.9.2.1.4 Material Properties

The NUHOMS®-OS187H Transfer Cask is primarily constructed from SA-240 Type 304 stainless steel. The top cover is constructed to SA-240 Type XM-19. SA-540 Grade B24 Class 1 is used for the top cover and bottom cover bolts. Chemical lead is used for radial gamma shielding, a proprietary polyester based polymer resin material is used for the solid axial neutron shielding, and liquid water is used for radial neutron shielding.

Since various temperature distributions are applied to the transfer cask model, temperature dependent Modulus of Elasticity, E , and Coefficient of Thermal Expansion, α , are used to model each material. The following material properties are used in the transfer cask model.

Transfer Cask Body (SA-240, type 304 Stainless Steel)

Temperature	Modulus of Elasticity, E (psi) [6]	Coefficient of Thermal Expansion, α (in./in.°F) [6]	Density, ρ (lb. /in ³ .) [7]	Poisson's ratio, ν [7]
70° F	28.3×10^6	8.5×10^{-6}	0.29	0.3
200° F	27.6×10^6	8.9×10^{-6}	0.29	0.3
300° F	27.0×10^6	9.2×10^{-6}	0.29	0.3
400° F	26.5×10^6	9.5×10^{-6}	0.29	0.3
500° F	25.8×10^6	9.7×10^{-6}	0.29	0.3
600° F	25.3×10^6	9.8×10^{-6}	0.29	0.3

Top Cover (SA-240, type XM-19 Stainless Steel)

Temperature	Modulus of Elasticity, E (psi) [6]	Coefficient of Thermal Expansion, α (in./in.°F) [6]	Density, ρ (lb. /in ³ .) [7]	Poisson's ratio, ν [7]
70° F	28.3×10^6	8.2×10^{-6}	0.29	0.3
200° F	27.6×10^6	8.5×10^{-6}	0.29	0.3
300° F	27.0×10^6	8.8×10^{-6}	0.29	0.3
400° F	26.5×10^6	8.9×10^{-6}	0.29	0.3
500° F	25.8×10^6	9.1×10^{-6}	0.29	0.3
600° F	25.3×10^6	9.2×10^{-6}	0.29	0.3

Top Cover Bolts and RAM Access Cover Bolts (SA-540 Grade B24 Class 1)

Temperature	Modulus of Elasticity, E (psi) [6]	Coefficient of Thermal Expansion, α (in./in.°F) [6]	Density, ρ (lb. /in ³ .) [7]	Poisson's ratio, ν [7]
70° F	27.8×10^6	6.4×10^{-6}	0.29	0.3
200° F	27.1×10^6	6.7×10^{-6}	0.29	0.3
300° F	26.7×10^6	6.9×10^{-6}	0.29	0.3
400° F	26.1×10^6	7.1×10^{-6}	0.29	0.3
500° F	25.7×10^6	7.3×10^{-6}	0.29	0.3
600° F	25.2×10^6	7.4×10^{-6}	0.29	0.3

Gamma Shield (ASTM B-29, Chemical Lead)

Temperature	Modulus of Elasticity, E (psi) [8]	Coefficient of Thermal Expansion, α (in./in.°F) [8]	Density, ρ (lb. /in ³ .) [7]	Poisson's ratio, ν [7]
70° F	2.35×10^6	16.21×10^{-6}	0.41	0.45
200° F	2.28×10^6	16.70×10^{-6}	0.41	0.45
300° F	2.06×10^6	17.34×10^{-6}	0.41	0.45
400° F	$1.92 \times 10^{6*}$	$18.12 \times 10^{-6*}$	0.41	0.45

* Extrapolated from available Reference 8 Data.

The resin material properties used to model the bottom neutron shield plate for the axisymmetric load cases are taken from Table 3-11 and are as follows.

Temperature	Modulus of Elasticity, E (psi)	Coefficient of Thermal Expansion, α (in./in.°F)	Density, ρ (lb. /in ³ .)	Poisson's ratio, ν
Room Temperature	0.16×10^6	—	0.065	0.20

Shell stresses are calculated at Trunnion-Pad intersection (in Table 3.9.2-2) and at Pad – Shell intersection (in Table 3.9.2-3).

Load Case 2. Transfer Loads

Load Case 2A. $DW + 1g$ Axial

The transfer loads are as follows:

Direction	g -load
Axial	1.0g
Vertical (DW)	1.0g
Lateral	0g

The top trunnion carries no axial load because it rests on a sliding support.

At the top and bottom trunnions the g -load per trunnion is:

$$1.0g \text{ (axial)} / 2 \text{ sides} / 1 \text{ set of trunnions} = 0.5g \text{ axial per bottom trunnion.}$$

$$1.0g \text{ (vertical)} / 2 \text{ sides} / 2 \text{ sets of trunnions} = 0.25g \text{ vertical per top and bottom trunnion}$$

Due to the above loads, stresses in the bottom trunnion locations will be critical since shell thickness at the bottom trunnion intersection is thinner relative to that of the top trunnions.

Trunnion loads:

$$P = 0 \text{ lb.}$$

$$M_L = 0.5 \times 250,000 \times 7.135 = 891,875 \text{ in. lb.}$$

$$M_C = 0.25 \times 250,000 \times 7.135 = 445,938 \text{ in. lb.}$$

$$M_T = 0.0 \text{ in. lb.}$$

$$V_L = 0.5 \times 250,000 = 125,000 \text{ lb.}$$

$$V_C = 0.25 \times 250,000 = 62,500 \text{ lb.}$$

At bottom trunnion locations:

$$\text{Trunnion radius, } r_0 = 8.575 \text{ in.}$$

$$\text{Mean radius, } R_m = 39.35 + 1.5/2 = 40.1 \text{ in.}$$

$$\text{Shell thickness, } T = 1.5 \text{ in}$$

See Table 3.9.2-4 for shell stress calculations and results.

Load Case 2C. *DW + 1g Transverse*

The transfer loads are as follows:

Direction	<i>g</i> -load
Axial	0 <i>g</i>
Vertical (DW)	1.0 <i>g</i>
Transverse	1.0 <i>g</i>

At the top and bottom trunnions the *g*-load per trunnion is:

$$1.0g \text{ (vertical)} / 2 \text{ sides} / 2 \text{ set trunnions} = 0.25g \text{ vertical per trunnion}$$

$$1.0g \text{ (transverse)} / 2 \text{ sides} / 1 \text{ set trunnions} = 0.5g \text{ transverse per trunnion}$$

Trunnion loads:

$$P = 0.5 \times 250,000 = 125,000 \text{ lb.}$$

$$M_L = 0 \text{ in. lb.}$$

$$M_C = 0.25 \times 250,000 \times 7.135 = 445,938 \text{ in. lb.}$$

$$M_T = 0.0 \text{ in. lb.}$$

$$V_L = 0 \text{ lb.}$$

$$V_C = 0.25 \times 250,000 = 62,500 \text{ lb.}$$

At bottom trunnion locations:

$$\text{Trunnion radius, } r_0 = 8.575 \text{ in.}$$

$$\text{Mean radius, } R_m = 39.35 + 1.5/2 = 40.1 \text{ in.}$$

$$\text{Shell thickness, } T = 1.5 \text{ in}$$

See Table 3.9.2-6 for shell stresses calculations and results.

Load Case 2D. $DW + 0.5g \text{ Axial} + 0.5g \text{ Vertical} + 0.5g \text{ Transverse}$

The transfer loads are as follows:

Direction	<i>g</i> -load
Axial	0.5 <i>g</i>
Vertical (DW)	$1.0g + 0.5 = 1.5g$
Transverse	0.5 <i>g</i>

The top trunnion carries no axial load because it rests on a sliding support.

At the top and bottom trunnions the *g*-load per trunnion is:

$$0.5g \text{ (axial)} / 2 \text{ sides} / 1 \text{ set of trunnions} = 0.25g \text{ axial per bottom trunnion}$$

$$1.5g \text{ (vertical)} / 2 \text{ sides} / 2 \text{ sets of trunnions} = 0.375g \text{ vertical per trunnion}$$

$$0.5g \text{ (transverse)} / 2 \text{ sides} / 1 \text{ set of trunnions} = 0.25g \text{ axial per trunnion}$$

Trunnion loads:

$$P = 0.25 \times 250,000 = 62,500 \text{ lb.}$$

$$M_L = 0.25 \times 250,000 \times 7.135 = 445,938 \text{ in. lb.}$$

$$M_C = 0.375 \times 250,000 \times 7.135 = 668,906 \text{ in. lb.}$$

$$M_T = 0.0 \text{ in. lb.}$$

$$V_L = 0.25 \times 250,000 = 62,500 \text{ lb.}$$

$$V_C = 0.375 \times 250,000 = 93,750 \text{ lb.}$$

At bottom trunnion locations:

$$\text{Trunnion radius, } r_0 = 8.575 \text{ in.}$$

$$\text{Mean radius, } R_m = 39.35 + 1.5/2 = 40.1 \text{ in.}$$

$$\text{Shell thickness, } T = 1.5 \text{ in}$$

See Table 3.9.2-7 for shell stress calculations and results.

These transfer load case parameter values are determined from tables in Reference 10. The following calculated parameters for load case 2D are given here to illustrate the typical procedure used in spreadsheet Tables 3.9.2-2 through 3.9.2-7.

$$\gamma = R_m/T = 26.7333$$

$$\beta = 0.875 \times r_0/R_m = 0.1871$$

$$\frac{P}{R_m T} = \frac{62,500}{40.1(1.5)} = 1,039$$

$$\frac{6P}{T^2} = \frac{6(62,500)}{1.5^2} = 166,667$$

$$\frac{M_C}{R_M^2 \beta T} = \frac{668,906}{40.1^2 (0.1871)(1.5)} = 1,482$$

$$\frac{6M_C}{R_M \beta T^2} = \frac{6(668,906)}{40.1(0.1871)(1.5^2)} = 237,747$$

$$\frac{M_L}{R_M^2 \beta T} = \frac{445,938}{40.1^2 (0.1871)(1.5)} = 988$$

$$\frac{6M_L}{R_M \beta T^2} = \frac{6(445,938)}{40.1(0.1871)(1.5^2)} = 158,498$$

$$\tau_{X\phi} \text{ for } V_C = \frac{V_C}{\pi r_o T} = \frac{93,750}{\pi(8.575)(1.5)} = 2,320$$

$$\tau_{X\phi} \text{ for } V_L = \frac{V_L}{\pi r_o T} = \frac{62,500}{\pi(8.575)(1.5)} = 1,546$$

It may be noted that some numbers in hand calculation do not exactly match the spreadsheet (Table 3.9.2-7) numbers. The reason is that hand calculation results are rounded as compared to the results in the spreadsheets.

3.9.2.6 References

1. 10CFR Part 72, Licensing Requirement for Storage of Spent Fuel in an Independent Spent Fuel Storage Installation.
2. ASME Code Section III, Subsection NC and Appendices, 1998, through 2000 addenda.
3. American Society of Mechanical Engineers, ASME Boiler and Pressure Vessel Code, Section III, Appendix F, 1998, through 2000 addenda.
4. ANSYS Users Manual, Rev. 5.6, 1998.
5. Not used.
6. American Society of Mechanical Engineers, ASME Boiler and Pressure Vessel Code, Section II, Part D, 1998, through 2000 addenda.
7. Baumeister & Marks, Standard Handbook for Mechanical Engineers, 7th Edition.
8. An Assessment of Stress-Strain Data Suitable for Finite Element Elastic-Plastic Analysis of Shipping Containers, NUREG/CR-0481.
9. Stress Analysis of Closure Bolts for Shipping Casks, NUREG/CR-6007, April 1992.
10. Welding Research Council (WRC), Local Stresses in Spherical and Cylindrical Shells Due To External Loadings, Bulletin 107.
11. Special Lifting Devices for Shipping Containers Weighing 10,000 Pounds or More, ANSI N14.6, 1993.

Table 3.9.2-1 (concluded)
OS-187H Transfer Cask Maximum Stresses

Load Case Number	Loading Condition	Service Level	Component		Maximum Stress Intensity (ksi)	Allowable Membrane Stress Intensity (ksi)
8	75g Top End Drop + Internal Pressure	D	Structural Shell		19.11	46.34
			Top Cover		27.89	65.94
			Inner Shell		10.07	44.80
			Bottom End plates		6.56	46.34
			RAM Access and Cover		4.83	48.00
9	75g Side Drop + Internal Pressure	D	Structural Shell	P_m	42.95	46.34
				$(P_m \text{ or } P_L) + P_b$	58.17	66.20 ⁽³⁾
			Top Cover	P_m	60.38	65.94
				P_L	77.81 ⁽⁴⁾	94.20 ⁽⁴⁾
				$(P_m \text{ or } P_L) + P_b$	91.90	94.20 ⁽³⁾
			Inner Shell	P_m	33.43	44.80
				$(P_m \text{ or } P_L) + P_b$	49.86	64.00 ⁽³⁾
			Bottom End plates	P_m	43.88	46.34
				P_L	51.26 ⁽⁴⁾	66.20 ⁽⁴⁾
				$(P_m \text{ or } P_L) + P_b$	48.28	66.20 ⁽³⁾
10	Transfer Thermal Accident (Fire)	D	Structural Shell	P_m	37.14	48.00
				$(P_m \text{ or } P_L) + P_b$	47.74	71.00 ⁽³⁾

(1) $P_L + P_b + Q$ allowable stress.

(2) $S_m = 16.2$ ksi. For SA-240 type 304 at a temperature of 650° F. (the maximum transfer cask temperature is 618° F during the thermal accident [Chapter 4]). The allowable is taken as $3.6S_m$.

(3) Membrane plus bending [$(P_m \text{ or } P_L) + P_b$] allowable stress.

(4) Stresses at the edge of the impact target support at the 15° location are considered local and are compared to P_L allowable stresses.

Table 3.9.2-4
Computation Spreadsheet for the (DW + 1.0g Axial) Transfer Load,
Bottom Trunnion – Local Shell Stresses

Allplied Loads		Geometry		Geometric Parameters									
W	250000	T	1.5	gamma	26.7333								
P	0	r0	8.575	beta	0.1871								
ML	891875	Rm	40.1										
MC	445938												
MT	0												
VL	125000												
VC	62500												
		column # =		1	2	3	4	5	6	7	8		
from fig	read curves	for	multiplier	abs. stress	values	Au	Al	Bu	Bl	Cu	Cl	Du	DI
3C AND 4C	3.5	4.5	0	0	0	0	0	0	0	0	0	0	0
1C AND 2C-1	0.088	0.054	0	0	0	0	0	0	0	0	0	0	0
3A	1.1		988	1087						-1087	-1087	1087	1087
1A	0.09		158490	14264						-14264	14264	14264	-14264
3B	3		1976	5929		-5929	-5929	5929	5929				
1B OR 1B-1	0.034		316979	10777		-10777	10777	10777	-10777				
Summation of phi stresses => sigma phi =						-16706	4849	16706	-4849	-15351	13177	15351	-13177
3C AND 4C	3.5	4.5	0	0	0	0	0	0	0	0	0	0	0
1C-1 AND 2C	0.084	0.052	0	0	0	0	0	0	0	0	0	0	0
4A	1.7		988	1680						-1680	-1680	1680	1680
2A	0.044		158490	6974						-6974	6974	6974	-6974
4B	1		1976	1976		-1976	-1976	1976	1976				
2B OR 2B-1	0.05		316979	15849		-15849	15849	15849	-15849				
Summation of X stresses => sigma X =						-17825	13873	17825	-13873	-8653	5294	8653	-5294
Shear stress due to torsion MT						0	0	0	0	0	0	0	0
Shear stress due to load VC						1547	1547	-1547	-1547				
Shear stress due to load VL						3093				-3093	-3093	3093	3093
Summation of shear stresses tau =						1547	1547	-1547	-1547	-3093	-3093	3093	3093
stress intensities =>						18910	14131	18910	14131	16561	14246	16561	14246
membrane components of sigma phi =>						-5929	-5929	5929	5929	-1087	-1087	1087	1087
membrane components of sigma X =>						-1976	-1976	1976	1976	-1680	-1680	1680	1680
tau =>						1547	1547	-1547	-1547	-3093	-3093	3093	3093
membrane stress intensities =>						6462	6462	6462	6462	6215	6215	6215	6215

Table 3.9.2-7
Computation Spreadsheet for the (DW + 0.5g axial + 0.5g vertical + 0.5g trans.) Transfer
Load, Bottom Trunnion – Local Shell Stresses

W	250000		T	1.5	gamma	26.7333							
P	62500		r0	8.575	beta	0.1871							
ML	445938		Rm	40.1									
MC	668906												
MT	0												
VL	62500												
VC	93750												
				column # =	1	2	3	4	5	6	7	8	
from fig	read curves	for	multiplier	abs. stress values	Au	Al	Bu	Bl	Cu	Cl	Du	DI	
3C AND 4C	3.5	4.5	1039	3637	4676	-4676	-4676	-4676	-4676	-3637	-3637	-3637	-3637
1C AND 2C-1	0.088	0.054	166667	14667	9000	-9000	9000	-9000	9000	-14667	14667	-14667	14667
3A	1.1		1482	1630						-1630	-1630	1630	1630
1A	0.09		237734	21396						-21396	21396	21396	-21396
3B	3		988	2964		-2964	-2964	2964	2964				
1B OR 1B-1	0.034		158490	5389		-5389	5389	5389	-5389				
Summation of phi stresses => sigma phi =					-22029	6749	-5323	1900	-41330	30796	4723	-8736	
3C AND 4C	3.5	4.5	1039	3637	4676	-3637	-3637	-3637	-3637	-4676	-4676	-4676	-4676
1C-1 AND 2C	0.084	0.052	166667	14000	8667	-14000	14000	-14000	14000	-8667	8667	-8667	8667
4A	1.7		1482	2520						-2520	-2520	2520	2520
2A	0.044		237734	10460						-10460	10460	10460	-10460
4B	1		988	988		-988	-988	988	988				
2B OR 2B-1	0.05		158490	7924		-7924	7924	7924	-7924				
Summation of X stresses => sigma X =					-26549	17300	-8724	3427	-26322	11932	-363	-3950	
Shear stress due to torsion MT					0	0	0	0	0	0	0	0	
Shear stress due to load VC					2320	2320	2320	-2320	-2320				
Shear stress due to load VL					1547				-1547	-1547	1547	1547	
Summation of shear stresses tau =					2320	2320	-2320	-2320	-1547	-1547	1547	1547	
stress intensities =>					27528	17787	9900	5106	41488	30922	5952	9192	
membrane components of sigma phi =>					-7640	-7640	-1712	-1712	-5267	-5267	-2006	-2006	
membrane components of sigma X =>					-4625	-4625	-2649	-2649	-7195	-7195	-2156	-2156	
tau =>					2320	2320	-2320	-2320	-1547	-1547	1547	1547	
membrane stress intensities =>					8899	8899	4734	4734	8054	8054	3630	3630	

Table 3.9.2-8
NUHOMS®-OS187H Transfer Cask Local Shell Stresses and Allowables

Load Case Number	Load	Maximum Local Stress		Allowable (ksi)	Reference Table
		Type	Magnitude (ksi)		
1	6g Lifting (Pad)	P_l	20.42	30.0	Table 3.9.2-2
		$P_l + P_b$	55.66	60.0	Table 3.9.2-2
	6g Lifting (Shell)	P_l	19.35	30.0	Table 3.9.2-3
		$P_l + P_b$	50.73	60.0	Table 3.9.2-3
2A.	Transfer, DW + 1g Axial	P_l	6.46	30.0	Table 3.9.2-4
		$P_l + P_b$	18.91	60.0	Table 3.9.2-4
2B.	Transfer, DW + 1g Vertical	P_l	6.19	30.0	Table 3.9.2-5
		$P_l + P_b$	30.70	60.0	Table 3.9.2-5
2C.	Transfer, DW + 1g Transverse	P_l	11.03	30.0	Table 3.9.2-6
		$P_l + P_b$	51.96	60.0	Table 3.9.2-6
2D.	Transfer, DW + 0.5g Axial + 0.5g Vertical + 0.5g Transverse	P_l	8.90	30.0	Table 3.9.2-7
		$P_l + P_b$	41.48	60.0	Table 3.9.2-7

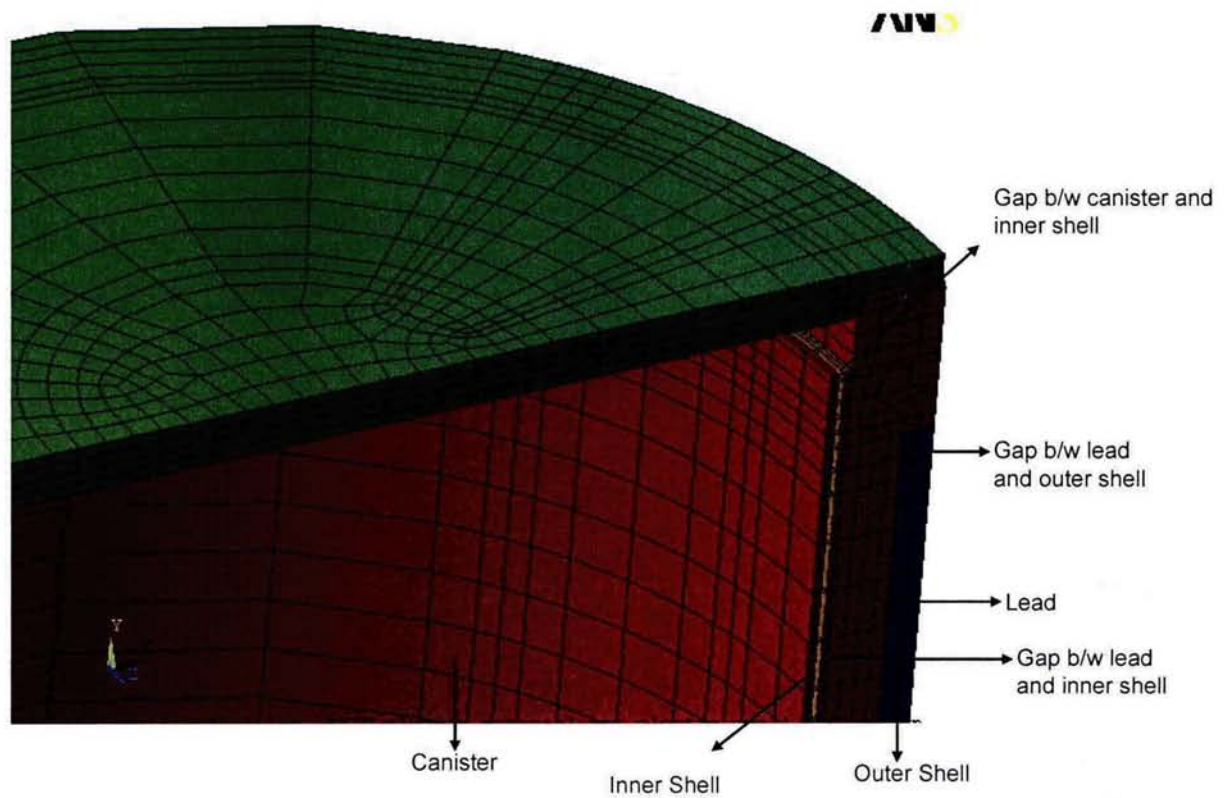


Figure 3.9.2-14
Canister/Cask Top Cover/Flange/CONTAC52 Element Representation

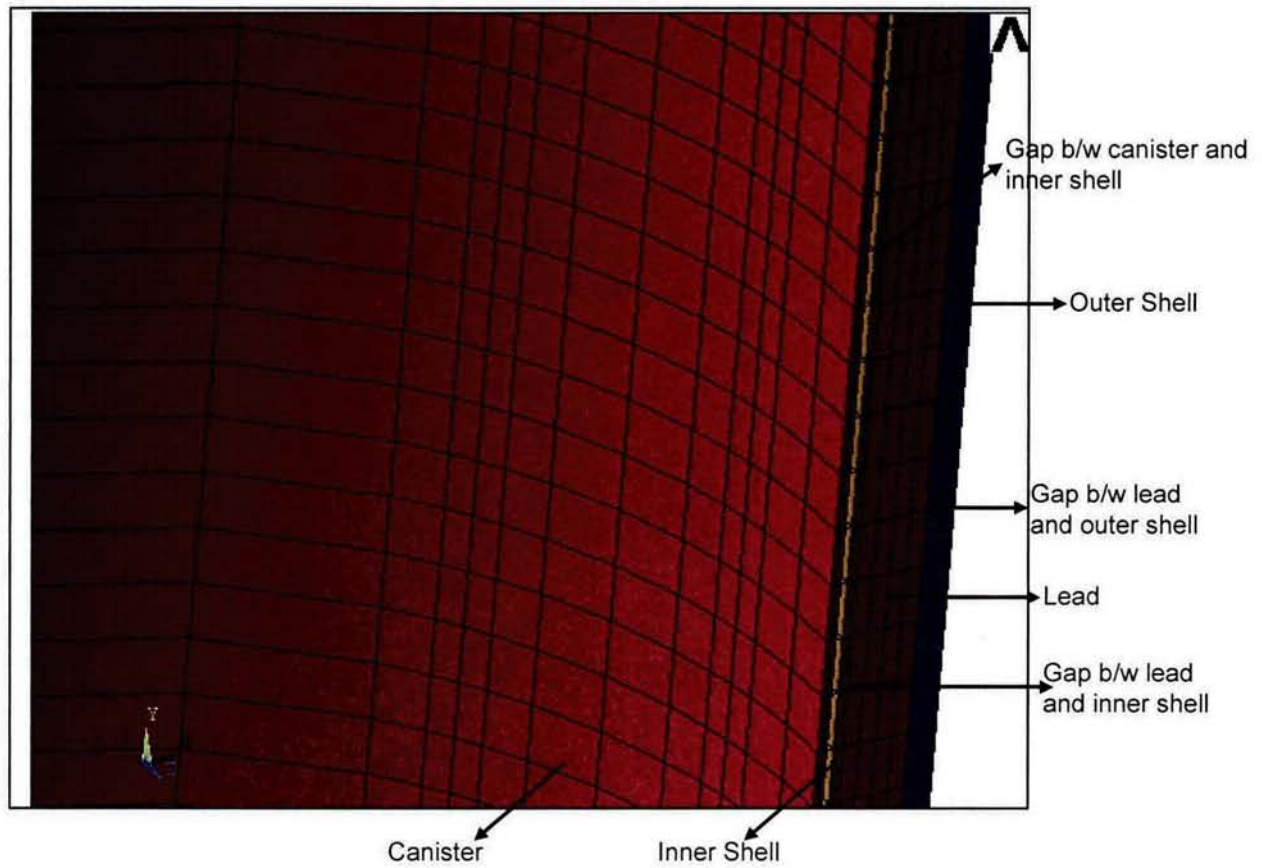


Figure 3.9.2-15
Canister/ Cask Shell /Lead /CONTAC52 Element Representation

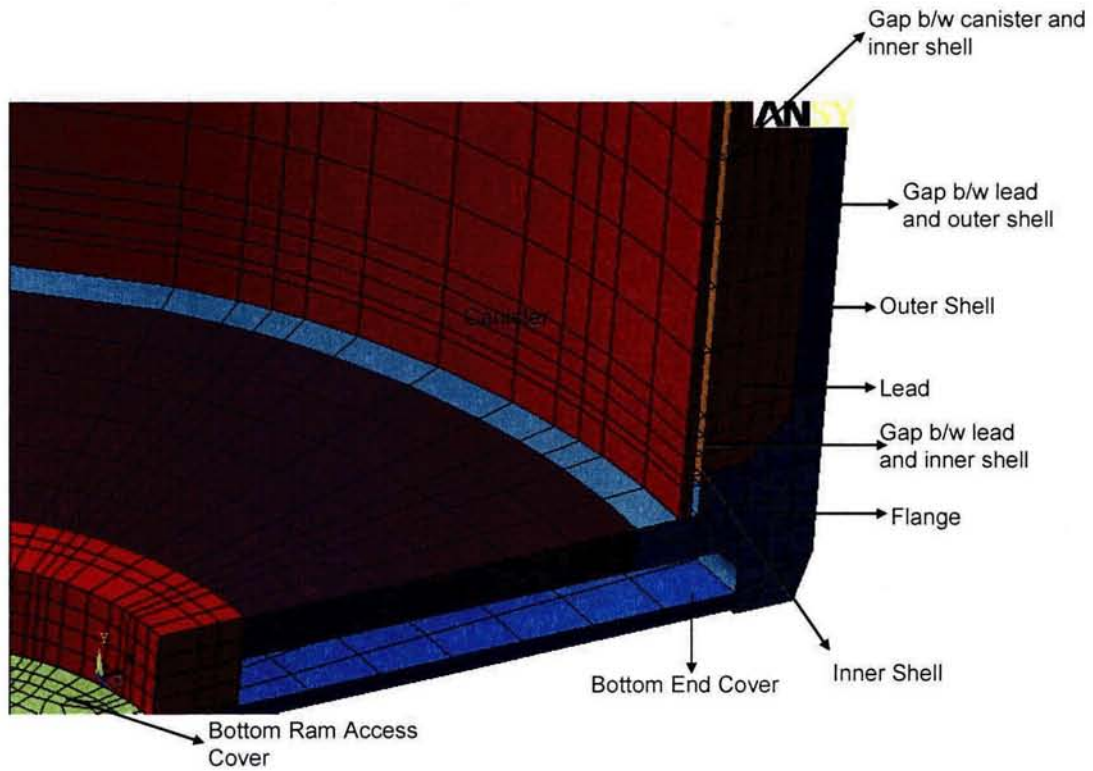


Figure 3.9.2-16

Canister/ Cask Bottom Access/Shell/ Flange/ Lead /CONTAC52 Element Representation

APPENDIX 3.9.3 OS187H TRANSFER CASK TOP COVER AND RAM COVER BOLT ANALYSES

TABLE OF CONTENTS

3.9.3	OS187H TRANSFER CASK TOP COVER AND RAM COVER BOLT ANALYSES	3.9.3-1
3.9.3.1	Introduction.....	3.9.3-1
3.9.3.2	Top Cover Bolt Load Calculations	3.9.3-3
3.9.3.3	Top Cover Bolt Load Combinations.....	3.9.3-8
3.9.3.4	Top Cover Bolt Stress Calculations.....	3.9.3-10
3.9.3.5	Top Cover Bolt Analysis Results.....	3.9.3-13
3.9.3.6	Minimum Engagement Length for Top Cover Bolt and Flange.....	3.9.3-14
3.9.3.7	RAM Access Cover Bolt Calculations	3.9.3-16
3.9.3.8	RAM Access Cover Bolt Load Combinations.....	3.9.3-21
3.9.3.9	RAM Access Cover Bolt Stress Calculations.....	3.9.3-23
3.9.3.10	RAM Access Cover Bolt Analysis Results.....	3.9.3-26
3.9.3.11	Minimum Engagement Length for RAM Access Cover Bolt	3.9.3-27
3.9.3.12	Brittle Fracture Analysis of Top Cover Bolt.....	3.9.3-29
3.9.3.13	Conclusions.....	3.9.3-32
3.9.3.14	References.....	3.9.3-33

LIST OF TABLES

3.9.3-1	Design Parameters for Top Cover Bolt Analysis
3.9.3-2	Design Parameters for Ram Access Cover Bolt Analysis
3.9.3-3	Bolt Data
3.9.3-4	Allowable Stresses in Closure Bolts for Normal Conditions
3.9.3-5	Allowable Stresses in Closure Bolts for Hypothetical Accident Conditions

3.9.3.12 Brittle Fracture Analysis of Top Cover Bolt

The transfer cask and its attachment bolts are designed and fabricated per ASME Subsection NC Code [6]. The fracture toughness requirements for the bolting material are specified in Section NC-2332.3. This section indicates that in order to meet the fracture toughness requirements, a Charpy V-notch test shall be performed. The test shall be performed at or below the Lowest Service Metal Temperature, and all three specimens shall meet the requirements of Table NC-2332.3-1. The size of lid bolt is 1.5" diameter, based on Table NC-2332.3-1 the required C_v value is 25 mils (lateral expansions).

In addition to the above Charpy V-notch test, a brittle fracture evaluation is performed to demonstrate that the brittle fracture is not a concern for the lid bolts.

The lid bolt is fabricated from SA-540 Gr. B24 Cl. 1 and has the following material properties.

Material Grade	Yield Strength, ksi (Room Temperature)	Ultimate Tensile Strength, ksi (Room Temperature)
SA-540 Gr. B24 Cl. 1	150	165

In accordance with the ASME Code, Section II, Part A [7], the bar stocks of these materials are quenched and fully tempered (1000 – 1100°F or higher) to produce a strong and tough microstructure.

ASM Metal Handbook [8], Figure 26 (reproduced here in Figure 3.9.3-1) shows that a 4340 steel tempered at 1035°F for 1 ½ hours to produce a yield strength of 158 ksi exhibits a very low Charpy impact transition temperature (< -20°F) and an upper shelf energy of about 45 ft-lbs at -20°F.

Figure 31 (reproduced here in Figure 3.9.3-2) shows that a medium carbon low alloy steel tempered to a yield strength of 107 ksi (like SA-193, Grade B7) would have an upper shelf energy of about 52 ft-lbs and absorb about 48 ft-lbs at -20°F while material at a yield strength of 149 ksi (like SA-540 Gr. B24 Cl. 1) would have an upper shelf energy of 35 ft-lbs and absorb about 30 ft-lbs at -20°F.

The following table summarizes the equivalent impact energy of the SA-540 Gr. B24 Cl. 1 at -20°F and the Charpy values used for the brittle fracture evaluation.

3.9.3.14 References

1. Stress Analysis of Closure Bolts for Shipping Cask, NUREG/CR-6007, 1992.
2. American Society of Mechanical Engineers, ASME Boiler and Pressure Vessel Code, Section II, Part D, 1998 through 2000 addenda.
3. Helicoil Catalog, Heli-Coil 8-Pitch Inserts, Bulletin 913B.
4. Machinery Handbook, 21st Ed, Industrial Press, 1979.
5. Baumeister, T., Marks, L. S., *Standard Handbook for Mechanical Engineers*, 7th Edition, McGraw-Hill, 1967.
6. American Society of Mechanical Engineers, ASME Boiler and Pressure Vessel Code, Section III, Division 1, Subsection NC, 1998, through 2000 addenda.
7. American Society of Mechanical Engineers, ASME Boiler and Pressure Vessel Code, Section II, Part A, 1998, through 2000 addenda.
8. American Society for Metals (ASM) Metal Handbook (Volume 1), Notch Toughness of Steels Section, 9th Edition, 1978.
9. Singular Integral Equation (Bueckner) and Asymptotic Approximation (Benthem)
- 10 NUREG/CR-1815 "Recommendation for Protecting Against Failure by Brittle Fracture in Ferritic Steel Shipping Containers Up to Four Inches Thick" Lawrence Livermore National Laboratory, June 15, 1981.
11. American Society of Mechanical Engineers, ASME Boiler and Pressure Vessel Code, Section XI, 1989.
12. American Society of Mechanical Engineers, ASME Boiler and Pressure Vessel Code, Section V, Article 6, 1998 through 2000 addenda.

3.9.4.6 References

1. ANSYS User's Manual, Rev 6.0
2. American Society of Mechanical Engineers, ASME Boiler and Pressure Vessel Code, Section II, Part D and Section III, Subsection NB and Appendix F, 1998, through 2000 addenda.
3. Baumeister & Marks, Standard Handbook for Mechanical Engineers, 7th Edition.
4. An Assessment of Stress-Strain Data Suitable for Finite-Element Elastic-Plastic Analysis of Shipping Containers, NUREG/CR-0481.
5. A Survey of Strain Rate Effects for some Common Structural Materials Used in Radioactive Material Packaging and Transportation Systems, U.S. Energy Research and Development Administration, Battelle Columbus Laboratories, August 1976.
6. "Stress Analysis of Closure Bolts for Shipping Casks", NUREG/CR-6007, April 1992
7. ANSYS User's Manual, Rev 5.6

3.9.5.6.2 Handling Load Stresses

All four trunnions carry the axial and vertical loads while only one top trunnion and one bottom trunnion on the same side of the cask will carry the transverse load. The axial load is carried only by the bottom trunnions because the top trunnions rest on sliding supports.

A. DW (1g vertical) + 1g Axial

At the top and bottom trunnions the g-loads per trunnion are:

$$\begin{aligned} 1.0g \text{ (axial)} / 2 \text{ sides} / 1 \text{ set trunnions} &= 0.5g \text{ axial per bottom trunnion.} \\ 1.0g \text{ (vertical)} / 2 \text{ sides} / 2 \text{ set trunnions} &= 0.25g \text{ vertical per trunnion} \end{aligned}$$

The bottom trunnions have a larger inner diameter (8 inch diameter of material is removed to reduce the weight, see Figure 3.9.5-1) than the top trunnions (4 inch diameter, see Figure 3.9.5-2). Also, the bottom trunnions material has lower yield and ultimate strengths relative to the top trunnions, and therefore has lower allowable stresses. Thus, the bottom trunnions are critical with respect to stress generated by the handling load. The transfer loads are therefore analyzed only for the weaker bottom trunnions, which are shown in Figure 3.9.5-1.

The vector sum of 0.25g vertical and 0.5g axial = $[0.25^2 + 0.5^2]^{1/2} g = 0.559g$

Therefore, the lateral load at each bottom trunnion, F_1 , is,

$$F_1 = 250,000 \text{ lb} \times 0.559g = 139,750 \text{ lb.}$$

Stresses at Trunnion Section B-B (See Figure 3.9.5-1)

The cross-section Area, A_{B-B} , is,

$$A_{B-B} = \pi/4 (12^2 - 8^2) = 62.83 \text{ in}^2$$

Area Moment of Inertia, I_{B-B} , is,

$$I_{B-B} = \pi/64 (12^4 - 8^4) = 816.81 \text{ in}^4$$

Therefore, the bending moment, M_{B-B} , is,

$$M_{B-B} = 139,750 \text{ lb} \times (3.25 \text{ in.} / 2) = 227,100 \text{ in-lb.}$$

The maximum shear stress due to bending for a hollow circular section, τ_{\max} , is the following.

$$\tau_{\max} = 2F_1 / A_{B-B} = 2 \times 139,750 \text{ lb} / 62.83 \text{ in}^2 = 4,450 \text{ psi}$$

The maximum bending stress due to lateral load, σ_x , is,

$$\begin{aligned}\sigma_x &= (M_{B-B} / I_{B-B}) \times (H_{B-B} / 2) \\ &= (227,100 \text{ in-lb} / 816.61 \text{ in}^4) (12 \text{ in.} / 2) = 1,670 \text{ psi.}\end{aligned}$$

The stress intensity, $S.I.$, is then,

$$\begin{aligned}S.I. &= [(\sigma_x^2 + 4(\tau_{\max})^2)]^{0.5} = [1,670^2 + 4(4,450)^2]^{0.5} \\ &= 9,055 \text{ psi} < S_m\end{aligned}$$

The stress intensity, $S.I.$, calculated here is conservatively considered to be primary membrane stress, P_m , and is evaluated against its allowable stress, S_m , as per ASME B&PV Section III-NC [3].

$$S_m = 20,000 \text{ psi (for SA-182 Gr.F304 at } 300^\circ \text{ F)}$$

Stresses at Section C-C (See Figure 3.9.5-1)

Cross-section Area, A_{C-C} , is,

$$A_{C-C} = \pi/4 (17.15^2 - 8^2) = 180.74 \text{ in}^2.$$

Area Moment of Inertia, I_{C-C} , is,

$$I_{C-C} = \pi/64 (17.15^4 - 8^4) = 4,045 \text{ in}^4.$$

The bending moment, M_{C-C} , is then,

$$\begin{aligned}M_{C-C} &= F \times L_{C-C} \\ &= 139,750 \text{ lb} \times (8.75 \text{ in.} - 3.25 \text{ in.} / 2) = 995,720 \text{ in-lb.}\end{aligned}$$

The maximum shear stress due to bending for a hollow circular section, τ_{\max} , is the following.

$$\tau_{\max} = 2 F / A_{C-C} = 2 \times 139,750 \text{ lb} / 180.74 \text{ in}^2 = 1,550 \text{ psi.}$$

The maximum bending stress due to lateral load, σ_x , is,

$$\begin{aligned}\sigma_x &= (M_{C-C} / I_{C-C}) \times (H_{C-C} / 2) + F_a / A_{C-C} \\ &= (995,720 \text{ in-lb} / 4,045 \text{ in}^4) (17.15 \text{ in.} / 2) = 2,111 \text{ psi}\end{aligned}$$

The stress intensity, $S.I.$, is,

$$\begin{aligned}S.I. &= [(\sigma_x^2 + 4(\tau_{\max})^2)]^{0.5} \\ &= [2,111^2 + 4(1,550)^2]^{0.5} = 3,751 \text{ psi} < S_m\end{aligned}$$

D. DW + 0.5g Axial + 0.5g Vertical + 0.5g Transverse

At the top and bottom trunnions the g-loads per trunnion are:

$$\begin{aligned} 0.5g \text{ (axial)} / 2 \text{ sides} / 1 \text{ set trunnions} &= 0.25g \text{ axial per trunnion} \\ 0.5g \text{ (transverse)} / 1 \text{ side} / 2 \text{ set trunnions} &= 0.25g \text{ transverse per trunnion} \\ 1.5g \text{ (vertical)} / 2 \text{ sides} / 2 \text{ set trunnions} &= 0.375g \text{ vertical per trunnion} \end{aligned}$$

The vector sum of 0.375g vertical and 0.125g axial = $[0.375^2 + 0.25^2]^{1/2} g = 0.451g$

Lateral Load at each bottom trunnion, F_1 , is,

$$F_1 = 250,000\text{lb} \times 0.451g = 112,750 \text{ lb}$$

Transverse Load at bottom trunnion, F_2 , is,

$$F_2 = 250,000\text{lb} \times 0.25g = 62,500 \text{ lb}$$

Where, the load, F_2 , acts as an axial load on the bottom trunnion.

Stresses at trunnion Section B-B (See Figure 3.9.5-1)

The bending moment, M_{B-B} , is,

$$M_{B-B} = 112,750 \text{ lb} \times (3.25 \text{ in.} / 2) = 183,219 \text{ in-lb.}$$

The maximum shear stress due to bending for a hollow circular section, τ_{\max} , is the following.

$$\tau_{\max} = 2F_1 / A_{B-B} = 2 \times 112,750 \text{ lb} / 62.83 \text{ in}^2 = 3,590 \text{ psi.}$$

The maximum normal stress, σ_x , is,

$$\begin{aligned} \sigma_x &= \text{max. bending stress due to lateral } (F_1) \text{ load} + \text{normal stress due to } F_2 \text{ load} \\ &= (M_{B-B} / I_{B-B}) \times (H_{B-B} / 2) + F_2 / A_{B-B} \\ &= (183,219 \text{ in-lb} / 816.61 \text{ in}^4) (12 \text{ in.} / 2) + 62,500 \text{ lb} / 62.83 \text{ in}^2 \\ &= 1,347 + 995 = 2,342 \text{ psi.} \end{aligned}$$

The stress intensity, $S.I.$, is,

$$\begin{aligned} S.I. &= [(\sigma_x^2 + 4(\tau_{\max})^2)]^{0.5} = [2,342^2 + 4(3,590)^2]^{0.5} \\ &= 7,553 \text{ psi.} < S_m \end{aligned}$$

Stresses at Section C-C (See Figure 3.9.5-1)

The bending moment, M_{C-C} , is,

$$\begin{aligned} M_{C-C} &= F_1 \times L_{C-C} \\ &= 112,750 \text{ lb} \times (8.75 \text{ in.} - 3.25 \text{ in.} / 2) = 803,344 \text{ in-lb.} \end{aligned}$$

The maximum shear stress due to bending for a hollow circular section, τ_{\max} , is the following.

$$\tau_{\max} = 2F_1 / A_{C-C} = 2 \times 112,750 \text{ lb} / 180.74 \text{ in}^2 = 1,248 \text{ psi.}$$

The maximum normal stress, σ_x , is,

$$\begin{aligned} \sigma_x &= \text{max. bending stress due to lateral load} + \text{normal stress due to axial load} \\ &= (M_{C-C} / I_{C-C}) \times (H_{C-C} / 2) + F_2 / A_{C-C} \\ &= (803,344 \text{ in-lb} / 4,045 \text{ in}^4) (17.15 \text{ in.} / 2) + 62,500 \text{ lb} / 180.74 \text{ in}^2 \\ &= 1,703 + 346 = 2,050 \text{ psi.} \end{aligned}$$

The stress intensity, $S.I.$, is,

$$\begin{aligned} S.I. &= [(\sigma_x^2 + 4(\tau_{\max})^2)]^{0.5} \\ &= [2,050^2 + 4(1,248)^2]^{0.5} = 3,230 \text{ psi.} < S_m \end{aligned}$$

3.9.5.9 References

1. "Special Lifting Devices for Shipping Containers Weighing 10,000 Pounds or More", ANSI N14.6, 1993.
2. American Society of Mechanical Engineers, ASME Boiler and Pressure Vessel Code, Section II, Part D, 1998, through 2000 addenda.
3. American Society of Mechanical Engineers, ASME Boiler and Pressure Vessel Code, Section III, Division 1, Subsection NC, 1998, through 2000 addenda.

Table 3.9.5-1
Summary of Computed and Allowable Trunnion Stresses

Case Number	Load	Maximum Stress		Allowable (ksi)
		Type	Magnitude (ksi)	
1	Lifting 6g	Shear	19.9	43.3 ⁽²⁾
		Tensile	29.8	43.3 ⁽²⁾
2	Lifting ⁽¹⁾ 10g	Shear	33.2	94.2 ⁽⁴⁾
		Tensile	49.6	94.2 ⁽⁴⁾
3	Handling DW + 1.0g Axial	P_m	9.1	20.0 ⁽³⁾
		$P_m + P_b$	9.1	20.0 ⁽³⁾
4	Handling DW + 1.0g Vertical	P_m	8.1	20.0 ⁽³⁾
		$P_m + P_b$	8.1	20.0 ⁽³⁾
5	Handling DW + 1.0g Transverse	P_m	4.8	20.0 ⁽³⁾
		$P_m + P_b$	4.8	20.0 ⁽³⁾
6	Handling DW + 0.5g Axial + 0.5g Vertical + 0.5g Transverse	P_m	7.6	20.0 ⁽³⁾
		$P_m + P_b$	7.6	20.0 ⁽³⁾

Notes:

- (1) Stresses in the trunnions are obtained by direct ratio from 6g load.
(2) Yield stress, S_y , for top trunnion material SA-182-FXM19 at 300° F per ANSI N14.6 [1] criterion.
(3) Design Stress Intensity, S_m , for bottom trunnion material SA-182-F304 at 300° F per ASME Section III-NC [3] criterion. Conservatively, $P_m + P_b$ is compared with S_m .
(4) Ultimate stress, S_u , for trunnion material SA-182-FXM19 at 300° F per ANSI N14.6 [1] criterion.

LIST OF TABLES

- 3.9.6-1 Summary of Calculated and Allowable Neutron Shield Shell Stresses

LIST OF FIGURES

- 3.9.6-1 Neutron Shield Shell Finite Element Model
- 3.9.6-2 Neutron Shield Shell Finite Element Model, Top Plate Region
- 3.9.6-3 Neutron Shield Shell Finite Element Model, Bottom Plate Region
- 3.9.6-4 Neutron Shield Shell Finite Element Model, 3g Lifting Boundary Conditions
- 3.9.6-5 3g Lifting Stress Intensity Distribution
- 3.9.6-6 Neutron Shield Shell Finite Element Model, Transfer Loads Boundary Conditions
- 3.9.6-7 Transfer Loads Stress Intensity Distribution
- 3.9.6-8 Cold Ambient Environment Temperature Distribution
- 3.9.6-9 Hot Ambient Environment Temperature Distribution
- 4.9.6-10 Transfer Loads plus Cold Ambient Condition Stress Intensity Distribution
- 4.9.6-11 Transfer Loads plus Hot Ambient Condition Stress Intensity Distribution

3.9.6.8 References

1. American Society of Mechanical Engineers, ASME Boiler and Pressure Vessel Code, Section II, Part D, 1998, through 2000 addenda. |
2. American Society of Mechanical Engineers, ASME Boiler and Pressure Vessel Code, Section III, Division 1, Subsection NC, 1998, through 2000 addenda. |

LIST OF TABLES

- 3.9.7-1 Spreadsheet for 80 inch Side Drop Impact Load Calculations (Using Non-Linear S vs. g relationship)
- 3.9.7-2 C. G. Over Corner Drop – L Calculations
- 3.9.7-3 C. G. Over Corner Drop – Area Calculations
- 3.9.7-4 C. G. Over Corner Drop – Energy Calculations

LIST OF FIGURES

- 3.9.7-1 Force vs. Displacement – End Drop (see Reference 1, Figure 14)
- 3.9.7-2 S vs. g Curve for 80 inch Height Side Drop
- 3.9.7-3 Geometry of C. G. Over Corner Drop
- 3.9.7-4 Geometry of C. G. Over Corner Drop
- 3.9.7-5 Geometry of the C. G. Over Corner Drop – Area Calculation
- 3.9.7-6 C. G. Over Corner Drop – L Dimension Calculation

The area of the impact surface is obtained by first writing the equation for the intersection curves between the cylinder and plane surfaces. We set up the following coordinate systems with the origin at the bottom center of the cask.

By transforming coordinates:

$$\begin{aligned}\alpha &= x \sin \theta + z \cos \theta & x &= \alpha \sin \theta - \beta \cos \theta \\ \beta &= -x \cos \theta + z \sin \theta & z &= \alpha \cos \theta + \beta \sin \theta\end{aligned}$$

The equation for a cylinder is,

$$x^2 + y^2 = R^2$$

Or by transforming coordinates,

$$\alpha^2 \sin^2 \theta - 2\alpha\beta \sin \theta \cos \theta + \beta^2 \cos^2 \theta + y^2 = R^2$$

By setting the intersection of this surface with target surface, $\beta = \Delta CL$, the equation of the intersection curve becomes the following.

$$\alpha^2 \sin^2 \theta - 2\Delta CL \sin \theta \cos \theta + \Delta CL^2 \cos^2 \theta + y^2 = R^2$$

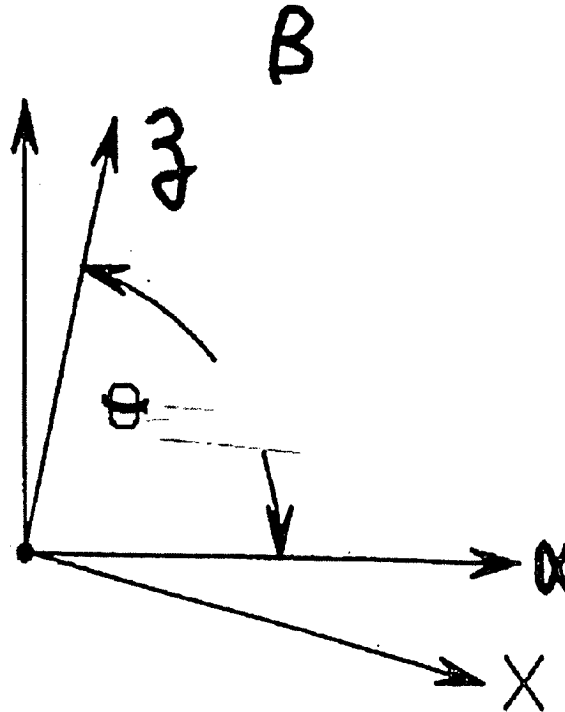


Figure 3.9.7-4
Geometry of C. G. Over Corner Drop

The area, A , as a function of the deformation is calculated by integrating the following.

$$\alpha^2 \sin^2 \theta - 2\alpha \Delta CL \sin \theta \cos \theta + \Delta CL^2 \cos^2 \theta + y^2 = R^2$$

$$A = 2 \int_{\alpha \min}^{\alpha \max} y d\alpha$$

Where y is given in above equation.

This is numerically integrated using 100 divisions and the trapezoidal rule. The results are tabulated in Table 3.9.7-4.

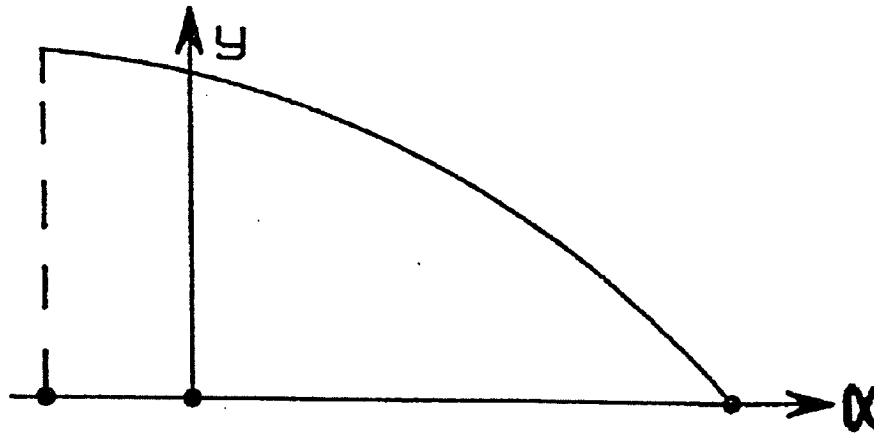


Figure 3.9.7-5
Geometry of the C. G. Over Corner Drop - Area Calculation

APPENDIX 3.9.8
DAMAGED FUEL CLADDING STRUCTURAL EVALUATION

TABLE OF CONTENTS

3.9.8	DAMAGED FUEL CLADDING STRUCTURAL EVALUATION	3.9.8-1
3.9.8.1	Introduction.....	3.9.8-1
3.9.8.2	Design Input / Data	3.9.8-2
3.9.8.3	Loads.....	3.9.8-3
3.9.8.4	Evaluation Criteria	3.9.8-5
3.9.8.5	Evaluation Methodology.....	3.9.8-6
3.9.8.6	Trailer Acceleration from 0 mph to 5 mph during Transfer	3.9.8-8
3.9.8.7	Trailer Deceleration from 0 mph to 5 mph during Transfer	3.9.8-11
3.9.8.8	Normal Loading Condition during Insertion/Retrieval of DSC into/from HSM.....	3.9.8-13
3.9.8.9	Off-Normal Jammed Canister Loading during Insertion of DSC into HSM	3.9.8-14
3.9.8.10	One Foot End Drop Damaged Fuel Evaluation	3.9.8-15
3.9.8.11	One Foot Side Drop Damaged Fuel Evaluation	3.9.8-16
3.9.8.12	Conclusions.....	3.9.8-20
3.9.8.13	Derivation of Fuel Assembly Material Properties	3.9.8-21
3.9.8.14	DELETED.....	6.9.8-24
3.9.8.15	References.....	6.9.8-29

LIST OF TABLES

3.9.8-1	WE and WES 15x15 - K_I Calculation using Fracture Geometry #2	
3.9.8-2	WE 17x17 - K_I Calculation using Fracture Geometry #2	
3.9.8-3	MK BW 17x17 - K_I Calculation using Fracture Geometry #2	
3.9.8-4	WEV 17x17 - K_I Calculation using Fracture Geometry #2	
3.9.8-5	WEO 17x17 - K_I Calculation using Fracture Geometry #2	
3.9.8-6	CE 14x14 - K_I Calculation using Fracture Geometry #2	
3.9.8-7	Summary - Maximum Fuel Rod Stresses and Stress Ratios	
3.9.8-8	Summary - Computed Fuel Tube Stress Intensity Factors and Ratios	
3.9.8-9	Derivation of Tensile Force (T) and Applied Moment (M) Relationship for a Circular Tube	
3.9.8-10	Tire Stiffness Calculation	

LIST OF FIGURES

3.9.8-1	Fracture Geometry #1: Ruptured Section	
3.9.8-2	Fracture Geometry #2: Through-Wall Circumferential Crack in Cylinder Under Bending	
3.9.8-3	Stress Intensity Factor Solutions For Several Specimen Configurations	
3.9.8-4	Temperature Vs Tensile and Yield Strength for Low Burn up Fuel	
3.9.8-5	Temperature Vs Tensile and Yield Strength for High Burn up Fuel	

Reference 15 reports a $K_{IC} = 35 \text{ ksi in}^{1/2}$ at approximately 300°F which is greater than highest computed stress intensity factor, K_I of 24.2 ksi in^{1/2} presented in the above table.

Therefore, the structural integrity of the damaged fuel rods, which are conservatively assumed to rupture as shown in Figure 3.9.8-1, will be maintained.

3.9.8.11.2 Structural Integrity Evaluation with Fracture Geometry #2

This geometry is shown in Figure 3.9.8-2. Stress intensity factors are computed for a crack in a fuel tube subjected to a uniform bending moment (M) using formulas given in "The Stress Analysis of Cracks Handbook" [13]:

$$K_I = \sigma (\pi R_m \theta)^{1/2} F(\theta)$$

where,

$$F(\theta) = 1 + 6.8*(\theta/\pi)^{3/2} - 13.6*(\theta/\pi)^{5/2} + 20.0*(\theta/\pi)^{7/2}$$

σ = Bending Stress due to Uniform Moment 'M'

R_m = Average radius of the fuel tube

2θ = Angle which the crack makes at the center of the tube

K_I = Stress Intensity Factor at the crack

The K_I is computed for all the different fuel assemblies, and the results for all the fuel assemblies are presented in Table 3.9.8-1, 3.9.8-2, 3.9.8-3, 3.9.8-4 and 3.9.8-5.

Based on the computed K_I using Fracture Geometries #1 & #2, a summary of the comparisons is presented as follows:

	Fracture Geometry #1 K_I	Fracture Geometry #2 K_I
WE & WES 15x15	24.2	33.8
WE 17x17	21.3	29.9
MK BW 17x17	19.9	28.0
WEV 17x17	21.3	29.9
WEO 17x17	22.6	31.8
CE 14x14	8.8	12.4

3.9.8.13 Derivation of Fuel Assembly Material Properties

Material property for low burnup fuel

The material properties used for the fuel cladding structural analysis is based on the LLNL report "Dynamic Impact Effects on Spent Fuel Assemblies" [3] and is for low burnup fuel. The material properties used for the drop analysis at elevated temperature are obtained from the following methodology.

Yield Strength of cladding: The yield stress vs. temperature is taken from Table 5 of [3, page 12] and is depicted in Figure 3.9.8-4. Since the relation between the yield strength vs. temperature is linear, the yield strength at higher temperature is obtained by extending the curve.

$$S_y = 81,500 \text{ psi (725}^\circ\text{F)}$$

$$S_y = 80,500 \text{ psi (750}^\circ\text{F)}$$

Tensile Strength of cladding: The tensile strength corresponding to the yield strength at the temperatures is obtained from Figure 5 of [3, page 17] and is also depicted in Figure 3.9.8-4.

$$S_u = 92,000 \text{ psi (725}^\circ\text{F)}$$

$$S_u = 91,800 \text{ psi (750}^\circ\text{F)}$$

Material property for high burnup fuel

Information Withheld Under 10 CFR 2.390

3.9.8.15 References

1. Transnuclear Calculation No. NUH24PTH.0209 Rev. 0, "NUHOMS® 24PTH Damaged Fuel Cladding Structural Evaluation to Demonstrate the Retrievability of the Fuel Subject to Normal and Off-Normal Loads".
2. Transnuclear, Inc., "Design Criteria Document (DCD) for the NUHOMS®-32PTH System for Transportation and Storage," NUH32PTH.0101, Revision 0.
3. UCID – 21246, "Dynamic Impact Effects on Spent Fuel Assemblies," Lawrence Livermore National Laboratory, October 20, 1987.
4. Transnuclear Calculation No. 10494-6, Rev. 0, "NUHOMS-32PTH DSC, Transfer Cask, and 'Under Hook' Nominal Weight Calculation".
5. ANSI N14.23, "Draft American National Standard Design Basis for Resistance to Shock and Vibration of Radioactive Material Packages Greater than One Ton in Truck Transport", May 1980.
6. NRC -12, SAND76-0427, NUREG766510, "Shock and Vibration Environments for Large Shipping Containers on Rail Cars and Trucks", June 1977.
7. Updated Final Safety Analysis Report, Standardized NUHOMS® Horizontal Modular Storage System for Irradiated Nuclear Fuel, Revision 9, Feb. 2006.
8. Transnuclear, Inc., "Technical Specification for the NUHOMS® 10' - 6" Wide Cask Transfer Trailer," Report No. NUH-07-106, Revision 5.
9. Baumeister, T., "Mark's Standard Handbook for Mechanical Engineers," McGraw-Hill Book Company, 8th Edition.
10. Transnuclear Calculation No. 10494-20, Rev. 1, "NUHOMS-32PTH Thermal Analysis of DSC in the HSM for Normal, Off-Normal, and Accident Storage Conditions".
11. Transnuclear Calculation No. 10494-46, Rev. 0, "NUHOMS-32PTH Thermal Expansions".
12. OCRWM Database, "Characteristics of spent fuel, high level waste, and other radioactive wastes which may require long term isolation" Appendix 2A, Volume 3 of 6, DOE/RW-0184, December 1987.
13. "The Stress Analysis of Cracks Handbook" Third Edition by Hiroshi Tada et al., ASME Press 2000.
14. R.W. Hertzberg, "Deformation and Fracture Mechanics of Engineering Material" John Wiley & Sons, New York, 1976.

Table 3.9.8-9 (concluded)

Derivation of Tensile Force (T) and Applied Moment (M) Relationship for a Circular Tube

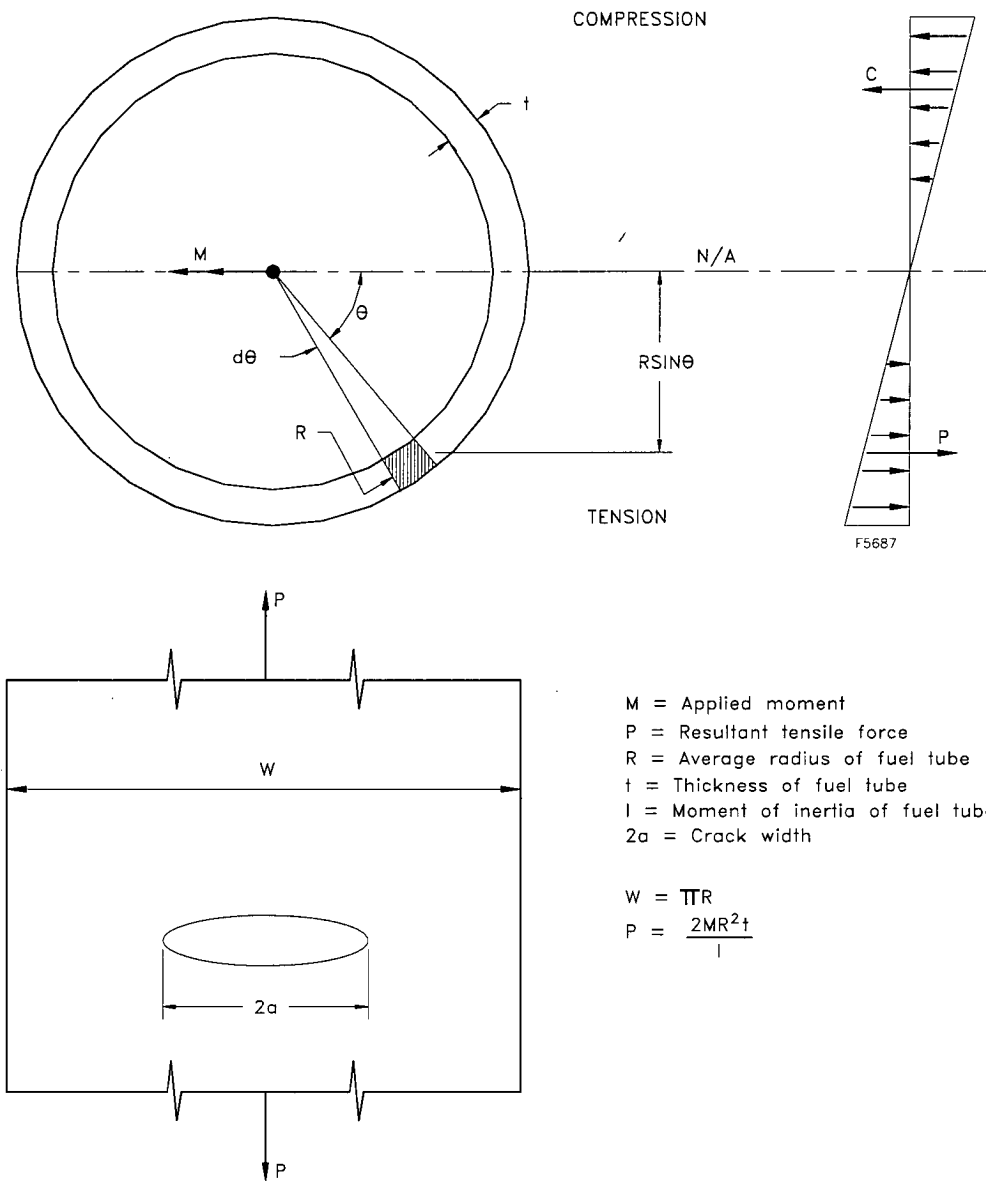


Table 3.9.8-10 (concluded)**Tire Stiffness Calculation**

All other tires: 2070 lbs/tire

Stiffness is determined as:

$$K_{\text{front}} = 3670 / (33 - 30.4) = 1411 \text{ lbs/in}$$

$$K_{\text{all others}} = 2070 / (33 - 31.4) = 1294 \text{ lbs/in}$$

Use $K/\text{tire} = 1500 \text{ lbs/inch}$.

$$\text{Total stiffness} = 32 \times 1500 = 4.8 \times 10^4 \text{ lbs/in}$$

LIST OF TABLES

3.9.9-1	Summary of HSM-H Component Design Loadings	
3.9.9-2	Summary of 32PTH DSC Support Structure Design Loadings	
3.9.9-3	HSM-H Concrete Load Combinations	
3.9.9-4	Ultimate Capacities of Concrete Components	
3.9.9-5	Structural Design Criteria for DSC Support structure	
3.9.9-6	HSM-H Support Steel Structure Load Combinations	
3.9.9-7	Design Pressure for Tornado Wind Loading	
3.9.9-8	Maximum HSM-H Concrete Component Forces and Moments for Normal & Off-Normal Loads	
3.9.9-9	Summary of Thermal Forces and Moments in the HSM-H Concrete Components	
3.9.9-10	Maximum HSM-H Concrete Component Forces and Moments for Accident Loads	
3.9.9-11	Comparison of Highest Combined Shear Forces/Moments with the Capacities	
3.9.9-12	Maximum/Minimum Forces/Moments in the Rail Components in the Local System	
3.9.9-13	Maximum/Minimum Forces/Moments in the Rail Extension Plates in the Local System	
3.9.9-14	Maximum/Minimum Axial Forces in the Cross member Components	
3.9.9-15	Rail Component Results	
3.9.9-16	Extension Plates and Cross Members Results	

3.9.9 HSM-H STRUCTURAL ANALYSIS

3.9.9.1 Introduction

The purpose of this appendix is to present the structural evaluation of the HSM-H due to all applied loads during storage loading operations.

The design of the HSM-H for 32PTH DSC is the same as the HSM-H which is under NRC review as Amendment 8 to CoC 1004 for 24PTH DSC. Analyses performed for HSM-H with 24PTH DSC used bounding values to envelop both 24PTH DSC and 32PTH DSC.

The HSM-H module design for 32PTH canister is identical to the HSM-H design for 24PTH canister except the following modifications:

1. The module for the 32PTH canister is designed such that the center line of the loaded 32PTH canister is approximately four inches higher compared to that of the 24PTH canister.
2. The diameter of the door openings in the front and rear of the front wall are approximately four inches and two inches larger for the 32PTH canister compared to those of the 24PTH canister.
3. The transfer cask docking surface in the module for the 32PTH canister transfer cask is approximately half inch wider compared to the cask docking surface for the 24PTH canister transfer cask.
4. The diameters of the front inner circular steel plate and rear circular concrete block of the shielded door for the 32PTH canister are approximately four inches and two inches larger compared to those of the 24PTH canisters.
5. For the 32PTH design the spacers at the canister stop plate of the module will be provided similar to the 24PTH short cavity design.

Analyses performed for HSM-H with 24PTH DSC used bounding values to envelop both 24PTH DSC and 32PTH DSC. The structural evaluation provided in this appendix is identical as the information provided in Amendment 8 to CoC 1004 for 24PTH DSC. Amendment 8 reference sections are indicated in this appendix for cross reference.

3.9.9.2 General Description of the HSM-H

The HSM-H is a free standing reinforced concrete structure designed to provide environmental protection and radiological shielding for the 32PTH DSC. Each HSM-H provides a self contained modular structure for the storage of a 32PTH DSC containing up to 32 PWR spent fuel

assemblies. The HSM-H provides heat rejection from the spent fuel decay heat by a combination of radiation, conduction and convection. Schematic sketch of the HSM-H showing the different components is provided in Chapter 1, Figure 1-1. The drawings in Chapter 1, Section 1.5 provide the principal dimensions and design parameters of the HSM-H.

The HSM-H is a reinforced concrete structure comprised of a base unit, where the 32 PTH DSC is stored and a roof unit that serves to provide environmental protection and radiation shielding. These two units are assembled together to form a single module.

The HSM-H modules may be prefabricated off-site, then transported to the ISFSI site and installed on a reinforced concrete basemat. The HSM-H is placed next to, and in contact with, adjacent module(s) to form a continuous single or double row arrays.

The 32PTH DSC is supported inside the HSM-H by the DSC support structure. The DSC support structure (rail support assembly) is comprised of two rail sections, two slotted plates and two rail support plates. The rail support assembly provides support for the DSC during storage and act as a sliding surface during DSC insertion and retrieval.

The air inlet vents are extending through the front on both sides of the front wall. The front wall and the rear wall of the base unit provide support for the rails and the rail extension flanges. The roof unit rests on the front, rear and side walls of the base unit. The air outlet vents are provided in the roof unit.

The HSM-H front standard door is a composite door, which consists of a rectangular steel face plate at the front attached to a circular thick steel plate and a circular reinforced concrete block at the rear. The rectangular steel face plate of the door is attached to the front wall concrete using four bolts anchored through four embedments. The alternate circular door is similar to the standard door except that the front face is a circular steel plate. The circular steel plate of the door is attached to the front wall concrete by four clamps which are located at the 45° line in each quadrant of the door. The clamps consist of four "L" shaped clips which are bolted to the front wall concrete through four embedments. The door provides missile protection and shielding for the DSC.

The concrete door provides missile protection and shielding. End shield walls are provided at the ends of a module array to provide the required missile and shielding protection. Similarly, an additional shield wall is used at the rear of the module for single module rows.

The side heat shields (with fins) consist of three panels. Each panel consists of anodized aluminum fins mounted on the stainless steel base plates. The base plates are provided with aluminum backing plates on the surface facing the concrete. The alternate side heat shields are made of stainless steel and consist of four flat panels. The top louvered heat shield under the roof consists of six panels. Each panel has two aluminum mounting bars. Horizontal louvers are mounted on these bars. The alternate top heat shields are made of stainless steel and consist of two flat panels. The heat shields provide thermal protection for the HSM-H concrete.

During DSC insertion/retrieval operations, the transfer cask is docked with the HSM-H docking surface and mechanically secured to the embedment provided in the front wall. The embedments are equally spaced on either side of the HSM-H access opening.

The drawings in Chapter 1, Section 1.5 provide the principal dimensions and design parameters of the HSM-H. The dimension differences between the HSM-H to be used for storing the 32PTH canister and 24PTH canister are listed in the following tables.

TN drawing No. 10494-72-104 (for 32PTH data)

Dimension	HSM-H	
	System Type	
	For 32PTH Canister	For 24PTH Canister [13]
A	8' – 10"	8' – 6"
B	Ø 5' – 11 5/8"	Ø 5' – 9"
C	Ø 7' – 5"	Ø 7' – 1 1/2"

TN drawing No. 10494-72-107 (for 32PTH data)

Dimension	HSM-H	
	System Type	
	For 32PTH Canister	For 24PTH Canister [13]
A	34.88"	33.60"

TN drawing No. 10494-72-108 (for 32PTH data)

Dimension	HSM-H	
	System Type	
	For 32PTH Canister	For 24PTH Canister [13]
A	8' – 1 1/2"	7' – 3 3/4"
B	Ø 7' – 3"	Ø 6' – 11 1/2"
C	Ø 5' – 8 5/8"	Ø 5' – 6"
D	Ø 7' – 7 1/4"	Ø 7' – 3 3/4"
E	1' – 10 1/2"	1' – 10 1/2"

3.9.9.3 Material Properties

The temperature dependent material properties for concrete and reinforcing steel are provided in Chapter 3, Tables 3-6, 3-7 and 3-7A. The material properties of the Type 304 Stainless Steel rails are identical to the ASME Code properties listed in Chapter 3, Table 3-5.

3.9.9.5 Design Criteria

Codes and Standards

The reinforced concrete HSM-H, including the 32PTH-DSC support structures, are important to safety NUHOMS® HD system components. Consequently, they are designed and analyzed to perform their intended functions under the extreme environmental and natural phenomena specified in 10CFR 72.122 [1] and ANSI 57.9 [2]. These include tornado, wind, seismic, and flood design criteria.

The following table summarizes Codes and Standards for design and fabrication of these components.

Component	Code of Construction
HSM-H and 32PTH DSC Support Structures	<ul style="list-style-type: none"> - ACI 349-97 (Concrete); ACI 318-95 (construction) - AISC Ninth Edition (Structural Steel) - AWS D1.1-98 (Structural Welds) - ASCE 7-95 (Loads) - ANSI 57.9-84 (Loads & Load Combinations)

Loadings

The loadings are listed in Tables 3.9.9-1 & 3.9.9-2 and discussed in details in Section 3.9.9.6.

Loading Criteria

The ultimate strength method of ACI 349 [3] is used for the design of the HSM-H reinforced concrete structural components. Required reinforcement is provided to meet the minimum flexural and shear reinforcement requirements of ACI 349 and to ensure that the provided design strength exceeds that required for the factored design loads specified in Table 3.9.9-3.

The following relationships from the ACI code are used to compute capacities of the concrete components:

Ultimate Moment Capacity (M_u)

$$M_u = \phi M_n = \phi A_s f_y (d-a/2)$$

3.9.9.7 Finite Element Model

3.9.9.7.1 ANSYS Finite Element Model of the Rail Assembly

Description of the Rail Assembly

The HSM-H support structure consists of two rail assemblies, each at 30 degrees from the vertical center line of the DSC. Two welded cross members connect the two rail assemblies by four gusset plates welded to the rail web and flanges. The steel support structure supports the DSC stored inside the module. Each rail assembly of the DSC support structure consists of the following components:

1. W 12x96 Rail Section 187" long made from ASTM A992 material and with twelve (12) 6" diameter holes for airflow cooling of the DSC. The depth of the section is 12.71", thickness of the web is 0.55", width of the flange is 12.16" and thickness of the flange is 0.9" (Ref. 4).
2. A 1" thick slotted rail support plate made from A572 Grade 50 material with 1/2"x2" slots normal to the plate axis.
3. A 3/16" thick support plate made from Nitronic 60 (RC 29-35) material which provides a smooth support for the DSC to slide.
4. A rail extension baseplate which consists of 1" thick plate ASTM A36 material.

The rail extension baseplate is attached to 1-1/2" diameter threaded embedments by two bolts.

Finite Element Model of the Rail Assembly

A three dimensional finite element model of the rail section, slotted plate, rail support plate and rail extension flange was developed for the computer program ANSYS [10]. The rail sections, slotted plates, rail support plates and extension plates were modeled using SOLID 73 element. Each element has 8 nodes with six degrees of freedom (three translational and three rotational) per node. The web of the W section and the stiffeners were modeled using Shell 63 element. In order to establish compatibility of the degrees of freedom between solid and plate elements, the ANSYS option for activating realistic in-plane rotational stiffness (Allman rotational stiffness, KEYOPT(3)=2) is used for the plate elements. The model is inclined by 30 degrees from the vertical. A plot of the partial model (front end) is shown in Figure 3.9.9-1.

The model is completely restrained at the bottom end of the extension plate and supported vertically and transversely approximately 6" from the end to simulate the connection between the

extension plate and the front wall. The model also is supported in the vertical and transverse directions at approximately 12" on either side of the W section at the bottom flange (to simulate the simple support condition of the concrete pedestals at the front and rear walls).

Finite element analysis of the above rail assembly model was performed to compute the maximum displacements of the model, subjected to unit load normal to rail axis in and out of plane of the curb and in the axial direction. The equivalent beam element properties such as area (A), moment of inertia about the major axis (I_{x-x}) and moment of inertia about the minor axis (I_{y-y}) are determined by equating the maximum deflection of the beam to displacement obtained from the finite element model.

3.9.9.7.2 ANSYS Finite Element Model of the HSM-H Combined Concrete and Steel Structure for Structural Analysis

The structural analysis of an individual module provides a conservative estimate of the response of the HSM-H structural elements under various static and dynamic loads for any HSM-H array configuration. Therefore, analytical models of a single free standing HSM-H is developed in this section for the computer program ANSYS [10]. The frame and shear wall action of the HSM-H concrete components are considered to be the primary structural system resisting the loads. The analytical models are evaluated for normal operating, off-normal and postulated accident loads acting on the HSM-H.

A three dimensional finite element model of the HSM-H which includes all the concrete components (rear wall, front wall, two side walls and the roof) was developed for the computer program ANSYS [10]. The eight node brick element type SOLID 73 element was used to model the concrete structure. Four layers of brick elements were used to model the concrete components. Each node of the eight node brick element has six degrees of freedom. The DSC was modeled using the beam elements (ANSYS element type BEAM4). The rails and the lateral bracing between the rails (Cross beams) were also modeled using beam elements with appropriate stiffness. The mass of the DSC was lumped at the nodes representing the DSC using lumped mass elements (ANSYS element type MASS21). Plots of the model which includes the concrete structure and the support structure are shown in Figures 3.9.9-2. A plot of the support structure model (which includes the DSC, rails and the cross beams) is shown in Figure 3.9.9-3.

The material properties used in the DSC support structure model are provided in Chapter 3. The DSC support structure model is attached to the concrete at several locations (four locations at the rear shelf, four locations in the front shelf and two locations on the front wall opening.) Each node of the support structure has three translational and three rotational degrees of freedoms. The rails are supported such that they are completely restrained at the front extension plate locations and free to rotate in all three directions and free to translate only in axial direction at the other supports in the rear and the front shelf locations.

The DSC support structure analytical model is incorporated into the HSM-H analytical model. The various normal, off-normal and accident loads are applied to the analytical model and

3.9.9.8 Normal Operation Structural Analysis

The evaluation of the HSM-H for 32PTH DSC is the same as the HSM-H which is under NRC review as Amendment 8 to CoC 1004 for the 24PTH DSC [13]. Analyses performed for the HSM-H with 24PTH DSC used bounding values to envelop both the 24PTH DSC and the 32PTH DSC. The following table shows how the bounding loads are used for structural evaluation of the HSM-H.

	Weight	Thermal
24PTH DSC (loaded weight)	93.7 kips	40.8 kw
32PTH DSC (loaded weight)	108.76 kips	34.8 kw
Weight used for HSM-H structural evaluation to envelop both 24PTH & 32PTH	110.0 kips (max.) ⁽¹⁾ 72.0 kips (min.) ⁽²⁾	
Thermal load used for HSM-H structural evaluation to envelop both 24PTH & 32PTH		40.8 kw

Notes:

1. Maximum weight is used for structural evaluation of the HSM-H.
2. Minimum weight is used for stability evaluation of the HSM-H.

The following table shows the normal operating loads for which the HSM-H components are designed. The table also lists the individual NUHOMS® HSM-H components which are affected by each loading.

Load Type	Affected Component	
	DSC Support Structure	HSM-H
Dead Weight	X	X
Normal Thermal	X	X
Normal Handling	X	X
Live Loads		X

The reinforced concrete and the support steel structure of the HSM-H are analyzed for the normal, off-normal, and postulated accident conditions using finite element models described in Section 3.9.9.7. These models are used to evaluate concrete and support structure forces and moments due to dead load, live load, normal thermal loads, and normal handling loads. The methodology used to evaluate the effects of these normal loads is addressed in the following paragraphs.

(A) HSM-H Dead Load (DW) Analysis (Section P.3.6.1.4(A) from CoC 1004 Amendment #8)

Dead loads are applied to the analytical model by application of 1.05g where g is the gravitational acceleration in the vertical direction (386.4 in/sec²). The 5% variation in the dead

HSM-H Seismic Evaluation (Section P.3.7.2.3 from CoC 1004 Amendment #8)Seismic Loads (EQ)

As described in Section 3.9.9.6.3, the design basis accelerations for the HSM-H are 0.3g in the horizontal directions and 0.2g in the vertical direction. These seismic accelerations are amplified based on the results of the frequency analysis of the HSM-H, as documented in Section 3.9.9.6.3. The resulting amplified accelerations are 0.37g and 0.33g in the transverse and longitudinal directions, respectively and 0.20g in the vertical direction. For conservatism, a value of 0.37g is used for both horizontal directions in the seismic analysis of the HSM-H.

Seismic Stress Analysis

An equivalent static analysis of the HSM-H is performed using the ANSYS model described in Section 3.9.9.7 and the seismic accelerations of 0.37g horizontally (longitudinal and transverse directions) and 0.2g vertically. These amplified accelerations are determined based on the frequency analysis of the HSM-H.

The responses for each orthogonal direction are combined using the SRSS method. The seismic analysis results are shown in Table 3.9.9-10 and are incorporated in the loading combination C4C (Table 3.9.9-3) and C4S (Table 3.9.9-6) for the concrete and support structure components, respectively.

HSM-H Seismic Overturning Analysis

The following conservative analysis is performed to show that a single freestanding HSM-H without an end shield wall (in an array of two or more loaded modules) will not overturn due to seismic loads. Overturning about the long axis (i.e., in the short direction of the module) is considered.

$$\text{Stabilizing moment} = M_{st} = (W_{hsm} + W_{dsc}) b/2$$

$$\text{Overturning moment} = M_{ot} = (W_{hsm} 0.4a_{v1} + W_{dsc} 0.4a_{v2})b/2 + W_{hsm} d_1 a_{h1} + W_{dsc} d_2 a_{h2}$$

(100% of horizontal acceleration is combined with 40% of vertical acceleration, Ref. [11])

Where:	W_{hsm}	=	310 K, Weight of the HSM-H (conservatively assumed)
	W_{dsc}	=	110 K, Weight of DSC (conservatively assumed)
	$b/2$	=	52 in, Horizontal distance from CG to corner (half width of the HSM-H)
	d_1	=	123.45 in, Height of CG of HSM-H without the DSC
	d_2	=	106 in, Height of the DSC center line
	a_{v1}	=	0.20g, HSM-H peak vertical seismic acceleration
	a_{v2}	=	0.20g, DSC peak vertical seismic acceleration
	a_{h1}	=	0.37g, HSM-H peak horizontal seismic acceleration
	a_{h2}	=	0.43g, DSC peak horizontal seismic acceleration (conservatively assumed)
	M_{st}	=	21,840 K-in
	M_{ot}	=	20,921 K-in

HSM-H Heat Shield

The top heat shield (louvers) consists of six panels. Each panel has two aluminum mounting bars. The aluminum louvers are mounted on the mounting bars. Each mounting bar is suspended from the roof by two threaded rods. The natural lateral frequency of a typical rod is conservatively estimated to be 9.0 Hz. The combined axial and bending stress in the hanger rods is 24.0 ksi. The allowable axial and bending stress is 84.3 ksi.

The alternate top heat shield consists of two panels made of stainless steel plate. The panels are suspended from the roof by fifteen 1/2" diameter rods threaded into concrete embedments. The combined axial and bending stress in the rods is 59.5 ksi. The allowable stress is 70.2 ksi.

The side heat shields consists of three panels. Each panel is suspended from the roof by two threaded rods, and supported laterally and longitudinally by four rods. The maximum axial plus bending stress in the lateral and longitudinal support rods is 83.7 ksi. The allowable axial and bending stress is 84.3 ksi. The maximum temperature used in the stress analysis of the heat shields bounds the maximum temperatures reported in Chapter 4.

The alternate side heat shields consists of four panels, attached to the base unit side wall by 34 threaded rod stand-offs. The maximum axial and bending stress in the rods is about 1.4 ksi and 79.3 ksi, respectively. The axial and bending stress allowable for the rods is 67.9 ksi and 112.3 ksi, respectively.

HSM-H Seismic Retainers

The seismic retainer consists of a capped tube steel embedment located within the bottom center of the round access opening of the HSM-H, and a tube steel retainer that drops into the embedment cavity after DSC transfer is complete. The drop-in retainer extends approximately 4" above the rail to provide axial restraint of the DSC. The maximum seismically induced shear load in the retainer is 61 kips. The maximum shear stress in the retainer is 15.25 ksi. The allowable shear stress is 17.8 ksi.

3.9.9.12 Conclusions

The load categories associated with normal operating conditions, off-normal conditions and postulated accident conditions are described and analyzed in previous sections. The load combination results for HSM-H components important to safety are also presented. Comparison of the results with the corresponding design capacity shows that the design strength of the HSM-H is greater than the strength required for the most critical load combination.

3.9.9.13 References

1. Title 10, Code of Federal Regulations, Part 72 (10CFR72), "Licensing Requirements for the Storage of Spent Fuel in the Independent Spent Fuel Storage Installation," U.S. Nuclear Regulatory Commission, August 31, 1988.
2. ANSI/ANS 57.9-1984, "Design Criteria for an Independent Spent Fuel Storage Installation (Dry Storage Type)," American Nuclear Society.
3. "Code Requirements for Nuclear Safety Related Concrete Structures," ACI 349-97, American Concrete Institute, Detroit, MI.
4. "Manual of Steel Construction," American Institute of Steel Construction, Ninth Edition, 1989.
5. American Society of Civil Engineers, ASCE 7-95, "Minimum Design Loads for Buildings and Other Structures" (formerly ANSI A58.1).
6. "Design Basis Tornado for Nuclear Power Plants," Regulatory Guide 1.76, U.S. Atomic Energy Commission, April 1974.
7. "Missiles Generated by Natural Phenomenon," Standard Review Plan, NUREG-0800, U.S. Nuclear Regulatory Commission
8. Bechtel Topical Report, "Design of Structures for Missile Impact," BC-TOP-9-A, Revision 2, September 1974.
9. Regulatory Guide 1.60, "Design Response Spectra for Seismic Design of Nuclear Power Plants," U.S. Atomic Energy Commission, Revision 1, December 1973.
10. ANSYS Engineering Analysis System, Users Manual for ANSYS Rev. 5.6 and 7.0, Swanson Analysis Systems, Inc., Houston, PA.
11. "Structural Analysis and Design of Nuclear Plant Facilities," ASCE Publication No. 58.
12. Regulatory Guide 1.61, "Damping Values for Seismic Design of Nuclear Power Plants", U.S. Atomic Energy Commission, October 1973.
13. Amendment No. 8 to NUHOMS® CoC 1004, addition of 24PTH DSC to Standardized NUHOMS® System.
14. "Fluid Mechanics", Raymond C. Binder, 4th Edition, Prentice-Hall, Inc.
15. "Thermal testing of the NUHOMS® Horizontal Storage Module, Model HSM-H", Transnuclear Report No. E-21625, Rev 1

Table 3.9.9-11
Comparison of Highest Combined Shear Forces/Moments with the Capacities

Component	Load Comb. ⁽¹⁾	Quantity	V ₁ kips/ft	V ₀₁ kips/ft	V ₀₂ kips/ft	M ₁ kip-in/ft	M ₂ kip-in/ft
Rear Wall (Upper)	Comb 1c thru 6c	Computed	14.52	7.71	9.16	147.35	267.10
		Capacity	75.2	14.5	14.5	298.2	298.2
		Ratio	0.19	0.53	0.63	0.49	0.90
	Comb 7c	Computed	18.44	11.37	6.08	131.14	264.5
		Capacity	69.6	13.8	13.8	273.8	273.8
		Ratio	0.26	0.82	0.44	0.48	0.97
Rear Wall (Lower)	Comb 1c thru 6c	Computed	17.34	9.48	13.25	159.40	167.70
		Capacity	96.8	36.2	36.2	757.9	757.9
		Ratio	0.18	0.26	0.37	0.21	0.22
	Comb 7c	Computed	9.49	6.40	20.84	154.30	251.80
		Capacity	90.1	34.3	34.3	696.3	696.3
		Ratio	0.11	0.19	0.61	0.22	0.36
Side Walls (Upper)	Comb 1c thru 6c	Computed	18.92	12.05	13.19	177.76	163.10
		Capacity	54.4	14.8	14.8	196.9	196.9
		Ratio	0.35	0.82	0.89	0.90	0.83
	Comb 7c	Computed	22.37	12.08	9.10	120.24	91.05
		Capacity	50.5	14.0	14.0	180.8	180.8
		Ratio	0.44	0.86	0.265	0.67	0.50
Side Walls (Lower)	Comb 1c thru 6c	Computed	36.17	22.33	21.12	308.10	261.55
		Capacity	63.0	23.4	23.4	314.6	314.6
		Ratio	0.57	0.95	0.91	0.98	0.83
	Comb 7c	Computed	19.28	21.12	15.34	97.25	180.24
		Capacity	58.7	22.2	22.2	289.0	289.0
		Ratio	0.33	0.95	0.69	0.34	0.63
Roof	Comb 1c thru 6c	Computed	13.18	9.44	28.73	487.01	1022.49
		Capacity	174.6	59.1	59.10	2475.0	2375.0
		Ratio	0.08	0.16	0.49	0.21	0.43
	Comb 7c	Computed	7.69	11.48	28.38	386.48	897.67
		Capacity	162.4	56.1	56.10	2181.7	2181.70
		Ratio	0.05	0.21	0.51	0.18	0.41
Front Wall (Upper)	Comb 1c thru 6c	Computed	41.82	44.83	37.00	1393.19	1895.08
		Capacity	174.7	56.3	56.3	2257.3	2317.3
		Ratio	0.24	0.80	0.66	0.62	0.84
	Comb 7c	Computed	32.63	48.95	26.29	1853.0	1906.74
		Capacity	159.6	53.4	53.4	2073.5	2073.5
		Ratio	0.20	0.92	0.49	0.89	0.92
Front Wall (Lower)	Comb 1c thru 6c	Computed	29.29	30.43	37.83	1783.50	836.92
		Capacity	189.0	73.6	73.6	2963.4	2963.4
		Ratio	0.16	0.42	0.52	0.60	0.28
	Comb 7c	Computed	48.04	45.95	41.38	1908.90	507.22
		Capacity	176.0	69.8	69.8	2722.4	2722.4
		Ratio	0.27	0.66	0.59	0.70	0.19

Note:

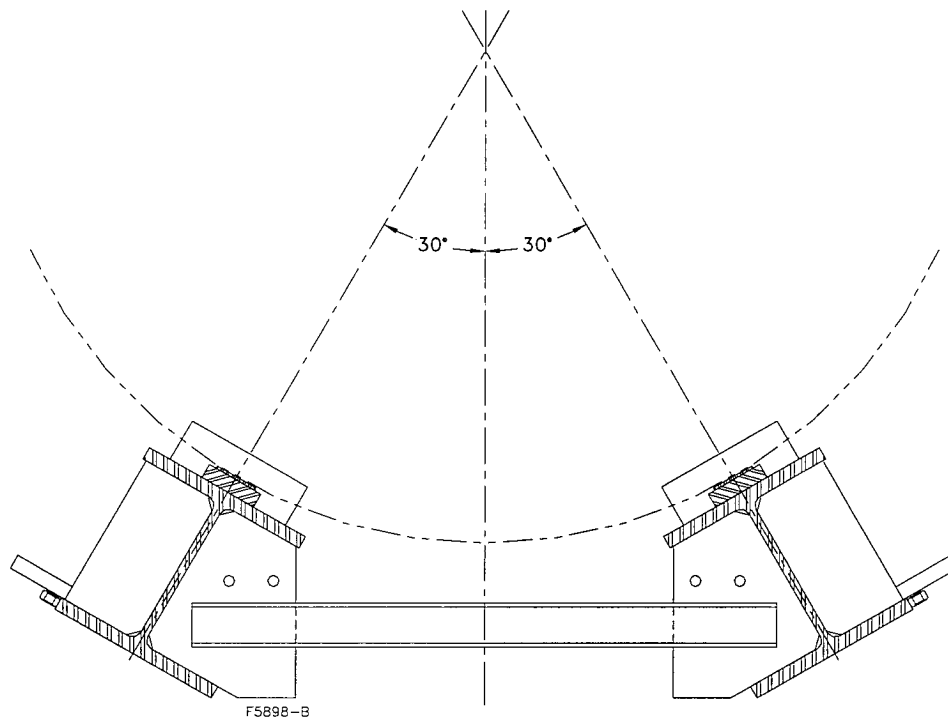
1. Comb 1c thru 6c includes normal thermal. Comb 7c includes accident thermal (see Table 3.9.9-3)

Table 3.9.9-16
Extension Plates and Cross Members Results

Load Comb.	Extension Plates Interaction Ratio⁽¹⁾	Cross Members Stress Ratio⁽²⁾
C1S	0.77	0.25
C2S	0.77	0.32
C3S	0.71	0.21
C4S	0.60	0.25
C5S	0.71	0.33

Notes:

- (1) Axial and bending stresses are computed using axial (F_x) and bending moment (M_y , M_z) results from Table 3.9.9-13. Interaction ratios are based on appropriate equations from Chapter H of AISC [4].
- (2) Axial stresses in the cross members are computed using axial (F_x) force results from Table 3.9.9-14. Cross member stress ratio is the axial stress in the member/axial allowable stress.



DSC SUPPORT STRUCTURE

Figure 3.9.9-6
Components of Support Structure

DSC (basket and canister) Material

The following material properties are used for the Dry Shielded Canister.

Stainless Steel (SA-240 Type 304)

$$E = 28.3 \times 10^6 \text{ psi}$$
$$\nu = 0.3$$

The density of the DSC is adjusted so that the actual weight of the DSC is properly accounted for. The effective density is computed in the following way.

$$\text{Weight of DSC} = \frac{1}{2} \times [28,191 \text{ lb (canister weight)} + 29,854 \text{ lb (basket weight)} + 50,720 \text{ lb (fuel weight)}] = 54,382.5 \text{ lb}$$

$$\text{Volume of F.E.M.} = 69,807.6 \text{ in}^3 \text{ (from ANSYS model)}$$

$$\rho_{\text{eff}} = 54,382.5 \text{ lb} / 69,807.6 \text{ in}^3 / (386.4 \text{ in/sec}^2) = 2.016 \times 10^{-3} \text{ lb-sec/in}^4$$

Concrete Material

The same concrete material properties used in the LLNL and TN-32 analyses, presented in Section 3.9.10.3, are also used for the OS187H transfer cask analysis. The concrete material properties used in the analysis are representative and do not constitute limits for the ISFSI Pad design or any other concrete which the loaded OS187H transfer cask is transported over. The OS187H transfer cask g-loads used for the stress evaluation given in the Table in Section 3.9.10.5 represent the limits that must be maintained for an 80 inch drop of the loaded OS187H transfer cask.

Soil Material

The same soil material properties used in the LLNL and TN-32 analyses, presented in Section 3.9.10.3, are also used for the OS187H transfer cask analysis. The soil material properties used in the analysis are representative and do not constitute limits for the ISFSI Pad design or any other concrete which the loaded OS187H transfer cask is transported over. The OS187H transfer cask g-loads used for the stress evaluation given in the Table in Section 3.9.10.5 represent the limits that must be maintained for an 80 inch drop of the loaded OS187H transfer cask.

Boundary Conditions

A 1/2 model is employed with symmetry boundary conditions used to simulate the full structure. Non-reflecting boundaries are used around the soil non-symmetry boundaries (bottom, left side, right side, and back) to prevent artificial stress waves from reflecting from the boundaries of the soil. Both dilatation and shear waves are damped as described in the LS-DYNA *BOUNDARY command [1].

Contact boundaries between the cask and DSC, cask and lead, cask and concrete, and concrete

and soil are modeled using surface-to surface contact elements in LS-DYNA. These contacts are defined using part numbers defined by the ANSYS macro that transfers the ANSYS finite element to the LS-DYNA model. A description of the LS-DYNA surface-to-surface contact elements are provided in Reference [1].

Damping Factor

As described in the above LLNL and TN-32 impact analyses (Section 3.9.10.3), the true damping characteristics of the cask impact event are very hard to quantify. Typical values for reinforced concrete structures subjected to dynamic loads are in the 5 to 10% range. A 6% damping factor is used for the LLNL and TN-32 impact analyses, for conservatism a lower bound damping factor of 5% is used for OS187H transfer cask impact analysis.

OS187H Transfer Cask Model LS-DYNA Impact Analysis

Two accident condition drop scenarios are evaluated which are considered to bound all credible transfer cask drops during fuel transfer:

- 80 inch, 0° side drop, and
- 80 inch, 60° CG over corner drop

The cask outer surface is initially placed in contact with the concrete pad, and an initial velocity is applied to the cask, lead, and DSC, to simulate the non-mechanistic drop events. The initial velocity is computed by equating potential and kinetic energies.

$$V = \text{potential energy} = mgh$$

$$T = \text{kinetic energy} = \frac{1}{2}mv^2$$

$$\Rightarrow mgh = \frac{1}{2}mv^2$$

$$\Rightarrow v = \sqrt{2gh} = \sqrt{2(386.4)(80)} = 248.644 \text{ in /sec}$$

With the above model, boundary conditions and initial conditions, the LS-DYNA program was run from $t_0 = 0$ seconds to $t_f = 0.04$ seconds for both the Side Drop and the C.G. Over Corner Drop runs. The time step was automatically chosen by the LS-DYNA program based on the minimum model element sizes.

Transfer Cask Sections Evaluated

The resulting nodal acceleration time histories, computed in the drop direction by LS-DYNA, are averaged over several cross sections of the transfer cask. For the side drop analysis, only the accelerations transverse to the transfer cask axis are computed since the resulting accelerations in the direction of the cask axis are negligible. For the CG over corner drop however, the accelerations in the drop direction are decomposed into accelerations in the longitudinal (parallel to the cask axis) and transverse directions, since significant impact accelerations are expected in

both orthogonal directions. Different nodal sections are selected as appropriate for each drop orientation.

Figures 3.9.10-12 and 3.9.10-13 show the nodal sections analyzed for the side drop and CG over corner drop.

Raw Data Filtering

As described in the TN-32 model LS-DYNA analysis, the LS-DYNA computes the nodal accelerations at 0.4 msec intervals. Therefore, by the Nyquist theorem, the frequency content of the nodal acceleration data, computed by LS-DYNA, ranges from zero Hz, up to the following maximum frequency, f_{\max} .

$$f_{\max} = 1/2 \times 1/(4 \times 10^{-4}) = 1,250 \text{ Hz}$$

The lowest natural frequencies of the OS187H Transfer Cask, which can be excited by an impact event, are much lower than this. These natural modes of the transfer cask involve small displacements (and therefore low stresses) at frequencies higher than that of the rigid body motion of the transfer cask. These high frequency accelerations mask the true rigid body motion of the transfer cask, because both the low frequency rigid body acceleration and the high frequency natural vibration accelerations superimpose. The net acceleration is contained in the raw data computed by LS-DYNA. Therefore, filtering is necessary to remove these high frequency accelerations.

In order to estimate the natural frequencies of the OS187H transfer cask, a modal analysis is performed by using the ANSYS 3D finite element model described in Appendix 3.9.2 (page 3.9.2-13). The weight densities used in Appendix 3.9.2 file are all changed to mass densities ($\rho_m = \rho_w / 386.4$).

The cask is oriented in the horizontal orientation and supported at the bottom. The cask finite element model and boundary conditions are shown in Figures 3.9.10-14 and 3.9.10-15.

The first five mode frequencies resulting from the ANSYS modal analysis are tabulated below:

Frequencies of the First Five Natural Modes of the OS187H Transfer Cask

Mode Number	Frequency (Hz)
1	69.17
2	125.00
3	130.52
4	141.07
5	147.23

The mode shapes of Mode 2, 3, and 4 are plotted in Figures 3.9.10-16 through 3.9.10-18.

The averaged raw data for each cross section is filtered using a low pass Butterworth filter with a

cutoff frequency of 180 Hz in order to recover the actual rigid body acceleration of the Transfer Cask. The Butterworth filter used in this analysis is characterized by its large number of coefficients, small pass band ripple, and slow roll off. The cutoff frequency of 180 Hz is conservative, because it is higher than at least the first five dominant modes of the OS187H Transfer Cask computed above. Therefore, the response predicted by the filtered results includes more dynamics than simply the rigid body motion of the transfer cask.

Results of LS-DYNA Analyses

The following table lists the LS-DYNA side drop results.

Summary of Impact g Load Due to Side Drop

Transfer Cask Section (see Figure 3.9.10-12)	G Load
Lid Section	62.9g
Top Trunnion Section	55.8g
Middle Section	57.3g
Bottom Trunnion Section	46.9g
Bottom Plate Section	44.0g

Based on the Results shown in above table, the maximum acceleration in the OS187H Transfer Cask during the 80 inch accident condition side drop event is 62.9g and occurs in the transfer cask lid section. Also from this table, the highest acceleration in the region of the transfer cask where the DSC rests is 57.3g during an 80 inch side drop event.

Figure 3.9.10-19 and 3.9.10-20 show the acceleration time history of the transfer cask lid section and middle section. Figure 3.9.10-21 shows the maximum effective stress of the transfer cask during the side drop event as computed by LS-DYNA.

The following table lists the LS-DYNA CG over corner drop results.

Summary of Impact g Load Due to CG Over Corner Drop

Transfer Cask Section (see Figure 3.9.10-13)	Axial Accelerations
Lid Section	15.5g

This table shows that the maximum axial acceleration during an 80 inch CG over corner drop accident event is 15.5g. Figure 3.9.10-23 shows the axial acceleration time history of the transfer cask lid section. Figure 3.9.10-23 shows the maximum effective stress of the transfer cask during the CG over corner drop event as computed by LS-DYNA.

3.9.10.5 Summary of g-Loads for the OS187H Transfer Cask Body and Lid Bolt Stress Analyses

Based on the dynamic analysis results shown on the above table, the following table summarizes the g loads to be used for the stress analyses of the transfer cask body and lid bolts.

Component	Drop Orientation	Maximum G Load Computed by LS-DYNA	G Load used for Stress Evaluation
Cask Body	Side Drop	62.9	75
	Corner Drop	15.5 ⁽¹⁾	75 ⁽¹⁾
Lid Bolt	Corner Drop	15.5	21.65 ⁽²⁾

Note:

1. The transfer cask is transferred in a horizontal position held by the transfer trailer. In the axial direction it is possible to slide into the ground and incur a corner drop. The maximum stress resulting from DYNA corner impact analysis is plot in Figure 3.9.10-23 of this Appendix and also compared with ASME code allowable as described in item 5 below. Additionally, a conservative 75g end drop analysis of the cask body was also performed in Appendix 3.9.2.
2. A conservative 21.65g was used in the lid bolt corner drop analysis (Appendix 3.9.3, page 3.9.3-6).

The g loads used for the static stress analyses of the cask and lid bolts are reasonable and conservative for following reasons:

1. The casks of OS187H and LLNL/TN-32 are very similar in both geometry and weight. However, the OS187H (0.5" SS + 4.5" lead + 2.5" SS) is less rigid than the LLNL/TN-32 (9.5" thick CS shell). The less rigidity results in a lower calculated g load for the OS187H cask than for the LLNL/TN32 cask from LS-DYNA analyses.
2. Like LLNL/TN-32 models, the OS187H model does not include the outer shell and resin. In reality, these relatively soft components will deform and absorb energy during a drop and will slow down the rate of deceleration to produce a lower g load.
3. All material properties at room temperature are used in the LS-DYNA analyses. In reality, the transfer cask loaded with spent fuels will be at temperatures higher than room temperature. The modulus of elasticity for the cask material decreases while its temperature increases. The lower modulus of elasticity for the cask materials at the real temperatures will produce a lower impact g-load than that calculated in this analysis for the cask at room temperature.

4. During the drop accident, the g loads vary along the cask length from the minimum occurred at the bottom end to the maximum occurred at the top surface of the lid. However, a uniform 75 g load along the cask length is conservatively used in the cask static stress analysis. The maximum stress intensity in the cask structural shell is calculated to be 58.17 ksi (see Table 3.9.2-1 of Appendix 3.9.2, structural shell) from the static stress analysis.
5. Comparably, the maximum effective stress (Von Mises stress) in the cask structure shell is calculated to be 29.12 ksi (see Figure 3.9.10-21 of this Appendix) from the LS-DYNA dynamic analysis. This indicates that the static stress analysis using drop load of 75g is a very conservative approach, which produces about twice stress value of that produced by the dynamic LS-DYNA analysis.
6. Figure 3.9.10-23 shows the maximum effective stress (Von Mises stress) in transfer cask due to CG over corner drop from LS-DYNA analysis. The maximum effective stress at cask top cover plate is about 34.49 ksi, which is less than its allowable stress of 94.2 ksi (SA-240, Type XM 19 at 300°F). The maximum effective stress in the structural shell is about 24.0 ksi, which is less than its allowable stress of 66.2 ksi (SA-240, Type 304 at 300°F).

The g loads (including dynamic load factor) to be used for canister and basket structural analyses are described in Appendix 3.9.11.

3.9.10.6 References

1. LS-DYNA Keyword User's Manual, Volumes 1 & 2, Version 970, April 2003, Livermore Software Technology Corporation.
2. Witte, M. et al., Evaluation of Low-Velocity Impact Testing of Solid Steel Billet onto Concrete Pads and Application to Generic ISFSI Storage Cask for Tipover and Side Drop, Lawrence Livermore National Laboratory, UCRL-ID-126295, Livermore, California. March 1997.
3. NUREG/CR-6608, UCRL-ID-12911, "Summary and Evaluation of Low-Velocity Impact Tests of Solid Steel/Billet onto Concrete Pad," LLNL, February, 1998
4. ANSYS User's Manual, Rev 5.6.
5. American Society of Mechanical Engineers, ASME Boiler and Pressure Vessel Code, Section II, Part D, 1998, through 2000 addenda.
6. Baumeister & Marks, Standard Handbook for Mechanical Engineers, 7th Edition.
7. American Society of Mechanical Engineers, ASME Boiler and Pressure Vessel Code, Section II, Part A, 1998, through 2000 addenda.
8. A Survey of Strain Rate Effects for some Common Structural Materials Used in Radioactive Material Packaging and Transportation Systems, U.S. Energy Research and Development Administration, Battelle Columbus Laboratories, August 1976.
9. Dilger, etc., Ductility of Plain and Confined Concrete under Different Stain Rates, ACI Journal, January-February, 1984.
10. Structural Design of Concrete Storage Pads for Spent Fuel Casks, Electric Power Research Institute, EPRI NP-7551, RP 2813-28, August 1991.
11. Matthiesen, R. B., Observations of Strong Motions from Earthquakes, ASCE Convention and Exposition, Portland, Oregon, April 1980.
12. Dove, R. C., Endebrock, E. G., Dunwoody, W. E., Bennet, J. G., Seismic Tests on Models of Reinforced-Concrete Category 1 Buildings, Structural Mechanics in Reactor Technology, SMIRT 8, Brussels, Belgium 1985.
13. ANSYS User's Manual, Rev 6.0.
14. Harris and Crede, Shock and Vibration Handbook, Second Edition, McGraw-Hill.
15. Methods for Impact Analysis of Shipping Containers, NUREG/CR-3966, UCID-20639, LLNL, 1987.
16. Clough and Penzien, "Dynamics of Structures" McGraw-Hill, 2nd Edition, 1993.

APPENDIX 3.9.11

TABLE OF CONTENTS

	<u>Page</u>
3.9.11 32PTH DSC DYNAMIC AMPLIFICATION FACTOR (DAF) CALCULATION	3.9.11-1
3.9.11.1 DAF Analysis Introduction	3.9.11-1
3.9.11.2 DAF Analysis Notations	3.9.11-2
3.9.11.3 End Drop Modal Analysis.....	3.9.11-2
3.9.11.4 Side Drop Modal Analysis.....	3.9.11-3
3.9.11.5 Dynamic Load Factor Calculations.....	3.9.11-5
3.9.11.6 Summary of g-Loads for 32PTH Canister and Basket Impact Analyses..	3.9.11-6
3.9.11.7 References	3.9.11-8

LIST OF FIGURES

3.9.11- 1	NUHOMS 32 PTH Basket – Finite Element Model
3.9.11- 2	NUHOMS 32 PTH Basket – First Mode Shape, 0 Degree Orientation
3.9.11- 3	NUHOMS 32 PTH Basket – First Mode Shape, 45 Degree Orientation
3.9.11- 4	Spring – Mass Finite Element Model
3.9.11-5	Cask Side Drop, Acceleration Time-History
3.9.11-6	Cask Corner Drop, Acceleration Time-History
3.9.11-7	Side Drop – Canister Dynamic Acceleration Response
3.9.11-8	Side Drop – Basket Dynamic Acceleration Response
3.9.11-9	Corner Drop – Canister Dynamic Acceleration Response
3.9.11-10	Corner Drop – Basket Dynamic Acceleration Response

Boundary Conditions

Since modal analysis is a linear analysis, all gap elements (and canister shell elements) used in the Appendix 3.9.1 finite element model are deleted and the rails are supported at periphery. Thus this model yields only the natural frequencies of the fuel supporting basket plates and the rail panels.

For the 0° basket orientation, fuel is supported only by the horizontal panels, but for the 45° basket orientation, fuel is supported by both horizontal and vertical panels. Since only the lateral modes of vibration are significant, the master degree-of-freedom is applied on horizontal panels in y-direction and on vertical panels in x-direction.

Resulting Modes and Frequencies from the ANSYS Analysis

The first four natural frequencies of the 32PTH basket, resulting from the ANSYS modal analysis are tabulated below.

32PTH Finite Element Modal Analysis Results

Mode Number	Frequency for the 0° Analysis (Hz)	Frequency for the 45° Analysis (Hz)
1	110.29	112.32
2	113.58	112.95
3	114.54	117.44
4	115.86	117.47

The first mode shape of the 0° and 45° modal analyses are plotted on Figures 3.9.11- 2 and 3.9.11- 3, respectively.

3.9.11.5 Dynamic Load Factor Calculations

An ANSYS [1] spring-mass model is developed using COMBIN14 Spring-Damper element and MASS21 Structural Mass element (See Figure 3.9.11-4). The spring stiffness and mass are adjusted to produce fundamental natural frequencies for canister and basket in axial and transverse orientations. Acceleration time-history from cask side and corner drops from Figures 3.9.11-5 and 3.9.11-6 (taken from Appendix 3.9.10) are impressed on the canister and basket spring-mass models in a transient dynamic analysis. A damping ratio of 5% is used in these transient dynamic analyses. The resulting canister and basket acceleration response for side and corner drops is presented in Figures 3.9.11-7 to 3.9.11-10. Using the maximum response values from these figures, the dynamic load factors for both side drop and corner drop are computed in the following table.

Dynamic Load Factor Calculation Results

Drop Orientation	Component	Maximum Cask Acceleration (From Figs. 3.9.11-5 and 3.9.11-6) (g)	Maximum Response Acceleration (From Figs. 3.9.11-7 to 3.9.11-10) (g)	Dynamic Load Factor
Side Drop	Basket	57.3	67.5	1.18
	Canister		59.2	1.03
Corner Drop	Basket	15.5	17.5	1.10
	Canister		20.8	1.30

3.9.11.6 Summary of g-Loads for 32PTH Canister and Basket Impact Analyses

Appendix 3.9.10 summarizes the maximum g-loads computed for the OS187H Transfer Cask during an 80 inch side drop and a CG over corner drop events. The dynamic amplification factor of 1.11 is used to compute g-loads for canister and basket impact loads for side drops and 1.34 for corner drops. These impact loads are computed in the following table:

Drop Orientation	Acceleration Direction	Maximum G Load From LS-DYNA Analysis	Maximum Basket and Canister G-Load	G-Load Used for Canister and Basket Evaluation
Side Drop	Transverse	57.3G ⁽¹⁾	57.3 G x 1.18 = 67.6G	75G
Corner Drop	Axial	15.5G	15.5G x 1.3 = 20.2G	75G ⁽²⁾ 22G ⁽³⁾

Note:

1. A total of five sections ranging from the lid down to the bottom plate (see Figure 3.9.10-12 of Appendix 3.9.10) are selected in order to capture all possible g-load ranges seen by the OS187H Transfer Cask. However, only the middle three sections (top trunnion, middle, and bottom trunnion sections) will transmit inertial loads to the canister and basket. Therefore, only the maximum g load in these sections is used to compute the g-loads seen by the canister and basket.
2. The transfer cask is transferred in the horizontal position held by the transfer trailer. In the axial direction it is possible to slide into ground and incur a corner drop. During the corner drop, the canister with basket is supported by the cask body in the horizontal position and the top end of the canister will slide into the cask lid and supported by the lid. The maximum worst condition in the axial direction is end drop and transverse condition is side drop, therefore the canister and basket were analyzed for 75g end drop and 75g side drop in Appendix 3.9.1 to bound the corner drop.
3. For canister end closure weld shear stress calculation, it was conservatively assumed that the internal weight (basket + fuel assemblies) will impact the inner surface of the canister inner top cover without any support from transfer cask lid. 22 g in the axial direction was used for weld stresses calculations.

3.9.11.7 References

1. ANSYS User's Manual, Rev 8.0.
2. Blevins, Formulas for Natural Frequency and Mode Shape, Krieger Publishing Company, 1995.
3. American Society of Mechanical Engineers, ASME Boiler and Pressure Vessel Code, Section II, Part D, 1998, through 2000 addenda.
4. Baumeister & Marks, Standard Handbook for Mechanical Engineers. 7th Edition.

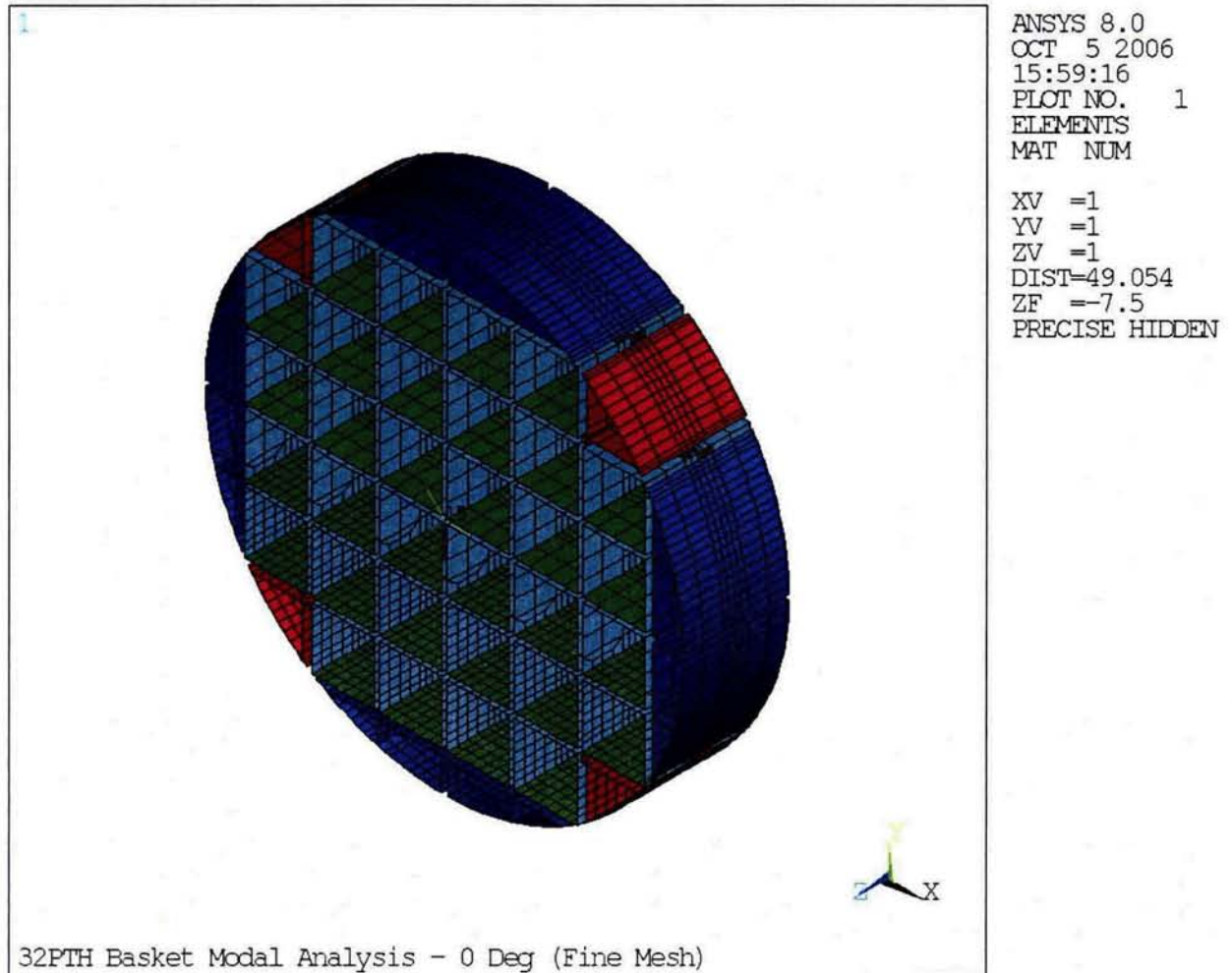


Figure 3.9.11-1
 NUHOMS 32 PTH Basket – Finite Element Model

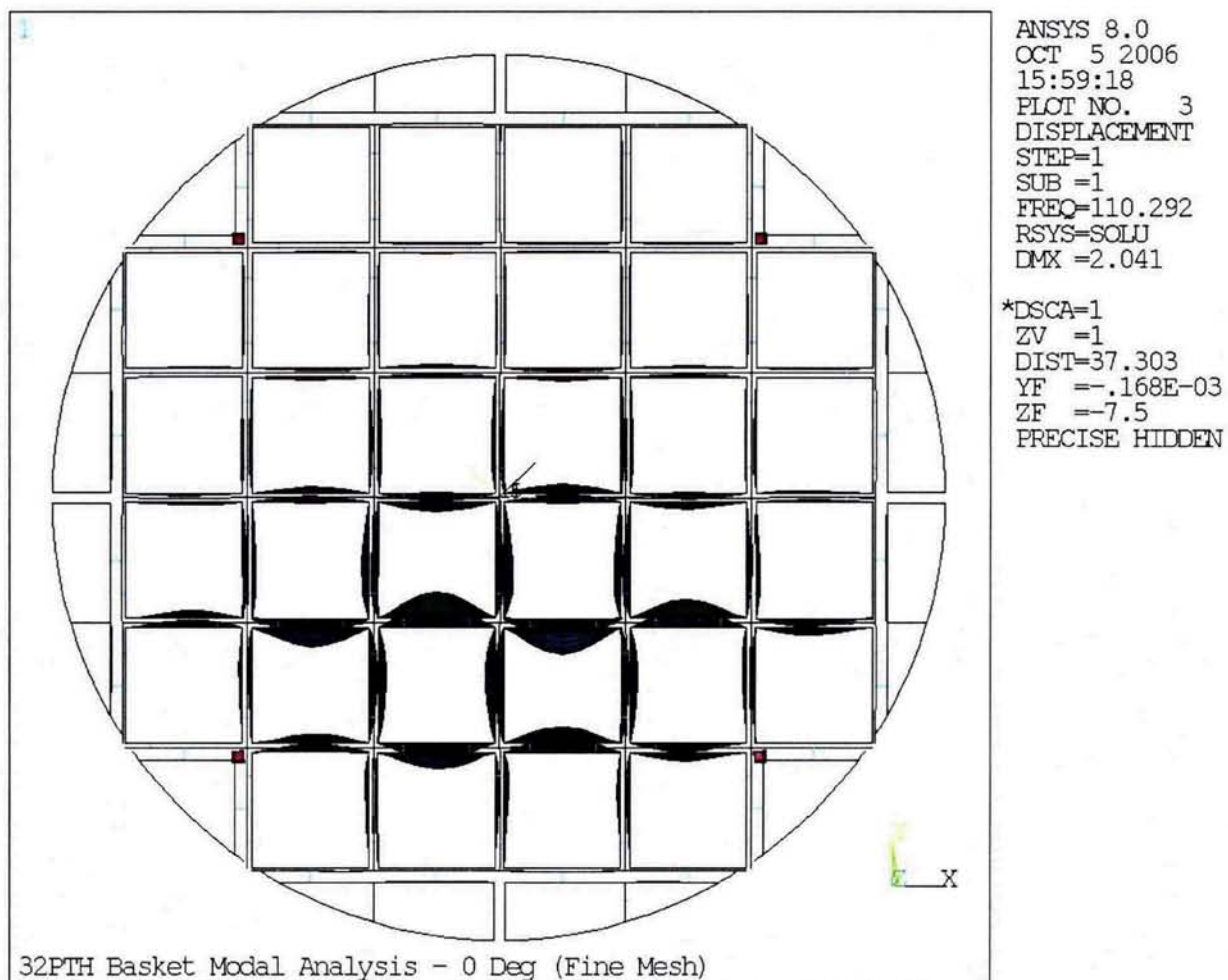


Figure 3.9.11-2
 NUHOMS 32 PTH Basket – First Mode Shape, 0 Degree Orientation

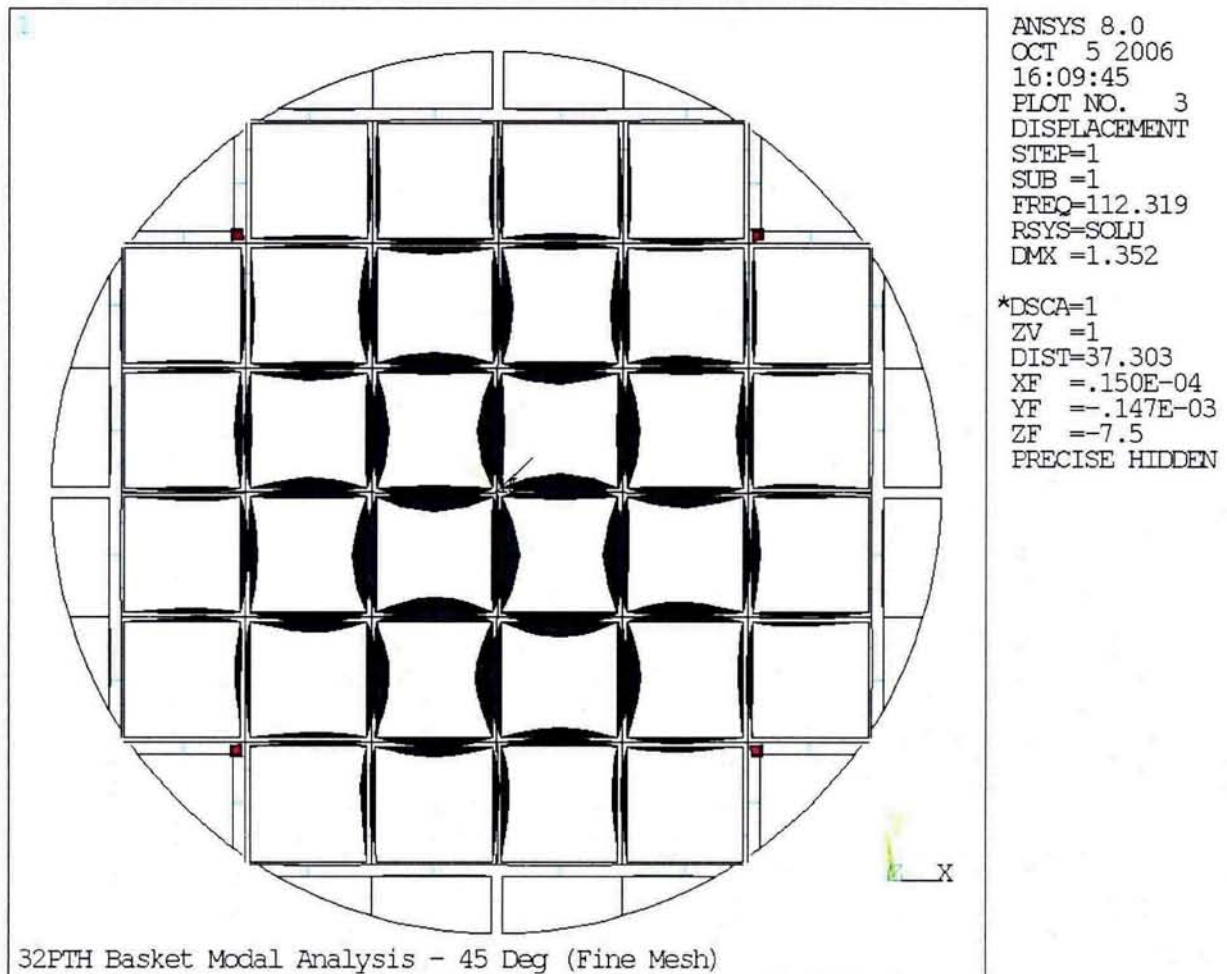


Figure 3.9.11-3
 NUHOMS 32 PTH Basket – First Mode Shape, 45 Degree Orientation

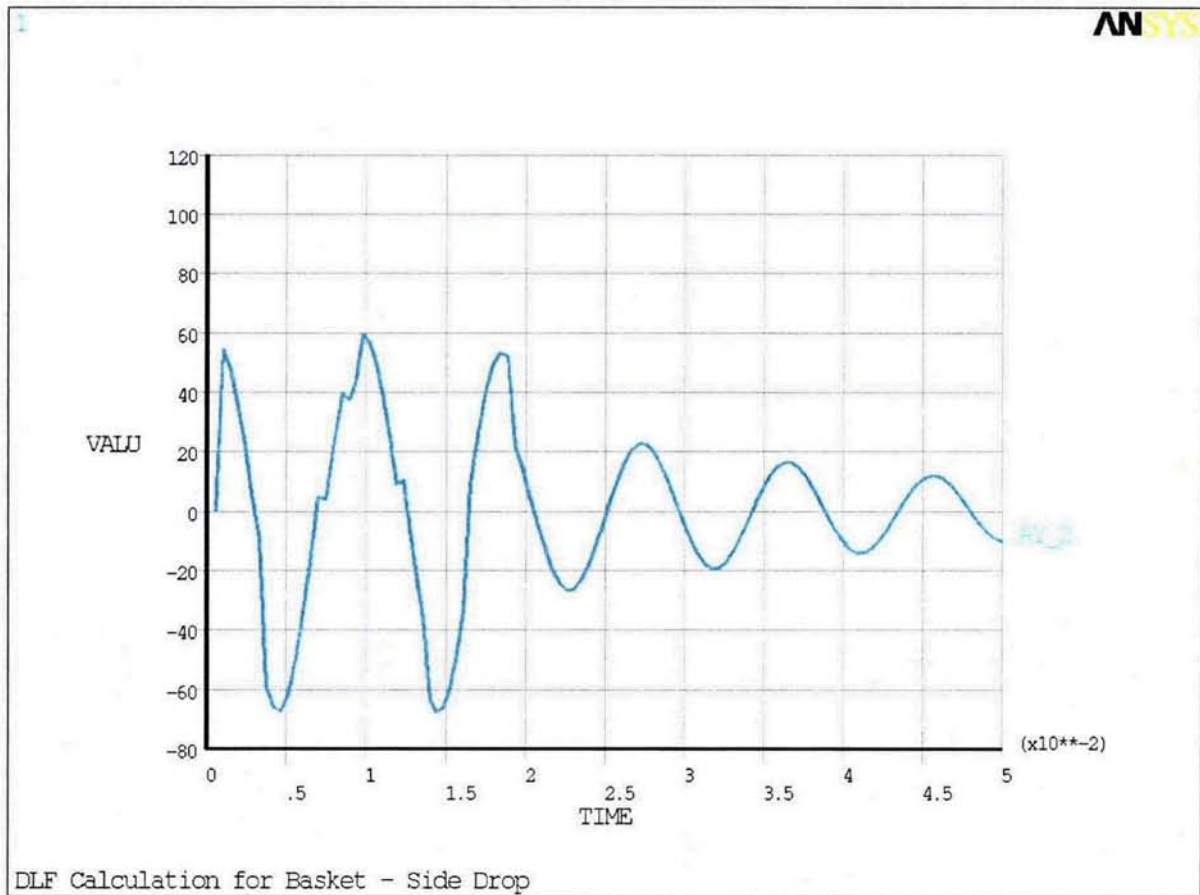


Figure 3.9.11-8
Side Drop – Basket Dynamic Acceleration Response

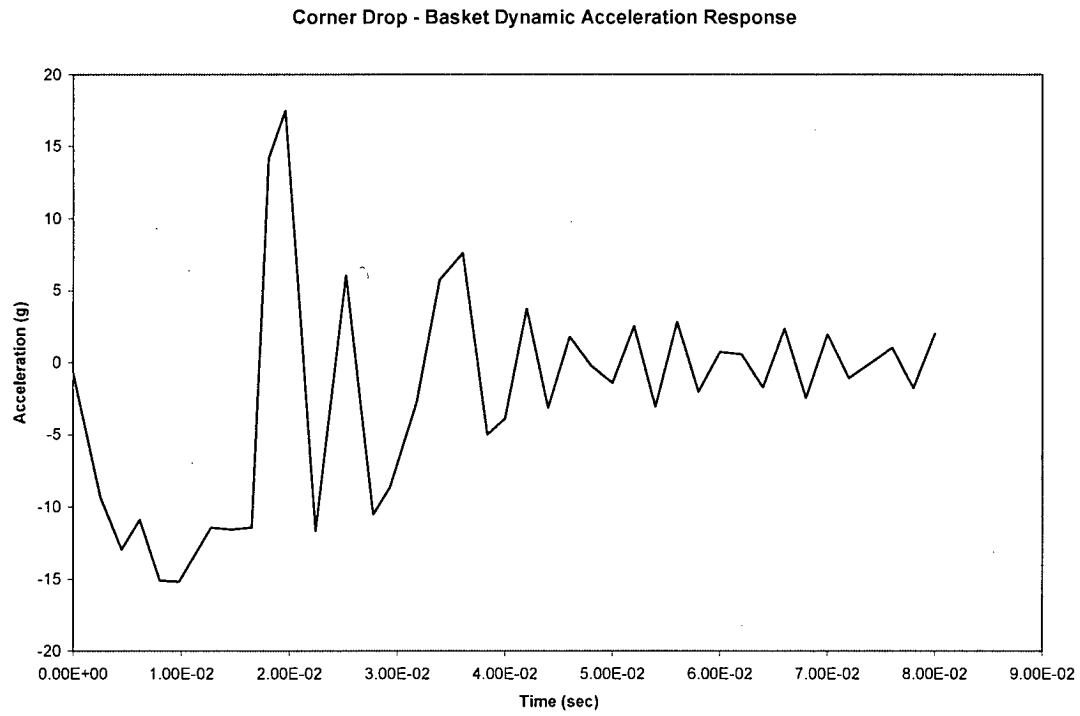


Figure 3.9.11-10
Corner Drop – Basket Dynamic Acceleration Response

CHAPTER 4 THERMAL EVALUATION

Table of Contents

4.	THERMAL EVALUATION.....	4-1
4.1	Discussion.....	4-1
4.2	Summary of Thermal Properties of Materials.....	4-3
4.3	Thermal Evaluation for Normal and Off-Normal Conditions	4-9
4.3.1	Thermal Models for Normal and Off-Normal Conditions.....	4-9
4.3.2	Maximum Temperatures for Normal and Off-Normal Conditions.....	4-20
4.3.3	Minimum Temperatures for Normal and Off-Normal Conditions	4-21
4.3.4	Maximum Internal Pressures for Normal and Off-Normal Conditions	4-21
4.3.5	Maximum Thermal Stresses for Normal and Off-Normal Conditions	4-21
4.3.6	Evaluation of Thermal Performance for Normal and Off-Normal Conditions.....	4-21
4.4	Thermal Evaluation for Accident Conditions	4-22A
4.4.1	Thermal Models for Accident Conditions	4-22A
4.4.2	Maximum Temperatures for Accident Conditions	4-27
4.4.3	Maximum Internal Pressures for Accident Conditions.....	4-28
4.4.4	Maximum Thermal Stresses for Accident Conditions.....	4-28
4.4.5	Evaluation of Thermal Performance for Accident Conditions	4-28
4.5	Thermal Evaluation for Loading and Unloading Conditions.....	4-29
4.5.1	Vacuum Drying.....	4-29
4.5.2	Reflooding.....	4-34
4.6	Maximum Internal Pressure.....	4-36
4.6.1	Average Gas Temperature	4-36
4.6.2	Amount of Initial Helium Backfill.....	4-37
4.6.3	Free Gas within Fuel Assemblies / BPRA.....	4-38
4.6.4	Total Amount of Gas within DSC	4-38
4.6.5	Maximum DSC Internal Pressures.....	4-39
4.6.6	Maximum Pressure in Annulus.....	4-39
4.7	Axial Decay Heat Profile	4-40
4.8	Effective Fuel Properties	4-43
4.8.1	Discussion.....	4-43
4.8.2	Summary of Material Properties	4-43
4.8.3	Effective Fuel Conductivity	4-45
4.8.4	Effective Fuel Density and Specific Heat.....	4-46
4.8.5	Conclusion	4-47
4.9	Effective Conductivity of Fluids in the Transfer Cask.....	4-48
4.9.1	Effective Conductivity in the Shielding Panel.....	4-48
4.9.2	Effective Water Conductivity in Annulus between TC and DSC.....	4-50
4.10	Justification of the Assumed Hot Gap Sizes	4-52
4.10.1	Radial Gap between Basket Rails and DSC shell.....	4-52
4.10.2	Radial Gap between Lead and the Cask Structural Shell	4-53

LIST OF TABLES

4-1	Maximum Component Temperatures during Transfer Operations at 115°F ambient	
4-2	Maximum Component Temperatures for Storage Conditions at 115°F ambient	
4-3	Maximum Component Temperatures during Transfer Operations at -20°F ambient	
4-4	Maximum Component Temperatures for Storage Conditions at -20°F ambient	
4-5	Maximum Component Temperatures for Fire Accident Case Transfer Cask, 34.8 kW	
4-6	Maximum Component Temperatures for Blocked Vent Accident Case	
4-7	Average Heat up Rates	
4-8	Maximum Temperatures during Vacuum Drying Process	
4-9	Maximum Decay Heat Load without Time Limitation for Vacuum Drying	
4-10	32PTH DSC Internal Pressure	
4-11	Average Peaking Factors for Active Fuel Length of 144" and 137" (2 pages)	
4-12	Characteristics of Fuel Assemblies	
4-13	Effective Fuel Properties	
4-14	Effective Conductivity of Liquid Neutron Shielding	
4-15	Verification of the Calculated Effective Conductivities for Liquid Neutron Shielding	
4-16	Effective Conductivity of Liquid Neutron Shield during Burning Period	
4-17	Effective Conductivity of Air within Shielding Panel during Cool Down Period	
4-18	Verification of the Selected k_{eff} Value for Water in the Annulus	
4-19	Total Heat Transfer Coefficient during Fire	
4-20	Deleted	
4-21	Summary of the Energy-Hydraulic Calculation Results for 34.8 kW	
4-22	Summary of the Energy-Hydraulic Calculation Results for 32.0 kW	
4-23	Summary of the Energy-Hydraulic Calculation Results for 26.1 kW	
4-24	Minimum Height of the Fuel Rubble	
4-25	Transverse Effective Fuel Conductivity at Various Fuel Rod Pitches	
4-26	Transverse Effective Conductivity of Damaged Fuel	
4-27	Maximum Component Temperatures in DSC containing 16 Damaged Fuel Assemblies	
4-28	Internal DSC Pressure during Transferring of Damaged Fuel	

LIST OF FIGURES

- 4-1 Position of the DSC in the Transfer Cask
- 4-2 Finite Element Model of Transfer Cask OS187H
- 4-3 FEM of Transfer Cask OS187H, Details
- 4-4 Top and Bottom Sub-Models of Transfer Cask OS187H
- 4-5 Typical Boundary Conditions on the TC Model
- 4-6 Finite Element Model of HSM-H
- 4-7 FEM of HSM-H, Concrete Structure
- 4-8 FEM of HSM-H, DSC and Support Rails
- 4-9 DSC Circumferential Convection Regions in the HSM-H Model
- 4-10 Typical Convection Boundary Conditions in the HSM-H Model
- 4-11 Typical Heat Flux and Fixed Temperature Boundary Conditions for HSM-H Model
- 4-12 Finite Element Model of the DSC
- 4-13 FEM of DSC Basket, Details
- 4-14 FEM of DSC Rails, Details
- 4-15 Thermally Bounding Loading Configurations Considered in the DSC Model
- 4-16 Typical Boundary Conditions in the DSC Model
- 4-17 Transfer Cask Temperature Distributions, 115°F Ambient
- 4-18 Temperature Distributions in Transfer Cask Sub-Models
- 4-19 DSC Temperature Distribution during Transfer Operation Basket Type I, Loading Configuration 1, 115°F Ambient
- 4-20 Temperature Distribution of DSC and Fuel Assemblies during Transfer Operations, 115°F Ambient
- 4-21 HSM-H Temperature Distribution 115°F Ambient with Finned Aluminum Side Heat Shields, 34.8 kW
- 4-22 HSM-H Temperature Distribution 115°F Ambient with Unfinned Side Heat Shields
- 4-23 DSC Temperature Distribution during Storage – 115°F Ambient, 34.8 kW, in HSM-H with Finned Aluminum Side Heat Shields
- 4-24 Temperature Distribution during Transfer Operations, Ambient -20°F
- 4-25 Temperature Distributions during Storage, Ambient -20°F, 34.8 kW
- 4-26 FEM of Transfer Cask for Fire Accident Case
- 4-27 Basket Model for Calculation of Effective Conductivities (HSM-H Model Blocked Vent Accident Case)
- 4-28 Temperature Distribution on TC Slice Model for Fire Accident Case
- 4-29 Time-History of TC Component Temperatures for the Fire Accident Case
- 4-30 Temperature Distribution for HSM-H with Finned Aluminum Side Heat Shields - 34 hours after Blockage of the Vents, 34.8 kW
- 4-31 Deleted
- 4-32 Temperature Distribution of DSC Model for Blocked Vent Accident Case
- 4-33 Temperature-Time History of HSM-H Components for Blocked Vent Accident Case
- 4-34 Temperature Distribution at the End of Vacuum Drying Process
- 4-35 Time-Temperature History for Vacuum Drying Procedure A
- 4-36 Time-Temperature History for Vacuum Drying Procedure B
- 4-37 Time-Temperature History for Vacuum Drying Procedure C

- 4-38 Total Free Gas Volume versus Burnup Rate
- 4-39 Comparison of the Axial Heat Profiles in the FE Model and in Ref. [4]
- 4-40 Finite Element Model of Fuel Assemblies
- 4-41 Effective Transverse Fuel Conductivity in Helium
- 4-42 Effective Transverse Fuel Conductivity for Vacuum Conditions
- 4-43 Effective Axial Fuel Conductivity
- 4-44 Schematic Flow Paths through HSM-H
- 4-45 Deleted |
- 4-46 Location of the Damaged Fuel Assemblies in the Basket
- 4-47 Typical FE Models of Damaged (Reconfigured) Fuel WEO 17x17
- 4-48 Transverse Effective Fuel Conductivity versus Pitch Size
- 4-49 Effective Transverse Conductivity of Damaged (Reconfigured) Fuel
- 4-50 Temperature Distributions in the DSC containing 16 Damaged Fuel Assemblies for
Normal / Off-Normal Transfer Conditions
- 4-51 Temperature Distributions in the DSC containing 16 Damaged (Rubble) Fuel
Assemblies for Accident Conditions |

THERMAL EVALUATION

The thermal evaluation described in this chapter 4.0 is applicable to the 32PTH DSC loaded inside the OS187H TC and HSM-H. See Appendix A, Chapter A.4 for discussion of applicability of these analyses for the 32PTH Type 1 DSC inside the OS187H Type 1 TC and HSM-H.

4.1 Discussion

The NUHOMS®-32PTH DSC is designed to passively reject decay heat during storage and transfer for normal, off-normal, and accident conditions while maintaining temperatures and pressures within specified limits. Objectives of the thermal analyses performed for this evaluation include:

- Determination of maximum and minimum temperatures with respect to material limits to ensure components perform their intended safety functions,
- Determination of temperature distributions to support the calculation of thermal stresses,
- Determination of maximum DSC internal pressures for normal, off-normal, and accident conditions, and
- Determination of the maximum fuel cladding temperature, and to confirm that this temperature will remain sufficiently low to prevent unacceptable degradation of the fuel during storage.

To establish the heat removal capability, several thermal design criteria are established for the System. These are:

- Maximum temperatures of the containment structural components must not adversely affect the containment function.
- To maintain the stability of the neutron shield resin in the transfer cask (TC) during normal transfer conditions, a maximum allowable temperature of 300°F is set for the neutron shield material [1].
- A maximum fuel cladding temperature limit of 400°C (752°F) has been established for normal conditions of storage and for short-term storage operations such as transfer and vacuum drying [2]. During off-normal storage and accident conditions, the fuel cladding temperature limit is 570°C (1058°F) [2].
- A maximum temperature limit of 327°C (620°F) is considered for the lead in the transfer cask, corresponding to the melting point [3].

6. SA-240, Type 304 Stainless Steel

Temperature (°F)	Conductivity (Btu/hr-ft-°F) [6]	Conductivity (Btu/hr-in-°F)	Diffusivity (ft²/hr) [6]	Specific Heat (Btu/lbm-°F)²	Density (lbm/in³) [3]
70	8.6	0.717	0.151	0.117	0.29
100	8.7	0.725	0.152	0.117	
150	9.0	0.750	0.154	0.120	
200	9.3	0.775	0.156	0.122	
250	9.6	0.800	0.158	0.125	
300	9.8	0.817	0.160	0.126	
350	10.1	0.842	0.162	0.128	
400	10.4	0.867	0.165	0.129	
450	10.6	0.883	0.167	0.130	
500	10.9	0.908	0.170	0.131	
550	11.1	0.925	0.172	0.132	
600	11.3	0.942	0.174	0.133	
650	11.6	0.967	0.177	0.134	
700	11.8	0.983	0.179	0.135	
750	12.0	1.000	0.181	0.136	
800	12.2	1.017	0.184	0.136	

7. Aluminum

Al-1100

Temperature (°F)	Conductivity (Btu/hr-ft-°F) [6]	Conductivity (Btu/hr-in-°F)	Diffusivity (ft²/hr) [6]	Specific Heat (Btu/lbm-°F)²	Density (lbm/in³) [6]
70	133.1	11.092	3.67	0.214	0.098
100	131.8	10.983	3.61	0.216	
150	130.0	10.833	3.50	0.219	
200	128.5	10.708	3.42	0.222	
250	127.3	10.608	3.35	0.224	
300	126.2	10.517	3.28	0.227	
350	125.3	10.442	3.23	0.229	
400	124.5	10.375	3.17	0.232	

Al-6061

Temperature (°F)	70	100	150	200	250	300	350	400
Conductivity (Btu/hr-ft-°F) [6]	96.1	96.9	98.0	99.0	99.8	100.6	101.3	101.9
Conductivity (Btu/hr-in-°F)	8.00	8.08	8.17	8.25	8.32	8.38	8.44	8.49

8. Lead

Temperature (K)	Conductivity (W/m-K) [5]	Temperature (°F)	Conductivity (Btu/hr-in-°F)	Specific Heat (Btu/lbm-°F) [3]	Density (lbm/in³) [3]
200	36.7	-100	1.767	0.03	0.393
250	36.0	10	1.733		
300	35.3	80	1.700		
400	34.0	260	1.637		
500	32.8	440	1.579		
600	31.4	620	1.512		

² Thermal diffusivity is $\alpha = \frac{k}{\rho c_p}$, this equation is used to calculate the specific heat.

9. Poison Plates

Neutron poison plates in the basket type I are borated aluminum alloy or MMC. The minimum conductivity of the borated material must be equal or larger than the 145 W/m-K at 100°C. It is assumed that the conductivity of the borated aluminum alloy/MMC remains unchanged at higher temperatures. The measured conductivities of the available borated aluminum alloys for the entire range of 20°C to 400°C are much higher than the above requirement [7 and 8].

Basket type II is designed to use Boral® absorber as neutron poison plate. The Boral® absorber possesses orthotropic thermal conductivity. To avoid any uncertainty, conductivity values of Boral® are set conservatively to zero. An equivalent conductivity is calculated for a pair of Boral® and aluminum-1100 plates in thermal analyses. For calculation of the equivalent conductivity, the paired plates are considered as parallel thermal resistances. Since the temperature gradients along the plates are much higher than the temperature gradients across the plates, this assumption is reasonable. The following equation is used to calculate the equivalent thermal conductivity of paired plates.

$$k_{eq} = \frac{k_{Al} t_{Al} + k_p t_p}{t_{total}} = \frac{k_{Al} t_{Al}}{t_{total}}$$

t_{total} = Total thickness of the basket plate = 0.5"

k_{Al} = Thermal conductivity of aluminum plate (Al 1100)

t_{Al} = Thickness of the aluminum plate ($t_{total} - t_p$ -tolerance)

t_p = Thickness of the Boral® plate = 0.075"

Temp (°F)	k - Al-1100 [6] (Btu/hr-ft-°F)	k_{eq} for Basket Type II (Btu/hr-in-°F)
70	133.1	9.34
100	131.8	9.25
150	130.0	9.12
200	128.5	9.02
250	127.3	8.93
300	126.2	8.86
350	125.3	8.79
400	124.5	8.74
650	121.3 ³	8.51

Basket type II contains Boral® plates with a nominal core thickness of 0.05 in.

Total Boral® plate thickness is 0.075±0.004 in. from reference [9]

The minimum thickness of the Al-1100 plate (0.421") is considered to calculate the equivalent conductivity.

The minimum required thermal conductivities of the paired aluminum and poison plates will be verified via testing as described in Chapter 9.

To minimize the thermal resistance of the basket during fire period, the conductivity of poison plate is considered to be equal to the aluminum conductivity. Conductivity of the poison plate is set equal to the minimum value of 145 W/m-K (6.98 Btu/hr-in-°F) during the cool down period to maximize the thermal resistance. Specific heat and density of poison plate is set equal to those of aluminum for transient runs.

³ Extrapolated from the values in [ASME]

4.3.1.2 Steady State HSM-H Model

Horizontal Storage Module (HSM-H) is designed to provide an independent, passive system with substantial structural capacity to ensure safe storage of spent fuel assemblies in NUHOMS®-32PTH canisters. The decay heat load from stored canisters is removed via radiation, free convection and conduction. Natural draft of air within the HSM-H cavity is created by the temperature difference between ambient and the DSC surface, and the height difference between the HSM-H vents. Ambient air enters the HSM-H through the inlet openings in the lower part of the HSM-H side walls and circulates around the DSC and the side heat shields. Warm air passes through or around the top heat shield and exits the HSM-H through the outlet openings in the upper part of the HSM-H side walls.

Decay heat is rejected from the DSC to the HSM-H air space by convection and then is removed from the HSM-H by natural air circulation. Heat is also radiated from the DSC surface to the heat shields and HSM-H walls, where again natural air circulation and conduction through the walls remove the heat. Typical flow paths are shown in Figure 4-44.

A half symmetric, three dimensional, finite element model of the HSM-H is developed using ANSYS [16]. The model represents one module among adjacent HSM-H's containing DSCs with the maximum heat load of 34.8kW. Therefore, adiabatic boundary conditions are applied over the outer surfaces of the HSM-H side walls and back wall. The HSM-H model includes the DSC shell and shield plugs, the concrete structure, and the heat shields. The DSC content is not considered for the steady state runs. The basket and its content are homogenized for the transient runs. The homogenized basket properties are discussed in Section 4.4.1.1.

Conduction through components is modeled using SOLID70 elements. Conduction through air within the HSM-H cavity is not considered for the steady state runs. Radiation between the DSC shell, heat shields, and HSM-H walls is modeled using /AUX12 methodology. SHELL57 elements were superimposed on radiating surfaces to create the Super-element MATRIX50. The SHELL57 elements were unselected prior to solving the model. The finite element model of HSM-H is shown in Figures 4-6 to 4-8.

For the design basis heat load, 34.8 kW, the side heat shields are equipped with fins on the surface facing the DSC. In this case, the fins and the surface facing the DSC are anodized. The side shields are modeled as flat plates with a thickness of 0.3125" at the position of shield base plate. Convection from the fins attached to the side shields is modeled using equivalent convection coefficient. Calculation of the effective convection coefficients is discussed in Section 4.11. Optionally, the alternative side heat shields without the fins may be utilized. For this un-finned configuration, the convection coefficient for a flat, vertical plate replaces the effective convection coefficient over the fins. Flat side heat shields may be made from stainless steel, aluminum or galvanized steel. If aluminum is used, the surface of the side heat shield facing the DSC is anodized.

The top heat shield is a louver plate attached to the ceiling or a flat stainless steel plate for HSM-H modules with stainless steel side heat shields. The louvered heat shield is modeled in its exact geometry. The convection coefficient for the louvered top heat shield is discussed in

Section 4.11. The convection coefficients for flat, horizontal plate facing up or downwards are considered for the flat stainless steel top heat shield. These convection coefficients are discussed in Section 4.11 as well.

Steady State Boundary conditions for the HSM-H Model

Ambient temperatures between 0 and 100°F are considered as normal storage conditions. The maximum day temperature of 115°F and the minimum temperature of -20°F are considered as the maximum and minimum off-normal storage condition respectively.

Because of the large thermal inertia, the temperature responses of the HSM-H and DSC to maximum day temperature are relatively slow. Therefore, considering an average maximum temperature over a 24 hour period is reasonable to calculate the maximum component temperatures during storage using steady state boundary conditions.

In order to calculate a daily average temperature given a maximum day temperature, a minimum daily range must be specified. Reference [18] shows that the minimum daily range in the contiguous United States is 27°F for a maximum summer ambient above 110°F. the hourly temperature is defined in [18] as:

$$T_{\text{hour}} = T_{\text{max}} - (\text{percentage of the daily range}) \times (\text{min daily range})$$

The percentages of the daily range are shown as a function of day time in [18]. The average of the hourly temperatures over the 24 hour period gives the daily average temperature. The following table shows the calculated daily average temperature for a maximum day temperature of 115°F and a daily minimum range of 27°F.

Maximum day temperature = 115°F
Minimum daily range = 27°F

Time, hr	% daily range [16]	T _{hour} (°F)	Time, hr	% daily range [16]	T _{hour} (°F)
1	87	91.5	13	11	112.0
2	92	90.2	14	3	114.2
3	96	89.1	15	0	115.0
4	99	88.3	16	3	114.2
5	100	88.0	17	10	112.3
6	98	88.5	18	21	109.3
7	93	89.9	19	34	105.8
8	84	92.3	20	47	102.3
9	71	95.8	21	58	99.3
10	56	99.9	22	68	96.6
11	39	104.5	23	76	94.5
12	23	108.8	24	82	92.9

Daily average temperature = 100°F

A daily average temperature 105°F is used in this analysis to bound the maximum temperatures for normal and off-normal storage conditions. To maximize the temperature gradients in the

HSM-H concrete structure, only the off-normal storage condition of -20°F ambient is considered for the evaluation.

The circumference of the DSC model is divided into three regions for convection boundary conditions as shown in Figure 4-9. If the bar located on the supporting beam is slotted, the surface of the DSC shell from -64.2° to -60° is located above the upper edge of the slots in the slotted plate. The free convection is therefore restricted over this area. For conservatism, this area is considered as a dead zone with no free convection. In the case that no slot is provided on the supporting bar, the dead zone is increased to 18.9° as shown in Figure 4-9. Calculation of free convection coefficients for the DSC regions is discussed in Section 4.11.

Similar to the DSC circumference, the cross section of the HSM-H cavity is divided into different regions to apply the convection boundary conditions. Energy and hydraulic equations are combined to calculate the exit and the average bulk air temperatures for various ambient temperatures. Section 4.13 shows the regions and describes briefly the methodology to calculate the exit and the average bulk air temperatures in the HSM-H cavity.

Convection on HSM-H end walls is calculated using free convection correlations for vertical surfaces at HSM-H average bulk air temperature (T_c). Convection on the lower part of the side wall, below the side heat shield, is determined using free convection correlation for vertical surfaces at ambient temperature (T_c). For the space between the side wall and the side heat shield, free convection correlation for a narrow channel is used to determine the free convection coefficient. For the HSM-H ceiling and the HSM-H basemat, correlations for flat horizontal surfaces are used to determine free convection coefficients. Air temperatures for the convection on the basemat and ceiling are ambient temperature (T_c) and exit air temperature (T_{exit}) respectively. The calculation methods of free convection coefficients are discussed in detail in Section 4.11. Figure 4-10 shows the convection boundary conditions applied in the HSM-H model.

The thermal test reported in reference [25] shows that the HSM-H thermal analysis methodology conservatively predicts the DSC and the HSM-H component temperatures.

Insolance is applied as a constant heat flux on the roof and front wall of the HSM-H, which are exposed to the ambient. The value of the solar heat flux is taken from [17] averaged over a 24 hour period. The insolance is applied as a constant heat flux over the SURF152 elements superimposed on the SOLID70 elements on the HSM-H roof and front wall. A solar absorptivity of 1.0 is assumed for the concrete surface. The values of the applied heat fluxes are listed below:

Shape	Insolance [17] (gcal/cm ²)	Averaged over 24 hr (Btu/hr-in ²)
HSM roof	800	0.8537
HSM front wall	200	0.2134

Insolance is not considered for the minimum ambient temperature of -20°F.

Convection and radiation from the roof and the front wall are combined together as a total convection coefficient. The calculation of the total convection coefficient is discussed in Section 4.11.

The decay heat load is considered to be distributed evenly on the radial inner surface of the DSC for the steady state runs in this analysis. The applied decay heat flux is:

$$\text{Decay heat flux} = \frac{Q}{\pi D_i L} = 3.34 \quad \text{Btu/hr-in}^2 \quad \text{or} \quad 3.25 \text{ Btu/hr-in}^2 \text{ for CE 14x14 only}$$

where,

Q = total decay heat load = 34.8 kW = (118,748 Btu/hr) or 33.8 kW (115,336 Btu/hr) for CE 14x14 only

Di = inner DSC diameter = 68.75"

L = DSC cavity length = 164.5"

HSM-H modules with finned aluminum side shields and HSM-H modules with stainless steel heat shields are evaluated with the maximum decay heat load of 34.8 kW. In order to limit the maximum concrete temperature below the values considered for the HSM-H with finned aluminum side heat shields, the maximum decay heat load is decreased for the HSM-H modules with flat aluminum or flat galvanized steel side heat shields. The maximum decay heat load for the HSM-H modules with un-finned aluminum side heat shields is 32.0 kW, which gives a uniform heat flux of 3.07 Btu/hr-in².

$$\text{Decay heat flux} = \frac{Q}{\pi D_i L} = 3.07 \quad \text{Btu/hr-in}^2 \text{ for HSM-H with un-finned aluminum side heat shields}$$

$$Q_1 = 32.0 \text{ kW} = 109,194 \quad \text{Btu/hr}$$

For the HSM-H modules with galvanized side heat shields, the maximum decay heat load is limited to 26.1 kW.

$$\text{Decay heat flux} = \frac{Q}{\pi D_i L} = 2.51 \quad \text{Btu/hr-in}^2 \text{ for HSM-H with galvanized steel side heat shields}$$

$$Q_2 = 26.1 \text{ kW} = 89,061 \quad \text{Btu/hr}$$

It is assumed that soil has a temperature of 70°F at 10' below the HSM-H basemat for hot conditions. The soil temperature for cold condition (-20°F) is assumed to be 45°F. These assumptions are consistent with the assumptions in the thermal analysis of the standardized HSM design [19]. The HSM-H basemat is considered to be a 4' thick concrete slab. Due to low conductivity of concrete and soil, the model is insensitive to the thickness of the basemat / soil and the soil temperature. The heat flux and fixed temperature boundary conditions applied in the model are shown in Figure 4-11.

4.3.1.3 Steady State 32PTH DSC Model

The 32PTH DSC is a high integrity stainless steel welded pressure vessel that provides confinement of radioactive material, encapsulates the fuel in a helium atmosphere, and when placed in the transfer cask, provides radiological shielding.

A three dimensional finite element model of the 32PTH DSC is developed using ANSYS [16] to determine the maximum fuel cladding temperature. The DSC model includes the DSC shell, shield plugs, basket rails, basket, and fuel assemblies. The fuel assemblies are modeled as

homogenized regions within the fuel compartments. The effective thermal properties for the homogenized fuel are calculated in Section 4.8.

The following conservative assumptions are considered in developing the finite element model to maximize the fuel cladding temperature:

- No convection occurs within the DSC cavity,
- The basket containing the fuel assemblies is centered axially in the DSC cavity,
- Heat transfer across the contact gaps within the basket occurs only by gaseous conduction.

The following gaps are considered between components in the model at thermal equilibrium:

- 0.010" gap between each two adjacent basket plates except for the following cases:
 - between the aluminum inserts and the stainless steel rails – this gap is considered to be at least 0.020"
 - between the aluminum and the poison plates, when applicable. The aluminum plate and the poison plate are sandwiched between fuel compartments. For ease of modeling the 0.010" gaps are placed on both sides of the paired plates. These gaps account for the total contact resistance between the four plates shown in Figure 4-13, Detail B.
- 0.010" gap between the basket plates and aluminum rails
- 0.100" radial gap between rails and inner shell (see Section 4.11 for justification)

The axial cold gap of 0.07" between the stainless steel support plates and the aluminum plates is divided into a 0.01" axial gap at the bottom and a 0.060" axial gap at the top of the stainless steel plate. All dimensions of the canister are at nominal values. Details of the finite element model are shown in Figures 4-12 to 4-14.

Five basket types in two categories are designed for NUHOMS-32PTH DSC. Relevant characteristics of these basket types are listed below.

Basket type	I	II
A	Boron Aluminum, or Metal Matrix Composites (MMC) Maximum thickness 0.187"	Boral® Maximum thickness 0.075"
B		
C		
D		Not applicable
E		Not applicable

Aluminum plates are to be paired with the poison plates to make a nominal thickness of 0.5". The conductivity of the borated aluminum/MMC plate depends on the boron content and the fabrication procedure. To bound the maximum component temperature, the maximum thickness of the boron containing plate (0.1875") is considered in the model for basket type I.

Paired Boral®/ aluminum plates are used in basket type II. An effective conductivity is calculated for the paired Boral®/ aluminum plates, as discussed in Section 4.2. Other combination of aluminum and poison plates that satisfies the conductivity requirements in Chapter 9 can be used in the basket.

Heat transfer from the fuel regions occurs only by conduction through the basket plates and the rails. Conduction and radiation heat transfer are considered between the rails and the DSC shell. Conduction through components is modeled using SOLID70 elements.

Radiation between the rails and the DSC shell is modeled using radiation LINK31 elements using the same methodology as described in Section 4.3.1.1. Axial radiation is also considered between the top and bottom surfaces of the fuel assemblies to the shield plugs. The emissivity of the heavily oxidized top and bottom surfaces of the fuel assemblies are considered to be 0.9.

The material properties of Al-1100 are considered for the rail inserts and back plates in the DSC model. Alternately, Al-6061 can be used to fabricate these components.

The DSC model is modified to evaluate the thermal effects of using alternate material Al-6061. The conductivity of rail inserts and back plate is changed from Al-1100 to Al-6061 in the modified model. All other material properties and boundary conditions remain unchanged. The results are discussed in Section 4.3.2.

Steady State Boundary conditions for the DSC Model

The nodal temperatures of the DSC shell are retrieved from the transfer cask or HSM-H models described in Sections 4.3.1.1 and 4.3.1.2, and applied to the corresponding nodes in the DSC model via a macro described in Appendix 4.16.1.

The SOLID70 elements representing the homogenized fuel are given heat generating boundary conditions in the region of the active fuel length. Active fuel length is considered to be 144" [20] beginning at approximately 4.0" above the bottom of the fuel assembly [20]. Fuel assembly has a total length of 162" in the model. Peaking factors to apply the axial decay heat profile for the homogenized fuel region are calculated in Section 4.7.

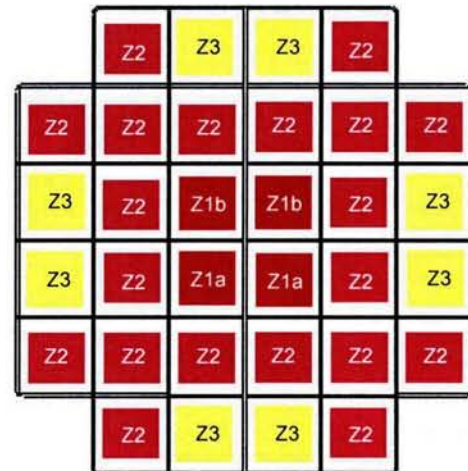
The maximum heat load per canister is 33.8 kW for CE 14x14 fuel assemblies and 34.8 kW for other fuel assemblies. Since CE 14x14 fuel assembly has a shorter active fuel length than the other assemblies, a lower total heat load is considered for CE 14x14 assembly to avoid a high heat generating rate. The maximum decay heat per assembly is 1.5 kW. Heat load zoning, as illustrated below, is used to maximize the number of higher heat load assemblies per DSC. The loading requirements are as follows.

For CE 14x14 Assemblies

- Q_{zi} is the maximum decay heat per assembly in zone i
- Total Decay Heat ≤ 33.8 kW
- 4 fuel assemblies in zone 1 with $Q_{z1} \leq 0.775$ kW
- 20 fuel assemblies in zone 2 with $Q_{z2} \leq 1.068$ kW
- 8 fuel assemblies in zone 3 with $Q_{z3} \leq 1.5$ kW

For other fuel Assemblies

- Q_{zi} is the maximum decay heat per assembly in zone i
- Total Decay Heat ≤ 34.8 kW
- 4 fuel assemblies in zone 1 with
 - total decay heat ≤ 3.2 kW
 - $Q_{z1a} \leq 1.05$ kW in the lower compartments
 - $Q_{z1b} \leq 0.8$ kW in the upper compartments
- 20 fuel assemblies in zone 2 with $Q_{z2} \leq 1.1$ kW
- 8 fuel assemblies in zone 3 with $Q_{z3} \leq 1.5$ kW



Heat generation rates as a function of spent fuel parameters are calculated in Appendix 4.16.2. Five extreme loading configurations are considered to bound the maximum component temperatures. The loading configurations are shown in Figure 4-15. In the first configuration, the heat load in the core compartments is maximized, so that zone 1 has a uniform heat load of 0.8 kW per assembly and zone 2 has a heat load of 1.1 kW per assembly. Since the total heat load is limited to 34.8 kW, the heat load of zone 3 is 1.2 kW per assembly.

The heat load in the peripheral compartments is maximized in loading configuration 2, so that zone 3 has a heat load of 1.5 kW per assembly and zone 2 has a heat load of 1.1 kW per assembly. Since the total heat load is limited to 34.8 kW, the heat load of zone 1 is 0.2 kW per assembly. A heat load of 0.2 kW per assembly for a fuel assembly in zone 1 is rather unrealistic. To have a more realistic estimation of maximum component temperatures loading configuration 3 is considered, in which zone 1 has a heat load of 0.55 kW per assembly and zone 3 has a heat load of 1.5 kW per assembly. Zone 2 is divided into two subdivisions. The first subdivision includes the fuel assemblies around the central assemblies with a heat load of 0.925 kW per assembly and the second subdivision located at the periphery has a heat load of 1.1 kW per assembly.

In loading configuration 4, the heat load in zone 1 and zone 3 are maximized, so that the central and peripheral compartments have maximum heat load. The heat load is 1.5 kW per assembly in zone 3 and 0.8 kW per assembly in zone 1. The remaining heat load is divided uniformly over assemblies in zone 2, which gives a heat load of 0.98 kW per assembly.

To investigate the effect of non-uniform loading in zone 1, loading configuration 5 is considered, in which the two lower compartments in zone 1 have a heat load of 1.05 kW per assembly. It gives a heat load of 0.55 kW per assembly for the two upper compartments in zone 1 based on the loading restrictions.

Similar to load configuration 1, the heat load in the core compartments is maximized for CE 14x14 assemblies in load configuration 6. The heat load of zone 3 is 1.17 kW per assembly.

Load configuration 7 is similar to configuration 4, the heat load in zones 1 and 3 are maximized to investigate the effect of the maximum heat load in zone 3 on the cladding temperature.

The sevenfive loading configurations discussed above are considered only for the maximum ambient temperature of 115°F during transfer operation. For the other conditions loading configuration 1 is evaluated, which gives the maximum DSC component temperatures for high enriched fuel assemblies in basket type I.

Heat generating rate for each segment of the active fuel region is calculated as follows:

$$\dot{q}''' = \frac{\left(\frac{Q}{4a^2 L_a} \right)}{0.984}$$

where

Q = Heat load per assembly defined for each loading zone

a = half width of fuel compartment = Width of the modeled fuel assembly = 8.7"/2 = 4.35"

L_a = Active fuel length = 137 for CE 14x14 / 144" for other assemblies

PF = Peaking Factor from Section 4.7

The area beneath the peaking factor curve shown in Section 4.7 is 0.984. The heat generating value is divided by this factor to avoid any reduction of the total heat load in the model. The total heat load applied in the model is verified by retrieving the reaction solution from the solved model and comparing it to the maximum heat load value. Typical applied boundary conditions are shown in Figure 4-16

4.3.2 Maximum Temperatures for Normal and Off-Normal Conditions

Steady state thermal analyses are performed using the maximum decay heat load of 34.8 kW (33.8 kW for CE 14x14) per canister, 115°F ambient temperature, and the maximum insolation per reference [17]. Insolation is averaged over a 12 hour period for transfer conditions and over a 24 hour period for storage conditions.

The temperature distributions within the TC, the HSM-H, and the DSC models are shown in Figures 4-17 to 4-23. Summaries of the maximum component temperatures are listed in Tables 4-1 and 4-2. The maximum component temperatures for 34.8 kW heat load bounds the temperatures calculated for 33.8 kW heat load as shown in Table 4-1.

The maximum basket component temperatures for normal and off-normal storage conditions in Table 4-2 and Table 4-4 are calculated based on DSC shell temperature profiles with the maximum temperature of 422°F and 319°F for off-normal hot and cold conditions, respectively. These maximum temperatures bound the maximum DSC shell temperatures resulted for HSM-H with stainless steel heat shields. Therefore, the maximum basket component temperatures including the maximum fuel cladding temperatures reported in Table 4-2 and Table 4-4 are the bounding temperatures for all HSM-H variations discussed in Section 4.3.1.2.

As seen from Table 4-2, using Al-6061 instead of Al-1100 for rail inserts and back plates increases the maximum cladding temperature by 4 °F. The temperature increase for the basket components due to use of Al-6061 is bounded by 4 °F as well.

The maximum temperatures calculated for off-normal conditions bound the values for the normal conditions. Therefore, thermal stress and DSC internal pressures for both normal and off-normal conditions are calculated based on the temperatures resulted from the maximum off-normal conditions (115°F ambient) for conservatism.

4.3.3 Minimum Temperatures for Normal and Off-Normal Conditions

Temperature distributions under the minimum ambient temperatures of -20°F with no insolation and the maximum design heat load are determined under steady state conditions to maximize the temperature gradients in the TC, the HSM-H and the DSC. Figures 4-24 and 4-25 show the temperature distributions for transfer operations and storage conditions at -20°F respectively. Tables 4-3 and 4-4 summarize the results of these analyses.

The resultant DSC and transfer cask temperatures for the -20°F ambient during transfer and storage are used to calculate the thermal stresses for the normal conditions at 0°F ambient.

4.3.4 Maximum Internal Pressures for Normal and Off-Normal Conditions

Maximum internal pressure within the NUHOMS®-32PTH DSC is calculated in Section 4.6.

4.3.5 Maximum Thermal Stresses for Normal and Off-Normal Conditions

Maximum thermal stresses during normal and off-normal conditions of storage and transfer are calculated in Chapter 3.

4.3.6 Evaluation of Thermal Performance for Normal and Off-Normal Conditions

The thermal analysis for normal and off-normal conditions of transfer and storage concludes that the NUHOMS®-32PTH System design meets all applicable requirements.

The maximum component temperatures calculated using conservative assumptions are lower than the allowable limits. The maximum TC seal temperature (255°F / 124°C) during off-normal transfer conditions is well below the 400°F long-term limit specified for continued seal function. The maximum solid neutron shield temperature (265°F / 129°C) is below allowable limit of 300°F (149°C) and no degradation of the solid neutron shielding material is expected. The maximum pressure within the neutron shielding panel (38.5 psia / 23.8 psig) corresponding to the average temperature of the liquid neutron shield (265°F / 129°C) is below the set point of the pressure relief valve (54.7 psia / 40 psig).

For all the side heat shield configurations, the maximum local temperature of the HSM-H concrete structure is lower than 300°F as required in [22]. The concrete structure of the HSM-H is made using Type II cement with fine aggregates satisfying ASTM C33 or equivalents as defined in NUREG-1536 [22].

The calculated maximum fuel cladding temperature is lower than the temperature limit of 752°F (400°C) considered for normal conditions of storage and short-term operations in [2]. The comparison of the resultant maximum temperatures with the allowable limits is listed below:

Component	Transfer Conditions ¹	Allowable / Design Limit
Cask Lid Seal	205°F	400°F
Cask Bottom Plate Seal	190°F	400°F
Lead	337°F	621°F
Liquid Neutron Shield (Temp / Press)	265°F / 23.8 psig	45 psig
Solid Neutron Shield	213 °F	300°F
Fuel Cladding	727°F	752°F

Component	Storage Conditions ¹	Allowable / Design Limit
Concrete in module with finned aluminum side heat shields @ 34.8 kW	213°F	300°F
Concrete in module with flat stainless side heat shields @ 34.8 kW	248°F	300°F
Concrete in module with un-finned aluminum side heat shields @ 32.0 kW	219°F	300°F
Concrete in module with un-finned galvanized steel side heat shields @ 26.1 kW	213°F	300°F
Fuel Cladding @ 34.8 kW	684°F	752°F for normal conditions / 1058°F for off-normal conditions

The maximum DSC internal pressures for normal and off-normal storage conditions are 5.9 and 10.7 psig respectively. The maximum DSC internal pressure for normal transfer conditions is 6.4 psig and for off-normal transfer conditions is 11.2 psig. The DSC internal pressures are lower than the design pressure limits of 15 psig for normal and 20 psig for off-normal storage and transfer conditions.

¹ The TC and HSM-H models are run only with off-normal conditions at 115°F ambient. The resultant temperatures are used to evaluate the thermal performance for both normal and off-normal conditions. The fuel cladding temperature remains in all cases below the normal allowable limit of 752°F.

4.4 Thermal Evaluation for Accident Conditions

Three hypothetical accident cases during transfer operation are relevant for thermal evaluation:

- Loss of the TC liquid neutron shield due to damages on the shielding panel
- Loss of helium gas in annulus between the DSC and the TC
- Postulated fire engulfing the TC

It is considered in all the above cases that the transfer cask contains a fully loaded DSC. The fire accident is postulated in which maximum amount of 300 gallons of diesel fuel is spilled onto the ground in such a way as to completely engulf the transfer cask. Subsequent to the fire accident, it is assumed that the seals for the TC lid and the bottom cover plate will burn, and the liquid neutron shield will be released and evaporates completely. Therefore, the fire accident scenario bounds the loss of liquid neutron shield and the loss of helium gas in the accident cases. The fire accident case is analyzed to give the bounding fuel cladding temperature for the transfer accident cases.

Since the HSM-H is located outdoors, there is a remote probability that the air inlet and outlet openings will become blocked by snow or by debris from events such as flooding, high wind, and tornados. The perimeter security fence around ISFSI and the location of the air inlet and outlet openings reduces the probability of such an event. Nevertheless, it is conservatively considered in this analysis that all the inlet and outlet openings become blocked.

The thermal mass of the HSM-H, the construction of the vent openings, and the location of the fuel on the transfer vehicle limit the effect of a fire accident for the HSM-H. Therefore, the worst case fire accident is bounded by the fire accident case during transfer operation.

A new model is developed to evaluate the fire accident case during transfer operation. The HSM-H model described in Section 4.3 is slightly modified to evaluate the blocked vent accident case during storage. The DSC model is unchanged for this evaluation. Details of the models are discussed in section 4.4.1.

4.4.1 Thermal Models for Accident Conditions

4.4.1.1 Transient Transfer Cask Model

To determine the temperature distribution in the transfer cask and the DSC for fire accident case, a three dimensional model is developed using ANSYS [16]. This model is created by selecting the nodes and elements of the DSC model described in Section 4.3 at z-axis from 56.06" to 86.07". The shells of TC including the annulus are then modeled around the DSC using SOLID70 elements. LINK31 elements are created using the same methodology as described in Section 4.3.1.1 to simulate the radiation between the DSC shell and the TC inner shell. The three dimensional model represents a slice of the DSC within the transfer cask. The TC slice model is shown in Figure 4-26. Axial length of the slice model is 30".

The insolation on the HSM-H surfaces exposed to the ambient and the soil temperature are applied also in the same way as described in Section 4.3.1.2. Uniform heat generating boundary conditions are applied over the elements representing the homogenized basket. The heat generating rate for the basket elements is calculated as follows.

$$\text{Heat generating rate} = \frac{Q}{\left(\frac{\pi}{4} D_i^2 L\right)} = 0.1945 \quad \text{Btu/hr-in}^3$$

where,

Q = total decay heat load = 34.8 kW = 118748 Btu/hr

Di = inner DSC diameter = 68.75"

L = DSC cavity length = 164.5"

During the blockage of the vents, air within the HSM-H cavity is trapped. The convection heat transfer under these circumstances reduces to free convection in closed cavities. However, closed cavity convection is conservatively ignored and all convection boundary conditions within the HSM-H cavity are removed. Only the conductivity of air is considered for this analysis. The effect of the thermal radiation exchange between the top heat shield and the DSC is studied to calculate the bounding component temperatures for the blocked vent conditions.

The DSC shell temperatures are retrieved from the transient HSM-H model and applied as steady state boundary conditions to the 32PTH DSC model. This methodology over predicts the fuel cladding temperature since the fuel assemblies heat up faster than the DSC shell. The heat generating rates and peaking factors for the homogenized fuel regions in the DSC model are calculated in the same way as described in 4.3.1.3. The maximum decay heat load of 34.8 kW and loading configuration 1 (Figure 4-15) are considered for this evaluation. The DSC temperatures for 34.8 kW decay heat load bound the temperatures for lower decay heat loads of 32.0 and 26.1 kW cases.

4.4.2 Maximum Temperatures for Accident Conditions

The maximum component temperatures resulted from the transient run of the transfer cask model are listed in Table 4-5. Figure 4-28 shows the temperature distributions for the transfer cask fire accident. The temperature-time histories of major components in the transfer cask OS187H during fire accident are shown in Figure 4-29.

The transient model of the HSM-H simulates 36 hours of the blocked vents accident case. 34 hours after complete blockage of the inlet and outlet vents, the maximum concrete temperature rises to 364°F for the HSM-H equipped with finned aluminum side heat shields and to 377°F for the HSM-H equipped with flat stainless steel heat shields. Since lower heat loads are specified for the HSM-H with un-finned side heat shields (aluminum or galvanized steel), it takes longer than 34 hours of vent blockage until the maximum concrete temperature of these modules exceed the above temperature. Typical temperature distributions for the HSM-H model during blockage of the vents are shown in Figure 4-30.

The DSC shell temperatures at 34 hours after blockage of the vents are retrieved from the transient model and applied as steady-state boundary conditions to the DSC model. The typical resultant temperature distributions are shown in Figure 4-32.

The maximum component temperatures for the blocked vent cases are listed in Table 4-6. Since the DSC shell temperature resulted for HSM-H with finned aluminum side heat shields is higher, the maximum basket component temperatures including the maximum fuel cladding temperature are bounded by this case. Figure 4-33 shows the temperature-time history of major components in the HSM-H during blockage of the vents, for the bounding case.

4.4.3 Maximum Internal Pressures for Accident Conditions

Maximum internal pressure within the NUHOMS®-32PTH DSC is calculated in section 4.6.

4.4.4 Maximum Thermal Stresses for Accident Conditions

Maximum thermal stresses during accident conditions of storage and transfer are calculated in Chapter 3.

4.4.5 Evaluation of Thermal Performance for Accident Conditions

The thermal analysis for the accident conditions during storage or transfer operation concludes that the NUHOMS®-32PTH System design meets all applicable requirements.

The conservative model of the transfer cask for the fire accident case shows that the maximum fuel cladding temperature does not exceed 1036°F. This maximum temperature is lower than the allowable limit of 1058°F.

The maximum fuel cladding temperature after blockage of the vents for 34 hours is 823°F in the HSM-H with the design basis heat load of 34.8 kW. This temperature is well below the maximum allowable limit of 1058°F set for fuel cladding in accident conditions.

The analysis for the blocked vent accident conditions limits the block vent duration to 34 hours. This time limit is adequate for a combination of inspection and reaction times to remove any vent blockage. Since the maximum concrete temperature is higher than 350°F suggested in reference [21], the strength of the concrete structure will be verified by a test as described in Chapter 12.

The maximum DSC internal pressure 34 hours after blockage of the HSM-H vents is 14.1 psig, which is lower than the design pressure of 70 psig. The maximum DSC internal pressure for fire accident case during transfer operation is 91.0 psig, which is well below 120 psig design pressure considered for the transfer accident cases.

4.6 Maximum Internal Pressure

The following methodology is used to determine the maximum pressures within the 32PTH DSC during storage and transfer conditions:

- Average cavity gas temperatures are derived from component temperatures.
- The amount of helium present within the canister after the initial backfilling is determined via the ideal gas law.
- The total amount of free gas within the fuel assemblies, including both fill and fission gases, is calculated based on data reported in [28].
- The amount of released gas from the fuel rods into the DSC cavity is determined based on the maximum fraction of the ruptured fuel rods considered in NUREG 1536 [22].
- The amount of helium gas is added to the amount of released gases to make the total amount of gases in the 32PTH DSC cavity.
- Finally, the maximum cavity pressures are determined via the ideal gas law.

The design pressures for the NUHOMS®-32PTH DSC are summarized in the following table.

Condition	Maximum Allowable Pressure For Storage (psig)	Maximum Allowable Pressure for Transfer (psig)
Normal	15	15
Off-Normal	20	20
Accident	70	120

Based on the ideal gas law, the internal pressure of the DSC increases as the average gas temperature increases. Since the DSC normal operating temperatures are bounded by the off-normal temperatures, the maximum internal pressure of the DSC is conservatively calculated based on the off-normal temperatures for both the normal and the off-normal conditions. The average cavity gas temperatures are calculated for transfer and storage conditions with 34.8 kW, which give the bounding maximum component temperatures. (See Table 4-1 and Table 4-2.)

The maximum fractions of the fuel rods that can rupture and release their free gases to DSC cavity for normal, off-normal, and accident cases are 1, 10, and 100% respectively as considered in NUREG 1536 [22].

4.6.1 Average Gas Temperature

To determine the average gas temperature, volume average temperatures of the elements representing the helium gaps (T_{void}) and the homogenized fuel assemblies (T_{fuel}) are calculated discretely from the thermal models. Although the average temperature of the homogenized fuel elements includes the fuel rods and the helium gas between them, this average temperature is considered as the average gas temperature within fuel compartments. The following volumes are considered to calculate the gas average temperature:

$$\begin{aligned}
 \text{Gas volume in the fuel compartments} &= \text{Volume of the fuel compartments} - \text{Volume of the fuel rods} \\
 \text{Volume of the fuel compartment} &= 8.7 \times 8.7 \times 162 \times 32 = 392,377 \text{ in}^3 \\
 \text{Volume of the fuel rods} &= 148,488 \text{ in}^3 \quad [\text{Chapter 3}] \\
 \text{Gas volume in the fuel compartments (V}_{\text{He,comp}}) &= 243,889 \text{ in}^3
 \end{aligned}$$

Gas volume in the void space of DSC = Total DSC cavity volume – Gas volume in the fuel compartments
 Total DSC cavity volume (V_{cavity}) = 308,146 in³ [Chapter 3]
 Gas volume in fuel compartments = 243,889 in³
 Gas volume in void space of DSC (V_{void}) = 64,257 in³

The average gas temperature in the 32PTH DSC is calculated as follows:

$$\bar{T}_{DSC} = \frac{T_{\text{avg, fuel}} \times V_{\text{He, comp}} - T_{\text{avg, void}} \times V_{\text{void}}}{V_{\text{cavity}}}$$

For an average gas temperature, the mass and volume average temperatures are equal. The results are summarized below.

Operating Condition		$\bar{T}_{DSC} (^{\circ}F)$
Storage	Normal	515
	Off-Normal	515
	Accident ⁷	647
Transfer	Normal	537
	Off-Normal	537
	Accident ⁸	961

Using Al-6061 instead of Al-1100 for rail inserts and back plates increases the DSC component temperature by at most 4 °F as discussed in Section 4.3.2. As noted in Table 4-2, the DSC component temperatures for normal and off-normal storage conditions are based on maximum DSC shell temperature of 422°F instead of 407°F for conservatism. This conservatism compensates more than adequate the temperature increase due to use of Al-6061. Therefore, the average gas temperatures in the above table remain bounding for storage conditions.

The temperature increase of 4°F for transfer conditions results in an increase of at most 0.3% for absolute average gas temperature within DSC cavity.

$$\text{Temp. Increase / Absolute Fuel Cladding Temp. [Table 4-2]} = 4/(723 + 460) = 0.3\%$$

4.6.2 Amount of Initial Helium Backfill

The initial helium fill pressure within the canister is 2.5±1.0 psig after vacuum drying. An initial pressure of 3.5 psig (18.2 psia) is considered here to maximize the amount of helium gas. The finite element model developed to analyze the vacuum drying process (Section 4.5.1) is run for steady state conditions with helium atmosphere to consider the minimum initial DSC temperature before backfilling, which gives the maximize amount of initial helium gas. Procedure A for vacuum drying (circulation of cool water around DSC) is considered in this run to have the lowest DSC temperature after vacuum drying. The average gas temperature is then calculated using the same methodology described in section 4.6.1. The initial temperature of the backfill gas within the canister is 469°F.

⁷ After 48 hours of vent blockage

⁸ At the end of cool down period, 120 hours after beginning of the fire

From the backfill pressure and initial backfill gas temperature, the amount of helium backfill gas can be calculated using the ideal gas law.

$$n = \frac{PV}{RT}$$

P = maximum initial canister fill pressure = 18.2 psia

V = DSC cavity volume (loaded) = 308,146 in³ = 178.3 ft³ [Chapter 3]

T = initial fill temperature = 469°F = 929 R

R = universal gas constant = 10.730 psia-ft³/lbmoles-R [3]

$$n_{\text{back}} = 0.326 \text{ lb-moles}$$

4.6.3 Free Gas within Fuel Assemblies / BPRA

Maximum volume of free gas per assembly is bounded by WE 15x15 fuel assembly with 204 fuel rods for burnup rates from 35,000 to 55,000 MWd/MTU as concluded in [28]. The reported total free gas volumes from reference [28] are extrapolated to evaluate the free gas volume at the maximum design burnup rate of to 60,000 MWd/MTU. Figure 4-38 illustrates this extrapolation. Based on extrapolation results, the total free gas volume at 60,000 MWd/MTU burnup rate is 1123 cc per fuel rod at standard pressure and temperature (0°C and 760 mmHg). The amount of free gases in the fuel rods based on the ideal gas law is then:

$$\begin{aligned} n_{\text{fuel}} &= (204 \text{ rods/assy})(32 \text{ assy})[(760 \times 1123/1000)/(62.361 \times 273.15)] (2.2046\text{E-}3 \text{ lbm/g}) \\ &= 0.721 \text{ lbmoles} \end{aligned}$$

$$\text{with } R = 62.361 \text{ (mmHg-lit/gmoles-K)}$$

Customer supplied data [29] states that the Westinghouse BPRA has the largest displacement volume and the most amount of free gas among the applicable BPRA types. The amount of free gas in each BPRA rod is 2.0E-4 lbmoles per reference [29].

The amount of free gas in the BPRA rods is:

$$\begin{aligned} n_{\text{BPRA}} &= (2.0\text{E}4 \text{ lbmole/rod})(20 \text{ rod/assy})(32 \text{ assy}) \\ &= 0.128 \text{ lbmoles} \end{aligned}$$

Total amount of free gas is:

$$n_{\text{free}} = n_{\text{fuel}} + n_{\text{BPRA}}$$

4.6.4 Total Amount of Gas within DSC

The total amount of gas within the DSC is equal to the amount of the initial helium backfill gas plus any free gases within the ruptured fuel assembly rods or BPRA. All free gases within the ruptured fuel rods/BPRAs will be released into the canister. It is assumed that the fractions of the ruptured BPRA rods are the same as those considered for the fuel rods, i.e., 1, 10, and 100% for normal, off-normal, and accident case respectively.

Total amount of free gas released to the DSC cavity is:

$$n_{\text{total}} = n_{\text{back}} + f_B (n_{\text{free}})$$

n_{total} = total amount of gas (lbmoles)
 f_B = fraction of the ruptured fuel rods

4.6.5 Maximum DSC Internal Pressures

Displacement volume of the BPRA is 480 in³ per reference [29]. Maximum DSC internal pressures are determined via the ideal gas law:

$$P = (n_{\text{total}} R \bar{T}_{\text{DSC}}) / V$$

P = pressure (psia)
 V = Cavity volume = 178.3 (ft³) without BPRAs
 V = Cavity volume – BPRA volume = (308,146 – 32*480)/12³ = 169.4 (ft³) with BPRAs
 R = universal gas constant = 10.73 (psia-ft³/lbmoles-R)

The results are summarized in Table 4-10.

The temperature increase of 0.3% for transfer conditions discussed in Section 4.6.1 due to use of Al-6061 for rail inserts and back plates increases the DSC internal pressure by the same ratio according to the above equation. This small increase remains bounded by the design pressures in Table 4-10.

4.6.6 Maximum Pressure in Annulus

The pressure in the annulus between the transfer cask and the DSC is calculated using the ideal gas law:

$$P_{\text{ann}} = P_{\text{init}} \frac{T}{T_{\text{init}}}$$

P_{ann} = Annulus pressure (psia)
 P_{init} = initial pressure = 3.0 psig = 16.7 psia
 T = annulus average temperature (R)
 T_{init} = annulus initial temperature = 70°F = 530 R

Average annulus temperature is the volume average temperature of the annulus elements retrieved from the transfer cask model. The results are summarized below.

Transfer Condition	\bar{T}_{ann} (°F)	P_{ann} (psia)	P_{ann} (psig)
Normal and Off-Normal	349	27.0	12.3
Accident	682	38.1	23.4

$$Nu_{l,H} = \frac{0.527 Ra^{1/5}}{[1 + (1.9/Pr)^{9/10}]^{2/9}}$$

$$Nu_l = \max[Nu_{l,V}, Nu_{l,H}] \quad \text{Nusselt number for laminar flow}$$

$$Nu_t = C_t Ra^{1/3} \quad \text{Nusselt number for turbulent flow with}$$

$$C_t = C_t^V \cos^{1/3} \phi \quad \text{for} \quad -90^\circ \leq \phi \leq \tan^{-1} \left(\frac{C_t^V}{C_t^H} \right)^3$$

$$C_t = C_t^H \sin^{1/3} \phi \quad \text{for} \quad \tan^{-1} \left(\frac{C_t^V}{C_t^H} \right)^3 \leq \phi \leq 90^\circ$$

$$\text{with} \quad C_t^V \approx \frac{0.13 Pr^{0.22}}{(1 + 0.61 Pr^{0.81})^{0.42}}$$

$$C_t^H \approx 0.14 \quad \text{for} \quad Pr < 100$$

$$Nu = [(Nu_t)^m + (Nu_l)^m]^{1/m} \quad \text{with} \quad m = 6 \quad \text{for} \quad 1 < Ra < 10^{12}$$

$$h_c = \frac{Nu k}{L} \quad \text{with}$$

L = length of the inclined plate

k = air conductivity

The above correlations are incorporated in ANSYS [16] model via macro "HC_IPLD.mac" listed in Appendix 4.16.1.

4.11.2.7 Convection Coefficient for the Louvered Top Heat Shield

The louvered top shield consists of six pieces each containing 70 inclined plates. Because of the relatively large opening between the plates and their short length, the interference of the thermal boundary layers is minimal, so that a convection coefficient can be calculated separately for each plate as follows.

h_{up} = convection coefficient on upper surface of louver plates (positive angled)

h_{down} = convection coefficient on lower surface of louver plates (negative angled)

h_{up} and h_{down} are calculated using the correlations described in Sections 4.11.2.5 and 4.11.2.6 for inclined plates. The above correlations are incorporated in ANSYS [16] model via macro "HC_LL.mac" listed in Appendix 4.16.1.

The average bulk temperature (T_{mean}) is calculated as follows to use for the convection boundary conditions within the HSM-H cavity.

$$T_{\text{mean}} = (T_c + T_{\text{exit}})/2$$

The temperature of the air leaving region 8 is equal to the exit air temperature.

The HSM-H is divided into three following sections to calculate the dynamic loss coefficients.

- 1: from air entrance opening to the inlet vent at the lower part of the HSM-H sidewall
- 2: HSM-H cavity from inlet opening to outlet opening
- 3: from outlet opening at the upper part of the HSM-H sidewall to the exhaust opening on the roof.

Each section is divided into subsections. Hydraulic loss coefficients in subsections are calculated using corresponding correlations from [35] and [36]. Serial loss coefficients of subsections are

added together to make the equivalent total loss coefficient ($\sum \frac{K_{Ei}}{A_{Ei}^2}$). For calculation of the

equivalent loss coefficient for parallel flow paths see footnote on Table 4-21. Table 4-21 summarizes the results for 34.8 kW decay heat load for both HSM-H with louvered top heat shield and finned aluminum side heat shields and for HSM-H with flat stainless steel top and side heat shields. The results for 32.0 kW and 26.1 kW decay heat loads are listed in Tables 4-22 and 4-23 respectively.

The concentration of the decay heat for the rubble fuels is maximized, when the rubble is compressed to a minimum height at one end of the fuel compartment.

To bound the maximum cladding temperature of the intact fuel assemblies, it is assumed that all the 16 damaged fuel assemblies transform to rubble. The cladding is considered as powder but the pellets are assumed to keep their shape in the rubble. An approximate void volume between the pellets can be evaluated considering the area ratio of the pellet cross-section to the square area with a width equal to the pellet outer diameter. The increased volume due to the void spaces between pellets is then:

$$\{(\text{OD}_{\text{pellet}}^2 - \pi \text{OD}_{\text{pellet}}^2 / 4) / (\pi \text{OD}_{\text{pellet}}^2 / 4)\} \times 100 = (4/\pi - 1) \times 100 = 27.32 \%$$

The minimum height of the fuel rubble is calculated as follows.

$$H_{\min} = \frac{V_{\text{UO}_2} \times 1.2732 + V_{\text{Zr4}}}{A}$$

where

A = cross-sectional area of the fuel compartment = $8.7 \times 8.7 = 75.69 \text{ in}^2$

V_{UO_2} = volume of fuel pellets from Section 4.8

V_{Zr4} = volume of fuel cladding from Section 4.8

Table 4-24 summarizes the calculation of H_{\min} for all the fuel types. The shortest height of 61" is used for the fuel rubble.

The thermal model of the transfer cask described in Section 4.3 is modified for the purpose of the evaluation. It is assumed that the seals of the transfer cask and the shielding shell will be damaged as a consequence of the hypothetical drop accident. In this event, the helium in the annulus and the water in the shielding shell will be released to the ambient. To evaluate the thermal effects of this accident, the transfer cask model developed in Section 4.3 is used to determine the DSC shell temperature when the DSC contains fuel rubble. Helium conductivity in the annulus is replaced with air conductivity. The effective conductivity in the shielding panel is also recalculated based on air properties.

To stabilize the ANSYS run and shorten the run time, the LINK31 elements simulating the radiation between the DSC and transfer cask are replaced with equivalent effective conductivity. Calculations of the effective conductivities for air in annulus and in the shielding shell are based on the methodologies described in Section 4.9. The equivalency of the applied effective conductivities to the radiation elements (LINK31) is verified by hand comparison of the maximum temperatures resulting from separate runs of the transfer cask slice model using LINK31 elements and equivalent effective conductivities.

Steady state boundary conditions are used to run the transfer cask model. Total heat load of 34.8 kW is applied uniformly on the DSC inner radial surface. The resultant DSC shell temperatures are transferred then to the DSC model to determine the maximum fuel temperature for this accident case.

4.15 References

1. Cogema Logistics, Personnel Communication.
2. USNRC, SFPO, Interim Staff Guidance – 11, Rev. 3, “Cladding Considerations for the Transportation and Storage of Spent Fuel.”
3. Perry, R. H., Chilton, C. H., “Chemical Engineers’ Handbook,” 5th Edition, 1973.
4. USDOE, “Topical Report on Actinide-Only Burnup Credit for PWR Spent Nuclear Fuel Packages,” Department of Energy, Report No. DOE / RW0472, Rev. 2, 1998.
5. Rohsenow, W. M., Hartnett, J. P., Ganic, E. N. , “Handbook of Heat Transfer Fundamentals,” 2nd Edition, 1985.
6. ASME Boiler and Pressure Vessel Code, Section II, Part D, “Material Properties,” 1998 and 2000 addenda.
7. Issard, Herve, “ACL Progress on Boralyn Development,” Cogema Logistics presented in “Transnuclear Group Technical Exchange Meeting,” October 11, 2002.
8. Final Documentation Package TN-68, P.O. # EP-2001-022, Section G, “Thermal Conductivity Measurements of Borated Aluminum Specimens,” Rev. 0.
9. AAR Brooks & Perkins Advanced Structures Division, “Boral® The Neutron Absorber – Product Performance,” Report 624.
10. Zoldners, N. G., “Thermal Properties of Concrete under Sustained Elevated Temperatures,” ACI Publications, Paper SP 25-1, American Concrete Institute, Detroit, MI, 1970.
11. Cavanaugh, Kevin, “Guide to Thermal Properties of Concrete and Masonry Systems,” Reported by ACI Committee 122, Report # ACI 122R-02, American Concrete Institute, Detroit, MI, 2002.
12. Bentz, D. P., “A Computer Model to Predict the Surface Temperature and Time-of-wetness of Concrete Pavements and Bridge Decks,” Report # NISTIR 6551, National Institute of Standards and Technology, 2000.
13. Siegel, Robert, Howell, R. H., “Thermal Radiation Heat Transfer,” 4th Edition, 2002.
14. Azzazy Technology Inc., “Emissivity Measurements of 304 Stainless Steel,” Report Number ATI-2000-09-601, 2000.
15. Kreith, Frank, “Principles of Heat Transfer,” 3rd Edition, 1973.
16. ANSYS Computer Code and User’s Manuals, Rev. 6.0.
17. USNRC, Code of Federal Regulations, Part 71, “Packaging and Transportation of Radioactive Material,” 2003.
18. “ASHRAE Handbook Fundamentals,” 4th Edition, 1983.
19. Updated Final Safety Analysis Report, Standardized NUHOMS® Horizontal Modular Storage System for Irradiated Nuclear Fuel, Rev. 9, Feb. 2006.
20. Viebrock, J. M., Douglas, H. M., “Domestic Light Water Reactor Fuel Design Evolution,” Vol. III, Nuclear Assurance Corporation, 1981.
21. American Concrete Institute, “Code Requirements for Nuclear Safety Related Concrete Structures (ACI 349-97) and Commentary (ACI 349R-97),” 1997.
22. USNRC, SFPO, NUREG-1536, “Standard Review Plan for Dry Cask Storage Systems - Final Report,” 1997.
23. Gregory, J. J., Mata, R., Keltner, N. R., “Thermal Measurements in a Series of Long Pool Fires,” SANDIA Report, SAND 85-0196, TTC-0659, 1987.
24. Parker O-Ring Handbook, 5700, Y2000 Edition, 1999.

25. Transnuclear, Inc., "Thermal Testing of the NUHOMS® Horizontal Storage Module, Model HSM-H," Doc. No. E-21625, Rev. 1.
26. Chun, R., Witte, M., Schwartz, M., "Dynamic Impact Effects on Spent Fuel Assemblies," Lawrence Livermore National Laboratory, Report UCID-21246, 1987.
27. Young, W. C., "Roark's Formulas for Stress and Strain," 6th Edition, 1989.
28. Plannel, et al., "Extended Fuel Burnup Demonstration Program – Topical Report – Transport Considerations for Transnuclear Casks," DOE/ET 34014-11, TN-E4226, Transnuclear, Inc. 1983.
29. Brookmire, et al., "Storage of Burnable Poison Rod Assemblies and Thimble Plug Devices in Dry Storage Casks Surry ISFSI," NE-1162, Rev. 0, 1998.
30. Oak Ridge National Laboratory, RSIC Computer Code Collection, "SCALE, A Modular Code System for Performing Standardized Computer Analysis for Licensing Evaluation for Workstations and Personal Computers," NUREG/CR-0200, Rev. 6, ORNL/NUREG/CSD-2/V3/R6.
31. USNRC, SFPO, NUREG/CR-0497, "A Handbook of Materials Properties for Use in the Analysis of Light Water Reactor Fuel Rod Behavior," MATPRO - Version 11, EG&G Idaho, Inc., TREE-1280, 1979.
32. SANDIA Report, SAND90-2406, "A Method for Determining the Spent Fuel Contribution to Transport Cask Containment Requirements," 1992.
33. Diament, R.M.E., "Thermal and Acoustic Insulation," 1986.
34. Kreith, Frank, "The CRC Handbook of Thermal Engineering," 2000.
35. "ASHRAE Handbook, Fundamentals," – SI Edition, 1997.
36. I.E. Idelchik, "Handbook of Hydraulic Resistance," 3rd Edition, 1994.

Table 4-1
Maximum Component Temperatures during Transfer Operations at 115°F ambient

Component	Maximum Temperature 34.8 kW (°F)	Allowable Maximum Temperature (°F)
DSC shell	475	
Cask inner shell	340	
Lead gamma shielding	337	621 [3]
Cask structural shell	280	
Neutron shield panel	263	
Cask lid inner plate *	275	
Cask lid outer plate	217	
Solid neutron shield	265	300 [1]
Cask lid seal †	240	400 [24]
Bottom plate seal ‡	255	400 [24]
Liquid neutron shield (Bulk temperature) §	265	286.9 **
Liquid neutron shield (Maximum temperature)	275	

	Maximum Temperature (°F) 34.8 kW						Allowable Max. Temp. (°F)
Basket Type	Type I				Type II		
Component	Conf. # 1	Conf. # 2	Conf. # 3	Conf. # 4	††	‡‡	
Fuel cladding	719	705	700	715	723	727	752 [2]
Fuel compartment	693	667	673	689	697	700	
Basket Al plates	692	666	672	688	696	699	
Basket rails	561	559	559	558	561	565	

	Maximum Temperature (°F) 33.8 kW for CE 14x14 Fuel Assembly		Allowable Max. Temp. (°F)
Basket Type	Type I		
Component	Configuration # 6	Configuration # 7	
Fuel cladding	717	712	752 [2]
Fuel compartment	689	685	
Basket Al plates	689	684	
Basket rails	555	552	
DSC Shell	467	467	

* Temperatures of cask lid, solid neutron absorber, and seals are from the transfer cask sub-models.

† Maximum temperature of cask body at seal location

‡ Maximum temperature of ram access ring at seal location

§ Bulk temperature is the volumetric average temperature of the elements in shielding segments 8 and 9, see Figure 4-2.

** 286.9°F is the saturated water temperature at 40 psig.

†† Conf. #1 with Al-1100 for rail inserts and back-plates

‡‡ Conf. #1 with Al-6061 for rail inserts and back-plates

Table 4-2
Maximum Component Temperatures for Storage Conditions at 115°F ambient

HSM-H with Finned Aluminum Side Heat Shields		
Component	Maximum Temperature @ 34.8 kW (°F)	Allowable Max. Temp. (°F)
Fuel cladding	684*	752 [2]†
Fuel compartment	656	
Basket Al plates	655	
Basket rails	511	
DSC shell	407	
Concrete structure	213	300‡
Top heat shield	199	
Side heat shield	188	
DSC supporting structure	268	

	Flat Stainless Side Heat Shields @ 34.8 kW	Un-finned Aluminum Side Heat Shields @ 32.0 kW	Un-finned Galvanized Steel Side Heat Shields @ 26.1 kW	
Component	Maximum Temperature (°F)	Maximum Temperature (°F)	Maximum Temperature (°F)	Allowable Max. Temp. (°F)
Fuel cladding	§	§	§	752 [2]
DSC shell	420	394	368	
Concrete structure	248	219	213	300
Top heat shield	245	196	186	
Side heat shield	239	241	190	
DSC supporting structure	311	264	247	

* The fuel cladding temperature is calculated based on bounding DSC shell temperatures with the maximum temperature of 422°F.

† The ambient temperature of 115°F is the maximum off-normal temperature. Based on reference [2], maximum allowable fuel cladding temperature is 1058°F (570°C) for off-normal storage conditions and 752°F (400°C) for normal storage conditions. The maximum fuel cladding temperatures in Table 4-2 are all below 752°F.

‡ The cement type and concrete aggregates satisfy the guidelines in NUREG 1536, Section V.2 [22]

§ Bounded by 34.8 kW case in the upper part of the table

Table 4-3
Maximum Component Temperatures during Transfer Operations
at -20°F ambient

Component	Maximum Temperature (°F)
Fuel cladding	650
Fuel compartment	620
Basket Al plates	619
Basket rails	487
DSC shell	398
Cask inner shell	249
Lead gamma shielding	245
Cask structural shell	178
Neutron shield panel	157
Cask lid inner plate	76
Cask lid outer plate	65
Solid neutron shield	97
Cask lid seal	88
Cask bottom plate seal	70
Liquid neutron shield (Bulk temperature)	162
Liquid neutron shield (Maximum temperature)	172

Table 4-4
Maximum Component Temperatures for Storage Conditions
at -20°F ambient, 34.8 kW

Component	Maximum Temperature (°F) (Finned Aluminum Side Heat Shields)	Maximum Temperature (°F) (Flat Stainless Steel Side Heat Shields)
Fuel cladding*	596	†
Fuel compartment	565	†
Basket Al plates	564	†
Basket rails	418	†
DSC shell	292	306
Concrete structure	49	117
Top heat shield	50	91
Side heat shield	41	85
DSC supporting structure	135	183

* The fuel cladding temperature is calculated based on bounding DSC shell temperatures with the maximum temperature of 319°F.

† Bounded by the values for HSM-H with finned aluminum side heat shields since the maximum DSC shell temperature is lower than 319°F.

Table 4-5
Maximum Component Temperatures for Fire Accident Case
Transfer Cask, 34.8 kW

Component	Maximum Temperature (°F)	Time (hr)	Allowable Max. Temp. (°F)
Fuel cladding	1036	200	1058 [2]
Basket Al plates	1021	200	
Basket rails	878	200	
DSC shell	790	200	
Gamma shell (lead)	618	200	
Cask structural shell	553	200	
Shielding shell	598	0.25	

Table 4-6
Maximum Component Temperatures for Blocked Vent Accident Case

	HSM-H with Finned Aluminum Side Heat Shields, 34.8 kW	HSM-H with Flat Stainless Steel Heat Shields, 34.8 kW	
Component	Max. Temp (°F) 34 hours after complete blockage		Allowable Max. Temp. (°F)
Fuel Cladding	823	-	1058 [2]
Fuel Compartment	801	*	
Basket Al Plates	800	*	
Basket Rails	662	*	
DSC Shell	600	582	
Concrete Structure	364	377	350 [21] †
Top Heat Shield	366	431	
Side Heat Shield	471	385	
DSC support Str.	497	505	

* These temperatures are bounded by the values resulted for HSM-H with finned aluminum side heat shields.

† Capability of concrete will be verified at elevated temperatures above 350°F via test, see Chapter 12.

Table 4-10
32PTH DSC Internal Pressure

Operating Condition Without BPRA		n_{back}	f_B	n_{free}	n_{total}	\bar{T}_{DSC}	P_{DSC}		Design Pressure
		(lbmoles)	(---)	(lbmoles)	(lbmoles)	(°F)	(psia)	(psig)	(psig)
Storage	Normal	0.326	0.01	0.721	0.333	515	19.5	4.8	15
	Off-Normal	0.326	0.1	0.721	0.398	515	23.3	8.6	20
	Accident	0.326	0.1	0.721	0.398	647	26.5	11.8	70
Transfer*	Normal	0.326	0.01	0.721	0.333	537	20.0	5.3	15
	Off-Normal	0.326	0.1	0.721	0.398	537	23.9	9.2	20
	Accident	0.326	1.0	0.721	1.047	961	89.5	74.8	120

Operating Condition With BPRA		n_{back}	f_B	n_{free}	n_{total}	\bar{T}_{DSC}	P_{DSC}		Design Pressure
		(lbmoles)	(---)	(lbmoles)	(lbmoles)	(°F)	(psia)	(psig)	(psig)
Storage	Normal	0.326	0.01	0.849	0.334	515	20.6	5.9	15
	Off-Normal	0.326	0.1	0.849	0.411	515	25.4	10.7	20
	Accident	0.326	0.1	0.849	0.411	647	28.8	14.1	70
Transfer*	Normal	0.326	0.01	0.849	0.334	537	21.1	6.4	15
	Off-Normal	0.326	0.1	0.849	0.411	537	25.9	11.2	20
	Accident	0.326	1.0	0.849	1.175	961	105.7	91.0	120

* The average gas temperature within DSC cavity for transfer conditions increase by 0.3% if Al-6061 is used for rail inserts and back-plates as discussed in Section 4.6.1. The DSC absolute pressure will be increased by the same ratio. This small change remains bounded by the design pressures.

Table 4-11 – Concluded
Average Peaking Factors for Active Fuel Length of 137”

	Height from Bottom of Active Fuel (in)	P_i [4]	P_i (interpolated)	A_i	$P_{avg, i}$
1	0	0.000			
	5.5675		0.725	2.452	0.441
2	11.41	0.967			
	13		0.989	6.497	0.874
3	19.03	1.074			
	20.5675		1.080	7.877	1.041
4	26.63	1.103			
	34.25	1.108			
5	35.5675		1.108	16.500	1.100
6	41.87	1.106			
	49.47	1.102			
7	56.19		1.098	22.757	1.103
8	57.09	1.097			
	59.82		1.096	3.981	1.097
9	64.69	1.094			
	72.31	1.094			
10	73.01		1.094	14.435	1.094
11	79.91	1.095			
	87.53	1.096			
12	89.82		1.096	18.410	1.095
13	95.13	1.095			
	102.75	1.086			
14	104.82		1.079	16.366	1.091
15	110.37	1.059			
	114.5		1.011	10.207	1.054
16	117.97	0.971			
	119.82		0.914	5.183	0.974
17	125.59	0.738			
	131.25		0.532	8.362	0.732
18	133.19	0.462			
	137		0.000	1.845	0.321
19	137	0.000			

Table 4-13 – Concluded
Effective Fuel Properties for CE 14x14

Transverse Effective Fuel Conductivity in Helium

Fuel Type			CE 14x14	
T _o (°F)	T _c (°F)	T _{avg} (°F)	Q _{react} (Btu/hr-in)	k (Btu/hr-in-°F)
100	181	140	19.968	0.0182
225	291	258	19.969	0.0222
350	404	377	19.969	0.0271
475	519	497	19.970	0.0331
600	637	618	19.970	0.0402
725	755	740	19.970	0.0483
850	875	863	19.970	0.0577

Axial Effective Conductivity

Fuel type	CE 14x14
No of fuel rods	176
OD fuel rod (in)	0.440
Clad thickness (in)	0.028
No of guide tubes	5
OD guide tubes (in)	1.115
Wall thickness (in)	0.04
No of instrument tubes	---
OD instrument tube (in)	---
Wall thickness (in)	---
Fuel type	CE 14x14
Cladding area (in ²)	7.05
Compartment area (in ²)	75.69
Temperature (°F)	k-axial (Btu/hr-in-°F)
212	0.0610
392	0.0642
572	0.0682
752	0.0736
932	0.0808

Table 4-14 – Concluded
Effective Conductivity of Liquid Neutron Shielding – Sections 13 to 15

Ti	To	Tavg	Tavg	k	β	ν	Pr	C _l	Ra	Nu_COND	Nu _l	Nu	k _{eff}
(°F)	(°F)	(°F)	(K)	(W/m-K)	(1/K)	(m ² /s)	(--)	(--)	(--)	(--)	(--)	(--)	(Btu/hr-in-°F)
135	125	130	328	0.648	4.159E-04	5.171E-07	3.29	0.5883	5.938E+08	1.00	22.83	22.83	0.712
145	135	140	333	0.653	4.501E-04	4.815E-07	3.04	0.5852	6.846E+08	1.00	23.54	23.54	0.740
155	145	150	339	0.658	4.844E-04	4.460E-07	2.79	0.5819	7.880E+08	1.00	24.24	24.24	0.768
165	155	160	344	0.663	5.186E-04	4.104E-07	2.54	0.5780	9.066E+08	1.00	24.94	24.94	0.796
175	165	170	350	0.668	5.528E-04	3.749E-07	2.29	0.5737	1.044E+09	1.00	25.64	25.64	0.825
185	175	180	356	0.671	5.858E-04	3.552E-07	2.16	0.5712	1.162E+09	1.00	26.22	26.22	0.847
195	185	190	361	0.674	6.187E-04	3.355E-07	2.03	0.5684	1.291E+09	1.00	26.79	26.79	0.869
205	195	200	367	0.677	6.517E-04	3.158E-07	1.90	0.5654	1.436E+09	1.00	27.37	27.37	0.892
215	205	210	372	0.680	6.846E-04	2.962E-07	1.77	0.5622	1.597E+09	1.00	27.94	27.94	0.914
225	215	220	378	0.682	7.167E-04	2.802E-07	1.66	0.5593	1.755E+09	1.00	28.46	28.46	0.934
235	225	230	383	0.683	7.481E-04	2.681E-07	1.58	0.5570	1.906E+09	1.00	28.94	28.94	0.952
245	235	240	389	0.685	7.794E-04	2.559E-07	1.50	0.5545	2.069E+09	1.00	29.40	29.40	0.970
255	245	250	394	0.686	8.108E-04	2.437E-07	1.42	0.5518	2.246E+09	1.00	29.87	29.87	0.987
265	255	260	400	0.688	8.421E-04	2.315E-07	1.34	0.5490	2.439E+09	1.00	30.33	30.33	1.005
275	265	270	406	0.688	8.815E-04	2.231E-07	1.29	0.5471	2.647E+09	1.00	30.85	30.85	1.022
285	275	280	411	0.688	9.210E-04	2.147E-07	1.24	0.5451	2.870E+09	1.00	31.37	31.37	1.039
295	285	290	417	0.688	9.604E-04	2.063E-07	1.19	0.5430	3.111E+09	1.00	31.88	31.88	1.056
305	295	300	422	0.687	9.906E-04	1.990E-07	1.15	0.5411	3.325E+09	1.00	32.31	32.31	1.069

Table 4-15 – Concluded
Verification of the Calculated Effective Conductivities for Liquid Neutron Shielding

At -20°F Ambient Temperature

Sec. #	T _i	T _o	\bar{T}	\bar{T}	k	β	ν	Pr	C _l	Ra	Nu	Calculated k _{eff}	k _{eff} in Model	Diff. %
(---)	(°F)	(°F)	(°F)	(K)	(W/m-K)	(1/K)	(m ² /s)	(---)	(---)	(---)	(---)	(Btu/hr-in-°F)	(Btu/hr-in-°F)	(---)
1	100	90	95	308	0.623	2.11E-04	7.519E-07	5.04	0.6030	2.232E+08	18.35	0.551	0.674	22.4%
2	121	107	113	319	0.637	3.33E-04	6.117E-07	3.99	0.5952	5.807E+08	23.01	0.706	0.761	7.8%
3	138	124	130	328	0.648	4.19E-04	5.141E-07	3.27	0.5880	8.705E+08	25.15	0.785	0.762	2.9%
4	152	136	143	336	0.655	4.64E-04	4.672E-07	2.94	0.5839	1.134E+09	26.68	0.841	0.801	4.8%
5	161	145	152	340	0.659	4.94E-04	4.359E-07	2.72	0.5808	1.325E+09	27.59	0.876	0.827	5.5%
6	167	150	158	344	0.662	5.13E-04	4.162E-07	2.58	0.5787	1.457E+09	28.15	0.897	0.844	6.0%
7	170	153	161	345	0.664	5.24E-04	4.047E-07	2.50	0.5774	1.539E+09	28.48	0.910	0.854	6.2%
8	171	155	162	346	0.664	5.29E-04	3.992E-07	2.46	0.5767	1.580E+09	28.63	0.916	0.858	6.3%
9	172	155	163	346	0.665	5.30E-04	3.986E-07	2.46	0.5767	1.585E+09	28.65	0.917	0.859	6.3%
10	170	154	161	346	0.664	5.26E-04	4.028E-07	2.49	0.5772	1.554E+09	28.53	0.912	0.855	6.2%
11	168	151	159	344	0.663	5.17E-04	4.126E-07	2.56	0.5783	1.479E+09	28.24	0.901	0.847	6.0%
12	162	146	154	341	0.660	4.99E-04	4.311E-07	2.69	0.5803	1.293E+09	27.40	0.871	0.832	4.5%
13	153	138	145	336	0.655	4.68E-04	4.627E-07	2.91	0.5835	1.073E+09	26.26	0.829	0.753	9.1%
14	140	126	133	329	0.649	4.26E-04	5.065E-07	3.22	0.5874	8.544E+08	24.97	0.780	0.719	7.9%
15	122	110	116	320	0.639	3.44E-04	5.985E-07	3.90	0.5944	5.077E+08	22.18	0.682	0.712	4.4%
16	102	92	97	309	0.625	2.25E-04	7.357E-07	4.92	0.6023	2.361E+08	18.59	0.559	0.674	20.5%

Note: The applied k_{eff} values in the model for sections 1 and 16 at -20°F ambient are accepted, because these values are higher than the calculated values, which cause higher temperature gradient in the model for minimum ambient conditions.

Table 4-17 - Concluded
Effective Conductivity of Air within Shielding Panel during Cool Down Period – Verification

time	Ti*	To†	T _{avg} ‡	T _{avg}	k	β	ν	Pr	C _l	Ra	Nu	Calculated k _{eff} §	k _{eff} in Model**	Diff. %
(hr)	(°F)	(°F)	(°F)	(K)	(W/m-K)	(1/K)	(m ² /s)	(—)	(—)	(—)	(—)	(Btu/hr-in-°F)	(Btu/hr-in-°F)	(—)
0.26	370	559	456	509	0.041	120E-03	4.00E-05	0.69	0.513	1.86E+06	4.7	0.066	0.064	2.3%
1	356	255	308	427	0.035	2.4E-03	2.97E-05	0.69	0.513	2.18E+06	4.9	0.040	0.038	4.4%
2	352	227	292	418	0.035	2.4E-03	2.86E-05	0.69	0.513	2.97E+06	5.3	0.039	0.036	6.7%
5	357	219	290	417	0.035	2.4E-03	2.85E-05	0.69	0.513	3.30E+06	5.4	0.039	0.036	7.4%
10	378	227	305	425	0.035	2.4E-03	2.95E-05	0.69	0.513	3.29E+06	5.4	0.041	0.038	6.9%
15	399	235	320	433	0.036	2.3E-03	3.05E-05	0.69	0.513	3.27E+06	5.4	0.043	0.040	6.6%
20	415	243	333	440	0.036	2.3E-03	3.14E-05	0.69	0.513	3.22E+06	5.4	0.045	0.042	6.2%
50	491	277	391	473	0.039	2.1E-03	3.54E-05	0.69	0.513	2.92E+06	5.3	0.053	0.050	5.3%
80	521	292	415	486	0.039	2.1E-03	3.70E-05	0.69	0.513	2.76E+06	5.2	0.057	0.055	2.0%
120	535	299	426	492	0.040	2.0E-03	3.78E-05	0.69	0.513	2.68E+06	5.2	0.058	0.058	0.6%
175	540	302	430	494	0.040	2.0E-03	3.81E-05	0.69	0.513	2.65E+06	5.2	0.059	0.059	0.3%
200	540	302	430	495	0.040	2.0E-03	3.81E-05	0.69	0.513	2.65E+06	5.2	0.059	0.059	0.2%

*This value is the average temperature of the structural shell retrieved from the solid elements in the model

†This value is the average temperature of the shielding shell retrieved from the solid elements in the model

‡This value is the average temperature of the air within the shielding shell retrieved from the model

§This value is calculated using the correlations discussed in Section 4.9.

**This value is resulted from interpolation between the values used in the ANSYS model

Table 4-20

, TABLE IS DELETED IN ITS ENTIRETY

Table 4-21
Summary of the Energy-Hydraulic Calculation Results for 34.8 kW
(HSM-H with Finned Aluminum Side Shields)

Section	No. of Flow Paths	Subsection	Type of Flow Resistance	Ref.	K_{Ei} at 115°F	K_{Ei} at -20°F	$\Sigma(K_{Ei}/A_{Ei}^2)$ at 115°F (in ⁻⁴)	$\Sigma(K_{Ei}/A_{Ei}^2)$ at -20°F (in ⁻⁴)
1	Two parallel flows *	Entrance $A_0 = 30 \times 36 = 1080 \text{ in}^2$	Entrance effect	[35]	0.5	0.5	9.26×10^{-7}	9.26×10^{-7}
			Screen	[35]	0.58	0.58		
		Inlet channel $A_{0,1} = 12 \times 30 = 360 \text{ in}^2$ $A_{0,2} = 8 \times 12 = 96 \text{ in}^2$	First Contraction & Friction	[36]	0.03	0.03	7.84×10^{-6}	7.68×10^{-6}
			Second Contraction & Friction	[36]	0.04	0.02		
			Splitting	[36]	0.63	0.63		
		Inlet opening $A_0 = 8 \times 148 = 1184 \text{ in}^2$	Friction thru Sidewall **	[35]	0.04	0.04	7.43×10^{-6}	7.41×10^{-6}
			Discharge	[35]	1	1		
Equivalent Losses in Section 1 for two parallel flows							2.38×10^{-6}	2.34×10^{-6}
2	Two parallel flows	Flow direction change $A_0 = 8 \times 148 = 1184 \text{ in}^2$	Bend	[36]	0.75	0.71	1.35×10^{-7}	1.27×10^{-7}
	One flow	Lower part of HSM-H cavity $A_0 = 68 \times 185.25 = 12597 \text{ in}^2$	Friction through lower part	[35]	0.01	0.01	6.26×10^{-11}	5.64×10^{-11}
	One flow	HSM-H cavity below DSC $A_0 = 82.4 \times 185.25 = 15260 \text{ in}^2$	Expansion	[36]	0.03	0.03	1.57×10^{-10}	1.54×10^{-10}
			Friction after expansion	[35]	0.006	0.005		
	3 parallel flow couples	Flow thru holes of the beam $A_0 = 12.7 \times 185.25 = 2355 \text{ in}^2$	Orifice or perforated plates	[36]	112.5	112.5	2.07×10^{-9}	2.07×10^{-9}
		Flow through slotted bar $A_0 = 1 \times 185.25 = 185.25 \text{ in}^2$	Orifice or perforated plates	[36]	18.19	18.19		
		Flow bypassing Support rails $A_0 = 12 \times 185.25 = 2223 \text{ in}^2$	Contraction with $\alpha = 30^\circ$	[36]	0.04	0.04		
	One flow	Middle part of HSM-H cavity $A_0 = 82.375 \times 185.25 = 15260 \text{ in}^2$	DSC as solid object in flow	[36]	4.20	4.65	1.82×10^{-8}	2.01×10^{-8}
			Friction on side heat shields	[35]	0.03	0.03		
	One flow	Upper part of HSM-H cavity $A_0 = 82.375 \times 185.25 = 15260 \text{ in}^2$	Top heat shields as louver	[36]	5.44	5.44	2.61×10^{-8}	2.61×10^{-8}
			Splitting to outlets	[36]	0.63	0.63		
Equivalent Losses in Section 2 for one flow path							1.81×10^{-7}	1.76×10^{-7}

Table 4-21 – Continued
Summary of the Energy-Hydraulic Calculation Results for 34.8 kW
(HSM-H with Finned Aluminum Side Shields)

Section	No. of Flow Paths	Subsection	Type of Flow Resistance	Ref.	K_{Ei} at 115°F	K_{Ei} at -20°F	$\Sigma(K_{Ei}/A_{Ei}^2)$ at 115°F (in ⁻⁴)	$\Sigma(K_{Ei}/A_{Ei}^2)$ at -20°F (in ⁻⁴)
3	Two parallel flows	Outlet opening $A_0 = 8 \times 148 = 1184 \text{ in}^2$	Entrance	[35]	0.5	0.5	1.86×10^{-6}	1.78×10^{-6}
			Friction thru sidewall	[35]	0.03	0.03		
			First bend (friction included)	[36]	2.08	1.97		
		Exhaust channel $A_0 = 4 \times 148 = 592 \text{ in}^2$	Friction	[35]	0.25	0.24	3.14×10^{-6}	2.97×10^{-6}
			Second bend (friction included)	[36]	0.85	0.81		
		Exhaust to Ambient $A_0 = 6 \times 148 = 888 \text{ in}^2$	Screen	[35]	0.58	0.58	2.00×10^{-6}	2.00×10^{-6}
			Discharge	[35]	1	1		
Equivalent Losses in Section 3 for two Parallel Flows							1.75×10^{-6}	1.69×10^{-6}
Total Equivalent Losses (in ⁻⁴)							4.31×10^{-6}	4.20×10^{-6}
Total Equivalent Losses (ft ⁻⁴)							0.089	0.087

Ambient (°F)	$\Sigma(K_{Ei}/A_{Ei}^2)$ (ft ⁻⁴)	T_{exit} (°F)	T_{mean} (°F)
115	0.089	188	147
-20	0.087	43	12

* The equivalent loss coefficient for parallel flow paths can be expressed as follows:

$$\frac{K_E}{A_E^2} = \frac{1}{\left(\sum \frac{A_j}{\sqrt{K_j}} \right)^2} \quad \text{using continuity and pressure loss equations. } \Delta p_E = \Delta p_j = K_j \frac{\rho V_j^2}{2}; \dot{m}_j = \rho A_j V_j$$

** Friction loss coefficient is $K_f = f \frac{L}{D_h}$ with L=channel length, D_h = hydraulic diameter,

$$f = \begin{cases} f' & \text{if } f' \geq 0.018 \\ \frac{f'}{0.85 f' + 0.0028} & \text{if } f' < 0.018 \end{cases}, \text{ and } f' = 0.11 \left[\frac{\varepsilon}{D_h} + \frac{64}{\text{Re}} \right]^{0.25} \quad [35]$$

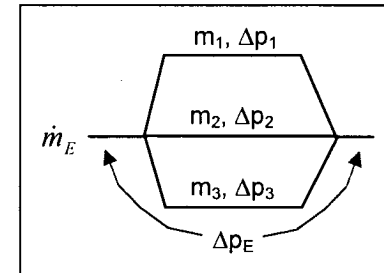


Table 4-21 – Continued
Summary of the Energy-Hydraulic Calculation Results for 34.8 kW
 (HSM-H with Flat Stainless Steel Shields)

Section	No. of Flow Paths	Subsection	Type of Flow Resistance	Ref.	K_{Ei} at 115°F	K_{Ei} at -20°F	$\Sigma(K_{Ei}/A_{Ei}^2)$ at 115°F (in ⁻⁴)	$\Sigma(K_{Ei}/A_{Ei}^2)$ at -20°F (in ⁻⁴)
1	Two parallel flows *	Entrance $A_0 = 30 \times 36 = 1080 \text{ in}^2$	Entrance effect	[35]	0.5	0.5	9.26×10^{-7}	9.26×10^{-7}
			Screen	[35]	0.58	0.58		
		Inlet channel $A_{0,1} = 12 \times 30 = 360 \text{ in}^2$ $A_{0,2} = 8 \times 12 = 96 \text{ in}^2$	First Contraction & Friction	[36]	0.02	0.02	7.86×10^{-6}	7.69×10^{-6}
			Second Contraction & Friction	[36]	0.02	0.01		
			Splitting	[36]	0.63	0.63		
		Inlet opening $A_0 = 8 \times 148 = 1184 \text{ in}^2$	Friction thru Sidewall **	[35]	0.04	0.04	7.44×10^{-7}	7.42×10^{-7}
			Discharge	[35]	1	1		
Equivalent Losses in Section 1 for two parallel flows							2.38×10^{-6}	2.34×10^{-6}
2	Two parallel flows	Flow direction change $A_0 = 8 \times 148 = 1184 \text{ in}^2$	Bend	[36]	0.76	0.72	1.35×10^{-7}	1.28×10^{-7}
	One flow	Lower part of HSM-H cavity $A_0 = 68 \times 179.75 = 12223 \text{ in}^2$	Friction through lower part	[35]	0.01	0.01	6.74×10^{-11}	6.06×10^{-11}
	One flow	HSM-H cavity below DSC $A_0 = 87.5 \times 179.75 = 15773 \text{ in}^2$	Expansion	[36]	0.05	0.05	2.27×10^{-10}	2.25×10^{-10}
			Friction after expansion	[35]	0.006	0.005		
	Two parallel flow couples	Flow thru holes of the beam $A_0 = 12.7 \times 179.75 = 2283 \text{ in}^2$	Orifice or perforated plates	[36]	105.4	105.4	2.24×10^{-9}	2.24×10^{-9}
		Flow through slotted bar $A_0 = 0 \text{ in}^2$	Orifice or perforated plates	[36]	0	0		
		Flow bypassing Support rails $A_0 = 12 \times 179.75 = 2157 \text{ in}^2$	Contraction with $\alpha = 30^\circ$	[36]	0.04	0.04		
	One flow	Middle part of HSM-H cavity $A_0 = 87.5 \times 179.75 = 15773 \text{ in}^2$	DSC as solid object in flow	[36]	3.40	3.81	1.38×10^{-8}	1.54×10^{-8}
			Friction on side heat shields	[35]	0.03	0.03		
	One flow	Upper part of HSM-H cavity $A_0 = 87.75 \times 179.75 = 15260 \text{ in}^2$	Splitting below top heat shield	[36]	0.63	0.63	2.53×10^{-9}	2.53×10^{-9}
	Two parallel flows	$A_0 = 4.88 \times 179.75 = 1753 \text{ in}^2$	Contraction between shields	[36]	0.62	0.62	2.02×10^{-7}	2.02×10^{-7}
	Two parallel flows	$A_0 = 4.88 \times 148 = 722 \text{ in}^2$	Bend toward outlet	[36]	0.84	0.79	4.03×10^{-7}	3.81×10^{-7}
Equivalent Losses in Section 2 for one flow path							7.59×10^{-7}	7.31×10^{-7}

Table 4-21 – Concluded
Summary of the Energy-Hydraulic Calculation Results for 34.8 kW
 (HSM-H with Flat Stainless Steel Shields)

Section	No. of Flow Paths	Subsection	Type of Flow Resistance	Ref.	K_{Ei} at 115°F	K_{Ei} at -20°F	$\Sigma(K_{Ei}/A_{Ei}^2)$ at 115°F (in ⁻⁴)	$\Sigma(K_{Ei}/A_{Ei}^2)$ at -20°F (in ⁻⁴)
3	Two parallel flows	Outlet opening $A_0 = 8 \times 148 = 1184 \text{ in}^2$	Entrance	[35]	0.5	0.5	1.87×10^{-6}	1.79×10^{-6}
			Friction thru sidewall	[35]	0.03	0.03		
			First bend (friction included)	[36]	2.09	1.98		
		Exhaust channel $A_0 = 4 \times 148 = 592 \text{ in}^2$	Friction	[35]	0.25	0.24	3.15×10^{-6}	2.99×10^{-6}
			Second bend (friction included)	[36]	0.86	0.81		
		Exhaust to Ambient $A_0 = 6 \times 148 = 888 \text{ in}^2$	Screen	[35]	0.58	0.58	2.00×10^{-6}	2.00×10^{-6}
			Discharge	[35]	1	1		
		Equivalent Losses in Section 3 for two Parallel Flows						
Total Equivalent Losses (in ⁻⁴)							4.90×10^{-6}	4.77×10^{-6}
Total Equivalent Losses (ft ⁻⁴)							0.102	0.099

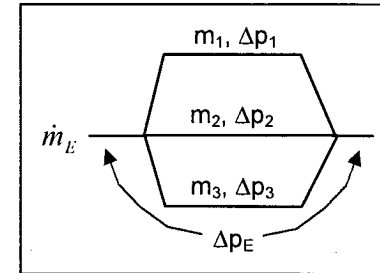
Ambient (°F)	$\Sigma(K_{Ei}/A_{Ei}^2)$ (ft ⁻⁴)	T_{exit} (°F)	T_{mean} (°F)
115	0.102	192	148
-20	0.099	46	13

* The equivalent loss coefficient for parallel flow paths can be expressed as follows:

$$\frac{K_E}{A_E^2} = \frac{1}{\left(\sum \frac{A_j}{\sqrt{K_j}} \right)^2} \quad \text{using continuity and pressure loss equations. } \Delta p_E = \Delta p_j = K_j \frac{\rho V_j^2}{2}; \dot{m}_j = \rho A_j V_j$$

** Friction loss coefficient is $K_f = f \frac{L}{D_h}$ with L=channel length, D_h = hydraulic diameter,

$$f = \begin{cases} f' & \text{if } f' \geq 0.018 \\ \frac{f'}{0.85f' + 0.0028} & \text{if } f' < 0.018 \end{cases}, \text{ and } f' = 0.11 \left[\frac{\varepsilon}{D_h} + \frac{64}{\text{Re}} \right]^{0.25} \quad [35]$$



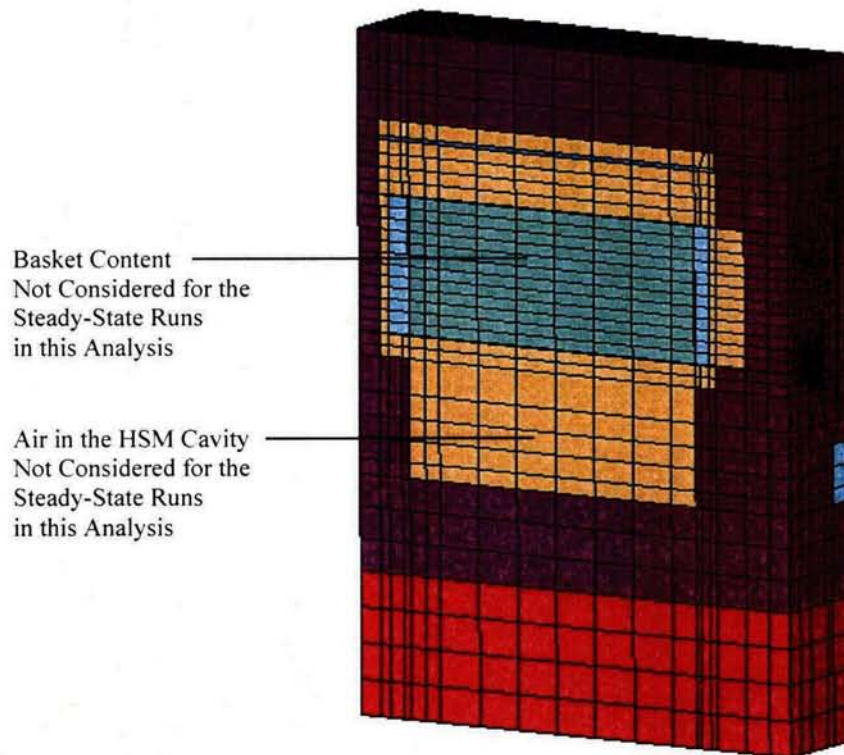
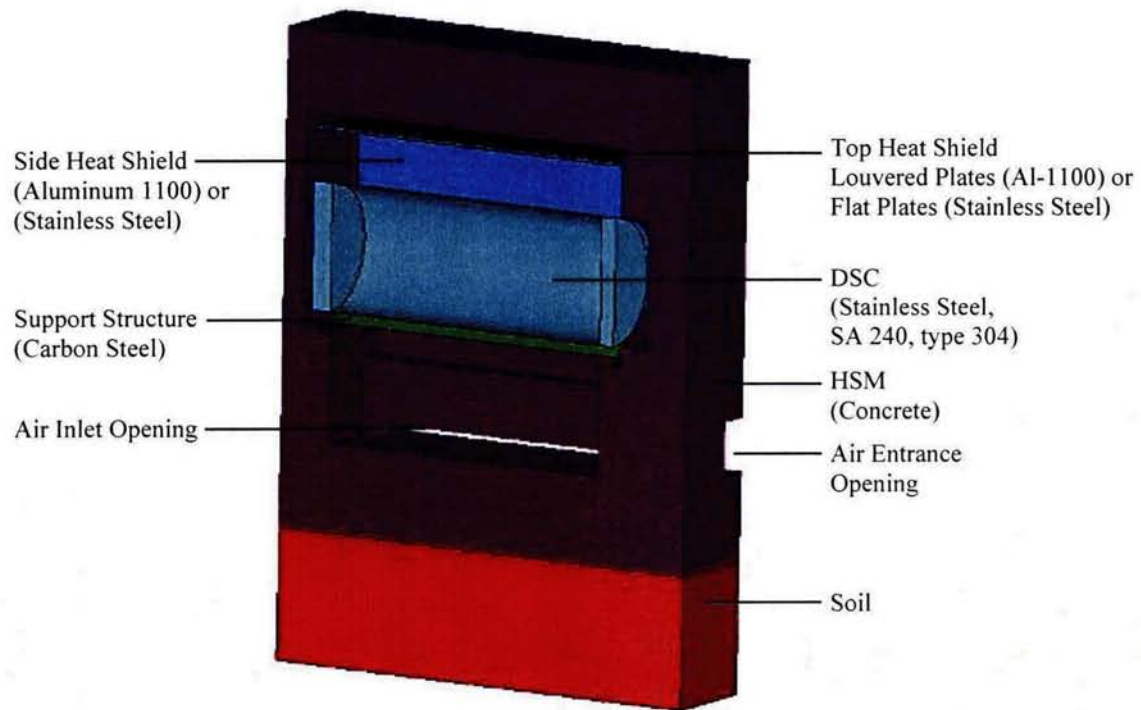


Figure 4-6
Finite Element Model of HSM-H

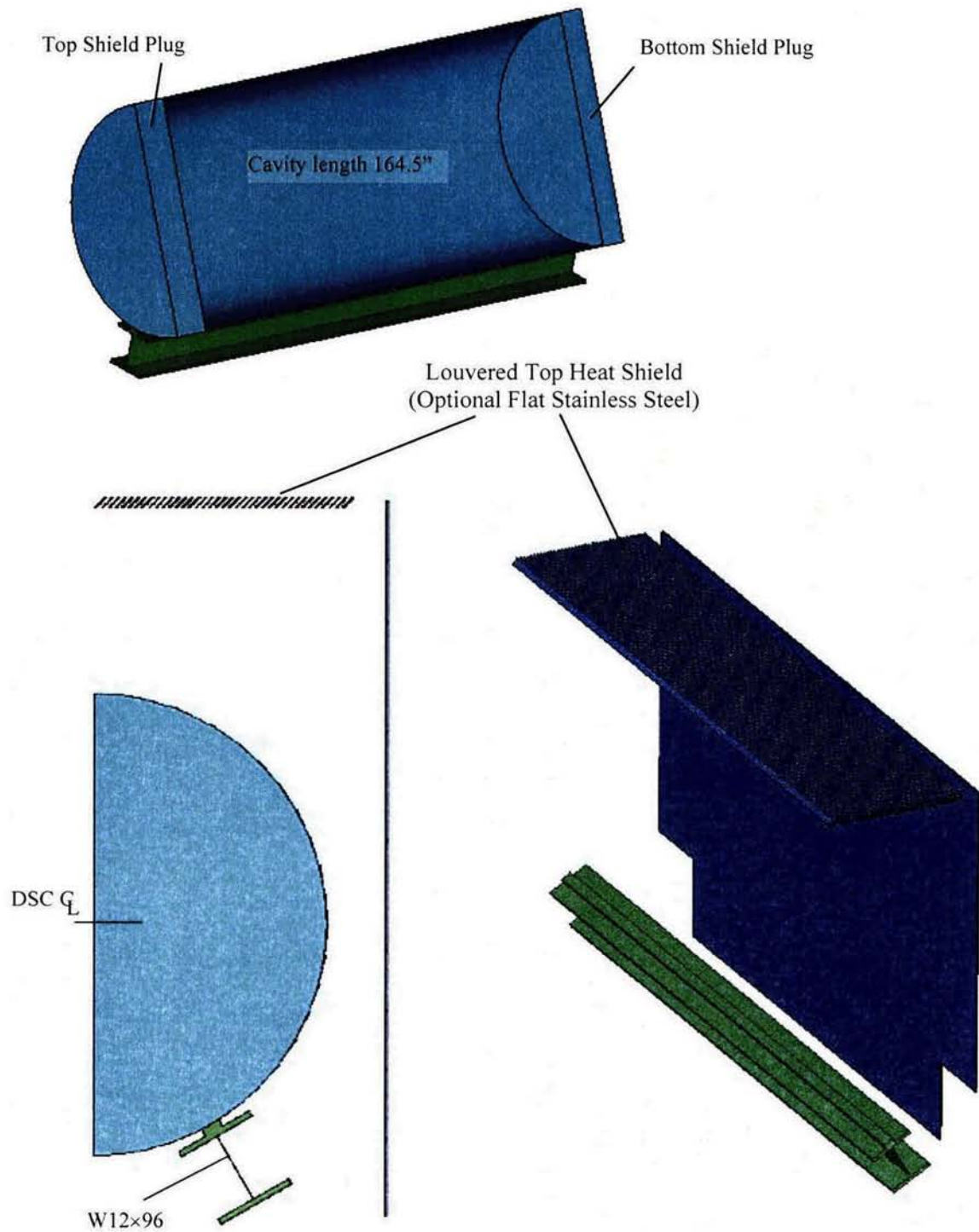
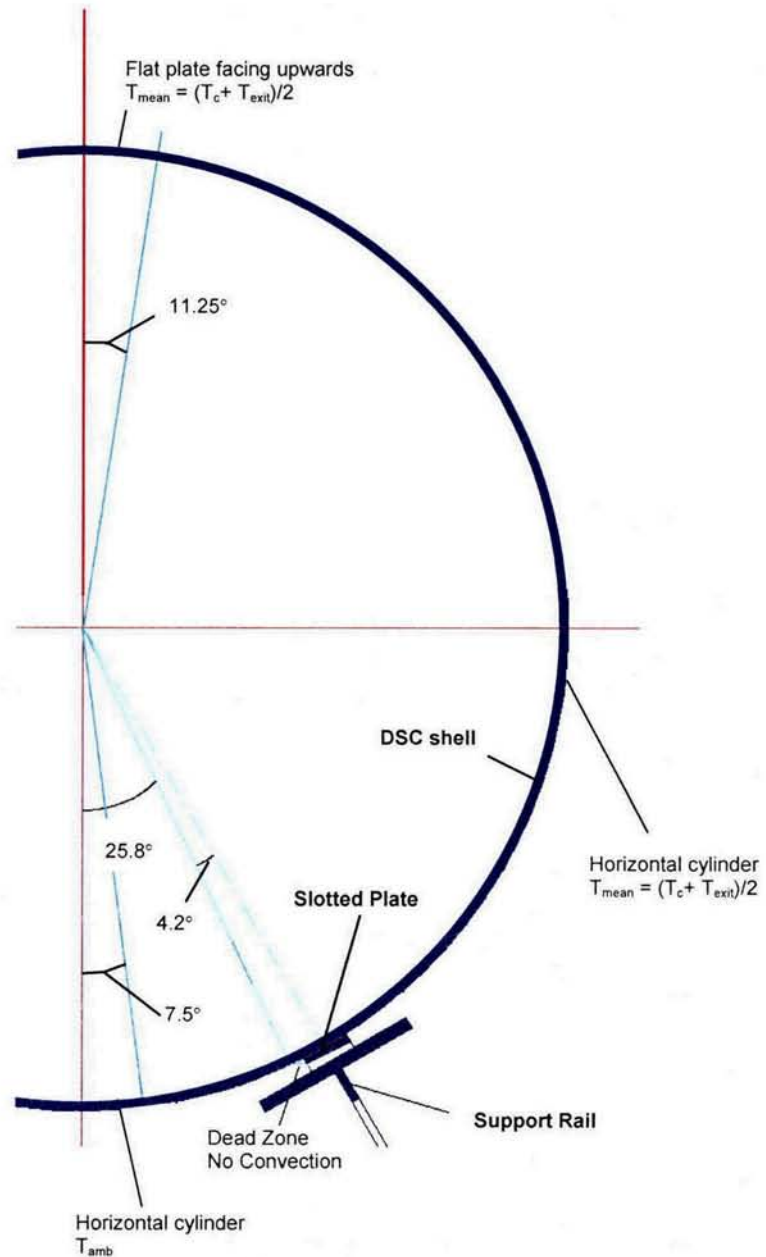


Figure 4-8
FEM of HSM-H, DSC and Support Rails



For option with slotted plate on support rail

Figure 4-9
DSC Circumferential Convection Regions in the HSM-H Model

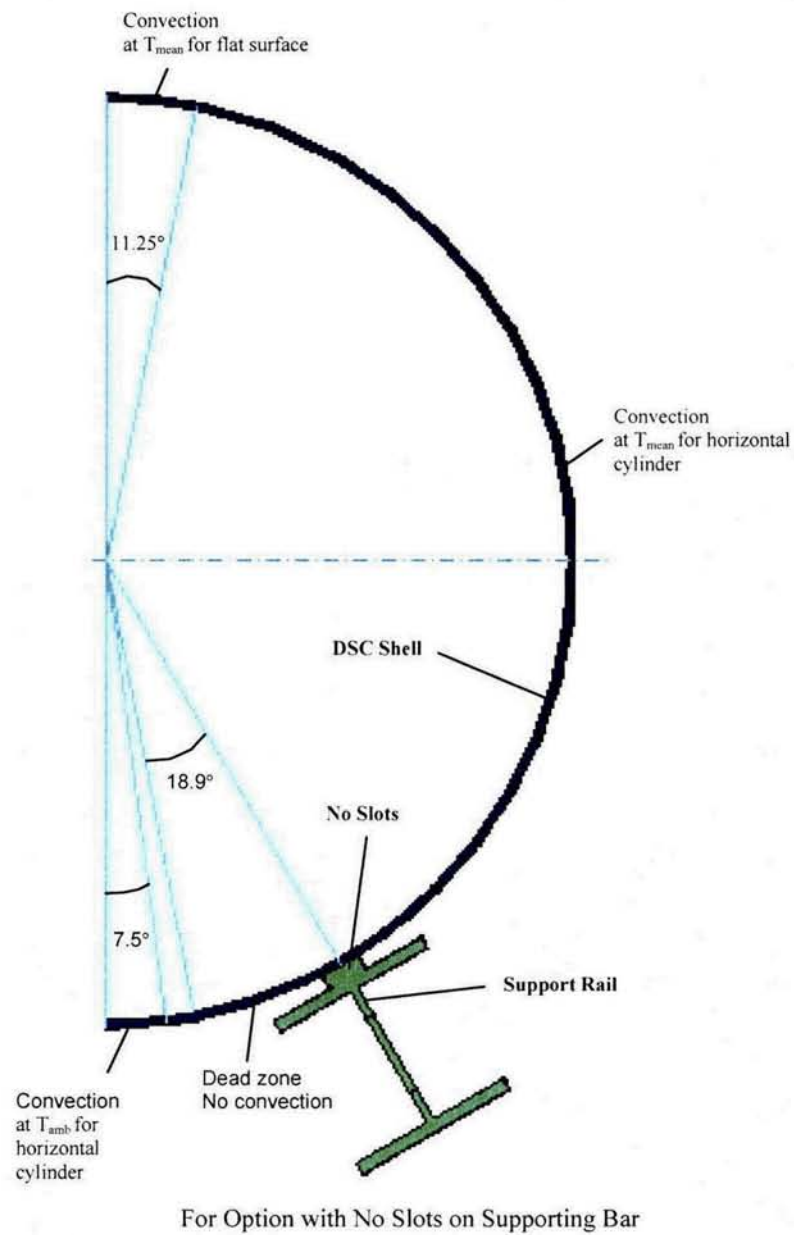


Figure 4-9-continued
DSC Circumferential Convection Regions in the HSM-H Model

Convection for a narrow strip (22.5°) at top as flat plate to T_{mean}
 Convection at a narrow strip (15°) at bottom to T_c
 Convection on other areas as horizontal cylinder to T_{mean}

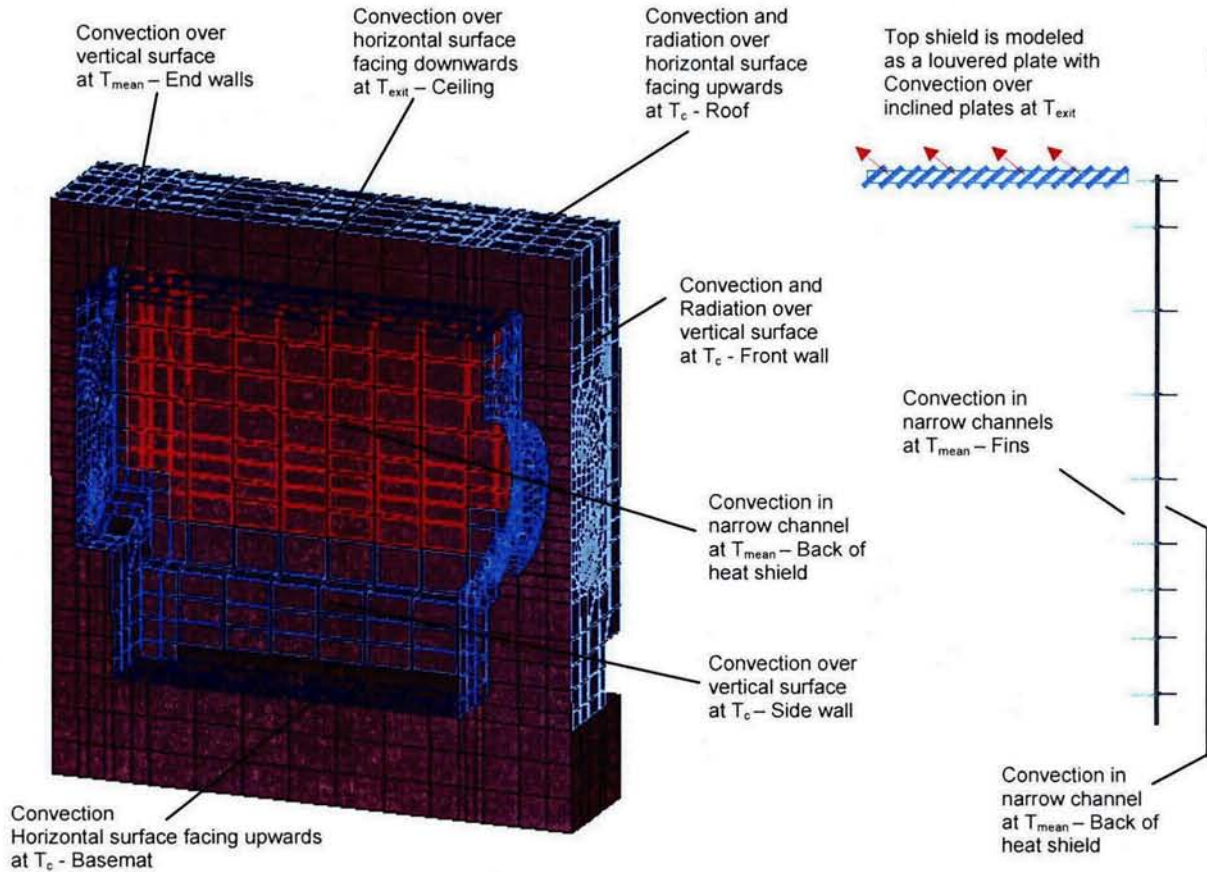
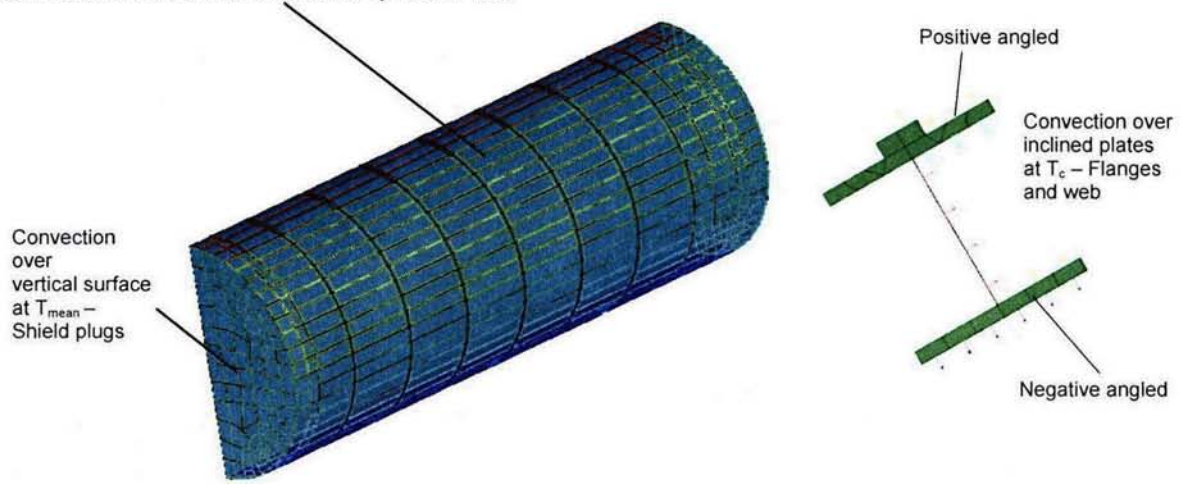


Figure 4-10
Typical Convection Boundary Conditions in the HSM-H Model

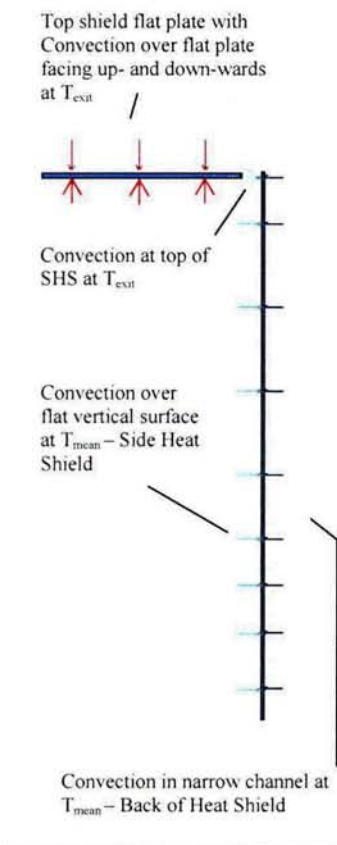


Figure 4-10 – continued
Typical Convection boundary Conditions in the HSM-H Model

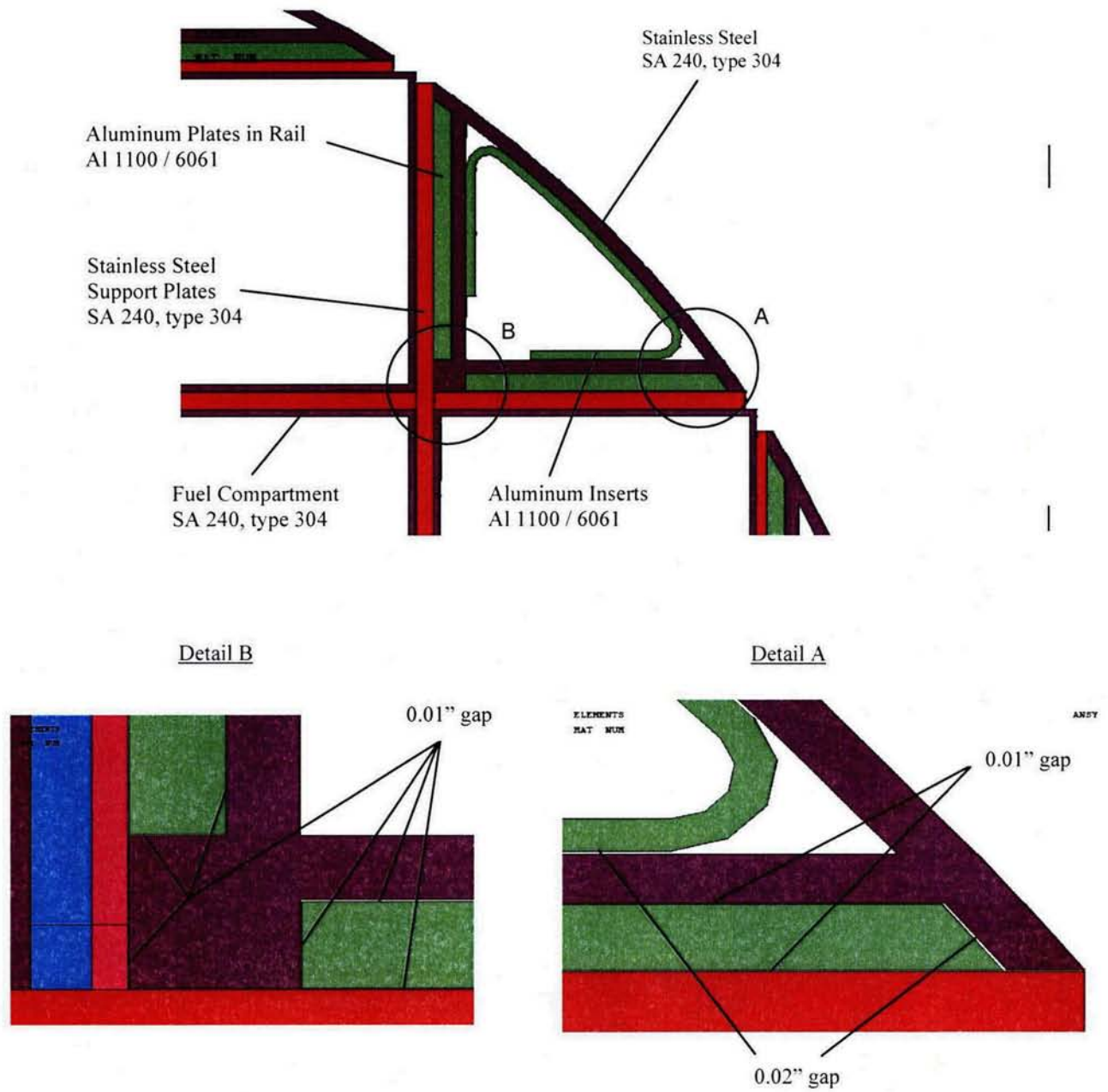


Figure 4-14
FEM of DSC Rails, Details

Configuration 6

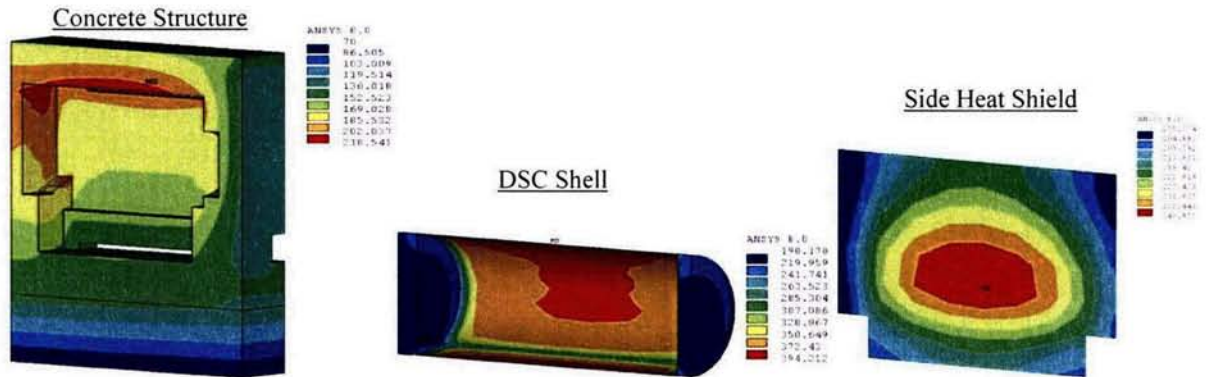
	1.068	1.168	1.168	1.068	
1.068	1.068	1.068	1.068	1.068	1.068
1.168	1.068	0.755	0.755	1.068	1.168
1.168	1.068	0.755	0.755	1.068	1.168
1.068	1.068	1.068	1.068	1.068	1.068
	1.068	1.168	1.168	1.068	

Configuration 7

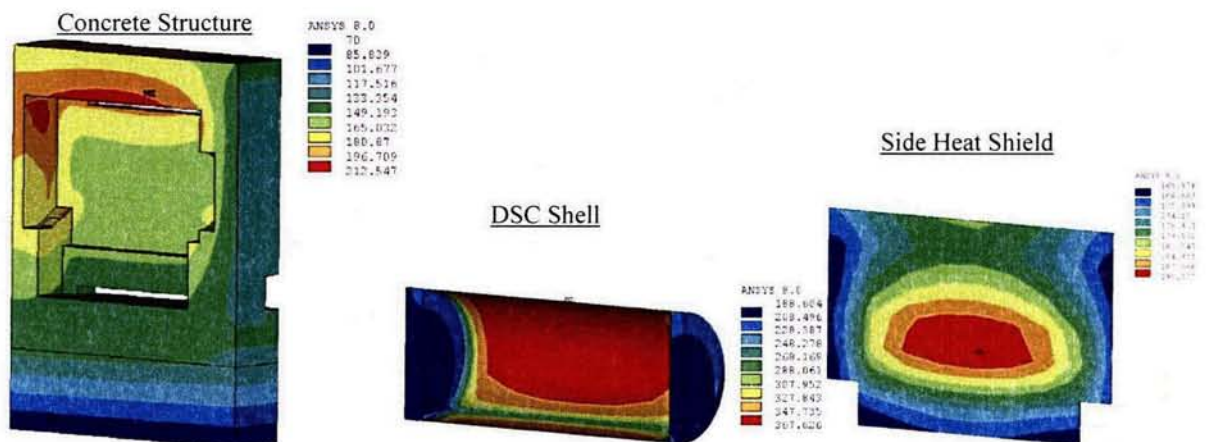
	0.935	1.5	1.5	0.935	
0.935	0.935	0.935	0.935	0.935	0.935
1.5	0.935	0.775	0.775	0.935	1.5
1.5	0.935	0.775	0.775	0.935	1.5
0.935	0.935	0.935	0.935	0.935	0.935
	0.935	1.5	1.5	0.935	

Figure 4-15 – Concluded
Thermally Bounding Loading Configurations Considered in the DSC Model
For Total Decay Heat Load of 33.8 kW, CE14x14 Fuel Assemblies

HSM-H with Un-finned Aluminum Side Heat Shield – 32.0 kW



HSM-H with Un-finned Galvanized Steel Side Heat Shield – 26.1 kW



HSM-H with Flat Stainless Steel Top & Side Heat Shields – 34.8 kW

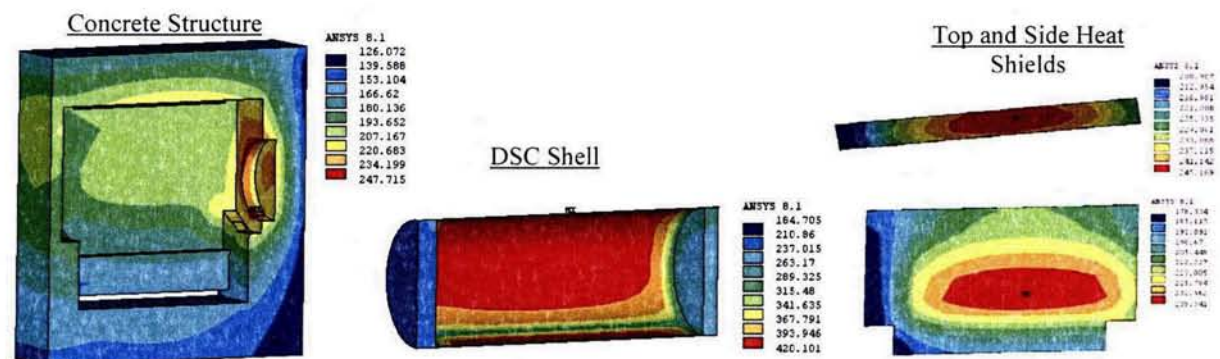


Figure 4-22
HSM-H Temperature Distribution 115°F Ambient
with Un-finned Side Heat Shields

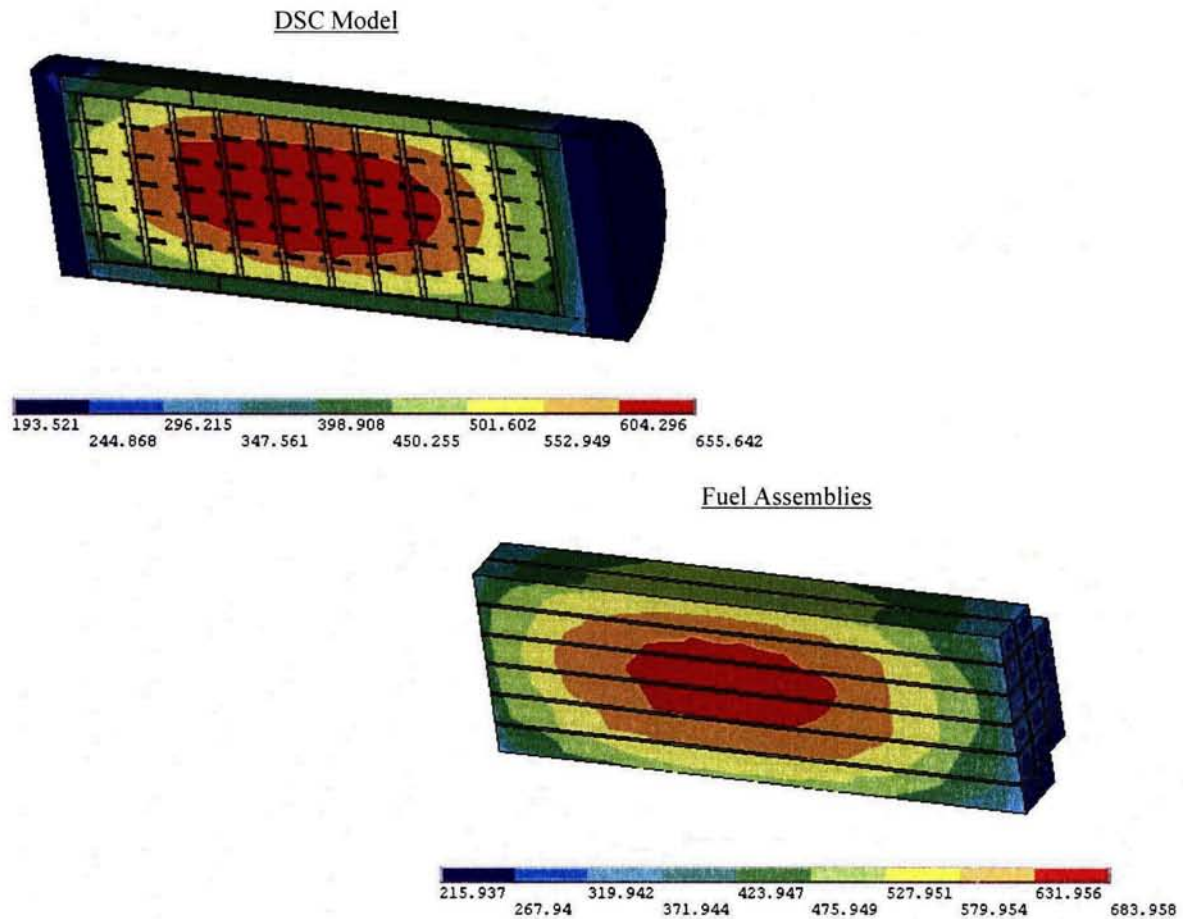


Figure 4-23
DSC Temperature Distribution during Storage, 115°F Ambient, 34.8 kW
In HSM-H with Finned Aluminum Side Heat Shields*

*These temperature distributions are calculated based on DSC maximum shell temperature of 422°F. Therefore, these profiles are bounding for the HSM-H with flat stainless steel heat shields with maximum DSC shell temperature of 420°F reported in Table 4-2.

HSM-H with Finned Aluminum Side Heat Shields and Louvered Top Heat Shield

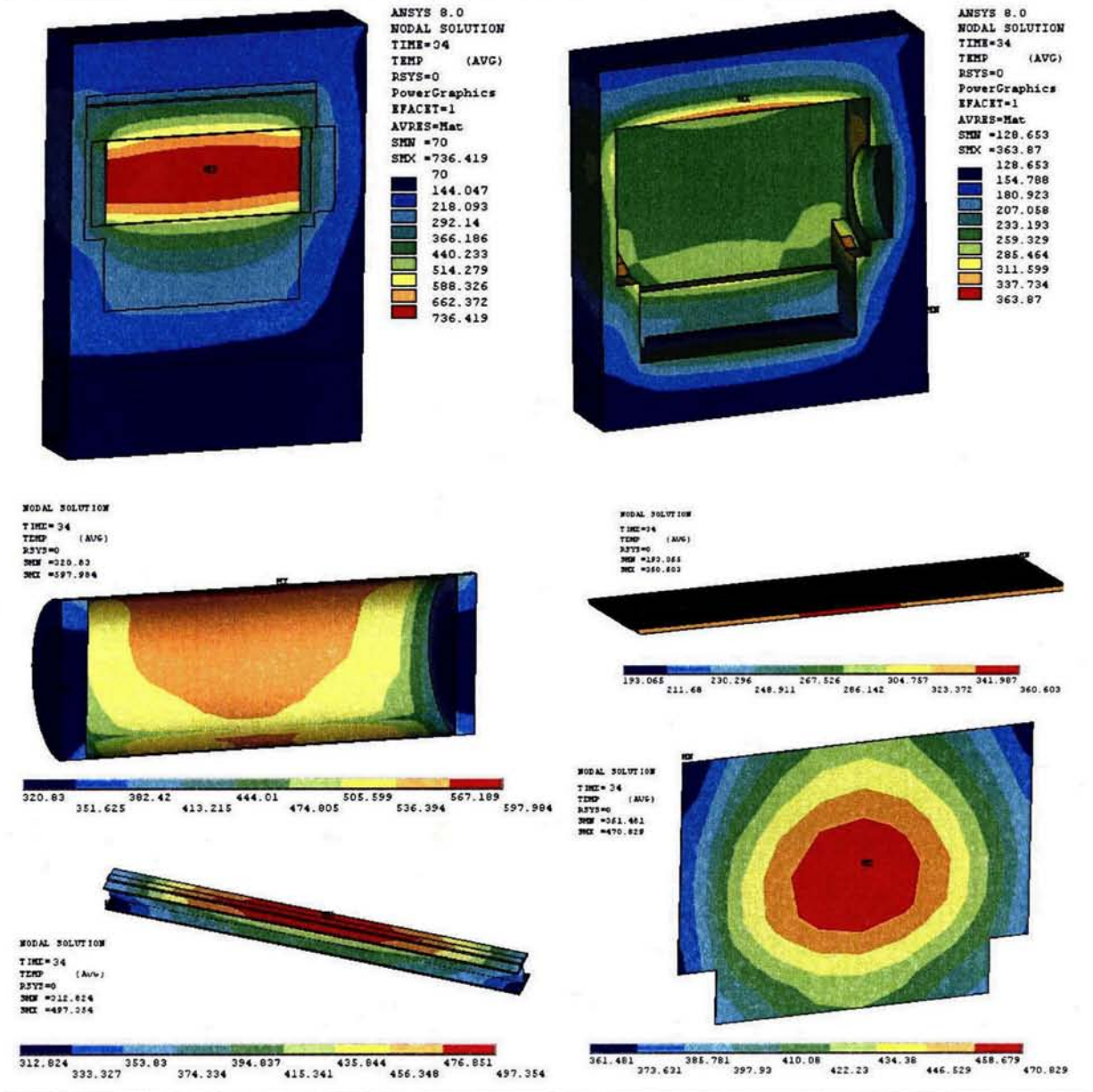


Figure 4-30

Temperature Distribution for HSM-H 34 hours after Blockage of the Vents, 34.8 kW

HSM-H with Flat Stainless Steel Top and Side Heat Shields

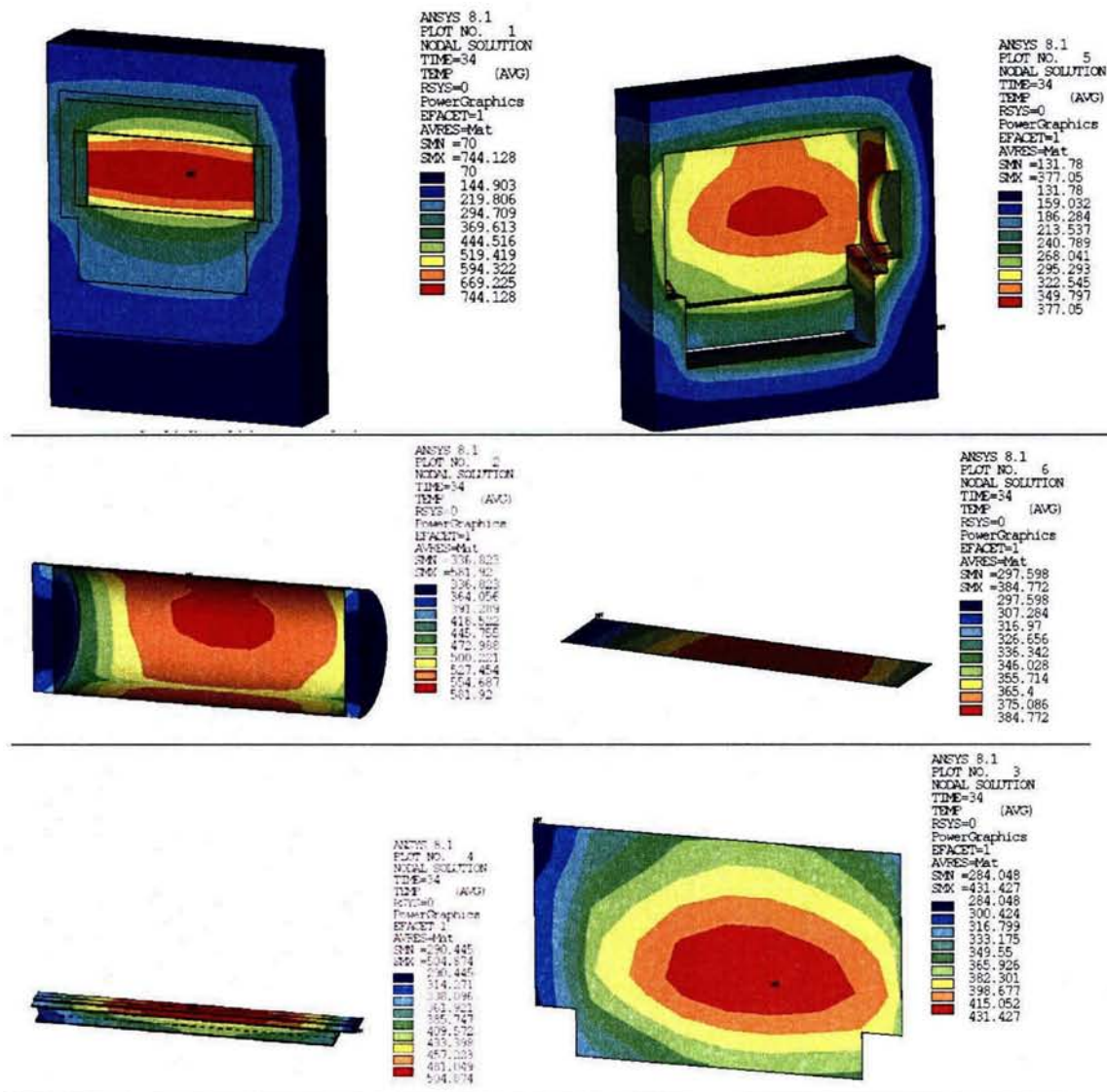


Figure 4-30—continued
Temperature Distribution for HSM-H 34 hours after Blockage of the Vents, 34.8 kW

FIGURE IS DELETED IN ITS ENTIRETY

Figure 4-31

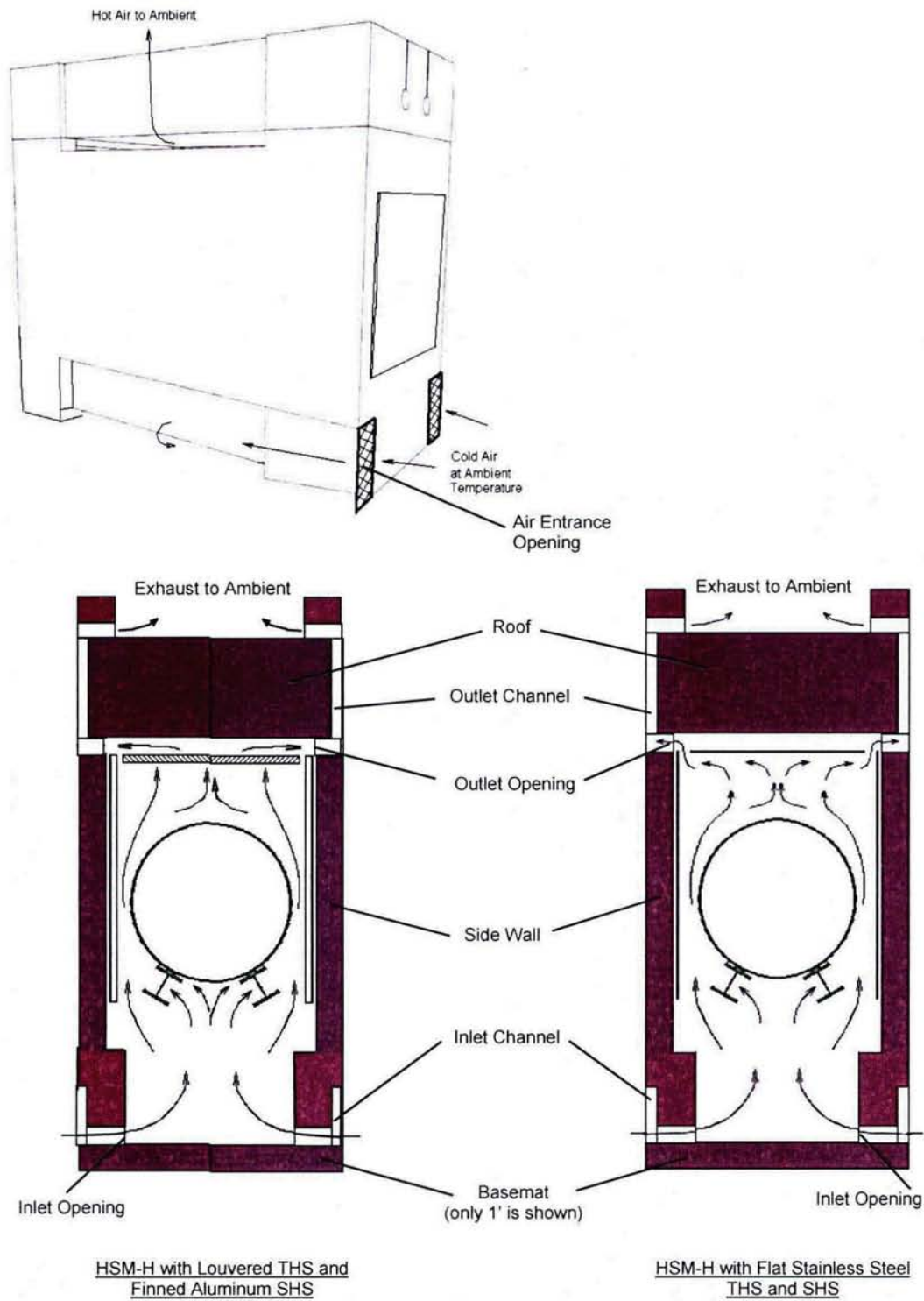


Figure 4-44
Schematic Flow Paths through HSM-H

FIGURE IS DELETED IN ITS ENTIRETY

Figure 4-45

LIST OF TABLES

5-1	NUHOMS® HD 32PTH System Shielding Materials	
5-2	Summary HSM-H Dose Rates	
5-3	Transfer Cask (Loading/Unloading/Transfer Operations) Side Dose Rate Summary	
5-4	Transfer Cask (Loading/Unloading/Transfer Operations) Top End Dose Rate Summary	
5-5	Cask (Loading/Unloading/Transfer Operations) Bottom End Dose Rate Summary	
5-6	Flux Factor by Fuel Assembly Region	
5-7	Westinghouse Fuel Assembly Materials and Masses	
5-8	NFAH Materials and Masses	
5-9	Fuel Assembly Material Masses	
5-10	SAS2H Gamma Sources for 60 GWd/MTU, 7-Year Cooled MK BW 17x17 Fuel Assembly	
5-11	SAS2H Gamma Sources for 210 GWd/MTU, 20-Year Cooled TPA	
5-12	SAS2H Gamma Sources for 30 GWd/MTU, 4-Day Cooled BPRA	
5-13	SAS2H Neutron Sources for 60 GWd/MTU, 7-10 yr Cooled MK BW 17x17 Fuel Assembly	
5-14	ANSI Standard-6.1.1-1977 Flux-to-Dose Factors	
5-15	Material Densities for Fuel Assembly Regions (dry)	
5-16	Material Densities for Fuel Assembly Regions (wet)	
5-17	NUHOMS® HD 32PTH DSC and OS-187H Material Composition	
5-18	NUHOMS® HD 32PTH DSC and OS-187H Material Composition	

5. SHIELDING EVALUATION

The shielding evaluation presented for the NUHOMS® 32PTH System demonstrates adequacy of the shielding design for the payload described in Chapter 2. The geometry of the NUHOMS® System is described in Chapter 1. The heavy concrete walls and roof of the Horizontal Storage Module (HSM-H) provide the bulk of the shielding for the payload in the storage condition. During fuel loading and transfer operations, the combination of thick steel shield plugs at the ends of the 32PTH-DSC and heavy steel/lead/neutron shield material of the OS187H transfer cask provide shielding for personnel loading and transferring the 32PTH-DSC to the HSM-H. Figure 5-1 through Figure 5-4 and Table 5-1 provide the general configuration and material thicknesses of the important components of the NUHOMS® 32PTH System.

For this shielding evaluation, source terms are calculated for the bounding Framatome ANP Advanced MK BW 17x17 (MK BW 17x17) fuel assembly. This fuel assembly is bounding because it contains the greatest mass of fuel.

Also included in the source term is the bounding Non-Fuel Assembly Hardware (NFAH) which is the BPRA.

Several burnup/enrichment combinations with minimum 5 year cooling times are addressed for the fuel to provide more flexibility in qualifying fuel for storage. These combinations form the basis for the NUHOMS® 32PTH System fuel specifications in Chapter 12. Bounding operating histories are assumed for the NFAH with a minimum cooling time of 4 days. The methodology, assumptions, and criteria used in this evaluation are summarized in the following subsections.

Section 5.4 provides a three dimensional (3-D) shielding analysis for the NUHOMS® 32PTH System using MCNP [2,6]

The shielding evaluation described in this chapter 5.0 is applicable to the 32PTH DSC in the OS187H TC and HSM-H. See Appendix A, Chapter A.5 for discussion of applicability of these analyses for the 32PTH Type 1 DSC in the OS187H Type 1 TC and HSM-H.

The mass of materials in each fuel assembly region is homogenized over the volume of the region (x-section = 71 in²). Tables 5-17 and 5-18 provide the shield regional densities for the 32PTH-DSC and OS187H TC.

The concrete for the HSM-H is chosen to be “plain” concrete with a density of 143 lbs/ft³ with the rebar conservatively neglected. Table 5-19 provides the concrete densities.

The actual fuel layout in the 32PTH-DSC is a cartesian array of fuel assemblies inside stainless steel compartments surrounded by sheets of aluminum material. These regions are modeled discretely as are the rails on the periphery of the basket. A source is modeled for each of the four homogenized fuel assembly regions for all 32 fuel assemblies. The source regions are cuboid in shape with the same 8.426” x 8.426” (17 times the Pitch) x-section and the appropriate axial length.

When the transfer cask/32PTH-DSC annulus and 32PTH-DSC are filled with water, the wet axial densities are used for the homogenized regions.

5.5.2 Sample Input Files

(PROPRIETARY INFORMATION)

Figure Withheld Under 10 CFR 2.390

Table 5-9
Fuel Assembly Material Masses

(kg/assembly)					
Scaling Factors	0.1	0.2	1	0.2	
	Top Fitting	Plenum	Active Fuel	Bottom Fitting	Total
<u>15x15</u>					
Chromium	0.1501	0.0555	2.2972	0.2166	2.7194
Manganese	0.0138	0.0060	0.1059	0.0228	0.1485
Iron	0.4879	0.2121	4.4512	0.7848	5.9360
Cobalt	0.0011	0.0003	0.0328	0.0009	0.0350
Nickel	0.1178	0.0268	4.3714	0.1017	4.6177
Zirconium	0.0000	1.1945	97.128	0.0000	98.322
Aluminum	0.0007	0.0000	0.0380	0.0000	0.0387
Silicon	0.0070	0.0030	0.0124	0.0000	0.0224
Titanium	0.0009	0.0000	0.0473	0.0000	0.0481
Niobium	0.0061	0.0000	0.3272	0.0000	0.3333
Molybdenum	0.0033	0.0000	0.1768	0.0000	0.1801
Tin	0.0000	0.0195	1.6608	0.0182	1.6986
<u>17x17</u>					
Chromium	0.1551	0.0698	2.3018	0.2166	2.7433
Manganese	0.0139	0.0076	0.1060	0.0228	0.1503
Iron	0.4927	0.2676	4.4595	0.7848	6.0047
Cobalt	0.0012	0.0003	0.0329	0.0009	0.0353
Nickel	0.1317	0.0339	4.3715	0.1017	4.6388
Zirconium	0.0000	1.0770	100.75	0.0000	101.83
Aluminum	0.0008	0.0000	0.0381	0.0000	0.0389
Silicon	0.0071	0.0038	0.0124	0.0182	0.0415
Titanium	0.0011	0.0000	0.0473	0.0000	0.0484
Niobium	0.0076	0.0000	0.3272	0.0000	0.3348
Molybdenum	0.0041	0.0000	0.1768	0.0000	0.1809
Tin	0.0000	0.0176	1.7200	0.0182	1.7558

Table 5-17
NUHOMS® HD 32PTH DSC and OS-187H Material Composition

(% weight)

Element	Atomic Weight	Carbon Steel ¹	Stainless Steel 304 ¹	Aluminum ¹	Lead ¹	Water ¹ (atm fraction)	Air ²	Polyester Resin ³
H	1.008					0.666		5.05
B	10.811							1.05
C	12.011	1.00					0.01	35.1
N	14.0067						75.53	
O	15.9994					0.333	23.18	41.7
Al	26.9815			100.00				14.9
Ar	39.948						1.28	
Cr	51.996		19.00					
Mn	54.938		2.00					
Fe	55.847	99.00	68.375					
Ni	58.71		9.50					
Zn	65.37							2.11
Pb	207.19				100.00			
density (g/cc)		7.8212	7.92	2.702	11.17 ⁴	0.9982	0.0012	1.58

1. Ref [1], 2. Ref [3], 3. Proprietary resin formulation, 4. Use 98.5% of TD (11.344 g/cc)

Table 5-18
NUHOMS® HD 32PTH DSC and OS-187H Material Composition

(atm/b-cm)

Element	Carbon Steel	Stainless Steel 304	Aluminum	Lead	Water	Dry Air	Polyester Resin
H					6.673E-02		4.767E-02
B-10							2.098E-04
C	3.921E-03					6.016E-09	3.168E-02
N						3.897E-05	
O					3.337E-02	1.047E-05	2.825E-02
Al			6.031E-02				5.986E-03
Ar						2.315E-07	
Cr		1.743E-02					
Mn		1.736E-03					
Fe	8.349E-02	5.935E-02					
Ni		7.718E-03					
Zn*							3.499E-04
Pb				3.248E-02			

*- Ignored,

LIST OF TABLES

Table 6-1 Maximum Assembly Average Initial Enrichment for Each Fuel Design for both Intact and Damaged Fuel Assemblies	
Table 6-2 Summary of Limiting Criticality Evaluations for all Fuel Assemblies	
Table 6-3 Authorized Contents for NUHOMS®-32PTH DSC	
Table 6-4 Fuel Assembly Design Parameters for Criticality Analysis	
Table 6-5 NUHOMS®-32PTH - Basket and DSC Dimensions	
Table 6-6 NUHOMS® OS187H Transfer Cask Dimensions	
Table 6-7 NUHOMS®-32PTH - Fixed Poison Loading Requirements	
Table 6-8 Description of the Basic KENO Model Units	
Table 6-9 Material Property Data	
Table 6-10 Results of the Fuel Assembly Positioning Studies	
Table 6-11 Results of the Rail Material Variation Studies	
Table 6-12 Results of the Poison Plate Thickness Variation Studies	
Table 6-13 Results of the Fuel Compartment Width Variation Studies	
Table 6-14 Results of the Fuel Compartment Thickness Variation Studies	
Table 6-15 WE 15x15 Class Intact Assemblies Without BPRAs - Final Results	
Table 6-16 WE 15x15 Class Intact Assemblies With BPRAs - Final Results	
Table 6-17 WE 17x17 Class Intact Assemblies Without BPRAs - Final Results	
Table 6-18 WE 17x17 Class Intact Assemblies With BPRAs - Final Results	
Table 6-19 Limiting Parameters for Damaged Fuel Calculations	
Table 6-20 Results of Optimum Pitch Studies	
Table 6-21 Results of the Single Ended Rod Shear Studies	
Table 6-22 Results of the Double Ended Rod Shear Studies	
Table 6-23 Evaluation of the Shifting of Fuel Rods Beyond the Poison	
Table 6-24 Most Reactive Damaged Assembly Configuration	
Table 6-25 Double Ended Rod Shear Study with BPRAs	
Table 6-26 WE 15x15 Class Damaged Assemblies With BPRAs - Final Results	
Table 6-27 WE 17x17 Class Damaged Assemblies With BPRAs - Final Results	
Table 6-28 Maximum k_{eff} for Intact Assemblies - Final Results	
Table 6-29 Maximum k_{eff} for Damaged Assemblies - Final Results	
Table 6-30 Benchmark Results	
Table 6-31 USL-1 Results	
Table 6-32 USL Determination for Criticality Analysis	
Table 6-33 CE 14x14 Class Intact Assemblies - Final Results	
Table 6-34 CE 14x14 Class Damaged Assemblies - Final Results	

6. CRITICALITY EVALUATION

The NUHOMS® HD System is designed to meet 10CFR 72.124 1 criticality safety limits during worst case wet loading/unloading operations with the use of fixed neutron absorbing materials (poisons) in the flooded Dry Shielded Canister (32PTH DSC) and credit for soluble boron in the spent fuel pool. The design assures criticality safety under all normal, off-normal and accident conditions associated with fuel handling, 32PTH DSC handling, on-site transfer and 32PTH DSC storage.

The NUHOMS® 32PTH DSC criticality safety is ensured by fixed neutron absorbers, soluble boron in the pool and favorable geometry. Burnup credit is not taken in this criticality evaluation. The basket uses a Borated-Aluminum alloy, Aluminum/B₄C metal matrix composite, or Boral® as its fixed neutron poison material. These materials are ideal for long-term use in the radiation and thermal environments of a DSC. The minimum required boron-10 loading for the metallic plates is 7.0 mg/cm² (90% credit taken in the criticality analysis or 6.3 mg/cm²). Metal Matrix Composites (MMCs) at a minimum areal density of 7.0 mg/cm² have been qualified for use as a neutron absorber with 90% credit as justified in Section 9.1.7.2 of this SAR. Similarly, Section 9.1.7.1 provides the justification for the use of 90% credit for borated aluminum. The maximum poison loading for the metallic plates is 50.0 mg B-10/cm² (90% credit taken in the analysis or 45.0 mg B-10/cm²). The minimum required poison loading for Boral® plates is 9.0 mg B-10/cm² (75% credit). The maximum poison loading for Boral® plates is 25.0 mg B-10/cm² (75% credit). In addition to utilizing five different fixed poison loadings, the soluble boron concentration credited in the analysis is also varied from a minimum of 2000 ppm to a maximum of 2500 ppm.

The results of the detailed analyses demonstrate that the NUHOMS® HD System is criticality safe under normal, off normal and accident conditions including all applicable biases and uncertainties.

The criticality evaluation described in this chapter 6.0 is applicable to the 32PTH DSC and the OS187H TC. See Appendix A, Chapter A.6 for discussion of applicability of these analyses for the 32PTH Type 1 DSC and OS187H Type 1 TC.

6.1 Discussion and Results

The NUHOMS®-32PTH DSC stainless steel basket consists of an egg-crate plate design. The fuel assemblies are housed in 32 stainless steel fuel compartments with the damaged fuel assemblies occupying the positions shown in Chapter 12. The basket structure, including the fuel compartments, is held together with stainless steel insert plates and the poison and aluminum plates that form the egg crate structure. The basket compartment structure is connected to perimeter rail assemblies, portions of it comprising of a solid aluminum interface. The fuel compartment structure is connected to perimeter transition rail assemblies as described shown on the drawings in Section 1.5. The poison/aluminum plates are located between the fuel compartments.

The analysis presented herein is performed for a NUHOMS®-32PTH DSC in the NUHOMS®-OS187H transfer cask (TC) during normal and accident loading conditions. The NUHOMS®-OS187H TC consists of an inner stainless steel shell, lead gamma shield, a stainless steel structural shell and a water neutron shield. This analysis is applicable to any licensed cask of similar construction. The NUHOMS®-32PTH DSC/TC configuration is shown to be subcritical under normal and accident conditions of loading, transfer and storage.

The 32PTH DSC contents are limited to the fuel designs listed in Section 6.1. Computer models of the 32PTH DSC are discussed in Section 6.3. The criticality evaluation is presented in Section 6.4. The 32PTH DSC was evaluated for the following conditions that bound normal conditions and the off-normal and accident events listed in Chapter 11:

- varied internal moderator density (IMD) within the basket with borated water (water density evaluated includes steam which may be generated during loading and unloading operations),
- variations in material tolerances,
- variations in fuel assembly position in the compartment tubes,
- fresh water in the fuel pellet - cladding annulus,
- postulated change of pin pitch due to fuel grid crushing in a drop accident,
- postulated failures for damaged fuel payloads.

The various effects are evaluated individually, and are combined as required to demonstrate compliance with the requirement of 10CFR 72.124 that "before a criticality accident is possible, at least two unlikely, independent, and concurrent or sequential changes have occurred in the conditions essential to nuclear criticality safety."

The criticality analysis determines the most reactive configuration for the basket and fuel assembly position. Then criticality calculations evaluate a variety of fuel assembly types, initial enrichments and poison loadings (fixed and soluble poison). Finally, the maximum allowed initial enrichment for each fuel assembly type as a function of soluble boron concentration and fixed poison loading is determined and is listed in Table 6-1.

Additionally, calculations are carried out to determine the most reactive damaged fuel assembly (design basis damaged fuel assembly) configuration for each fuel assembly class.

Then criticality calculations evaluate a variety of fuel assembly types, initial enrichments and poison loadings (fixed and soluble poison). Finally, the maximum allowed initial enrichment and the number of damaged assemblies per DSC for each fuel assembly type as a function of soluble boron concentration and fixed poison loading is determined and is also shown in Table 6-1.

These calculations determine k_{eff} with the CSAS25 control module of SCALE-4.4 [3] for each assembly type and initial enrichment, including all uncertainties to assure criticality safety under all credible conditions.

The results of these calculations demonstrate that the maximum expected k_{eff} , including statistical uncertainty, will be less than the Upper Subcritical Limit (USL) determined from a statistical analysis of benchmark criticality experiments. The statistical analysis procedure includes a confidence band with an administrative safety margin of 0.05. A series of benchmark calculations were performed with the SCALE 4.4 PC/CSAS25 [3] package using the 44-group cross-section library as presented in Section 6.5. The minimum value of the Upper Subcritical Limit (USL) was determined to be 0.9419.

The results of the limiting criticality analyses are summarized in Table 6-2. The maximum k_{eff} for the normal fuel geometry is 0.9404 ($k_{\text{eff}}+2\sigma$) and is based on the Westinghouse 17x17 (WE 17x17) fuel assembly design. The maximum k_{eff} for the damaged fuel geometry is 0.9402 ($k_{\text{eff}}+2\sigma$) and is based on the WE 17x17 fuel assembly design.

6.4 Criticality Calculation

This section describes the analysis methodology utilized for the criticality analysis. The analyses are performed with the CSAS25 module of the SCALE system. A series of calculations are performed to determine the relative reactivity of the various fuel assembly designs evaluated and to determine the most reactive configuration without BPRAs. The most reactive intact fuel design, for a given enrichment, as demonstrated by the analyses, is the WE 17x17 standard assembly. The most reactive credible configuration is an infinite array of flooded casks, each containing 32 fuel assemblies, with minimum fuel compartment ID, minimum basket structure thickness and minimum assembly-to-assembly pitch.

A series of calculations are also performed to determine the relative reactivity of the various damaged fuel configurations for each fuel assembly class. The most reactive damaged fuel configuration for the WE17 and WE15 class occurs due to a postulated double-ended shear. The most reactive damaged fuel configuration for the CE14 class occurs when the fuel rods are arranged in an optimum pitch configuration. The most reactive credible configuration analyzed in this calculation is an infinite array of flooded casks, each containing a maximum of 32 damaged fuel assemblies with BPRAs, with minimum fuel compartment ID, minimum basket structure thickness and minimum assembly-to-assembly pitch.

As mentioned in Section 6.1, the NUHOMS®-32PTH DSC is evaluated to determine the maximum initial enrichment of the fuel assemblies (both damaged and intact) per DSC for each assembly class as a function of fixed poison loading and soluble boron concentration levels.

6.4.1 Calculational Method

6.4.1.1 Computer Codes

Criticality analyses were performed using the microcomputer application KENO-Va and the 44 neutron group library based on ENDF-B Version 5 cross-section data that are part of the SCALE 4.4 code package [3]. Validation and benchmarking of these codes is performed in accordance with applicable QA program requirements (see Chapter 13) and is discussed in Section 6.5.

SCALE 4.4 [3] is an extensive computer package which has many applications including cross section processing, criticality studies, and heat transfer analyses among others. The package is comprised of many functional modules, which can be run independently of each other. Control Modules were created to combine certain functional modules in order to make the input requirements less complex. For the purpose of criticality analysis, only four functional modules are used and one control module. These Modules are CSAS25, which includes the three dimensional criticality code KENO-Va and the preprocessing codes BONAMI-S, NITAWL-II and XSDRNPM-S.

KENO-Va, in conjunction with a suitable working library of nuclear cross section data, is used to calculate the multiplication factor, k_{eff} , of systems of fissile material. It can also compute lifetime and generation time, energy dependent leakages, energy and region-dependent absorptions, fissions, fluxes, and fission densities. KENO-Va utilizes a three-dimensional Monte-Carlo computation scheme. KENO-Va is capable of modeling complex geometries including facilities for handling arrays, arrays of arrays, and holes.

SCALE 4.4 is set up so that any number of cross-section libraries may be used with the preprocessing functional and control modules. For the purpose of this analysis, only the 44-group ENDF/B Version 5 library is used.

The preprocessing codes used for this analysis are the functional modules BONAMI-S, NITAWL-II and XSDRNPM-S. They are consolidated into the control module CSAS25. BONAMI-S has the function of performing Bondarenko calculations for resonance self-shielding. The cross sections and Bondarenko factor data are pulled from an AMPX master library. The output is placed into a master library as well. Dancoff approximations allow for different fuel lattice cell geometries. The main function of NITAWL-II is to change the format of the master cross-section libraries to one which the criticality code (KENO-Va) can access. It also provides the Nordheim Integral Treatment for resonance self-shielding. XSDRNPM-S provides cell-weighted cross sections based on the specified unit cell.

The criticality analysis, using the above computer codes, is performed in compliance with the 10CFR 72 [1] requirements. Specifically, all cases are analyzed assuming that the basket is fully flooded with borated water and the neutron shield of the transfer cask is eliminated and the cask is flooded with fresh water. Finally, KENO V.a calculates the k_{eff} of the system that is modeled. A sufficiently large number of neutron histories are run so that the standard deviation is below 0.0010 for all calculations.

6.4.1.2 Physical and Nuclear Data

The physical and nuclear data required for the criticality analysis include the fuel assembly data and cross-section data as described below.

Table 6-4 provides the pertinent data for criticality analysis for each fuel assembly evaluated for the NUHOMS® HD System.

The criticality analysis used the 44-group cross-section library built into the SCALE system. ORNL used ENDF/B-V data to develop this broad-group library specifically for criticality analysis of a wide variety of thermal systems.

- (5) The single-ended fuel rod shear cases assume that fuel rods that form one assembly face shear in one place and are displaced to new locations. The fuel pellets are assumed to remain in the fuel rods.
- (6) The double-ended fuel rod shear cases assume that the fuel rods that form one assembly face shear in two places and the intact fuel rod pieces are separated from the parent fuel rods.
- (7) Although only 16 damaged fuel assemblies are authorized contents for the DSC, all 32 fuel assemblies are considered to be damaged in the criticality analyses for damaged fuel.

6.4.1.4 Determination of k_{eff}

The Monte Carlo calculations performed with CSAS25 (KENO V.a) use a flat neutron starting distribution. The total number of histories traced for each calculation is approximately 800,000. This number of histories is sufficient to achieve source convergence and produce standard deviations of less than 0.10% in k_{eff} . The maximum k_{eff} for the calculation is determined with the following formula:

$$k_{eff} = k_{KENO} + 2\sigma_{KENO}.$$

These results also indicate that there would be no significant effect on k_{eff} due to the presence of aluminum cladding in case of Boral® poison due to the fact that this study also evaluates the effect of aluminum plate thickness.

The next set of analyses determines the effect of fuel compartment size on the system reactivity. The model starts with the most reactive geometry determined from the previous study. For this evaluation, the compartment size is varied from 8.650 square inches to 8.750 square inches. These results are shown in Table 6-13. These results indicate that the most reactive configuration is with the minimum fuel compartment size because the assembly-to-assembly pitch is minimized.

The next set of analyses determines the effect of fuel compartment box thickness on the system reactivity. The model starts with the minimum fuel compartment width from the previous study and the compartment thickness is varied from 0.1775 inches to 0.2325 inches. The results in Table 6-14 show that the most reactive calculated condition occurs with nominal compartment box thickness. The results indicate that the system reactivity is not very sensitive to the box thickness and that the difference in k_{eff} between the nominal and minimum thickness cases is within statistical uncertainty. The balance of this evaluation uses the nominal box thickness because it represents the most reactive configuration from this study.

6.4.2.3 Determination of Maximum Initial Enrichment for Intact Assemblies

The most reactive configuration determined based on parametric studies is with the rail structure represented with Composition 3, poison and aluminum plates at nominal thickness, fuel compartment at minimum width and nominal thickness and the fuel assemblies positioned in the “inward” position. The following analysis uses this configuration to determine the maximum allowable initial enrichment as a function of poison plate loading and soluble boron concentration for the two fuel assembly classes. Only the fuel assembly type, the fixed and soluble poison loading is changed for each model. In addition, the internal moderator density is varied to determine the peak reactivity for the specific configuration.

The canister / cask model for this evaluation differs from the actual design in the following ways:

- the boron-10 content in the borated aluminum poison plates is 10% lower than the minimum required and the boron-10 content in the Boral® poison plates is 25% lower than the minimum required
- the neutron shield and the skin of the cask are conservatively replaced with water between the casks, and
- the worst case geometry and material conditions, as determined in the previous sections, are modeled.

Five different fixed poison loadings are analyzed in the criticality calculations as described in Section 6.3, corresponding to the five different types of basket based on fixed poison loading (Type A, B, C, D and E). Four different soluble boron concentration levels are analyzed: 2000 ppm, 2300 ppm, 2400 ppm and 2500 ppm. The maximum analyzed initial enrichment is 5.0 wt. % U-235.

6.6 Supplemental Information

6.6.1 References

1. Title 10 Code of Federal Regulations, Part 72, "Licensing Requirements for the Independent Storage of Spent Nuclear Fuel and High-Level Radioactive Waste."
2. Not Used
3. "SCALE, A Modular Code System for Performing Standardized Computer Analyses for Licensing Evaluation," NUREG/CR-0200, Rev. 6 (ORNL/NUREG/CSD-2/R6), Vol. I-III, September 1998.
4. ANSI/ANS 57.2, Design Requirements for Light Water Reactor Spent Fuel Storage Facilities at Nuclear Power Plants, 1983.
5. ANS/ANSI-8.1, American National Standard for Nuclear Criticality Safety in Operations with Fissionable Materials Outside Reactors, 1983.
6. U.S. Nuclear Regulatory Commission, "Criticality Benchmark Guide for Light-Water-Reactor Fuel in Transportation and Storage Packages," NUREG/CR-6361, ORNL-TM-13211, March 1997.
7. U.S. Nuclear Regulatory Commission, "Recommendations for Preparing the Criticality Safety Evaluation of Transportation Packages," NUREG/CR-5661, ORNL/TM-11936, April 1997.
8. Transnuclear Specification, "Design Criteria Document for the 10494 NUHOMS®-32PTH System for Transportation and Storage."
9. Transnuclear Calculation 1095-42, Rev. 0, "Criticality Benchmarks."

Table 6-3
Authorized Contents for NUHOMS®-32PTH DSC

Assembly Type ⁽¹⁾	Array
Westinghouse 17x17 Standard (WE 17x17)	17x17
Westinghouse 17x17 Vantage 5H (WEV 17x17)	17x17
Westinghouse 17x17 OFA (WEO 17x17)	17x17
Framatome ANP Advanced MK BW 17x17 (MK BW 17x17)	17x17
Westinghouse 15x15 Standard (WE 15x15)	15x15
Westinghouse 15x15 Surry Improved (WES 15x15)	15x15
CE 14x14 Standard (CE 14x14)	14x14

- (1) Equivalent reload fuel assemblies that are enveloped by the fuel assembly design characteristics listed above are also acceptable.

Table 6-4
Fuel Assembly Design Parameters for Criticality Analysis

Manufacturer ⁽¹⁾	Array	Version	Active Fuel Length (inches)	# Fuel Rods per Assembly	Pitch (inches)	Fuel Pellet OD (inches)
Westinghouse	17x17	Standard Vantage	144	264	0.4960	0.3225
Westinghouse	17x17	OFA	144	264	0.4960	0.3088
Framatome	17x17	MK BW	144	264	0.4960	0.3195
Westinghouse	15x15	Std / Surry	144	204	0.5630	0.3669
CE	14x14	Std	137	176	0.5800	0.3765
CE	14x14	Ft. Calhoun	128	176	0.5800	0.3815
Manufacturer ⁽¹⁾	Array	Version	Clad Thickness (inches)	Clad OD (inches)	Guide Tube OD Inst. Tube OD (inches)	Guide Tube ID Inst. Tube ID (inches)
Westinghouse	17x17	Standard Vantage	0.0225	0.374	24 @ 0.4820 1 @ 0.4740	24 @ 0.4500 1 @ 0.4440
Westinghouse	17x17	OFA	0.0225	0.360	24 @ 0.4820 1 @ 0.4740	24 @ 0.4500 1 @ 0.4440
Framatome	17x17	MK BW	0.0225	0.374	24 @ 0.4820 1 @ 0.4820	24 @ 0.4500 1 @ 0.4500
Westinghouse	15x15	Std / Surry	0.0243	0.422	20 @ 0.5450 1 @ 0.5450	20 @ 0.5100 1 @ 0.5100
CE	14x14	Std	0.0280	0.440	5 @ 1.115	5 @ 1.035
CE	14x14	Ft. Calhoun	0.0280	0.440	5 @ 1.115	5 @ 1.035

Note: All dimensions shown are nominal

- (1) Equivalent reload fuel assemblies that are enveloped by the fuel assembly design characteristics listed above are also acceptable.

Table 6-10
Results of the Fuel Assembly Positioning Studies
 (Concluded)

Description	K_{keno}	σ_{keno}	K_{eff}	Filename
Westinghouse 17x17 Standard Fuel Assembly				
Centered, 70% IMD	0.9212	0.0008	0.9228	we17std_c070.out:
Centered, 80% IMD	0.9264	0.0007	0.9278	we17std_c080.out:
Centered, 90% IMD	0.9233	0.0007	0.9247	we17std_c090.out:
Centered, 100% IMD	0.9194	0.0007	0.9208	we17std_c100.out:
Inward, 70% IMD	0.9245	0.0008	0.9261	we17std_o070.out:
Inward, 80% IMD	0.9289	0.0008	0.9305	we17std_o080.out:
Inward, 90% IMD	0.9277	0.0007	0.9291	we17std_o090.out:
Inward, 100% IMD	0.9217	0.0007	0.9231	we17std_o100.out:
CE 14x14 Standard Fuel Assembly				
Centered, 60% IMD	0.8799	0.0007	0.8813	ce14std_c060.out:
Centered, 70% IMD	0.8834	0.0007	0.8848	ce14std_c070.out:
Centered, 80% IMD	0.8807	0.0007	0.8821	ce14std_c080.out:
Centered, 90% IMD	0.8723	0.0007	0.8737	ce14std_c090.out:
Centered, 100% IMD	0.8619	0.0007	0.8633	ce14std_c100.out:
Inward, 60% IMD	0.8826	0.0008	0.8842	ce14std_o060.out:
Inward, 70% IMD	0.8862	0.0007	0.8876	ce14std_o070.out:
Inward, 80% IMD	0.8842	0.0007	0.8856	ce14std_o080.out:
Inward, 90% IMD	0.8772	0.0008	0.8788	ce14std_o090.out:
Inward, 100% IMD	0.8676	0.0007	0.8690	ce14std_o100.out:
CE 14x14 Fort Calhoun Fuel Assembly				
Centered, 60% IMD	0.8808	0.0008	0.8824	ce14ftc_c060.out:
Centered, 70% IMD	0.8851	0.0007	0.8865	ce14ftc_c070.out:
Centered, 80% IMD	0.8828	0.0007	0.8842	ce14ftc_c080.out:
Centered, 90% IMD	0.8756	0.0008	0.8772	ce14ftc_c090.out:
Centered, 100% IMD	0.8679	0.0007	0.8693	ce14ftc_c100.out:
Inward, 60% IMD	0.8826	0.0008	0.8842	ce14ftc_o060.out:
Inward, 70% IMD	0.8883	0.0007	0.8897	ce14ftc_o070.out:
Inward, 80% IMD	0.8865	0.0008	0.8881	ce14ftc_o080.out:
Inward, 90% IMD	0.8815	0.0008	0.8831	ce14ftc_o090.out:
Inward, 100% IMD	0.8717	0.0008	0.8733	ce14ftc_o100.out:

Table 6-15
WE 15x15 Class Intact Assemblies Without BPRAs - Final Results
(Concluded)

Description	K _{keno}	σ _{keno}	K _{eff}	Filename
Type D Basket (32.0 mg B-10/cm ²), 2400 ppm Boron, 4.7 wt. % U-235				
60% IMD	0.9115	0.0007	0.9129	we15b24_p32e47_060.out:
70% IMD	0.9263	0.0008	0.9279	we15b24_p32e47_070.out:
80% IMD	0.9338	0.0007	0.9352	we15b24_p32e47_080.out:
90% IMD	0.9333	0.0007	0.9347	we15b24_p32e47_090.out:
100% IMD	0.9305	0.0008	0.9321	we15b24_p32e47_100.out:
Type E Basket (50.0 mg B-10/cm ²), 2400 ppm Boron, 5.0 wt. % U-235				
60% IMD	0.9050	0.0009	0.9068	we15b24_p50e50_060.out:
70% IMD	0.9219	0.0010	0.9239	we15b24_p50e50_070.out:
80% IMD	0.9299	0.0009	0.9317	we15b24_p50e50_080.out:
90% IMD	0.9340	0.0011	0.9362	we15b24_p50e50_090.out:
100% IMD	0.9319	0.0010	0.9339	we15b24_p50e50_100.out:
Type A Basket (7.0 mg B-10/cm ²), 2500 ppm Boron, 3.9 wt. % U-235				
60% IMD	0.9270	0.0007	0.9284	we15b25_p07e39_060.out:
70% IMD	0.9326	0.0007	0.9340	we15b25_p07e39_070.out:
80% IMD	0.9301	0.0007	0.9315	we15b25_p07e39_080.out:
90% IMD	0.9215	0.0008	0.9231	we15b25_p07e39_090.out:
100% IMD	0.9119	0.0008	0.9135	we15b25_p07e39_100.out:
Type B Basket (15.0 mg B-10/cm ²), 2500 ppm Boron, 4.4 wt. % U-235				
60% IMD	0.9282	0.0008	0.9298	we15b25_p15e44_060.out:
70% IMD	0.9355	0.0007	0.9369	we15b25_p15e44_070.out:
80% IMD	0.9357	0.0008	0.9373	we15b25_p15e44_080.out:
90% IMD	0.9353	0.0006	0.9365	we15b25_p15e44_090.out:
100% IMD	0.9273	0.0008	0.9289	we15b25_p15e44_100.out:
Type D Basket (32.0 mg B-10/cm ²), 2500 ppm Boron, 4.9 wt. % U-235				
60% IMD	0.9171	0.0008	0.9187	we15b25_p32e49_060.out:
70% IMD	0.9316	0.0007	0.9330	we15b25_p32e49_070.out:
80% IMD	0.9364	0.0007	0.9378	we15b25_p32e49_080.out:
90% IMD	0.9383	0.0008	0.9399	we15b25_p32e49_090.out:
100% IMD	0.9336	0.0008	0.9352	we15b25_p32e49_100.out:

Table 6-16
WE 15x15 Class Intact Assemblies With BPRAs - Final Results
 (Concluded)

Description	K_{keno}	σ_{keno}	K_{eff}	Filename
Type A Basket (7.0 mg B-10/cm ²), 2000 ppm Boron, 3.50 wt. % U-235				
60% IMD	0.9200	0.0007	0.9214	we15bp20_p07e35_060.out:
70% IMD	0.9312	0.0008	0.9328	we15bp20_p07e35_070.out:
80% IMD	0.9362	0.0007	0.9376	we15bp20_p07e35_080.out:
90% IMD	0.9370	0.0007	0.9384	we15bp20_p07e35_090.out:
100% IMD	0.9318	0.0007	0.9332	we15bp20_p07e35_100.out:
Type B Basket (15.0 mg B-10/cm ²), 2000 ppm Boron, 3.80 wt. % U-235				
60% IMD	0.9037	0.0008	0.9053	we15bp20_p15e38_060.out:
70% IMD	0.9204	0.0009	0.9222	we15bp20_p15e38_070.out:
80% IMD	0.9290	0.0007	0.9304	we15bp20_p15e38_080.out:
90% IMD	0.9335	0.0008	0.9351	we15bp20_p15e38_090.out:
100% IMD	0.9328	0.0007	0.9342	we15bp20_p15e38_100.out:
Type D Basket (32.0 mg B-10/cm ²), 2000 ppm Boron, 4.20 wt. % U-235				
60% IMD	0.8903	0.0007	0.8917	we15bp20_p32e42_060.out:
70% IMD	0.9105	0.0007	0.9119	we15bp20_p32e42_070.out:
80% IMD	0.9255	0.0007	0.9269	we15bp20_p32e42_080.out:
90% IMD	0.9324	0.0007	0.9338	we15bp20_p32e42_090.out:
100% IMD	0.9354	0.0007	0.9368	we15bp20_p32e42_100.out:
Type E Basket (50.0 mg B-10/cm ²), 2000 ppm Boron, 4.50 wt. % U-235				
60% IMD	0.8827	0.0008	0.8843	we15bp20_p50e45_060.out:
70% IMD	0.9063	0.0008	0.9079	we15bp20_p50e45_070.out:
80% IMD	0.9236	0.0008	0.9252	we15bp20_p50e45_080.out:
90% IMD	0.9320	0.0008	0.9336	we15bp20_p50e45_090.out:
100% IMD	0.9380	0.0008	0.9396	we15bp20_p50e45_100.out:

Table 6-17
WE 17x17 Class Intact Assemblies Without BPRAs - Final Results
(Concluded)

Description	K_{keno}	σ_{keno}	K_{eff}	Filename
Type D Basket (32.0 mg B-10/cm ²), 2400 ppm Boron, 4.7 wt. % U-235				
60% IMD	0.9122	0.0007	0.9136	we17b24_p32e47_060.out:
70% IMD	0.9271	0.0009	0.9289	we17b24_p32e47_070.out:
80% IMD	0.9360	0.0008	0.9376	we17b24_p32e47_080.out:
90% IMD	0.9383	0.0007	0.9397	we17b24_p32e47_090.out:
100% IMD	0.9373	0.0008	0.9389	we17b24_p32e47_100.out:
Type E Basket (50.0 mg B-10/cm ²), 2400 ppm Boron, 4.9 wt. % U-235				
60% IMD	0.8992	0.0007	0.9006	we17b24_p50e49_060.out:
70% IMD	0.9165	0.0008	0.9181	we17b24_p50e49_070.out:
80% IMD	0.9285	0.0007	0.9299	we17b24_p50e49_080.out:
90% IMD	0.9335	0.0007	0.9349	we17b24_p50e49_090.out:
100% IMD	0.9339	0.0007	0.9353	we17b24_p50e49_100.out:
Type A Basket (7.0 mg B-10/cm ²), 2500 ppm Boron, 3.9 wt. % U-235				
60% IMD	0.9299	0.0006	0.9311	we17b25_p07e39_060.out:
70% IMD	0.9350	0.0008	0.9366	we17b25_p07e39_070.out:
80% IMD	0.9333	0.0008	0.9349	we17b25_p07e39_080.out:
90% IMD	0.9278	0.0007	0.9292	we17b25_p07e39_090.out:
100% IMD	0.9193	0.0007	0.9207	we17b25_p07e39_100.out:
Type B Basket (15.0 mg B-10/cm ²), 2500 ppm Boron, 4.3 wt. % U-235				
60% IMD	0.9224	0.0007	0.9238	we17b25_p15e43_060.out:
70% IMD	0.9327	0.0007	0.9341	we17b25_p15e43_070.out:
80% IMD	0.9341	0.0007	0.9355	we17b25_p15e43_080.out:
90% IMD	0.9325	0.0007	0.9339	we17b25_p15e43_090.out:
100% IMD	0.9279	0.0008	0.9295	we17b25_p15e43_100.out:
Type D Basket (32.0 mg B-10/cm ²), 2500 ppm Boron, 4.8 wt. % U-235				
60% IMD	0.9137	0.0009	0.9155	we17b25_p32e48_060.out:
70% IMD	0.9282	0.0009	0.9300	we17b25_p32e48_070.out:
80% IMD	0.9358	0.0008	0.9374	we17b25_p32e48_080.out:
90% IMD	0.9373	0.0007	0.9387	we17b25_p32e48_090.out:
100% IMD	0.9356	0.0007	0.9370	we17b25_p32e48_100.out:
Type E Basket (50.0 mg B-10/cm ²), 2500 ppm Boron, 5.0 wt. % U-235				
60% IMD	0.8996	0.0007	0.9010	we17b25_p50e50_060.out:
70% IMD	0.9174	0.0008	0.9190	we17b25_p50e50_070.out:
80% IMD	0.9273	0.0009	0.9291	we17b25_p50e50_080.out:
90% IMD	0.9326	0.0008	0.9342	we17b25_p50e50_090.out:
100% IMD	0.9329	0.0008	0.9345	we17b25_p50e50_100.out:

Table 6-18
WE 17x17 Class Intact Assemblies with BPRAs – Final Results
 (Concluded)

Description	K_{keno}	σ_{keno}	K_{eff}	Filename
Type D Basket (32.0 mg B-10/cm ²), 2500 ppm Boron, 4.7 wt. % U-235				
60% IMD	0.8992	0.0007	0.9006	we17bp25_p32e47_060.out:
70% IMD	0.9154	0.0007	0.9168	we17bp25_p32e47_070.out:
80% IMD	0.9272	0.0007	0.9286	we17bp25_p32e47_080.out:
90% IMD	0.9341	0.0007	0.9355	we17bp25_p32e47_090.out:
100% IMD	0.9356	0.0008	0.9372	we17bp25_p32e47_100.out:
Type E Basket (50.0 mg B-10/cm ²), 2500 ppm Boron, 5.0 wt. % U-235				
60% IMD	0.8871	0.0008	0.8887	we17bp25_p50e50_060.out:
70% IMD	0.9102	0.0007	0.9116	we17bp25_p50e50_070.out:
80% IMD	0.9260	0.0007	0.9274	we17bp25_p50e50_080.out:
90% IMD	0.9343	0.0008	0.9359	we17bp25_p50e50_090.out:
100% IMD	0.9379	0.0008	0.9395	we17bp25_p50e50_100.out:

Table 6-19
Limiting Parameters for Damaged Fuel Calculations

Fuel Assembly Type	Enrichment	Boron Concentration	Fixed Poison Loading
CE 14x14	4.90 wt. % U-235	2300 ppm	15 mg B-10/cm ²
Westinghouse 15x15	4.90 wt. % U-235	2500 ppm	32 mg B-10/cm ²
Westinghouse 17x17	4.80 wt. % U-235	2500 ppm	32 mg B-10/cm ²

Table 6-20
Results of Optimum Pitch Studies
 (Concluded)

Description	K_{keno}	σ_{keno}	K_{eff}	Filename
CE 14x14, 4.9 wt. % U-235, 2300 ppm, 15 mg B-10/cm ² (Type B Basket)				
Pitch = 0.4400", 70% IMD	0.6852	0.0007	0.6866	ce14_pitch_min_070.out:
Pitch = 0.4400", 80% IMD	0.6915	0.0008	0.6931	ce14_pitch_min_080.out:
Pitch = 0.4700", 70% IMD	0.7560	0.0008	0.7576	ce14_pitch_470_070.out:
Pitch = 0.4700", 80% IMD	0.7626	0.0009	0.7644	ce14_pitch_470_080.out:
Pitch = 0.5000", 70% IMD	0.8196	0.0008	0.8212	ce14_pitch_500_070.out:
Pitch = 0.5000", 80% IMD	0.8245	0.0008	0.8261	ce14_pitch_500_080.out:
Pitch = 0.5400", 70% IMD	0.8872	0.0008	0.8888	ce14_pitch_540_070.out:
Pitch = 0.5400", 80% IMD	0.8886	0.0009	0.8904	ce14_pitch_540_080.out:
Pitch = 0.5800", 70% IMD	0.9337	0.0007	0.9351	ce14_pitch_nom_070.out:
Pitch = 0.5800", 80% IMD	0.9336	0.0007	0.9350	ce14_pitch_nom_080.out:
Pitch = 0.6000", 70% IMD	0.9473	0.0007	0.9487	ce14_pitch_600_070.out:
Pitch = 0.6000", 80% IMD	0.9468	0.0007	0.9482	ce14_pitch_600_080.out:
Pitch = 0.6100", 60% IMD	0.9457	0.0008	0.9473	ce14_pitch_610_060.out:
Pitch = 0.6100", 70% IMD	0.9491	0.0008	0.9507	ce14_pitch_610_070.out:
Pitch = 0.6100", 80% IMD	0.9467	0.0007	0.9481	ce14_pitch_610_080.out:
Pitch = 0.6100", 90% IMD	0.9383	0.0008	0.9399	ce14_pitch_610_090.out:
Pitch = 0.6100", 100% IMD	0.9290	0.0007	0.9304	ce14_pitch_610_100.out:
Pitch = 0.6200", 60% IMD	0.9500	0.0007	0.9514	ce14_pitch_620_060.out:
Pitch = 0.6200", 70% IMD	0.9512	0.0007	0.9526	ce14_pitch_620_070.out:
Pitch = 0.6200", 80% IMD	0.9471	0.0007	0.9485	ce14_pitch_620_080.out:
Pitch = 0.6200", 90% IMD	0.9368	0.0008	0.9384	ce14_pitch_620_090.out:
Pitch = 0.6200", 100% IMD	0.9250	0.0007	0.9264	ce14_pitch_620_100.out:
Pitch = 0.6250", 60% IMD	0.9499	0.0007	0.9513	ce14_pitch_625_060.out:
Pitch = 0.6250", 70% IMD	0.9506	0.0007	0.9520	ce14_pitch_625_070.out:
Pitch = 0.6250", 80% IMD	0.9476	0.0008	0.9492	ce14_pitch_625_080.out:
Pitch = 0.6250", 90% IMD	0.9372	0.0007	0.9386	ce14_pitch_625_090.out:
Pitch = 0.6250", 100% IMD	0.9234	0.0008	0.9250	ce14_pitch_625_100.out:
Pitch = 0.6315", 60% IMD	0.9499	0.0007	0.9513	ce14_pitch_max_060.out:
Pitch = 0.6315", 70% IMD	0.9500	0.0008	0.9516	ce14_pitch_max_070.out:
Pitch = 0.6315", 80% IMD	0.9445	0.0007	0.9459	ce14_pitch_max_080.out:
Pitch = 0.6315", 90% IMD	0.9340	0.0008	0.9356	ce14_pitch_max_090.out:
Pitch = 0.6315", 100% IMD	0.9187	0.0007	0.9201	ce14_pitch_max_100.out:

Table 6-21
Results of the Single Ended Rod Shear Studies
 (Concluded)

Description	K_{keno}	σ_{keno}	K_{eff}	Filename
CE 14x14, 4.9 wt. % U-235, 2300 ppm, 15 mg B-10/cm ² (Type B Basket)				
D=1.20 cm, 60% IMD	0.9336	0.0007	0.9350	ce14_ss120_060.out:
D=1.20 cm, 70% IMD	0.9402	0.0008	0.9418	ce14_ss120_070.out:
D=1.20 cm, 80% IMD	0.9384	0.0007	0.9398	ce14_ss120_080.out:
D=1.20 cm, 90% IMD	0.9325	0.0007	0.9339	ce14_ss120_090.out:
D=1.20 cm, 100% IMD	0.9235	0.0007	0.9249	ce14_ss120_100.out:
D=1.35 cm, 60% IMD	0.9341	0.0007	0.9355	ce14_ssmax_060.out:
D=1.35 cm, 70% IMD	0.9386	0.0007	0.9400	ce14_ssmax_070.out:
D=1.35 cm, 80% IMD	0.9363	0.0008	0.9379	ce14_ssmax_080.out:
D=1.35 cm, 90% IMD	0.9291	0.0008	0.9307	ce14_ssmax_090.out:
D=1.35 cm, 100% IMD	0.9203	0.0007	0.9217	ce14_ssmax_100.out:

Table 6-22
Results of the Double Ended Rod Shear Studies

CE 14x14, 4.9 wt. % U-235, 2300 ppm, 15 mg B-10/cm ² (Type B Basket)				
Description	K_{keno}	σ_{keno}	K_{eff}	Filename
No Shear				
Ratio=0, 60% IMD	0.9289	0.0008	0.9305	ce14_ds000_060.out:
Ratio=0, 70% IMD	0.9340	0.0008	0.9356	ce14_ds000_070.out:
Ratio=0, 80% IMD	0.9336	0.0007	0.9350	ce14_ds000_080.out:
Ratio=0, 90% IMD	0.9284	0.0008	0.9300	ce14_ds000_090.out:
Ratio=0, 100% IMD	0.9224	0.0007	0.9238	ce14_ds000_100.out:
Double Ended Shear with Minimum Distance Between the Sheared and Intact Rows				
Ratio=5/10, 60% IMD	0.9349	0.0007	0.9363	ce14_ds001_060.out:
Ratio=5/10, 70% IMD	0.9406	0.0009	0.9424	ce14_ds001_070.out:
Ratio=5/10, 80% IMD	0.9442	0.0007	0.9456	ce14_ds001_080.out:
Ratio=5/10, 90% IMD	0.9398	0.0008	0.9414	ce14_ds001_090.out:
Ratio=5/10, 100% IMD	0.9328	0.0008	0.9344	ce14_ds001_100.out:
Double Ended Shear with Maximum Distance Between the Sheared and Intact Rows				
Ratio=5/10, 60% IMD	0.9373	0.0007	0.9387	ce14_ds011_060.out:
Ratio=5/10, 70% IMD	0.9453	0.0008	0.9469	ce14_ds011_070.out:
Ratio=5/10, 80% IMD	0.9492	0.0008	0.9508	ce14_ds011_080.out:
Ratio=5/10, 90% IMD	0.9443	0.0007	0.9457	ce14_ds011_090.out:
Ratio=5/10, 100% IMD	0.9365	0.0007	0.9379	ce14_ds011_100.out:

Table 6-22
Results of the Double Ended Rod Shear Studies
 (Concluded)

Description	K_{keno}	σ_{keno}	K_{eff}	Filename
WE 17x17, 4.8 wt. % U-235, 2500 ppm, 32 mg B-10/cm ² (Type D Basket)				
Ratio=0, 60% IMD	0.9149	0.0007	0.9163	we17_ds000_060.out:
Ratio=0, 70% IMD	0.9304	0.0009	0.9322	we17_ds000_070.out:
Ratio=0, 80% IMD	0.9354	0.0007	0.9368	we17_ds000_080.out:
Ratio=0, 90% IMD	0.9369	0.0007	0.9383	we17_ds000_090.out:
Ratio=0, 100% IMD	0.9355	0.0008	0.9371	we17_ds000_100.out:
Ratio=2/10, 60% IMD	0.9159	0.0008	0.9175	we17_ds210_060.out:
Ratio=2/10, 70% IMD	0.9299	0.0007	0.9313	we17_ds210_070.out:
Ratio=2/10, 80% IMD	0.9371	0.0008	0.9387	we17_ds210_080.out:
Ratio=2/10, 90% IMD	0.9386	0.0008	0.9402	we17_ds210_090.out:
Ratio=2/10, 100% IMD	0.9372	0.0008	0.9388	we17_ds210_100.out:
Ratio=3/10, 60% IMD	0.9184	0.0008	0.9200	we17_ds310_060.out:
Ratio=3/10, 70% IMD	0.9319	0.0008	0.9335	we17_ds310_070.out:
Ratio=3/10, 80% IMD	0.9382	0.0007	0.9396	we17_ds310_080.out:
Ratio=3/10, 90% IMD	0.9415	0.0007	0.9429	we17_ds310_090.out:
Ratio=3/10, 100% IMD	0.9386	0.0008	0.9402	we17_ds310_100.out:
Ratio=5/10, 60% IMD	0.9179	0.0008	0.9195	we17_ds510_060.out:
Ratio=5/10, 70% IMD	0.9324	0.0008	0.9340	we17_ds510_070.out:
Ratio=5/10, 80% IMD	0.9404	0.0007	0.9418	we17_ds510_080.out:
Ratio=5/10, 90% IMD	0.9444	0.0008	0.9460	we17_ds510_090.out:
Ratio=5/10, 100% IMD	0.9403	0.0007	0.9417	we17_ds510_100.out:

Table 6-26
WE 15x15 Class Damaged Assemblies With BPRAs - Final Results
 (Concluded)

Description	K_{keno}	σ_{keno}	K_{eff}	Filename
Type A Basket (7.0 mg B-10/cm ²), 2000 ppm Boron, 3.40 wt. % U-235				
60% IMD	0.9101	0.0008	0.9117	we15bpds_p07e34_060.out:
70% IMD	0.9249	0.0007	0.9263	we15bpds_p07e34_070.out:
80% IMD	0.9321	0.0008	0.9337	we15bpds_p07e34_080.out:
90% IMD	0.9324	0.0007	0.9338	we15bpds_p07e34_090.out:
100% IMD	0.9297	0.0008	0.9313	we15bpds_p07e34_100.out:
Type B Basket (15.0 mg B-10/cm ²), 2000 ppm Boron, 3.75 wt. % U-235				
60% IMD	0.9007	0.0007	0.9021	we15bpds_p15e38_060.out:
70% IMD	0.9205	0.0007	0.9219	we15bpds_p15e38_070.out:
80% IMD	0.9290	0.0007	0.9304	we15bpds_p15e38_080.out:
90% IMD	0.9352	0.0007	0.9366	we15bpds_p15e38_090.out:
100% IMD	0.9372	0.0007	0.9386	we15bpds_p15e38_100.out:
Type D Basket (32.0 mg B-10/cm ²), 2000 ppm Boron, 4.10 wt. % U-235				
60% IMD	0.8863	0.0008	0.8879	we15bpds_p32e41_060.out:
70% IMD	0.9088	0.0008	0.9104	we15bpds_p32e41_070.out:
80% IMD	0.9211	0.0008	0.9227	we15bpds_p32e41_080.out:
90% IMD	0.9307	0.0007	0.9321	we15bpds_p32e41_090.out:
100% IMD	0.9337	0.0008	0.9353	we15bpds_p32e41_100.out:
Type E Basket (50.0 mg B-10/cm ²), 2000 ppm Boron, 4.35 wt. % U-235				
60% IMD	0.8760	0.0007	0.8774	we15bpds_p50e44_060.out:
70% IMD	0.9020	0.0008	0.9036	we15bpds_p50e44_070.out:
80% IMD	0.9177	0.0008	0.9193	we15bpds_p50e44_080.out:
90% IMD	0.9274	0.0007	0.9288	we15bpds_p50e44_090.out:
100% IMD	0.9336	0.0008	0.9352	we15bpds_p50e44_100.out:

Table 6-27
WE 17x17 Class Damaged Assemblies With BPRAs - Final Results
 (Concluded)

Description	K_{keno}	σ_{keno}	K_{eff}	Filename
Type D Basket (32.0 mg B-10/cm ²), 2500 ppm Boron, 4.60 wt. % U-235				
60% IMD	60% IMD	60% IMD	60% IMD	60% IMD
70% IMD	70% IMD	70% IMD	70% IMD	70% IMD
80% IMD	80% IMD	80% IMD	80% IMD	80% IMD
90% IMD	90% IMD	90% IMD	90% IMD	90% IMD
100% IMD	100% IMD	100% IMD	100% IMD	100% IMD
Type E Basket (50.0 mg B-10/cm ²), 2500 ppm Boron, 4.9 wt. % U-235				
60% IMD	60% IMD	60% IMD	60% IMD	60% IMD
70% IMD	70% IMD	70% IMD	70% IMD	70% IMD
80% IMD	80% IMD	80% IMD	80% IMD	80% IMD
90% IMD	90% IMD	90% IMD	90% IMD	90% IMD
100% IMD	100% IMD	100% IMD	100% IMD	100% IMD

Table 6-33
CE 14x14 Class Intact Assemblies – Final Results
 (Concluded)

Description	K_{keno}	σ_{keno}	K_{eff}	Filename
Type C Basket (20.0 mg B-10/cm ²), 2300 ppm Boron, 5.00 wt. % U-235				
60% IMD	0.9196	0.0007	0.9210	ce14b23_p20e50_060.out:
70% IMD	0.9295	0.0007	0.9309	ce14b23_p20e50_070.out:
80% IMD	0.9305	0.0008	0.9321	ce14b23_p20e50_080.out:
90% IMD	0.9285	0.0008	0.9301	ce14b23_p20e50_090.out:
100% IMD	0.9223	0.0007	0.9237	ce14b23_p20e50_100.out:
Type A Basket (07.0 mg B-10/cm ²), 2400 ppm Boron, 4.45 wt. % U-235				
60% IMD	0.9317	0.0007	0.9331	ce14b24_p07e44_060.out:
70% IMD	0.9347	0.0007	0.9361	ce14b24_p07e44_070.out:
80% IMD	0.9305	0.0008	0.9321	ce14b24_p07e44_080.out:
90% IMD	0.9221	0.0007	0.9235	ce14b24_p07e44_090.out:
100% IMD	0.9124	0.0008	0.9140	ce14b24_p07e44_100.out:
Type B Basket (15.0 mg B-10/cm ²), 2400 ppm Boron, 5.00 wt. % U-235				
60% IMD	0.9290	0.0007	0.9304	ce14b24_p15e50_060.out:
70% IMD	0.9358	0.0008	0.9374	ce14b24_p15e50_070.out:
80% IMD	0.9358	0.0007	0.9372	ce14b24_p15e50_080.out:
90% IMD	0.9306	0.0007	0.9320	ce14b24_p15e50_090.out:
100% IMD	0.9238	0.0007	0.9252	ce14b24_p15e50_100.out:
Type A Basket (07.0 mg B-10/cm ²), 2500 ppm Boron, 4.55 wt. % U-235				
60% IMD	0.9345	0.0007	0.9359	ce14b25_p07e45_060.out:
70% IMD	0.9370	0.0008	0.9386	ce14b25_p07e45_070.out:
80% IMD	0.9295	0.0008	0.9311	ce14b25_p07e45_080.out:
90% IMD	0.9237	0.0007	0.9251	ce14b25_p07e45_090.out:
100% IMD	0.9139	0.0007	0.9153	ce14b25_p07e45_100.out:

Table 6-34
CE 14x14 Class Damaged Assemblies – Final Results
 (Concluded)

Description	K_{keno}	σ_{keno}	K_{eff}	Filename
Type A Basket (07.0 mg B-10/cm ²), 2500 ppm Boron, 4.35 wt. % U-235				
60% IMD	0.9364	0.0007	0.9378	ce14d25_p07e43_060.out:
70% IMD	0.9323	0.0007	0.9337	ce14d25_p07e43_070.out:
80% IMD	0.9235	0.0006	0.9247	ce14d25_p07e43_080.out:
90% IMD	0.9087	0.0007	0.9101	ce14d25_p07e43_090.out:
100% IMD	0.8926	0.0007	0.8940	ce14d25_p07e43_100.out:
Type B Basket (15.0 mg B-10/cm ²), 2500 ppm Boron, 4.90 wt. % U-235				
60% IMD	0.9375	0.0009	0.9393	ce14d25_p15e49_060.out:
70% IMD	0.9380	0.0007	0.9394	ce14d25_p15e49_070.out:
80% IMD	0.9327	0.0008	0.9343	ce14d25_p15e49_080.out:
90% IMD	0.9220	0.0007	0.9234	ce14d25_p15e49_090.out:
100% IMD	0.9077	0.0008	0.9093	ce14d25_p15e49_100.out:
Type C Basket (20.0 mg B-10/cm ²), 2500 ppm Boron, 5.00 wt. % U-235				
60% IMD	0.9297	0.0007	0.9311	ce14d25_p20e50_060.out:
70% IMD	0.9326	0.0007	0.9340	ce14d25_p20e50_070.out:
80% IMD	0.9277	0.0007	0.9291	ce14d25_p20e50_080.out:
90% IMD	0.9178	0.0007	0.9192	ce14d25_p20e50_090.out:
100% IMD	0.9059	0.0007	0.9073	ce14d25_p20e50_100.out:

CHAPTER 7
CONFINEMENT

TABLE OF CONTENTS

7. **CONFINEMENT** 7-1

7.1 Confinement Boundary 7-1

 7.1.1 Confinement Vessel..... 7-1

 7.1.2 Confinement Penetrations 7-2

 7.1.3 Seals and Welds..... 7-2

 7.1.4 Closure..... 7-2

7.2 Requirements for Normal Conditions of Storage 7-3

 7.2.1 Release of Radioactive Material..... 7-3

 7.2.2 Pressurization of Confinement Vessel..... 7-3

7.3 Confinement Requirements for Hypothetical Accident Conditions 7-4

 7.3.1 Fission Gas Products 7-4

 7.3.2 Release of Contents 7-4

7.4 Supplemental Data..... 7-5

 7.4.1 Confinement Monitoring Capability 7-5

 7.4.2 References 7-5

LIST OF FIGURES

7-1 Typical 32PTH DSC Confinement Boundaries and Welds

7. CONFINEMENT

The confinement evaluation described in this chapter 7.0 is applicable to the 32PTH DSC. See Appendix A, Chapter A.7, for discussion of applicability of these analyses to the 32PTH Type 1 DSC.

7.1 Confinement Boundary

The 32PTH DSC is a high integrity stainless steel welded vessel that provides confinement of radioactive materials encapsulates the fuel in a helium atmosphere and provides biological shielding during 32PTH DSC closure and transfer and storage operations. The 32PTH DSC is designed to maintain confinement of radioactive material within the limits of 10CFR 72.104(a), 10CFR 72.106(b) and 10CFR 20 under normal, off-normal, and credible accident conditions. Chapter 3 concludes that the design including the helium atmosphere within the 32PTH DSC will adequately protect the spent fuel cladding against degradation that might otherwise lead to gross ruptures during storage. The design ensures that fuel degradation during storage will not pose operational safety problems with respect to removal of the fuel from storage.

The DSC cylindrical shell, the inner top cover/shield plug¹, and shell bottom form the confinement boundary for the spent fuel. The vent and siphon covers and welds are also included in the confinement boundary. The outer top cover plate is a structural attachment to the confinement boundary. The dimensions and material descriptions for the confinement boundary assemblies and the redundantly welded barriers are discussed in Chapter 1. The components important to safety are identified in Chapter 2.

7.1.1 Confinement Vessel

The cylindrical shell and inner shell to bottom cover plate welds are made during fabrication of the 32PTH DSC and are fully compliant to ASME Section III, Subsection NB. The welds between the shell and inner top cover/shield plug¹ (including siphon and vent cover welds and option 2 or option 3 design welds shown in Figure 7-1) are made after fuel loading. These welds are designed, fabricated, inspected and tested using alternatives to the ASME code specified in SAR Section 3.10.

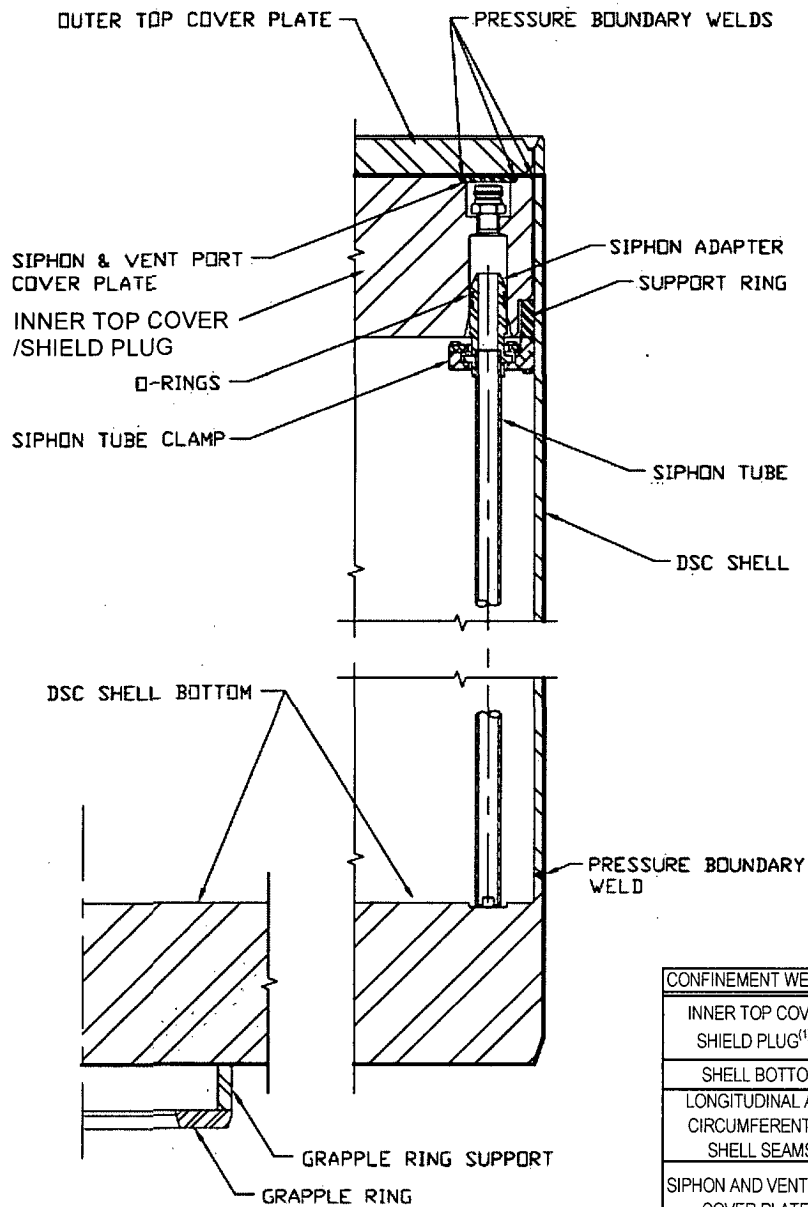
Stringent design and fabrication requirements ensure that the confinement function of the 32PTH DSC is maintained. The cylindrical shell and shell bottom are pressure tested in accordance with the ASME Code, Section III, Subarticle NB-6300. This pressure test is performed after installation of the shell bottom at the fabricator's facility and may be performed concurrently with the leak test, provided the requirements of NB-6300 are met.

A leak test of the shell assembly, including the shell bottom, is performed in accordance with ANSI N14.5 [2] and the ASME Code, Section V, Article 10. These tests are typically performed at the fabricator's facility. The acceptance criteria for the test are "leaktight" as defined in [2].

The process involved in leak testing the 32PTH DSC involves temporarily sealing the shell from the top end. The gas filled envelope and evacuated envelope testing methodologies have the

¹ For option 2 design (described in Chapter 1 drawings): Top casing plate, siphon/vent block, alignment pin block and lifting post are included in the confinement boundary

For option 3 design (described in Chapter 1 drawings): Top shield plug outer plate is included in the confinement boundary



NDE REQUIREMENTS FOR
CONFINEMENT BOUNDARY WELDS

CONFINEMENT WELD	NDE REQUIREMENTS	WELD TYPE
INNER TOP COVER/ SHIELD PLUG ^{(1) (2)}	MULTI-LEVEL PT	PARTIAL PENETRATION
SHELL BOTTOM	RT OR UT AND PT	FULL PENETRATION
LONGITUDINAL AND CIRCUMFERENTIAL SHELL SEAMS	RT AND PT	FULL PENETRATION
SIPHON AND VENT PORT COVER PLATES	MULTI-LEVEL PT	PARTIAL PENETRATION

⁽¹⁾ Includes shell to the top casing plate weld, shell to the siphon/vent block weld, and shell to the alignment pin block weld for option 2 design described in Chapter 1 drawings

⁽²⁾ Includes shell to the top shield plug outer plate weld for option 3 design described in Chapter 1 drawings

Figure 7-1
Typical 32PTH DSC Confinement Boundaries and Welds

8.0 OPERATING PROCEDURES

This chapter outlines a sequence of operations to be incorporated into procedures for preparation of the NUHOMS® HD System DSC, loading of fuel, closure of the DSC, transport to the ISFSI, transfer into the HSM-H, monitoring operations, and retrieval and unloading. Operations are presented in their anticipated approximate performance sequence. Alternate sequencing that achieves the same purpose is acceptable. Temporary shielding may be used throughout as appropriate to maintain doses as low as reasonably achievable (ALARA). Use nitrogen or helium to assist in removal of water. After water is drained from the DSC, (sections 8.1.1.2 & 8.1.1.3), the DSC shall be backfilled with nitrogen or helium.

As stated in Appendix A, Chapter A.8, the operational steps described here in Chapter 8 apply in their entirety and without change to the 32PTH Type 1 DSC (described in Appendix A) when the optional two-part top end closure assembly (which is similar to the 32PTH DSC) is used. The 32PTH Type 1 DSC also features a three-part top end closure assembly. Appendix A, Chapter A.8 provides a description of the changes in operational sequences that are applicable when using that alternative.

8.1 Procedures for Loading the DSC and Transfer to the HSM-H

8.1.1 Narrative Description

The following steps describe the recommended generic operating procedures for the NUHOMS® System. A list of major equipment used during loading and unloading operations is provided in Table 8-1. A pictorial representation of key phases of this process is provided in Figure 8-1.

8.1.1.1 Transfer Cask and DSC Preparation

1. Verify by plant records or other means that candidate fuel assemblies meet the physical, thermal and radiological criteria specified in the Technical Specifications.
2. Clean or decontaminate the transfer cask as necessary to meet licensee pool and ALARA requirements, and to minimize transfer of contamination from the cask cavity to the DSC exterior.
3. Examine the transfer cask cavity for any physical damage.
4. Verify specified lubrication of the transfer cask rails.
5. Examine the DSC for any physical damage and for cleanliness. Verify that bottom fuel spacers or damaged fuel bottom end caps, if required, are present in all fuel compartments. Remove damaged fuel top end caps if they are in place. Record the DSC serial number which is located on the grappling ring. Verify the basket type by identifying the last character in the serial number.
6. If not already installed, install lifting rods into the four threaded sockets in the bottom of the DSC cavity in accordance with the design drawing.
7. Lift the DSC into the cask cavity and rotate the DSC to match the transfer cask alignment marks.
8. Remove the lifting rods.
9. Fill the transfer cask/DSC annulus with clean water.
10. Seal the top of the annulus, using for example an inflatable seal.

11. A tank filled with clean water, and kept above the pool surface may be connected to the top vent port of the transfer cask via a hose to provide a positive pressure in the annulus. This is an optional arrangement, which provides additional assurance that contaminated water from the fuel pool will not enter the annulus. Do not pressurize this tank, nor raise it sufficiently high to float the DSC. For the 32PTH DSC with a 69.75 inch OD, and an empty weight of 49,000 lb, a differential pressure of 12.8 psi, equivalent to 29.6 ft of pure water, would be sufficient to lift the DSC.
12. If the DSC top covers were trial fitted, they must be removed prior to filling the DSC with water. The vent port quick connect fitting in the inner top cover may be removed to facilitate hydrogen monitoring later. The drain port fitting may be either left in place or removed – water may be pumped from the DSC either with or without the fitting.
13. The licensee shall develop procedures to verify that the boron content of the water added to the DSC conforms to the Technical Specifications. Fill the DSC with water from the fuel pool or an equivalent source meeting the minimum boron concentration required by the Technical Specifications. Optionally, this may be done at the time of immersing the cask in the pool. If the pool water is allowed flow over the transfer cask lip and into the DSC, provision must be made to protect the annulus seal from being dislodged by the water running over it.
- 14a. Optionally, secure a sheet of suitable material to the bottom of the cask to minimize the potential for ground-in contamination. This step may be done at any convenient time prior to immersion.
- 14b. Drain or fill the transfer cask liquid neutron shield, as required by licensee ALARA requirements and crane weight limits. This step may be done at any convenient time prior to immersion.
15. Prior to the cask being lifted into the fuel pool, the water level in the pool should be adjusted as necessary to accommodate the transfer cask and DSC volume. If the water placed in the DSC cavity was obtained from the fuel pool, a level adjustment may not be necessary.

8.1.1.2 DSC Fuel Loading

1. Verify proper engagement of the lifting yoke with the transfer cask lifting trunnions.
2. Lift the transfer cask / DSC and position them over the cask loading area of the spent fuel pool.
3. Lower the cask into the fuel pool until the bottom of the cask is at the height of the fuel pool surface. As the cask is lowered into the pool, spray the

exterior surface of the cask with clean water to minimize surface adhesion of contamination.

4. Place the cask in the location of the fuel pool designated as the cask loading area.
5. Disengage the lifting yoke from the transfer cask lifting trunnions and move the yoke clear of the cask. Spray the lifting yoke with clean water if it is raised out of the fuel pool.
6. Load pre-selected spent fuel assemblies into the DSC basket compartments. The licensee shall develop procedures to verify that the boron content of the water conforms to the Technical Specifications, and that fuel identifications are verified and documented. Damaged fuel must be loaded only in designated compartments fitted with a damaged fuel bottom end cap.
7. After all the fuel assemblies have been placed into the DSC and their identities verified, install damaged fuel top end caps into designated compartments containing damaged fuel.
8. Lower the inner top cover/shield plug¹ in the DSC, aligning it with the guide on the DSC wall, and engaging the drain tube, until it seats on its support ring.
9. Visually verify that the inner top cover/shield plug is properly seated in the DSC. Reseat if necessary.
10. Position the lifting yoke and verify that it is properly engaged with the transfer cask trunnions.
11. Lift the transfer cask to the pool surface and spray the exposed portion of the cask with clean water.
12. Drain any water from above the inner top cover/shield plug back to the spent fuel pool. Up to 1300 gallons of water may be removed from the DSC prior to lifting the transfer cask clear of the pool surface. Up to 15 psig of nitrogen or helium may be used to assist the removal of water. The DSC shall be backfilled with nitrogen or helium after drainage of bulk water.
13. Lift the cask from the fuel pool, continuing to spray the cask with clean water.
14. Move the cask with loaded DSC to the area designated for DSC draining and closure operations. The set-down area should be level, or if slightly sloped, the transfer cask and DSC should be placed with the slope down toward the DSC drain/siphon tube.

¹ Including option 2 or option 3 inner top cover as described in Chapter 1 drawings.

8.1.1.3 DSC Closing, Drying, and Backfilling

1. Fill the transfer cask liquid neutron shield if it was drained for weight reduction during preceding operations.
2. Decontaminate the transfer cask exterior.
3. Disengage the rigging from the inner top cover/shield plug, and remove the eyebolts. Disengage the lifting yoke from the trunnions.
4. Disconnect the annulus overpressure tank if one was used, decontaminate the exposed surfaces of the DSC shell perimeter, remove any remaining water from the top of the annulus seal, and remove the seal.
5. Open the cask cavity drain port and allow water from the annulus to drain out until the water level is approximately twelve inches below the top of the DSC shell. Take swipes around the outer surface of the DSC shell to verify conformance with Technical Specification limits.
6. Cover the transfer cask / DSC annulus to prevent debris and weld splatter from entering the annulus.
7. If water was not drained from the DSC earlier, connect a pump to the DSC drain port and remove up to 1300 gallons of water. Use nitrogen or helium to assist the removal of water. This lowers the water sufficiently to allow welding of the inner top cover/shield plug, while keeping a sufficient volume of the water in the DSC to cool the spent fuel (Pay special attention to step 14 below). Up to 15 psig of nitrogen, or helium gas may be applied at the vent port to assist the water pump down.

CAUTION: Radiation dose rates are expected to be high at the vent and siphon port locations. Use proper ALARA practices (e.g., use of temporary shielding, appropriate positioning of personnel, etc.) to minimize personnel exposure.

8. Install the automated welding machine onto the inner top cover/shield plug.
9. Hydrogen monitoring is required prior to commencing and continuously during the welding of the inner top cover / shield plug [1]. Insert a hydrogen monitor intake line through the vent port such that it terminates just below the inner top cover/shield plug. Temperature monitoring of the TC cavity/annulus water is also required, see step 14.
10. Verify that the hydrogen concentration does not exceed 2.4% [1]. If this limit is exceeded, stop all welding operations and purge the DSC cavity with helium (or other inert gas) via the vent port to reduce hydrogen concentration safely below the 2.4% limit.

11. Complete the inner top cover/shield plug welding and perform the non-destructive examinations as required by the Technical Specifications. The weld must be made in at least two layers.
12. Remove the automated welding machine.
13. Pump remaining water from the DSC. Remove as much free standing water as possible to shorten vacuum drying time. Up to 15 psig of nitrogen, or helium gas may be applied at the vent port to assist the water pump down.
14. There are three methods described in Chapter 4 to assure that the fuel temperature limit is not exceeded during vacuum drying. Each method is associated with a time limit for vacuum drying, starting from the time that pumping of liquid water from the DSC is complete as required by the Technical Specifications for vacuum drying. As required by the technique chosen, either
 - a) install annulus water circulation equipment, or
 - b) drain annulus water if temperature exceeds 180°F
 - c) for either a or b, the DSC may be evacuated to 100 mbar or lower, and backfilled with helium to atmospheric pressure prior to start of vacuum drying.

All helium used in backfilling operations shall be at least 99.99% pure (this may be done as part of step 15).

NOTE: Proceed cautiously when evacuating the dry shielded canister (DSC) to avoid freezing consequences.

15. Connect a vacuum pump / helium backfill manifold to the vent port or to both the vent and drain ports. The quick connect fittings may be removed and replaced with stainless steel pipe nipple / vacuum hose adapters to improve vacuum conductance. Make provision to prevent icing, for example by avoiding traps (low sections) in the vacuum line. Provide appropriate measures as required to control any airborne radionuclides in the vacuum pump exhaust. Purge air from the helium backfill manifold.

Optionally, leak test the manifold and the connections to the DSC. The DSC may be pressurized to no more than 15 psig for leak testing.

CAUTION: Radiation dose rates are expected to be high at the vent and siphon port locations. Use proper ALARA practices (e.g., use of temporary shielding, appropriate positioning of personnel, etc.) to minimize personnel exposure.

16. Evacuate the DSC to the pressure required by the Technical Specification for vacuum drying, and isolate the vacuum pump. The isolation valve should be

as near to the DSC as practicable, with a pressure gauge on the DSC side of the valve. Prior to performing the vacuum hold for 30 minutes as required by the Technical Specification, the vacuum pump must be turned off; or if the pump is not turned off, provide a tee and valve (or other means) to open the line to atmosphere between the pump and the DSC isolation valve.

17. Maintain the water condition in the transfer cask / DSC annulus as required by the technique chosen (step 14).
18. If the Technical Specification is satisfied, i.e., if the pressure remains below the specified limit for the required duration with the pump isolated, continue to the next step. If not, repeat steps 16 and 17.
- 19a. Purge air from the backfill manifold, open the isolation valve, and backfill the DSC cavity with helium to 16.5 to 18 psig and hold for 10 minutes.
- 19b. Reduce the DSC cavity pressure to atmospheric pressure, or slightly over.
20. If the quick connect fittings were removed for vacuum drying, remove the vacuum line adapters from the ports, and re-install the quick connect fittings using suitable pipe thread sealant.

CAUTION: Radiation dose rates are expected to be high at the vent and siphon port locations. Use proper ALARA practices (e.g., use of temporary shielding, appropriate positioning of personnel, etc.) to minimize personnel exposure.

21. Evacuate the DSC through the vent port quick connect fitting to a pressure 100 mbar or less.
22. Backfill the DSC with helium to the pressure specified in the Technical Specifications, and disconnect the vacuum / backfill manifold from the DSC.
23. Repeat steps 21 and 22 if the DSC interior is exposed to nitrogen during any succeeding operations.
- 24a. Weld the covers over the vent and drain ports, performing non-destructive examination as required by the Technical Specifications. The welds shall have at least two layers.
- 24b. Install a temporary test head fixture (or any other alternative means). Perform a leak test of the inner top cover/shield plug to the DSC shell welds and siphon/vent cover welds in accordance with the Technical Specification limits. Verify that the personnel performing the leak test are qualified in accordance with SNT-TC-1A.
25. Place the outer top cover plate onto the DSC and verify correct rotational alignment of the cover and the DSC shell. Install the automated welding

machine onto the outer top cover plate. As an option, the welding machine may be mounted onto the cover plate and then placed together on the DSC.

26. Complete the outer top cover welding and perform the non-destructive examinations as required by the Technical Specifications. The weld must be made in at least two layers.
27. Remove everything except the DSC from the transfer cask cavity: welding machine, protective covering from the transfer cask / DSC annulus, annulus temperature monitoring or water circulation equipment, temporary shielding, etc.
28. Install the transfer cask lid and bolt it.
29. Evacuate the transfer cask cavity to below 100 mbar, and backfill the transfer cask annulus with helium in accordance with the Technical Specifications pressure tolerance and time limit.

8.1.1.4 Transfer Cask Downending and Transport to ISFSI

1. Deleted.
2. The transfer trailer should be positioned so that the cask support skid is accessible to the crane with the trailer supported on its vertical jacks. If required due to space limitations, the crane may remain in a stationary position while the cask support skid and trailer translate underneath the cask as it is downended, (the trailer cannot be supported on the vertical jacks.)
3. Engage the lifting yoke and lift the transfer cask over the cask support skid onto the transfer trailer.
4. Position the cask lower trunnions onto the transfer trailer support skid pillow blocks.
5. Move the crane while simultaneously lowering the cask until the cask upper trunnions are just above the support skid upper trunnion pillow blocks. Alternatively, if the crane is to remain stationary as identified above, slowly move the trailer and support skid as the cask is lowered until the upper trunnions are just above the support skid upper trunnion pillow blocks.
6. Verify that the cask and trunnion pillow blocks are properly aligned.
7. Lower the cask onto the skid until the weight of the cask is distributed to the trunnion pillow blocks.
8. Verify the trunnions are properly seated onto the skid and install the trunnion tower closure plates. Refill the cask liquid neutron shield, if it was drained in step 1 above.

8.1.1.5 DSC Transfer to the HSM-H

1. The maximum lifting height and ambient temperature requirements of the Technical Specifications must be met during transfer from the fuel building to the HSM-H.
2. Prior to loading the DSC into the HSM-H, verify that there is no debris in the HSM-H, the air inlet and outlets are not blocked, the air inlet and outlet screens are not damaged, and the rails are lubricated as specified.

CAUTION: The inside of empty modules have the potential for high dose rates due to adjacent loaded modules. Proper ALARA practices should be followed for these operations. Do not leave the HSM door open except during DSC transfer. If DSC transfer is delayed after HSM door removal, a temporary cover shall be installed.

3. Tow the transfer trailer with the loaded cask to the ISFSI.
4. Position the transfer trailer to within a few feet of the HSM-H to maintain doses ALARA when the cask lid is removed.
5. Verify that the centerline of the HSM-H and cask approximately coincide. Reposition the trailer as necessary following appropriate ALARA practices.
6. Using a portable crane, unbolt and remove the cask lid.
7. Back the trailer to within a few inches of the HSM-H, set the trailer brakes and disengage the tractor. Drive the tractor clear of the trailer and extend the transfer trailer vertical jacks.
8. Remove the skid tie-down bracket fasteners and use the hydraulic skid positioning system to bring the cask into approximate vertical and horizontal alignment with the HSM-H. Using optical survey equipment and the alignment marks on the cask and the HSM-H, adjust the position of the cask until it is aligned with the HSM-H.
9. Using the skid positioning system, fully insert the cask into the HSM-H access opening docking collar.
10. Secure the cask to the front wall embedments of the HSM-H using the cask restraints.
11. Verify the alignment of the transfer cask is within specified tolerance using the optical survey equipment.
12. Remove the bottom ram access cover plate from the transfer cask. Extend the ram through the bottom cask opening into the DSC grapple ring.

13. Activate the hydraulic cylinder on the ram grapple and engage the grapple arms with the grapple ring.
14. Activate the hydraulic ram to initiate insertion of the DSC into the HSM-H. Stop the ram when the DSC reaches the support rail stops at the back of the module.
15. Disengage the ram grapple mechanism from the DDC grapple ring, and retract the hydraulic ram system from the transfer cask.
16. Remove the cask restraints from the HSM-H. Replace the bottom ram access cover plate. Optionally, a temporary cover may be used to cover the ram access opening.
17. Using the skid positioning system, disengage the cask from the HSM-H access opening.
18. Install the DSC seismic restraint.
19. Secure the skid to the trailer, retract the vertical jacks. Tow the trailer and cask a few feet to provide access for door installation.
20. Install the HSM-H door and secure it in place.
21. Replace the transfer cask lid.
22. Tow the trailer and cask from the ISFSI.

8.1.1.6 Monitoring Operations

1. Perform routine security surveillance in accordance with the licensee's ISFSI security plan.
2. Perform a daily visual surveillance of the HSM-H air inlets and outlets (bird screens) to verify that no debris is obstructing the HSM-H vents in accordance with Technical Specification requirements.
3. Perform a temperature measurement for each HSM-H in accordance with Technical Specification requirements.

8.2 Procedures for Unloading the DSC

The following section outlines the procedures for retrieving the DSC from the HSM-H and for removing the fuel assemblies from the DSC.

8.2.1 DSC Retrieval from the HSM-H

1. The maximum lifting height and ambient temperature requirements of the Technical Specifications must be met during transfer from the HSM-H to the fuel building.
2. Ready the transfer cask, transfer trailer, and support skid for service and tow the trailer to the HSM-H. Fill the transfer cask liquid neutron shield and remove the bottom access plate from the transfer cask.
3. Remove HSM-H door and seismic restraint. Remove the transfer cask lid. Back the trailer to within a few inches of the HSM-H.
4. Using the skid positioning system align the transfer cask with the HSM-H and position the skid until the transfer cask is docked with the HSM-H access opening.
5. Using optical survey equipment verify alignment of the transfer cask with respect to the HSM-H within specified tolerance. Install the transfer cask restraints.
6. Install and align the hydraulic ram with the transfer cask.
7. Extend the ram through the transfer cask into the HSM-H until it is inserted in the DSC grapple ring.
8. Activate the arms on the ram grapple mechanism to engage the grapple ring.
9. Retract the ram and pull the DSC into the transfer cask.
10. Disengage the ram grapple arms.
11. Retract the ram from the transfer cask.
12. Replace the cask ram access cover plate and remove the transfer cask restraints.
13. Using the skid positioning system, disengage the transfer cask from the HSM-H.
- 14a. Install the transfer cask top cover plate and ready the trailer for transfer/transport.

CAUTION: Radiation dose rates are expected to be high at the vent and siphon port locations. Use proper ALARA practices (e.g., use of temporary shielding, appropriate positioning of personnel, etc.) to minimize personnel exposure.

12. Obtain a sample of the DSC atmosphere. Confirm acceptable hydrogen concentration and check for presence of fission gas indicative of degraded fuel cladding.
13. If degraded fuel is suspected, additional measures appropriate for the specific conditions are to be planned, reviewed, and implemented to minimize exposures to workers and radiological releases to the environment.
14. Verify that the boron content of the fill water conforms to the Technical Specifications. Fill the DSC with water from the fuel pool or equivalent source through the drain port with the vent port open. The vented cavity gas may include steam, water, and radioactive material, and should be routed accordingly. Monitor the vent pressure and regulate the water fill rate to ensure that the pressure does not exceed 15 psig.
15. Provide for continuous hydrogen monitoring of the DSC cavity atmosphere during all subsequent cutting operations to ensure that hydrogen concentration does not exceed 2.4%. Purge with helium (or any other inert gas) as necessary to maintain the hydrogen concentration below this limit.
16. Provide suitable protection for the transfer cask during cutting operations.
17. Using a suitable method, such as mechanical cutting, remove the weld of the outer top cover plate to the DSC shell.
18. Remove the outer top cover plate.
19. Remove the weld of the inner top cover/shield plug to the shell in the same manner as the outer cover plate. Do not remove the inner top cover/shield plug at this time unless the removal is being done remotely in a dry transfer system.
20. Remove any remaining excess material on the inside shell surface by grinding.
21. Clean the transfer cask surface of dirt and any debris which may be on the transfer cask surface as a result of the weld removal operation.
22. Engage the yoke onto the trunnions, install eyebolts or other lifting attachment(s) into the inner top cover/shield plug, and connect the rigging cables to the eyebolts/lifting attachment(s).
23. Verify that the lifting hooks of the yoke are properly positioned on the trunnions.

24. Lift the transfer cask just far enough to allow the weight of the transfer cask to be distributed onto the yoke lifting hooks. Verify that the lifting hooks are properly positioned on the trunnions.
25. Optionally install suitable protective material onto the bottom of the transfer cask to minimize cask contamination. Move the transfer cask to the spent fuel pool.
26. Prior to lowering the transfer cask into the pool, adjust the pool water level, if necessary, to accommodate the volume of water which will be displaced by the transfer cask during the operation.
27. Position the transfer cask over the cask loading area in the spent fuel pool.
28. Lower the transfer cask into the pool. As the transfer cask is being lowered, the exterior surface of the transfer cask should be sprayed with clean water.
29. Disengage the lifting yoke from the transfer cask and lift the inner top cover/shield plug from the DSC.
30. Remove any failed fuel top end caps.
31. Remove the fuel from the DSC.

8.3 Supplemental Information

8.3.1 Other Operating Systems

The NUHOMS® System is a passive storage system and requires no operating systems other than those systems used in transferring the DSC to and from the HSM-H.

8.3.2 Operation Support System

The NUHOMS® System is a self contained passive system and requires no effluent processing systems during storage conditions.

8.3.3 Surveillance and Maintenance

Surveillance and maintenance requirements are discussed in Chapters 9 and 12. The only required surveillances during storage are monitoring of the HSM-H air exhaust temperature, and visual verification that the inlet and outlet vents are not blocked. There is no normally required maintenance of the HSM-H or DSC.

8.4 References

1. U.S. Nuclear Regulatory Commission, Office of the Nuclear Material Safety and Safeguards, "Safety Evaluation of VECTRA Technologies' Response to Nuclear Regulatory Commission Bulletin 96-04 for NUHOMS®-24P and NUHOMS®-7P Dry Spent Fuel Storage System," November 1997 (Dockets 72-1004, 72-3, 72-4, 72-8, and 72-14).
2. NUREG-0612, "Control of Heavy Loads at Nuclear Power Plants," USNRC, July 1980.

9. ACCEPTANCE TESTS AND MAINTENANCE PROGRAM

As noted in Chapter A.9, this chapter is also applicable to the 32PTH Type 1 DSC and OS187H Type 1 TC.

9.1 Acceptance Criteria

9.1.1 Visual Inspection and Non-Destructive Examination (NDE)

Visual inspections are performed at the fabricator's facility to ensure that the 32PTH DSC, the OS187H Transfer Cask and the HSM-H conform to the drawings and specifications. The visual inspections include weld, dimensional, surface finish, and cleanliness inspections. Visual inspections specified by codes applicable to a component are performed in accordance with the requirements and acceptance criteria of those codes.

All weld inspection is performed using qualified processes and qualified personnel according to the applicable code requirements, e.g., ASME or AWS. Non-destructive examination (NDE) requirements for welds are specified on the drawings provided in Chapter 1; acceptance criteria are as specified by the governing code. NDE personnel are qualified in accordance with SNT-TC-1A [2].

The confinement welds on the DSC are inspected in accordance with ASME B&PV Code Subsection NB [1] including alternatives to ASME Code specified in SAR Section 3.10.

DSC non-confinement welds are inspected to the NDE acceptance criteria of ASME B&PV Code Subsection NG or NF, based on the applicable code for the components welded.

The Transfer Cask welds are inspected in accordance with ASME B&PV Code Subsection NC for class 2 components, as modified by code alternates identified in Section 3.10 of Chapter 3.

9.1.2 Structural and Pressure Tests

The DSC confinement boundary except inner top cover/shield plug (including option 2 or option 3 inner top cover as described in the SAR) to the DSC shell weld is pressure tested at the fabricator's shop in accordance with ASME Article NB-6300. For future transportation licensing considerations, a conservative pressure of 20 psig is substituted for the design pressure (Section 4.1) to determine compliance test pressures during fabrication.

The inner top cover/shield plug (including option 2 or option 3 inner top cover) to the DSC shell weld is also pressure tested between 16.5 to 18 psig at the field after the fuel assemblies are loaded in the canister. This test is in accordance with the alternatives to the ASME code specified in SAR Section 3.10.

HSM-H reinforcement and concrete are tested as described in Section 2.5.2 and footnotes to Tables 4.1-5 and 4.4-3.

The Transfer Cask lifting (top) trunnions will be load tested in accordance with ANSI N14.6 [3] for a single failure proof design, i.e., three times the design load. The design load is conservatively set at 250,000 lbs (Section 3.2.2); therefore, the test load is 750,000 lbs (375,000 lbs/trunnion).

9.1.3 Leak Tests

DSC confinement welds in the DSC shell and bottom are leak tested at the fabricator's shop to an acceptance criterion of 1×10^{-7} ref cm³/s, i.e., "leaktight" as defined in ANSI N14.5 [4]. Personnel performing the leak test are qualified in accordance with SNT-TC-1A [2].

The weld between the DSC shell and inner top cover/shield plug (including option 2 or option 3 inner top cover) and siphon/vent cover welds are also leak tested to an acceptance criteria of 1×10^{-7} ref cm³/s at the field after the fuel assemblies are loaded in the canister.

The Transfer Cask lid, ram access, vent, and drain cover o-rings, vent and drain quick connect fittings, neutron shield welds, and neutron shield fittings are leak tested prior to first use.

If bubble leak testing is used, no leak indication is allowed. If pressure drop or helium leak testing is used, the maximum allowable leak for each of the components listed is 10^{-3} ref cm³/s.

9.1.4 Components

The NUHOMS® System does not include any components such as valves, rupture discs, pumps, or blowers. The gaskets in the Transfer Cask do not require acceptance testing other than the leak testing cited above. No other components of the NUHOMS® System require testing, except as discussed in this chapter.

9.1.5 Shielding Integrity

The Transfer Cask poured lead shielding integrity will be confirmed via gamma scanning or approved equivalent prior to first use. The detector and examination grid will be matched to provide coverage of the entire lead-shielded surface area. The acceptance criterion is attenuation greater than or equal to that of a test block matching the cask through-wall configuration with lead and steel thicknesses equal to the design minimum less 5%.

The radial neutron shielding is provided by filling the neutron shield shell with water during operations. No testing is necessary. The neutron shield material in the lid and bottom end is a proprietary polymer resin. The shielding performance of the resin will be assured by written procedures controlling temperature, measuring, and mixing of the components, degassing of the resin, and verification of the mass or volume of resin installed.

The gamma and neutron shielding materials of the storage system itself are limited to concrete HSM components and steel shield plugs in the DSC. The integrity of these shielding materials is ensured by the control of their fabrication in accordance with the appropriate ASME, ASTM or ACI criteria. No additional acceptance testing is required.

9.1.6 Thermal Acceptance

No thermal acceptance testing is required to verify the performance of each storage unit other than that specified in the Technical Specifications for initial loading of each HSM-H.

The heat transfer analysis for the basket includes credit for the thermal conductivity of neutron-absorbing materials, as specified in Section 4.3. Because these materials do not have publicly documented values for thermal conductivity, testing of such materials will be performed in accordance with Section 9.5.1.

one of the corners of the sheet produced from each ingot. If the measured areal density is below that specified, all the material produced from that ingot will be either rejected, or accepted only on the basis of alternate verification of B10 areal density for each of the final pieces produced from that ingot.

Visual inspections shall verify that the Boral® core is not exposed through the face of the sheet at any location.

9.2 Maintenance Program

The NUHOMS® HD System is designed to be totally passive with minimal maintenance requirements. The 32PTH DSC does not require any maintenance once it is loaded into the HSM-H. The HSM-H does not require any maintenance other than that indicated in off-normal operations, Chapter 11, such as clearing of blocked air inlets. Periodic inspection is therefore limited to the Transfer Cask.

9.2.1 Inspection

The following inspections of the transfer cask should be performed prior to each fuel loading or unloading campaign:

- A. Visual inspection of the transfer cask trunnions for damaged bearing surfaces
- B. Visual or functional inspection of all taps, threaded inserts, and bolts
- C. Functional inspection of all quick-connect fittings
- D. Visual inspection of the interior surface of the cask for any indications of excessive wear.
- E. Visual inspection of the neutron shield jacket for indications of damage
- F. Visual inspection of all Transfer Cask o-rings for indications of damage

Within the year prior to any loading or unloading campaign, the top trunnion bearing surfaces and accessible welds shall be examined by dye penetrant. No linear indications shall be acceptable other than surface scratches and wear.

9.2.2 Tests

The Transfer Cask lid and ram access cover o-rings, vent and drain quick connect fittings, and neutron shield fittings shall be leak tested within the year before the start of any fuel loading or unloading campaign. If bubble leak testing is used, no leak indication is allowed. If pressure drop or helium leak testing is used, the maximum allowable leak for each of the components listed is 10^{-3} ref cm³/s. If any of the listed components is replaced, that component shall be leak tested before use in fuel loading or unloading operations.

No periodic testing of the 32PTH DSC, HSM-H or routine support equipment is required.

Temperature and radiation monitoring is provided in accordance with the Technical Specifications. Periodic calibration of the monitoring equipment shall be as required by the licensee's quality program.

9.2.3 Repair, Replacement, and Maintenance

Any parts which fail inspections listed in 9.1.2 shall be repaired or replaced. Such parts may be also be accepted as-is if determined appropriate by engineering and licensing review.

9.3 Marking

The HSM-H and 32PTH DSC are marked with the model number, unique identification number, and empty weight in accordance with 10 CFR 72.236(k). The 32PTH DCS nameplate is shown in drawing 10494-72-7.

9.4 Pre-Operational Testing and Training Exercise

A dry run training exercise of the loading, closure, handling, unloading, and transfer of the NUHOMS® HD System shall be performed by each licensee prior to their first use of the system to load spent fuel assemblies. The dry run shall be conducted with simulated fuel to match the weight of the actual fuel. The dry run need not be performed in the sequence of operations in Chapter 8. The dry run shall include:

- (a) Loading of mock-up fuel
- (b) DSC draining, vacuum drying, welding, and backfilling
- (c) Loading of the Transfer Cask onto the Transfer Trailer, and transfer to the ISFSI
- (d) DSC transfer to the HSM-H
- (e) DSC retrieval from the HSM-H
- (f) Re-flooding of a sealed 32PTH DSC
- (g) Removal of the covers from a sealed 32PTH DSC

The dry run will simulate, as nearly as possible, the detailed written procedures developed by the licensee for NUHOMS® HD System operations. Guidelines for the dry run follow.

- A. An actual or a mock-up 32PTH DSC loaded with mock-up fuel is typically utilized. The 32PTH DSC is loaded into the transfer cask; the transfer cask/DSC annulus seal is installed.
- B. Functional testing is performed with the transfer cask and lifting equipment. These tests are to ensure that the transfer cask can be safely lifted from the plant's cask receiving area to the cask washdown area. The cask is partially lowered into the spent fuel pool and positioned in the cask loading area to verify clearances and travel path. The inner top cover is installed to verify handling and alignment operations.
- C. The transfer cask is placed on the transfer trailer, which is moved to the ISFSI aligned with an HSM-H. Compatibility of the transfer trailer with the transfer cask, verification of the transfer route to the ISFSI, and maneuverability within the confines of the ISFSI are verified.

9.6 References

1. ASME Boiler and Pressure Vessel Code, Section III, 1998 Edition through 2000 addenda.
2. SNT-TC-1A, "American Society for Nondestructive Testing, Personnel Qualification and Certification in Nondestructive Testing," 1992.
3. ANSI N14.6, "American National Standard for Special Lifting Devices for Shipping Containers Weighing 10,000 Pounds or More for Nuclear Materials," New York, 1996.
4. ANSI N14.5-1997, "American National Standard for Leakage Tests on Packages for Shipment of Radioactive Materials", February 1998.
5. "Aluminum Standards and Data, 2003" The Aluminum Association.
6. Topical report: Credit for 90% of the 10B in Boral[®], AAR Report 1829, AAR Manufacturing, Oct 2004
7. Natrella, "Experimental Statistics," Dover, 2005

CHAPTER 10
RADIATION PROTECTION

TABLE OF CONTENTS

10.	RADIATION PROTECTION	10-1
10.1	Ensuring That Occupational Radiation Exposures Are As Low As Reasonably Achievable (ALARA).....	10-1
10.1.1	Policy Considerations.....	10-1
10.1.2	Design Considerations.....	10-1
10.1.3	Operational Considerations	10-3
10.2	Radiation Protection Design Features	10-4
10.2.1	NUHOMS® HD System Design Features	10-4
10.2.2	Offsite Dose Calculations.....	10-4
10.3	Estimated Onsite Collective Dose Assessment	10-8
10.3.1	DSC Loading, Transfer and Storage Operations.....	10-8
10.3.2	DSC Retrieval Operations.....	10-8
10.3.3	Fuel Unloading Operations.....	10-9
10.3.4	Maintenance Operations.....	10-9
10.3.5	Doses During ISFSI Array Expansion	10-9
10.4	References.....	10-10

10. RADIATION PROTECTION

The applicability of these analyses to the 32PTH Type 1 DSC and OS187H Type 1 TC described in Appendix A are discussed in Appendix A, Chapter A.10, along with any necessary additional details.

10.1 Ensuring That Occupational Radiation Exposures Are As Low As Reasonably Achievable (ALARA)

10.1.1 Policy Considerations

The licensee's radiation safety and ALARA policies should be applied to the ISFSI. The ALARA program should follow the general guidelines of Regulatory Guides 1.8 [4], 8.8 [1], 8.10 [3] and 10 CFR 20 [6]. ISFSI personnel should be trained in the proper operation, inspection, repair and maintenance of the NUHOMS® HD System and updated on ALARA practices and dose reduction techniques. Implementation of ISFSI procedures should be reviewed by the licensee to ensure ALARA exposure.

10.1.2 Design Considerations

The thick inner cover of the DSC is designed to minimize exposure during draining, drying, and closure operations. The vent and drain ports are designed for maximum water flow rate and vacuum conductance to minimize the time (and thereby the exposure) associated with draining and vacuum drying. The design of the cover welds minimizes exposure during closure operations. The welds are designed to be easily performed by remote welding equipment. Because the cover welds are not used to lift the canister, they are relatively small, reducing the time needed to complete them. Because they are austenitic welds, no pre-heating is required. These welds are tested to be leak-tight as described in Chapter 7. Therefore, exposure associated with a leaking DSC is eliminated.

Lead, steel, water, and borated plastic in the transfer cask provide required gamma and neutron shielding during transfer activities. The exterior of the transfer cask is decontaminated prior to transfer to the ISFSI, thereby minimizing exposure of personnel to surface contamination.

The NUHOMS® HSM-H storage modules include no active components which require periodic maintenance thereby minimizing potential personnel dose due to maintenance activities.

The shielding design features of the storage modules storage minimize occupational exposure for any activities on or near the ISFSI. These features are:

- The DSCs are loaded and sealed prior to transfer to the ISFSI. Seals are austenitic stainless welds with at least two layers.
- The fuel will not be unloaded nor will the DSCs be opened at the ISFSI unless the ISFSI is specifically licensed for these purposes.
- The fuel is stored in a dry inert environment inside the DSCs so that no radioactive liquid is available for leakage.

- The DSCs are sealed with a helium atmosphere to prevent oxidation of the fuel. The leaktight design features are described in Chapter 7.
- The DSCs are heavily shielded on both ends to reduce external dose rates. The shielding design features are discussed in Chapter 5.
- No radioactive material will be discharged during storage since the DSC is designed, fabricated, and tested to be leaktight.
- The DSC outside surface is contamination free due to the use of clean water sealed in the annulus between the cask and DSC during loading operations.
- HSMs provide thick concrete shielding, while placement of modules immediately adjacent to one another enhances the effectiveness of this shielding.

Regulatory Position 2 of Regulatory Guide 8.8 [1], is incorporated into the design considerations, as described below:

- Regulatory Position 2a on access control is met by use of a fence with a locked gate that surrounds the ISFSI and prevents unauthorized access.
- Regulatory Position 2b on radiation shielding is met by the heavy shielding of the NUHOMS® System which minimizes personnel exposures.
- Regulatory Position 2c on process instrumentation and controls is met by designing the instrumentation for a long service life and locating readouts in a low dose rate location. The use of thermocouples for temperature measurements located in embedded thermowells provides reliable, easily maintainable instrumentation for this monitoring function.
- Regulatory Position 2d on control of airborne contaminants may be applicable for vacuum drying operations of DSCs containing damaged fuel. Diversion of the vacuum pump exhaust to an appropriate filtration system is recommended in the Chapter 8 operations. The regulatory position does not apply during transfer or storage because neither gaseous releases nor significant surface contamination are expected.
- Regulatory Position 2e on crud control is not applicable to the ISFSI because there are no systems at the ISFSI that could transport crud. The leaktight DSC design ensures that spent fuel crud will not be released or transferred from the DSC. Draining back to the spent fuel pool provides control over any crud that could be entrained in the outflow from the DSC draining operations.
- Regulatory Position 2f on decontamination is met because the transfer cask is decontaminated prior to transfer to the ISFSI. The transfer cask accessible surfaces are designed to facilitate decontamination.
- Regulatory Position 2g on radiation monitoring does not apply. There is no need for airborne radioactivity monitoring because the DSCs are sealed by leaktight welds. Airborne radioactivity due to damaged fuel is discussed under Regulatory Position 2d

11 ACCIDENT ANALYSIS

The applicability of these analyses to the 32PTH Type 1 DSC and OS187H Type 1 TC described in Appendix A are discussed in Appendix A, Chapter A.11, including additional evaluations specific to the OS187H Type 1 TC.

11.1 Introduction

This Chapter describes the postulated off-normal and accident events that might occur during transfer/storage of the 32PTH DSC in an HSM-H at an ISFSI. In addition, this chapter also addresses the potential causes of these events, their detection and consequences, and the corrective course of action to be taken by ISFSI personnel. Accident analyses demonstrate that the functional integrity of the system is maintained by:

1. Maintaining sub-criticality within margins defined in Chapter 6.
2. Maintaining confinement boundary integrity
3. Ensuring fuel retrievability and
4. Maintaining doses within 10CFR 72.106 [1] limits (<5 rem).

The Accident Dose Calculations sections report the expected doses resulting from the postulated event in terms of whole body doses only. The leaktight canister design and the maintenance of confinement boundary integrity under all credible off-normal and accident scenarios ensures no radiation leakage from the 32PTH DSC, thereby limiting dose consequences to direct and scattered radiation doses without any associated inhalation or ingestion doses.

11.2.1 Off-Normal Transfer Load

Although unlikely, the postulated off-normal handling event assumes that the leading edge of the 32PTH DSC becomes jammed against some element of the support structure during transfer between the transfer cask and the HSM-H.

Cause of the Event

It is postulated that if the transfer cask is not accurately aligned with respect to the HSM-H, the 32PTH DSC could bind or jam during transfer operations.

The interiors of the transfer cask and the HSM-H are inspected prior to transfer operations to ensure there are no obstacles, and the 32PTH DSC has beveled lead-ins on each end, designed to avoid binding or sticking on small (less than 1/4 inch) obstacles. The transfer cask and the 32PTH DSC support rails inside the HSM-H are also designed with lead-ins to minimize binding or obstruction during 32PTH DSC transfer. The postulated off-normal handling load event assumes that the leading edge of the 32PTH DSC becomes jammed against some element of the support structure because of gross misalignment of the transfer cask.

The interfacing dimensions of the top end of the transfer cask and the HSM-H access opening sleeve are specified such that docking of the transfer cask with the HSM-H is not possible should gross misalignments between the transfer cask and HSM-H exist.

Detection of the Event

The normal load to push/pull the DSC in and out of the Transfer Cask/HSM-H is less than 32 kips ($110 \text{ kips} \times 0.2/\cos 30$). This movement is performed at a very low speed. System operating procedures and technical specification limits defining the safeguards to be provided ensure that the system design margins are not compromised. If the 32PTH DSC were to jam or bind during transfer, the hydraulic pressure in the ram would increase. The off-normal load set for the "jammed 32PTH DSC" for both push/pull is 80 kips. This load is administrative controlled to ensure that during the transfer operation this load will not be exceeded.

NOTE: Even though the DSC and HSM are designed and analyzed for off-normal transfer loads of 80 kips, the DSC is conservatively analyzed for accident transfer loads of 110 kips.

During the transfer operation, the force exerted on the 32PTH DSC by the hydraulic ram is that required to first overcome the static frictional resisting force between the transfer cask rails and the 32PTH DSC. Once the 32PTH DSC begins to slide, the resisting force is a function of the sliding friction coefficient between the 32PTH DSC and the transfer cask rails and/or between the 32PTH-DSC and the HSM-H support rails. If motion is prevented, the hydraulic pressure increases, thereby increasing the force on the 32PTH DSC until the hydraulic ram system pressure limit is reached. This limit is controlled so that adequate force is available to overcome variations in surface finish, etc., but is sufficiently low to ensure that component damage does not occur.

Analysis of Effects and Consequences

The 32PTH DSC and the HSM-H are designed and analyzed for off-normal transfer loads of 80 kips during insertion (loading) and during retrieval (unloading) operations. These analyses are discussed in Chapter 3, Appendix 3.9.1, Load Cases 21 & 22 for off-normal conditions (page 3.9.1-53). For either loading or unloading of the 32PTH DSC under off-normal conditions, the stresses on the shell assembly components are demonstrated to be within the ASME allowable stress limits. Therefore, permanent deformation of the 32PTH DSC shell components does not occur. The internal basket assembly components are unaffected by these loads based on clearances provided between support rods and 32PTH DSC internal envelope.

There is no breach of the confinement pressure boundary and, therefore, no potential for release of radioactive material exists.

Corrective Actions

The required corrective action is to reverse the direction of the force being applied to the 32PTH DSC by the ram, and return the 32PTH DSC to its previous position. Since no permanent deformation of the 32PTH DSC occurs, the sliding of the 32PTH DSC back to its previous position is unimpeded. The transfer cask alignment is then rechecked, and the transfer cask repositioned as necessary before attempts at transfer are renewed.

APPENDIX A

32PTH Type 1 DSC and OS187H Type 1 TC

Chapter A.1 General Information

TABLE OF CONTENTS

A.1	GENERAL INFORMATION	A.1-1
A.1.1	Introduction.....	A.1-2
A.1.2	General Description of the NUHOMS® HD System with the 32PTH Type 1 DSC and OS187H Type 1 TC	A.1-3
A.1.2.1	NUHOMS® HD System Characteristics.....	A.1-3
A.1.2.2	Operational Features	A.1-4
A.1.2.3	32PTH Type 1 DSC Contents.....	A.1-5
A.1.3	Identification of Agents and Contractors	A.1-6
A.1.4	Generic Cask Arrays	A.1-7
A.1.5	Supplemental Data.....	A.1-8
A.1.5.1	References.....	A.1-8
A.1.5.2	Drawings	A.1-8

LIST OF TABLES

Table A.1-1	Key Design Parameters of the NUHOMS® HD System Components	A.1-9
-------------	---	-------

LIST OF FIGURES

Figure A.1-1	32PTH Type 1 Dry Shielded Canister (Optional two-part top end configuration shown)	A.1-10
Figure A.1-2	OS187H Type 1 On-Site Transfer Cask.....	A.1-11

A.1 GENERAL INFORMATION

Appendix A to this NUHOMS® HD System Final Safety Analysis Report (FSAR) documents the addition of the 32PTH Type 1 dry shielded canister (DSC) and the OS187H Type 1 transfer cask (TC) to the NUHOMS® HD System. These two components are similar but longer length versions of the 32PTH DSC and the OS187H TC described in the main body of this FSAR.

The general information presented in Chapter 1 remains applicable when the 32PTH Type 1 DSC and the OS187H Type 1 TC are added to the NUHOMS® HD System.

The format and content of this appendix follows the format and content of the main body of this FSAR. Generally, the same chapters and section numbers as in the main body have been kept in this appendix, preceded with a letter A. In addition, in several sections of this appendix reference is made to the corresponding section/chapter in the main body of the FSAR to avoid repetition of documentation that is also applicable to this appendix. For the sections in this appendix which have been identified as "No change," the description or analysis presented in the corresponding sections of the FSAR for the 32PTH and OS187H are also applicable to the 32PTH Type 1 DSC or the OS187H Type 1 transfer cask. Table and figures presented in the FSAR which remain unchanged due to the addition of the 32PTH Type 1 DSC and OS187H Type 1 transfer cask are not repeated in this appendix.

Note: References to sections or chapters within this appendix are identified with a prefix A (e.g., Section A.2.1 or Chapter A.2). References to sections or chapters of the FSAR outside of this appendix (main body of the FSAR) are identified with the applicable FSAR section or chapter number (e.g., Section 2.1 or Chapter 2).

A.1.1 Introduction

There is no change to the generic description presented in Section 1.1 of the FSAR when the 32PTH Type 1 dry shielded canister (DSC) and the OS187H Type 1 transfer cask (TC) are used instead of the 32PTH DSC and the OS187H TC. When used with the Type 1 components, the NUHOMS® HD System consists of the 32PTH Type 1 DSC, the OS187H Type 1 TC, and the HSM-H Horizontal Storage Module. Sketches for the 32PTH Type 1 DSC and the OS187H Type 1 TC are shown in Figure A.1-1 and Figure A.1-2.

The 32PTH Type 1 DSC and the OS187H Type 1 TC are similar to but longer length versions of the 32PTH DSC and OS187H TC described in the main body of this FSAR. The main design changes associated with these longer length NUHOMS® HD System components are summarized in Sections A.1.2.1.1 and A.1.2.1.3.1 for the 32PTH Type 1 DSC and OS187H Type 1 TC, respectively. The authorized contents and overall design criteria as described in the main body of this FSAR is the same for these added components with the exception that an elastic-plastic analysis methodology is used for the accident pressure load case evaluation of the 32PTH Type 1 DSC (instead of elastic analysis methodology used for the 32PTH DSC). The application of the elastic-plastic analysis methodology to the 32PTH Type 1 DSC is similar to that used for the NUHOMS® 32P DSC in Reference [2].

A.1.2 General Description of the NUHOMS® HD System with the 32PTH Type 1 DSC and OS187H Type 1 TC

The general arrangement of NUHOMS® HD System shown in Figure 1-3 and Figure 1-4 and the general description presented in Section 1.2 remain applicable when the 32PTH Type 1 DSC and the OS187H Type 1 TC are used instead of the 32PTH DSC and OS187H TC. The confinement boundary of the 32PTH Type 1 DSC is shown in Figure A.7-1 when the standard three-piece top end assembly configuration is used. For the optional two-piece top end assembly configuration, the confinement boundary is the same as that for the 32PTH DSC as shown in Figure 7-1.

The 32PTH Type 1 DSC is identified as follows: XXX-32PTH-YYY-Z-1, where XXX, YYY, and Z are as described in Section 1.2. The basket types are the same as for the 32PTH DSC and are described in drawing 10494-72-2003-SAR.

A.1.2.1 NUHOMS® HD System Characteristics

A.1.2.1.1 Dry Shielded Canister (32PTH Type 1 DSC)

No change to the generic description for the 32PTH DSC presented in Section 1.2.1.1. Table A.1-1 summarizes the key design parameters for the 32PTH Type 1 DSC.

The major changes implemented in the 32PTH Type 1 DSC relative to the 32PTH DSC are as follows:

- The interior cavity length of the 32PTH Type 1 DSC is increased, approximately 7½", with a corresponding increase in basket length.
- Since the thicknesses of the top and bottom shield assemblies remain unchanged, the overall DSC length also is increased. The DSC diameter is unchanged.
- The top end assembly of the 32PTH Type 1 DSC consists of a three-part closure design (top shield plug, inner top cover, and outer top cover). This design is the same as other standardized NUHOMS® canister designs described in Reference [1]. The two-part top end closure design of the 32PTH DSC is an alternate design in the 32PTH Type 1 DSC.
- Lifting lugs are used to lift the empty 32PTH Type 1 DSC into the OS187H Type 1 transfer cask. The lifting lugs are welded to the shell and are located at the support ring elevation, similar to other standardized NUHOMS® canister designs [1]. Lifting lugs are used in lieu of the lifting rods with welded bosses, located at the inner bottom cover plate, in the 32PTH design. The lifting lugs are non-safety components as they are used to lift the DSC prior to fuel load.

The 32PTH Type 1 DSC is shown on drawings 10494-2001-SAR through 10494-2005-SAR in Section A.1.5.2.

A.1.2.1.2 Horizontal Storage Module (HSM-H)

No change to the generic description presented in Section 1.2.1.2. Only a small ($\frac{1}{2}$ ") increase in the overall length of the DSC support rail is required to accommodate the 32PTH Type 1 DSC. The key design parameters for the HSM-H as presented in Table 1-1 are not changed.

A.1.2.1.3 Transfer Systems

A.1.2.1.3.1 OS187H Type 1 On-Site Transfer Cask

No change to the generic description presented in Section 1.2.1.3.1 for the OS187H TC. Table A.1-1 summarizes the key design parameters for the OS187H Type 1 TC. The major changes incorporated into the OS187H Type 1 transfer cask are:

- In order to accommodate the longer 32PTH Type 1 DSC, the minimum internal cavity length of the TC is increased from 186.60" (OS187H) to 198.75" (OS187H Type 1). As a result of the increased cavity length, the overall length is increased and the distance between upper and lower trunnions is also increased. The 70.5" inside diameter and the thicknesses of the top and bottom end assemblies are unchanged.
- The thickness of the inner liner is increased from $\frac{1}{2}$ " to a nominal $\frac{5}{8}$ ". The thickness of the upper shell course is increased from 2.00" to $2 \frac{3}{8}$ ".
- The transfer cask trunnions are revised to remove the resin-filled voids. The material for the lower trunnions is changed from SA-182 Type F304 to SA-182 Type F304N.
- The separate resin-filled and removable upper trunnion pocket shielding has been deleted and the water neutron shield extended to mate with the trunnion.

The OS187H Type 1 TC has a payload capacity of 120,000 lbs (determined based on its evaluated capacity of 250,000 lbs and its total weight of 130,000 lbs).

A.1.2.1.3.2 Transfer Equipment

No change to the transfer equipment description presented in Section 1.2.1.3.2.

A.1.2.2 Operational Features

A.1.2.2.1 Dry Run Operations

No change.

A.1.2.2.2 SFA Loading Operations

No change in the primary operations (in sequence of occurrence) for the NUHOMS® HD System described in Section 1.2.2.2, except for placement of the cask spacer (if required) prior to placing the 32PTH Type 1 DSC into the transfer cask, and, for a 32PTH Type 1 DSC with a three-part top end closure, the inner top cover plate is placed following placement of the top shield plug

(step 8) and lifting of the transfer cask from the pool (step 9). The inner top cover is sealed in Step 10 instead of the top shield plug.

A.1.2.2.3 Identification of Subjects for Safety and Reliability Analysis

A.1.2.2.3.1 Criticality Prevention

No change.

A.1.2.2.3.2 Chemical Safety

No change.

A.1.2.2.3.3 Operation Shutdown Modes

The NUHOMS® HD System is a totally passive system so that consideration of operation shutdown modes is unnecessary.

A.1.2.2.3.4 Instrumentation

No change.

A.1.2.2.3.5 Maintenance and Surveillance

No change. All maintenance and surveillance tasks are described in Chapter A.9.

A.1.2.3 32PTH Type 1 DSC Contents

No change. The DSC contents described in Section 1.2.3 for the 32PTH DSC are applicable for the 32PTH Type 1 DSC.

A.1.3 Identification of Agents and Contractors

No change.

A.1.4 Generic Cask Arrays

No change.

A.1.5 Supplemental Data

A.1.5.1 References

1. Updated Final Safety Analysis Report, Standardized NUHOMS® Horizontal Modular Storage System for Irradiated Nuclear Fuel, Revision 9, February 2006, USNRC Docket No. 72-1004.
2. USNRC Safety Evaluation Report, SNM-2505, Amendment 7, Dated 11/2/2005, Docket 72-8

A.1.5.2 Drawings

32PTH Type 1 DSC:

- 10494-72-2001-SAR, (3 sheets), (PROPRIETARY)
- 10494-72-2002-SAR, (2 sheets), (PROPRIETARY)
- 10494-72-2003-SAR, (5 sheets), (PROPRIETARY)
- 10494-72-2004-SAR, (3 sheets), (PROPRIETARY)
- 10494-72-2005-SAR, (5 sheets) (PROPRIETARY)

OS187H Type 1 TC:

- 10494-72-9001-SAR, (3 sheets), (PROPRIETARY)
- 10494-72-9002-SAR, (3 sheets), (PROPRIETARY)
- 10494-72-9003-SAR, (3 sheets) (PROPRIETARY)

Table A.1-1 Key Design Parameters of the NUHOMS® HD System Components

Dry Shielded Canister (32PTH Type 1 DSC)	
Overall length (in.)	193.00 (max), increased from 185.75 (max)
Outside diameter (in.)	69.75 (unchanged)
Cavity length (in.)	171.63 (min), increased from 164.5 (min.)
Shell thickness (in.)	0.5 (unchanged)
Design weight of loaded 32PTH Type 1 DSC (lb)	109,000 ⁽¹⁾
Materials of construction	Stainless steel shell assembly and internals, carbon steel and/or stainless steel shield plugs, aluminum
Neutron absorbing material	Boral™, borated aluminum, metal matrix composite (MMC)
Internal atmosphere	Helium

Horizontal Storage Module (HSM-H)	
Overall length (without back shield wall)	20'-8"
Overall width (without end shield walls)	9'-8"
Overall height	18' 6"
Total weight (not including 32PTH Type 1 DSC) (lbs.)	307,200 ⁽¹⁾
Materials of construction	Reinforced concrete and structural steel
Heat removal	Conduction, convection, and radiation

On-Site Transfer Cask (OS187H Type 1)	
Overall length (in.)	210.50, increased from 197.1
Outside diameter (in.)	92.11, changed from 92.2
Cavity length (in.)	198.75, increased from 186.6
Lead thickness (in.)	3.56 (nom), changed from 3.60 (nom)
Gross weight (including 32PTH Type 1 DSC) (tons)	120.0 ⁽¹⁾ (increased from 114.5)
Materials of construction	Stainless steel shell assemblies and closures with lead shielding
Internal atmosphere	Helium

Note:

(1) Rounded up values

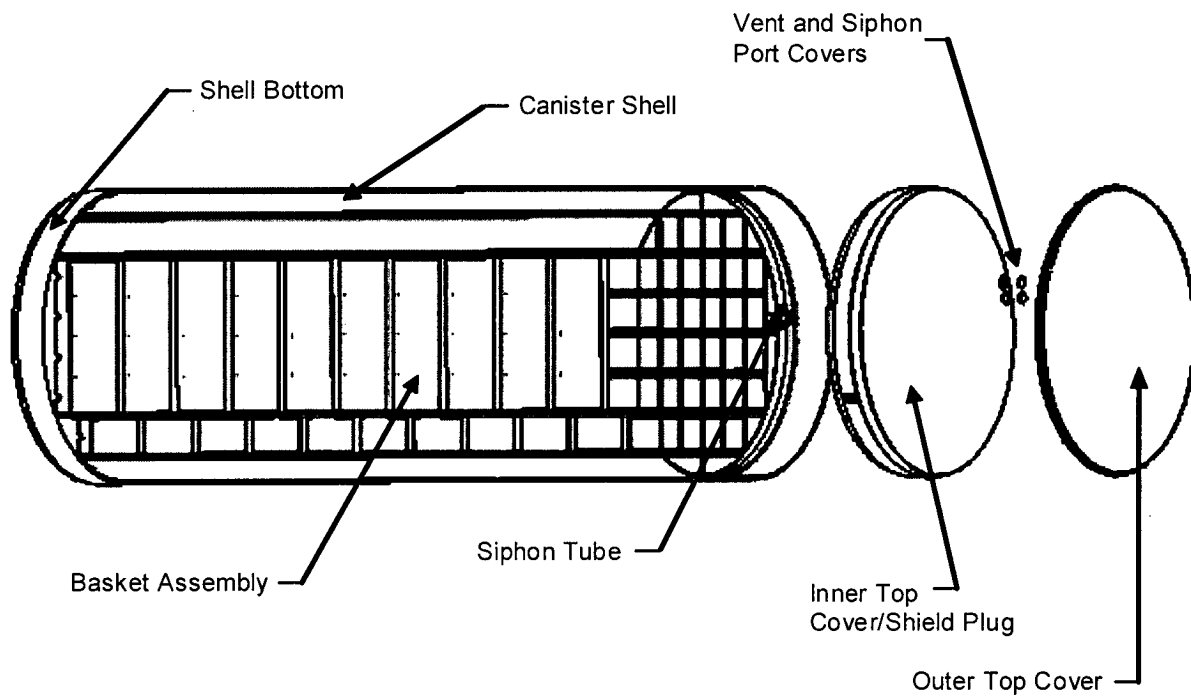


**Figure A.1-1 32PTH Type 1 Dry Shielded Canister
(Optional two-part top end configuration shown)**

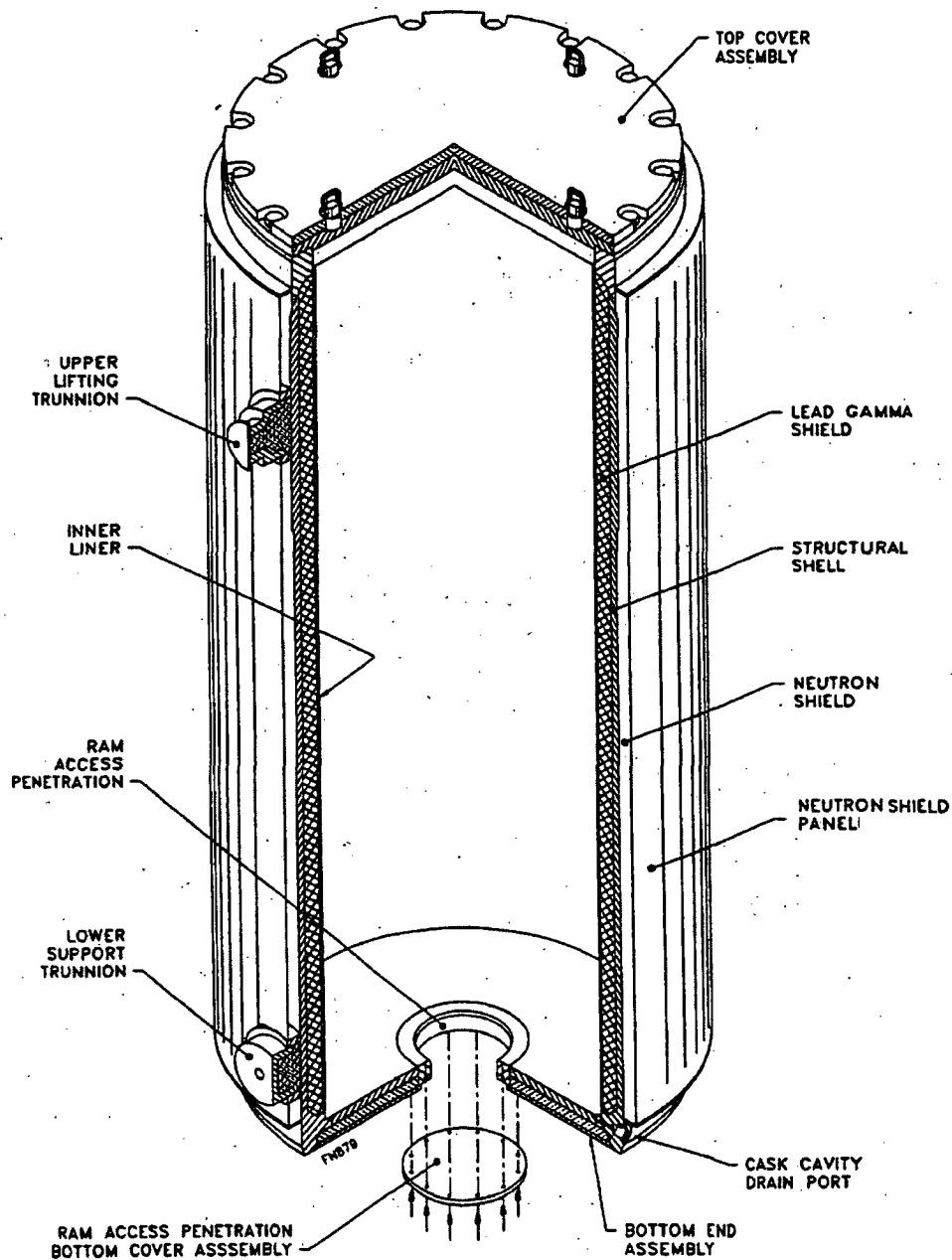


Figure A.1-2 OS187H Type 1 On-Site Transfer Cask

**PROPRIETARY AND
SECURITY RELATED
INFORMATION
WITHHELD UNDER 10 CFR 2.390**

ALL DIMENSIONS ARE NOMINAL UNLESS
A SPECIFIC TOLERANCE IS INDICATED
WITH THE DRAWING DIMENSION

DIMENSIONS ARE IN INCHES AND DEGREES
UNLESS OTHERWISE SPECIFIED.
DIMENSIONING IN ACCORDANCE WITH
ASME Y14.5M

PROPRIETARY AND
SECURITY RELATED INFORMATION
WITHHELD UNDER 10 CFR 2.390

**PROPRIETARY AND
SECURITY RELATED INFORMATION
WITHHELD UNDER 10 CFR 2.390**

PROPRIETARY AND
SECURITY RELATED INFORMATION
WITHHELD UNDER 10 CFR 2.390

ALL DIMENSIONS ARE NOMINAL UNLESS
A SPECIFIC TOLERANCE IS INDICATED
WITH THE DRAWING DIMENSION

DIMENSIONS ARE IN INCHES AND DEGREES
UNLESS OTHERWISE SPECIFIED.
DIMENSIONING IN ACCORDANCE WITH
ASME Y14.5M

PROPRIETARY AND
SECURITY RELATED INFORMATION
WITHHELD UNDER 10 CFR 2.390

PROPRIETARY AND
SECURITY RELATED INFORMATION
WITHHELD UNDER 10 CFR 2.390

ALL DIMENSIONS ARE NOMINAL UNLESS
A SPECIFIC TOLERANCE IS INDICATED
WITH THE DRAWING DIMENSION

DIMENSIONS ARE IN INCHES AND DEGREES
UNLESS OTHERWISE SPECIFIED.
DIMENSIONING IN ACCORDANCE WITH
ASME Y14.5M

PROPRIETARY AND
SECURITY RELATED INFORMATION
WITHHELD UNDER 10 CFR 2.390

PROPRIETARY AND
SECURITY RELATED INFORMATION
WITHHELD UNDER 10 CFR 2.390

PROPRIETARY AND
SECURITY RELATED INFORMATION
WITHHELD UNDER 10 CFR 2.390

PROPRIETARY AND
SECURITY RELATED INFORMATION
WITHHELD UNDER 10 CFR 2.390

PROPRIETARY AND
SECURITY RELATED INFORMATION
WITHHELD UNDER 10 CFR 2.390

ALL DIMENSIONS ARE NOMINAL UNLESS
A SPECIFIC TOLERANCE IS INDICATED
WITH THE DRAWING DIMENSION

DIMENSIONS ARE IN INCHES AND DEGREES
UNLESS OTHERWISE SPECIFIED.
DIMENSIONING IN ACCORDANCE WITH
ASME Y14.5M

PROPRIETARY AND
SECURITY RELATED INFORMATION
WITHHELD UNDER 10 CFR 2.390

PROPRIETARY AND
SECURITY RELATED INFORMATION
WITHHELD UNDER 10 CFR 2.390

PROPRIETARY AND
SECURITY RELATED INFORMATION
WITHHELD UNDER 10 CFR 2.390

ALL DIMENSIONS ARE NOMINAL UNLESS
A SPECIFIC TOLERANCE IS INDICATED
WITH THE DRAWING DIMENSION

DIMENSIONS ARE IN INCHES AND DEGREES
UNLESS OTHERWISE SPECIFIED.
DIMENSIONING IN ACCORDANCE WITH
ASME Y14.5M

PROPRIETARY AND
SECURITY RELATED INFORMATION
WITHHELD UNDER 10 CFR 2.390

PROPRIETARY AND
SECURITY RELATED INFORMATION
WITHHELD UNDER 10 CFR 2.390

PROPRIETARY AND
SECURITY RELATED INFORMATION
WITHHELD UNDER 10 CFR 2.390

PROPRIETARY AND
SECURITY RELATED INFORMATION
WITHHELD UNDER 10 CFR 2.390

PROPRIETARY AND
SECURITY RELATED INFORMATION
WITHHELD UNDER 10 CFR 2.390

ALL DIMENSIONS ARE NOMINAL UNLESS
A SPECIFIC TOLERANCE IS INDICATED
WITH THE DRAWING DIMENSION

DIMENSIONS ARE IN INCHES AND DEGREES
UNLESS OTHERWISE SPECIFIED.
DIMENSIONING IN ACCORDANCE WITH
ASME Y14.5M

PROPRIETARY AND
SECURITY RELATED INFORMATION
WITHHELD UNDER 10 CFR 2.390

PROPRIETARY AND
SECURITY RELATED INFORMATION
WITHHELD UNDER 10 CFR 2.390

PROPRIETARY AND
SECURITY RELATED INFORMATION
WITHHELD UNDER 10 CFR 2.390

ALL DIMENSIONS ARE NOMINAL UNLESS
A SPECIFIC TOLERANCE IS INDICATED
WITH THE DRAWING DIMENSION

DIMENSIONS ARE IN INCHES AND DEGREES
UNLESS OTHERWISE SPECIFIED.
DIMENSIONING IN ACCORDANCE WITH
ASME Y14.5M

PROPRIETARY AND
SECURITY RELATED INFORMATION
WITHHELD UNDER 10 CFR 2.390

PROPRIETARY AND
SECURITY RELATED INFORMATION
WITHHELD UNDER 10 CFR 2.390

PROPRIETARY AND
SECURITY RELATED INFORMATION
WITHHELD UNDER 10 CFR 2.390

ALL DIMENSIONS ARE NOMINAL UNLESS
A SPECIFIC TOLERANCE IS INDICATED
WITH THE DRAWING DIMENSION

DIMENSIONS ARE IN INCHES AND DEGREES
UNLESS OTHERWISE SPECIFIED.
DIMENSIONING IN ACCORDANCE WITH
ASME Y14.5M

PROPRIETARY AND
SECURITY RELATED INFORMATION
WITHHELD UNDER 10 CFR 2.390

PROPRIETARY AND
SECURITY RELATED INFORMATION
WITHHELD UNDER 10 CFR 2.390

Chapter A.2

Principal Design Criteria

No change. The design criteria described in Chapter 2 for the 32PTH DSC and OS187H TC are applicable to the 32PTH Type 1 DSC and the OS187H Type 1 TC. The contents authorized for storage in the 32PTH Type 1 DSC are the same as the authorized contents for the 32PTH DSC described in Section 2.1. The number of fuel assemblies per DSC, maximum heat load per DSC and heat load configurations, basket poison types, and basket geometric configuration are not changed. Similarly, there is no change to the design criteria for environmental conditions and natural phenomena as described in Section 2.2, or to the safety protection systems as described in Section 2.3. Section 2.4 (Decommissioning Considerations), Section 2.5 (Structures, Systems and Components Important to Safety), and Section 2.6 (References) are not changed. As described in Section A.1.1, an elastic-plastic analysis methodology is used for the accident pressure load case of the 32PTH Type 1 DSC. As with the 32PTH DSC, the details of the 32PTH Type 1 DSC evaluation criteria are described in Chapter A.3.

Chapter A.3 Structural Evaluation

TABLE OF CONTENTS

A.3	STRUCTURAL EVALUATION.....	A.3-1
A.3.1	Structural Design	A.3-1
A.3.1.1	Discussion.....	A.3-1
A.3.1.2	Design Criteria.....	A.3-6
A.3.2	Weights.....	A.3-7
A.3.2.1	32PTH Type 1 DSC Weight.....	A.3-7
A.3.2.2	OS187H Type 1 Transfer Cask Weight.....	A.3-8
A.3.2.3	HSM-H Weight.....	A.3-8
A.3.3	Mechanical Properties of Materials	A.3-9
A.3.4	General Standards for 32PTH Type 1 DSC, HSM-H, and OS187H Type 1 TC.....	A.3-10
A.3.4.1	Chemical and Galvanic Reactions	A.3-10
A.3.4.2	Positive Closure	A.3-10
A.3.4.3	Lifting Devices.....	A.3-10
A.3.4.4	Heat.....	A.3-10
A.3.4.5	Cold.....	A.3-11
A.3.5	Fuel Rods General Standards for 32PTH Type 1 DSC.....	A.3-12
A.3.6	Normal Conditions of Storage and Transfer.....	A.3-13
A.3.6.1	32PTH Type 1 DSC Normal Conditions Structural Analysis	A.3-13
A.3.6.2	HSM-H Normal Conditions Structural Analysis.....	A.3-15
A.3.6.3	OS187H Type 1 Transfer Cask Normal Conditions Structural Analysis	A.3-15
A.3.7	Off-Normal and Hypothetical Accident Conditions.....	A.3-18
A.3.7.1	32PTH Type 1 DSC Off-Normal and Accident Conditions Structural Analysis A.....	A.3-18
A.3.7.2	HSM-H Off-Normal and Accident Conditions Structural Analysis	A.3-21
A.3.7.3	OS187H Type 1 Transfer Cask Off Normal and Accident Conditions Structural Analysis.....	A.3-22
A.3.8	References.....	A.3-24
A.3.9	Appendices.....	A.3-25
A.3.10	ASME Code Alternatives	A.3-25

A.3 STRUCTURAL EVALUATION

A.3.1 Structural Design

This chapter, including its appendices, summarizes the structural evaluation of the NUHOMS® HD System Type 1 components, i.e., the 32PTH Type 1 DSC and the OS187H Type 1 transfer cask (TC).

The 32PTH Type 1 DSC is similar to but a longer version of the 32PTH DSC documented in the main body of this FSAR. As with the 32PTH DSC, the 32PTH Type 1 DSC is designed to accommodate up to 32 intact PWR fuel assemblies (or up to 16 damaged assemblies, with the remaining intact) with the same total heat load of up to 34.8 kW. Similarly, the OS187H Type 1 TC is similar to but a longer version of the OS187H TC.

The structural evaluation criteria for the 32PTH Type 1 DSC and the OS187H Type 1 TC are the same as the evaluation criteria for the 32PTH DSC and OS187H TC described in the main body of this FSAR, with the exception of the analysis methodology used for the evaluation of the accident pressure load case in the 32PTH Type 1 DSC, where an elastic-plastic analysis was used instead of an elastic analysis used for the 32PTH DSC.

A.3.1.1 Discussion

No change.

A.3.1.1.1 General Description of the 32PTH Type 1 DSC

The principal characteristics of the 32PTH Type 1 DSC are described in Chapter A.1, Section A.1.2.1, including the changes implemented in the 32PTH Type 1 DSC relative to the 32PTH DSC. The 32PTH Type 1 DSC is shown on drawings 10494-72-2001-SAR to 10494-72-2005-SAR in Section A.1.5.

For purposes of the structural analysis, the 32PTH Type 1 DSC is divided into the 32PTH Type 1 DSC shell assembly and the internal basket assembly.

A. DSC Shell Assembly Description

The 32PTH Type 1 canister shell assembly and design details are shown on drawings 10494-72-2001-SAR (main assembly), 10494-72-2002-SAR (shell assembly), and 10494-72-2005-SAR (alternate two-piece top end assembly design) in Section A.1.5. As with the 32PTH DSC, the 32PTH Type 1 DSC shell assembly is a high integrity stainless steel (SA-240 Type 304 or SA-182 Type F304) welded vessel that provides confinement of radioactive materials, encapsulates the fuel in an inert atmosphere (the canister is backfilled with helium before being seal welded closed), and provides biological shielding (in axial direction).

The 32PTH Type 1 main structural components include the welded cylindrical shell and the top and bottom end assemblies. The top end assembly may be a three-piece assembly, (a solid shield plug, made of A36 carbon steel, and the inner cover and outer cover plates, both made of SA-240 Type 304 stainless steel) or, as an alternate, a two-piece assembly, consisting of a combined top

shield plug/inner cover assembly, and an outer cover plate. The combined top shield plug/inner cover may be a single stainless steel piece (SA-240 Type 304 or SA-182 Type F304), or two stainless steel plates welded together, or a carbon steel shield plug encased within welded stainless steel plates. The various top end assembly design options for the alternate design are similar to those of the 32PTH DSC, as described in Section 3.1.1.1. For the bottom end assembly, the four optional design configurations present in the 32PTH are kept for the 32PTH Type 1 DSC. Although the total thickness of the bottom end assembly remains the same (8.75"), the minimum thicknesses of the bottom end inner and outer cover plates have increased from 1.69" and 1.70", respectively, in the 32PTH DSC to 2.25" and 2.00" in the 32PTH Type 1 DSC.

The remaining 32PTH Type 1 shell assembly structural components include the grapple ring assembly, the support ring and the lifting lugs (in the three-piece top end assembly design), or lifting blocks (in the two-piece alternate top end assembly design). The grapple ring assembly, which is welded to the shell bottom or outer bottom cover plate, is used to insert/extract the DSC to and from the Horizontal Storage Module (HSM-H). The grapple ring minimum thickness is increased from 1.00" to 1.20" in the 32PTH Type 1 DSC. The support ring, welded to the cylindrical shell, supports the shield plug. The 32PTH Type 1 DSC with the three-piece top end assembly design option incorporates four lifting lugs (welded to the shell and to the support ring) in lieu of the four lifting blocks which are welded to the inside of the shell bottom in the alternate design. The lifting lugs/lifting blocks are used to lift the DSC into the transfer cask prior to fuel loading operations.

The 32PTH Type 1 DSC shell assembly is designed, fabricated, examined, and tested in accordance with the same ASME Code Subsection NB [6] requirements as for the 32PTH DSC presented in Section 3.1.1.1.A. The 32PTH Type 1 DSC top closure is designed, fabricated, and inspected using the same alternatives to the ASME code specified in Section 3.10. The outer top cover plate and inner top cover plate are sealed by separate, redundant closure welds. The inner top cover (or inner top cover/top shield plug in the alternate two-piece top end design) is welded to the 32PTH Type 1 DSC shell to form the confinement boundary at the top end of the 32PTH Type 1 DSC, as shown in Chapter A.7, Figure A.7-1 (or Chapter 7, Figure 7-1 for the alternate top end design). The outer top cover plate provides structural support to the confinement boundary. All closure welds are multiple layer welds. Both, the inner and outer top cover plates to shell welds are examined by multi-level liquid penetrant to effectively eliminate through wall leaks. The three-piece top end assembly incorporates a vent and siphon block, welded to the shell, that is similar to that in other NUHOMS® canister designs [9]. The vent and siphon block weld to the shell and the inner top cover plate weld to the vent and siphon block are part of the confinement boundary. These welds are also multiple layer welds and receive multi-level liquid penetrant examination.

The leak test and the acceptance criterion of 1×10^{-7} ref. cm^3/sec as defined in ANSI N14.5 [2] of the DSC shell and bottom end assembly during fabrication and of the inner top closure weld (including vent/siphon cover welds) after loading of the fuel assemblies, have not changed from those of the 32PTH DSC.

The use of a strongback is not required during fuel loading operations when using the 32PTH Type 1 DSC.

B. Fuel Basket Assembly Description

The details of the 32PTH Type 1 basket assembly are shown in drawings 10494-72-2003-SAR and 10494-72-2004-SAR, provided in Section A.1.5. The overall length of the 32PTH Type 1 DSC basket is increased from 162.00" to 169.00". The internal canister cavity length is also increased from 164.50" minimum to 171.63" minimum to allow for thermal expansion, tolerances, and access to the top of the fuel assemblies.

The description for the basket assembly presented in Section 3.1.1.1 (B) for the 32PTH basket is applicable to the 32PTH Type 1 basket assembly. Additionally, when lifting blocks are not used, the circumferential orientation of the basket is maintained by the use of a key welded to the inside diameter of the shell at two opposite azimuths, and two accompanying slots in the basket rails. The purpose of the basket key is non-safety and is intended to prevent rotation during fabrication and during shipment of the empty canister.

A.3.1.1.2 General Description of the HSM-H

The general description of the HSM-H presented in Section 3.1.1.2 is applicable when the HSM-H is loaded with a 32PTH Type 1 DSC. The spacer mounted on the support rails used to accommodate shorter length DSCs is not needed for storage of the 32PTH Type 1 DSC. Additionally, the HSM-H support rail structure length has been slightly increased. The changes to the HSM-H support rail are shown in drawings 10494-72-100 and 10494-72-107.

A.3.1.1.3 General Description of the OS187H On-Site Transfer Cask

The NUHOMS® OS187H Type 1 On-Site transfer cask consists of a structural shell, gamma shielding material, and solid and liquid (water) neutron shield. The OS187H Type 1 TC is similar to the OS187H TC described in Section 3.1.1.3. The OS187H Type 1 TC is approximately 13 inches longer than the OS187H TC due to an increase in the interior cavity length to accommodate the longer 32PTH Type 1 DSC. Other main changes include:

- The OS187H Type 1 TC trunnions are made of monolithic solid steel forgings (the OS187H trunnions have a cutout that is filled with resin material) to accommodate the increased weight of the 32PTH Type 1 DSC and provide additional margins. The lower trunnion material is changed from SA-182 Type F304 to SA-182 Type F304N.
- The upper course of the structural shell thickness is increased from 2.00" to 2.38". Similarly, the upper trunnions pad plate is increased from 1.00" to 1.375".
- The inner liner thickness is increased from 1/2" to 5/8".

The overall dimensions of the OS187H Type 1 TC are 210.50" long and 92.11" in diameter. The TC structural shell is 83.63" in diameter (upper course). The TC cavity is 198.75" long and 70.50" in diameter. Detailed design drawings for the OS187H Type 1 TC are provided in drawings 10494-72-9001-SAR through 10494-72-9003-SAR on Chapter A.1, Section A.1.5. The materials used to fabricate the TC are shown in the parts list on each drawing. Where more than one material has been specified for a component, the most limiting properties are used in the analyses in the subsequent chapters of this Final Safety Analysis Report.

The gross weight of the loaded transfer cask is approximately 120.0 tons including a DSC payload of 54.3 tons. Section A.3.2.2 summarizes the weights of the NUHOMS® OS187H Type 1 packaging components.

The TC is fabricated primarily of stainless steel. Non-stainless steel members include the cast lead shielding between the inner radial shell and the structural shell, the O-ring seals, the NS-3 shielding material in the top and bottom end assemblies, and the carbon steel closure bolts. The top cover is bolted to the top flange by 24-1 1/2 in. diameter high strength bolts and sealed with O-ring. A cover plate is provided to seal the bottom hydraulic ram access penetration of the cask (by 12-1/2 in. high strength bolts with O-rings) during fuel loading and transferring the canister to the ISFSI. The dimensions and design details of the OS187H Type 1 TC are provided in drawings 10494-72-9001-SAR through 10494-72-9003-SAR in Chapter A.1, Section A.1.5.

The geometry and dimensions of the OS176H Type 1 TC trunnions are shown on Sheet 2 of Drawing 10494-72-9002-SAR. Some details/features of the OS187H Type 1 TC trunnions are different from those of the OS187H TC, e.g., the bearing width in each trunnion cylinder has been increased for ease of operations. In addition, the trunnion shielding pockets which are machined cavities filled with resin shielding material in the OS187H TC are deleted. Instead, the OS187H Type 1 TC trunnions are solid steel components.

The following sections provide physical and functional descriptions of each major component of the transfer cask.

A. Transfer Cask Body and Structural Components

The shell or cask body cylinder assembly is an open ended (at the top) cylindrical unit with an integral closed bottom end. This assembly consists of concentric inner shell and outer shell (both SA-240 Type 304), welded to massive closure flanges (SA-182 Type F304N) at the top and bottom ends. The inner shell is 0.625 inches thick and has a 70.50 inch inside diameter. The outer shell is the primary structural shell and is 1.5 inches (lower course) to 2.38 inches thick (upper course), and has a 78.87 inch inside diameter. The annulus between the shells is filled with lead shielding. The lead gamma shield is 3.56 inches (nominal) thick and is poured into the annulus in a molten state using a carefully controlled procedure.

The transfer cask bottom end assembly and top cover assembly are similar to the OS187H transfer cask with the exception that the resin neutron shield in the OS187H transfer cask is replaced with NS-3, a castable neutron shielding material. As with the OS187H, the OS187H Type 1 transfer cask is designed to maintain a helium atmosphere in the cask cavity.

The OS187H Type 1 transfer cask is designed, fabricated, examined, and tested in accordance with the requirements of Subsection NC [3] of the ASME Code to the maximum practical extent. The alternatives to the ASME Code presented in Section 3.10 for the OS187H TC are also applicable to the OS187H Type 1 TC.

B. Gamma and Radial Neutron Shielding

The description provided in Section 3.1.1.3 (B) is applicable to the OS187H Type 1 TC except that the resin material in the top and bottom assemblies, which provides axial neutron shielding in

the OS187H, is replaced with NS-3, a castable cementitious material. NS-3 has been used in other NUHOMS® applications, e.g., the OS197 transfer cask [9]. The radial neutron shielding provided by liquid water enclosed in a radial outer stainless steel shell welded to the structural shell is of similar design as the OS187H transfer cask.

C. Tiedown and Lifting Devices

The description provided in Section 3.1.1. 3 (C) is applicable to the OS187H Type 1 TC. The OS187H Type 1 trunnions are solid steel forgings as opposed to the OS187H trunnions that incorporate a neutron shield plug. The top trunnions are designed, fabricated, and tested in accordance with ANSI N14.6 [4] as single failure proof lifting devices. Consequently, they are designed with a factor of safety of 6 against the material yield strength and a factor of safety of 10 against the material ultimate strength.

D. Operational Features

The NUHOMS® OS187H Type 1 transfer cask is not considered to be operationally complex and is designed to be compatible with spent fuel pool loading/unloading methods. All operational features are readily apparent from inspection of the General Arrangement Drawings provided in Chapter A.1, Section A.1.5. The sequential steps to be followed for cask loading, testing, and unloading operations are provided in Chapter A.8.

A.3.1.1.4 Discussion of NUHOMS® HD System Drop Analysis

All lifting of the TC loaded with the DSC must be made within the existing heavy loads requirements and procedures of the licensed nuclear power plant.

The transfer cask is transported to the ISFSI in a horizontal configuration. Therefore, the only credible drop accident during storage or transfer operations is a side drop. The transfer cask, canister and basket assemblies and fuel cladding are analyzed for this accident in the following sections.

In addition, a vertical drop or corner drop accident scenarios may need to be evaluated under 10CFR50 should the user not be able to demonstrate that this accident drop is not credible during loading operations, or during transport operations governed under 10CFR71. Similarly, the fuel cladding integrity has not been demonstrated for this accident scenario. An additional safety review by the user is required to demonstrate fuel cladding integrity under 10CFR50 or to demonstrate that the end drop accidents are not credible.

The drop analyses of the NUHOMS® HD 32PTH Type 1 DSC and OS187H Type 1 transfer cask components are performed in the following appendices.

Appendix A.3.9.1

This appendix describes the detailed analysis of the 32PTH Type 1 DSC shell assembly and basket assembly for all the loading conditions. For the drop loads, the DSC shell assembly is analyzed for the 75g side and end drops. The basket assembly is also analyzed for the 75g side

and end drops. The 75g side drop in conjunction with the 75g end drop is considered to bound the 22g corner drop.

Appendix A.3.9.2

This appendix describes the detailed analysis of the OS187H Type 1 TC for all the loading conditions. For the drop loads, the TC is analyzed for the 75g side and end drops. The results for the TC side drop using LS-DYNA are reported in Appendix A.3.9.10.

Appendix A.3.9.3

This appendix describes the detailed analysis of the TC top cover bolt and ram cover bolt due to the 22g corner drop. The stress analysis is performed in accordance with NUREG/CR-6007.

Appendix A.3.9.4

Since the end and corner drops are not credible under 10CFR Part 72 the OS187H Type 1 TC lead slump and inner shell buckling analysis for the 75g end drop load are not evaluated. Vertical drop or corner drop accident scenarios may need to be evaluated under 10CFR50 should the user not be able to demonstrate that this accident drop is not credible during loading operations, or during transport operations governed under 10CFR71.

Appendix A.3.9.8

No change to the structural evaluations of the fuel cladding presented in Appendix 3.9.8.

Appendix A.3.9.10

This appendix provides the justification for the rigid body accident drop accelerations applicable to the OS187H Type 1 TC based on the LS-DYNA accident drop analysis documented in Appendix 3.9.10.

Appendix A.3.9.11

This appendix computes the dynamic amplification factor (DAF) to be applied to the response accelerations obtained from the side drop accident dynamic analysis of the transfer cask (TC) when applying those accelerations as input to an equivalent static analysis of the 32PTH Type 1 DSC.

A.3.1.2 Design Criteria

No change. The design criteria described in Section 3.1.2 is not changed and remains applicable to the 32PTH Type 1 DSC and OS187H Type 1 TC.

A.3.2 Weights

The nominal 32PTH Type 1 DSC, HSM-H and OS187H Type 1 transfer cask geometry is used to compute the weights of the NUHOMS® HD system components. Material densities are unchanged and are provided in Chapter 3.

A.3.2.1 32PTH Type 1 DSC Weight

The bounding weight of the loaded 32PTH Type 1 DSC is 108.61 kips (54.3 tons). The weights of the major individual subassemblies are listed in following table.

32PTH Type 1 DSC Summary of Nominal Component Weights

Component	Nominal Weight (lb x 1000)
Canister shell	5.81
Outer top cover plate	2.14
Inner top cover plate	2.15
Top shield plug and support ring	8.57
Bottom end assembly	9.70
Grapple ring	0.075
Total canister assembly	28.44
Fuel compartments (32)	10.48
Aluminum/poison plates	4.67
Stainless steel plates	2.36
Small support rails	3.08
Large support rails	8.86
Total Fuel Basket	29.45
Total Empty DSC (Basket & Canister)	57.89
Fuel assembly weight (32) @ 1585 lb/assembly	50.72
Total loaded DSC weight	108.61

A.3.2.2 OS187H Type 1 Transfer Cask Weight

The total weight of the loaded NUHOMS® OS187H Type 1 transfer cask is 239.47 kips (119.7 tons). The weights of the major individual subassemblies are listed in following table.

OS187H Type 1 Transfer Cask Summary of Nominal Component Weights

Component	Nominal Weight (lb x 1000)
Structural shell	23.73
Inner shell	7.89
Lead gamma shield	66.65
Top flange	2.63
Bottom flange	3.40
Top cover assembly	5.36
Bottom assembly	3.94
Neutron shield panel assembly	5.14
Radial neutron shield (water)	8.67
Upper trunnion pair	1.45
Lower trunnion pair	1.06
Total Empty Transfer Cask Weight	130.00⁽¹⁾
Total Transfer Cask with Empty DSC Weight	188.00⁽¹⁾
Total Transfer Cask with Loaded DSC Weight (Dry)	240.00⁽¹⁾⁽²⁾⁽³⁾

Notes:

- (1) Rounded up to nearest 1,000 lbs.
- (2) Includes a cask spacer with an approximate weight of 900 lbs.
- (3) 250.0 kips is conservatively used for the trunnion analysis.

A.3.2.3 HSM-H Weight

No change. See Section 3.2.3 for details of the HSM-H weight.

A.3.3 Mechanical Properties of Materials

No change. The material properties described in Section 3.3 remain applicable to the 32PTH Type 1 DSC and OS187H Type 1 TC. The properties for the resin shielding material used in the stress analysis of the OS187H TC are similar to those of the NS-3 material in the OS187H Type 1 TC.

A.3.4 General Standards for 32PTH Type 1 DSC, HSM-H, and OS187H Type 1 TC

A.3.4.1 Chemical and Galvanic Reactions

No change. The information provided in Section 3.4.1 is unchanged and applicable to the 32PTH Type 1 DSC and OS187H Type 1 TC.

A.3.4.2 Positive Closure

No change. The information provided in Section 3.4.2 is unchanged and applicable to the 32PTH Type 1 DSC and OS187H Type 1 TC.

A.3.4.3 Lifting Devices

No change. The information provided in Section 3.4.3 is unchanged and applicable to the 32PTH Type 1 DSC and OS187H Type 1 TC.

A.3.4.4 Heat

A.3.4.4.1 Summary of Pressures and Temperatures

No change. As documented in Chapter A.4, the heat transfer analyses documented in Chapter 4 for the 32PTH DSC inside the OS187H TC during transfer and in the HSM-H during storage are bounding relative to the 32PTH Type 1 DSC in the HSM-H and in the OS187H Type 1 TC. Therefore, the pressures and temperatures used for the stress analyses of the 32PTH DSC and the OS187H TC in Chapter 3 are also applicable for the 32PTH Type 1 DSC and the OS187H Type 1 TC. As discussed in Section A.3.6 and Section A.3.7, the Chapter 4 temperature distributions are conservatively applied (considering the longer length of the 32PTH Type 1 DSC and OS187H Type 1 TC) for the structural evaluations.

Thus, the maximum and minimum temperatures for the various components for normal, off-normal, and accident conditions are the same as those summarized in Tables 4-1 to Table 4-6. Similarly, the maximum pressures are the same as those summarized in Table 4-10. The Table 4-10 pressures bound those used in the structural analysis of the 32PTH Type 1 DSC.

A.3.4.4.2 Differential Thermal Expansion

Potential interference due to differential thermal expansion between the 32PTH Type 1 DSC shell assembly, the basket assembly, and transfer cask components is evaluated in Appendix A.3.9.1, Section A.3.9.1.4.

A.3.4.4.3 Stress Calculations

The stress analyses have been performed using the acceptance criteria presented in Section 3.1.2. The structural analyses for the 32PTH Type 1 DSC and OS187H Type 1 TC are summarized in Sections A.3.6 and A.3.7, for normal, off-normal, and hypothetical accident conditions, respectively.

A.3.4.5 Cold

No change.

A.3.5 Fuel Rods General Standards for 32PTH Type 1 DSC

No change. The fuel rod evaluations presented in Section 3.5 are unchanged for the 32PTH Type 1 DSC.

A.3.6 Normal Conditions of Storage and Transfer

This section presents the structural analyses of the 32PTH Type 1 DSC, and the OS187H Type 1 TC subjected to normal conditions of storage and transfer. The analyses performed evaluate these two major NUHOMS® HD System components for the design criteria described in Section A.3.1.2 of this appendix. The structural analyses of the HSM-H presented in Chapter 3.6 are bounding and thus, not changed.

The 32PTH Type 1 DSC is subjected to both storage and transfer loading conditions and the OS187H Type 1 TC is only subjected to transfer loading conditions.

Numerical analyses have been performed for the normal and accident conditions, as well as for the lifting loads. In general, numerical analyses have been performed for the regulatory events. These analyses are summarized in Section A.3.6 and Section A.3.7, and described in detail in the Appendices A.3.9.1 through A.3.9.10 listed below.

The detailed structural analysis of the NUHOMS® HD System is included in the following appendices:

- Appendix A.3.9.1 32PTH Type 1 DSC (Canister and Basket) Structural Analysis
- Appendix A.3.9.2 OS187H Type 1 Transfer Cask Body Structural Analysis
- Appendix A.3.9.3 OS187H Type 1 Transfer Cask Top Cover and Ram Access Cover Bolts Analyses
- Appendix A.3.9.4 Not used (since the end and corner drops are not credible under 10CFR Part 72, the lead slump and inner shell buckling analysis of the OS187H Type 1 TC for the 75g end drop load are not documented).
- Appendix A.3.9.5 OS187H Type 1 Transfer Cask Trunnion Analysis
- Appendix A.3.9.6 OS187H Type 1 Transfer Cask Shield Panel Structural Analysis
- Appendix A.3.9.7 Deleted (superseded by Appendix A.3.9.10)
- Appendix A.3.9.8 No change. (Damaged Fuel Cladding Structural Evaluation)
- Appendix A.3.9.9 No change. (HSM-H Structural Analysis)
- Appendix A.3.9.10 OS187H Type 1 Transfer Cask Dynamic Impact Analysis
- Appendix A.3.9.11 32PTH Type 1 DSC Dynamic Amplification Factors

A.3.6.1 32PTH Type 1 DSC Normal Conditions Structural Analysis

Details of the structural analysis of the 32PTH Type 1 DSC are provided in Appendix A.3.9.1. The fuel basket assembly and canister shell assembly are analyzed independently. The structural evaluation of the 32PTH Type 1 fuel basket assembly is described in Section A.3.6.1.1. The structural evaluation of the canister shell assembly is described in Section A.3.6.1.2.

A.3.6.1.1 32PTH Type 1 DSC Fuel Basket Assembly Normal Condition Structural Evaluation

No change. As described in Appendix A.3.9.1, Section A.3.9.1.2, the ANSYS models, material properties, and design criteria used for the evaluation of the fuel basket assembly are the same

between the 32PTH and the 32PTH Type 1 DSCs, and, therefore, the stress analysis results documented in Section 3.9.1.2 for the 32PTH fuel basket assembly are applicable to the 32PTH Type 1 fuel basket assembly. As described in Section 3.9.1.2, a 360° finite element model of a 15 inch segment of the basket assembly is constructed for the structural evaluation of the basket assembly.

Based on the results of these analyses, the design of the 32PTH Type 1 DSC basket is structurally adequate with respect to normal condition transfer and storage loads.

A.3.6.1.2 32PTH Type 1 DSC Canister Shell Assembly Normal Condition Structural Evaluation

This section summarizes the evaluation of the structural adequacy of the 32PTH Type 1 DSC canister shell assembly under all applied normal condition loads. Detailed evaluation of the stresses generated in the canister is presented in Appendix A.3.9.1, Section A.3.9.1.3.2. The DSC canister shell buckling evaluation is presented in Appendix A.3.9.1, Section A.3.9.1.3.3.

Elastic and elastic-plastic analyses are performed to calculate the stresses in the 32PTH Type 1 DSC canister under the transfer and storage loads. These detailed load cases are summarized in Appendix A.3.9.1, Tables A.3.9.1-3, A.3.9.1-4 and A.3.9.1-13.

The calculated stresses in the canister shell due to normal transfer loading conditions are summarized in Appendix A.3.9.1, Tables A.3.9.1-5, A.3.9.1-6, A.3.9.1-9, and A.3.9.1-10. The stresses due to normal storage loading conditions are summarized in Appendix A.3.9.1, Tables A.3.9.1-14, and A.3.9.1-15.

The 32PTH Type 1 DSC with the three-piece top end assembly configuration (separate inner cover plate, shield plug, and outer cover plate) is considered to bound the alternate design with a two-piece top end assembly (combined top shield plug/inner cover plate and outer cover plate). Similarly, the bottom end assembly configuration, consisting of separate inner bottom, shield plug and outer bottom plates is considered the bounding configuration relative to that of a DSC with the optional single or two piece bottom end configurations. See discussion in Section A.3.9.1.3.4.

As described in Chapter A.8, Section A.8.1.1.3, operation steps 7 and 13, a maximum of 15.0 psig air pressure may be applied at the canister vent port to assist draining of the water. The canister is structurally evaluated for a bounding 25 psig internal pressure using the 2-D ANSYS finite element model described in Appendix A.3.9.1, Section A.3.9.1.3.2. The outer cover plate of the canister is removed from the 2-D model, since it is not yet installed during the application of this 25 psig air pressure. The maximum stress intensity in the canister is calculated to as 7.09 ksi. The stress limit for membrane stress per ASME B&PV Code Subsection NB [6] is 16.40 ksi. Therefore, the application of 25 psig air pressure to the canister is acceptable.

Based on the results of these analyses, the design of the 32PTH Type 1 DSC canister is structurally adequate with respect to both transfer and storage loads under the normal conditions.

A.3.6.2 HSM-H Normal Conditions Structural Analysis

No change. The DSC weight used for the structural evaluation of the HSM-H (110,000 lb) bounds the calculated weight of the 32PTH Type 1 DSC (108,610 lb). In addition, as discussed in Chapter A.4, the temperature distributions of the HSM-H loaded with a 32PTH Type 1 DSC are bounded by those of the HSM-H loaded with a 32PTH DSC documented in Chapter 4. Therefore, the structural evaluation of the HSM-H loaded with a 32PTH DSC, as documented in Section 3.6.2 and Appendix 3.9.9, are applicable for a HSM-H loaded with the 32PTH Type 1 DSC.

A.3.6.3 OS187H Type 1 Transfer Cask Normal Conditions Structural Analysis

Details of the structural analysis of the OS187H Type 1 transfer cask are provided in Appendices A.3.9.2 through A.3.9.6. The contents of each of these appendices are as follows.

Appendix A.3.9.2 OS187H Type 1 Transfer Cask Body Structural Analysis

Appendix A.3.9.3 OS187H Type 1 Transfer Cask Lid and Ram Access Cover Bolt Analyses

Appendix A.3.9.5 OS187H Type 1 Transfer Cask Trunnion Analysis

Appendix A.3.9.6 OS187H Type 1 Transfer Cask Shield Panel Structural Analysis

A.3.6.3.1 Structural Analysis of the Transfer Cask Body under Normal Conditions

The details of the structural analyses of the NUHOMS® OS187H Type 1 TC body including the cylindrical shell assembly and bottom assembly, the top cover, and the local stresses at the trunnion/cask body interface are presented in Appendix A.3.9.2. The specific methods, models and assumptions used to analyze the cask body for the various individual loading conditions specified in 10CFR72 [1] are described in that appendix.

The OS187H Type 1 TC body structural analyses for normal conditions use static or quasistatic linear elastic methods. The stresses and deformations due to the applied loads are generally determined using the ANSYS [7] computer program.

Table A.3.9.2-1 of Appendix A.3.9.2 summarizes the maximum stresses in the transfer cask body computed for normal conditions of transfer. The maximum stresses in each component are listed along with the normal loading condition that generates the stress. The results are evaluated against the ASME Code [3] design criteria described in Section A.3.1.2 of this chapter.

Based on the results of these analyses, the design of the OS187H Type 1 TC is structurally adequate with respect to normal condition (Level A) transfer loads.

A.3.6.3.2 Transfer Cask Top Cover and Ram Access Cover Bolt Normal Condition Analysis

The detailed calculations for the top cover and ram access cover bolts are presented in Appendix A.3.9.3. The analysis is based on NUREG/CR-6007 [8]. The bolts are analyzed for the following normal loading conditions: operating pre-load, gasket seating load, internal pressure, and temperature changes.

The bolt preload is calculated to withstand the worst case load combination and to maintain a clamping (compressive) force on the closure joint, under normal conditions. Based upon the load combination results (see Appendix A.3.9.3, Sections A.3.9.3.3 and A.3.9.3.8), it is shown that a positive (compressive) load is maintained on the clamped joint for all normal condition load combinations.

A summary of the calculated top cover bolt stresses is provided in Appendix A.3.9.3, Section A.3.9.3.5. The calculations result in a maximum average tensile stress of 37.4 ksi, which is below the allowable tensile stress of 92.4 ksi for normal conditions. The maximum average shear stress in the bolts is due to torsion during pre-loading. This stress is 6.8 ksi, which is well below the allowable shear stress of 55.4 ksi. The maximum combined stress intensity due to tension plus shear plus bending is 72.9 ksi, which is also less than the maximum allowable stress intensity of 124.7 ksi.

A summary of the calculated ram access bolt stresses is provided in Appendix A.3.9.3, Section A.3.9.3.10. The analysis results in a maximum average tensile stress of 70.8 ksi, which is below the allowable tensile stress of 92.4 ksi for normal conditions. The maximum normal condition shear stress is 15.9 ksi, which is well below the allowable shear stress of 55.4 ksi. The maximum combined stress intensity due to tension plus shear plus bending is 97.3 ksi, which is also less than the maximum allowable stress intensity of 124.7 ksi.

A.3.6.3.3 Transfer Cask Normal Condition Trunnion Analysis

Appendix A.3.9.5 presents the evaluation of the trunnion stresses in the NUHOMS® OS187H Type 1 TC due to all applied loads during fuel loading and transfer operations.

The NUHOMS® OS187H Type 1 TC has two upper trunnions constructed from SA-182 Type FXM-19 and two lower trunnions constructed from SA-182 Type F304N stainless steel material. Both sets of trunnions are solid forged components welded to the structural shell of the transfer cask, which is constructed from SA240 Type 304 stainless steel. The upper trunnions are used to lift the cask with an empty DSC into a fuel pool. After the spent fuel has been loaded into the DSC, the upper trunnions are used to lift the cask to the decontamination area. After draining, drying, and closure welding of the DSC, the cask lid is bolted onto the transfer cask and the cask is vertically lifted to the transfer trailer where the cask is mated with the transfer skid front trunnion towers and pivoted about the lower trunnions into its horizontal position. In its horizontal position, the cask is supported by its four trunnions which are mounted on the four trunnion towers of the transfer skid.

Based on the loading and transfer scenario described above, the top trunnions are analyzed for 6g vertical lifting loads, and both sets of trunnions are evaluated for a prescribed set of transfer handling loads.

The transfer cask shell and trunnions are assumed to be at 300 °F during transfer. This assumption is conservative based on the thermal evaluation performed in Chapter 4.

The calculated maximum trunnion stresses are summarized in Appendix A.3.9.5, Table A.3.9.5-1 and compared with their corresponding allowable stresses. Table A.3.9.5-1 shows that all

calculated trunnion stresses are less than their corresponding allowable stresses. Therefore, the NUHOMS® OS187H Type 1 TC top and bottom trunnions are structurally adequate to withstand loads during lifting and transfer operations.

A.3.6.3.4 Transfer Cask Shield Panel Structural Analysis for Normal Conditions

Appendix A.3.9.6 presents the evaluation of the stresses in the NUHOMS® OS187H Type 1 TC neutron shield shell due to all applied loads during fuel loading and transfer operations.

A finite element model, similar to that of the OS187H TC neutron shield panel, is developed for the structural analysis of the outer neutron shield shell, end closure, central plates and structural shell. These structural components were modeled with two dimensional axisymmetric elements. The same finite element model is used for all loading conditions.

Table A.3.9.6-1 of Appendix A.3.9.6 summarizes the calculated stresses for the transfer cask lifting and transfer loads. Based on the results of the analysis, it is concluded that the outer shell structure is structurally adequate for the specified transfer loads.

A.3.7 Off-Normal and Hypothetical Accident Conditions

This section presents the structural analyses of the 32PTH Type 1 DSC, the HSM-H and the OS187H Type 1 TC subjected to off normal and hypothetical accident conditions of storage and transfer. The analyses are summarized in Sections A.3.7.1, A.3.7.2 and A.3.7.3 of this appendix and are evaluated against the design criteria described in Section A.3.1.2 of this chapter.

The 32PTH Type 1 DSC is subjected to both storage and transfer loading conditions, while the HSM-H is only subjected to storage loading conditions and the OS187H Type 1 TC is only subjected to transfer loading conditions.

A.3.7.1 32PTH Type 1 DSC Off-Normal and Accident Conditions Structural Analysis

Details of the structural analysis of the 32PTH Type 1 DSC are provided in Appendix A.3.9.1. The fuel basket assembly and canister shell assembly are analyzed independently. The structural analysis of the fuel basket assembly is described in Appendix A.3.9.1, Section A.3.9.1.2, while the structural analysis of the canister shell assembly is described in Section A.3.9.1.3. A 360° finite element model of a 15" segment of the basket assembly is constructed for the structural evaluation of the fuel basket assembly. Four finite element models are used for the structural evaluation of the canister shell assembly. A 2-D axisymmetric model used for the analysis of axisymmetric loads, two 3-D models modeling the top and bottom halves of the shell assembly, respectively, used for the analysis of non-axisymmetric loads, and a 3-D local model of the lifting lugs welded to the shell assembly to evaluate stresses during lifting of the DSC and placement into the transfer cask prior to fuel loading.

A.3.7.1.1 32PTH Type 1 DSC Fuel Basket Assembly Off Normal and Accident Condition Structural Analysis

A.3.7.1.1.1 32PTH Type 1 Fuel Basket Off-Normal and Accident Condition Stress Analysis

The fuel basket assembly stress analyses are performed for off-normal and accident condition loads during fuel transfer and storage.

The mechanical properties of structural materials used in the basket and canister are shown in Section 3, Table 3-5, and Appendix 3.9.1, Table 3.9.1-1, as a function of temperature. All structural components of the fuel basket and support rails are constructed from SA-240, Type 304 stainless steel, with properties taken from AMSE B&PV Code [5].

The load cases used for the analyses of the 32PTH Type 1 fuel basket assembly are the same as for the 32PTH fuel basket assembly and are as summarized in Section 3.9.1.2.2.

The details of the stress analysis of the basket assembly, as presented in Appendix 3.9.1, Section 3.9.1.2.3 are applicable without change to the 32PTH Type 1 fuel basket assembly. As discussed in Section 3.9.1.2.3, the basket stress analyses are performed using a 3-dimensional finite element model of the cross section of the basket assembly. The model is a 15" long segment of the basket assembly and is described in detail in Appendix 3.9.1, Section 3.9.1.2.3 (A). This model is used for the analysis of the transfer side drop impact loads, storage seismic loads, and both, transfer

and storage thermal load cases. Hand calculations are used for the evaluation of the transfer end drop load cases.

The stresses calculated for the 32PTH DSC fuel basket assembly and summarized in Tables 3.9.1-4a and 3.9.1-4b for the transfer accident loads and Table 3.9.1-5 for the storage accident loads are applicable to the 32PTH Type 1 basket assembly.

The maximum shear load in the fusion welds for the 75g side drop accident loading condition is calculated in Appendix 3.9.1, Section 3.9.1.2.3.B.5. The calculated maximum shear force during side drop is 7,208 lb. The fusion weld is qualified by a pull test (shear). The minimum test load is 17.1 kips. This test load includes a safety factor of 2 and a correction for material strength for room temperature testing.

Based on the results of these analyses, the design of the 32PTH Type 1 DSC basket is structurally adequate with respect to off-normal and accident conditions of transfer and storage loads.

A.3.7.1.1.2 32PTH Type 1 DSC Fuel Basket Accident Condition Buckling Analysis

As stated in Section A.3.9.1.2.4, the details of the buckling analysis of the fuel basket plates and support rails as presented in detail in Appendix 3.9.1, Section 3.9.1.2.4 are applicable without change to the 32PTH Type 1 fuel basket assembly. The buckling evaluation is performed using the 3-D finite element model of the basket assembly used for the stress analysis, as described in Section 3.9.1.2.3.

Nonlinear stress analyses are conducted in order to evaluate the plastic buckling loads for the 32PTH DSC basket. The three critical azimuth drop orientations analyzed are:

1. 0° (load applied in the direction parallel to the basket plates)
2. 30° (load applied at 30° relative to the basket plate direction)
3. 45° (load applied at 45° relative to the basket plate direction)

The following table summarizes the input load and last converged load for all three load cases analyzed using the local finite element model of the critical basket region:

Basket Orientation	150g loads			Last Converged Load (g)
	Vertical Pressure (psi)	Lateral Pressure (psi)	Applied Acceleration	
Vertical	171.12	0	(0, 150, 0)	102.5
30°	148.19	85.56	(-75, 129.9, 0)	83.9
45°	121.00	121.00	(-106.1, 160.1, 0)	85.6

Per the stability criteria described in Section 3.1.2.1.2 the load applied in the last converged load sub-step is considered to be the buckling load of the structure, therefore the allowable buckling load for the basket is 83.9g.

Since the critical collapse load for the 32PTH Type 1 DSC basket (83.9g for the 30° orientation) is greater than the maximum design acceleration of 75g, the basket will not fail in buckling during the accident condition events.

A.3.7.1.1.3 32PTH Type 1 DSC Fuel Basket Support Rail Accident Condition Buckling Analysis

No change.

A.3.7.1.2 32PTH Type 1 DSC Canister Shell Off Normal and Accident Condition Structural Evaluation

A.3.7.1.2.1 32PTH Type 1 Canister Shell Assembly Off-Normal and Accident Condition Stress Analysis

The description of the off-normal and accident analysis for the 32PTH DSC shell assembly presented in Section 3.7.1.2.1 is applicable without change to the 32PTH Type 1 canister shell assembly.

Elastic and elastic-plastic analyses are performed to calculate the stresses in the 32PTH Type 1 DSC shell assembly under the transfer and storage loads. These load cases are summarized in Appendix A.3.9.1, Tables A.3.9.1-3, A.3.9.1-4 and A.3.9.1-13. The accident side drop load case and the accident pressure load case are analyzed by elastic-plastic analyses and the rest by elastic analyses.

Two finite element model types are used for the analysis of the 32PTH Type 1 DSC shell assembly. The first type is a 2-Dimensional axisymmetric model used for the analysis of symmetric loads (e.g., pressure, dead weight). The second type is a 3-Dimensional model of the top and bottom halves of the shell assembly and is used for the analysis of non-axisymmetric loads (e.g., side drops). The 2-D model is shown in Figures A.3.9.1-1. The 3-D models are shown in Figure A.3.9.1-4 and A.3.9.1-5 for the top and bottom halves, respectively. As shown in Figure A.3.9.1-2, the three-part top end assembly is modeled (separate shield plug, inner cover, and outer cover plates). Similarly, as shown in Figure A.3.9.1-3, the design option with separate inner bottom cover plate, bottom shield plug, and outer bottom cover plate is modeled. This configuration is expected to be the bounding as the pressure load is resisted by the inner top and inner bottom plates, and supported by the outer top cover plate (at the top) and, through the stiff bottom shield plug by the outer bottom cover plate (at the bottom).

The calculated stresses in the canister shell assembly due to off-normal and accident transfer loading conditions are summarized in Appendix A.3.9.1, Tables A.3.9.1-6, 7, 8, 10, 11, and 12. The stresses due to accident storage loading conditions are summarized in Appendix A.3.9.1, Tables A.3.9.1-14, and 15.

The alternate top closure assembly of the 32PTH Type 1 DSC which consists of the two-part combined shield plug/inner cover assembly (including the optional configurations), as well as the optional bottom end configurations are not analyzed explicitly. The results of the 32PTH DSC for the side drop accident load case are applicable for these alternate configurations. See discussion in Section A.3.9.1.3.4.

Based on the results of these analyses, the design of the 32PTH Type 1 DSC canister is structurally adequate with respect to off-normal and accident condition transfer and storage loads.

A.3.7.1.2.2 32PTH Type 1 DSC Canister Shell Accident Condition Buckling Analysis

This section summarizes the evaluation of the 32PTH Type 1 DSC canister against buckling under a vertical end drop during transfer operations. The details of the DSC canister shell buckling analysis are provided in Appendix A.3.9.1, Section A.3.9.1.3.3. A finite element elastic-plastic analysis with large displacement option is performed to monitor occurrence of canister shell buckling under the specified loads.

The thermal evaluation presented in Chapter 4 shows that the metal temperatures of the entire canister are below 500 °F during transfer operations. The material properties of the canister at 500 °F are therefore conservatively used for the canister buckling analysis.

The following three hypothetical accident load cases for the canister are considered in this buckling analysis.

Buckling Load Case 1: 15 psig external pressure and 75g axial acceleration due to end drop

Buckling Load Case 2: 30 psig internal pressure and 75g axial acceleration due to end drop

Buckling Load Case 3: 0 psig internal pressure and 75g axial acceleration due to end drop

The same two-dimensional axisymmetric finite element model used for the stress analysis of the canister shell assembly and described in Appendix A.3.9.1, Section A.3.9.1.3.2.D.2 is used for the buckling accident analysis. Since the top end of the canister is heavier than the bottom end, it is a more severe case when the canister drops on its bottom end. A bottom end drop is therefore chosen for analysis in this calculation.

Load Case 1 converged at 173.5g load. Load Case 2 converged at 174.9g load. Load Case 3 converged at a load corresponding to 174.0g. This load is much higher than the required 75g load in either Load Case 1 or 2. The analysis shows that the canister does not buckle up to an end drop load of 173.5g, which is well beyond the design 75g load. It is, therefore, concluded that buckling of the canister will not occur during a hypothetical accident end drop.

A.3.7.2 HSM-H Off-Normal and Accident Conditions Structural Analysis

No change. As discussed in Section 3.7.2, the HSM-H is evaluated for a DSC weight and heat loads that bound those of the 32PTH Type 1 DSC. Thus, the evaluations of the 32PTH inside the HSM-H documented in Section 3.7.2 are bounding for the 32PTH Type 1 DSC inside the HSM-H.

A.3.7.3 OS187H Type 1 Transfer Cask Off Normal and Accident Conditions Structural Analysis

A.3.7.3.1 Structural Analysis of the Transfer Cask Body for Off Normal and Accident Conditions

The details of the structural analyses of the NUHOMS® OS187H Type 1 TC body including the cylindrical shell assembly and bottom assembly, the top cover, and the local stresses at the trunnion/cask body interface are presented in Appendix A.3.9.2. The specific methods, models and assumptions used to analyze the cask body for the various individual loading conditions specified in 10CFR72 [1] are described in that appendix.

The OS187H transfer cask body structural analyses generally use static or quasistatic linear elastic methods. The stresses and deformations due to the applied loads are generally determined using the ANSYS [7] computer program.

The maximum stresses in each of the major components of the transfer cask are reported for each load case and load combination in Appendix A.3.9.2, Table A.3.9.2-1. The results are evaluated against the ASME Code [3] design criteria described in Section A.3.1.2 of this chapter.

Based on the results of these analyses, the design of the OS187H Type 1 TC is structurally adequate with respect to off normal and hypothetical accident transfer loads.

A.3.7.3.2 Transfer Cask Top Cover and Ram Access Cover Bolt Accident Condition Analysis

The detailed calculations for the top cover and ram access cover bolts are presented in Appendix A.3.9.3. The analysis is based on NUREG/CR-6007 [8]. The bolts are analyzed for the hypothetical accident condition impact loads and load combinations.

A summary of the calculated top cover bolt stresses is listed in Appendix A.3.9.3, Section A.3.9.3.5. The calculations result in a maximum average tensile stress of 110.6 ksi, which is below the allowable tensile stress of 115.5 ksi for accident conditions. The maximum average shear stress in the bolts is due to torsion during pre-loading. This stress is 6.8 ksi, which is well below the allowable shear stress of 69.3 ksi.

A summary of the calculated ram access bolt stresses is listed in Appendix A.3.9.3, Section A.3.9.3.10. The analysis results in a maximum average tensile stress of 70.8 ksi, which is below the allowable tensile stress of 115.5 ksi for accident conditions. The maximum accident shear stress is 15.9 ksi, which is well below the allowable shear stress of 69.3 ksi.

A.3.7.3.3 Transfer Cask Lead Slump Analysis

As described in Section 3.1.1.4, the only credible drop accident during storage or transfer operations is a side drop. Thus, lead slump evaluation under top or bottom end drop accident is not performed for the OS187H Type 1 TC.

A.3.7.3.4 Transfer Cask Inner Containment Buckling Analysis

As described in Section 3.1.1.4, the only credible drop accident during storage or transfer operations is a side drop. Thus, inner liner buckling evaluation under top or bottom end drop accidents is not performed for the OS187H Type 1 TC.

A.3.7.3.5 Transfer Cask Trunnion Analysis

Appendix A.3.9.5 presents the evaluation of the trunnion stresses in the NUHOMS® OS187H Type 1 TC due to all applied loads during fuel loading and transfer operations. The calculated maximum normal condition trunnion stresses are summarized in Table A.3.9.5-1 and compared with their corresponding allowable stresses.

A.3.7.3.6 Transfer Cask Shield Panel Structural Analysis for Accident Conditions

Appendix A.3.9.6 presents the evaluation of the stresses in the NUHOMS® OS187H Type 1 TC neutron shield shell due to all applied loads during fuel loading and transfer operations. The calculated maximum normal condition neutron shield shell stresses are summarized in Table A.3.9.6-1 of Appendix A.3.9.6.

A.3.7.3.7 Transfer Cask Impact Analysis

Appendix A.3.9.10 presents the computation of the peak decelerations of NUHOMS® OS187H Type 1 TC during impact, subsequent to the hypothetical accident drop onto the concrete pad/soil system during transfer operations.

A.3.8 References

1. Title 10, Code of Federal Regulations, Part 72, "Licensing Requirements for the Storage of Spent Fuel in an Independent Spent Fuel Storage Installation."
2. American National Standards Institute, ANSI N14.5-1997, Leakage Tests on Packages for Shipment of Radioactive Materials.
3. American Society of Mechanical Engineers, ASME Boiler and Pressure Vessel Code, Section III, Subsection NC, 1998 through 2000 addenda.
4. American National Standards Institute, ANSI N14.6, American National Standard for Special Lifting Devices for Shipping Containers Weighing 10,000 Pounds or More for Nuclear Materials, 1993.
5. American Society of Mechanical Engineers, ASME Boiler and Pressure Vessel Code, Section II, Parts A, B, C and D, 1998, through 2000 addenda.
6. American Society of Mechanical Engineers, ASME Boiler and Pressure Vessel Code, Section III, Subsection NB, 1998 through 2000 addenda.
7. ANSYS Users Manual, Rev. 5.6 and 6.0, 8.0, 8.1, and 10A1
8. NUREG/CR-6007 "Stress Analysis of Closure Bolts for Shipping Casks", By Mok, Fischer, and Hsu, Lawrence Livermore National Laboratory, 1992.
9. Updated Final Safety Analysis Report (UFSAR), Standardized NUHOMS® Horizontal Modular Storage System for Irradiated Nuclear Fuel, Rev. 9, Feb. 2006.

A.3.9 Appendices

The detailed structural analyses of the NUHOMS® HD system Type 1 components are included in the following appendices:

- Appendix A.3.9.1 32PTH Type 1 DSC (Canister and Basket) Structural Analysis
- Appendix A.3.9.2 OS187H Type 1 Transfer Cask Body Structural Analysis
- Appendix A.3.9.3 OS187H Type 1 Transfer Cask Top Cover and Ram Access Cover Bolts Analyses
- Appendix A.3.9.4 Not used (since the end and corner drops are not credible under 10CFR Part 72, the lead slump and inner shell buckling analysis of the OS187H Type 1 TC for the 75g end drop load are not documented).
- Appendix A.3.9.5 OS187H Type 1 Transfer Cask Trunnion Analysis
- Appendix A.3.9.6 OS187H Type 1 Transfer Cask Shield Panel Structural Analysis
- Appendix A.3.9.7 Deleted (superseded by Appendix A.3.9.10)
- Appendix A.3.9.8 No change (Damaged Fuel Cladding Structural Evaluation)
- Appendix A.3.9.9 No change (HSM-H Structural Analysis)
- Appendix A.3.9.10 OS187H Type 1 Transfer Cask Dynamic Impact Analysis
- Appendix A.3.9.11 32PTH Type 1 DSC Dynamic Amplification Factors

A.3.10 ASME Code Alternatives

No change to the ASME Code Alternatives provided in Section 3.10.

Appendix A.3.9.1

32PTH Type 1 Type 1 DSC (Canister and Basket) Structural Analysis

TABLE OF CONTENTS

A.3.9.1	32PTH TYPE 1 DSC (CANISTER AND BASKET) STRUCTURAL ANALYSIS	A.3.9.1-1
A.3.9.1.1	Introduction.....	A.3.9.1-1
A.3.9.1.2	32PTH Type 1 DSC Fuel Basket Assembly Structural Evaluation.....	A.3.9.1-2
A.3.9.1.2.1	Approach.....	A.3.9.1-2
A.3.9.1.2.2	Loading Conditions.....	A.3.9.1-2
A.3.9.1.2.3	Fuel Basket Assembly Stress Analysis	A.3.9.1-2
A.3.9.1.2.4	32PTH Type 1 Fuel Basket Assembly Buckling Analysis	A.3.9.1-2
A.3.9.1.3	32PTH Type 1 DSC Shell Assembly Structural Evaluation	A.3.9.1-3
A.3.9.1.3.1	Approach.....	A.3.9.1-3
A.3.9.1.3.2	DSC Canister Shell Assembly Stress Analysis.....	A.3.9.1-3
A.3.9.1.3.3	DSC Shell Buckling Evaluation.....	A.3.9.1-20
A.3.9.1.3.4	Evaluation of Alternate DSC Top and Bottom Closure Assembly Design.....	A.3.9.1-23
A.3.9.1.4	32PTH Type 1 DSC and OS187H Type 1 Transfer Cask Thermal Expansion Evaluation.....	A.3.9.1-24
A.3.9.1.4.1	Introduction.....	A.3.9.1-24
A.3.9.1.4.2	Approach.....	A.3.9.1-24
A.3.9.1.4.3	Mechanical Properties of Materials	A.3.9.1-24
A.3.9.1.4.4	Thermal Expansion Computation	A.3.9.1-24
A.3.9.1.4.5	Thermal Expansion Analysis Conclusions	A.3.9.1-25
A.3.9.1.5	References.....	A.3.9.1-26

LIST OF TABLES

Table A.3.9.1-1	Temperature Dependent Material Properties for ASTM A-36.....	A.3.9.1-27
Table A.3.9.1-2	Material Stress Limits for 32PTH Type 1 DSC	A.3.9.1-28
Table A.3.9.1-3	32PTH Type 1 DSC Canister Load Combinations during Transfer	A.3.9.1-29
Table A.3.9.1-4	32PTH Type 1 DSC Canister Load Combinations during Lifting, Testing, and Hydraulic Loads	A.3.9.1-30
Table A.3.9.1-5	Summary of Calculated Stresses for Testing Condition Loads.....	A.3.9.1-31
Table A.3.9.1-6	Summary of Calculated Stress for Normal and Off-Normal Condition Transfer Loads	A.3.9.1-32
Table A.3.9.1-7	Summary of Calculated Stress for Accident Condition Transfer Loads (Axisymmetric Loads)	A.3.9.1-33
Table A.3.9.1-8	Summary of Stresses for Accident Condition Transfer Loads (3-D Inertial Loads)	A.3.9.1-34
Table A.3.9.1-9	Summary of Calculated Stress at End Closure Welds for Testing Condition Loads.....	A.3.9.1-35
Table A.3.9.1-10	Summary of Calculated Stress at the End Closure Welds for Normal and Off-Normal Condition Transfer Loads	A.3.9.1-36
Table A.3.9.1-11	Summary of Calculated Stresses at End Closure Welds for Accident Condition Transfer Loads (Axisymmetric Loads)	A.3.9.1-37
Table A.3.9.1-12	Summary of Calculated Stresses at End Closure Welds for Accident Condition Transfer Loads (3-D Inertial Loads).....	A.3.9.1-38
Table A.3.9.1-13	32PTH Type 1 DSC Canister Load Combinations during Storage	A.3.9.1-39
Table A.3.9.1-14	Summary of Calculated Stresses for Normal and Accident Condition Loads (canister in horizontal position)	A.3.9.1-40
Table A.3.9.1-15	Summary of Calculated Stresses at the End Closure Welds for Normal and Accident Condition Storage Loads	A.3.9.1-41

LIST OF FIGURES

Figure A.3.9.1-1 2-D Canister Axisymmetrical Thermal and Stress Finite
Element Model..... A.3.9.1-42

Figure A.3.9.1-2 Top End of the 2-D Axisymmetrical Canister Model A.3.9.1-43

Figure A.3.9.1-3 Bottom End of the 2-D Axisymmetrical Canister Model..... A.3.9.1-44

Figure A.3.9.1-4 3-D DSC Canister Top End Assembly Finite Element Model..... A.3.9.1-45

Figure A.3.9.1-5 3-D DSC Canister Bottom End Assembly Finite Element
Model A.3.9.1-46

Figure A.3.9.1-6 32PTH Type 1 DSC Canister Finite Element Model used for
Pressure Test Analysis A.3.9.1-47

A.3.9.1 32PTH TYPE 1 DSC (CANISTER AND BASKET) STRUCTURAL ANALYSIS

A.3.9.1.1 Introduction

The NUHOMS® 32PTH Type 1 DSC consists of a fuel basket assembly and a canister shell assembly. The canister shell assembly consists of a cylindrical shell, top end assembly (outer top cover plate, inner top cover plate, top shield plug), and a bottom end assembly (inner bottom cover plate, bottom shield plug, outer bottom cover plate). An alternate design for the top end assembly includes a two-part top end (combined shield plug/inner top cover and the outer cover plate). Similarly, the bottom end may consist of a single forged piece or two-piece, or three-piece assembly. The primary confinement boundary for the 32PTH Type 1 DSC consists of the DSC shell, the inner top cover plate, and shell bottom or inner bottom cover plate of the shell bottom assembly.

The canister shell thickness is 0.50 inches, and the top and bottom closure assemblies are 12.0 inches and 8.75 inches, respectively. The canister is constructed entirely from SA-240 Type 304 stainless steel and SA-182 Type F304. The shield plugs are constructed from ASTM A-36. There are no penetrations through the confinement vessel. The draining and venting systems are covered by the port plugs, and the outer top cover plate and the inner top cover plate are welded to the cylindrical shell with multi-layer welds. The canister cavity is pressurized above atmospheric pressure with helium. The 32PTH Type 1 DSC shell assembly geometry and the materials used for its analysis and fabrication are shown on drawings 10492-72-2001-SAR to 2005-SAR included in Chapter A.1.

The basket structure consists of assemblies of stainless steel fuel compartments and support rails. The borated aluminum or boron carbide/aluminum metal matrix composite plates (neutron poison plates) provide the necessary criticality control and also provide a portion of the heat conduction paths from the fuel assemblies to the cask cavity wall. This method of construction forms a very strong structure of compartment assemblies which provide for storage of 32 PWR fuel assemblies. The open dimension of each fuel compartment is 8.70 in. × 8.70 in., which provides clearance around the fuel assemblies.

The fuel basket assembly and the canister assembly are analyzed separately. The fuel basket assembly is analyzed in Section A.3.9.1.2, while the canister shell assembly is analyzed in Section A.3.9.1.3. The full 360° 3-dimensional finite element model of the basket assembly used for the evaluation of the 32PTH basket is applicable to the 32PTH Type 1 basket assembly. The analyses performed in Section 3.9.1.2 for the 32PTH basket are applicable for the 32PTH Type 1 basket (See Section A.3.9.1.2 for details).

Three finite element models are used for the structural evaluation of the canister shell assembly. A 2-dimensional axisymmetric model of the DSC canister shell assembly is used to evaluate axial inertial loads as well as internal pressure, external pressure, and thermal loads. Two 3-dimensional finite element models of the DSC shell assembly are used to evaluate the effects of transverse inertial loads (e.g., side drop). These are separate models of the top half and bottom half assemblies of the 32PTH Type 1 DSC.

A.3.9.1.2 32PTH Type 1 DSC Fuel Basket Assembly Structural Evaluation

A.3.9.1.2.1 Approach

The basket design for the NUHOMS® 32PTH Type 1 DSC is identical to the 32PTH DSC except that the length of the 32PTH Type 1 basket is longer (the length of the 32PTH DSC basket is 162 inches, whereas the length of the 32PTH Type 1 DSC basket is 169 inches). In addition, the fuel compartment tubes at the top of the basket are also connected with support bars and fusion welds in the 32PTH Type 1 design. The 15 inch pitch between support bars (where the fuel compartments are connected to each other by fusion welds), which is the basis for the selection of the axial length of the analysis model, is the same for the 32PTH and 32PTH Type 1 baskets. The material properties, maximum fuel assembly weight, and the temperature profiles used in the 32PTH basket analyses (Section 3.9.1.2) have not changed. Thus, the analyses performed for the 32PTH basket assembly, documented in Section 3.9.1.2, are also applicable for the 32PTH Type 1 basket.

Therefore, the analysis results for the 32PTH basket in Section 3.9.1.2 are also applicable to the 32PTH Type 1 basket.

A. Material Properties

No change. The material properties for the 32PTH DSC in Section 3.9.1.2.1(A) are also applicable to the 32PTH Type 1 DSC.

B. Design Criteria

No change. The design criteria for the 32PTH DSC described in Section 3.9.1.2.1 (B) are also applicable to the 32PTH Type 1 DSC.

A.3.9.1.2.2 Loading Conditions

No change. The loading conditions for the 32PTH DSC described in Section 3.9.1.2.2 are also applicable to the 32PTH Type 1 DSC.

A.3.9.1.2.3 Fuel Basket Assembly Stress Analysis

No change. The 32PTH basket stress analysis model and analysis results in Section 3.9.1.2.3 are applicable to the 32PTH Type 1.

A.3.9.1.2.4 32PTH Type 1 Fuel Basket Assembly Buckling Analysis

The buckling evaluation for the 32PTH DSC performed using the full 360° 3-dimensional model of the basket assembly documented in Section 3.9.1.2.4 (A.3) is also applicable to the 32PTH Type 1 DSC.

A.3.9.1.3 32PTH Type 1 DSC Shell Assembly Structural Evaluation

A.3.9.1.3.1 Approach

This section evaluates the structural adequacy of the 32PTH Type 1 DSC canister under all applicable normal and hypothetical accident condition loads. Evaluation of the stresses generated in the DSC is presented in Section A.3.9.1.3.2, and the DSC shell assembly buckling evaluation is presented in Section A.3.9.1.3.3.

A.3.9.1.3.2 DSC Canister Shell Assembly Stress Analysis

A. Methodology

An enveloping technique of combining various individual loads in a single analysis is used in this evaluation for several load combinations. This approach greatly reduces the number of computer runs while remaining conservative. However, for some load combinations, the stress intensities under individual loads are added to obtain resultant stress intensities for the specified combined loads. This stress addition at the stress intensity level for the combined loads, instead of at component stress level, is also a conservative way to reduce the number of analyses runs.

The ANSYS calculated stresses are the total stresses of the combined membrane, bending, and peak stresses. These total stresses are conservatively taken to be membrane stresses (P_m) as well as membrane plus bending stresses ($P_L + P_b$) and are evaluated against their corresponding ASME code stress limits. In the case where the total stresses, evaluated in this manner, exceed the ASME allowable stresses, a detailed stress linearization is performed to separate the membrane, bending, and peak stresses. The linearized stresses are then compared to their proper Code allowable stresses. ASME B&PV Code Subsection NB [8] is used for evaluation of loads under normal conditions and Appendix F [3] for evaluation of loads under hypothetical accident conditions.

The thermal stress intensities are classified as secondary stress intensities, Q , for code evaluations.

B. Canister Material Properties

Temperature dependent material properties obtained from Reference 1 for the NUHOMS® 32PTH Type 1 canister materials are summarized as follows.

Elastic Material Properties

Elastic properties are tabulated in Table 3-5 for SA-240 Type 304/SA-182 F304 (DSC Shell, Support Ring, Outer Top Cover, Inner Top Cover, Bottom Grapple Ring, Inner Bottom Cover and Outer Bottom Cover) and in Table A.3.9.1-1 for ASTM A-36 (top and bottom shield plugs).

Elastic-Plastic Material Properties

The ANSYS Bilinear Kinematic Hardening option of inelastic analysis is employed for Transfer Load Case 4 (120 psig internal pressure and hypothetical accident fire). Tangent modulus of 5% of elastic modulus is assumed after yield stress.

The ANSYS Multilinear Kinematic Hardening material option of inelastic analysis is employed in the analyses of all canister accident side drops. A multi-linear stress-strain curve for Type 304 stainless steel at 500 °F is constructed using the yield and tensile stress values taken from Reference 1 and the elongation value from Reference [9]. The stress-strain curve used for all canister materials is as follows.

Point	1	2	3	4	5
Strain (in/in)	0.0004845	0.000768	0.001164	0.00275	0.46
Stress (psi)	12,500	14,660	17,120	19,400	63,400

C. DSC Shell Assembly Stress Criteria

Allowable stresses given in ASME B&PV Code Subsection NB [8] and Appendix F [3] are used to evaluate the calculated stresses in the canister under normal, off-normal, and accident conditions, respectively. The stress criteria are summarized in Table 3-2. The allowable stresses are summarized in Table A.3.9.1-2. The closure welds between the inner top cover to the shell and the outer top cover to the shell use a stress reduction factor of 0.8 in accordance with ISG-15 [14].

D. DSC Shell Assembly Stress Analysis for Transfer Loads

The evaluation of the stresses generated in the NUHOMS® 32PTH Type 1 canister during transfer operations is presented here. During fuel transfer, the canister is oriented horizontally inside the OS187H Type 1 Transfer Cask. The OS187H Type 1 Transfer Cask is mounted to the transfer skid and transferred from the fuel building to the ISFSI.

The maximum temperature in the canister under vacuum drying operation is calculated to be 522 °F in the thermal stress analysis (see Chapter 4). This temperature occurs in the shell center where stresses are low. The maximum temperature in critical stress areas (top and bottom canister regions) are below 500 °F. However, the stress evaluations are conservatively performed at 500 °F.

D.1. DSC Shell Assembly Transfer Load Cases

Elastic and elastic-plastic analyses are performed to calculate the stresses in the NUHOMS® 32PTH Type 1 canister under the transfer loads. These load cases are summarized in Table A.3.9.1-3 and Table A.3.9.1-4. The accident side drop and the accident pressure load cases are analyzed by elastic-plastic analyses and the rest by elastic analyses.

D.2. DSC Shell Assembly Finite Element Model Descriptions

DSC Temperature Distribution

The DSC metal temperatures which are calculated in Chapter 4 are extracted and directly applied as temperature loads to the 2-D stress model using ANSYS macros. Since the 32PTH Type 1 DSC is longer than the 32PTH DSC, the temperature distribution at the maximum temperature location was extended in the middle of the canister, thus maximizing thermal gradients and hence thermal stresses at the top and bottom of the canister shell.

2-D Canister Stress Models

A two-dimensional (2-D) axisymmetric ANSYS finite element model, constructed from PLANE42 elements, is used for the elastic analyses of all axisymmetrical loading on the canister. ANSYS contact elements CONTAC12 are generated by connecting the nodes of two adjacent solids along their boundary. The real constant of each contact element is defined for the initial gap at each contact element.

At the weld locations between two joined solids, the contacting nodes are coupled in all directions. These coupled-nodes are applied to the welds between the shell and the support ring and between the shell and the inner top cover plate. The larger ½ inch weld between the shell and the top cover is modeled with PLANE42 elements. The normal stiffness of all contact elements are calculated using guidelines in the ANSYS manual [10]. The applied boundary conditions for this 2-D model under each load case are described in the following sections. Figures A.3.9.1-1, A.3.9.1-2, and A.3.9.1-3 show the ANSYS 2-D finite element model, which includes the canister shell, outer and inner top covers, support ring and outer and inner bottom covers. This model is used for analyses of all axisymmetric loads during the transfer operations of the canister.

The normal stiffness, K_N , for the contact elements were estimated according to the ANSYS manual [10] as follows.

$$K_N \approx f E h$$

Where, f = Factor that controls contact compatibility (ranging between 0.01 to 100), use 1

E = Young's modulus, use 25.8×10^6 psi

h = average radius where contact to occur (for 2-D axisymmetrical model), use 34 in.

$K_N = 1 \times 25.8 \times 10^6 \times 34 = 8.8 \times 10^8$ lb/in. Conservatively used 1×10^9 lb/in.

3-D Canister Stress Model

A three-dimensional (3-D) ANSYS stress model is created using ANSYS elements SOLID45 and CONTAC178. The 3-D model is used for the analysis of accident side drops. To help reduce the ANSYS run time and assure numerical convergence, the whole canister is split into two portions, namely, the top and the bottom end sections. These two sections are represented by two different ANSYS models. Each end model includes the canister shell at a length beyond which the un-modeled shell will have no significant impact on the stress levels at the junction between the shell and its end closures. The DSC canister top end assembly finite element model is shown in Figure A.3.9.1-4 and the canister bottom end assembly model is shown in Figure A.3.9.1-5.

These 3-D models are used for analyses of side drops only. The postulated side drops will occur when the canister is resting inside the OS187H Type 1 transfer cask during transfer. Two side drops with the impact points located at 0° (i.e., the cask drops onto a target at 180° opposite to its four canister support pads) and at 180° (i.e., the cask drops onto a target between its two bottom canister support pads) are analyzed.

Load cases 6, 7, 10, and 11 consider the side drop loads at 0° and load cases 8, 9, 12, and 13 at 180° (see Table A.3.9.1-3). Elastic-plastic analyses, using multi-linear hardening material properties, are performed for both side drops. In addition to the contact areas generated from the 2-D model, new contact elements are generated connecting the inner diameter of the cask and the outer diameter of the canister in the radial direction. The nodes of these contact elements are located either on the inner diameter of the cask or on the outer diameter of the canister at the moment when the cask hits the side drop target. The actual gaps for these contact elements are defined by their initial location in conjunction with the contact element real constants. The contact element nodes located on the inner diameter of the cask are held fixed in all directions, simulating a rigid cask on which the canister drops.

Weak link elements are added to each contact element in the model to help numerical convergence. Zero density of these link elements is used to avoid adding any non-existing weights. This model does not calculate the stress levels in the middle section of the canister shell, which are calculated and evaluated as part of the basket stress analysis in Section 3.9.1.2.3.

Only half of the canister in circumferential direction is included in the 3-D model. Symmetry boundary conditions are applied to the plane of symmetry (global Cartesian x - z plane) during a side drop. Symmetry boundary conditions are also applied to the cut-off plane at the canister shell to provide proper diametrical rigidity of the shell during side drops.

During the 75 g side drop, the canister internals are accounted for by applying a cosine varying pressure distribution on the inside surface of the canister shell. Assuming that the canister internals react upon a 90° arc of the inside surface, then the inertial load of the internals, $P_{(\theta)}$, which varies with angle, θ , ($\theta = 0$ is at the impact point), is governed by the following expression.

$$P_{(\theta)} = P_{max} \cos(2\theta) \quad (0^\circ < \theta < 45^\circ)$$

Where P_{max} is the maximum pressure at the impact point ($\theta = 0$). Assuming the axial length of the applied load is L , the inside radius of the canister shell is R , and the load distribution, $P_{(\theta)}$ above, then the total inertial load generated by the internals, F , is the following.

$$F = \int_{-\frac{\pi}{4}}^{\frac{\pi}{4}} P_{max} \cos(2\theta) \cos(\theta) LR d\theta$$

or,

$$F = \frac{P_{max} LR}{2} \int_{-\frac{\pi}{4}}^{\frac{\pi}{4}} \cos((2+1)\theta) + \cos((2-1)\theta) d\theta$$

By integrating we get the following:

$$F = \left[\frac{P_{\max} LR}{2} \right] \left[\frac{\sin(3\theta)}{3} + \sin(\theta) \right] \Bigg|_{-\frac{\pi}{4}}^{\frac{\pi}{4}}$$

Therefore,

$$F = \left[\frac{P_{\max} LR}{2} \right] \left[\frac{\sin\left(\frac{3\pi}{4}\right)}{3} + \sin\left(\frac{\pi}{4}\right) - \frac{\sin\left(\frac{-3\pi}{4}\right)}{3} - \sin\left(\frac{-\pi}{4}\right) \right]$$

$$F = P_{\max} LR \left[\frac{\sin\left(\frac{3\pi}{4}\right)}{3} + \sin\left(\frac{\pi}{4}\right) \right]$$

The canister shell inner diameter, $R = 34.375$ in., the axial length of the applied load, $L = 169$ in. The total applied force, F , is equal to the inertial load of the canister internals, which is the following.

Basket weight = 29,451 lb,

Fuel assembly weight = 50,720 lb

Total weight of canister internals = 29,451 lb + 50,720 lb = 80,171 lb (use 83,000 lb).

Then,

$$F = 83,000 \times 75 \text{ g} = 6,225,000 \text{ lb.}$$

Therefore, P_{\max} is the following:

$$P_{\max} = \frac{6,225,000}{(169)(34.375)} \left[\frac{\sin\left(\frac{3\pi}{4}\right)}{3} + \sin\left(\frac{\pi}{4}\right) \right]^{-1} = 1136.54 \text{ psi.}$$

The equivalent pressure applied on the canister inside shell surface is therefore,

$$P_{(\theta)} = 1136.54 \cos(2\theta),$$

Where, θ is the angle from the bottom ($\theta = 0$) of the horizontal canister shell to the center of the shell element, up to 45° .

D.3. DSC Shell Assembly Stress Evaluation for Transfer Loads

All analyzed load cases in this section are identified in Tables A.3.9.1-3 and A.3.9.1-4 and are described in detail in the following sections.

Transfer Load Case 1: Deadweight + 15 psig external pressure + thermal (vacuum drying)

The temperature profile utilized for the analysis of Transfer Load Case 1 for the 32PTH DSC described in Section 3.9.1.3.2 (D.3) was adjusted by linearly scaling to the maximum vacuum drying temperature of 522 °F, which corresponds to the maximum temperature for vacuum drying Procedure B, as calculated in Chapter 4. This adjusted temperature profile is used for the analysis of Transfer Load Case 1 for the 32PTH Type 1 DSC.

The weight of the canister internals (basket and fuel assemblies) is accounted for by applying equivalent pressures on the support surfaces of the canister. The actual weights of the basket and fuel assemblies are 29,451 lb and 50,720 lb, respectively (see Section A.3.2.1). Therefore, the total weight of the canister internals is 80,171 lbs. A weight of 83,000 lbs is conservatively used in this analysis. The canister cavity inner radius is 34.375 in. Therefore, the pressure load equivalent to the inertial load of the internals, P_{ia} , is,

$$P_{ia} = [83,000 / (\pi \times 34.375^2)] = 22.36 \text{ psi.}$$

An elastic analysis is performed using the ANSYS 2-D axisymmetric model. The analysis was run in 2 load steps. The first load step includes dead weight, 15 psig external pressure, and the temperature profile discussed above, but it does not include coefficient of thermal expansion. The second load step includes the coefficient of thermal expansion and all of the above mentioned loads. The results from the first load step are compared against the P_m and $P_m + P_b$ allowable stresses and the results from the second load step are compared against the $P_m + P_b + Q$ allowable stresses.

The maximum primary stress intensity in the canister was calculated to be 2.05 ksi in Load Step 1. The maximum primary stress intensity in the closure welds is calculated to be 1.52 ksi.

The maximum primary plus secondary stress intensity in the canister was calculated to be 22.69 ksi in Load Step 2. These stresses are summarized in Table A.3.9.1-6. The maximum primary stress intensity in the closure welds is calculated to be 2.07 ksi.

Transfer Load Case 2: Handling, 2 g axial + 2 g transverse + 2 g vertical + 30 psig int. pressure + thermal (115 °F ambient)

The handling 2 g inertial loads applied to the canister when inside the transfer cask in the horizontal orientation are analyzed as part of the basket model described in Section 3.9.1.2.3 (B.2) (the basket model includes a segment of the canister shell). It is judged that under the relatively light handling loads the maximum stresses in the canister will occur in the shell section and can be obtained from the results calculated in Section 3.9.1.2.3 (B.2). The maximum primary membrane stress intensity and primary membrane plus bending stress intensity in the canister shell due to the handling load of 2 g, calculated in Section 3.9.1.2.3 (B.2), are 880 psi and 9740 psi, respectively. These stresses are summarized in Table A.3.9.1-6.

The stress intensities calculated in Section 3.9.1.2.3 (B.2) for the canister shell due to the 2 g handling loads are combined with the stresses due to internal pressure of 30 psig, and the 115 °F ambient environment temperature loads resulting from the thermal analysis in Chapter 4.

The stress analysis for the 30 psig internal pressure and 115 °F thermal loads is performed using the ANSYS 2-D axisymmetric model. The stress analysis contains two load steps. Load step 1 includes the primary loads of 30 psig internal pressure. Load step 2 includes the primary pressure load plus the secondary thermal load.

The maximum primary stress intensity in the canister was calculated to be 14.97 ksi in Load Step 1 analysis. The maximum primary stress intensity in the closure welds is calculated to be 11.75 ksi. The maximum primary plus secondary stress intensity in the canister is calculated to be 41.70 ksi under load step 2. The maximum primary plus secondary stress intensity in the closure welds is calculated to be 14.94 ksi.

The maximum primary stress intensities in the canister shell calculated in Section 3.9.1.2.3 (B.2) are added to the maximum primary and primary plus secondary stress intensities calculated from the 2-D axisymmetric model and the combined results are evaluated against the corresponding ASME stress limits (See Table A.3.9.1-6). The direct addition of stresses at the stress intensities level, instead of at the component level, as well as the addition of the maximum stress intensities at different locations is very conservative. This enveloping technique is used to minimize the computer runs.

Transfer Load Case 3: Handling 2 g axial + 2 g transverse + 2 g vertical + 15 psig ext. pressure + thermal (-20 °F ambient)

The same methodology described for load case 2 is used in this load case.

The maximum stress intensity in the canister for the primary load of 15 psig external pressure in load step 1 is calculated to be 2.75 ksi. The maximum stress intensity in the closure welds is calculated to be 1.46 ksi.

The maximum stress intensity in the canister for the primary load of 15 psig external pressure plus the secondary temperature load in load step 2, is calculated to be 31.63 ksi. These stresses combined with the stresses due to the handling loads as well as the evaluation against the ASME stress limits are summarized in Table A.3.9.1-6. The maximum stress intensity in the closure welds is calculated to be 2.32 ksi.

Transfer Load Case 4: 120 psig internal pressure and hypothetical accident fire

Stresses in the canister under an internal pressure of 120 psig are calculated in this load case. ASME code [3] requires only primary stresses be evaluated under accident conditions. The secondary thermal stresses are therefore not calculated. The ANSYS 2-D axisymmetric model is used for analysis of this accident pressure load. This is an elastic-plastic analysis with large deformations.

The maximum calculated stress in the entire canister for the pressure load is 23.92 ksi. This maximum stress intensity is conservatively treated both as primary membrane stress intensity

and as primary membrane plus bending stress intensity and so evaluated against ASME code limits at the maximum metal temperature of the canister (See Table A.3.9.1-7).

The maximum metal temperature in the canister during fire accident is calculated to be 790 °F (see Chapter 4). Canister material properties at 800 °F are used for the ANSYS model. The maximum stress intensity in the closure welds is calculated to be 21.71 ksi.

Transfer Load Case 5: 25 psig external pressure and flood hypothetical accident

The external pressure of 25 psig on the canister is analyzed using material properties taken at 500 °F for the entire model.

The maximum stress intensity in the canister for this load case is calculated to be 4.56 ksi. The maximum stress intensity in the closure welds is calculated to be 2.42 ksi.

Transfer Load Case 6: Accident condition 75 g side drop at 0° (no rail) at ambient temperature of 115 °F (75 g side drop + 30 psig internal pressure)—top end portion of canister

The canister internal pressure of 30 psig plus a side acceleration of 75 g is analyzed in this load case. A multi-linear elastic-plastic stress-strain curve for material 304 SS at 500 °F is applied to all materials. The stress-strain curve is obtained from Reference 9. ASME code requires only primary stresses be evaluated under accident conditions. The values of the thermal expansion coefficients for all materials are therefore set to 0 to eliminate any secondary thermal stresses in the canister.

The maximum stress intensity in the canister for this load case is calculated to be 25.5 ksi. The maximum stress intensity in the closure welds is calculated to be 23.3 ksi.

Transfer Load Case 7: Accident condition 75 g side drop at 0° (no rail) at ambient temperature of 115 °F (75 g side drop + 30 psig internal pressure)—bottom end portion of canister

The methodology of the analysis and stress evaluation used in this load case is the same as that described for Load Case 6.

The maximum stress intensity in the canister for this load case is calculated to be 24.0 ksi.

Transfer Load Case 8: Accident 75 g side drop at 180° (drop between two transfer cask bottom support pads) at ambient temperature of 115 °F (75 g side drop + 30 psig internal pressure)—top end portion of canister

The same methodology of the analysis and stress evaluation used for Load Case 6 is used for this load case except that the gaps between the canister and the rigid cask are different due to the orientation of the transfer cask support pads.

The maximum stress intensity in the canister for this load case is calculated to be 27.3 ksi. The maximum stress intensity in the closure welds is calculated to be 24.3 ksi.

Transfer Load Case 9: Accident 75 g side drop at 180° (drop between two cask bottom rails) at ambient temperature of 115 °F (75 g side drop + 30 psig internal pressure)—bottom end portion of canister

The same methodology of the analysis and stress evaluation used for Load Case 7 is used for this load case except that the gaps between the canister and the rigid cask are different.

The maximum stress intensity in the canister for this load case is calculated to be 24.7 ksi.

Transfer Load Case 10: Accident 75 g side drop at 0° (drop at no cask rail) at ambient temperature of -20 °F (75 g side drop + 15 psig external pressure)—top end portion of canister

The same methodology of the analysis and stress evaluation used for Load Case 6 is used for this load case except that external pressure instead of internal pressure is applied.

The maximum stress intensity in the canister for this load case is calculated to be 25.9 ksi. The maximum stress intensity in the closure welds is calculated to be 23.4 ksi.

Transfer Load Case 11: Accident 75 g side drop at 0° (drop at no cask rail) at ambient temperature of -20 °F (75 g side drop + 15 psig external pressure)—bottom end portion of canister

The same methodology of the analysis and stress evaluation used for Load Case 7 are used for this load case except external pressure instead of internal pressure is applied.

The maximum stress intensity in the canister for this load case is calculated to be 24.1 ksi.

Transfer Load Case 12: Accident 75 g side drop at 180° (drop between two cask bottom rails) at ambient temperature of -20 °F (75 g side drop + 15 psig external pressure)—top end portion of canister

The same methodology of the analysis and stress evaluation used for Load Case 8 is used for this load case except that external pressure instead of internal pressure is applied.

The maximum stress intensity in the canister for this load case is calculated to be 27.3 ksi. The maximum stress intensity in the closure welds is calculated to be 24.2 ksi.

Transfer Load Case 13: Accident 75 g side drop at 180° (drop between two cask bottom rails) at ambient temperature of -20 °F (75 g side drop + 15 psig external pressure)—bottom end portion of canister

The same methodology of the analysis and stress evaluation used for Load Case 9 is used for this load case except that the external pressure instead of the internal pressure is applied.

The maximum stress intensity in the canister is calculated to be 24.9 ksi.

Transfer Load Case 14: Accident 75 g top end drop (75 g + internal pressure of 30 psig)

The top end drop is not considered credible during storage and transfer operations under 10 CFR Part 72 because the transfer cask is always in the horizontal orientation. The top end drop

evaluation documented below is performed in support of a 10 CFR Part 50 evaluation that may be performed by the user if the user cannot demonstrate that this accident drop is not credible.

The weight of the canister internals (basket and fuel assemblies) during end drop is accounted for by applying equivalent pressures on canister components that support them. The actual weights of the canister basket and fuel assemblies are 29,451 lb. and 50,720 lb. (see Section A.3.2.1). Therefore, the total actual weight of the canister internals is 80,171 lb. The weight of the canister internals used in this analysis is conservatively increased to 83,000 lb.

The canister cavity inner radius at the top end is 34.375 in. The pressure load equivalent to the inertial load of the internals at 75 g under accident condition, P_{ia} , is,

$$P_{ia} = [83,000 / (\pi \times 34.375^2)] \times 75 \text{ g} = 1676.89 \text{ psi.}$$

The top face of the canister outer top cover is held in the axial direction in order to simulate the rigid support provided by the transfer cask top cover. An inertial load of 75 g in the negative y-direction is applied to the model. An internal pressure of 30 psig and the metal temperatures from the 115 °F ambient condition are also included in this analysis. Temperature-dependent material properties are selected based on the temperature distribution in the canister. The values of thermal expansion coefficients for all materials are set to zero so that secondary thermal stresses, which are not required for evaluation under an accident condition per Reference 3, are not calculated.

The maximum stress intensity in the canister for this load case is calculated to be 17.68 ksi. The maximum stress intensity in the closure welds is calculated to be 6.43 ksi.

Transfer Load Case 15: Accident 75 g bottom end drop (75 g + internal pressure of 30 psig)

The bottom end drop is not considered credible during storage and transfer operations under 10 CFR Part 72 because the transfer cask is always in the horizontal orientation. The bottom end drop evaluation documented below is performed in support of a 10 CFR Part 50 evaluation that may be performed by the user if the user cannot demonstrate that this accident drop is not credible.

The weight of the canister internals used in this analysis is 83,000 lb. The canister cavity inner radius at the bottom end is 34.375 in. The pressure load equivalent to the weight of the internals under the accident condition 75 g drop, P_{ia} , is,

$$P_{ia} = [83,000 / (\pi \times 34.375^2)] \times 75 \text{ g} = 1676.89 \text{ psi}$$

The bottom face of the canister is held in the axial direction in order to simulate the rigid support provided by the transfer cask bottom. An inertial load of 75 g in the positive y-direction is applied to the model. An internal pressure of 30 psig and the metal temperatures from the 115 °F ambient condition are included in this analysis. Temperature-dependent material properties are selected based on the temperature distribution in the canister. The values of thermal expansion coefficients for all materials are set to zero so that secondary thermal stresses, which are not required for evaluation under an accident condition per Reference 3, are not calculated.

The maximum stress intensity in the canister for this load case is calculated to be 21.05 ksi. The maximum stress intensity in the closure welds is calculated to be 4.27 ksi.

Transfer Load Case 16: Accident 75 g top end drop (75 g + external pressure of 15 psig)

The top end drop is not considered credible during storage and transfer operations under 10 CFR Part 72 because the transfer cask is always in the horizontal orientation. The top end drop evaluation documented below is performed in support of a 10 CFR Part 50 evaluation that may be performed by the user if the user cannot demonstrate that this accident drop is not credible.

This load case is similar to Load Case 14 with different pressure loadings and metal temperatures. An external pressure of 15 psig and material properties at 500 °F are used in this analysis. The values of thermal expansion coefficients for all materials are set to zero so that secondary thermal stresses, which are not required for evaluation under an accident condition per Reference 3, are not calculated.

The maximum stress intensity in the canister for this load case is calculated to be 30.7 ksi. The maximum stress intensity in the closure welds is calculated to be 8.7 ksi.

Transfer Load Case 17: Accident 75 g bottom end drop in accident condition (75 g + external pressure of 15 psig)

The bottom end drop is not considered credible during storage and transfer operations under 10 CFR Part 72 because the transfer cask is always in the horizontal orientation. The bottom end drop evaluation documented below is performed in support of a 10 CFR Part 50 evaluation that may be performed by the user if the user cannot demonstrate that this accident drop is not credible.

This load case is similar to Load Case 15 with different pressure loadings and metal temperatures. An external pressure of 15 psig and material properties at 500 °F are used in this analysis. The values of thermal expansion coefficients for all materials are set to zero so that secondary thermal stresses, which are not required for evaluation under an accident condition per Reference 3, are not calculated.

The maximum stress intensity in the canister for this load case is calculated to be 26.1 ksi. The maximum stress intensity in the closure welds is calculated to be 6.1 ksi.

Transfer Load Case 18: Fabrication test condition (DW + 18 psig internal pressure + 155 kips axial load)

After the canister bottom is welded to the shell a pressure test is conducted by applying an internal pressure of 18 psig with a top seal plate being held by an axial force of 155 kips. The canister bottom may be made, as an option, of composite plates. For each of these options the bottom inner plate, which is to be first welded to the shell and tested, has a minimum thickness of 2.25 inches. An ANSYS model, shown in Figure A.3.9.1-6, is generated that simulates the canister shell with the bottom inner plate for analysis of pressure and axial loads under the test condition. The deadweight load on the horizontal canister is manually analyzed using Roark's formulas [7]. The stresses calculated from both manual and ANSYS analyses are conservatively added for ASME Code stress evaluation.

(1) 1g deadweight load

It is conservatively assumed that the horizontal shell's own weight is line supported at its base.

From Case 15 of Table 9.2 in Roark's Formulas for Stress & Strains, 7th Edition:

$$R \text{ (mean radius)} = \frac{1}{2} (69.75 \text{ in.} - 0.5 \text{ in.}) = 34.625 \text{ in.}$$

$$t \text{ (wall thickness)} = 0.5 \text{ in.}$$

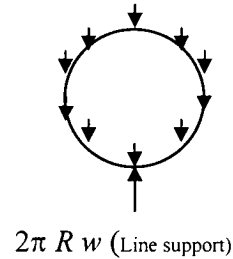
$$\rho \text{ (density)} = 0.29 \text{ lb/in}^3$$

Take unit length ($L = 1 \text{ in.}$) of shell,

The weight per unit length of circumference of shell, w , is,

$$\begin{aligned} w &= (2 \times \pi \times R \times t \times L \times \rho) / (2 \times \pi \times R) \\ &= t \times L \times \rho = 0.5 \times 1 \text{ in.} \times 0.29 \text{ lb/in}^3 = 0.145 \text{ lb/in} \end{aligned}$$

$$\text{For a thin ring, } I = \frac{t^3}{12(1-\nu^2)} = 0.01145, \text{ where } \nu = 0.3$$



$$K_T = 1 + \frac{I}{AR^2} \approx 1$$

$$K_2 = 1 - \alpha = 1 - \frac{I}{AR^2} \approx 1$$

$$\text{Max. } -M = -wR^2(1.6408 - K_2) = -0.145 \times 34.625^2 (1.6408 - 1) = -111.4 \text{ in-lb/in}$$

or,

$$\text{Max. } +M = (3/2) wR^2 = 1.5 \times 0.145 \times 34.625^2 = 260.76 \text{ in-lb/in}$$

$$\text{Max. bending stress, } \sigma_b = (6M)/(t^2) = (6 \times 260.76) / (0.5^2) = 6,258 \text{ psi}$$

$$N = N_A \cos(x) + V_A \sin(x) + LT_N$$

$$V_A = 0$$

$$LT_N = -Wr(x)(\sin(x))$$

$$N_A = wR/2 = 2.51 \text{ lb/in}$$

$$N = 2.51 \cos(x) - 0.145 \times 34.625 \times (x) \times \sin(x) \text{ lb/in}$$

$$N_{\max} = 2.51 \text{ lb/in at } x = 0^\circ$$

$$\text{Max. membrane stress, } \sigma_m = N_{\max} / t = (2.51 \text{ lb/in}) / (0.5 \text{ in}) = 5 \text{ psi}$$

(2) 18 psig internal pressure + 155 kips axial load

An internal pressure of 18 psig is applied while an axial force of 155 kips is applied to a seal plate on the top of the shell. The net force applied to the entire circumference of the shell at the top will be 88,180 lb ($155,000 \text{ lb} - 18 \text{ lb/in}^2 \times [\pi/4 \times 68.75^2] \text{ in}^2 = 88,180 \text{ lb}$). A nodal force of 22,045 lb ($88,180 / 4 = 22,045 \text{ lb}$) is applied at each node on the top end of the shell.

Figure A.3.9.1-6 shows the model with the applied pressure of 18 psig and the nodal forces of 88,180 lb.

The maximum stress intensity in the canister is calculated to be 9.36 ksi under these testing loads.

The resultant stresses calculated in (1) and (2) above are conservatively added and evaluated against ASME Code allowable stresses in Table A.3.9.1-5.

Transfer Load Case 19: Normal 80 kip push hydraulic load (internal pressure of 30 psig + 80 kip push + thermal load of 115 °F ambient)

During transfer of the canister from the transfer cask to the HSM a normal maximum push force of 80 kip is applied by a hydraulic ram over an area of 9 inch diameter on the canister bottom. A uniform pressure of 1258 psig $[= 80,000 \text{ lb} / ((\pi/4) \times 9^2)]$ is applied over this area. The periphery of the top cover outer surface is held as boundary condition. The sustained loads of an internal pressure of 30 psig plus the equivalent push load pressure of 1,258 psi are applied in load step 1. The sustained loads plus the temperature load from fuel decay heat are applied in load step 2.

The maximum stress intensity for load step 1 is calculated to be 15.73 ksi. The maximum stress intensity in the closure welds is calculated to be 10.75 ksi.

The maximum stress intensity in the canister for load step 2 is calculated to be 38.19 ksi. The maximum stress intensity in the closure welds is calculated to be 14.91 ksi.

Transfer Load Case 20: Normal 60 kip pull hydraulic load (internal pressure of 30 psig + 60 kip pull + thermal of 115 °F ambient)

During retrieval of the canister from the HSM into the transfer cask a normal maximum pull force of 60 kips is applied by a hydraulic ram over an annulus area of 12.62 inches outer diameter and 10 inches inner diameter on the inside surface of grapple ring. A uniform pressure of 1,289 psig $[= 60,000 \text{ lb} / ((\pi/4) \times (12.62^2 - 10^2))]$ is applied over this area. The periphery of the top cover outer surface is held as boundary condition. The sustained loads of an internal pressure of 30 psig plus the equivalent pull load pressure of 1,289 psi are applied in load step 1. The sustained loads plus the temperature load from fuel decay heat are applied in load step 2.

Stresses in the grapple ring, outer bottom cover plate, and the bottom 2 inches of the canister shell are linearized in ANSYS. The membrane stress results are compared against the general membrane stress, P_m , stress limits. The membrane plus bending stress results are compared against the primary membrane plus bending, $P_m/P_L + P_B$, stress limits. The maximum stress intensity in the rest of the canister is compared against the general membrane stress, P_m , and primary membrane plus bending stress, $P_m/P_L + P_B$, stress limit.

The maximum membrane and membrane plus bending stress in the grapple ring, outer bottom cover plate, and the bottom 2 inches of the canister shell are 9.30 ksi and 25.80 ksi, respectively for Load Case 1. Maximum stress intensity in all other components is 14.97 ksi for Load Case 1. The maximum stress intensity in the closure welds is calculated to be 11.75 ksi.

The maximum stress intensity in the canister is calculated to be 41.64 ksi for load step 2. The maximum stress intensity in the closure welds is calculated to be 14.94 ksi.

Transfer Load Case 21: Off-normal 80 kip push hydraulic load (internal pressure of 30 psig + 80 kip push + thermal load of 115 °F ambient)

The same 80 kip push hydraulic load analyzed in Load Case 19 is also designated as an off-normal condition. Evaluation of this load in Load Case 19 as normal condition covers this off-normal condition.

Transfer Load Case 22: Off-normal 80 kip pull hydraulic load (internal pressure of 30 psig + 80 kip pull + thermal of 115 °F ambient)

During retrieval, the canister from the HSM into the transfer cask a normal maximum pull force of 80 kips is applied by a hydraulic ram over an annulus area of 12.62 inches outer diameter and 10 inches inner diameter on the inside surface of grapple ring. A uniform pressure of 1,719 psig $[= 80,000 \text{ lb} / ((\pi/4) \times (12.62^2 - 10^2))]$ is applied over this area. The periphery of the top cover outer surface is held as boundary condition. The sustained loads of an internal pressure of 30 psig plus the equivalent pull load pressure of 1,719 psi are applied as the loading. ASME code requires only primary stresses to be evaluated under off-normal condition Service Level C, therefore the secondary thermal stresses are not evaluated.

Stresses in the grapple ring, outer bottom cover plate, and the bottom 2 inches of the canister shell are linearized in ANSYS. The membrane stress results are compared against the general membrane stress, P_m , stress limits. The membrane plus bending stress results are compared against the primary membrane plus bending, $P_m/P_L + P_B$, stress limits. The maximum stress intensity in the rest of the canister is compared against the general membrane stress, P_m , and primary membrane plus bending stress, $P_m/P_L + P_B$, stress limit.

The maximum membrane and membrane plus bending stress in the grapple ring, outer bottom cover plate, and the bottom 2 inches of the canister shell are 12.41 ksi and 34.43 ksi, respectively. The maximum stress intensity in all other components is 14.97 ksi. The maximum stress intensity in the closure welds is calculated to be 11.75 ksi.

Transfer Load Case 23: Accident 110 kip push hydraulic load (internal pressure of 30 psig + 110 kip push)

The maximum accident hydraulic force applied by the ram to push the canister from its transfer cask to the HSM is set at 110 kips. The load will be applied over an area with a 9 inch diameter on the canister bottom. A uniform pressure of 1,729.1 psig $[= 110,000 \text{ lb} / ((\pi/4) \times 9^2)]$ is applied over this area in the 2-D ANSYS canister model. The periphery of the canister top cover outer surface is held as boundary condition. The sustained loads of an internal pressure of 30 psig plus the equivalent push force pressure of 1,729 psi are applied as the loading. The secondary temperature load is not required by ASME code for an accident condition analysis.

The maximum stress intensity in the canister for this load case is calculated to be 16.36 ksi. The maximum stress intensity in the closure welds is calculated to be 10.49 ksi.

Transfer Load Case 24: Accident 110 kip pull hydraulic load (internal pressure of 30 psig + 110 kip pull)

The maximum accident condition hydraulic force applied by the ram to pull the canister out of the HSM into the transfer cask is set at 110 kips. This pull force is applied over an annulus area of 12.62 inches outer diameter and 10 inches inner diameter on the inside surface of grapple ring. A uniform pressure of 2,363 psig $[=110,000 \text{ lb} / ((\pi/4) \times (12.62^2 - 10^2))]$ is applied over this area in the 2-D ANSYS canister model. The periphery of the top cover outer surface is held as a boundary condition. The sustained loads of an internal pressure of 30 psig plus the equivalent pull force pressure of 2,363 psi are applied as loading. The secondary temperature load is not required by ASME code for an accident condition analysis.

Stresses in the grapple ring, outer bottom cover plate, and the bottom 2 inches of the canister shell are linearized in ANSYS. The membrane stress results are compared against the general membrane stress, P_m , stress limits. The membrane plus bending stress results are compared against the primary membrane plus bending, $P_m/P_L + P_B$, stress limits. The maximum stress intensity in the rest of the canister is compared against the general membrane stress, P_m , and primary membrane plus bending stress, $P_m/P_L + P_B$, stress limit.

The maximum membrane and membrane plus bending stress in the grapple ring, outer bottom cover plate, and the bottom 2 inches of the canister shell are 17.03 ksi and 47.25 ksi, respectively. The maximum stress intensity in all other components is 15.99 ksi. The maximum stress intensity in the closure welds is calculated to be 11.75 ksi.

Transfer Load Case 25: Canister lifting**Three-Piece Top End Assembly Design**

For the three-piece top end assembly design, four lifting lugs are used for lifting the empty canister into the transfer cask. The lifting lugs, support ring, reinforcing pad, connecting welds, and local stresses in the canister shell are evaluated using an empty DSC weight of 45,234 lbs and a dynamic load factor of 1.15.

Since lifting using internal lugs is an infrequent event (normally the DSC would be lifted for placement into the cask only once prior to fuel loading and will never occur after the DSC is in service), Service Level B allowable stresses are applied. Level B allowables are identical to Level A allowables for the components (shell, support ring, and lug). However, for the welds, Level B allowables are 33% greater than Level A values.

The evaluation is performed using a combination of hand calculations and ANSYS finite element analyses. Hand calculations are used to evaluate the local stresses in the lifting lugs near the pin-hole; finite element analyses are used to determine loads and/or stresses in all other components.

The shell, support ring and lug components are modeled using ANSYS solid elements and welds are modeled by coupling the translational degrees of freedom for the coincident nodes.

Results of the stress evaluation are calculated for different lifting configurations. The maximum stress ratio is 0.909 for the spreader bar assembly, 8' sling, and 10' sling lifting configurations. Therefore, the lug design and required welds are acceptable for the 32PTH Type 1 DSC.

Alternate Two-piece Top End Assembly Design

For the alternate two-piece top end assembly design, the evaluations performed for the 32PTH DSC are bounding.

Canister Corner Drop Analysis

As stated in [16], the end and corner drops are generally not considered credible during storage and transfer operations because the transfer cask will always be in horizontal orientation. Thus, corner drop load cases are not evaluated.

D.4. Summary of Results for DSC Shell Assembly Stress Evaluation for Transfer Loads

The calculated maximum stress intensities in the DSC shell assembly components are summarized in Tables A.3.9.1-5 through A.3.9.1-8. These tables also show that the stress intensity results are below the ASME code stress intensity allowables.

The stresses in the closure welds are summarized in Tables A.3.9.1-9 through A.3.9.1-12. These tables also show that the stress results are below the ASME code stress allowables.

Based on the results of these analyses, the design of the 32PTH Type 1 DSC shell assembly is structurally adequate under transfer loads of testing, normal (Service Level A), and accident (Level D) conditions.

E. DSC Shell Assembly Stress Evaluation for Storage Loads

This section evaluates the structural adequacy of the 32PTH Type 1 DSC shell assembly when it is in the horizontal storage position within an HSM-H. This section considers storage loads on the canister under both normal and hypothetical accident conditions.

The evaluation of the stresses in the canister for storage loads employs an ANSYS 2-D axisymmetrical model to analyze three thermal conditions specified for the canister during storage. This 2-D model is the same model described in Section A.3.9.1.3.2 (D.2) used to compute stresses due to axisymmetric transfer loads. The analyses of axisymmetric loads such as internal and external pressure loads for transfer conditions are also valid for a horizontal storage canister. Their results are therefore used in this section for stress combinations and evaluations.

The fuel basket stress analysis for storage loads (Section 3.9.1.2.3 (C)) uses an ANSYS 3-D model, which includes the DSC canister shell, to calculate the non-axisymmetrical seismic and deadweight loads. The calculated stress intensities in the canister under the seismic and deadweight loads from Section 3.9.1.2.3 (C) are used in this section for stress combinations and evaluations.

The temperatures in the canister under 115 °F and -20 °F ambient conditions of and under HSH-H blocked vent conditions for 34 hours are computed in Chapter 4. These temperatures are imposed on the stress model in this evaluation for thermal stress calculations.

E.1. DSC Shell Assembly Storage Load Cases

The storage load cases considered in this section are summarized in Table A.3.9.1-13.

E.2. DSC Shell Assembly Finite Element Model Descriptions

The 2-D axisymmetrical stress models described in Section A.3.9.1.3.2 (D.2) for the transfer load analysis are also used for the storage load analysis. Figures A.3.9.1-1, A.3.9.1-2 and A.3.9.1-3 show this model. This model is used to evaluate the three specified thermal cases for storage, which are the -20 °F and 115 °F ambient conditions, and the blocked vent hypothetical accident condition. The temperature profiles in the canister for the three storage thermal cases are calculated in Chapter 4.

E.3. DSC Shell Assembly Stress Analysis for Storage Loads

All individual load cases specified in Table A.3.9.1-13 are described in detail in the following sections.

Storage Load Case 1: Deadweight (1 g down)

The canister shell and fuel basket containing the fuel assemblies, resting horizontally on the rails of an HSM-H is analyzed in Section 3.9.1.2.3 (C) for storage loads. The maximum primary membrane and membrane plus bending stress intensities in the canister shell due to the deadweight load are calculated to be 0.4 ksi, and 4.05 ksi, respectively (see Table 3.9.1-5). These stress intensities are also used as maximum stress intensities at closures welds (see Table A.3.9.1-15).

Storage Load Case 2: Internal pressure of 30 psig

The internal pressure of 30 psig applied on the canister is analyzed in load step 1 of Transfer Load Case 2 in Section A.3.9.1.3.2 (D). The maximum membrane plus bending stress intensities in the canister, calculated in Section A.3.9.1.3.2.D is 14.97 ksi. The maximum stress intensity in the closure welds is calculated to be 11.75 ksi calculated in section A.3.9.1.3.2 (D).

Storage Load Case 3: Seismic loads (0.65 g axial + 0.65 g transverse + 1.3g vertical down)

The seismic loads on the canister, containing the basket and the fuel assemblies and resting on the rails of an HSM-H, are analyzed in Section 3.9.1.2.3 (C). The maximum primary membrane and membrane plus bending stress intensities are calculated in Section 3.9.1.2.3 (C) to be 0.63 ksi, and 6.08 ksi, respectively (see Table 3.9.1-5). This specified seismic load includes a 1g deadweight load.

Storage Load Case 4: Thermal load at -20 °F ambient

The maximum temperature in the canister for this thermal case is calculated in Chapter 4 to be 318 °F. The temperatures in the canister calculated in Chapter 4 are applied to the stress model in order to compute the thermal stress intensities in the canister. The maximum secondary thermal stress intensity is calculated to be 22.49 ksi. The 22.49 ksi stress is calculated based on canister maximum temperature of 324 °F. Since the revised temperature of 318 °F is less than 324 °F, 22.49 ksi is conservatively used for load combination and compared with the allowables. The maximum stress intensity in the closure welds is calculated to be 2.47 ksi.

Storage Load Case 5: Thermal load at 115 °F ambient

The thermal load case with the canister stored in the HSM-H with fins, described in Chapter 4, is selected for this evaluation. The maximum temperature in the canister for this thermal case is calculated in Chapter 4 to be 407 °F. The same procedure used for calculating the thermal stress intensities for the Load Case 4 is repeated for the 115 °F ambient thermal load. The secondary thermal stress intensity is calculated to be 20.51 ksi. The 20.51 ksi stress is calculated based on canister maximum temperature of 434 °F. Since the revised temperature of 407 °F is less than 434 °F, 20.51 ksi is conservatively used for load combination and compare with the allowables. The maximum stress intensity in the closure welds is calculated to be 2.50 ksi.

Storage Load Case 6: Blocked vent thermal accident condition

The thermal evaluation presented in Chapter 4 reports four thermal cases for the canister stored in the HSM with blocked vent. The maximum temperature of 600 °F in the canister is reached after 34 hours of complete vent blockage in an HSM with fins. The 34 hour vent blockage is a conservative scenario, since the vent is visually checked at least every 24 hours. However, this case is reported in the thermal evaluation and is therefore selected for analysis in this section. The same procedure used for obtaining the thermal load in Load Case 4 is used in this load case. The secondary thermal stress intensity is calculated to be 20.96 ksi. The maximum stress intensity in the closure welds is calculated to be 7.12 ksi.

Storage Load Case 7: Accident internal pressure of 70 psig (in the event of blocked vent)

The internal pressure of 70 psig in the canister is analyzed for enveloping the accident condition internal pressures during the blocked vent scenario. The maximum primary membrane plus bending stress intensity in the canister is calculated to be 34.96 ksi. The maximum stress intensity in the closure welds is calculated to be 27.44 ksi.

Storage Load Case 8: Accident flood load (enveloped by external pressure of 30 psig)

The hypothetical accident condition flood load is enveloped by an external pressure of 30 psig. The maximum primary membrane plus bending stress intensity in canister is calculated to be 5.48 ksi. The maximum stress intensity in the closure welds is calculated to be 2.90 ksi.

E.4. Summary of the Stress Calculation Results for All Storage Load Cases

Tables A.3.9.1-14 and A.3.9.1-15 summarize the calculated stresses in the entire canister and their corresponding ASME code evaluations.

Based on the results of this calculation, the 32PTH Type 1 DSC canister is structurally adequate under all normal (Service Level A), off-normal (Service Level C), and hypothetical accident (Service Level D) conditions during storage.

A.3.9.1.3.3 DSC Shell Buckling Evaluation

This section evaluates the structural adequacy of the 32PTH Type 1 DSC canister against buckling during a vertical end drop during transfer operations.

For the NUHOMS HD® System, the vertical end drops are not considered credible during storage and transfer operations under 10 CFR Part 72 because the transfer cask is always in the horizontal orientation. The vertical end drop buckling evaluation documented below is performed in support of a 10 CFR Part 50 evaluation that may be performed by the user if the user cannot demonstrate that this accident drop is not credible.

A. Approach

A finite element plastic analysis with large displacement option is performed to monitor occurrence of canister shell buckling under the specified loads.

The thermal evaluation presented in Chapter 4 shows that the metal temperatures of the entire canister are below 500 °F during the transfer operations. The material properties of canister at 500 °F are therefore conservatively used in this calculation.

B. Material Properties used for Canister Buckling Evaluation

The material properties of the canister materials, SA-240 Type 304 stainless steel, at 500 °F are as follows.

Property	@ 500 °F
S_m (ksi)	17.5
S_y (ksi)	19.4
S_u (ksi)	63.4
E (psi)	25.8×10^6

For the elastic-plastic finite element analysis, bilinear kinematic hardening material properties are used. Tangent modulus of 5% of elastic modulus is assumed after yield stress.

The material properties for the top and bottom shield plug, A-36, at 500 °F are as follows:

Property	@ 500 °F
S_m (ksi)	19.3
S_y (ksi)	29.3
S_u (ksi)	58.0
E (psi)	27.3×10^6

C. Finite Element Buckling Analysis

The following three hypothetical accident load cases for the canister are considered in this buckling analysis.

Buckling Load Case 1: End drop + 15 psig external pressure

Buckling Load Case 2: End drop + 30 psig internal pressure

Buckling Load Case 3: End drop + 0 psig internal pressure

The two-dimensional axisymmetric finite element model of the canister described in Appendix A.3.9.1, Section A.3.9.1.3.2 (D.2) for the DSC canister stress analysis is used for this analysis.

The gap element real constants, node couplings and displacement boundary conditions are also the same as those used in Section A.3.9.1.3.2 (D.2). The weight of the canister's outer and inner top cover plus the top shield plug and its support ring is 12,856 lb, and the bottom shield plug is 9,696 lb (see Section A.3.2.1). Since the top end of the canister is heavier than the bottom end, it is a more severe case when the canister drops on its bottom end. A drop on the bottom end is therefore chosen for analysis in this calculation.

For load case with external pressure or internal pressure, a quasi-static plastic analysis consisting of two load steps is performed to monitor buckling of the canister. The first load step applies external pressure or internal pressure alone. A subsequent inertial load of 300g is added in the second load step. The outer surface of the canister bottom is held in order to simulate the case that the canister drops on a rigid cask bottom face.

In the load step 1, the stepped external or internal pressure is applied as a static load.

In the load step 2, the weight of the canister internals (basket and fuel assemblies) is accounted for by applying an equivalent internal pressure on the canister bottom. The actual total weight of the canister internals is 80,171 lb (basket 29,451 lb + fuel assemblies 50,720 lb) (Chapter A.3, Section A.3.2.1). A total weight of 83,000 lb for the canister internals is conservatively used in this analysis. This inertial load is uniformly distributed over the bottom surface of the canister cavity with a radius of 34.375 in. This equivalent uniform pressure, P_{in} , exerted on the canister bottom by the weight of the internals under a 1 g load is calculated as follows.

$$P_{in} = [83,000 / (\pi \times 34.375^2)] = 22.3585 \text{ psi.}$$

An equivalent pressure of 6707.55 psig on the canister bottom corresponding to the 300g load ($P_{in} = 300 \times 22.3585 = 6707.55 \text{ psi}$) is, therefore, applied to the canister bottom along with the 300g acceleration load in the load step 2.

A bilinear stress-strain relationship (with kinematic hardening) is used to obtain stresses and deflections beyond the elastic limit of the material. The large displacement option in ANSYS is activated to monitor the buckling response.

D. Summary Canister Buckling Analysis Results

The following table summarizes the last converged load for the three load cases:

Load Case	Last Converged Load (g)	g Load Used for Basket Structural Analysis	Factor of Safety
1	173.5	75	2.31
2	174.9	75	2.33
3	174.0	75	2.32

The analysis shows that the critical buckling load for the canister end drop is 173.5g, which is well beyond the design 75g load. It is, therefore, concluded that buckling of the canister will not occur during a hypothetical accident end drop.

A.3.9.1.3.4 Evaluation of Alternate DSC Top and Bottom Closure Assembly Design

The alternate top closure assembly of the 32PTH Type 1 DSC which consists of the two-part combined shield plug /inner cover assembly (including the optional configurations), as well as the optional bottom end configurations (consisting of two-plate or single forging bottom assembly) are not analyzed explicitly.

The evaluations for the 32PTH Type 1 DSC consider a DSC with a three-part top end configuration (with separate inner cover plate, shield plug, and outer cover plate) and a three-part bottom end configuration (with separate inner bottom cover, bottom shield plug, outer bottom cover plate). The results from these evaluations are documented in Sections A.3.9.1.3.2 and A.3.9.1.3.3, and are considered to be bounding relative to those for a DSC with the alternate two-part top end assembly or the optional bottom end configurations for cases involving internal pressure and handling loads. For side drop accident loads, the results of the 32PTH DSC for the side drop accident load case are also applicable for the alternate top end and the optional bottom end configurations of the 32PTH Type 1 DSC. This is justified because the side drop analyses are performed using two separate 3-D models which model the top and the bottom regions of the DSC shell assembly, respectively. These models include a segment of the DSC shell and are intended to capture the maximum stresses that occur near the transition between the shell and the stiffer top and bottom ends, and, therefore, are not sensitive to the length differences between the 32PTH and 32PTH Type 1 DSCs. Furthermore, the loaded canister weight used in the 32PTH DSC analysis is the same as in the 32PTH Type 1 analyses.

A.3.9.1.4 32PTH Type 1 DSC and OS187H Type 1 Transfer Cask Thermal Expansion Evaluation

A.3.9.1.4.1 Introduction

The purpose of this section is to determine the thermal growths among components of fuel cladding, basket, canister, and transfer cask in the 32PTH Type 1 DSC and OS187H TC. This thermal expansion calculation covers events of vacuum drying, transfer, storage, and storage with blocked vent.

A.3.9.1.4.2 Approach

The temperatures of the fuel cladding, basket, canister, and transfer cask under various events calculated in the thermal analyses of Chapter 4 are applicable for the 32PTH Type 1 DSC and OS187H Type 1 transfer cask. Transient thermal analyses are conducted for the vacuum drying and blocked vent events. Steady-state thermal analyses are conducted for the normal and off-normal conditions during transfer and storage. This section computes the thermal expansions at the steady-state temperatures in the events of transfer and storage.

In the vacuum drying load case, the profiles of transient temperature versus time computed in Chapter 4 are studied for selection of the critical time points at which the corresponding component temperatures would generate a minimum clearance between two nested components. For the blocked vent load case, the maximum temperatures from Chapter 4 are used in this calculation.

The cold dimensions of each pair of nested components are so determined, based on design tolerances, which generates a minimum cold clearance between the two components.

Unless otherwise stated, nominal dimensions of basket, canister, and cask are used for the thermal expansion calculations.

A.3.9.1.4.3 Mechanical Properties of Materials

The coefficient of thermal expansion of structural materials used for the fuel basket, canister shell, and transfer cask are provided in Table 3.9.1-6 as a function of temperature. The properties of SA-240 Type 304 are taken from Reference 1, and the zircaloy properties are taken from Reference 4.

A.3.9.1.4.4 Thermal Expansion Computation

A. Thermal Expansion between the Length of Fuel Assembly and Canister Cavity

The cavity for the 32PTH Type 1 DSC is larger than the cavity for the 32PTH. Since the length of the fuel assemblies remain unchanged, additional thermal expansion calculations are not needed.

B. Thermal Expansion between the Outer Diameter of the Basket and the Inner Diameter of the Canister Cavity

The diametrical gap between the outer diameter of the basket and the inner diameter of the canister remains the same as for the 32PTH DSC. With the same radial temperature profile, the thermal expansion values calculated in Section 3.9.1.4.4.B are applicable for the 32PTH Type 1 DSC. These calculations show that the gap will allow free thermal expansion.

C. Thermal Expansion between the Length of Basket and Canister Cavity

The length of the basket is increased by 4.3% $((169-162)/162)$ for the 32PTH Type 1 DSC relative to the 32PTH DSC. The cold gap is increased by 5.2% $((2.63-2.5)/2.5)$ for the 32PTH Type 1 DSC relative to the 32PTH DSC. The percent increase in the cold gap is more than the increase in the length of the basket; therefore, the current gap will allow for free thermal expansion.

D. Thermal Expansion between the Outer Diameter of the Canister and the Inner Diameter of the Cask Body

The diametrical gap between the outer diameter of the canister and the inner diameter of the cask remains the same as for the 32PTH DSC and OS187H transfer cask. With the same radial temperature profile, the thermal expansion values calculated in Section 3.9.1.4.4.D are applicable for the 32PTH Type 1 DSC and OS187H transfer cask. These values show that the current gap will allow free thermal expansion.

E. Thermal Expansion between the Length of the Canister and the Transfer Cask Cavity

The maximum length of the canister at room temperature is 193.0 inches, while the transfer cask cavity at room temperature is 200.5 inches. A spacer will be used at the bottom of the cask. The length of the cask spacer is designed to permit free thermal expansion of the DSC without interference with the transfer cask.

A.3.9.1.4.5 Thermal Expansion Analysis Conclusions

This evaluation demonstrates that adequate clearance is provided between the 32PTH Type 1 DSC fuel basket and canister shell, and between the 32PTH Type 1 DSC canister and the OS87H Type 1 transfer cask to permit free thermal expansions among these components due to all specified design and service conditions.

A.3.9.1.5 References

- [1] American Society of Mechanical Engineers, ASME Boiler and Pressure Vessel Code, Section II, Part D, 1998, through 2000 addenda.
- [2] Not used
- [3] American Society of Mechanical Engineers, ASME Boiler and Pressure Vessel Code, Section III, Appendix F, 1998 through 2000 addenda.
- [4] NUREG/CR-0497-Rev 2, MATPRO-Version 11 (Revision 2), A handbook of materials properties for use in the analysis of light water reactor fuel rod behavior.
- [5] Not used
- [6] Manual of Steel Construction, Ninth Edition, American Institute of Steel Construction, Inc., 1989.
- [7] Roark, Formulas for Stress and Strain, Seventh Edition.
- [8] American Society of Mechanical Engineers, ASME Boiler and Pressure Vessel Code, Section III, Division 1, Subsection NB, 1998, through 2000 addenda.
- [9] NUREG/CR-0481 SAND77-1872 R-7, "An Assessment of Stress-Strain Data Suitable for Finite-Element Elastic-Plastic Analysis of Shipping Containers," September 1978.
- [10] ANSYS Engineering Analysis System and Users Manual, Release 8.0 and 10A1, Swanson Analysis Systems, Inc., Houston, PA.
- [11] Not used
- [12] Not used
- [13] Not used
- [14] USNRC Spent Fuel Project Office, Interim Staff Guidance – 15, "Materials Evaluation."
- [15] Roark, Formulas for Stress and Strain, Sixth Edition.
- [16] Safety Evaluation Report, Transnuclear, Inc., NUHOMS® HD Horizontal Modular Storage System for Irradiated Nuclear fuel, Docket No. 72-1030.

Table A.3.9.1-1 Temperature Dependent Material Properties for ASTM A-36

Temp (°F)	E (10³ ksi)	S_m (ksi)	S_y (ksi)	S_u (ksi)	α_{INST} (10⁻⁶°F⁻¹)	α_{AVG} (10⁻⁶°F⁻¹)
70	29.5	19.3	36.0	58.0	6.4	6.4
200	28.8	19.3	33.0	58.0	6.9	6.7
300	28.3	19.3	31.8	58.0	7.3	6.9
400	27.7	19.3	30.8	58.0	7.7	7.1
500	27.3	19.3	29.3	58.0	8.0	7.3
600	26.7	17.7	27.6	58.0	8.4	7.4
700	25.5	17.3	25.8	58.0	8.6	7.6

**Table A.3.9.1-2 Material Stress Limits for 32PTH Type 1 DSC
SA-240/SA-479 304 & SA-182 F304**

Temp (°F)	Level A			Level C		Level D			
						Elastic		Elastic-Plastic	
	P_m	$P_m + P_b$	$P_m + P_b + Q$	P_m	$P_m + P_b$	P_m	$P_m + P_b$	P_m	$P_m + P_b$
70	20.0	30.0	60.0	30.0	45.0	48.0	72.0	52.5	67.5
200	20.0	30.0	60.0	25.0	37.5	48.0	71.0	49.7	63.9
300	20.0	30.0	60.0	24.0	36.0	46.3	66.2	46.3	59.6
400	18.7	28.1	56.1	22.4	33.7	44.8	64.0	44.8	57.6
500	17.5	26.3	52.5	21.0	31.5	42.0	63.0	44.4	57.1
600	16.4	24.6	49.2	19.7	29.5	39.4	59.0	44.4	57.1
700	16.0	24.0	48.0	19.2	28.8	38.4	57.6	44.4	57.1
800	15.2	22.8	45.6	18.2	27.4	36.5	54.7	44.0	56.5

Table A.3.9.1-3 32PTH Type 1 DSC Canister Load Combinations during Transfer

Loading	Canister w/Transfer Cask Orientation	Service Level	Load for Analysis	Load Combinations	Analyzed Load Case No.	ANSYS Model
Dead weight	Vertical ⁽¹⁾	A	1 g down (axial)	1 g down + 15 psig ext. press. + thermal (vacuum dry)	1	2-D
External pressure	Vertical ⁽¹⁾	A	15 psig			
Thermal	Vertical ⁽¹⁾	A	Vacuum dry			
Dead weight	Horizontal ⁽²⁾	A	2 g axial + 2 g trans. + 2 g vertical	A = 2 g axial + 2 g trans. + 2 g vertical	2	2-D
Handling load in transfer cask	Horizontal ⁽²⁾	A		A+ 30 psig int. pressure + thermal (115 °F)		
				A+ 15 psig ext. pressure + thermal (-20 °F)	3	2-D
Internal pressure	Horizontal ⁽²⁾	A		30 psig ⁽⁶⁾	Pressure stress	[2] ⁽⁵⁾
External pressure	Horizontal ⁽²⁾	A	15 psig	Pressure stress	[3] ⁽⁵⁾	2-D
Thermal	Horizontal ⁽²⁾	A	Thermal stress (-20 °F Ambient)	Thermal stress	[3] ⁽⁵⁾	2-D
Thermal	Horizontal ⁽²⁾	A	Thermal stress (115 °F ambient)	Thermal stress	[2] ⁽⁵⁾	2-D
Internal pressure	Horizontal	D	120 psig ⁽³⁾	Pressure stress	4	2-D
External pressure	Horizontal	D	25 psig ⁽⁴⁾	Pressure stress	5	2-D
Side drop	Horizontal	D	75 g multiple orientations (0°, 30°, 45°, impact on two rails, impact on one rail) Drop angles are enveloped by 0° (no rail) and 180° (two rails)	75 g side drop at 0° (no rail) + 30 psig int. press. of top/bottom ends	6/7	3-D
				75 g side drop at 180° (two rails) + 30 psig int. press. of top/bottom ends	8/9	3-D
				75 g side drop at 0° (no rail) + 15 psig ext. press. of top/bottom ends	10/11	3-D
				75 g side drop at 180° (two rails) + 15 psig ext. press. of top/bottom ends	12/13	3-D
Corner drop	Horizontal	D	Enveloped by 75 g Side Drop and 75 g End Drop			
End drop	Vertical	D	75 g End Drop	75 g top/bottom + 30 psig int. pressure	14/15	2-D
				75 g top/bottom + 15 psig ext. pressure	16/17	2-D

Notes:

- (1) Transfer cask supported at the bottom.
- (2) Transfer cask supported at 4 trunnion location.
- (3) Under accident fire condition.
- (4) Under accident flood condition.
- (5) [#] indicates this individual load case is enveloped in the analyzed load case No.
- (6) From Chapter 4, Table 4-10, the maximum normal operating pressure is 6.4 psig during transfer operation. However, a design pressure of 15 psig is used. Conservatively, 30 psig is used for structural evaluation of the canister.

Table A.3.9.1-4 32PTH Type 1 DSC Canister Load Combinations during Lifting, Testing, and Hydraulic Loads

Loading	Canister w/Transfer Cask Orientation	Service Level	Load for Analysis	Load Combinations	Analyzed Load Case No.	ANSYS Model
Dead weight	Horizontal	A	1 g	1 g + 18 psig int. pressure + 155 kips axial loads	18	2-D
Test pressure	Horizontal	A	18 psig ⁽³⁾			
Seal plate axial load	Horizontal	A	155 kips			
Hydraulic loads ⁽¹⁾⁽²⁾ (push/pull)	Horizontal	A	80/60 kips	30 psig int. pressure + 80 kips push/60 kips pull + thermal (115 °F)	19/20	2-D
Hydraulic loads ⁽¹⁾⁽²⁾ (push/pull)	Horizontal	C	80/80 kips	30 psig int. pressure + 80 kips + thermal (115 °F)	21/22	2-D
Hydraulic loads ⁽¹⁾⁽²⁾ (push/pull)	Horizontal	D	110/110 kips	30 psig int. pressure + 110 kips	23/24	2-D
Lifting	Vertical	A	1g	1 g	25	3-D

Notes:

- (1) The hydraulic push loads are applied at the canister bottom surface within the grapple ring support.
- (2) The hydraulic pull loads are applied at the inner surface of the grapple ring.
- (3) From Chapter 4, Table 4-10, the maximum normal operating pressure is 6.4 psig during transfer operation. The test pressure is $1.5 \times \text{MNOP} = 1.5 \times 6.4 = 9.6$ psig. The canister is conservatively using 18 psig as the test pressure.

Table A.3.9.1-5 Summary of Calculated Stresses for Testing Condition Loads

Load Case	Combination of Loads	Canister Orientation	Service Level	Component	Stress Category	Stress ⁽²⁾ (ksi)	Stress Limit (ksi)
18	DW + 18 psig int. press. + 155 kip axial load	Horizontal	A	All ⁽¹⁾	P _m	9.36+0.005 = 9.36	16.4
					P _m + P _b	9.36+6.26 = 15.62	24.6

Notes:

- (1) Conservatively the stress limits at 600 °F are used.
- (2) Conservatively the maximum stress intensity was used for both P_m and P_m + P_b stresses.

Table A.3.9.1-6 Summary of Calculated Stress for Normal and Off-Normal Condition Transfer Loads

Load Case	Combination of Loads	Canister Orientation	Service Level	Components	Stress Category	Stress ⁽³⁾ (ksi)	Stress Limit (ksi)
1	1 g down + 15 psig ext. press. + vacuum drying thermal	Vertical	A	All ⁽²⁾	P_m	2.05	17.5
					$P_m + P_b$	2.05	26.3
					$P_m + P_b + Q$	22.69	52.5
2	Handling 2 g + 30 psig int. press. + thermal (115 °F)	Horizontal	A	All ⁽²⁾	P_m	$14.97+0.88 = 15.85$	17.5
					$P_m + P_b$	$14.97+9.74 = 24.71$	26.3
					$P_m + P_b + Q$	$41.70+9.74 = 51.44$	52.5
3	Handling 2 g + 15 psig ext. press. + thermal (-20 °F)	Horizontal	A	All ⁽²⁾	P_m	$2.75+0.88 = 3.63$	17.5
					$P_m + P_b$	$2.75+9.74 = 12.49$	26.3
					$P_m + P_b + Q$	$31.63+9.74 = 41.37$	52.5
19	30 psig int. press + 80 kips push + thermal (115 °F)	Horizontal	A	All ⁽²⁾	P_m	15.73	17.5
					$P_m + P_b$	15.73	26.3
					$P_m + P_b + Q$	38.19	52.5
20	30 psig int. press + 60 kips pull + thermal (115 °F)	Horizontal	A	GR, BOCP, and bottom 2" CS ⁽¹⁾	P_m	9.30	20.0
					$P_m + P_b$	25.80	30.0
					$P_m + P_b + Q$	27.45	60.0
				All except GR, BOCP, and bottom 2" CS ⁽³⁾	P_m	14.97	17.5
					$P_m + P_b$	14.97	26.3
					$P_m + P_b + Q$	41.64	52.5
21	30 psig int. press + 80 kips push + thermal (115 °F)	Horizontal	C	All ⁽²⁾	P_m	15.73	21.0
					$P_m + P_b$	15.73	31.5
					$P_m + P_b + Q$	-	-
22	30 psig int. press + 80 kips pull + thermal (115 °F)	Horizontal	C	GR, BOCP, and bottom 2" CS ⁽¹⁾	P_m	12.41	24.0
					$P_m + P_b$	34.43	36.0
					$P_m + P_b + Q$	-	-
				All except GR, BOCP, and bottom 2" CS ⁽³⁾	P_m	14.97	21.0
					$P_m + P_b$	14.97	31.5
					$P_m + P_b + Q$	-	-

Notes:

- (1) GR—grapple ring; BOCP—bottom outer cover plate; CS—canister shell. Except for the vacuum drying and fire accident load cases, the temperature in the grapple ring, the bottom outer cover plate and the bottom 2 inches of the canister shell do not exceed 300 °F. Conservatively stress limits at 300 °F are used.
- (2) Conservatively the stress limits at 500 °F are used.
- (3) Conservatively the maximum stress intensity was used for both P_m and $P_m + P_b$ stresses for all analyses except for grapple pull load cases, 20 and 22, where the stresses were linearized in the grapple ring, bottom outer cover plate and bottom 2 in of the canister shell.

**Table A.3.9.1-7 Summary of Calculated Stress for Accident Condition Transfer Loads
(Axisymmetric Loads)**

Load Case	Combination of Loads	Canister Orientation	Service Level	Components	Stress Category	Stress ⁽⁴⁾ (ksi)	Stress Limit (ksi)
4	120 psig int. press. under fire accident	Horizontal	D	All ⁽²⁾	P_m	23.92	44.0
					$P_m + P_b$	23.92	56.5
5	25 psig ext. press. under flood accident	Horizontal	D	All ⁽³⁾	P_m	4.56	42.0
					$P_m + P_b$	4.56	63.0
14	75 g top end drop + 30 psig int. press.	Vertical	D	All ⁽³⁾	P_m	17.68	42.0
					$P_m + P_b$	17.68	63.0
15	75 g bottom end drop + 30 psig int. press.	Vertical	D	All ⁽³⁾	P_m	21.05	42.0
					$P_m + P_b$	21.05	63.0
16	75 g top end drop + 15 psig ext. press.	Vertical	D	All ⁽³⁾	P_m	30.68	42.0
					$P_m + P_b$	30.68	63.0
17	75 g bottom end drop + 15 psig ext. press.	Vertical	D	All ⁽³⁾	P_m	26.09	42.0
					$P_m + P_n$	26.9	63.0
23	30 psig int. press. + 110 kips push	Horizontal	D	All ⁽³⁾	P_m	16.36	42.0
					$P_m + P_b$	16.36	63.0
24	30 psig int. press. + 110 kips pull	Horizontal	D	GR, BOCP, and bottom 2" CS ⁽¹⁾	P_m	17.03	46.3
					$P_m + P_b$	47.25	66.2
				All except GR, BOCP, and bottom 2" CS ⁽³⁾	P_m	15.99	42.0
					$P_m + P_b$	15.99	63.0

Notes:

- (1) GR—grapple ring; BOCP—bottom outer cover plate; CS—canister shell. Except for the vacuum drying and fire accident load cases, the temperature in the grapple ring, the bottom outer cover plate, and bottom 2 inches of the canister shell do not exceed 300 °F. Conservatively stress limits at 300 °F are used for elastic analysis.
- (2) Conservatively the stress limits at 800 °F are used for elastic-plastic analysis.
- (3) Conservatively the stress limits at 500 °F are used for elastic analysis.
- (4) Conservatively the maximum stress intensity was used for both P_m and $P_m + P_b$ stresses for all analyses except for grapple pull load cases, 23, where the stresses were linearized in the grapple ring, bottom outer cover plate and bottom 2 inches of the canister shell.

Table A.3.9.1-8 Summary of Stresses for Accident Condition Transfer Loads (3-D Inertial Loads)

Load Case	Load Combination	Canister	Maximum Stress Intensity ⁽¹⁾ [ksi]	Stress Limits	
				PM	PM+PB
6	Side drop 75 g + 30 psig internal pressure	Top end, no rails (orientation 0°)	25.5	44.4 ksi	57.1 ksi
7	Side drop 75 g + 30 psig internal pressure	Bottom end, no rails (orientation 0°)	24.0	44.4 ksi	57.1 ksi
8	Side drop 75 g + 30 psig internal pressure	Top end, rails (orientation 180°)	27.3	44.4 ksi	57.1 ksi
9	Side drop 75 g + 30 psig internal pressure	Bottom end, rails (orientation 180°)	24.7	44.4 ksi	57.1 ksi
10	Side drop 75 g + 15 psig external pressure	Top end, no rails (orientation 0°)	25.9	44.4 ksi	57.1 ksi
11	Side drop 75 g + 15 psig external pressure	Bottom end, no rails (orientation 0°)	24.1	44.4 ksi	57.1 ksi
12	Side drop 75 g + 15 psig external pressure	Top end, rails (orientation 180°)	27.3	44.4 ksi	57.1 ksi
13	Side drop 75 g + 15 psig external pressure	Bottom end, rails (orientation 180°)	24.9	44.4 ksi	57.1 ksi

Note:

(1) Shield plug component excluded in stress evaluation.

Table A.3.9.1-9 Summary of Calculated Stress at End Closure Welds for Testing Condition Loads

Load Case	Combination of Loads	Canister Orientation	Service Level	Stress Category	Stress ⁽¹⁾ (ksi)	Stress Limit (ksi)
18	DW + 18 psig int. press. + 155 kip axial load	Horizontal	A	P_m	-	-
				$P_m + P_b$	-	-

Note:

- (1) There are no closure welds during pressure test.

Table A.3.9.1-10 Summary of Calculated Stress at the End Closure Welds for Normal and Off-Normal Condition Transfer Loads

Load Case	Combination of Loads	Canister Orientation	Service Level	Stress Category	Stress ⁽²⁾ (ksi)	Stress Limit ⁽¹⁾ (ksi)
1	1 g down + 15 psig ext. press. + vacc. dry thermal	Vertical	A	P_m	1.52	16
				$P_m + P_b$	1.52	24
				$P_m + P_b + Q$	2.07	48
2	Handling 2 g + 30 psig int. press. + thermal (115 °F)	Horizontal	A	P_m	$11.75+0.88 = 12.63$	16
				$P_m + P_b$	$11.75+9.74 = 21.49$	24
				$P_m + P_b + Q$	$14.94+9.74 = 24.68$	48
3	Handling 2 g + 15 psig ext. press. + thermal (-20 °F)	Horizontal	A	P_m	$1.46+0.88 = 2.34$	16
				$P_m + P_b$	$1.46+9.74 = 11.20$	24
				$P_m + P_b + Q$	$2.32+9.74 = 12.06$	48
19	30 psig int. press + 80 kips push + thermal (115 °F)	Horizontal	A	P_m	10.75	16
				$P_m + P_b$	10.75	24
				$P_m + P_b + Q$	14.91	48
20	30 psig int. press + 60 kips pull + thermal (115 °F)	Horizontal	A	P_m	11.75	16
				$P_m + P_b$	11.75	24
				$P_m + P_b + Q$	14.94	48
21	30 psig int. press + 80 kips push + thermal (115 °F)	Horizontal	C	P_m	10.75	19.2
				$P_m + P_b$	10.75	28.8
				$P_m + P_b + Q$	-	-
22	30 psig int. press + 80 kips pull + thermal (115 °F)	Horizontal	C	P_m	11.75	19.2
				$P_m + P_b$	11.75	28.8
				$P_m + P_b + Q$	-	-

Notes:

- (1) Since the temperatures at the closure welds do not exceed 300 °F, the allowable stresses at 300 °F are used.
- (2) Conservatively the maximum stress intensity was used for both P_m and $P_m + P_b$ stresses for all analyses

Table A.3.9.1-11 Summary of Calculated Stresses at End Closure Welds for Accident Condition Transfer Loads (Axisymmetric Loads)

Load Case	Combination of Loads	Canister Orientation	Service Level	Stress Category	Stress ⁽²⁾ (ksi)	Stress Limit ⁽¹⁾ (ksi)
4	120 psig int. press. under fire accident	Horizontal	D	P_m	21.71	37.04
				$P_m + P_b$	21.71	47.68
5	25 psig ext. press. under flood accident	Horizontal	D	P_m	2.42	37.04
				$P_m + P_b$	2.42	52.96
14	75 g top end drop + 30 psig int. press.	Vertical	D	P_m	6.43	37.04
				$P_m + P_b$	6.43	52.96
15	75 g bottom end drop + 30 psig int. press.	Vertical	D	P_m	4.27	37.04
				$P_m + P_b$	4.27	52.96
16	75 g top end drop + 15 psig ext. press.	Vertical	D	P_m	8.67	37.04
				$P_m + P_b$	8.67	52.96
17	75 g bottom end drop + 15 psig ext. press.	Vertical	D	P_m	6.10	37.04
				$P_m + P_b$	6.10	52.96
23	30 psig int. press. + 110 kips push	Horizontal	D	P_m	10.49	37.04
				$P_m + P_b$	10.49	52.96
24	30 psig int. press. + 110 kips pull	Horizontal	D	P_m	11.75	37.04
				$P_m + P_b$	11.75	52.96

Notes:

- (1) Since the temperatures at the closure welds do not exceed 300 °F, the allowable stresses at 300 °F are used.
- (2) Conservatively the maximum stress intensity was used for both P_m and $P_m + P_b$ stresses for all analyses.

Table A.3.9.1-12 Summary of Calculated Stresses at End Closure Welds for Accident Condition Transfer Loads (3-D Inertial Loads)

Load Case	Load Combination	Canister	Maximum Stress Intensity (ksi)	Stress Limits
6	Side drop 75 g + 30 psig internal pressure	Top end, no rails (orientation 0°)	23.3	35.52 ksi
8	Side drop 75 g + 30 psig internal pressure	Top end, rails (orientation 180°)	24.3	35.52 ksi
10	Side drop 75 g + 15 psig external pressure	Top end, no rails (orientation 0°)	23.4	35.52 ksi
12	Side drop 75 g + 15 psig external pressure	Top end, rails (orientation 180°)	24.2	35.52 ksi

Table A.3.9.1-13 32PTH Type 1 DSC Canister Load Combinations during Storage

Loading	Canister Orientation	Service Level	Load	Enveloped Load for Analysis	Load Combinations
Dead weight	Horizontal ⁽¹⁾	A	1 g down	.65 g axial + .65 g trans. + 1.3 g vertical	.65 g axial + .65 g trans. + 1.3 g vertical down
Seismic loads	Horizontal ⁽¹⁾	C ⁽²⁾	0.43 g axial + 0.43 g trans. + 0.20 g vertical		.65 g axial + .65 g trans. + 1.3 g vertical down + 30 psig + thermal (115 °F) .65 g axial + .65 g trans. + 1.3 g vertical down + 30 psig + thermal (-20 °F)
Internal pressure	Horizontal ⁽¹⁾	A	15 psig	30 psig	Pressure
Thermal	Horizontal ⁽¹⁾	A	Thermal (-20 °F ambient)	Thermal (-20 °F ambient)	Thermal
Thermal	Horizontal ⁽¹⁾	A	Thermal (115 °F ambient)	Thermal (115 °F ambient)	Thermal
Thermal	Horizontal ⁽¹⁾	D	Blocked vent	Blocked vent	1 g down + 70 psig int. pressure + thermal (blocked vent)
Internal pressure	Horizontal ⁽¹⁾	D	< 67 psig due to blocked vent	Enveloped by 70 psig internal pressure	
Flood	Horizontal ⁽¹⁾	D ^t	50 ft water (≈22 psig)	Enveloped by 30 psig external pressure design	

Notes:

- (1) Canister supported at HSM rails and axial restrained by the seismic restraint devices.
- (2) Levels C loads are conservatively treated as Level A loads and so evaluated.

**Table A.3.9.1-14 Summary of Calculated Stresses for Normal and Accident Condition Loads
(canister in horizontal position)**

Load Case	Combination of Loads	Canister Orientation	Service Level	Components	Stress Category	Stress (ksi)	Stress Limit (ksi)
S1	Dead weight (1 g down)	Horizontal	A	All ⁽²⁾	P_m	0.40	17.5
					$P_m + P_b$	4.05	26.3
S2	30 psig internal pressure	Horizontal	A	All ⁽²⁾	$P_m^{(3)}$	14.97	17.5
					$P_m + P_b^{(3)}$	14.97	26.3
S3	Seismic (0.65 g axial + 0.65 trans. + 1.3 vert. down)	Horizontal	A ⁽¹⁾	All ⁽²⁾	P_m	0.63	17.5
					$P_m + P_b$	6.08	26.3
S4	Thermal (-20 °F amb.)	Horizontal	A	All ⁽²⁾	Q	22.49	52.5
S5	Thermal (115 °F amb.)	Horizontal	A	All ⁽²⁾	Q	20.51	52.5
S6	Thermal (blocked vent)	Horizontal	D	All ⁽⁴⁾	Q	20.96	63.0
S7	Accident 70 psig internal pressure	Horizontal	D	All ⁽²⁾	$P_m^{(3)}$	34.96	42.0
					$P_m + P_b^{(3)}$	34.96	63.0
S8	Accident flood (enveloped by 30 psig ext. pressure)	Horizontal	D	All ⁽²⁾	$P_m^{(3)}$	5.48	42.0
					$P_m + P_b^{(3)}$	5.48	63.0
SC1	S2 + S3 + S4	Horizontal	A ⁽¹⁾	All ⁽²⁾	P_m	15.60	17.5
					$P_m + P_b$	21.05	26.3
					$P_m + P_b + Q$	43.54	52.5
SC2	S2 + S3 + S5	Horizontal	A ⁽¹⁾	All ⁽²⁾	P_m	15.60	17.5
					$P_m + P_b$	21.05	26.3
					$P_m + P_b + Q$	41.56	52.5
SC3	S1 + S7 + S6	Horizontal	D	All ⁽⁴⁾	P_m	35.36	42.0
					$P_m + P_b$	39.01	63.0
					$P_m + P_b + Q$	59.97	63.0
SC4	S1 + S8	Horizontal	D	All ⁽²⁾	P_m	5.88	42.0
					$P_m + P_b$	9.53	63.0

Notes:

- (1) Seismic loads are conservatively treated as Level A loads.
- (2) Conservatively the stress limits at 500 °F are used.
- (3) Conservatively the maximum stress intensity was used for both P_m and $P_m + P_b$ stresses for all analyses.
- (4) ASME code requires only primary stresses be evaluated under accident conditions, conservatively secondary stresses were evaluated and compared against the $P_m + P_b$ stress limits. The peak stresses occur at the top and bottom of the canister where the maximum temperature is lower than 500 °F. The stress limits at 500 °F are used.

Table A.3.9.1-15 Summary of Calculated Stresses at the End Closure Welds for Normal and Accident Condition Storage Loads

Load Case	Combination of Loads	Canister Orientation	Service Level	Stress Category	Stress (ksi)	Stress Limit ⁽²⁾ (ksi)
S1	Dead weight (1 g down)	Horizontal	A	P_m	0.40	16
				$P_m + P_b$	4.05	24
S2	30 psig internal pressure	Horizontal	A	$P_m^{(3)}$	11.75	16
				$P_m + P_b^{(3)}$	11.75	24
S3	Seismic (0.65 g axial + 0.65 trans. + 1.3 vert. down)	Horizontal	A ⁽¹⁾	P_m	0.63	16
				$P_m + P_b$	6.08	24
S4	Thermal (-20 °F amb.)	Horizontal	A	Q	2.47	48
S5	Thermal (115 °F amb.)	Horizontal	A	Q	2.50	48
S6	Thermal (blocked vent)	Horizontal	D	Q ⁽⁴⁾	7.12	52.96
S7	Accident 70 psig internal pressure	Horizontal	D	$P_m^{(3)}$	27.44	37.04
				$P_m + P_b^{(3)}$	27.44	52.96
S8	Accident flood (enveloped by 30 psig ext. pressure)	Horizontal	D	$P_m^{(3)}$	2.90	37.04
				$P_m + P_b^{(3)}$	2.90	52.96
SC1	S2 + S3 + S4	Horizontal	A ⁽¹⁾	P_m	12.38	16
				$P_m + P_b$	17.83	24
				$P_m + P_b + Q$	20.30	48
SC2	S2 + S3 + S5	Horizontal	A ⁽¹⁾	P_m	12.38	16
				$P_m + P_b$	17.83	24
				$P_m + P_b + Q$	20.33	48
SC3	S1 + S7 + S6	Horizontal	D	P_m	27.84	37.04
				$P_m + P_b$	31.49	52.96
				$P_m + P_b + Q^{(4)}$	38.61	52.96
SC4	S1 + S8	Horizontal	D	P_m	3.30	37.04
				$P_m + P_b$	6.95	52.96

Notes:

- (1) Seismic loads are conservatively treated as Level A loads.
- (2) Since the temperatures at the closure welds do not exceed 300 °F, the stress limits at 300 °F are used.
- (3) Conservatively the maximum stress intensity was used for both P_m and $P_m + P_b$ stresses for all analyses.
- (4) ASME code requires only primary stresses be evaluated under accident conditions, conservatively secondary stresses were also included and compared against the $P_m + P_b$ stress limits.

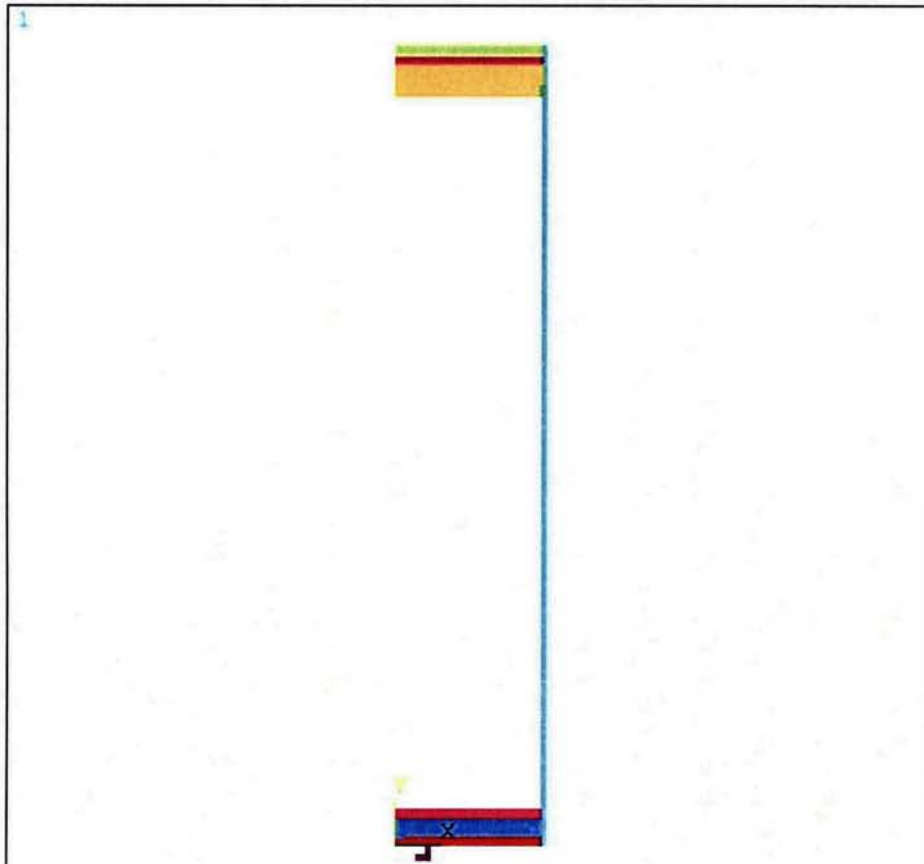


Figure A.3.9.1-1 2-D Canister Axisymmetrical Thermal and Stress Finite Element Model

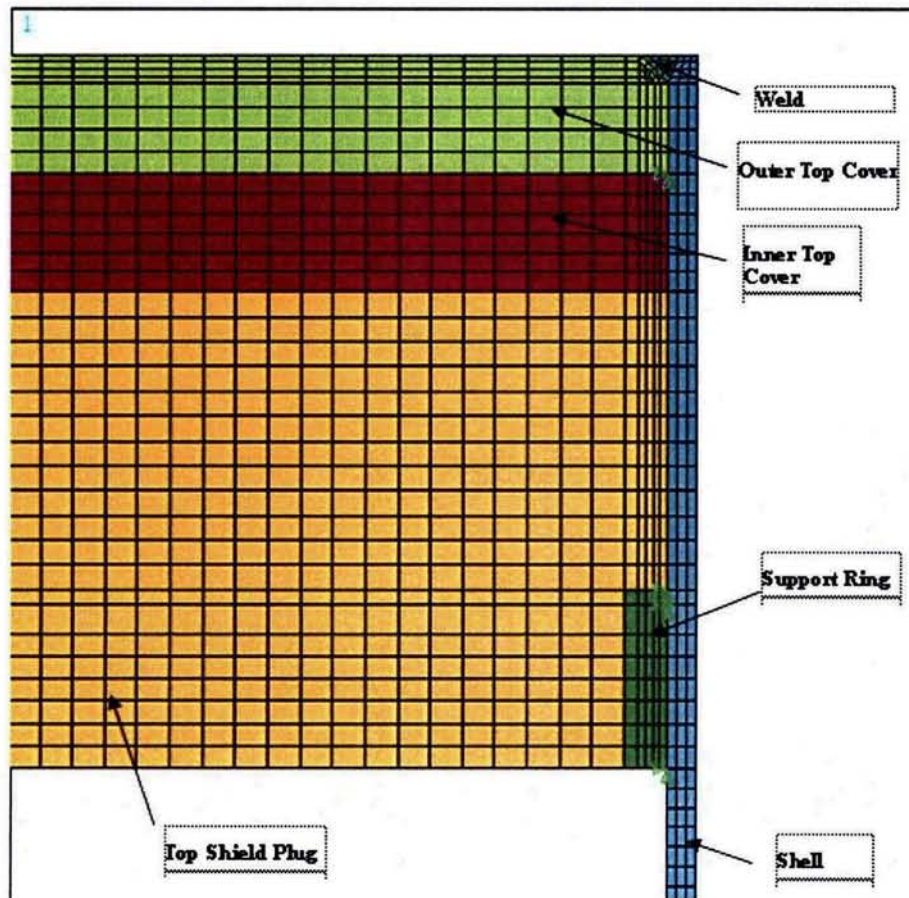


Figure A.3.9.1-2 Top End of the 2-D Axisymmetrical Canister Model

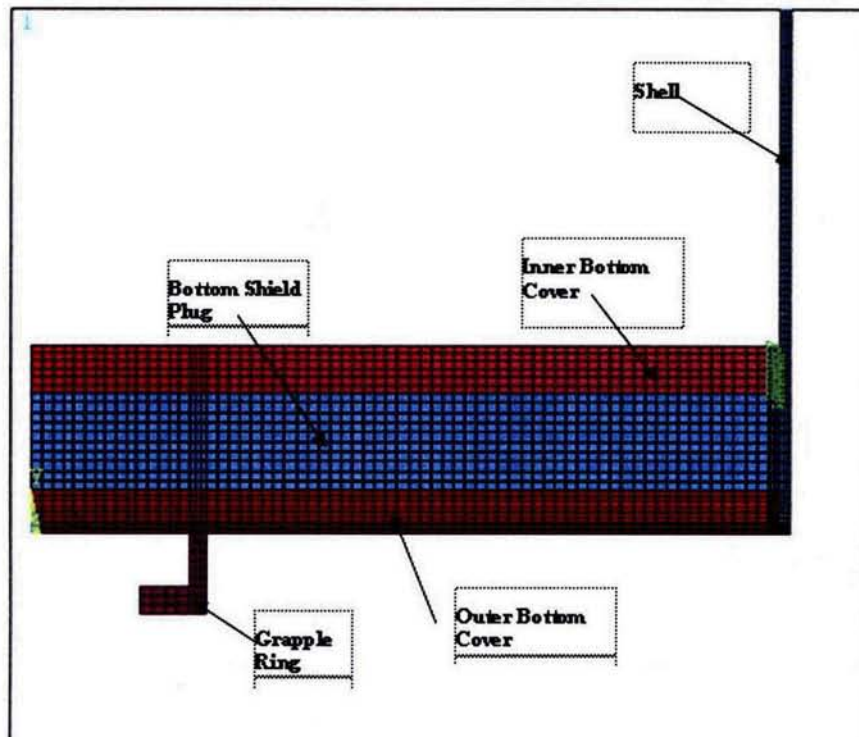


Figure A.3.9.1-3 Bottom End of the 2-D Axisymmetrical Canister Model

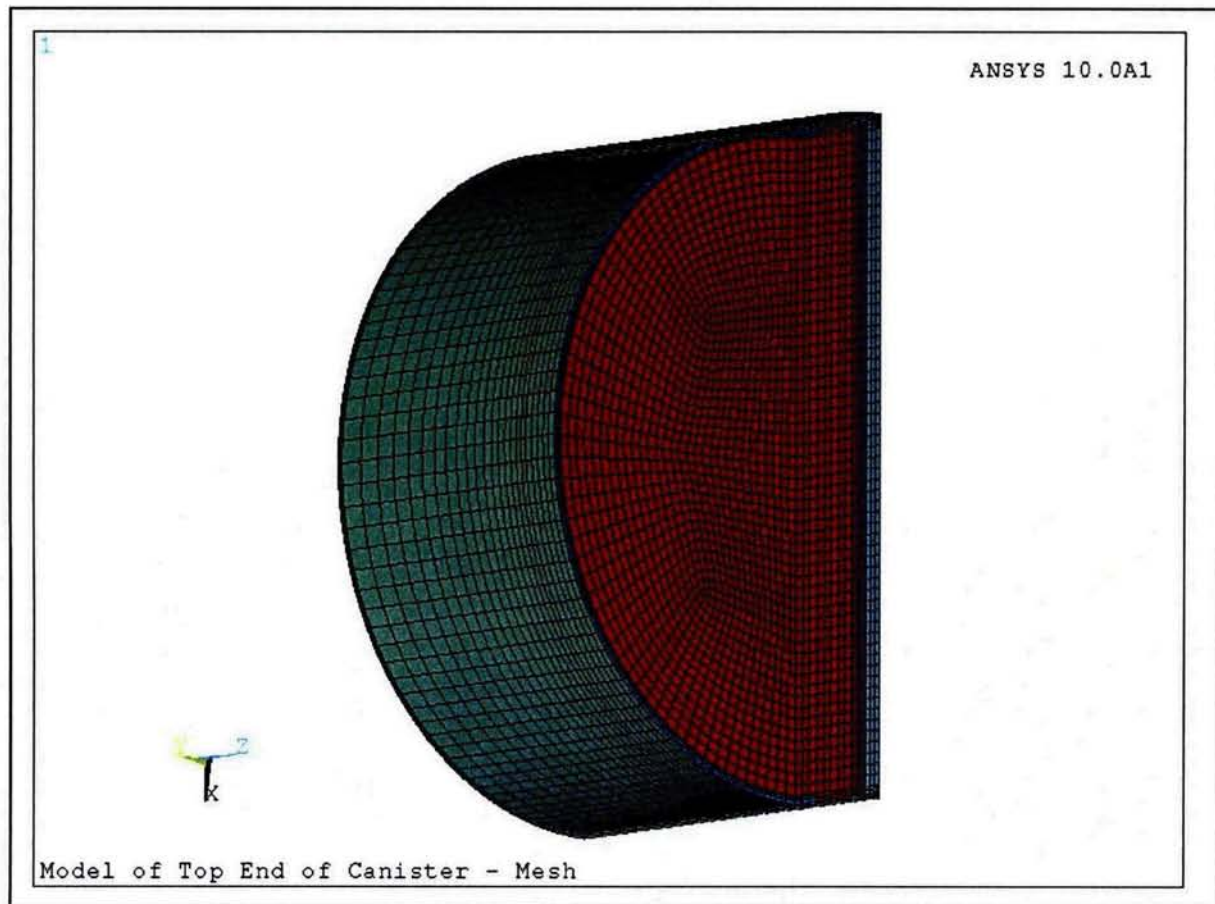


Figure A.3.9.1-4 3-D DSC Canister Top End Assembly Finite Element Model

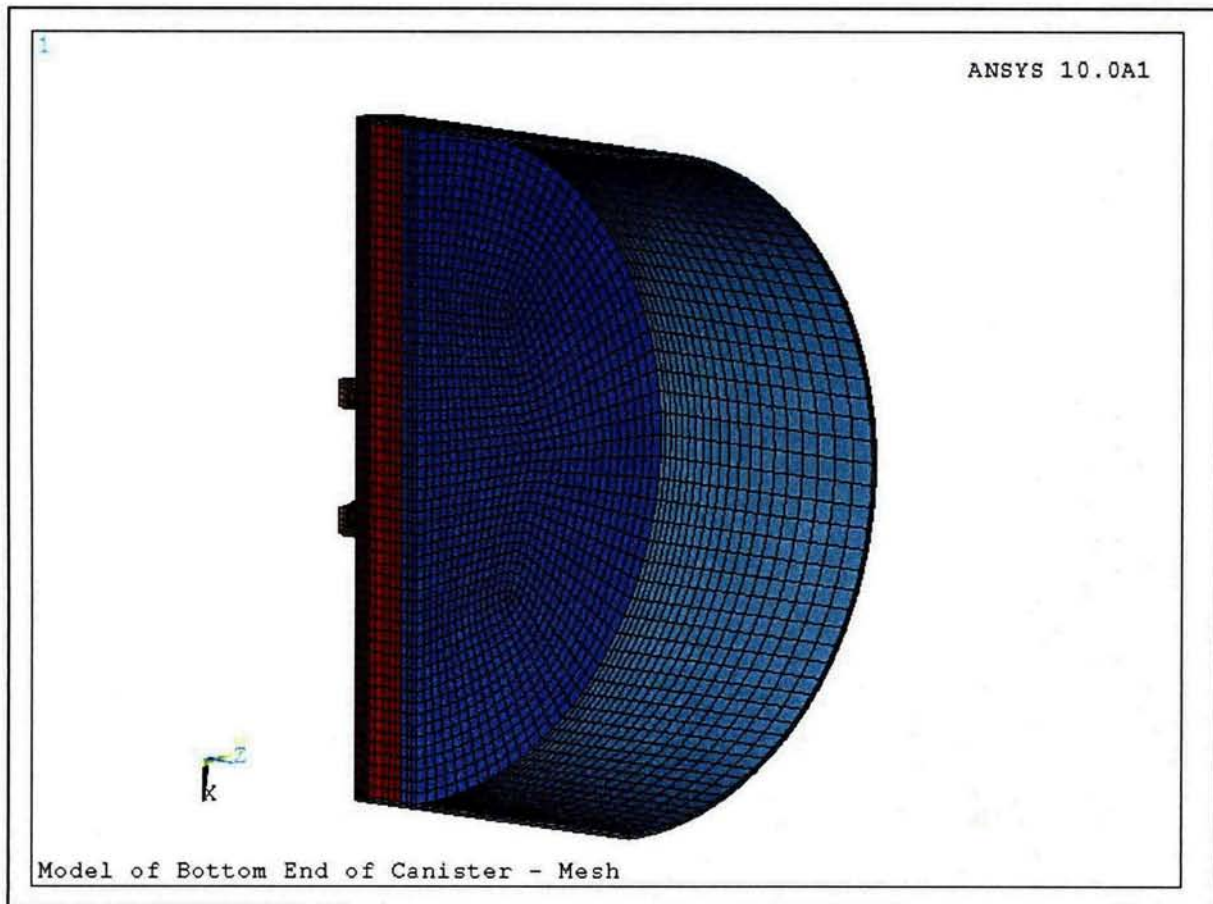


Figure A.3.9.1-5 3-D DSC Canister Bottom End Assembly Finite Element Model

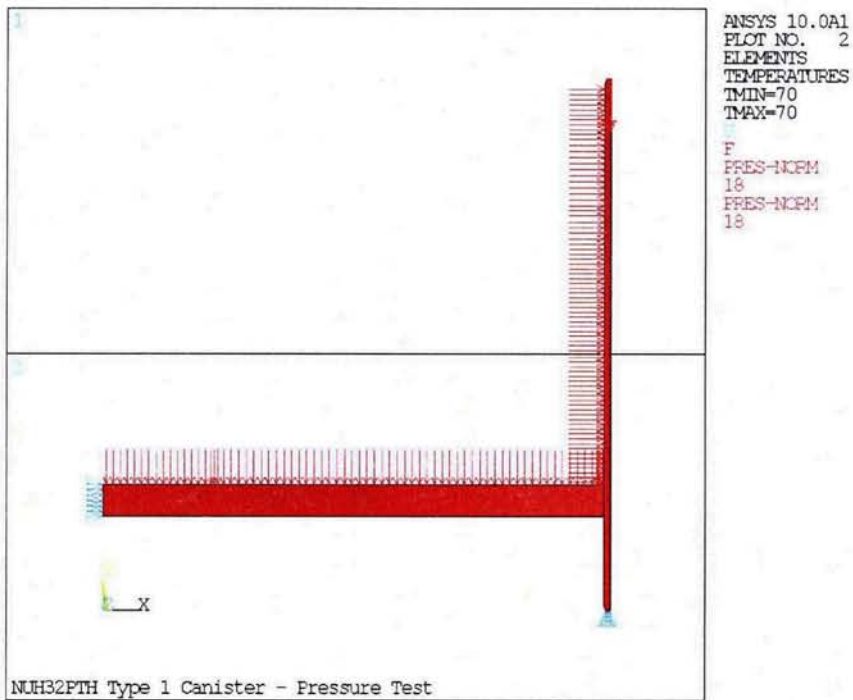
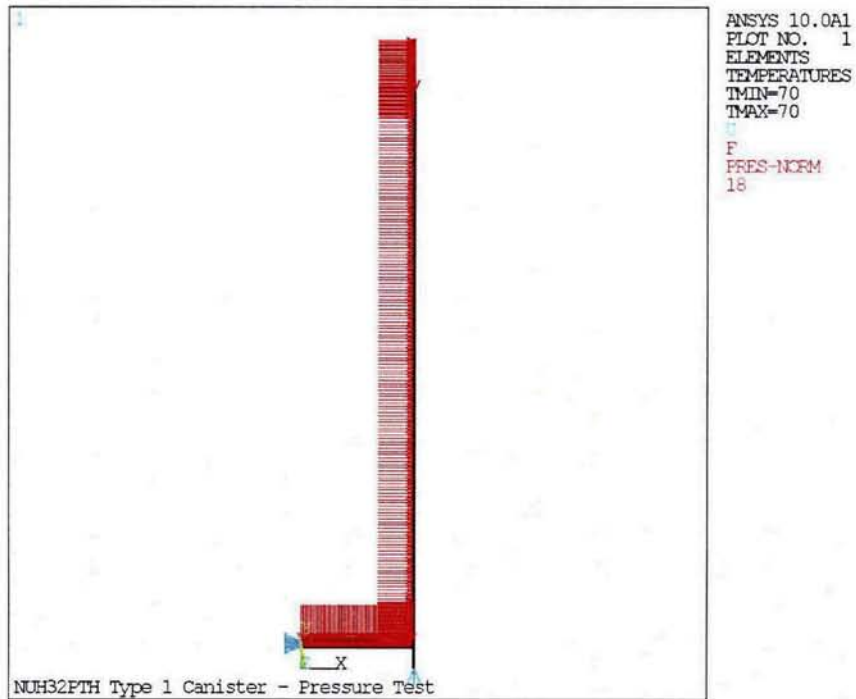


Figure A.3.9.1-6 32PTH Type 1 DSC Canister Finite Element Model used for Pressure Test Analysis

Appendix A.3.9.2 OS187H Type 1 Transfer Cask Body Structural Analysis

TABLE OF CONTENTS

A.3.9.2	OS187H TYPE 1 TRANSFER CASK BODY STRUCTURAL ANALYSIS	A.3.9.2-1
A.3.9.2.1	Introduction.....	A.3.9.2-1
A.3.9.2.2	ANSYS Analysis.....	A.3.9.2-4
A.3.9.2.3	ANSYS Analysis Results and Reporting Methodology	A.3.9.2-18
A.3.9.2.4	Evaluation of OS187H Type 1 Transfer Cask Trunnion Local Stresses	A.3.9.2-19
A.3.9.2.5	Stress and Deflection of Transfer Cask Inner Shell Support Rails...	A.3.9.2-26
A.3.9.2.6	References.....	A.3.9.2-28

LIST OF TABLES

Table A.3.9.2- 1	Transfer Cask Components Stress—Summary of Results.....	A.3.9.2-29
Table A.3.9.2- 2	Local Shell Stress at Trunnion Locations—Computation Spreadsheet for Case UT1	A.3.9.2-32
Table A.3.9.2- 3	Local Shell Stress at Trunnion Locations—Computation Spreadsheet for Case UT2	A.3.9.2-33
Table A.3.9.2- 4	Local Shell Stress at Trunnion Locations—Computation Spreadsheet for Case UT3	A.3.9.2-34
Table A.3.9.2- 5	Local Shell Stress at Trunnion Locations—Computation Spreadsheet for Case UT4	A.3.9.2-35
Table A.3.9.2- 6	Local Shell Stress at Trunnion Locations—Computation Spreadsheet for Case UT5	A.3.9.2-36
Table A.3.9.2- 7	Local Shell Stress at Trunnion Locations—Computation Spreadsheet for Case UT6	A.3.9.2-37
Table A.3.9.2- 8	Local Shell Stress at Trunnion Locations—Computation Spreadsheet for Case UT7	A.3.9.2-38
Table A.3.9.2- 9	Local Shell Stress at Trunnion Locations—Computation Spreadsheet for Case UT8	A.3.9.2-39
Table A.3.9.2- 10	Local Shell Stress at Trunnion Locations—Computation Spreadsheet for Case UT9	A.3.9.2-40
Table A.3.9.2- 11	Local Shell Stress at Trunnion Locations—Computation Spreadsheet for Case UT10	A.3.9.2-41

Table A.3.9.2– 12	Local Shell Stress at Trunnion Locations—Computation Spreadsheet for Case LT1	A.3.9.2-42
Table A.3.9.2– 13	Local Shell Stress at Trunnion Locations—Computation Spreadsheet for Case LT2	A.3.9.2-43
Table A.3.9.2– 14	Local Shell Stress at Trunnion Locations—Computation Spreadsheet for Case LT3	A.3.9.2-44
Table A.3.9.2– 15	Local Shell Stress at Trunnion Locations—Computation Spreadsheet for Case LT4	A.3.9.2-45
Table A.3.9.2– 16	Local Shell Stress at Trunnion Locations—Summary of Results	A.3.9.2-46

LIST OF FIGURES

Figure A.3.9.2– 1	Transfer Cask Key Components and Dimensions	A.3.9.2-47
Figure A.3.9.2– 2	2-Dimensional Finite Element Model, Element Plot.....	A.3.9.2-48
Figure A.3.9.2– 3	3-Dimensional Finite Element Model, Element Plot.....	A.3.9.2-49
Figure A.3.9.2– 4	115 °F Ambient Temperature Distribution.....	A.3.9.2-50
Figure A.3.9.2– 5	-20 °F Ambient Temperature Distribution	A.3.9.2-51
Figure A.3.9.2– 6	6 g Lifting Boundary Conditions (3D Half Model).....	A.3.9.2-52
Figure A.3.9.2– 7	30 psi Internal Pressure Boundary Conditions (2D Model)	A.3.9.2-53
Figure A.3.9.2– 8	Transfer Loads Boundary Conditions (3D Full Model)	A.3.9.2-54
Figure A.3.9.2– 9	75 g Bottom End Drop Boundary Conditions (2D Model)	A.3.9.2-55
Figure A.3.9.2– 10	75 g Top End Drop Boundary Conditions (2D Model).....	A.3.9.2-56
Figure A.3.9.2– 11	75 g Side Drop Boundary Conditions (3D Model)	A.3.9.2-57
Figure A.3.9.2– 12	Computational Worksheet for WRC 107 Bulletin Evaluation	A.3.9.2-58
Figure A.3.9.2– 13	NUHOMS OS187H Type 1 Transfer Cask Side Drop– 3D Finite Element Model.....	A.3.9.2-59
Figure A.3.9.2– 14	Transfer Cask Side Drop Model Top Cover/Flange/Lead Interface.....	A.3.9.2-60
Figure A.3.9.2– 15	Transfer Cask Side Drop Model Canister/Cask Shell/Lead/Interface	A.3.9.2-61
Figure A.3.9.2– 16	Transfer Cask Side Drop Model Canister/ Bottom Access Ram/Lead/Interface	A.3.9.2-62
Figure A.3.9.2– 17	Transfer Cask Side Drop Model—Rail Locations for Load Case 1	A.3.9.2-63
Figure A.3.9.2– 18	Transfer Cask Side Drop Model—Rail Locations for Load Case 2	A.3.9.2-64

Figure A.3.9.2– 19	Transfer Cask Side Drop—Sketch of Drop Modeling for Load Case 1	A.3.9.2-65
Figure A.3.9.2– 20	Transfer Cask Side Drop—Sketch of Drop Modeling for Load Case 2	A.3.9.2-66
Figure A.3.9.2– 21	Transfer Cask Side Drop Results—Inner Shell Stress Intensity for Load Case 1	A.3.9.2-67
Figure A.3.9.2– 22	Transfer Cask Side Drop Results—Outer Shell Stress Intensity for Load Case 1	A.3.9.2-68
Figure A.3.9.2– 23	Transfer Cask Side Drop Results—Inner Shell Stress Intensity for Load Case 2	A.3.9.2-69
Figure A.3.9.2– 24	Transfer Cask Side Drop Results—Outer Shell Stress Intensity for Load Case 2	A.3.9.2-70

A.3.9.2 OS187H TYPE 1 TRANSFER CASK BODY STRUCTURAL ANALYSIS

A.3.9.2.1 Introduction

This appendix presents the structural analyses of the NUHOMS® OS187H Type 1 transfer cask (TC) body including the top cover, cylindrical shell assembly, bottom assembly, and the local stresses at the trunnion/cask body interface. The specific methods, models, and assumptions used to analyze the cask body for the various individual loading conditions specified in 10CFR72 [1] are described. The maximum stresses in each of the major components of the TC are reported in Section A.3.9.2.2.4 for each analyzed load case and load combination. The results are evaluated against the ASME Code [2] design criteria described in Section A.3.9.2.1.3.

The OS187H Type 1 TC body structural analyses use static linear elastic analysis and elastic-plastic analysis methods. The stresses and deformations due to the applied loads are determined using finite element models developed using the ANSYS [4] computer program and/or hand calculations.

Other components associated with the TC are described and analyzed in the following appendices:

Appendix A.3.9.3—OS187H Type 1 Transfer Cask Top Cover and Ram Access Cover Bolt Analyses

Appendix A.3.9.4—Not used (since the end and corner drops are not credible under 10CFR Part 72, the lead slump and inner shell buckling analysis of the OS187H Type 1 TC for the 75g end drop load are not documented).

Appendix A.3.9.5—OS187H Type 1 Transfer Cask Trunnion Analysis

Appendix A.3.9.6—OS187H Type 1 Transfer Cask Shield Shell Panel Structural Analyses

A.3.9.2.1.1 OS187H Type 1 Transfer Cask Geometry Description

Key dimensions of the OS187H Type 1 TC are shown in Figure A.3.9.2-1. As with the OS187H TC described in Section 3.9.2.1, the shell, or cask body of the cylinder assembly, is an open ended (at the top) cylindrical unit with an integral closed bottom end. This assembly consists of a concentric inner shell (SA-240, Type 304) and an outer shell (SA-240, Type 304) welded to a massive closure flange (SA-182, Type F304N) at the top and bottom ends. The annulus between the shells is filled with lead shielding. The top cover is bolted to the top flange by 24-1 1/2 in. diameter high strength bolts and sealed with an O-ring. A cover plate is provided to seal the bottom hydraulic ram access penetration of the cask (by 12-1/2 in. high strength bolts with an O-ring) during fuel loading and transferring of the canister to the ISFSI.

Two upper trunnions are provided for handling the TC in the plant's fuel/reactor building using a lifting yoke and an overhead crane. Two lower support trunnions are provided for pivoting the TC from/to the vertical and horizontal positions on the support skid/transport trailer.

The overall dimensions of the OS187H Type 1 TC are 210.5 inches long and 92.11 inches in diameter. The TC structural shell is 83.63 inches in diameter. The TC cavity is 198.75 inches long and 70.50 inches in diameter. A detailed physical description of the TC is provided in

Chapter A.1. Chapter A.1, Section A.1.5 also contains reference drawings of the NUHOMS® OS187H Type 1 TC which are the source of dimensions and other information used to develop analysis models.

The gross weight of the loaded TC is approximately 120 tons (240 kips) including a 32PTH Type 1 DSC payload (dry) of 54.3 tons (108.61 kips), and a cask spacer (0.89 kips). Sections A.3.9.2.1.2 and Figure A.3.9.2-1 summarize the component weights and key dimensions of the NUHOMS® OS187H Type 1 TC, respectively.

This appendix evaluates the structural integrity of the OS187H Type 1 TC main structural members during all normal and hypothetical accident condition loadings.

A.3.9.2.1.2 Transfer Cask Component Weights

The following tables summarize the component weights of the NUHOMS® OS187H Type 1 TC as well as the dry loaded NUHOMS®-DSC weight, that are used for the TC structural evaluation.

OS187H Type 1 Transfer Cask Component Weights

Transfer Cask Component	Weight (lb x 1000)
Structural shell	23.73
Inner shell	7.89
Lead gamma shield	66.65
Top flange	2.63
Bottom flange	3.40
Top cover	5.36
Bottom assembly	3.94
Neutron shield panel (including water)	13.81
Upper trunnions (2)	1.45
Lower trunnions (2)	1.06
Total Transfer Cask Empty Weight	130.00⁽¹⁾
Total 32PTH Type 1 Weight (dry)	108.61
Cask Spacer	0.89
Total Transfer Cask Loaded Weight (dry)	240.00⁽¹⁾

Note:

(1) Rounded up to nearest 1000 lbs.

Dry Loaded 32PTH Type 1 DSC Weight

Transfer Cask Payload	Weight (lb x 1000)	Weight Used for Analysis (lb x 1000)
32PTH Type 1 canister	28.44	
32PTH Type 1 basket	29.45	
Fuel assemblies (32)	50.72	
Total 32PTH Type 1 DSC Weight	108.61	110.00
Cask spacer	0.89	5.00
Total Payload	109.5	115.00

A.3.9.2.1.3 Stress Criteria

The stress criteria used for the OS187H Type 1 TC is summarized in the table below. The resulting stresses are compared with the allowable stresses set forth by ASME B&PV Code, Section III, Subsection NC [2] for normal conditions and ASME B&PV Code, Section III, Appendix F [3] for accident conditions.

Service Level	Analysis Method	Stress Category	Stress Criteria
A (Normal Conditions)	Elastic Analysis	Primary Membrane Stress, P_m	S_m
		Primary Membrane + Bending Stress, $P_m + P_b$	$1.5 S_m$
		Primary + Secondary Stress, $P_m + P_b + Q$	$3 S_m$
D (Accident Conditions)	Elastic Analysis	Primary Membrane Stress, P_m	Lesser of $2.4 S_m$ or $0.7 S_u$
		Primary Local Membrane Stress, P_L	Lesser of 150% of P_m Stress Limit, or S_u
		Primary Membrane + Bending Stress, $P_m + P_b$	Lesser of $3.6 S_m$ or S_u
	Elastic Plastic Analysis	Primary Membrane Stress, P_m	Greater of $0.7 S_u$ and $S_y + 1/3(S_u - S_y)$
		Primary Membrane + Bending Stress, $P_m + P_b$	$0.9 S_u$

A.3.9.2.1.4 Material Properties

The material properties used for the analysis of the OS187H Type 1 TC are the same as those provided in Section 3.3 and Section 3.9.2.1.4 for the OS187H TC with the exception of the shielding material used in the top and bottom covers of the OS187H Type 1 TC, which uses a castable neutron shielding (NS-3) material instead of the resin material used in the OS187H TC. As discussed in Section A.3.3, the mechanical properties of these two shielding materials are not significantly different.

The NUHOMS® OS187H Type 1 TC is primarily constructed from SA-240 Type 304 stainless steel. The massive flanges at the top and bottom ends are machined forgings made of SA-182 Type 304N. The upper and lower trunnions are solid monolithic steel components made of SA-182 Type FXM-19 and SA-182 Type 304N, respectively. The top cover is constructed from SA-240 Type XM-19, or SA-182 Type FXM-19 (material properties for SA 240 Type XM-19 are bounding and used in the analysis). SA-540 Grade B23 Class 1 is used for the top cover and bottom cover bolts. Chemical lead is used for radial gamma shielding; NS-3 [5] is used for the solid axial neutron shielding, and liquid water is used for radial neutron shielding.

A.3.9.2.2 ANSYS Analysis

A.3.9.2.2.1 Geometry Description

The top cover, inner shell, structural shell, and bottom assembly are the primary structural members of the cask. Key components and dimensions of the confinement vessel are shown in Figure A.3.9.2-1. Chapter A.1 contains reference drawings of the NUHOMS® OS187H Type 1 TC which are the source of dimensions and other information used to develop analysis models.

A.3.9.2.2.2 Allowable Stresses

No change. The allowable stresses used for the stress evaluation of the OS187H Type 1 TC are the same as those for the OS187H TC, documented in Section 3.9.2.2.2. These allowables are based on conservative bounding temperatures of 300 °F and 400 °F for the outer and inner shells, respectively (the maximum temperatures from Chapter 4 thermal analysis are 280 °F and 340 °F, respectively). For the elastic-plastic analysis documented in Section A.3.9.2.5, the allowable stresses for the outer and inner shells are based on a bounding temperatures of 350 °F.

A.3.9.2.2.3 OS187H Type 1 Transfer Cask Finite Element Models

Three separate finite element models (FEMs) were constructed. The first is a 2-dimensional, axisymmetric representation of the cask, which is constructed with plane elements. The second model is a 180° (or half-symmetry model) 3-dimensional representation of the TC using “brick” elements. The third model is a 360° (or full model) 3-dimensional representation using “brick” elements.

A. 2-Dimensional Finite Element Model Description

A 2-dimensional axisymmetric ANSYS [4] finite element model, constructed primarily from PLANE42 elements, is used to analyze all axisymmetric load cases. The basic dimensions of the OS187H Type 1 TC are provided in Figure A.3.9.2-1. An element plot of the 2-dimensional FEM is shown in Figure A.3.9.2-2.

Model Material Properties

No change. The temperature dependent material properties used for the analysis of the OS187H Type 1 TC are based on the same temperature distributions applied to the OS187H TC. The temperature distributions applied to the OS187H Type 1 TC are shown in Figure A.3.9.2-4 and Figure A.3.9.2-5 for the 115 °F and -20 °F ambient conditions.

Unmodeled Components

As with the OS187H TC, only the structural steel section of the top cover (3 in. thick.) is modeled. The top neutron shield material, the ¼ in. thickness top cover outer plate, and hoist ring standoffs are not modeled since they are not intended to provide any structural support. However, their inertial load is accounted for by increasing the density of the structural portion of the top cover.

The weight of the unmodeled top cover components (neutron shield, 1/4" top cover, and hoisting standoffs) is approximately 1,114 lb. The weight of the structural steel portion of the top cover is 4,246 lb. Thus, the total top cover weight, including the unmodeled components, is 5,360 lb. The density of the top cover is calculated in the ANSYS model based on this total weight.

The radial neutron shield (water) and neutron shield panel are also not modeled, because they are not considered structural components of the transfer cask. Therefore, the density of the structural shell of the transfer cask is increased to account for these unmodeled components. The weight of the unmodeled radial neutron shield assembly is 13,806 lb. The weight of the structural shell is 23,729 lb. Thus, the total weight, including the unmodeled neutron shield assembly is 37,535 lb. This total weight is used to calculate the density of the structural shell in the ANSYS model.

Top Cover and Ram Access Cover Bolts

No change. The top cover and ram access cover bolts are modeled with axisymmetric BEAM3 elements, and are only used in the model to simulate the overall behavior of the closure joints. The stresses in the top cover and ram access cover bolts are evaluated separately in Appendix A.3.9.3. The element real constants for the top cover and the ram access cover bolts used in the ANSYS analysis are not changed from those used in the OS187H analysis.

The initial strains in BEAM3 elements are adjusted to match the minimum preload values of 27,270 lb and 6,364 lb for the top cover bolts and for the ram access cover bolts, respectively.

Contact Elements

CONTAC12 elements are placed between all surfaces of the top flange and top cover, between the ram access cover and ram access penetration that contact each other, and between the lead gamma shielding and the inner and structural shells. These contact elements are used to model the reaction forces that occur between these surfaces.

The contact elements introduce nonlinearities in the analysis depending on whether they are open or closed. Initially, at all contact surfaces, the gaps are closed. The contact element spring constant, K_n , is calculated in the following way.

$$K_n = f E h [4]$$

Where,

f = A factor usually between 0.01 to 100.

E = Modulus of elasticity (27.0×10^6 psi for SA-240, Type 304 @ 300 °F)

E_{lead} = Modulus of Elasticity (2.06×10^6 psi for ASTM B-29 chemical lead @ 300 °F)

h = contact target length.

Average radius of lead, $h \approx 37.66$ in.

Therefore,

$$K_n = 27.0 \times 10^6 \times 37.66 \times f \approx 1.0 \times 10^7 \text{ to } 1.0 \times 10^{11} \text{ lb/in. for steel}$$

$$K_n = 2.06 \times 10^6 \times 37.66 \times f \approx 7.8 \times 10^5 \text{ to } 7.8 \times 10^9 \text{ lb/in. for lead}$$

Thus, there is a very wide range for the K_n value. For the 2-D finite element model, the structure responded well with a spring constant value of 1.0×10^6 lb/in. for the lead shield contact elements and 1.0×10^7 lb/in. for the top cover and ram access cover contact elements.

Boundary Conditions

Separate sets of boundary conditions are required for the various loading cases analyzed. The boundary condition sets are used to prevent rigid body motion and are assigned based on the specific loading configuration. In each of the boundary condition sets, displacement constraints are fixed such that no displacement is permitted in the prescribed direction.

B. 3-Dimensional Finite Element Models Description

A 3-dimensional ANSYS [4] finite element model, constructed primarily from SOLID45 elements, is used to analyze all non-axisymmetric load cases. A 180° version (half symmetry model) is used for symmetric load cases such as the 6 g lifting and side drop load cases. A 360° version (full model) is used for asymmetric load cases such as the transfer load cases. A plot of the 3-dimensional FEM (half model) is shown in Figure A.3.9.2-3.

Model Material Properties

No change. As in the 2-dimensional model, the temperature dependent material properties used for the analysis of the OS187H Type 1 TC are based on the same temperature distributions applied to the OS187H TC.

Unmodeled Components Weights

Only the structural steel section of the top cover (3 in. thick.) is modeled. The top neutron shield material, the $\frac{1}{4}$ in. thickness top cover outer plate, and hoist ring standoffs are not modeled since they are not intended to provide any structural support. However, their inertial load is accounted for by increasing the density of the structural portion of the top cover.

The weight of the unmodeled top cover components (neutron shield, $\frac{1}{4}$ " top cover, and hoisting standoffs) is approximately 1,114 lb. The weight of the structural steel portion of the top cover is 4,246 lb. Thus, the total top cover weight including the unmodeled components is 5,360 lb. The density of the top cover is calculated in the ANSYS model based on this total weight.

The radial neutron shield (water) and neutron shield panel are also not modeled, because they are not considered structural components of the TC. The weight of the unmodeled radial neutron shield assembly is 13,806 lb. Therefore, the density of the structural shell of the TC is increased by 13,806 lb to account for the unmodeled components.

The NS-3 material in the bottom cask cover weighs 554 lb and is not modeled. Therefore, the densities of the bottom end plate, the bottom neutron shield plate, and the bottom flange components in the ANSYS model are increased in proportion to their respective weights to account for the unmodeled bottom neutron shield weight.

Top Cover and Ram Access Cover Bolts

No change. The top cover and ram access cover bolts are modeled with BEAM4 elements, and are only used in the model to simulate the overall behavior of the closure joints. The stresses in the top cover and ram access cover bolts are evaluated separately in Appendix A.3.9.3. The element real constants for the top cover and the ram access cover bolts used in the ANSYS analysis are not changed from those used in the OS187H analysis.

The initial strains in BEAM4 elements are adjusted to match the minimum preload values of 27,270 lb and 6,364 lb for the top cover bolts and for the ram access cover bolts, respectively.

Contact Elements

CONTAC52 elements are placed between all surfaces of the top flange and top cover, between the ram access cover and ram access penetration that contact each other, and between the lead gamma shielding and the inner and structural shells. These contact elements are used to model the reaction forces that occur between closure surfaces. LINK8 elements with a very low modulus of elasticity and density are placed in all locations where CONTAC52 elements exist in order to maintain overall stability of the model. This is only required in the 3-dimensional model.

The contact elements introduce nonlinearities in the analysis depending on whether they are open or closed. Initially, at all contact surfaces, the gaps are closed. The contact element spring constant, K_n , is calculated in the following way [4].

$$K_n = f E h$$

Where,

f = A factor usually between 0.01 to 100.

E = Modulus of elasticity (27.0×10^6 psi for SA-240, type 304 @ 300 °F)

h = contact target length (i.e., the square root of target area).

Typical element length $\approx 1/2$ in.

Typical element width ≈ 1 in.

Typical target length, $h = (0.5 \times 1.0)^{0.5} = 1.22$ in.

Therefore,

$$K_n = 25.8 \times 10^6 \times 1.22 \times f \approx 3.39 \times 10^5 \text{ to } 3.39 \times 10^9 \text{ lb/in.}$$

Thus, there is a very wide range for the K_n value. For the 3-D finite element model, the structure responded well with a spring constant value of 1.0×10^7 lb/in. for the lead shield contact elements and 1.0×10^8 lb/in. for the top cover and ram access cover contact elements.

A.3.9.2.2.4 Load Cases

The following two tables describe the normal (Level A) and accident (Level D) condition load cases analyzed in this calculation. The load cases considered consist of 115 °F hot ambient and -20 °F cold ambient environments, 30 psig internal, vacuum drying conditions, transfer loads,

and 75 g accident condition end and side drops. The normal and accident load conditions are summarized in the following table.

Summary of Normal and Accident Load Conditions

Load Case Number	Loading Condition	Service Level	Case Description
1A	6 g vertical lifting	A	Cask vertical, supported at top trunnions, 6 g vertical acceleration + 30 psi internal pressure
1B	6 g vertical lifting + thermal loads	A	Cask vertical, supported at top trunnions, 6 g vertical acceleration + 30 psi internal pressure + 115 °F ambient
2	Vacuum drying	A	Cask vertical, supported at cask bottom, 15 psi external pressure + vacuum drying thermal loads
3	30 psi internal pressure	A	30 psi internal pressure
4	115 °F ambient hot thermal environment	A	115 °F ambient temperature
5	-20 °F ambient cold thermal environment	A	-20 °F ambient temperature
6A	Transfer inertial loads—axial accel. toward bottom	A	Cask horizontal, 2 g acceleration in all directions—axial acceleration toward the bottom of the cask
6B	Transfer inertial loads—axial accel. toward top	A	Cask horizontal, 2 g acceleration in all directions—axial acceleration toward the top of the cask
7A	Transfer loads—axial accel. toward bottom + internal pressure	A	Cask horizontal, 2 g acceleration in all directions—axial acceleration toward the bottom of the cask + 30 psi internal pressure
7B	Transfer loads—axial accel. toward top + internal pressure	A	Cask horizontal, 2 g acceleration in all directions—axial acceleration toward the top of the cask + 30 psi internal pressure
7C	Transfer loads + 115 °F ambient + internal pressure	A	Cask horizontal, supported at top and bottom trunnions, 2 g acceleration in all directions + 30 psi internal pressure + 115 °F ambient
8	Transfer loads + -20 °F ambient + internal pressure	A	Cask horizontal, supported at top and bottom trunnions, 2 g acceleration in all directions + 30 psi internal pressure + -20 °F ambient
9	75 g bottom end drop + internal pressure	D	Cask vertical, supported at bottom, 75 g vertical up acceleration + 30 psi internal pressure
10	75 g top end drop + internal pressure	D	Cask vertical, supported at top, 75 g vertical down acceleration + 30 psi internal pressure
11	75 g side drop + internal pressure	D	Cask horizontal, supported on side, 75 g transverse acceleration + 30 psi internal pressure
12	Transfer thermal accident (Fire)	D	30 psi internal pressure + thermal accident loads

Method of Applying Load to the Cask Body

Pressures applied in the axial direction are calculated based on load divided by pressure area calculation.

Pressures applied in the radial direction in the 3-dimensional finite element model are based on cosine distributed pressure functions. These pressure distributions simulate the internal cask contents applying pressure to the inner cask wall. The pressure distribution is assumed to be in the longitudinal direction over a specified length and vary with a cosine distribution around the circumference of the cask.

The following sections describe the boundary conditions used for each individual load case and load combination.

Load Case 1: 6 g Lifting (3-D FEM)

The 6 g Lifting Load case consists of the loaded OS187H Type 1 TC in the vertical position, supported by the two top trunnions. A 6 g vertical acceleration is conservatively used to bound the normal lifting load. An internal pressure of 30 psi is also applied.

The weight of the TC internals (canister, basket, and fuel assemblies) is accounted for by applying equivalent pressures. The weight of the cask internals used in this analysis is 115,000 lb. The TC inner radius is 35.25 in., and the inner radius of the ram access penetration is 11.00 in. The inertial load of the TC internals reacts against the annular surface bounded by these two radii during lifting. Therefore the area of the reaction surface, A_{6gi} , is as follows.

$$A_{6gi} = \pi(35.25^2 - 11.00^2) = 3,523.49 \text{ in}^2.$$

The pressure equivalent to the inertial load of the internals during a 6 g lift, P_{6gi} , is,

$$P_{6gi} = [115,000/3,523.49] \times 6 \text{ gs} = 195.83 \text{ psi}$$

Symmetry displacement boundary conditions are applied along the y-axis of the 3-dimensional axisymmetric model.

A depiction of the 6 g lifting load case boundary conditions is provided in Figure A.3.9.2-6.

Load Case 2: Vacuum Drying

The applied loads used to calculate the maximum stress in the TC during vacuum drying include a 15 psi external pressure, a maximum radial temperature gradient, and a 1g axial (gravity) load. The stresses generated in the TC shell by these three loads are computed using hand calculations. Since the primary load during vacuum drying is caused by the radial temperature gradient, the maximum TC stress is computed for the outer radial structural shell.

A uniform 15 psi pressure is applied to the external radial surface of the cask, generating a hoop stress in the cask structural shell. The hoop stress, σ_p , in the shell is computed in the following way.

$$\begin{aligned}\sigma_p &= \text{external pressure} \times \text{the mean structural shell radius} / \text{the minimum structural shell thickness} \\ &= 15 \text{ psi} \times (78.87 + 1.50)/2 \text{ in.} / 1.50 \text{ in.} = 402 \text{ psi}\end{aligned}$$

The stress generated in the structural shell by the 1g axial load is conservatively computed assuming that the weight of the entire TC is taken by the cross sectional area of the structural shell. The weight of the TC is conservatively taken to be 250,000 lb. The 1g axial stress in the structural shell, σ_g , is computed as follows.

$$\begin{aligned}\sigma_g &= 1g \times \text{maximum TC weight} / \text{minimum cross sectional area of the structural shell} \\ &= 1g \times 250,000 / [(\pi/4) \times (81.87^2 - 78.87^2)] = 660 \text{ psi}\end{aligned}$$

The maximum hoop stress generated by the radial thermal gradient during the vacuum drying process will occur in the outer structural shell due to the thermal expansion of the lead gamma shield. From Chapter 4, the maximum temperature difference between the lead gamma shield and the structural shell occurs during the drying process Procedure C at 42 hours, when the lead and structural shell are at 275 °F and 219 °F, respectively.

The change in the outer radius of the lead gamma shield, ΔR_l , is computed as follows.

$$\begin{aligned}\Delta R_l &= R_l \times \alpha_l \times \Delta T_l = 39.435 \text{ in.} \times 17.34 \times 10^{-6} \text{ in./in. } ^\circ\text{F} (@300 ^\circ\text{F}) \times (275 - 70) ^\circ\text{F} \\ &= 0.1402 \text{ in.}\end{aligned}$$

The change in the inner radius of the structural shell, ΔR_s , is computed as follows.

$$\begin{aligned}\Delta R_s &= R_s \times \alpha_s \times \Delta T_s = 39.435 \text{ in.} \times 8.9 \times 10^{-6} \text{ in./in. } ^\circ\text{F} (@200 ^\circ\text{F}) \times (219 - 70) ^\circ\text{F} \\ &= 0.0523 \text{ in.}\end{aligned}$$

Therefore the differential radial expansion between the lead and structural shell, ΔR , is as follows.

$$\Delta R = 0.1402 \text{ in.} - 0.0523 \text{ in.} = 0.0879 \text{ in.}$$

Therefore, the lead cylinder, if it were free, would grow 0.0879 in. more than the inner surface of the structural shell. If all of the differential expansion is accommodated in the lead, the lead strain, ϵ_l , would be the following.

$$\epsilon_l = \Delta R / R_l = 0.0879 \text{ in.} / 39.435 \text{ in.} = 0.00223 \text{ in./in.}$$

If the lead remained linear elastic, the maximum hoop stress in the lead would be,

$$\sigma_l = E_l \times \epsilon_l = 2.06 \times 10^6 \text{ psi} (@300 ^\circ\text{F}) \times 0.00223 \text{ in./in.} = 4,594 \text{ psi}$$

Conservatively assuming that the lead remains linear elastic, the interference pressure on the outer structural shell required to exert an average hoop stress of 4,594 psi in the lead can be determined in the following way.

$$P_{\text{interface}} = \sigma_l \times \text{lead thickness} / R_{\text{interface}} = 4,594 \text{ psi} \times 3.56 \text{ in.} / 39.435 \text{ in.} = 415 \text{ psi}$$

This interference pressure would generate the following hoop stress in the structural shell.

$$\sigma_s = P_{interface} \times R_{interface}/\text{shell thickness} = 415 \text{ psi} \times 39.435/1.50 = 10,910 \text{ psi}$$

The total combine maximum stress intensity, σ , in the TC during vacuum drying operations is then,

$$\sigma = 402 \text{ psi} + 660 \text{ psi} + 10,910 \text{ psi} = 11,972 \text{ psi}$$

Load Case 3: 30 psi Internal Pressure (2-D FEM)

A uniform 30 psi pressure is applied to the internal surface of the OS187H Type 1 TC up to the top cover and ram access cover seal locations. Symmetry displacement boundary conditions are applied along the y-axis of the 2-dimensional axisymmetric model, and the TC is held in the y-direction at one location to prevent rigid body motion. A depiction of the internal pressure load case boundary conditions is provided in Figure A.3.9.2-7.

Load Case 4: 115 °F Ambient Hot Thermal Environment (2-D FEM)

The temperature distribution resulting from a 115 °F ambient environment is shown in Figure A.3.9.2-4. The distribution is based on the temperature profile used in the OS187H TC which is bounding when applied to the OS187H Type 1 TC. The temperature dependent coefficients of thermal expansion are applied to each corresponding material type, in order to induce thermal stresses in the model.

Symmetry displacement boundary conditions are applied along the cut boundary of the 2-dimensional axisymmetric model, and the TC is held in the axial direction at one location to prevent rigid body motion.

Load Case 5: -20 °F Ambient Cold Thermal Environment (2-D FEM)

The temperature distribution resulting from a -20 °F ambient environment is shown in Figure A.3.9.2-5. The distribution is based on the temperature profile used in the OS187H TC which is bounding when applied to the OS187H Type 1 TC. The temperature dependent coefficients of thermal expansion are applied to each corresponding material type, in order to induce thermal stresses in the model.

Symmetry displacement boundary conditions are applied along the cut boundary of the 2-dimensional axisymmetric model, and the TC is held in the axial direction at one location to prevent rigid body motion.

Load Case 6-8: Transfer Loads (3-D FEM)

The transfer load cases consist of the loaded TC in the horizontal position, supported at both upper and lower trunnions in the vertical direction, supported at the bottom two trunnions in the axial direction, and supported at one side of the trunnion towers of the skid (the loaded side) in the lateral (transverse) direction.

An acceleration of 2 g in all directions (axial, vertical, and transverse) is applied to the TC model in order to bound all possible transfer accelerations. For the transverse and vertical directions, the

weights of the DSC and spacer are accounted for by applying a cosine varying pressure on the inside surface of the inner shell. The approach is explained below.

The vertical and transverse accelerations are combined, so that a single horizontal acceleration is applied to the finite element model in the following way.

$$\text{Resultant Acceleration} = [2 g^2 \text{ transverse} + 2 g^2 \text{ vertical}]^{1/2} = 2.828 g$$

The resultant inertial load of the TC internals is accounted for by applying a cosine varying pressure on the inside surface of the cask inner shell. Assuming that the TC internals react upon 90° arc of the inside surface, then the inertial load of the internals, $P_{(\theta)}$, which varies with angle, θ , ($\theta = 0$ is at the impact point), is governed by the following expression.

$$P_{(\theta)} = P_{\max} \cos(2\theta)$$

Where P_{\max} is the maximum load at the impact point ($\theta = 0$). Assuming the axial length of the applied load is L , the inside radius of the cask inner shell is R , and the load distribution, $P_{(\theta)}$ above, then the total inertial load generated by the internals, F , is the following.

$$F = \int_{-\frac{\pi}{4}}^{\frac{\pi}{4}} P_{\max} \cos(2\theta) \cos(\theta) LR d\theta$$

or,

$$F = \frac{P_{\max} LR}{2} \int_{-\frac{\pi}{4}}^{\frac{\pi}{4}} \cos((2+1)\theta) + \cos((2-1)\theta) d\theta$$

By integrating we get the following.

$$F = \left[\frac{P_{\max} LR}{2} \right] \left[\frac{\sin(3\theta)}{3} + \sin(\theta) \right]_{-\frac{\pi}{4}}^{\frac{\pi}{4}}$$

Therefore,

$$F = \left[\frac{P_{\max} LR}{2} \right] \left[\frac{\sin\left(\frac{3\pi}{4}\right)}{3} + \sin\left(\frac{\pi}{4}\right) - \frac{\sin\left(\frac{-3\pi}{4}\right)}{3} - \sin\left(\frac{-\pi}{4}\right) \right]$$

$$F = P_{\max} LR \left[\frac{\sin\left(\frac{3\pi}{4}\right)}{3} + \sin\left(\frac{\pi}{4}\right) \right]$$

The applied forces are the inertial load of the DSC, F_i , and the inertial load of the spacer and air wedges, F_s :

$$F_i = 110,000 \text{ lb} \times 2.828 g = 311,080 \text{ lb},$$

$$F_s = 5,000 \text{ lb} \times 2.828 g = 14,140 \text{ lb. (spacer weight of 5,000 lb is bounding; see section A.3.9.2.1.2)}$$

Additional input data are:

$$\begin{array}{ll} \text{TC inner shell inner diameter,} & R = 35.25 \text{ in.,} \\ \text{axial length of the applied DSC load,} & L_i = 190.25 \text{ in., and} \\ \text{axial length of the applied spacer load,} & L_s = 5.0 \text{ in., are applied} \end{array}$$

Therefore, P_{\max} for the DSC and spacer are the following:

$$P_{i\max} = \frac{311,080}{(190.25)(35.25)} \left[\frac{\sin\left(\frac{3\pi}{4}\right)}{3} + \sin\left(\frac{\pi}{4}\right) \right]^{-1} = 49.2 \text{ psi}$$

$$P_{s\max} = \frac{14,140}{(6)(35.25)} \left[\frac{\sin\left(\frac{3\pi}{4}\right)}{3} + \sin\left(\frac{\pi}{4}\right) \right]^{-1} = 70.9 \text{ psi}$$

The axial inertial load of the TC internals is accounted for by applying a pressure on the inside surface of the cask lid. For a 2 g inertial load, the applied axial pressure, P_a , is as follows.

$$P_{aBOT} = 115,000 \text{ lb} \times 2 g / [\pi \times (35.25^2 - 11^2)] = 65.28 \text{ psi} - \text{Cases 6A and 7A}$$

$$P_{aTOP} = 115,000 \text{ lb} \times 2 g / [\pi \times 35.83^2] = 57.03 \text{ psi} - \text{Cases 6B and 7B}$$

Transfer loads are run with and without internal pressure of 30 psi to bound any possible pressure build up inside the cask. Displacement constraints are applied at the trunnion locations to the 3-dimensional full model.

A depiction of the transfer loads load case boundary conditions is provided in Figure A.3.9.2-8.

Load Case 9: 75 g Bottom End Drop (2-D FEM)

The bottom end drop is not considered credible during storage and transfer operations under 10 CFR Part 72 because the TC will always be in the horizontal orientation. The bottom drop evaluation documented below is performed in support of a 10 CFR Part 50 evaluation that may be performed by the user if the user cannot demonstrate that this accident drop is not credible.

The weight of the TC internals (canister, basket, spacer, and fuel assemblies) is accounted for by applying equivalent pressures. The total actual weight of the cask internals is 109.50 kips. For conservatism, the weight of the cask internals used in this analysis is increased to 115 kips. The TC inner radius is 35.25 in., and the inner radius of the ram access penetration is 11.00 in. The inertial load of the TC internals reacts against the annular surface bounded by these two radii during a bottom end drop. The area of this reaction surface, A_{bi} , is as follows.

$$A_{bi} = \pi(35.25^2 - 11.00^2) = 3,523 \text{ in}^2.$$

The pressure equivalent to the inertial load of the internals under accident conditions, P_{bi} , is,

$$P_{in} = [115,000 / 3,523] \times 75 \text{ gs} = 2,447.86 \text{ psi}$$

Internal pressure of 30 psi is applied.

Symmetry displacement boundary conditions are applied along the y -axis of the 2-dimensional axisymmetric model. The bottom end of the TC is held in the axial direction in order to simulate the rigid reaction force generated by the impact target. A 75 g inertial load in the positive y -direction is also applied to the model for the accident condition load case.

A depiction of the Bottom End Drop load case boundary conditions is provided in Figure A.3.9.2-9.

Load Case 10: 75 g Top End Drop (2-D FEM)

The top end drop is not considered credible during storage and transfer operations under 10 CFR Part 72 because the TC will always be in the horizontal orientation. The top end drop evaluation documented below is performed in support of a 10 CFR Part 50 evaluation that may be performed by the user if the user cannot demonstrate that this accident drop is not credible.

The weight of the TC internals (canister, basket, spacer, and fuel assemblies) is accounted for by applying equivalent pressures. The weight of the canister internals used in this analysis is 115,000 lb. The inertial load of the TC internals reacts against the inside surface of the top cover assembly during a top end drop. The outer radius of the inside surface of the TC top cover assembly is 35.675 in. Therefore the area of the reaction surface, A_{bi} , is as follows.

$$A_{bi} = \pi(35.675^2) = 3,998.32 \text{ in}^2.$$

The pressure equivalent to the inertial load of the internals under accident conditions, P_{bi} , is,

$$P_{in} = [115,000/3,998.32] \times 75 \text{ gs} = 2,157.16 \text{ psi}$$

The internal pressure of 30 psi is also applied to the model.

Symmetry displacement boundary conditions are applied along the y-axis of the 2-dimensional axisymmetric model. The outer surface of the top cover is held in the axial direction in order to simulate the rigid reaction force generated by the impact target. A 75 g inertial load in the negative y-direction is also applied to the model for the accident condition load case.

A depiction of the top end drop load case boundary conditions is provided in Figure A.3.9.2-10.

Since the top end vertical drop will induce much higher shear stress in the weld between the TC inner shell and top flange, this load case is used to calculate the weld stresses. The ANSYS run result file from this load case is post processed to get the maximum shear stress at this weld location.

The maximum shear stress is 7,991 psi and the allowable shear stress is $0.42 S_u$ ($0.42 \times 64,000 = 26,880$ psi, for 304 SS at 400 °F). Factor of safety = $26,880/7,991 = 3.36$.

Load Case 11: 75 g Side Drop (3-D FEM)

During the 75 g side drop load case, the loaded TC is dropped onto a concrete target generating a transverse acceleration of 75 g.

The impact side of the TC is supported in the cask radial direction along the entire length of the cask. The radial support spans 15° of the 180° model. The radial support is intended to model the reaction of the concrete target during impact.

The inertial load of the TC internals is accounted for by applying a cosine varying pressure on the inside surface of the cask inner shell using the same method that was used for the transfer loads case. The applied forces are the inertial load of the DSC, F_i , and the inertial load of the spacer and air wedges, F_s :

$$F_i = 110,000 \text{ lb} \times 75 \text{ g} = 8,250,000 \text{ lb},$$

$$F_s = 5,000 \text{ lb} \times 75 \text{ g} = 375,000 \text{ lb}.$$

Therefore, P_{\max} for the DSC and spacer are the following:

$$P_{i\max} = \frac{8,250,000}{(190.25)(35.25)} \left[\frac{\sin\left(\frac{3\pi}{4}\right)}{3} + \sin\left(\frac{\pi}{4}\right) \right]^{-1} = 1,304.8 \text{ psi}$$

$$P_{s\max} = \frac{375,000}{(6)(35.25)} \left[\frac{\sin\left(\frac{3\pi}{4}\right)}{3} + \sin\left(\frac{\pi}{4}\right) \right]^{-1} = 1,880.6 \text{ psi}$$

Symmetry displacement boundary conditions are applied along the cut boundary of the 3-dimensional half model. An internal pressure of 30 psi is also applied to the model.

A depiction of the 75 g side drop load case boundary conditions is provided in Figure A.3.9.2-11.

Load Case 12: Transfer Thermal Accident (Fire)

The applied loads used to calculate the maximum stress in the transfer during fire accident event include a maximum radial temperature gradient and normal conditions transfer loads. The stresses generated in the TC shell by the temperature gradient are computed using hand calculations. The resulting stresses caused by the thermal temperature gradient are added to the stresses computed for the transfer load case. Since the primary load for the fire accident is caused by the radial temperature gradient, the maximum TC stress is computed for the outer radial structural shell.

The maximum stress generated by the radial thermal gradient fire accident will occur in the outer structural shell due to the thermal expansion of the lead gamma shield. From Chapter 4, the maximum temperature difference between the lead gamma shield and the structural shell occurs when the lead and structural shell are at 618 °F and 553 °F, respectively.

The change in the outer radius of the lead gamma shield, ΔR_l , is computed as follows.

$$\begin{aligned}\Delta R_l &= R_l \times \alpha_l \times \Delta T_l = 39.435 \text{ in.} \times 19.68 \times 10^{-6} \text{ in./in. } ^\circ\text{F} (@600 ^\circ\text{F}) \times (618 - 70) ^\circ\text{F} \\ &= 0.4253 \text{ in.}\end{aligned}$$

The change in the inner radius of the structural shell, ΔR_s , is computed as follows.

$$\begin{aligned}\Delta R_s &= R_s \times \alpha_s \times \Delta T_s = 39.435 \text{ in.} \times 9.7 \times 10^{-6} \text{ in./in. } ^\circ\text{F} (@500 ^\circ\text{F}) \times (553 - 70) ^\circ\text{F} \\ &= 0.1848 \text{ in.}\end{aligned}$$

Therefore the differential radial expansion between the lead and structural shell, ΔR , is as follows:

$$\Delta R = 0.4253 \text{ in.} - 0.1848 \text{ in.} = 0.241 \text{ in.}$$

Therefore, the lead cylinder, if it were free, would grow 0.241 in. more than the inner surface of the structural shell. If all of the differential expansion is accommodated in the lead, the lead strain, ε_l , would be the following.

$$\varepsilon_l = \Delta R / R_l = 0.241 \text{ in.} / 39.435 \text{ in.} = 0.006 \text{ in./in.}$$

If the lead remained linear elastic, the residual hoop stress in the lead would be,

$$\sigma_l = E_l \times \varepsilon_l = 1.64 \times 10^6 \text{ psi} (@600 ^\circ\text{F}) \times 0.006 \text{ in./in.} = 9,840 \text{ psi}$$

Conservatively assuming that the lead remains linear elastic, the interference pressure on the outer structural shell required to exert an average hoop stress of 9,840 psi in the lead can be determined in the following way.

$$P_{interface} = \sigma_l \times \text{lead thickness} / R_{interface} = 9,840 \text{ psi} \times 3.56 \text{ in.} / 39.435 \text{ in.} = 888 \text{ psi}$$

This interference pressure would generate the following hoop stress in the structural shell.

$$\sigma_s = P_{interface} \times R_{interface} / t_s = 888 \text{ psi} \times 39.435 / 1.50 = 23,346 \text{ psi} \approx 23.35 \text{ ksi}$$

The total combined maximum stress, σ , in the TC during the fire accident is then,

$$\begin{aligned} \sigma &= 5.06 \text{ ksi (stress due to 30 psi internal pressure from load case 3)} + 23.35 \text{ ksi} \\ &= 28.41 \text{ ksi} \end{aligned}$$

A.3.9.2.3 ANSYS Analysis Results and Reporting Methodology

The maximum nodal stress intensities in various components of the NUHOMS® OS187H Type 1 TC are extracted from the ANSYS results files for all load cases. These stresses are compared to the normal and accident condition allowable stresses set forth by ASME B&PV Code Section III, Subsection NC [2] and Appendix F [3]. Allowable stresses are derived from material properties taken from Reference 6 at the various component temperatures listed in the Material Properties section. A summary of the maximum TC component stresses and corresponding allowable stresses is presented in Table A.3.9.2-1.

The maximum nodal stress intensities ($P_m + P_b$) are conservatively compared to the allowable membrane stress intensities, unless otherwise stated. In load cases where the nodal stress intensity exceeds the membrane allowable stress, individual membrane and membrane plus bending stresses are computed by linearizing the maximum component stresses through the thickness of the component. The resulting linearized stresses are then compared to their corresponding P_m and $P_m + P_b$ allowable stresses.

For the load combinations involving mechanical loads and thermal loads (i.e., 6 g lifting plus 115 °F ambient), the maximum stresses from the mechanical load case and the maximum stress from the thermal load case are simply summed for each of the major cask components. This method of computing the maximum load combination stresses is very conservative, because, in general, the maximum stress caused by a mechanical load and the maximum stress caused by a thermal load will not occur at the same location in the TC.

Typically, fictitious stresses at nodes where point contact exists are ignored. These unrealistic stresses usually occur in the top cover at locations where the top cover bolts are fixed to the cover by node coupling (in all degrees of freedom) at a single node. Similarly, in the transfer loads analysis, the TC is held at the trunnion locations. This boundary condition creates fictitious stresses in the structural shell around the trunnions. Thus, stresses 4-inches around the trunnions are not evaluated. Local stresses in the shell due to trunnion loads are evaluated separately and are documented in Section A.3.9.2.4. For the 75 g side drop, high fictitious stresses are created due to the boundary condition discontinuity at the contact location. These stresses are also not evaluated.

A.3.9.2.4 Evaluation of OS187H Type 1 Transfer Cask Trunnion Local Stresses

The purpose of this section is to evaluate the local stress intensities in the NUHOMS® OS187H Type 1 TC radial shells near the upper and lower trunnions, due to all applied loads during fuel loading and transfer operations.

A.3.9.2.4.1 Approach

The NUHOMS® OS187H Type 1 TC has two upper trunnions made of SA-182 Gr. FXM19 forging and two lower trunnions made of SA-182 Gr. F304N. The OS187H Type 1 TC cylindrical shell and the reinforcing pad are made of SA-240 Type 304 stainless steel.

The two top trunnions are used to first lift the cask, containing an empty DSC, into a fuel pool for loading of the spent fuel. After the spent fuel has been loaded into the DSC, the cask is lifted to a decontamination area. After draining and drying of the pool water, welding of the canister cover, and bolting of the cask top cover, the cask is placed on a trailer for transfer to an onsite HSM-H.

The TC is vertically lifted into the trailer and rests its bottom trunnions on a support frame mounted to the top of the trailer. Then the cask is allowed to rotate, using the bottom trunnion supports as the pivot points, into a horizontal position until the top trunnions rest on their supports on the trailer. Throughout the operation the maximum total load is applied to the cask top trunnions. After the cask has been placed in the trailer, it is supported by all four trunnions and is subject to a set of specified handling loads.

The following two load cases are analyzed for the four cask trunnions and adjoining shell:

1. Lifting Loads (cask is in vertical position, lifted from the pool to the decontamination area and then to the trailer). The two top trunnions and interfacing structural shell are analyzed for vertical 6g load. The two bottom trunnions are not used during lifting of the cask.
2. Handling Loads (cask is in a horizontal position mounted on the trailer). All four trunnions rest on the supports in the trailer.

These four trunnion-shell interfaces are designed to resist the following transfer load combinations:

1. DW (dead weight) + 1 g axial (load resisted by lower trunnions only)
2. DW + 1 g transverse (load is resisted by trunnions on one side of the cask)
3. DW + 1 g vertical (load is distributed to all four trunnions)
4. DW + 1/2 g axial + 1/2 g transverse + 1/2 g vertical
(Directions of transfer loads are relative to a horizontal cask)

In load combination 4, the load components are distributed according to the direction used in load cases 1 through 3 above.

HSM insertion/withdrawal loads are bounded by the analyzed transfer loads. For the OS187H Type 1 TC, the maximum load that may be reacted by the trunnions during insertion/withdrawal of the DSC to/from the HSM is 80 kips. The evaluation of local stresses near the upper trunnions considers loads exceeding that magnitude.

The trunnions and cask shells are assumed to be at a 400° F uniform temperature during transfer, which is conservative compared to the maximum temperature computed in Chapter 4 for the 115 °F ambient environment condition (see Figure A.3.9.2-4).

The following calculations are based on the method described in Reference 10. A spreadsheet based on Figure 3.9.2-12, which implements the Reference 10 method, was developed to aid in the computations. The computation spreadsheets presented in Tables A.3.9.2-2 through A.3.9.2-15 document the evaluation of local shell stresses for the various load cases analyzed.

A.3.9.2.4.2 Load Cases

The weights of NUHOMS® OS187H Type 1 TC components are listed in Section A.3.9.2.1.2. The weight of the NUHOMS® OS187H Type 1 TC loaded with a 32PTH Type 1 DSC (dry) is 240,000 lbs. The wet weight of a loaded OS187H Type 1 TC (includes the weight of water in the DSC and TC/DSC annulus and excludes the weight of the TC lid and DSC top covers) is approximately 244,500 lbs. However, for conservatism, a weight of 250,000 lb is used in this analysis.

In the estimation of the magnitude of trunnion reactions it is assumed that:

- (a) Maximal load considered for vertical lift is 125 kips (per trunnion) plus the 15% allowance, or 143.75 kips.
- (b) The moment arm is measured from the center of the yoke of the (lifting) hook to the middle surface of the TC structural shell.
- (c) The cask weight is distributed proportionally between the upper and lower trunnions and the cask is analyzed as a simply supported beam.

The requirement given in (b) above is consistent with the methodology in WRC-107 Bulletin [10]. Based on geometry relations the median radius of cask shell, R_m , can be defined as:

$$R_m = R_I + (T_{\text{shell}} + T_{\text{pad}})/2$$

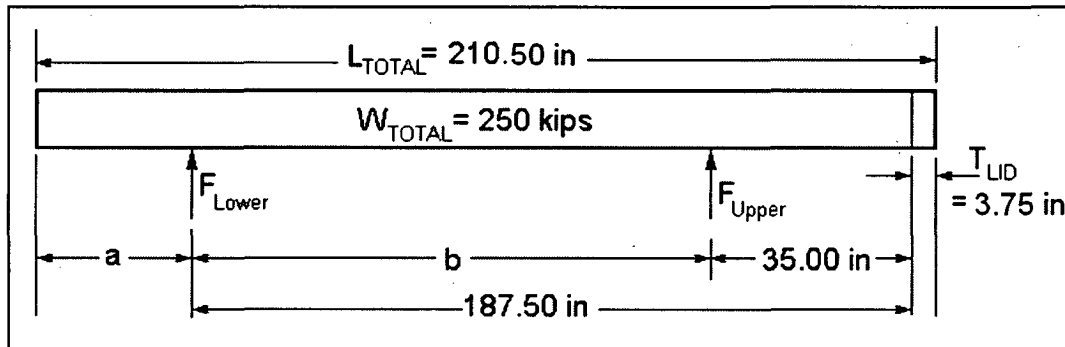
where:

- T_{shell} is nominal thickness of cask shell at trunnion location
- T_{pad} is the thickness of reinforcement pad
- R_I = 39.44 inch is inner radius of cask shell

The table below provides values of median radius of cask shell R_m and moment arms used in this calculation. Reinforcement pad thickness $T_{\text{pad}} = 1.31$ inches is used conservatively in the calculations (actual design thickness = 1.375 inches).

Upper Trunnion - Input Data for Reinforcement Pad-Trunnion Joint (Load Cases UT 1-5)						
R _l [in]	R _m [in]	T _{shell} [in]	T _{pad} [in]	Load Type	Moment Arm Definition	Moment Arm [in]
39.44	41.29	2.38	1.31	6g Lifting Load	46.3+3.75+ 3.25/2-R _m	10.390
				Transfer Loads	46.3+3.75/2-R _m	6.8900
Upper Trunnion - Input Data for Reinforcement Pad - Shell Joint (Load Cases UT 6-10)						
39.44	40.63	2.38	0	6g Lifting Load	46.3+3.75+ 3.25/2-R _m	11.045
				Transfer Loads	46.3+3.75/2-R _m	7.5450
Lower Trunnion Input Data for Trunnion-Shell Joint - No Reinforcement Pad (Load Cases LT 1- 4)						
39.44	40.19	1.5	0	Transfer Loads	46.3+3.5/2-R _m	7.8600

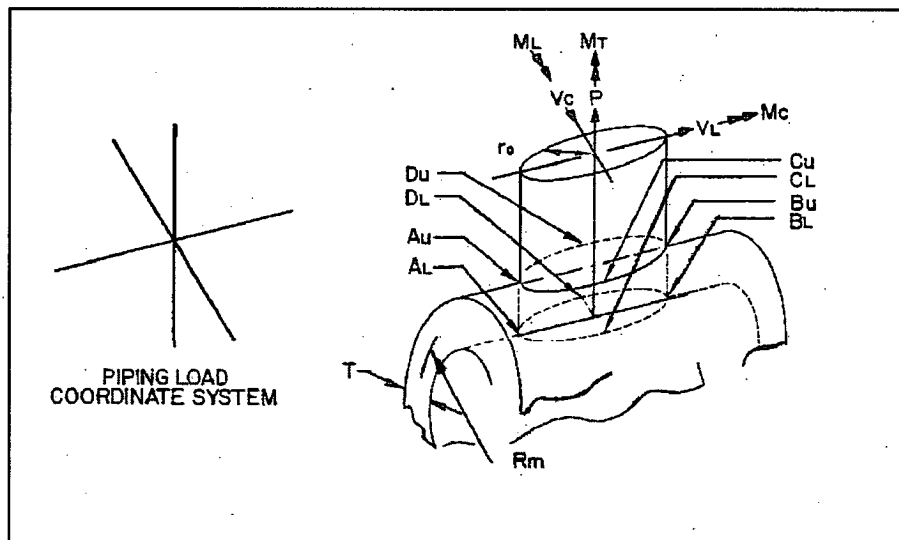
The figure below shows basic geometry relations, derived from the OS187H Type 1 TC drawings.



The above geometrical relations are used in the calculation of reaction forces for the upper and lower trunnions. The total length of the cask is 210.50 inches. The dimension $T_{LID} = 3.75$ inches denotes the thickness of the top cover above the top edge of the cask. Distance $a = 19.25$ inches, distance $b = 152.5$ inches.

Assuming a total weight of 250 kips, the reaction forces at trunnion locations can be calculated as $F_{upper} = 71$ kips for the upper trunnion, and $F_{lower} = 54$ kips for the lower trunnion.

The stress classification locations (A_U , B_U , C_U , D_U and A_L , B_L , C_L , D_L) as well as basic parameters used in WRC-107 Bulletin [10] are illustrated in the figure below:



In the WRC-107 Bulletin coordinate system convention, the radial load P is assumed positive when directed away from cylinder centerline. Axial loads (e.g., critical lifting loads for upper trunnions, axial transport loads for lower trunnions) are represented as V_L loads. When the transfer cask is supported in the horizontal position the vertical transfer loads and deadweight loads acting on the transfer cask are tangential loads V_C . The M_L loads are force moments generated by V_L loads, while M_C loads are force moments generated by V_C loads.

A.3.9.2.4.3 Material Properties

The following pertinent material properties are taken from Reference 6 corresponding to a (conservative) temperature of 400 °F.

Property	SA-240, Type 304 stainless steel (cask shells and pad)
S_m	18.7 ksi
S_y	20.7 ksi
S_u	64.0 ksi

A.3.9.2.4.4 Stress Criteria

All load cases analyzed are Service Level A load cases. According to ASME Code, Section III, Subsection NC [2], for Service Level A conditions, the maximum allowable general primary membrane stresses (P_m) shall be limited to S_m . Local primary membrane stresses (P_L) shall be limited to $1.5 S_m$, while maximum allowable primary plus secondary stresses, $P_L + P_b + Q$, shall be limited to $3.0 S_m$.

Primary stresses result from an imposed loading for which it is necessary to satisfy the laws of equilibrium between external and internal forces and moments. The basic characteristic of primary stress is that it is not self-limiting. If the primary stress exceeds yield through the entire thickness of the wall, the failure of the design depends entirely on strain hardening properties of

material. In the case of trunnion load, the primary stress is the membrane stress occurring near the trunnion, caused by mechanical load.

General primary stresses (P_m) are stresses that are located remote from any structural discontinuity. Such stresses should be derived as the average stresses through the thickness of the cask shell at the location remote from discontinuity. No redistribution of load occurs as a result of yielding of material of general primary stress.

Local primary stress (P_L) is also average stress across a solid section, but it includes the effect of gross structural discontinuities. This type of stress is self-limiting when it exceeds yield because the load is resisted by other parts of the structure, but it may result in excessive distortion of the structure because of the shift of the load to other parts. In the case of the WRC-107 methodology, the example of local primary stress is stress in the vicinity of a nozzle (trunnion) occurring as a result of external loads.

Secondary stresses (Q) are developed as a result of the strain pattern induced by the maintaining of structural continuity between structural members of the design. The basic characteristic of secondary stresses is that they are self-limiting. In the case of external loads imposed onto trunnions the secondary stresses are surface stresses caused by mechanical load in the vicinity of the trunnion. In the case of the WRC-107 methodology, these stresses are surface stresses at stress classification locations A_U , B_U , C_U , D_U and A_L , B_L , C_L , D_L .

For the upper trunnions region, stress levels for primary membrane and secondary stresses are checked in the trunnion to reinforcement pad juncture and the reinforcement pad to cask shell juncture. For the lower trunnions region, the primary membrane and secondary stresses are checked at the trunnion-to-shell juncture.

The TC shells and pad are constructed from stainless steel, SA-240, Type 304. The material properties are taken at 400 °F, which bounds the maximum inner shell and structural shell temperatures generated during 150 °F ambient transfer condition.

The table below shows a summary of stress acceptance criteria used in the stress evaluation:

Stress Location	Stress Description	Stress Classification	Criteria Limit	Criteria Limit [ksi]
Cask shell at both trunnion locations	Local membrane	P_L	$1.5*S_m$	28.1
	Surface stress	P_L+P_b+Q	$3.0*S_m$	56.1

A.3.9.2.4.5 Stress Computation

For the upper trunnion, stress levels for primary membrane and secondary stresses are checked in the trunnion-to-reinforcement pad juncture and the reinforcement pad-to-cask shell juncture. For the lower trunnion, the primary membrane and secondary stresses are checked at the trunnion-to-shell juncture. The detailed information about input loads V_L , M_L , V_C , M_C , and P at these locations is provided below. The definition of these input loads is presented in section A.3.9.2.4.2.

Stress results for the load combinations presented below are calculated in the attached spreadsheets (Table A.3.9.2-2 through Table A.3.9.2-15). Each spreadsheet contains the specification of all input parameters used in the stress calculation. The summary of stress results is provided in Table A.3.9.2-16.

The specification of input loads at the juncture of the upper trunnion and reinforcement pad is presented in the table below. Stress calculations for load cases UT1, UT2 UT3, UT4, and UT5 are documented in Table A.3.9.2-2 through Table A.3.9.2-6.

Load Type	Load Combination	Case ID	Axial Load	Axial Load Moment	Tangential Load	Tangential Load Moment	Radial Load
			V_L [kips]	M_L [in-kips]	V_C [kips]	M_C [in-kips]	P [kips]
Lifting Loads	Critical lifts	UT1	862.5	8961.4	0.0	0.0	0.0
Transfer Handling Loads	DW+1g Axial	UT2	0.0	0.0	71.0	489.2	0.0
	DW+1g Transverse	UT3	0.0	0.0	71.0	489.2	-142.0
	DW+1g Vertical	UT4	0.0	0.0	142.0	978.4	0.0
	1/2g Axial + 1/2g Transverse + 1/2g Vertical + DW	UT5	0.0	0.0	106.5	733.8	-71.0

The specification of input load at the juncture of the upper trunnion reinforcement pad and cask shell is shown in the following table. Stress calculations for load cases UT6, UT7 UT8, UT9, and UT10 are documented in Table A.3.9.2-7 through Table A.3.9.2-11.

Load Type	Load Combination	Case ID	Axial Load	Axial Load Moment	Tangential Load	Tangential Load Moment	Radial Load
			V_L [kips]	M_L [in-kips]	V_C [kips]	M_C [in-kips]	P [kips]
Lifting Loads	Critical lifts	UT6	862.5	9526.3	0.0	0.0	0.0
Transfer Handling Loads	DW+1g Axial	UT7	0.0	0.0	71.0	535.7	0.0
	DW+1g Transverse	UT8	0.0	0.0	71.0	535.7	-142.0
	DW+1g Vertical	UT9	0.0	0.0	142.0	1071.4	0.0
	1/2g Axial + 1/2g Transverse + 1/2g Vertical + DW	UT10	0.0	0.0	106.5	803.5	-71.0

Finally, the specification of input loads at the interface of the lower trunnion and cask shell is presented in the table below. Stress calculations for load cases LT1, LT2, LT3, and LT4 are documented in Table A.3.9.2-12 through Table A.3.9.2-15.

Load Type	Load Combination	Case ID	Axial Load	Axial Load Moment	Tangential Load	Tangential Load Moment	Radial Load
			V_L [kips]	M_L [in-kips]	V_C [kips]	M_C [in-kips]	P [kips]
Transfer Handling Loads	DW+1g Axial	LT1	125.0	982.5	54.0	424.4	0.0
	DW+1g Transverse	LT2	0.0	0.0	54.0	424.4	-108.0
	DW+1g Vertical	LT3	0.0	0.0	108.0	848.9	0.0
	1/2g Axial + 1/2g Transverse + 1/2g Vertical + DW	LT4	62.5	491.3	81.0	636.7	-54.0

A.3.9.2.4.6 Stress Intensity Calculation

Membrane plus bending stress intensities are calculated in the following way.

$$S.I. = \text{Max. of} \left\{ \begin{array}{l} \frac{1}{2} \left[(\sigma_x + \sigma_\phi) \pm \sqrt{(\sigma_x - \sigma_\phi)^2 + 4\tau^2} \right] \\ \sqrt{(\sigma_x - \sigma_\phi)^2 + 4\tau^2} \end{array} \right.$$

In order to calculate the membrane or bending stress intensity, only those components associated with membrane or bending stress, respectively, are summed to calculate σ_ϕ , σ_x and τ .

A.3.9.2.4.7 Local Shell Stress Results

Table A.3.9.2-16 summarizes the maximum stress intensities and compares them against applicable allowables.

A.3.9.2.4.8 Local Shell Stress Conclusions

All calculated local membrane stresses are less than the allowable local membrane stress of 28.1 ksi, and all local membrane plus bending stress intensities are less than the allowable local membrane plus bending stress of 56.1 ksi. Therefore, the NUHOMS® OS187H Type 1 TC shells adjoining the trunnions are structurally adequate with respect to local stresses generated during lifting and transfer operations.

A.3.9.2.5 Stress and Deflection of Transfer Cask Inner Shell Support Rails

The 3D finite element model used for side drop analyses as described in Appendix A.3.9.2, Section 3.9.2.2.3 (B) is modified as follows and used to calculate the stresses and deflections of the transfer cask inner shell along the support rail locations.

Finite Element Model Modifications

1. Include the 3" wide x 0.12" thick rails in the 3-D TC inner shell (SHELL 43 element)
2. Include canister shell (SOLID 45 element) in the 3-D model
3. Gap elements (CONTACT 52) are used between the canister shell and transfer cask inner shell and between the canister shell and inner shell rail

Radial gap elements (CONTACT 52) are used to simulate the interface between the outer radius of the canister and inner radius of the cask inner shell. Each gap element contains two nodes; one on each surface of the structure. The gap size at each gap element is determined by the difference between the canister outer radius and the inside radius of the cask (canister outer radius = 34.875" and cask inner radius = 35.25" to give a 0.375 inch mean gap). Radial gap elements are generated using an ANSYS macro. Actual gap sizes for the gap element, at each radial location, were determined and input into the model as real constants using another ANSYS macro. This macro accepts the drop orientation and model geometry as inputs and determines the circumferential position of each gap element. The macro then computes the appropriate real constants and applies to appropriate gap elements.

During drops on cask rails (180° side drop), the initial gaps between the canister and the cask are modified using the ANSYS macro. Two 3 inch wide and 0.12 inch thick rails are welded to the cask inner shell at 12° on both sides of the vertical center line of the model and another set of two rails are welded at 38° on both sides of the same vertical center line. For the 180° side drop onto the rails, the initial gaps at the two inner rail locations are assumed closed (0 gap). In-between these two rail locations, the initial gaps are set to 0.12 inches. On the other two rail locations, the gaps are initially set to open, and the gap sizes are generated by macro with consideration of the rail thickness.

The ANSYS 3-D finite element models including cask shell, lead, rails, canister, and gap elements are shown on Figures A.3.9.2-13 through A.3.9.2-18.

Loadings

Pressures applied in the radial direction to the inner surface of the canister in the 3-dimensional finite element model are based on a cosine distribution. This pressure distribution simulates the load which the internal canister contents exert on the inner canister wall. Two drop cases are analyzed: impact on two rails (Figure A.3.9.7-19) and impact on one rail (Figure A.3.9.2-20).

Materials

In order to properly calculate the deflections of the rails, elastic and inelastic material properties of the canister and cask at the temperatures are used for the analysis.

Results

The following table summarizes the maximum stress intensities at the TC inner and outer shells for the above two drop load cases.

Summary of Maximum Stress Intensities and Allowables

Load Case	Component	Stress Category	Calculated Max. Stress Intensity (ksi)	Allowable Membrane Stress Intensity (ksi) ⁽¹⁾	Factor of Safety
Impact on two rails	Inner Shell	$P_L + P_b$	43.786	45.57	1.04
	Outer Shell	$P_L + P_b$	37.674	45.57	1.21
Impact on one rail	Inner Shell	$P_L + P_b$	45.282	45.57	1.01
	Outer Shell	$P_L + P_b$	37.805	45.57	1.21

Note:

(1) Since the calculated maximum stress intensity is less than the allowable membrane stress intensity (P_m), therefore only maximum stress intensity is reported.

The calculated stresses are less than the code allowables and the calculated maximum deflection in the rail is 0.0725". This small deflection will not affect the retrieving of the canister from the TC after an accident drop.

The maximum stress intensity plots of the cask inner shell and outer shell for the impact to the two rails load case are shown on Figures A.3.9.2-21 and A.3.9.2-22, respectively. The maximum stress intensity plots of the inner shell and outer shell for the impact to the one rail load case are shown on Figures A.3.9.2-23 and A.3.9.2-24, respectively.

A.3.9.2.6 References

- [1] 10CFR Part 72, Licensing Requirement for Storage of Spent Fuel in an Independent Spent Fuel Storage Installation.
- [2] ASME Code Section III, Subsection NC and Appendices, 1998, through 2000 addenda.
- [3] American Society of Mechanical Engineers, ASME Boiler and Pressure Vessel Code, Section III, Appendix F, 1998, through 2000 addenda.
- [4] ANSYS Users Manual, Rev. 8.0 and Rev. 8.1.
- [5] Technical Report N3-3-012, Bisco Products Inc., April 1984.
- [6] American Society of Mechanical Engineers, ASME Boiler and Pressure Vessel Code, Section II, Part D, 1998, through 2000 addenda.
- [7] Not Used.
- [8] Not Used.
- [9] Not Used.
- [10] Welding Research Council (WRC), Local Stresses in Spherical and Cylindrical Shells Due to External Loadings, Bulletin 107, March 1979.
- [11] Not Used.

Table A.3.9.2- 1 Transfer Cask Components Stress—Summary of Results

Load Case Number	Loading Condition	Service Level	Component ⁽⁶⁾		Maximum Stress Intensity (ksi)	Allowable Stress (ksi)
1A	6 g vertical lifting	A	Structural shell	P_m	8.71	20.00
				$P_m + P_b$	27.48	30.00
			Top cover		8.92	31.40
			Inner shell		15.08	18.70
			Bottom end plates	P_m	15.22	20.00
				$P_m + P_b$	27.34	30.00
			Ram acc. and cover	P_m	19.51	20.00
				$P_m + P_b$	21.45	30.00
1B	6 g vertical lifting + thermal loads	A	Structural shell		53.6	60.00 ⁽¹⁾
			Top cover		19.54	94.20 ⁽¹⁾
			Inner shell		41.83	56.10 ⁽¹⁾
			Bottom end plates		39.79	60.00 ⁽¹⁾
			Ram access and cover		36.44	60.00 ⁽¹⁾
2	Vacuum drying	A	Structural shell		11.97	60.00 ⁽¹⁾
3	30 psi internal pressure	A	Structural shell		5.06	20.00
			Top cover		6.31	31.40
			Inner shell		3.89	18.70
			Bottom end plates		5.06	20.00
			Ram access and cover		3.93	20.00
4	115 °F ambient hot thermal environment	A	Structural shell		26.12	60.00 ⁽¹⁾
			Top cover		10.62	94.20 ⁽¹⁾
			Inner shell		23.70	56.10 ⁽¹⁾
			Bottom end plates		12.45	60.00 ⁽¹⁾
			Ram access and cover		14.99	60.00 ⁽¹⁾
5	-20 °F ambient cold thermal environment	A	Structural shell		10.97	60.00 ⁽¹⁾
			Top cover		9.34	94.20 ⁽¹⁾
			Inner shell		26.75	56.10 ⁽¹⁾
			Bottom end plates		11.83	60.00 ⁽¹⁾
			Ram access and cover		12.43	60.00 ⁽¹⁾
6A	Transfer inertial loads—axial accel. toward bottom	A	Structural shell		18.90	20.00
			Top cover		8.55	31.40
			Inner shell		12.81	18.70
			Bottom end plates		10.70	20.00
			Ram access and cover		9.09	20.00

Table A.3.9.2- 1 (continued) Transfer Cask Components Stress—Summary of Results

Load Case Number	Loading Condition	Service Level	Component ⁽⁶⁾		Maximum Stress Intensity (ksi)	Allowable Stress (ksi)
6B	Transfer inertial loads—axial accel. toward top	A	Structural shell	P_m	9.27	20.00
				$P_m + P_b$	22.85	30.00
			Top cover		12.14	31.40
			Inner shell	P_m	8.48	18.70
				$P_m + P_b$	17.66	28.05
			Bottom end plates		7.43	20.00
			Ram access and cover		6.50	20.00
7A	Transfer loads—axial accel. toward bottom + internal pressure	A	Structural shell		18.37	20.00
			Top cover		11.92	31.40
			Inner shell		12.38	18.70
			Bottom end plates		14.89	20.00
			Ram access and cover		12.23	20.00
7B	Transfer loads—axial accel. toward top + internal pressure	A	Structural shell	P_m	9.12	20.00
				$P_m + P_b$	21.17	30.00
			Top cover		15.74	31.40
			Inner shell		18.50	18.70
			Bottom end plates		6.85	20.00
			Ram access and cover		7.68	20.00
7C ⁽⁷⁾	Transfer loads + 115 °F ambient + internal pressure	A	Structural shell		48.97	60.00 ⁽¹⁾
			Top cover		26.36	94.20 ⁽¹⁾
			Inner shell		42.70	56.10 ⁽¹⁾
			Bottom end plates		27.34	60.00 ⁽¹⁾
			Ram access and cover		27.22	60.00 ⁽¹⁾
8 ⁽⁷⁾	Transfer loads + - 20 °F ambient + internal pressure	A	Structural shell		33.82	60.00 ⁽¹⁾
			Top cover		25.08	94.20 ⁽¹⁾
			Inner shell		45.25	56.10 ⁽¹⁾
			Bottom end plates		26.72	60.00 ⁽¹⁾
			Ram access and cover		24.66	60.00 ⁽¹⁾
9	75 g bottom end drop + internal pressure	D	Structural shell		39.62	46.34
			Top cover		46.41	65.94
			Inner shell		16.69	44.80
			Bottom end plates		26.50	46.34
			Ram access and cover		43.86	48.00

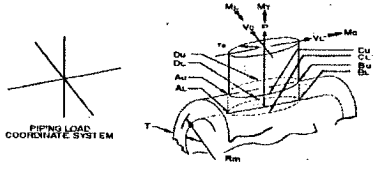
Table A.3.9.2- 1 (concluded) Transfer Cask Components Stress—Summary of Results

Load Case Number	Loading Condition	Service Level	Component ⁽⁶⁾	Maximum Stress Intensity (ksi)	Allowable Stress (ksi)
10	75 g top end drop + internal pressure	D	Structural shell	43.61	46.34
			Top cover	39.44	65.94
			Inner shell	18.11	44.80
			Bottom end plates	5.93	46.34
			Ram access and cover	4.87	48.00
11	75 g side drop + internal pressure	D	Structural shell ⁽⁵⁾	P_m	45.06
				$(P_m \text{ or } P_L) + P_b$	66.20 ⁽³⁾
			Top cover ⁽⁵⁾	P_m	63.82
				$(P_m \text{ or } P_L) + P_b$	94.20 ⁽³⁾
			Inner shell	P_m	35.43
				$(P_m \text{ or } P_L) + P_b$	64.00 ⁽³⁾
			Bottom end plates ⁽⁴⁾	P_m	45.96
				P_L	50.73
				$(P_m \text{ or } P_L) + P_b$	66.20 ⁽³⁾
			Ram access and cover	P_m	44.47
				$(P_m \text{ or } P_L) + P_b$	71.00 ⁽³⁾
12	Transfer thermal accident (fire)	D	Structural shell	28.41	58.32 ⁽²⁾

Notes

- (1) $P_L + P_b + Q$ allowable stress.
- (2) $S_m = 16.2$ ksi. For SA-240 type 304 at a temperature of 650 °F. (the maximum TC temperature is 618° during the thermal accident condition). The allowable stress is taken as $3.6S_m$.
- (3) Membrane plus bending $[(P_m \text{ or } P_L) + P_b]$ allowable stress.
- (4) Stresses at the edge of the impact target support at the 15° location is considered local and are compared to P_L allowable stresses.
- (5) High stresses due to boundary condition discontinuity and bearing stresses at contact locations are not evaluated for top cover and top flange.
- (6) See Figure A.3.9.2-1 for the stress reporting components. Structural Shell component includes the structural shell, the top flange and the bottom support ring components shown in Figure A.3.9.2-1. Bottom end plates component includes the bottom end plate and bottom neutron shield plate components.
- (7) Load cases 6A and 6B are transfer handling load cases without internal pressure; load cases 7A and 7B are transfer handling load cases with internal pressure. If the component stresses for transfer handling load cases without internal pressure is higher, conservatively the higher stress is used for load combination in load cases 7C and 8.

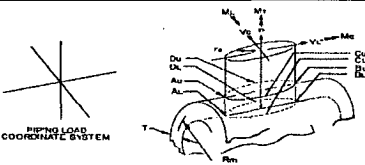
Table A.3.9.2-2 Local Shell Stress at Trunnion Locations—Computation Spreadsheet
for Case UT1

Applied Loads				Geometry											
V_L	862.5	[kips]		I [in]	3.690										
M_L	8961.4	[in-kips]		R_m [in]	41.285										
V_C	0.0	[kips]		r_o [in]	8.575										
M_C	0.0	[in-kips]		$\beta=0.875+0/R_m$	0.182										
P	0.0	[kips]		$\gamma=R_m/T$	11.188										
M_T	0	[in-kips]		$\lambda=d/D(T)^{1/2}$	0.983										
Figures	Read curves for		multiplier	abs. stress	values	1	2	3	4	5	6	7	8		
3C AND 4C	1.578	2.006	0.0	0.0	0.0	0.0	0.0	0.0	0.0	0.0	0.0	0.0	0.0	1	P-M
1C AND 2C-1	0.116	0.085	0.0	0.0	0.0	0.0	0.0	0.0	0.0	0.0	0.0	0.0	0.0	2	P-B
3A	0.324		0.0	0.0						0.0	0.0	0.0	0.0	3	M _C -M
1A	0.097		0.0	0.0						0.0	0.0	0.0	0.0	4	M _C -B
3B	1.161		7.8	9.1		-9.1	-9.1	9.1	9.1					5	M _L -M
1B (OR 1B-1)	0.048		526.3	25.1		-25.1	25.1	25.1	-25.1					6	M _L -B
Summation of circumferential stresses $\sigma_\theta \Rightarrow$						-34.2	16.0	34.2	-16.0	0.0	0.0	0.0	0.0	7	
4C AND 3C	2.006	1.578	0.0	0.0	0.0	0.0	0.0	0.0	0.0	0.0	0.0	0.0	0.0	8	P-M
2C AND 1C-1	0.085	0.116	0.0	0.0	0.0	0.0	0.0	0.0	0.0	0.0	0.0	0.0	0.0	9	P-B
4A	0.498		0.0	0.0						0.0	0.0	0.0	0.0	10	M _C -M
2A	0.057		0.0	0.0						0.0	0.0	0.0	0.0	11	M _C -B
4B	0.330		7.8	2.6		-2.6	-2.6	2.6	2.6					12	M _L -M
2B (OR 2B-1)	0.076		526.3	40.1		-40.1	40.1	40.1	-40.1					13	M _L -B
Summation of longitudinal stresses $\sigma_x \Rightarrow$						-42.7	37.5	42.7	-37.5	0.0	0.0	0.0	0.0	14	
WRC-107										8.68	8.68	-8.68	-8.68	15	
Shear stress τ due to V_L						8.6766								16	
Shear stress τ due to V_C						0	0.00	0.00	0.00	0.00				17	
Shear stress τ due to M_T						0.00	0.00	0.00	0.00	0.00	0.00	0.00	0.00	18	
Summation of shear stress $\tau \Rightarrow$						0.0	0.0	0.0	0.0	8.7	8.7	-8.7	-8.7	19	
Membrane components of $\sigma_\theta \Rightarrow$						-9.1	-9.1	9.1	9.1	0.0	0.0	0.0	0.0	20	
Membrane components of $\sigma_x \Rightarrow$						-2.6	-2.6	2.6	2.6	0.0	0.0	0.0	0.0	21	
Membrane stress intensities $S_I \Rightarrow$						9.1	9.1	9.1	9.1	17.4	17.4	17.4	17.4	22	
Stress intensities $S_I \Rightarrow$						42.7	37.5	42.7	37.5	17.4	17.4	17.4	17.4	23	
1. Curves 1B and 2B apply to rigid attachments						σ_1	-34.2	37.5	42.7	-16.0	8.7	8.7	8.7	8.7	
2. If $d/D(T)^{1/2} > 2.0$, then use 2c-1 for 1c and 1c-1 for 2c						σ_2	-42.7	16.0	34.2	-37.5	-8.7	-8.7	-8.7	-8.7	
Ref: Stearns Roger "Analysis of External Loadings on Pressure Vessels"						$ \sigma_1 - \sigma_2 $	8.5	21.5	8.5	21.5	17.4	17.4	17.4	17.4	
						$ \sigma_1 + \sigma_2 $	76.9	53.6	76.9	53.6	0.0	0.0	0.0	0.0	

OS187H Type 1 Trunnions WRC-107 Calculation

wrc107-case UT1

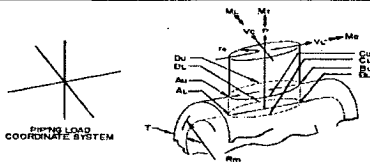
Table A.3.9.2-3 Local Shell Stress at Trunnion Locations—Computation Spreadsheet
for Case UT2

Applied Loads				Geometry											
V_L	0.0	[kps]		I [in]	3.690										
M_L	0.0	[in-kps]		R_m [in]	41.285										
V_C	71.0	[kps]		r_0 [in]	8.575										
M_C	489.2	[in-kps]		$\beta = 0.875 \cdot r_0 / R_m$	0.182										
P	0.0	[kps]		$\gamma = R_m / T$	11.188										
M_T	0	[in-kps]		$\lambda = d / (D(T))^{1/2}$	0.983										
Figures	Read curves for		multiplier	abs. stress	values	1	2	3	4	5	6	7	8		
3C AND 4C	1.578	2.006	0.0	0.0	0.0	0.0	0.0	0.0	0.0	0.0	0.0	0.0	0.0	1	P-M
1C AND 2C-1	0.116	0.085	0.0	0.0	0.0	0.0	0.0	0.0	0.0	0.0	0.0	0.0	0.0	2	P-B
3A	0.324		0.4	0.1						-0.1	-0.1	0.1	0.1	3	M _C -M
1A	0.097		28.7	2.8						-2.8	2.8	2.8	-2.8	4	M _C -B
3B	1.161		0.0	0.0		0.0	0.0	0.0	0.0					5	M _L -M
1B (OR 1B-1)	0.048		0.0	0.0		0.0	0.0	0.0	0.0					6	M _L -B
Summation of circumferential stresses $\sigma_\theta \Rightarrow$						0.0	0.0	0.0	0.0	-2.9	2.6	2.9	-2.6	7	
4C AND 3C	2.006	1.578	0.0	0.0	0.0	0.0	0.0	0.0	0.0	0.0	0.0	0.0	0.0	8	P-M
2C AND 1C-1	0.085	0.116	0.0	0.0	0.0	0.0	0.0	0.0	0.0	0.0	0.0	0.0	0.0	9	P-B
4A	0.498		0.4	0.2						-0.2	-0.2	0.2	0.2	10	M _C -M
2A	0.057		28.7	1.6						-1.6	1.6	1.6	-1.6	11	M _C -B
4B	0.330		0.0	0.0		0.0	0.0	0.0	0.0					12	M _L -M
2B (OR 2B-1)	0.076		0.0	0.0		0.0	0.0	0.0	0.0					13	M _L -B
Summation of longitudinal stresses $\sigma_x \Rightarrow$						0.0	0.0	0.0	0.0	-1.8	1.4	1.8	-1.4	14	
WRC-107						0				0.00	0.00	0.00	0.00	15	
Shear stress τ due to V_L						0								16	
Shear stress τ due to V_C						0.7142	0.71	-0.71	-0.71					17	
Shear stress τ due to M_T						0.00	0.00	0.00	0.00	0.00	0.00	0.00	0.00	18	
Summation of shear stress						$\tau \Rightarrow$	0.7	0.7	-0.7	-0.7	0.0	0.0	0.0	19	
Membrane components of						$\sigma_\theta \Rightarrow$	0.0	0.0	0.0	0.0	-0.1	-0.1	0.1	20	MAX
Membrane components of						$\sigma_x \Rightarrow$	0.0	0.0	0.0	0.0	-0.2	-0.2	0.2	21	1.4
Allowable						28.05	1.4	1.4	1.4	1.4	0.2	0.2	0.2	22	1.4
Allowable						56.1	1.4	1.4	1.4	1.4	2.9	2.6	2.9	22	2.9
1. Curves 1B and 2B apply to rigid attachments						σ_1	0.7	0.7	0.7	0.7	-1.8	2.6	2.9		
2. If $d/(D(T))^{1/2} > 2.0$, then use 2c-1 for 1c and 1c-1 for 2c						σ_2	-0.7	-0.7	-0.7	-0.7	-2.9	1.4	1.8		
Ref: Stearns Roger "Analysis of External Loadings on Pressure Vessels"						$ \sigma_1 - \sigma_2 $	1.4	1.4	1.4	1.4	1.1	1.2	1.1		
						$ \sigma_1 + \sigma_2 $	0.0	0.0	0.0	0.0	4.8	4.1	4.8		

OS187H Type 1 Trunnions WRC-107 Calculation

wrc107-case UT2

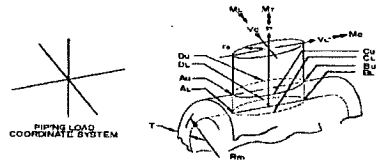
Table A.3.9.2-4 Local Shell Stress at Trunnion Locations—Computation Spreadsheet
for Case UT3

Applied Loads				Geometry											
V_L	0.0	[kips]		l [in]	3.690										
M_L	0.0	[in-kips]		R_m [in]	41.285										
V_c	71.0	[kips]		r_0 [in]	8.575										
M_c	489.2	[in-kips]		$\beta=0.875 \cdot d_0/R_m$	0.182										
P	-142.0	[kips]		$\gamma=R_m/T$	11.188										
M_T	0	[in-kips]		$\lambda=d/D(D/T)^{1/2}$	0.983										
Figures	Read curves for		multiplier	abs. stress	values	1	2	3	4	5	6	7	8		
3C AND 4C	1.578	2.006	-0.9	-1.5	-1.9	-1.9	-1.9	-1.9	-1.9	-1.5	-1.5	-1.5	-1.5	1	P-M
1C AND 2C-1	0.116	0.085	-62.6	-7.3	-5.3	-5.3	5.3	-5.3	5.3	-7.3	7.3	-7.3	7.3	2	P-B
3A	0.324		0.4	0.1						-0.1	-0.1	0.1	0.1	3	M _c -M
1A	0.097		28.7	2.8						-2.8	2.8	2.8	-2.8	4	M _c -B
3B	1.161		0.0	0.0		0.0	0.0	0.0	0.0					5	M _L -M
1B (OR 1B-1)	0.048		0.0	0.0		0.0	0.0	0.0	0.0					6	M _L -B
Summation of circumferential stresses $\sigma_\theta \Rightarrow$						-7.2	3.5	-7.2	3.5	-11.7	8.5	-5.8	3.2	7	
4C AND 3C	2.006	1.578	-0.9	-1.9	-1.5	-1.5	-1.5	-1.5	-1.5	-1.9	-1.9	-1.9	-1.9	8	P-M
2C AND 1C-1	0.085	0.116	-62.6	-5.3	-7.3	-7.3	7.3	-7.3	7.3	-5.3	5.3	-5.3	5.3	9	P-B
4A	0.498		0.4	0.2						-0.2	-0.2	0.2	0.2	10	M _c -M
2A	0.057		28.7	1.6						-1.6	1.6	1.6	-1.6	11	M _c -B
4B	0.330		0.0	0.0		0.0	0.0	0.0	0.0					12	M _L -M
2B (OR 2B-1)	0.076		0.0	0.0		0.0	0.0	0.0	0.0					13	M _L -B
Summation of longitudinal stresses $\sigma_x \Rightarrow$						-8.7	5.8	-8.7	5.8	-9.0	4.9	-5.4	2.1	14	
WRC-107						Shear stress τ due to V_L								15	
						Shear stress τ due to V_c								16	
						Shear stress τ due to M_T								17	
						Summation of shear stress $\tau \Rightarrow$								18	
						Membrane components of $\sigma_\theta \Rightarrow$								19	
						Membrane components of $\sigma_x \Rightarrow$								20	MAX
S_m	18.7	[kips]				2.4	2.4	2.4	2.4	2.1	2.1	1.7	1.7	21	2.4
Allowable	28.05	[kips]				9.0	6.0	9.0	6.0	11.7	8.5	5.8	3.2	22	11.7
Allowable	56.1	[kips]													
						Membrane stress intensities \Rightarrow									
						Stress intensities $SI \Rightarrow$									
						σ_1	-6.9	6.0	-6.9	6.0	-9.0	8.5	-5.4	3.2	
						σ_2	-9.0	3.3	-9.0	3.3	-11.7	4.9	-5.8	2.1	
						$ \sigma_1 - \sigma_2 $	2.1	2.7	2.1	2.7	2.6	3.6	0.4	1.1	
						$ \sigma_1 + \sigma_2 $	16.0	9.3	16.0	9.3	20.7	13.3	11.2	5.2	

OS187H Type 1 Trunnions WRC-107 Calculation

wrc107-case UT3

Table A.3.9.2-5 Local Shell Stress at Trunnion Locations—Computation Spreadsheet
for Case UT4

Applied Loads				Geometry											
V_L	0.0	[kips]		I [in]	3.690										
M_L	0.0	[in-kips]		R_m [in]	41.285										
V_C	142.0	[kips]		r_0 [in]	8.575										
M_C	978.4	[in-kips]		$\beta=0.875 \cdot r_0/R_m$	0.182										
P	0.0	[kips]		$\gamma=R_m/T$	11.188										
M_T	0	[in-kips]		$\lambda=d/D(D/T)^{1/2}$	0.983										
Figures	Read curves for		multiplier	abs. stress	values	1	2	3	4	5	6	7	8		
						A_U	A_L	B_U	B_L	C_U	C_L	D_U	D_L		
3C AND 4C	1.578	2.006	0.0	0.0	0.0	0.0	0.0	0.0	0.0	0.0	0.0	0.0	0.0	1	P-M
1C AND 2C-1	0.116	0.085	0.0	0.0	0.0	0.0	0.0	0.0	0.0	0.0	0.0	0.0	0.0	2	P-B
3A	0.324		0.9	0.3						-0.3	-0.3	0.3	0.3	3	M_C -M
1A	0.097		57.5	5.6						-5.6	5.6	5.6	-5.6	4	M_C -B
3B	1.161		0.0	0.0		0.0	0.0	0.0	0.0					5	M_L -M
1B (OR 1B-1)	0.048		0.0	0.0		0.0	0.0	0.0	0.0					6	M_L -B
Summation of circumferential stresses $\sigma_\theta \Rightarrow$						0.0	0.0	0.0	0.0	-5.8	5.3	5.8	-5.3	7	
4C AND 3C	2.006	1.578	0.0	0.0	0.0	0.0	0.0	0.0	0.0	0.0	0.0	0.0	0.0	8	P-M
2C AND 1C-1	0.085	0.116	0.0	0.0	0.0	0.0	0.0	0.0	0.0	0.0	0.0	0.0	0.0	9	P-B
4A	0.498		0.9	0.4						-0.4	-0.4	0.4	0.4	10	M_C -M
2A	0.057		57.5	3.2						-3.2	3.2	3.2	-3.2	11	M_C -B
4B	0.330		0.0	0.0		0.0	0.0	0.0	0.0					12	M_L -M
2B (OR 2B-1)	0.076		0.0	0.0		0.0	0.0	0.0	0.0					13	M_L -B
Summation of longitudinal stresses $\sigma_x \Rightarrow$						0.0	0.0	0.0	0.0	-3.7	2.8	3.7	-2.8	14	
WRC-107						Shear stress τ due to V_L	0			0.00	0.00	0.00	0.00	15	
						Shear stress τ due to V_C	1.4285	1.43	1.43	-1.43	-1.43			16	
						Shear stress τ due to M_T	0.00	0.00	0.00	0.00	0.00	0.00	0.00	0.00	17
Summation of shear stress $\tau \Rightarrow$						1.4	1.4	-1.4	-1.4	0.0	0.0	0.0	0.0	18	
S_m	18.7	[kips]	Membrane components of $\sigma_\theta \Rightarrow$			0.0	0.0	0.0	0.0	-0.3	-0.3	0.3	0.3	19	
S_x	20.7	[kips]	Membrane components of $\sigma_x \Rightarrow$			0.0	0.0	0.0	0.0	-0.4	-0.4	0.4	0.4	20	MAX
Allowable	28.05	[kips]	Membrane stress intensities \Rightarrow			2.9	2.9	2.9	2.9	0.4	0.4	0.4	0.4	21	2.9
Allowable	56.1	[kips]	Stress intensities SI \Rightarrow			2.9	2.9	2.9	2.9	5.8	5.3	5.8	5.3	22	5.8
1. Curves 1B and 2B apply to rigid attachments 2. If $d/D(D/T)^{1/2} > 2.0$, then use 2c-1 for 1c and 1c-1 for 2c Ref: Stearns Roger "Analysis of External Loadings on Pressure Vessels"						σ_1	1.4	1.4	1.4	1.4	-3.7	5.3	5.8	-2.8	
						σ_2	-1.4	-1.4	-1.4	-1.4	-5.8	2.8	3.7	-5.3	
						$ \sigma_1 - \sigma_2 $	2.9	2.9	2.9	2.9	2.2	2.5	2.2	2.5	
						$ \sigma_1 + \sigma_2 $	0.0	0.0	0.0	0.0	9.5	8.1	9.5	8.1	

OS187H Type 1 Trunnions WRC-107 Calculation

wrc107-case UT4

Table A.3.9.2-6 Local Shell Stress at Trunnion Locations—Computation Spreadsheet for Case UT5

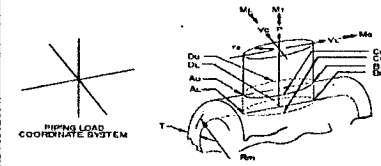
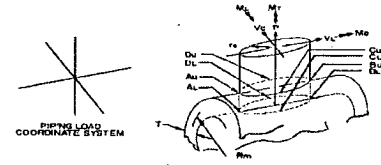
Applied Loads			Geometry													
V _L	0.0	[kips]	t	[in]	3.690											
M _L	0.0	[in-kips]	R _m	[in]	41.285											
V _C	106.5	[kips]	r ₀	[in]	8.575											
M _C	733.8	[in-kips]	β=0.875-t ₀ /R _m		0.182											
P	-71.0	[kips]	γ=R _m /T		11.188											
M _T	0	[in-kips]	λ=d/D(D/T) ^{1/2}		0.983											
Figures	Read curves for		multiplier	abs. stress	values	1	2	3	4	5	6	7	8			
						A _U	A _L	B _U	B _L	C _U	C _L	D _U	D _L			
3C AND 4C	1.578	2.006	-0.5	-0.7	-0.9	-0.9	-0.9	-0.9	-0.9	-0.7	-0.7	-0.7	-0.7	1	P-M	
1C AND 2C-1	0.116	0.085	-31.3	-3.6	-2.7	-2.7	2.7	-2.7	2.7	-3.6	3.6	-3.6	3.6	2	P-B	
3A	0.324		0.6	0.2						-0.2	-0.2	0.2	0.2	3	M _C -M	
1A	0.097		43.1	4.2						-4.2	4.2	4.2	-4.2	4	M _C -B	
3B	1.161		0.0	0.0		0.0	0.0	0.0	0.0					5	M _L -M	
1B (OR 1B-1)	0.048		0.0	0.0		0.0	0.0	0.0	0.0					6	M _L -B	
Summation of circumferential stresses α _y =>						-3.6	1.7	-3.6	1.7	-8.8	6.9	0.0	-1.1	7		
4C AND 3C	2.006	1.578	-0.5	-0.9	-0.7	-0.7	-0.7	-0.7	-0.7	-0.9	-0.9	-0.9	-0.9	8	P-M	
2C AND 1C-1	0.085	0.116	-31.3	-2.7	-3.6	-3.6	3.6	-3.6	3.6	-2.7	2.7	-2.7	2.7	9	P-B	
4A	0.498		0.6	0.3						-0.3	-0.3	0.3	0.3	10	M _C -M	
2A	0.057		43.1	2.4						-2.4	2.4	2.4	-2.4	11	M _C -B	
4B	0.330		0.0	0.0		0.0	0.0	0.0	0.0					12	M _L -M	
2B (OR 2B-1)	0.076		0.0	0.0		0.0	0.0	0.0	0.0					13	M _L -B	
Summation of longitudinal stresses α _x =>						-4.4	2.9	-4.4	2.9	-6.4	3.9	-0.8	-0.4	14		
WRC-107						Shear stress τ due to V _L								15		
						0								16		
						1.0714								17		
						Shear stress τ due to V _C								18		
						0.00								19		
						0.00								20		
						0.00								21		
						0.00								22		
						0.00								23		
						0.00								24		
						0.00								25		
						0.00								26		
						0.00								27		
						0.00								28		
						0.00								29		
						0.00								30		
						0.00								31		
						0.00								32		
						0.00								33		
						0.00								34		
						0.00								35		
						0.00								36		
						0.00								37		
						0.00								38		
						0.00								39		
						0.00								40		
						0.00								41		
						0.00								42		
						0.00								43		
						0.00								44		
						0.00								45		
						0.00								46		
						0.00								47		
						0.00								48		
						0.00								49		
						0.00								50		
						0.00								51		
						0.00								52		
						0.00								53		
						0.00								54		
						0.00								55		
						0.00								56		
						0.00								57		
						0.00								58		
						0.00								59		
						0.00								60		
						0.00								61		
						0.00								62		
						0.00								63		
						0.00								64		
						0.00								65		
						0.00								66		
						0.00								67		
						0.00								68		
						0.00								69		
						0.00								70		
						0.00								71		
						0.00								72		
						0.00								73		
						0.00								74		
						0.00								75		
						0.00								76		
						0.00								77		
						0.00								78		
						0.00								79		
						0.00								80		
						0.00								81		
						0.00								82		
						0.00								83		
						0.00								84		
						0.00								85		
						0.00								86		
						0.00								87		
						0.00								88		
						0.00								89		
						0.00								90		
						0.00								91		
						0.00								92		
						0.00								93		
						0.00								94		
						0.00								95		
						0.00								96		
						0.00								97		
						0.00								98		
						0.00								99		
						0.00								100		
						0.00								101		
						0.00								102		
						0.00								103		
						0.00								104		
						0.00								105		
						0.00								106		
						0.00								107		
						0.00								108		
						0.00								109		
						0.00								110		
						0.00								111		
						0.00								112		
						0.00								113		
						0.00								114		
						0.00								115		
						0.00								116		
						0.00								117		
						0.00								118		
						0.00								119		
						0.00								120		
						0.00								121		
						0.00								122		
						0.00								123		
						0.00								124		
						0.00								125		
						0.00								126		
						0.00								127		
						0.00								128		
						0.00								129		
						0.00								130		
						0.00								131		
						0.00								132		
						0.00								133		
						0.00								134		
						0.00								135		
						0.00								136		
						0.00								137		
						0.00								138		
						0.00								139		
						0.00								140		
						0.00								141		
						0.00								142		
						0.00								143		
						0.00								144		
						0.00								145		
						0.00								146		
						0.00								147		
						0.00								148		
						0.00								149		
						0.00								150		
						0.00								151		
						0.00								152		
						0.00								153		
						0.00								154		
						0.00								155		
						0.00								156		
						0.00								157		
						0.00								158		
						0.00								159		
						0.00								160		
						0.00								161		
						0.00								162		
						0.00								163		
						0.00								164		
						0.00								165		
						0.00								166		
						0.00								167		
						0.00								168		
						0.00								169		
						0.00								170		
						0.00								171		
						0.00								172		
						0.00								173		
						0.00								174		
						0.00								175		
						0.00								176		
						0.00								177		
						0.00								178		
						0.00								179		
						0.00								180		
						0.00								181		
						0.00								182		
						0.00								183		
						0.00								184		
						0.00								185		
						0.00								186		
						0.00								187		
						0.00								188		
						0.00								189		
						0.00								190		
						0.00								191		
						0.00								192		
						0.00								193		
						0.00								194		
						0.00								195		
						0.00								196		
						0.00								197		
						0.00								198		
						0.00								199		
						0.00								200		
						0.00								201		
						0.00								202		
						0.00								203		
						0.00								204		
						0.00								205		
						0.00								206		
						0.00								207		
						0.00								208		
						0.00								209		
						0.00								210		
						0.00								211		
						0.00								212		
						0.00								213		
						0.00								214		
						0.00								215		
						0.00								216		
						0.00								217		
						0.00								218		
						0.00								219		
						0.00								220		
						0.00								221		
						0.00								222		
						0.00								223		
						0.00								224		
						0.00								225		
						0.00								226		
						0.00								227		
						0.00								228		
						0.00								229		
						0.00								230		
						0.00								231		
						0.00								232		
						0.00								233		
						0.00								234		
						0.00								235		
						0.00								236		
						0.00								237		
						0.00								238		
						0.00								239		
						0.00								240		
						0.00								241		
						0.00								242		
						0.00								243		
						0.00								244		
						0.00								245		
						0.00								246		
						0.00								247		
						0.00								248		
						0.00								249		
						0.00								250		
						0.00								251		
						0.00								252		
						0.00								253		
						0.00								254		
						0.00								255		
						0.00								256		
						0.00								257		
						0.00								258		
						0.00								259		
						0.00								260		
						0.00								261		
						0.00								262		
						0.00								263		
						0.00								264		
						0.00								265		
						0.00								266		
						0.00								267		
						0.00								268		
						0.00								269		
						0.00								270		
						0.00								271		</

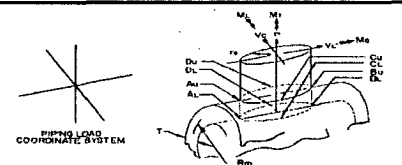
Table A.3.9.2-7 Local Shell Stress at Trunnion Locations—Computation Spreadsheet
for Case UT6

Applied Loads				Geometry											
V_L	862.5	[kips]		I [in]	2.380										
M_L	9526.3	[in-kips]		R_m [in]	40.630										
V_C	0.0	[kips]		r_0 [in]	15.000										
M_C	0.0	[in-kips]		$\beta=0.875 \cdot I_p/R_m$	0.323										
P	0.0	[kips]		$\gamma=R_m/T$	17.071										
M_T	0	[in-kips]		$\lambda=d/D \cdot (D/T)^{1/2}$	2.157										
Figures	Read curves for		multiplier	abs. stress	values	1	2	3	4	5	6	7	8		
						A_U	A_L	B_U	B_L	C_U	C_L	D_U	D_L		
3C AND 4C	1.718	2.346	0.0	0.0	0.0	0.0	0.0	0.0	0.0	0.0	0.0	0.0	0.0	1	P-M
1C AND 2C-1	0.056	0.032	0.0	0.0	0.0	0.0	0.0	0.0	0.0	0.0	0.0	0.0	0.0	2	P-B
3A	0.734		0.0	0.0						0.0	0.0	0.0	0.0	3	M _C -M
1A	0.077		0.0	0.0						0.0	0.0	0.0	0.0	4	M _C -B
3B	1.759		7.5	13.2		-13.2	-13.2	13.2	13.2					5	M _L -M
1B (OR 1B-1)	0.024		768.8	18.7		-18.7	18.7	18.7	-18.7					6	M _L -B
Summation of circumferential stresses $\sigma_\theta \Rightarrow$						-31.9	5.5	31.9	-5.5	0.0	0.0	0.0	0.0	7	
4C AND 3C	2.346	1.718	0.0	0.0	0.0	0.0	0.0	0.0	0.0	0.0	0.0	0.0	0.0	8	P-M
2C AND 1C-1	0.032	0.057	0.0	0.0	0.0	0.0	0.0	0.0	0.0	0.0	0.0	0.0	0.0	9	P-B
4A	1.459		0.0	0.0						0.0	0.0	0.0	0.0	10	M _C -M
2A	0.038		0.0	0.0						0.0	0.0	0.0	0.0	11	M _C -B
4B	0.709		7.5	5.3		-5.3	-5.3	5.3	5.3					12	M _L -M
2B (OR 2B-1)	0.042		768.8	32.6		-32.6	32.6	32.6	-32.6					13	M _L -B
Summation of longitudinal stresses $\sigma_x \Rightarrow$						-37.9	27.3	37.9	-27.3	0.0	0.0	0.0	0.0	14	
WRC-107				Shear stress τ due to V_L	7.6903					7.69	7.69	-7.69	-7.69	15	
				Shear stress τ due to V_C	0	0.00	0.00	0.00	0.00					16	
				Shear stress τ due to M_T	0.00	0.00	0.00	0.00	0.00	0.00	0.00	0.00	0.00	17	
				Summation of shear stress $\tau \Rightarrow$		0.0	0.0	0.0	0.0	7.7	7.7	-7.7	-7.7	18	
S_m	18.7	[kips]		Membrane components of $\sigma_\theta \Rightarrow$		-13.2	-13.2	13.2	13.2	0.0	0.0	0.0	0.0	19	
S_y	20.7	[kips]		Membrane components of $\sigma_x \Rightarrow$		-5.3	-5.3	5.3	5.3	0.0	0.0	0.0	0.0	20	MAX
Allowable	20.7	[kips]		Membrane stress intensities \Rightarrow		13.2	13.2	13.2	13.2	15.4	15.4	15.4	15.4	21	15.4
Allowable	56.1	[kips]		Stress intensities $SI \Rightarrow$		37.9	27.3	37.9	27.3	15.4	15.4	15.4	15.4	22	37.9
				σ_1		-31.9	27.3	37.9	-5.5	7.7	7.7	7.7	7.7		
				σ_2		-37.9	5.5	31.9	-27.3	-7.7	-7.7	-7.7	-7.7		
				$ \sigma_1 - \sigma_2 $		6.0	21.7	6.0	21.7	15.4	15.4	15.4	15.4		
				$ \sigma_1 + \sigma_2 $		69.9	32.8	69.9	32.8	0.0	0.0	0.0	0.0		

OS187H Type 1 Trunnions WRC-107 Calculation

wrc107-case UT6

Table A.3.9.2-8 Local Shell Stress at Trunnion Locations—Computation Spreadsheet
for Case UT7

Applied Loads				Geometry												
V_L	0.0	[kps]		I [in]	2.380											
M_L	0.0	[in-kps]		R_m [in]	40.630											
V_C	71.0	[kps]		r_0 [in]	15.000											
M_C	535.7	[in-kps]		$\beta=0.875-r_0/R_m$	0.323											
P	0.0	[kps]		$\gamma=R_m/T$	17.071											
M_T	0	[in-kps]		$\lambda=d/D(T)^{1/2}$	2.157											
Figures	Read curves for		multiplier	abs. stress	values	1	2	3	4	5	6	7	8			
						A_U	A_L	B_U	B_L	C_U	C_L	D_U	D_L			
3C AND 4C	1.718	2.346	0.0	0.0	0.0	0.0	0.0	0.0	0.0	0.0	0.0	0.0	0.0	1	P-M	
1C AND 2C-1	0.056	0.032	0.0	0.0	0.0	0.0	0.0	0.0	0.0	0.0	0.0	0.0	0.0	2	P-B	
3A	0.734		0.4	0.3						-0.3	-0.3	0.3	0.3	3	M_C -M	
1A	0.077		43.2	3.3						-3.3	3.3	3.3	-3.3	4	M_C -B	
3B	1.759		0.0	0.0		0.0	0.0	0.0	0.0					5	M_L -M	
1B (OR 1B-1)	0.024		0.0	0.0		0.0	0.0	0.0	0.0					6	M_L -B	
Summation of circumferential stresses $\sigma_x \Rightarrow$						0.0	0.0	0.0	0.0	-3.6	3.0	3.6	-3.0	7		
4C AND 3C	2.346	1.718	0.0	0.0	0.0	0.0	0.0	0.0	0.0	0.0	0.0	0.0	0.0	8	P-M	
2C AND 1C-1	0.032	0.057	0.0	0.0	0.0	0.0	0.0	0.0	0.0	0.0	0.0	0.0	0.0	9	P-B	
4A	1.459		0.4	0.6						-0.6	-0.6	0.6	0.6	10	M_C -M	
2A	0.038		43.2	1.7						-1.7	1.7	1.7	-1.7	11	M_C -B	
4B	0.709		0.0	0.0		0.0	0.0	0.0	0.0					12	M_L -M	
2B (OR 2B-1)	0.042		0.0	0.0		0.0	0.0	0.0	0.0					13	M_L -B	
Summation of longitudinal stresses $\sigma_x \Rightarrow$						0.0	0.0	0.0	0.0	-2.3	1.0	2.3	-1.0	14		
WRC-107						Shear stress τ due to V_L	0			0.00	0.00	0.00	0.00	15		
						Shear stress τ due to V_C	0.6331	0.63	-0.63	-0.63				16		
						Shear stress τ due to M_T	0.00	0.00	0.00	0.00	0.00	0.00	0.00	0.00	17	
						Summation of shear stress $\tau \Rightarrow$	0.6	0.6	-0.6	-0.6	0.0	0.0	0.0	0.0	18	
S_m	18.7	[kps]	Membrane components of $\sigma_x \Rightarrow$			0.0	0.0	0.0	0.0	-0.3	-0.3	0.3	0.3	19		
S_y	20.7	[kps]	Membrane components of $\sigma_y \Rightarrow$			0.0	0.0	0.0	0.0	-0.6	-0.6	0.6	0.6	20	MAX	
Allowable	28.05	[kps]	Membrane stress intensities \Rightarrow			1.3	1.3	1.3	1.3	0.6	0.6	0.6	0.6	21	1.3	
Allowable	56.1	[kps]	Stress intensities SI \Rightarrow			1.3	1.3	1.3	1.3	3.6	3.0	3.6	3.0	22	3.6	
1. Curves 1B and 2B apply to rigid attachments 2. If $d/D(T)^{1/2} > 2.0$, then use 2c-1 for 1c and 1c-1 for 2c Ref: Stearns Roger "Analysis of External Loadings on Pressure Vessels"						σ_1	0.6	0.6	0.6	0.6	-2.3	3.0	3.6	-1.0		
						σ_2	-0.6	-0.6	-0.6	-0.6	-3.6	1.0	2.3	-3.0		
						$ \sigma_1 - \sigma_2 $	1.3	1.3	1.3	1.3	1.4	2.0	1.4	2.0		
						$ \sigma_1 + \sigma_2 $	0.0	0.0	0.0	0.0	5.9	4.0	5.9	4.0		

OS187H Type 1 Trunnions WRC-107 Calculation

wrc107-case UT7

Table A.3.9.2-9 Local Shell Stress at Trunnion Locations—Computation Spreadsheet
for Case UT8

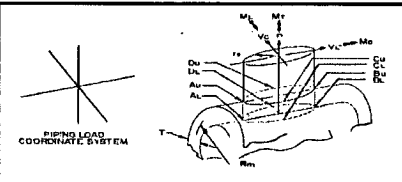
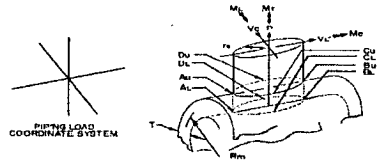
Applied Loads					Geometry													
V_L	0.0	[kips]	I [in]	2.380														
M_L	0.0	[in-kips]	R_m [in]	40.630														
V_C	71.0	[kips]	r_0 [in]	15.000														
M_C	535.7	[in-kips]	$\beta=0.875 \cdot f_y \cdot R_m$	0.323														
P	-142.0	[kips]	$\gamma=R_m/T$	17.071														
M_T	0	[in-kips]	$\lambda=d/D(T/1)^{1/2}$	2.157														
Figures	Read curves for		multiplier	abs. stress		values	1	2	3	4	5	6	7	8				
							A_U	A_L	B_U	B_L	C_U	C_L	D_U	D_L				
3C AND 4C	1.718	2.346	-1.5	-2.5	-3.4		-3.4	-3.4	-3.4	-3.4	-2.5	-2.5	-2.5	-2.5	1	P-M		
1C AND 2C-1	0.056	0.032	-150.4	-8.5	-4.8		-4.8	4.8	-4.8	4.8	-8.5	8.5	-8.5	8.5	2	P-B		
3A	0.734		0.4	0.3							-0.3	-0.3	0.3	0.3	3	M-C		
1A	0.077		43.2	3.3							-3.3	3.3	3.3	-3.3	4	M-C		
3B	1.759		0.0	0.0			0.0	0.0	0.0	0.0					5	M-L		
1B (OR 1B-1)	0.024		0.0	0.0			0.0	0.0	0.0	0.0					6	M-L		
Summation of circumferential stresses $\sigma_\theta \Rightarrow$							-8.2	1.3	-8.2	1.3	-14.6	9.0	-7.4	2.9	7			
4C AND 3C	2.346	1.718	-1.5	-3.4	-2.5		-2.5	-2.5	-2.5	-2.5	-3.4	-3.4	-3.4	-3.4	8	P-M		
2C AND 1C-1	0.032	0.057	-150.4	-4.8	-8.5		-8.5	8.5	-8.5	8.5	-4.8	4.8	-4.8	4.8	9	P-B		
4A	1.459		0.4	0.6							-0.6	-0.6	0.6	0.6	10	M-C		
2A	0.038		43.2	1.7							-1.7	1.7	1.7	-1.7	11	M-C		
4B	0.709		0.0	0.0			0.0	0.0	0.0	0.0					12	M-L		
2B (OR 2B-1)	0.042		0.0	0.0			0.0	0.0	0.0	0.0					13	M-L		
Summation of longitudinal stresses $\sigma_x \Rightarrow$							-11.0	6.0	-11.0	6.0	-10.5	2.4	-6.0	0.3	14			
WRC-107							Shear stress τ due to V_L											
							0											
							Shear stress τ due to V_C								0.6331	0.63	-0.63	-0.63
							Shear stress τ due to M_T											
							0.00	0.00	0.00	0.00	0.00	0.00	0.00	0.00	0.00	16		
							Summation of shear stress $\tau \Rightarrow$											
							0.6	0.6	-0.6	-0.6	0.0	0.0	0.0	0.0	0.0	17		
							Membrane components of $\sigma_\theta \Rightarrow$											
							-3.4	-3.4	-3.4	-3.4	-2.8	-2.8	-2.2	-2.2	19			
							Membrane components of $\sigma_x \Rightarrow$											
							-2.5	-2.5	-2.5	-2.5	-4.1	-4.1	-2.8	-2.8	20	MAX		
							Membrane stress intensities \Rightarrow											
							3.8	3.8	3.8	3.8	4.1	4.1	2.8	2.8	21	4.1		
Allowable	28.05	[kips]	Stress intensities $SI \Rightarrow$				11.2	6.1	11.2	6.1	14.6	9.0	7.4	2.9	22	14.6		
Allowable	56.1	[kips]																
							σ_1	-8.1	6.1	-8.1	6.1	-10.5	9.0	-6.0	2.9			
							σ_2	-11.2	1.3	-11.2	1.3	-14.6	2.4	-7.4	0.3			
							$ \sigma_1 - \sigma_2 $	3.1	4.8	3.1	4.8	4.1	6.6	1.4	2.6			
							$ \sigma_1 + \sigma_2 $	19.3	7.3	19.3	7.3	25.1	11.3	13.3	3.3			

Table A.3.9.2- 10 Local Shell Stress at Trunnion Locations—Computation Spreadsheet for Case UT9

Applied Loads				Geometry				<div></div>									
V_L	0.0	[kips]		I [in]	2.380												
M_L	0.0	[in-kips]		R_m [in]	40.630												
V_C	142.0	[kips]		r_0 [in]	15.000												
M_C	1071.4	[in-kips]		$\beta=0.875 \cdot d_p/R_m$	0.323												
P	0.0	[kips]		$\gamma=R_m/T$	17.071												
M_T	0	[in-kips]		$\lambda=d/D(T)^{1/2}$	2.157												
Figures	Read curves for		multiplier	abs. stress	values	1	2	3	4	5	6	7	8				
3C AND 4C	1.718	2.346	0.0	0.0	0.0	0.0	0.0	0.0	0.0	0.0	0.0	0.0	0.0	1	P-M		
1C AND 2C-1	0.056	0.032	0.0	0.0	0.0	0.0	0.0	0.0	0.0	0.0	0.0	0.0	0.0	2	P-B		
3A	0.734		0.8	0.6						-0.6	-0.6	0.6	0.6	3	M _C -M		
1A	0.077		86.5	6.6						-6.6	6.6	6.6	-6.6	4	M _C -B		
3B	1.759		0.0	0.0		0.0	0.0	0.0	0.0					5	M _L -M		
1B (OR 1B-1)	0.024		0.0	0.0		0.0	0.0	0.0	0.0					6	M _L -B		
Summation of circumferential stresses $\sigma_\theta \Rightarrow$						0.0	0.0	0.0	0.0	-7.3	6.0	7.3	-6.0	7			
4C AND 3C	2.346	1.718	0.0	0.0	0.0	0.0	0.0	0.0	0.0	0.0	0.0	0.0	0.0	8	P-M		
2C AND 1C-1	0.032	0.057	0.0	0.0	0.0	0.0	0.0	0.0	0.0	0.0	0.0	0.0	0.0	9	P-B		
4A	1.459		0.8	1.2						-1.2	-1.2	1.2	1.2	10	M _C -M		
2A	0.038		86.5	3.3						-3.3	3.3	3.3	-3.3	11	M _C -B		
4B	0.709		0.0	0.0		0.0	0.0	0.0	0.0					12	M _L -M		
2B (OR 2B-1)	0.042		0.0	0.0		0.0	0.0	0.0	0.0					13	M _L -B		
Summation of longitudinal stresses $\sigma_x \Rightarrow$						0.0	0.0	0.0	0.0	-4.5	2.1	4.5	-2.1	14			
WRC-107																	
Shear stress τ due to V_L						0				0.00	0.00	0.00	0.00	15			
Shear stress τ due to V_C						1.2661	1.27	1.27	-1.27	-1.27				16			
Shear stress τ due to M_T						0.00	0.00	0.00	0.00	0.00	0.00	0.00	0.00	17			
Summation of shear stress $\tau \Rightarrow$						1.3	1.3	-1.3	-1.3	0.0	0.0	0.0	0.0	18			
S_m	18.7	[kips]	Membrane components of $\sigma_\theta \Rightarrow$			0.0	0.0	0.0	0.0	-0.6	-0.6	0.6	0.6	19			
S_y	20.7	[kips]	Membrane components of $\sigma_x \Rightarrow$			0.0	0.0	0.0	0.0	-1.2	-1.2	1.2	1.2	20	MAX		
Allowable	28.05	[kips]	Membrane stress intensities \Rightarrow			2.5	2.5	2.5	2.5	1.2	1.2	1.2	1.2	21	2.5		
Allowable	56.1	[kips]	Stress intensities SI \Rightarrow			2.5	2.5	2.5	2.5	7.3	6.0	7.3	6.0	22	7.3		
1. Curves 1B and 2B apply to rigid attachments						σ_1	1.3	1.3	1.3	-4.5	6.0	7.3	-2.1				
2. If $d/D(T)^{1/2} > 2.0$, then use 2c-1 for 1c and 1c-1 for 2c						σ_2	-1.3	-1.3	-1.3	-7.3	2.1	4.5	-6.0				
Ref: Stearns Roger "Analysis of External Loadings on Pressure Vessels"						$ \sigma_1 - \sigma_2 $	2.5	2.5	2.5	2.5	7.3	3.9	2.7	3.9			
						$ \sigma_1 + \sigma_2 $	0.0	0.0	0.0	0.0	11.8	8.1	11.8	8.1			

OS187H Type 1 Trunnions WRC-107 Calculation

wrc107-case UT9

Table A.3.9.2- 11 Local Shell Stress at Trunnion Locations—Computation Spreadsheet
for Case UT10

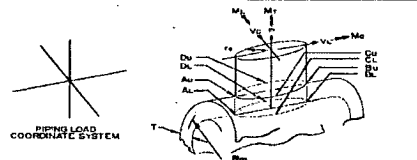
Applied Loads				Geometry															
V_L	0.0	[kps]		I [in ⁴]	2.380														
M_L	0.0	[in-kps]		R_m [in]	40.630														
V_C	106.5	[kps]		I_0 [in ⁴]	15.000														
M_C	803.5	[in-kps]		$\beta=0.875 \cdot I_0/R_m$	0.323														
P	-71.0	[kps]		$\gamma=R_m/T$	17.071														
M_T	0	[in-kps]		$\lambda=d(D/T)^{1/2}$	2.157														

Figures	Read curves for		multiplier	abs. stress	values	1	2	3	4	5	6	7	8		
						A_U	A_L	B_U	B_L	C_U	C_L	D_U	D_L		
3C AND 4C	1.718	2.346	-0.7	-1.3	-1.7	-1.7	-1.7	-1.7	-1.7	-1.3	-1.3	-1.3	-1.3	1 P-M	
1C AND 2C-1	0.056	0.032	-75.2	-4.2	-2.4	-2.4	2.4	-2.4	2.4	-4.2	4.2	-4.2	4.2	2 P-B	
3A	0.734		0.6	0.5						-0.5	-0.5	0.5	0.5	3 M _C -M	
1A	0.077		64.8	5.0						-5.0	5.0	5.0	-5.0	4 M _C -B	
3B	1.759		0.0	0.0		0.0	0.0	0.0	0.0					5 M _L -M	
1B (OR 1B-1)	0.024		0.0	0.0		0.0	0.0	0.0	0.0					6 M _L -B	
Summation of circumferential stresses $\sigma_\theta \Rightarrow$						-4.1	0.7	-4.1	0.7	-10.9	7.5	-0.1	-1.5	7	
4C AND 3C	2.346	1.718	-0.7	-1.7	-1.3	-1.3	-1.3	-1.3	-1.3	-1.7	-1.7	-1.7	-1.7	8 P-M	
2C AND 1C-1	0.032	0.057	-75.2	-2.4	-4.3	-4.3	4.3	-4.3	4.3	-2.4	2.4	-2.4	2.4	9 P-B	
4A	1.459		0.6	0.9						-0.9	-0.9	0.9	0.9	10 M _C -M	
2A	0.038		64.8	2.5						-2.5	2.5	2.5	-2.5	11 M _C -B	
4B	0.709		0.0	0.0		0.0	0.0	0.0	0.0					12 M _L -M	
2B (OR 2B-1)	0.042		0.0	0.0		0.0	0.0	0.0	0.0					13 M _L -B	
Summation of longitudinal stresses $\sigma_x \Rightarrow$						-5.5	3.0	-5.5	3.0	-7.5	2.2	-0.7	-0.9	14	
WRC-107						Shear stress τ due to V_L								15	
						Shear stress τ due to V_C								16	
						Shear stress τ due to M_T								17	
						Summation of shear stress $\tau \Rightarrow$								18	
						Membrane components of $\sigma_\theta \Rightarrow$								19	
						Membrane components of $\sigma_x \Rightarrow$								20	
						Membrane stress intensities \Rightarrow								21	
						Stress intensities $SI \Rightarrow$								22	
						σ_1	-3.6	3.3	-3.6	3.3	-7.5	7.5	-0.1	-0.9	
						σ_2	-6.0	0.3	-6.0	0.3	-10.9	2.2	-0.7	-1.5	
						$ \sigma_1 - \sigma_2 $	2.4	3.0	2.4	3.0	3.4	5.2	0.7	0.7	
						$ \sigma_1 + \sigma_2 $	9.6	3.7	9.6	3.7	18.5	9.7	0.8	2.4	
1. Curves 1B and 2B apply to rigid attachments															
2. If $d(D/T)^{1/2} > 2.0$, then use 2c-1 for 1c and 1c-1 for 2c															
Ref: Stearns Roger "Analysis of External Loadings on Pressure Vessels"															

OS187H Type 1 Trunnions WRC-107 Calculation

wrc107-case UT10

Table A.3.9.2- 12 Local Shell Stress at Trunnion Locations—Computation Spreadsheet for Case LT1

Applied Loads				Geometry				<div></div>											
V_L	125.0	[kips]		I [in]	1.500														
M_L	982.5	[in-kips]		R_m [in]	40.190														
V_C	54.0	[kips]		r_g [in]	7.315														
M_C	424.4	[in-kips]		$\beta=0.875 \cdot r_g/R_m$	0.159														
P	0.0	[kips]		$\gamma=R_m/T$	26.793														
M_T	0	[in-kips]		$\lambda=d/D(D/T)^{1/2}$	1.332														
Figures	Read curves for		multiplier	abs. stress	values	1	2	3	4	5	6	7	8						
						A_U	A_L	B_U	B_L	C_U	C_L	D_U	D_L						
3C AND 4C	3.154	4.336	0.0	0.0	0.0	0.0	0.0	0.0	0.0	0.0	0.0	0.0	0.0	1	P-M				
1C AND 2C-1	0.099	0.065	0.0	0.0	0.0	0.0	0.0	0.0	0.0	0.0	0.0	0.0	0.0	2	P-B				
3A	0.972		1.1	1.1						-1.1	-1.1	1.1	1.1	3	M_C -M				
1A	0.091		176.8	16.1						-16.1	16.1	16.1	-16.1	4	M_C -B				
3B	2.971		2.5	7.6		-7.6	-7.6	7.6	7.6					5	M_L -M				
1B (OR 1B-1)	0.039		409.3	16.1		-16.1	16.1	16.1	-16.1					6	M_L -B				
Summation of circumferential stresses $\sigma_\theta \Rightarrow$						-23.6	8.5	23.6	-8.5	-17.2	15.0	17.2	-15.0	7					
4C AND 3C	4.336	3.154	0.0	0.0	0.0	0.0	0.0	0.0	0.0	0.0	0.0	0.0	0.0	8	P-M				
2C AND 1C-1	0.065	0.102	0.0	0.0	0.0	0.0	0.0	0.0	0.0	0.0	0.0	0.0	0.0	9	P-B				
4A	1.506		1.1	1.7						-1.7	-1.7	1.7	1.7	10	M_C -M				
2A	0.047		176.8	8.4						-8.4	8.4	8.4	-8.4	11	M_C -B				
4B	0.932		2.5	2.4		-2.4	-2.4	2.4	2.4					12	M_L -M				
2B (OR 2B-1)	0.064		409.3	26.1		-26.1	26.1	26.1	-26.1					13	M_L -B				
Summation of longitudinal stresses $\sigma_x \Rightarrow$						-28.4	23.7	28.4	-23.7	-10.0	6.7	10.0	-6.7	14					
WRC-107						Shear stress τ due to V_L	3.6262				3.63	3.63	-3.63	-3.63	15				
						Shear stress τ due to V_C	1.5665	1.57	1.57	-1.57	-1.57							16	
						Shear stress τ due to M_T	0.00	0.00	0.00	0.00	0.00	0.00	0.00	0.00	0.00	17			
Summation of shear stress $\tau \Rightarrow$						1.6	1.6	-1.6	-1.6	3.6	3.6	-3.6	-3.6	18					
S_m	18.7	[kips]	Membrane components of $\sigma_\theta \Rightarrow$			-7.6	-7.6	7.6	7.6	-1.1	-1.1	1.1	1.1	19					
S_y	20.7	[kips]	Membrane components of $\sigma_x \Rightarrow$			-2.4	-2.4	2.4	2.4	-1.7	-1.7	1.7	1.7	20	MAX				
Allowable	28.05	[kips]	Membrane stress intensities \Rightarrow			8.0	8.0	8.0	8.0	7.3	7.3	7.3	7.3	21	8.0				
Allowable	56.1	[kips]	Stress intensities SI \Rightarrow			28.9	23.8	28.9	23.8	18.7	16.4	18.7	16.4	22	28.9				
1. Curves 1B and 2B apply to rigid attachments 2. If $d/D(D/T)^{1/2} > 2.0$, then use 2c-1 for 1c and 1c-1 for 2c Ref. Stearns Roger "Analysis of External Loadings on Pressure Vessels"						σ_1	-23.2	23.8	28.9	-8.3	-8.5	16.4	18.7	-5.3					
						σ_2	-28.9	8.3	23.2	-23.8	-18.7	5.3	8.5	-16.4					
						$ \sigma_1 - \sigma_2 $	5.7	15.5	5.7	15.5	10.2	11.1	10.2	11.1					
						$ \sigma_1 + \sigma_2 $	52.1	32.2	52.1	32.2	27.2	21.7	27.2	21.7					

OS187H Type 1 Trunnions WRC-107 Calculation

wrc107-case LT1

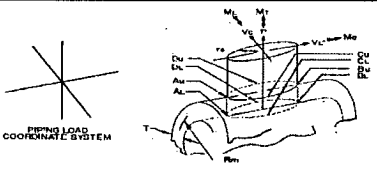
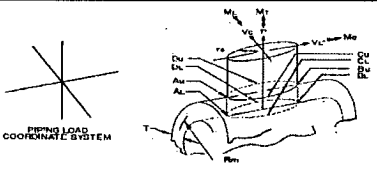
Table A.3.9.2-13 Local Shell Stress at Trunnion Locations—Computation Spreadsheet
for Case LT2

Applied Loads				Geometry											
V_L	0.0	[kips]		I [in]	1.500										
M_L	0.0	[in-kips]		R_m [in]	40.190										
V_C	54.0	[kips]		r_0 [in]	7.315										
M_C	424.4	[in-kips]		$\beta=0.875 \cdot r_0/R_m$	0.159										
P	-108.0	[kips]		$\gamma=R_m/T$	26.793										
M_T	0	[in-kips]		$\lambda=d/D(T)^{1/2}$	1.332										
Figures	Read curves for		multiplier	abs. stress	values	1	2	3	4	5	6	7	8		
						A_U	A_L	B_U	B_L	C_U	C_L	D_U	D_L		
3C AND 4C	3.154	4.336	-1.8	-5.7	-7.8	-7.8	-7.8	-7.8	-7.8	-5.7	-5.7	-5.7	-5.7	1	P-M
1C AND 2C-1	0.099	0.065	-288.0	-28.4	-18.9	-18.9	18.9	-18.9	18.9	-28.4	28.4	-28.4	28.4	2	P-B
3A	0.972		1.1	1.1						-1.1	-1.1	1.1	1.1	3	M_C -M
1A	0.091		176.8	16.1						-16.1	16.1	16.1	-16.1	4	M_C -B
3B	2.971		0.0	0.0		0.0	0.0	0.0	0.0					5	M_L -M
1B (OR 1B-1)	0.039		0.0	0.0		0.0	0.0	0.0	0.0					6	M_L -B
Summation of circumferential stresses $\sigma_\phi \Rightarrow$						-26.6	11.1	-26.6	11.1	-51.2	37.8	-16.8	7.7	7	
4C AND 3C	4.336	3.154	-1.8	-7.8	-5.7	-5.7	-5.7	-5.7	-5.7	-7.8	-7.8	-7.8	-7.8	8	P-M
2C AND 1C-1	0.065	0.102	-288.0	-18.9	-29.4	-29.4	29.4	-29.4	29.4	-18.9	18.9	-18.9	18.9	9	P-B
4A	1.506		1.1	1.7						-1.7	-1.7	1.7	1.7	10	M_C -M
2A	0.047		176.8	8.4						-8.4	8.4	8.4	-8.4	11	M_C -B
4B	0.932		0.0	0.0		0.0	0.0	0.0	0.0					12	M_L -M
2B (OR 2B-1)	0.064		0.0	0.0		0.0	0.0	0.0	0.0					13	M_L -B
Summation of longitudinal stresses $\sigma_x \Rightarrow$						-35.1	23.8	-35.1	23.8	-36.6	17.8	-16.6	4.4	14	
WRC-107						Shear stress τ due to V_L								15	
						Shear stress τ due to V_C								16	
						Shear stress τ due to M_T								17	
Summation of shear stress						1.6	1.6	-1.6	-1.6	0.0	0.0	0.0	0.0	18	
S_m 18.7 [kips]						Membrane components of $\sigma_\phi \Rightarrow$								19	
						-7.8	-7.8	-7.8	-7.8	-6.7	-6.7	-4.6	-4.6	20	MAX
S_y 20.7 [kips]						Membrane components of $\sigma_x \Rightarrow$								21	9.4
						-5.7	-5.7	-5.7	-5.7	-9.4	-9.4	-6.1	-6.1	22	51.2
Allowable 28.05 [kips]						Membrane stress intensities \Rightarrow									
Allowable 56.1 [kips]						Stress intensities $SI \Rightarrow$									
1. Curves 1B and 2B apply to rigid attachments 2. If $d/D(T)^{1/2} > 2.0$, then use 2c-1 for 1c and 1c-1 for 2c Ref. Stearns Roger "Analysis of External Loadings on Pressure Vessels"						σ_1	-26.3	24.0	-26.3	24.0	-36.6	37.8	-16.6	7.7	
						σ_2	-35.3	10.9	-35.3	10.9	-51.2	17.8	-16.8	4.4	
						$ \sigma_1 - \sigma_2 $	9.0	13.1	9.0	13.1	14.6	20.0	0.2	3.3	
						$ \sigma_1 + \sigma_2 $	61.7	34.9	61.7	34.9	87.8	55.6	33.5	12.1	

OS187H Type 1 Trunnions WRC-107 Calculation

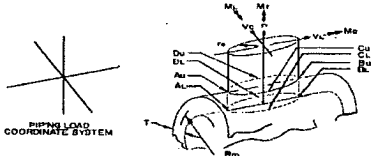
wrc107-case LT2

for Case LT3

Applied Loads			Geometry													
V_L	0.0	[kips]	I [in]	1.500												
M_L	0.0	[in-kips]	R_m [in]	40.190												
V_C	108.0	[kips]	t_0 [in]	7.315												
M_C	848.9	[in-kips]	$B=0.875 \cdot t_0 \cdot R_m$	0.159												
P	0.0	[kips]	$\gamma=R_m/T$	26.793												
M_T	0	[in-kips]	$\lambda=d/D(D/T)^{1/2}$	1.332												
Figures	Read curves for	multiplier	abs. stress	values		1	2	3	4	5	6	7	8			
						A_U	A_L	B_U	B_L	C_U	C_L	D_U	D_L			
3C AND 4C	3.154	4.336	0.0	0.0	0.0	0.0	0.0	0.0	0.0	0.0	0.0	0.0	0.0	1	P-M	
1C AND 2C-1	0.099	0.065	0.0	0.0	0.0	0.0	0.0	0.0	0.0	0.0	0.0	0.0	0.0	2	P-B	
3A	0.972		2.2	2.1						-2.1	-2.1	2.1	2.1	3	M-C	
1A	0.091		353.7	32.2						-32.2	32.2	32.2	-32.2	4	M-C	
3B	2.971		0.0	0.0		0.0	0.0	0.0	0.0					5	M-L	
1B (OR 1B-1)	0.039		0.0	0.0		0.0	0.0	0.0	0.0					6	M-L	
Summation of circumferential stresses $\sigma_\phi \Rightarrow$						0.0	0.0	0.0	0.0	-34.4	30.1	34.4	-30.1	7		
4C AND 3C	4.336	3.154	0.0	0.0	0.0	0.0	0.0	0.0	0.0	0.0	0.0	0.0	0.0	8	P-M	
2C AND 1C-1	0.065	0.102	0.0	0.0	0.0	0.0	0.0	0.0	0.0	0.0	0.0	0.0	0.0	9	P-B	
4A	1.506		2.2	3.3						-3.3	-3.3	3.3	3.3	10	M-C	
2A	0.047		353.7	16.7						-16.7	16.7	16.7	-16.7	11	M-C	
4B	0.932		0.0	0.0		0.0	0.0	0.0	0.0					12	M-L	
2B (OR 2B-1)	0.064		0.0	0.0		0.0	0.0	0.0	0.0					13	M-L	
Summation of longitudinal stresses $\sigma_x \Rightarrow$						0.0	0.0	0.0	0.0	-20.0	13.4	20.0	-13.4	14		
WRC-107 Shear stress τ due to V_L 0 Shear stress τ due to V_C 3.1331 Shear stress τ due to M_T 0.0001						3.13	3.13	-3.13	-3.13	0.00	0.00	0.00	0.00	15		
						0.00	0.00	0.00	0.00	0.00	0.00	0.00	0.00	16		
						3.1	3.1	-3.1	-3.1	0.0	0.0	0.0	0.0	17		
						0.0	0.0	0.0	0.0	-2.1	-2.1	2.1	2.1	18		
Summation of shear stress $\tau \Rightarrow$						3.1	3.1	-3.1	-3.1	0.0	0.0	0.0	0.0	19		
S_m	18.7	[kips]	Membrane components of $\sigma_\phi \Rightarrow$			0.0	0.0	0.0	0.0	-2.1	-2.1	2.1	2.1	20	MAX	
S_y	20.7	[kips]	Membrane components of $\sigma_x \Rightarrow$			0.0	0.0	0.0	0.0	-3.3	-3.3	3.3	3.3	21		
Allowable	28.05	[kips]	Membrane stress intensities \Rightarrow			6.3	6.3	6.3	6.3	3.3	3.3	3.3	3.3	22	6.3	
Allowable	56.1	[kips]	Stress intensities $S_I \Rightarrow$			6.3	6.3	6.3	6.3	34.4	30.1	34.4	30.1	22	34.4	
1. Curves 1B and 2B apply to rigid attachments 2. If $d/D(D/T)^{1/2} > 2.0$, then use 2c-1 for 1c and 1c-1 for 2c Ref. Stearns Roger "Analysis of External Loadings on Pressure Vessels"						σ_1	3.1	3.1	3.1	3.1	-20.0	30.1	34.4	-13.4		
						σ_2	-3.1	-3.1	-3.1	-3.1	-34.4	13.4	20.0	-30.1		
						$ \sigma_1 - \sigma_2 $	6.3	6.3	6.3	6.3	14.3	16.7	14.3	16.7		
						$ \sigma_1 + \sigma_2 $	0.0	0.0	0.0	0.0	54.4	43.5	54.4	43.5		

wrc107-case LT3

Table A.3.9.2- 15 Local Shell Stress at Trunnion Locations—Computation Spreadsheet
for Case LT4

Applied Loads				Geometry															
V_L	62.5	[kips]		t [in]	1.500														
M_L	491.3	[in-kips]		R_m [in]	40.190														
V_C	81.0	[kips]		r_0 [in]	7.315														
M_C	636.7	[in-kips]		$\beta=0.875 \cdot f_p/R_m$	0.159														
P	-54.0	[kips]		$\gamma=R_m/T$	26.793														
M_T	0	[in-kips]		$\lambda=d/(D/T)^{1/2}$	1.332														
Figures				Read curves for		multiplier	abs. stress	values	1	2	3	4	5	6	7	8			
									A_U	A_L	B_U	B_L	C_U	C_L	D_U	D_L			
3C AND 4C				3.154		4.3	-0.9	-2.8	-3.9	-3.9	-3.9	-3.9	-2.8	-2.8	-2.8	-2.8	1	P-M	
1C AND 2C-1				0.099		0.065	-144.0	-14.2	-9.4	-9.4	-9.4	-9.4	-14.2	14.2	-14.2	14.2	2	P-B	
3A				0.972			1.6	1.6					-1.6	-1.6	1.6	1.6	3	M-C	
1A				0.091			265.2	24.2					-24.2	24.2	24.2	-24.2	4	M-C	
3B				2.971			1.3	3.8									5	M-L	
1B (OR 1B-1)				0.039			204.7	8.0									6	M-L	
							Summation of circumferential stresses $\sigma_\phi \Rightarrow$		-25.1	9.8	-1.5	1.3	-42.8	33.9	8.8	-11.2	7		
4C AND 3C				4.336		3.2	-0.9	-3.9	-2.8	-2.8	-2.8	-2.8	-3.9	-3.9	-3.9	-3.9	8	P-M	
2C AND 1C-1				0.065		0.102	-144.0	-9.4	-14.7	-14.7	14.7	-14.7	-9.4	9.4	-9.4	9.4	9	P-B	
4A				1.506			1.6	2.5					-2.5	-2.5	2.5	2.5	10	M-C	
2A				0.047			265.2	12.5					-12.5	12.5	12.5	-12.5	11	M-C	
4B				0.932			1.3	1.2									12	M-L	
2B (OR 2B-1)				0.064			204.7	13.0									13	M-L	
							Summation of longitudinal stresses $\sigma_x \Rightarrow$		-31.8	23.7	-3.3	0.0	-28.3	15.6	1.7	-4.5	14		
WRC-107							Shear stress τ due to V_L		1.8131				1.81	1.81	-1.81	-1.81	15		
							Shear stress τ due to V_C		2.3498	2.35	2.35	-2.35	-2.35					16	
							Shear stress τ due to M_T		0.00	0.00	0.00	0.00	0.00	0.00	0.00	0.00	0.00	17	
							Summation of shear stress $\tau \Rightarrow$		2.3	2.3	-2.3	-2.3	1.8	1.8	-1.8	-1.8			18
S_m				18.7		[kips]	Membrane components of $\sigma_\phi \Rightarrow$		-7.7	-7.7	-0.1	-0.1	-4.4	-4.4	-1.2	-1.2	19		
S_y				20.7		[kips]	Membrane components of $\sigma_x \Rightarrow$		-4.0	-4.0	-1.6	-1.6	-6.4	-6.4	-1.4	-1.4	20	MAX	
Allowable				28.05		[kips]	Membrane stress intensities \Rightarrow		8.8	8.8	4.9	4.9	7.5	7.5	3.6	3.6	21	8.8	
Allowable				56.1		[kips]	Stress intensities $S_I \Rightarrow$		32.5	24.1	5.0	4.9	43.0	34.1	9.2	11.7	22	43.0	
							σ_1		-24.4	24.1	0.1	3.1	-28.1	34.1	9.2	-4.0			
							σ_2		-32.5	9.4	-4.9	-1.8	-43.0	15.4	1.3	-11.7			
							$ \sigma_1 - \sigma_2 $		8.1	14.7	5.0	4.9	14.9	18.7	7.9	7.6			
							$ \sigma_1 + \sigma_2 $		56.9	33.5	4.8	1.3	71.1	49.5	10.5	15.7			
1. Curves 1B and 2B apply to rigid attachments																			
2. If $d/(D(T))^{1/2} > 2.0$, then use 2c-1 for 1c and 1c-1 for 2c																			
Ref. Stearns Roger 'Analysis of External Loadings on Pressure Vessels'																			

OS187H Type 1 Trunnions WRC-107 Calculation

wrc107-case LT4

Table A.3.9.2– 16 Local Shell Stress at Trunnion Locations—Summary of Results

Case ID.	Location	Load Combination	Maximum Stress		Allowable [ksi]	Reference Table
			Type	Value [ksi]		
UT1	Upper trunnion pad	Critical lifting 6g axial	P_L	17.4	28.1	Table A.3.9.2-2
			P_L+P_b+Q	42.7	56.1	Table A.3.9.2-2
UT6	Upper trunnion shell	Critical lifting 6g axial	P_L	15.4	28.1	Table A.3.9.2-7
			P_L+P_b+Q	37.9	56.1	Table A.3.9.2-7
UT2	Upper trunnion pad	Transfer load DW+1g axial	P_L	1.4	28.1	Table A.3.9.2-3
			P_L+P_b+Q	2.9	56.1	Table A.3.9.2-3
UT7	Upper trunnion shell	Transfer load DW+1g axial	P_L	1.3	28.1	Table A.3.9.2-8
			P_L+P_b+Q	3.6	56.1	Table A.3.9.2-8
UT3	Upper trunnion pad	Transfer load DW+1g transverse	P_L	2.4	28.1	Table A.3.9.2-4
			P_L+P_b+Q	11.7	56.1	Table A.3.9.2-4
UT8	Upper trunnion shell	Transfer load DW+1g transverse	P_L	4.1	28.1	Table A.3.9.2-9
			P_L+P_b+Q	14.6	56.1	Table A.3.9.2-9
UT4	Upper trunnion pad	Transfer load DW+1g vertical	P_L	2.9	28.1	Table A.3.9.2-5
			P_L+P_b+Q	5.8	56.1	Table A.3.9.2-5
UT9	Upper trunnion shell	Transfer load DW+1g vertical	P_L	2.5	28.1	Table A.3.9.2-10
			P_L+P_b+Q	7.3	56.1	Table A.3.9.2-10
UT5	Upper trunnion pad	Transfer load 1/2g A+1/2gT+1/2gV +DW	P_L	2.2	28.1	Table A.3.9.2-6
			P_L+P_b+Q	8.8	56.1	Table A.3.9.2-6
UT10	Upper trunnion shell	Transfer load 1/2g A+1/2gT+1/2g V+DW	P_L	2.6	28.1	Table A.3.9.2-11
			P_L+P_b+Q	10.9	56.1	Table A.3.9.2-11
LT1	Lower trunnion shell	Transfer load DW+1g axial	P_L	8.0	28.1	Table A.3.9.2-12
			P_L+P_b+Q	28.9	56.1	Table A.3.9.2-12
LT2	Lower trunnion shell	Transfer load DW+1g transverse	P_L	9.4	28.1	Table A.3.9.2-13
			P_L+P_b+Q	51.2	56.1	Table A.3.9.2-13
LT3	Lower trunnion shell	Transfer load DW+1g vertical	P_L	6.3	28.1	Table A.3.9.2-14
			P_L+P_b+Q	34.4	56.1	Table A.3.9.2-14
LT4	Lower trunnion shell	Transfer load 1/2g A+1/2gT+1/2gV +DW	P_L	8.8	28.1	Table A.3.9.2-15
			P_L+P_b+Q	43.0	56.1	Table A.3.9.2-15

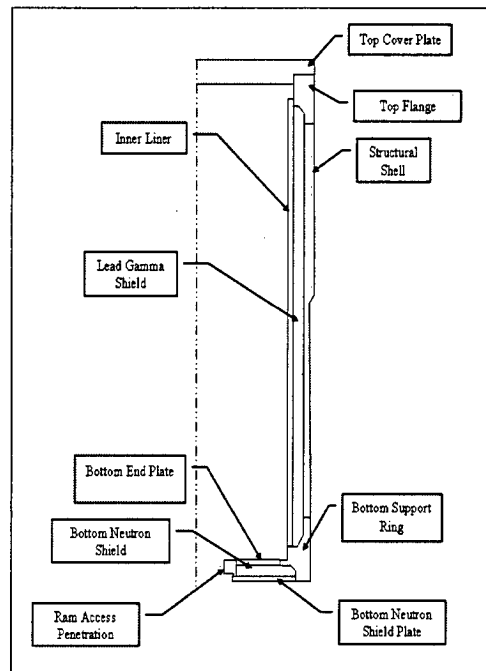


**Figure Withheld
under 10 CFR 2.390**

Figure A.3.9.2– 1 Transfer Cask Key Components and Dimensions

(Drawing Not to Scale)

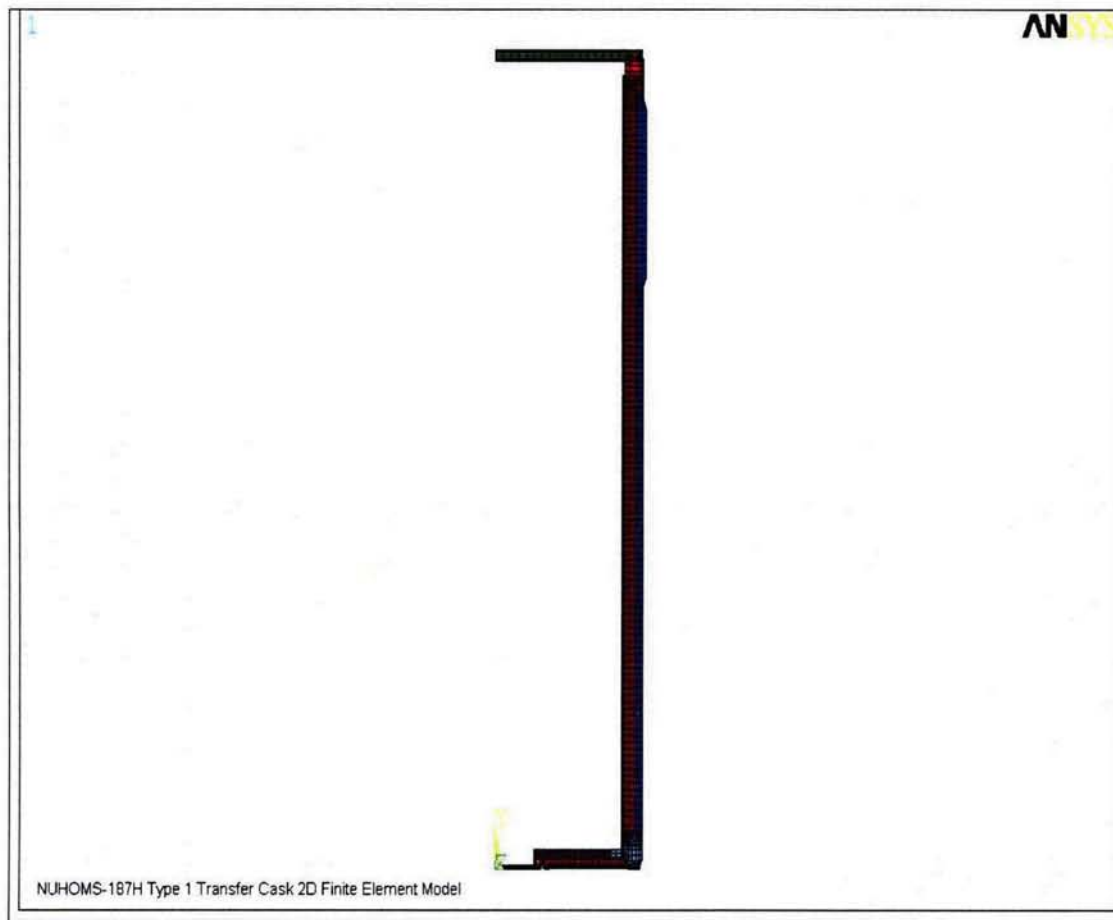


Figure A.3.9.2– 2 2-Dimensional Finite Element Model, Element Plot

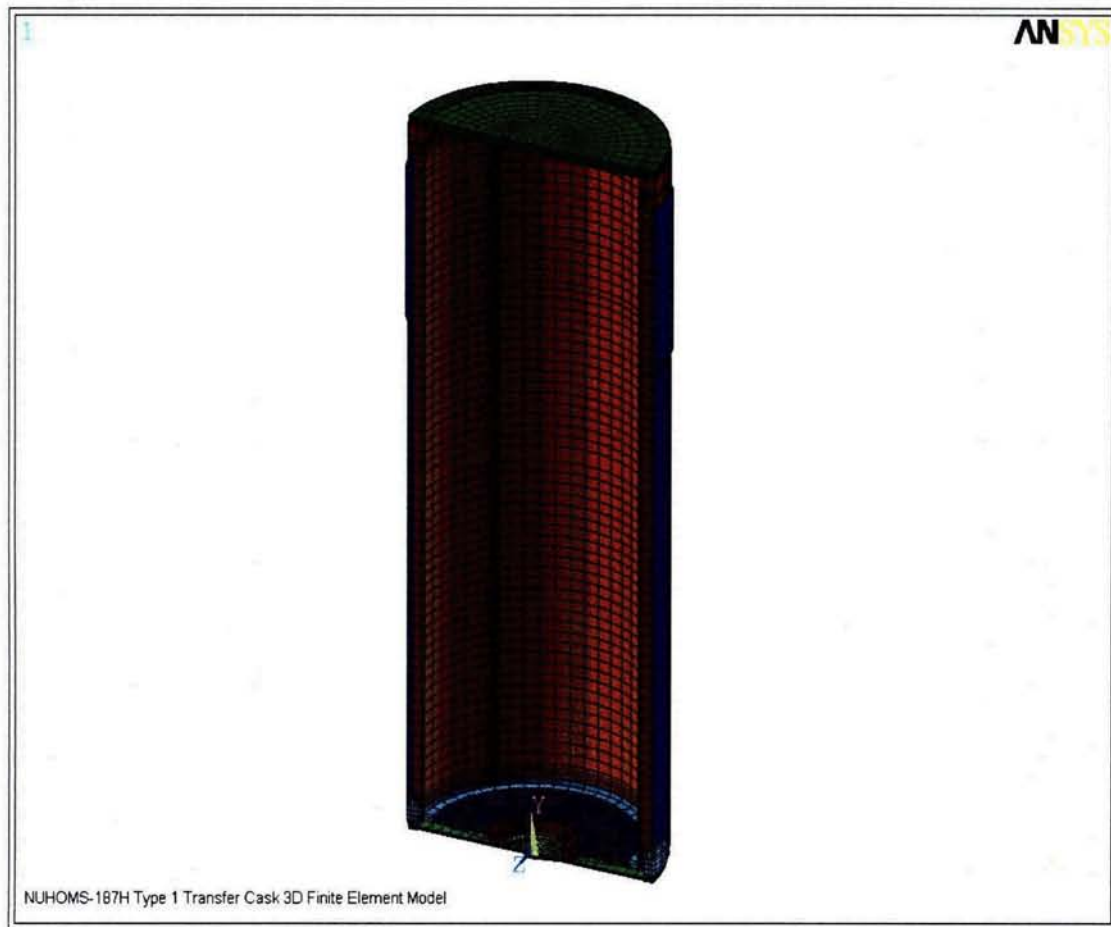


Figure A.3.9.2– 3 3-Dimensional Finite Element Model, Element Plot



Figure A.3.9.2- 4 115 °F Ambient Temperature Distribution

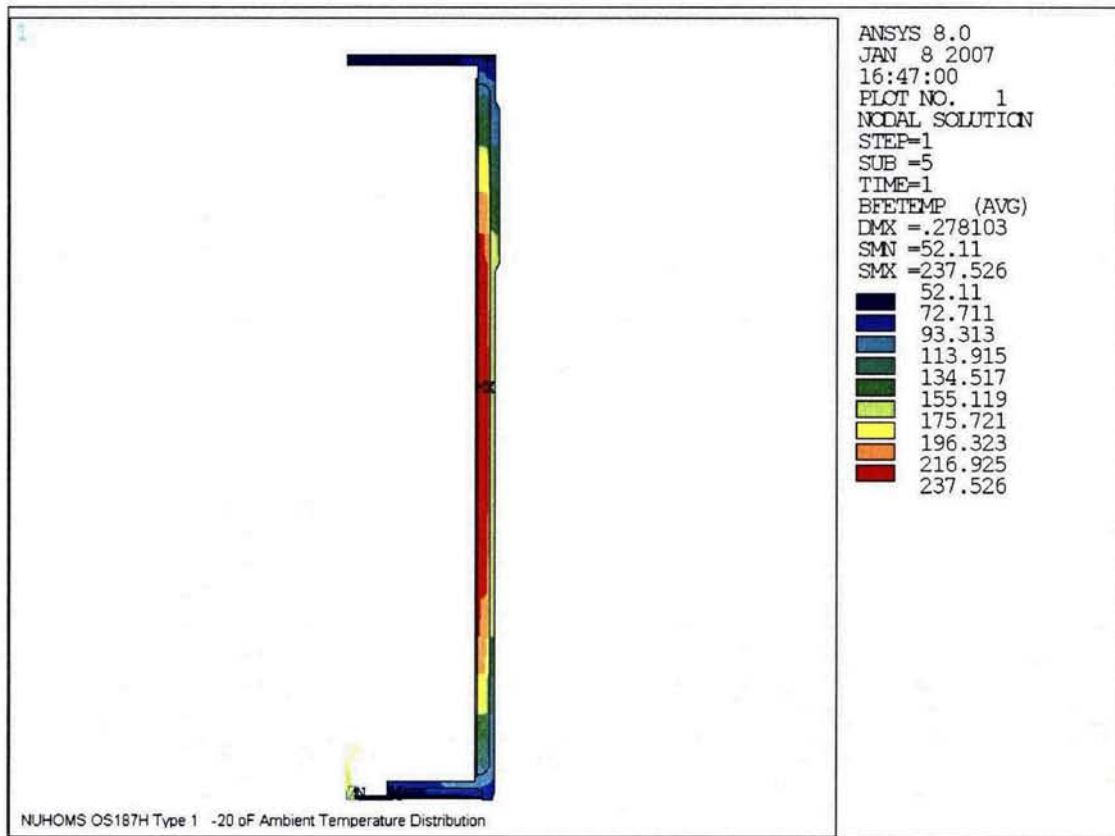


Figure A.3.9.2– 5 -20 °F Ambient Temperature Distribution

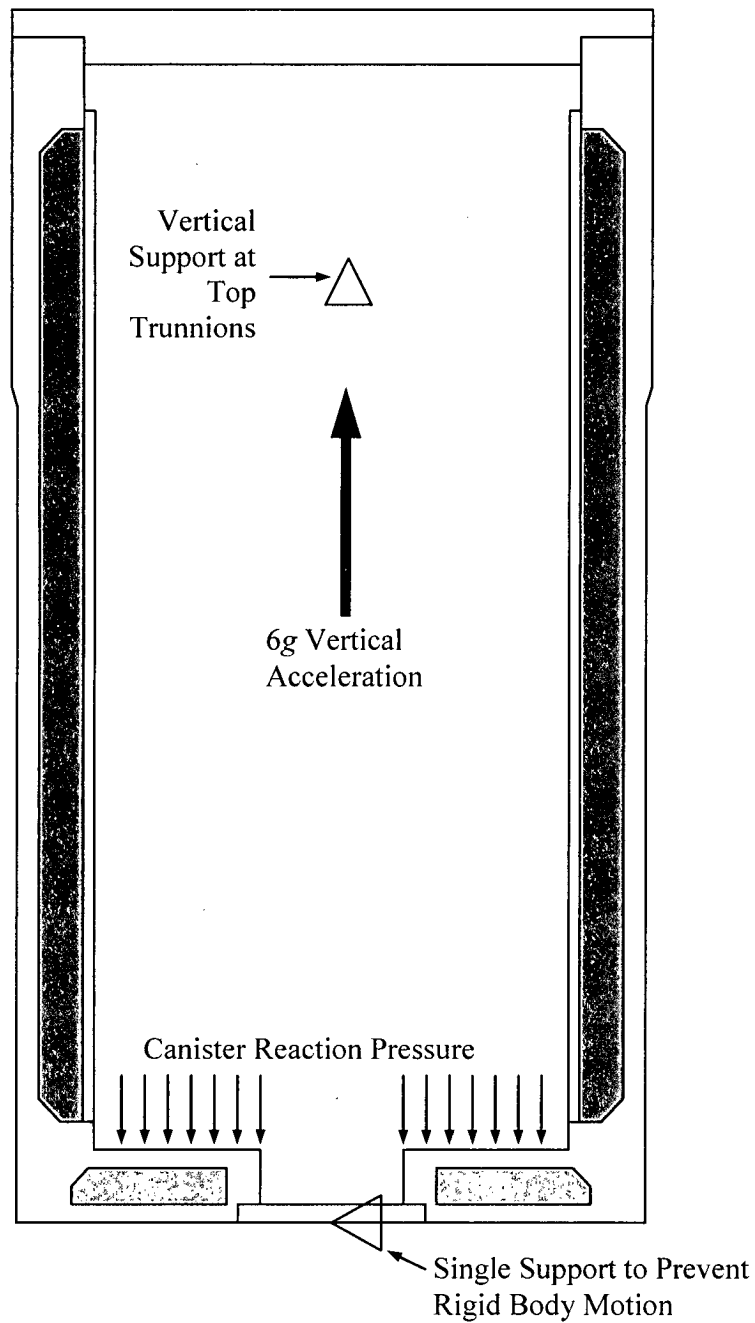


Figure A.3.9.2- 6 6 g Lifting Boundary Conditions (3D Half Model)

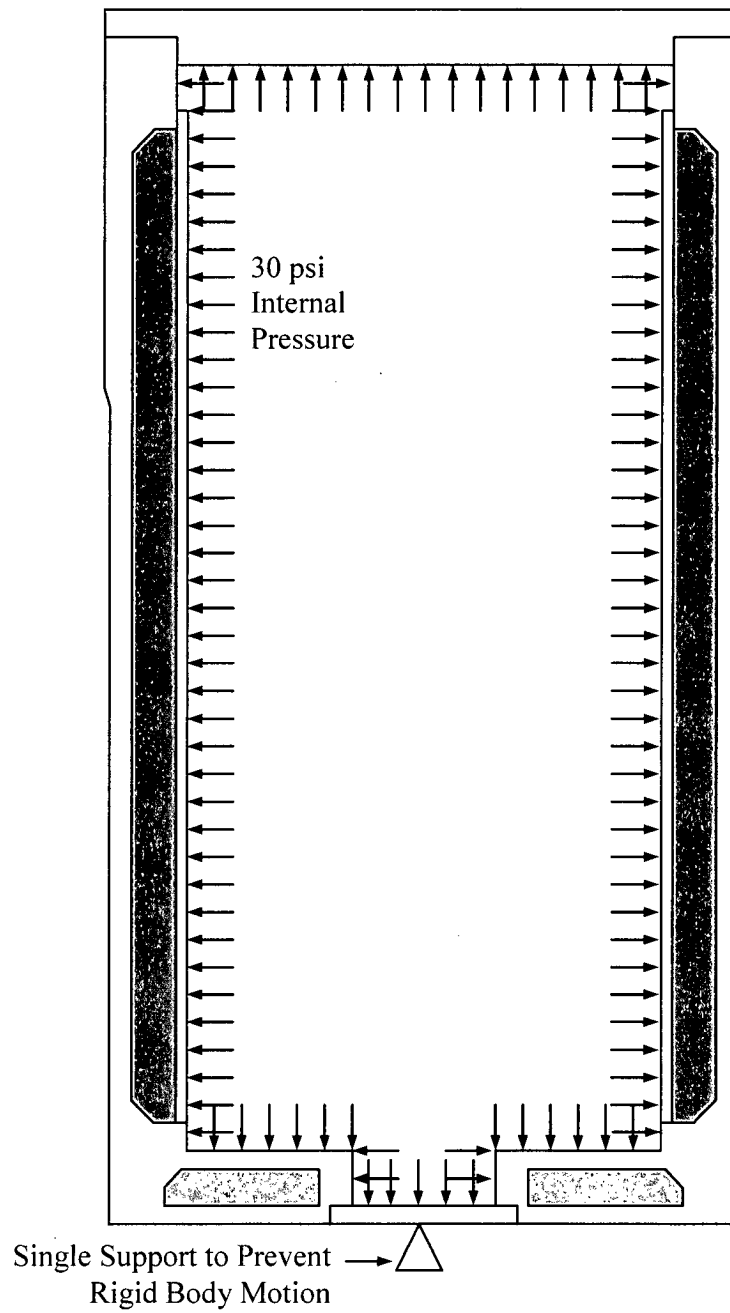


Figure A.3.9.2– 7 30 psi Internal Pressure Boundary Conditions (2D Model)

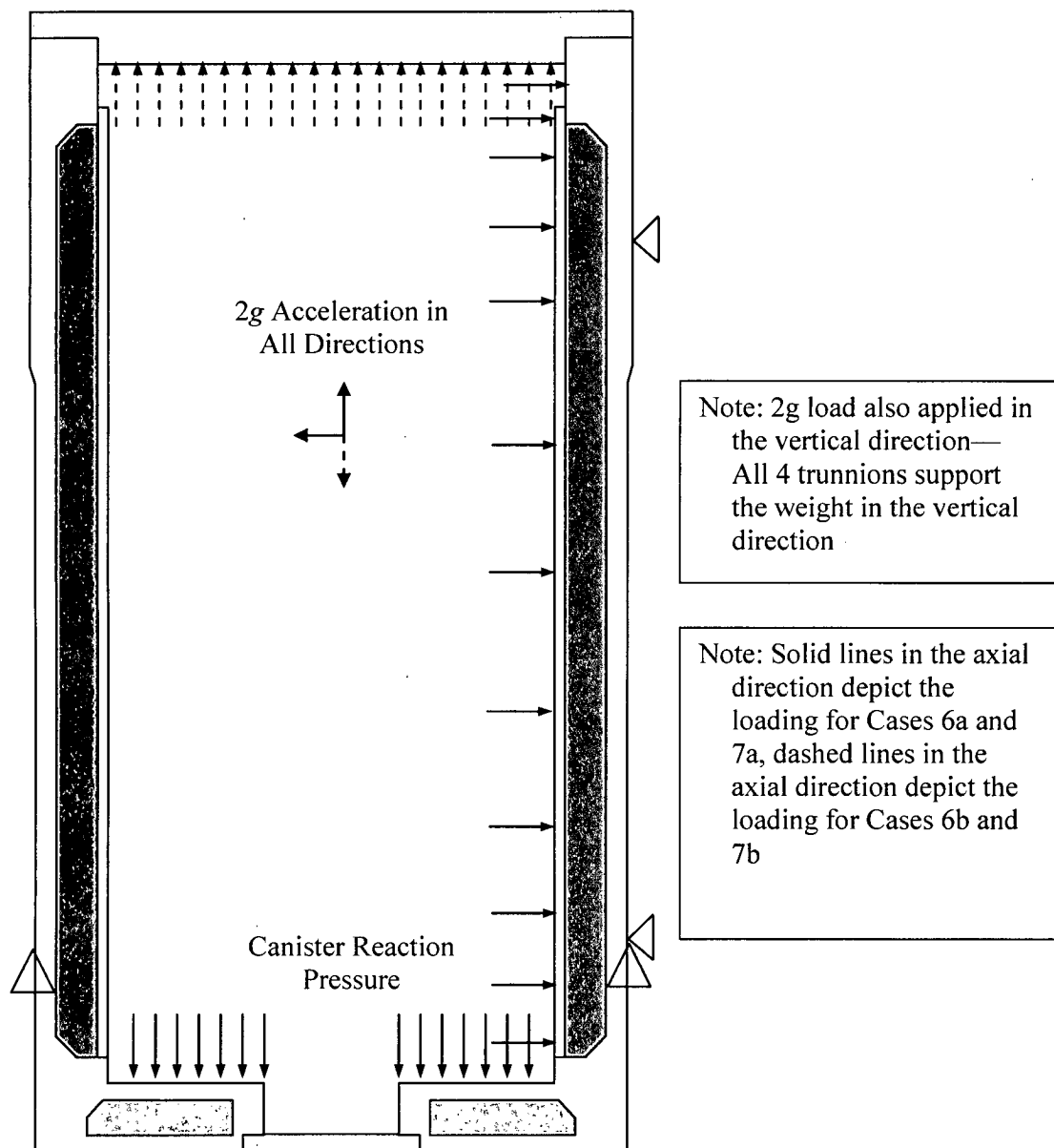


Figure A.3.9.2– 8 Transfer Loads Boundary Conditions (3D Full Model)

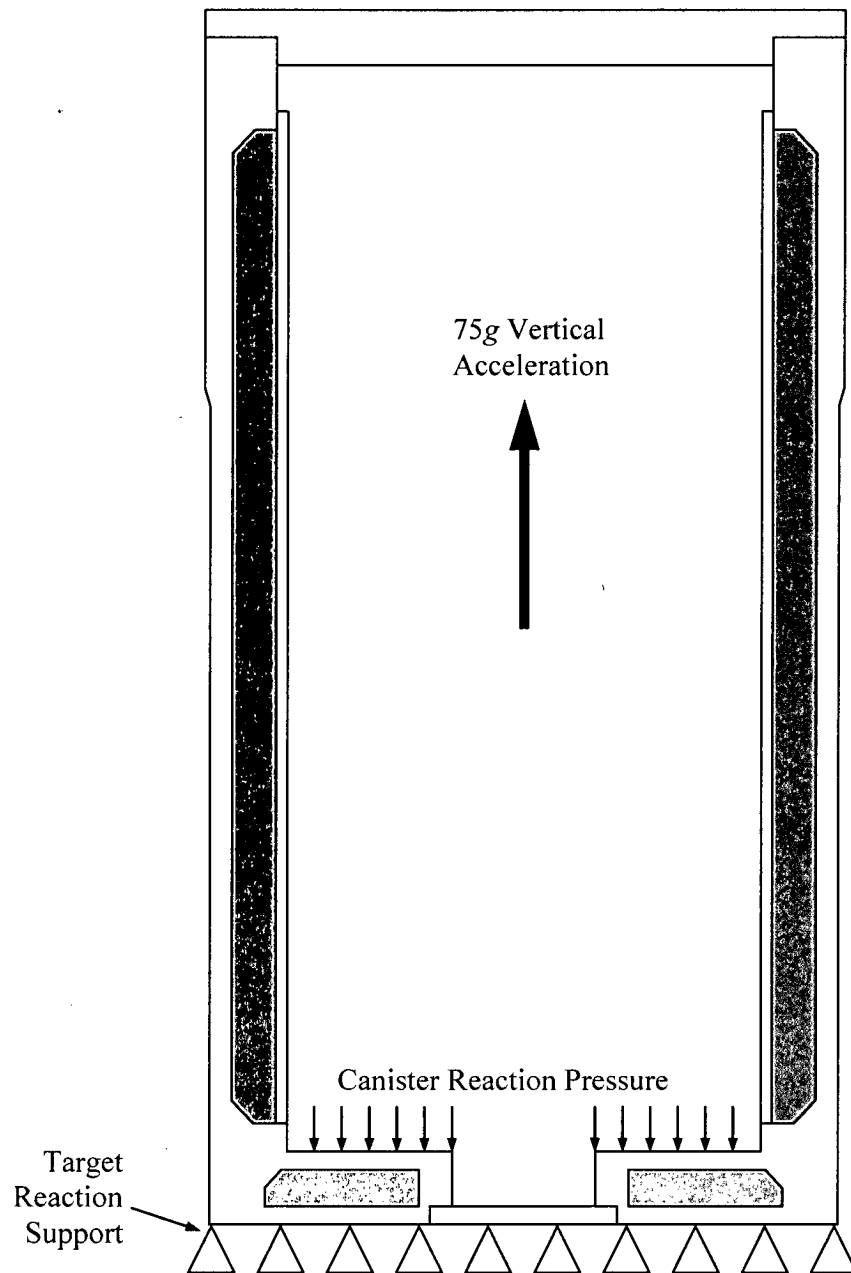


Figure A.3.9.2- 9 75 g Bottom End Drop Boundary Conditions (2D Model)

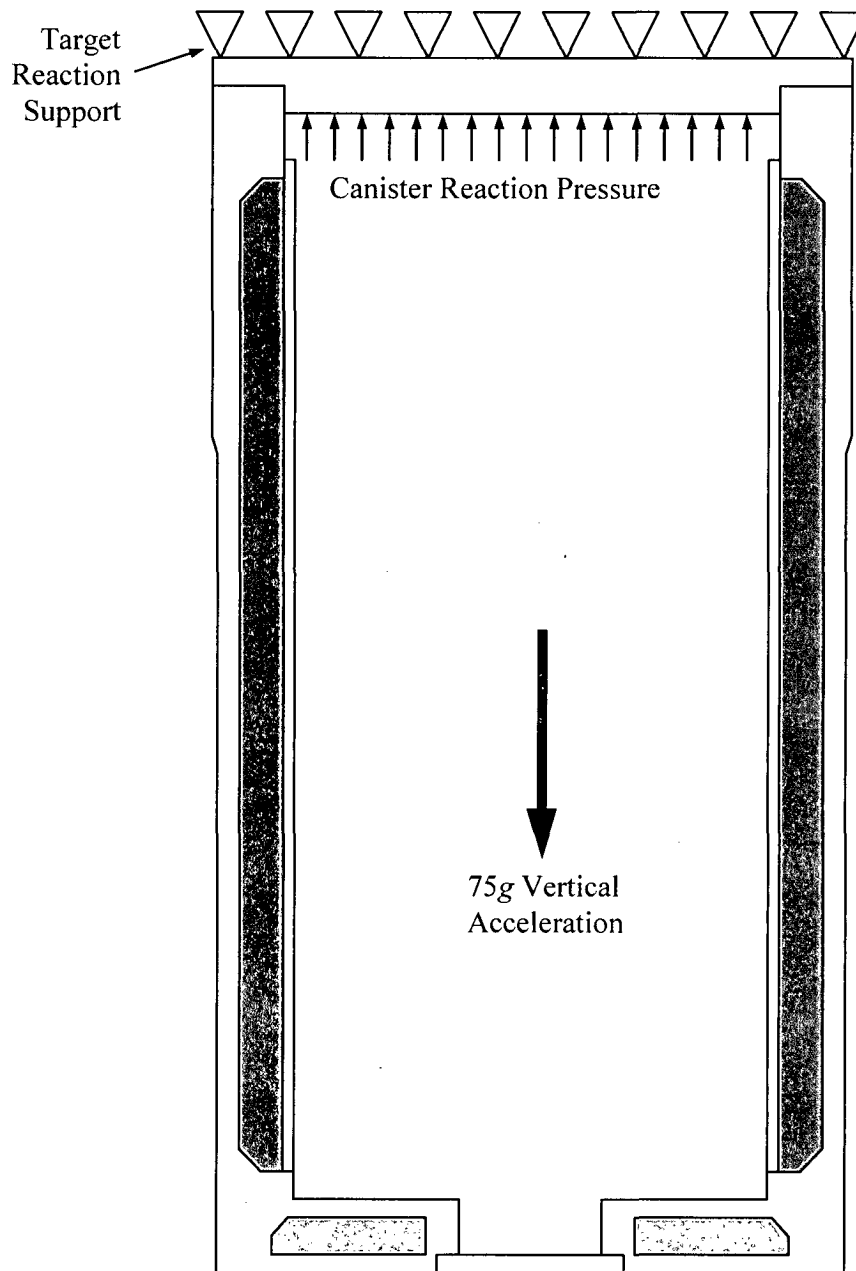


Figure A.3.9.2– 10 75 g Top End Drop Boundary Conditions (2D Model)

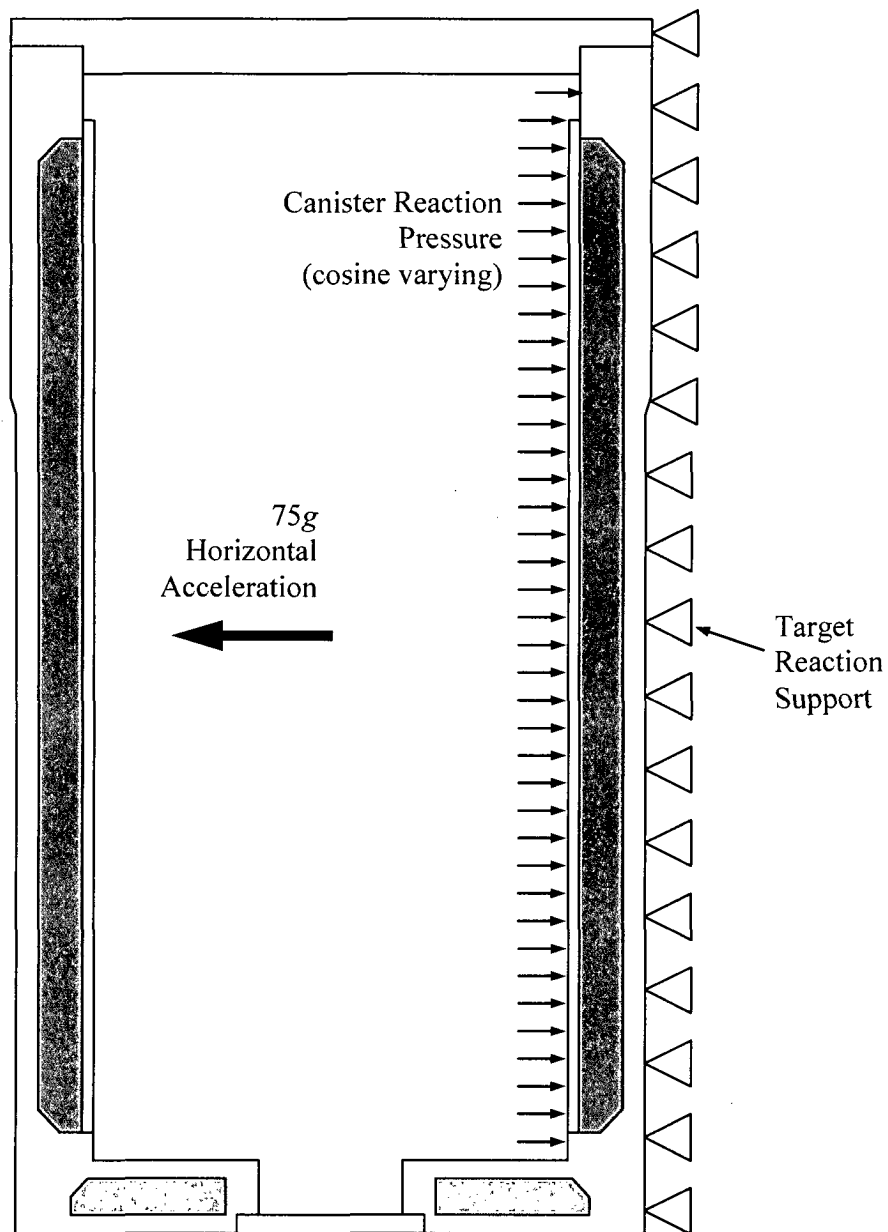


Figure A.3.9.2– 11 75 g Side Drop Boundary Conditions (3D Model)

1. APPLIED LOADS:

RADIAL LOAD P _____ LB

CIRC. MOMENT M_c _____ IN-LB

LONG. MOMENT M_L _____ IN-LB

TORSION MOMENT M_t _____ IN-LB

SHEAR LOAD W _____ LB

SHEAR LOAD V _____ LB

2. GEOMETRY:

VESSEL THICKNESS T _____ IN

ATTACHMENT RADIUS r_a _____ IN

VESSEL RADIUS R_v _____ IN

3. GEOMETRIC PARAMETERS:

$7 \cdot \frac{R_v}{T}$ _____

$\frac{r_a}{T}$ _____

$\frac{R_v}{T}$ _____

PUMP LOAD COORDINATE SYSTEM

* NOTE: ENTER ALL FORCE VALUES IN ACCORDANCE WITH SIGN CONVENTION

FROM FIG.	READ CURVES FOR	COMPUTE ABSOLUTE VALUES OF STRESS AND ENTER RESULT	STRESSES - IF LOADS OPPOSITE TWO SHOWN, REVERSE SIGNS SHOWN							
			σ_x	σ_y	σ_z	τ_{xy}	τ_{yz}	τ_{zx}	τ_{xy}	
3C AND 4C	$\frac{M_c}{W T}$	$\frac{M_c}{W T}$	+	+	+	+	+	+	+	
1C AND 2C-1	$\frac{M_L}{W T}$	$\frac{M_L}{W T}$	+	-	+	-	+	-	+	
3A	$\frac{M_t}{W T}$	$\frac{M_t}{W T}$								
1A	$\frac{M_c}{W T}$	$\frac{M_c}{W T}$								
3B	$\frac{M_t}{W T}$	$\frac{M_t}{W T}$								
1B OR 2B-1	$\frac{M_L}{W T}$	$\frac{M_L}{W T}$								
ADD ALGEBRAICALLY FOR SUMMATION OF 4 STRESSES σ_x										
3C AND 4C	$\frac{M_c}{W T}$	$\frac{M_c}{W T}$	+	+	+	+	+	+	+	
1C AND 2C	$\frac{M_L}{W T}$	$\frac{M_L}{W T}$	+	-	+	-	+	-	+	
3A	$\frac{M_t}{W T}$	$\frac{M_t}{W T}$								
1A	$\frac{M_c}{W T}$	$\frac{M_c}{W T}$								
3B	$\frac{M_t}{W T}$	$\frac{M_t}{W T}$								
1B OR 2B-1	$\frac{M_L}{W T}$	$\frac{M_L}{W T}$								
ADD ALGEBRAICALLY FOR SUMMATION OF 4 STRESSES σ_y										
3C AND 4C	$\frac{M_c}{W T}$	$\frac{M_c}{W T}$	+	+	+	+	+	+	+	
1C AND 2C	$\frac{M_L}{W T}$	$\frac{M_L}{W T}$	+	-	+	-	+	-	+	
3A	$\frac{M_t}{W T}$	$\frac{M_t}{W T}$								
1A	$\frac{M_c}{W T}$	$\frac{M_c}{W T}$								
3B	$\frac{M_t}{W T}$	$\frac{M_t}{W T}$								
1B OR 2B-1	$\frac{M_L}{W T}$	$\frac{M_L}{W T}$								
ADD ALGEBRAICALLY FOR SUMMATION OF 4 STRESSES σ_z										
SHEAR STRESS DUE TO TORSION M_t			τ_{xy}	τ_{yz}	τ_{zx}	τ_{xy}	τ_{yz}	τ_{zx}	τ_{xy}	
SHEAR STRESS DUE TO LOAD W			τ_{xy}	τ_{yz}	τ_{zx}	τ_{xy}	τ_{yz}	τ_{zx}	τ_{xy}	
SHEAR STRESS DUE TO LOAD V			τ_{xy}	τ_{yz}	τ_{zx}	τ_{xy}	τ_{yz}	τ_{zx}	τ_{xy}	
ADD ALGEBRAICALLY FOR SUMMATION OF SHEAR STRESSES τ_{xy}										

LONGITUDINAL σ_x

PRESSURE STRESS $\frac{P R_v}{T}$ _____

LONGITUDINAL BENDING STRESS _____

TOTAL MEMBRANE STRESS _____

TOTAL SURFACE STRESS _____

CIRCUMFERENTIAL σ_y

PRESSURE STRESS $\frac{P R_v}{T}$ _____

CIRCUMFERENTIAL BENDING STRESS _____

TOTAL MEMBRANE STRESS _____

TOTAL SURFACE STRESS _____

NOZZLE NO. _____

PUMP LOAD CODE _____

ANALYSIS POINT _____

COMPUTATION SHEET FOR LOCAL STRESSES IN CYLINDRICAL SHELLS

Figure A.3.9.2-12 Computational Worksheet for WRC 107 Bulletin Evaluation

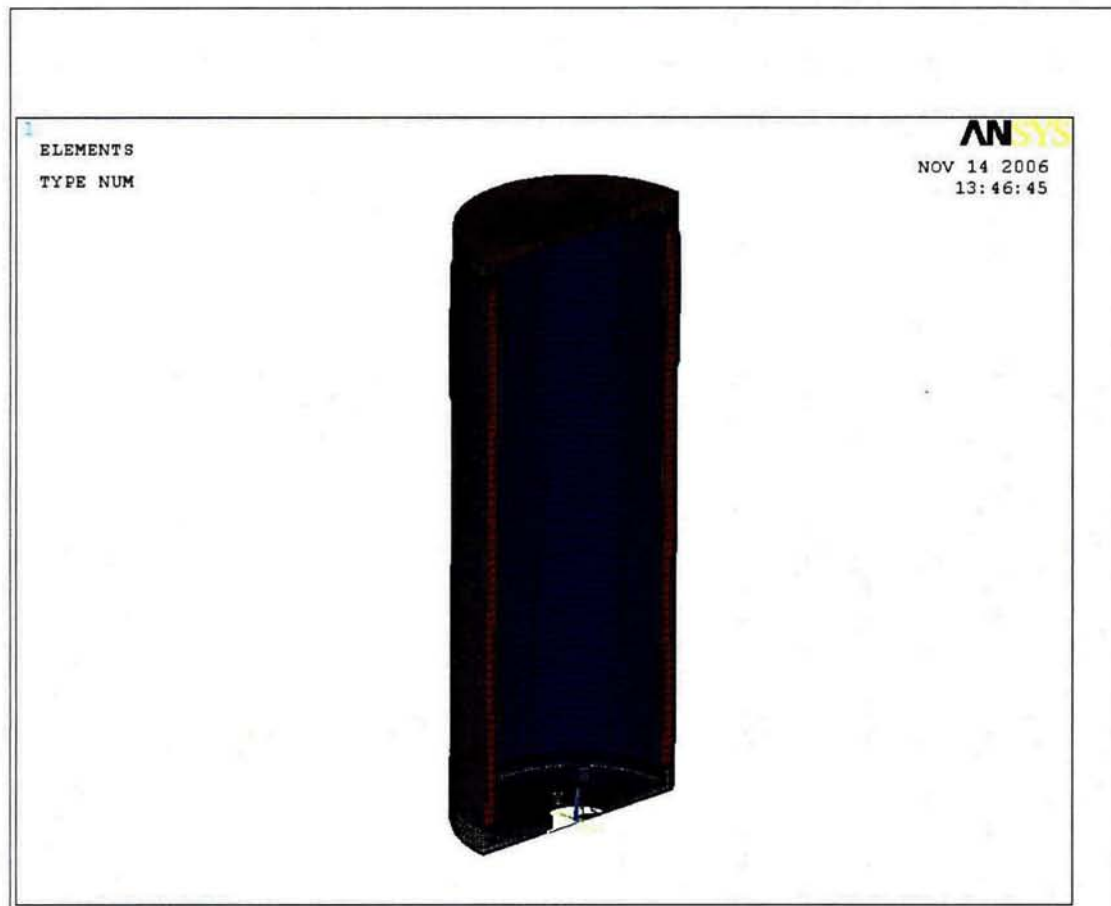


Figure A.3.9.2- 13 NUHOMS OS187H Type 1 Transfer Cask Side Drop- 3D Finite Element Model

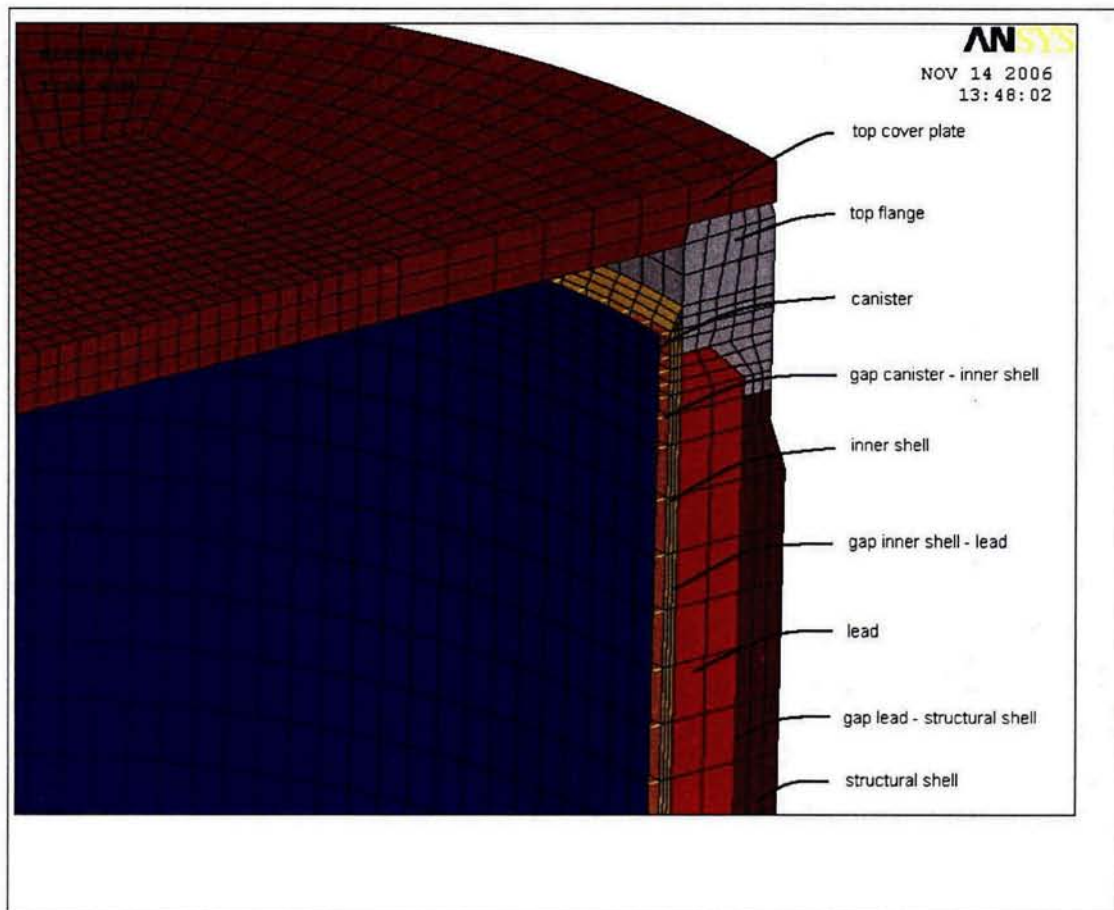


Figure A.3.9.2– 14 Transfer Cask Side Drop Model Top Cover/Flange/Lead Interface

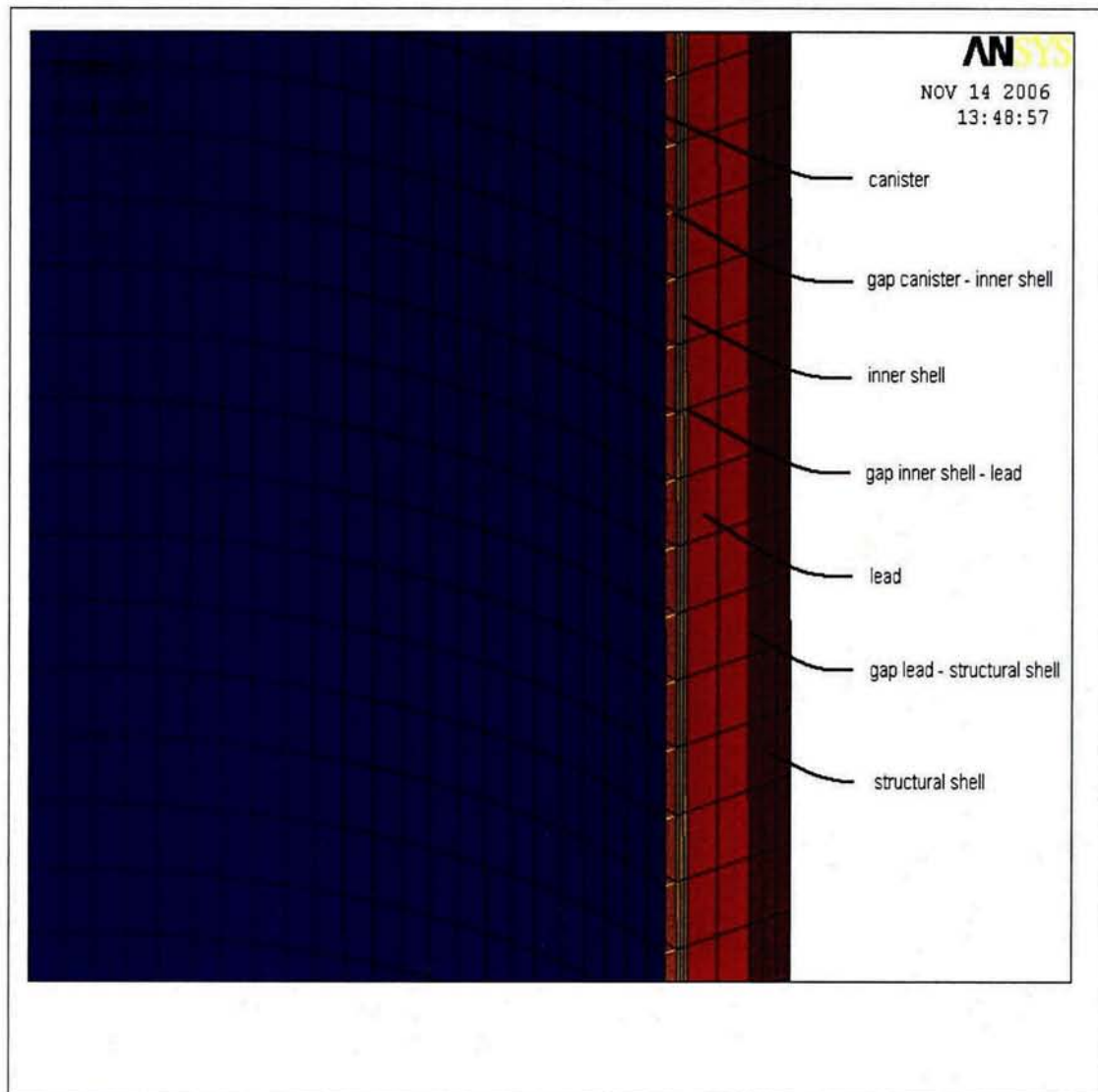


Figure A.3.9.2– 15 Transfer Cask Side Drop Model Canister/Cask Shell/Lead/Interface

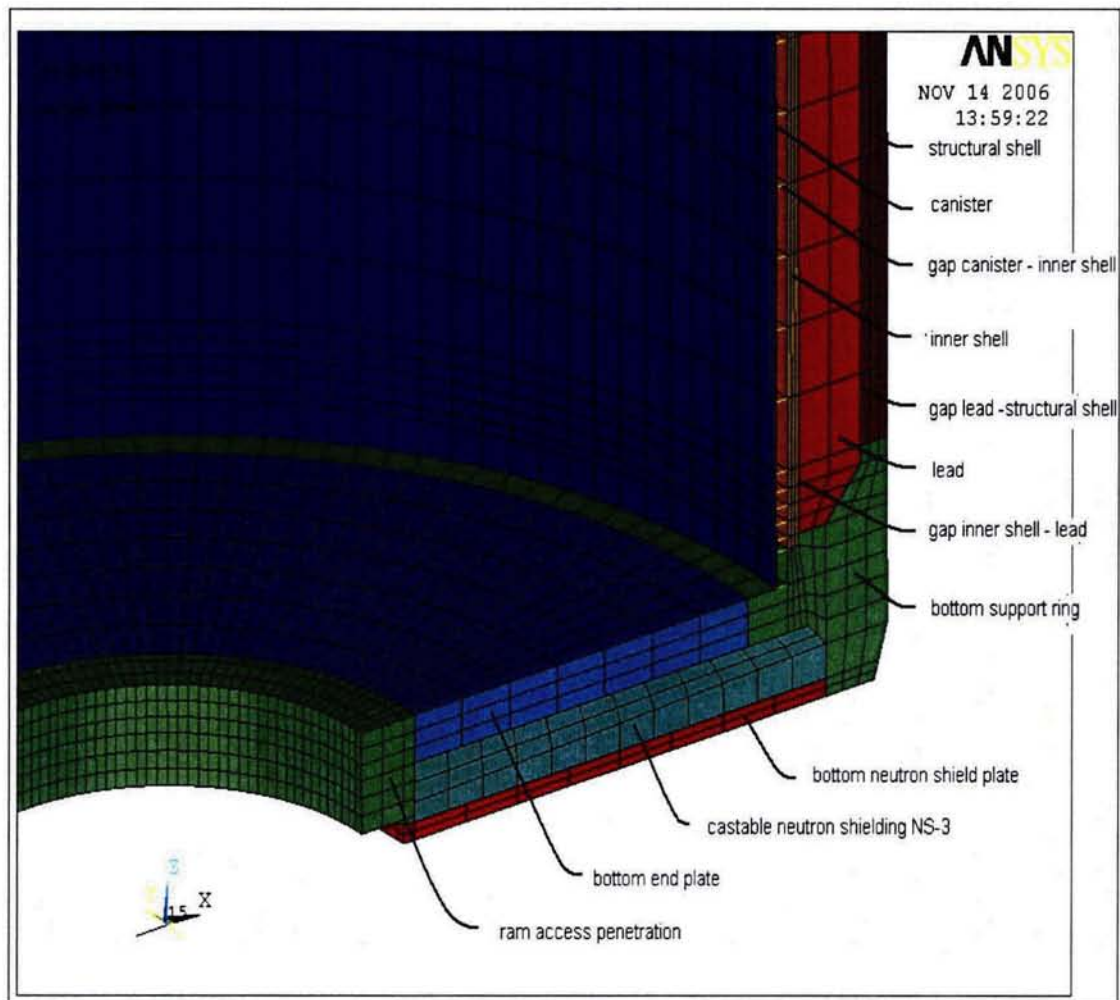


Figure A.3.9.2– 16 Transfer Cask Side Drop Model Canister/ Bottom Access Ram/Lead/Interface

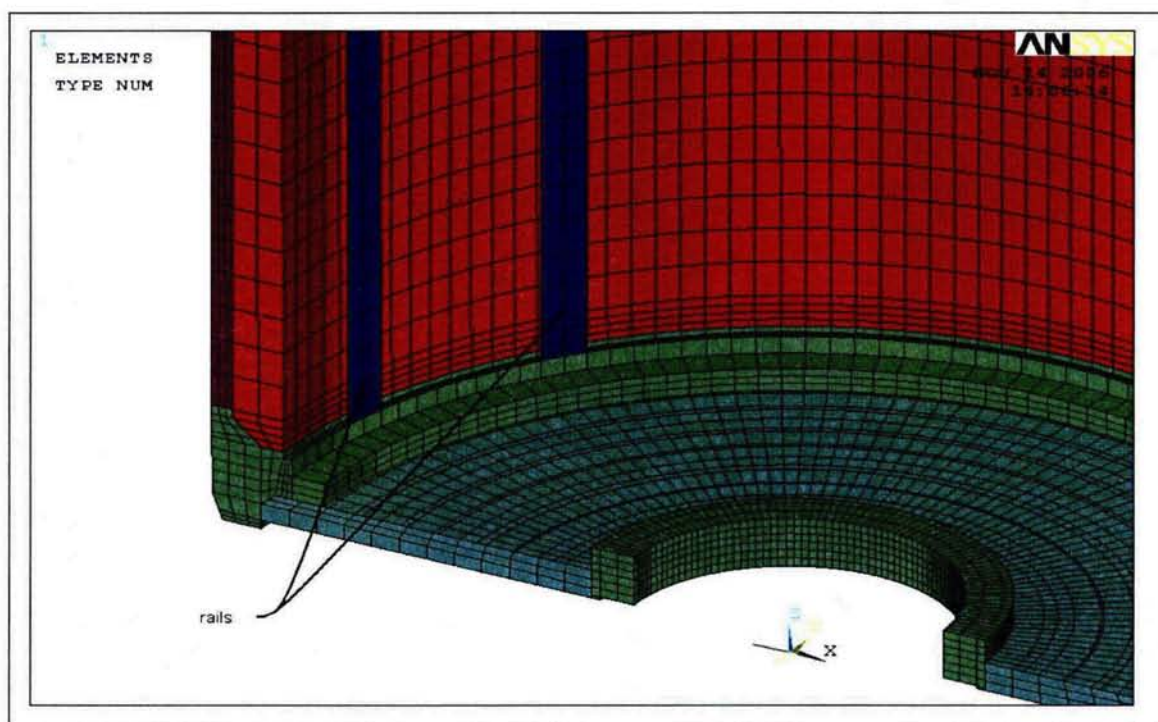
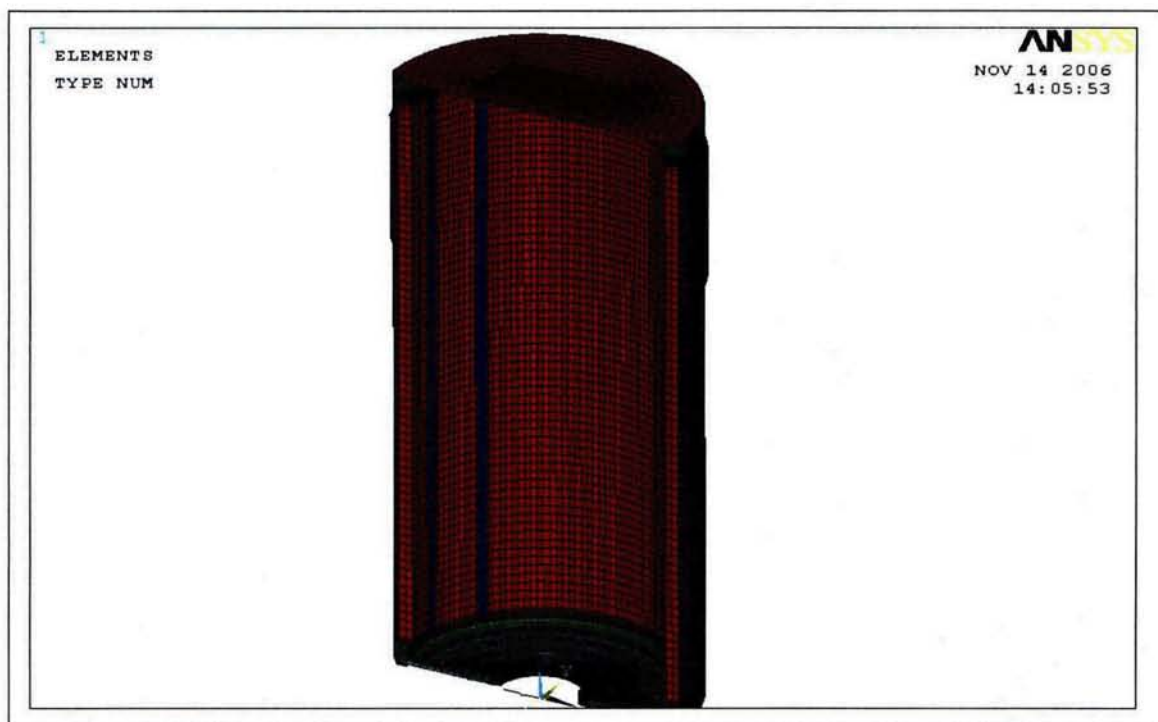


Figure A.3.9.2- 17 Transfer Cask Side Drop Model—Rail Locations for Load Case 1

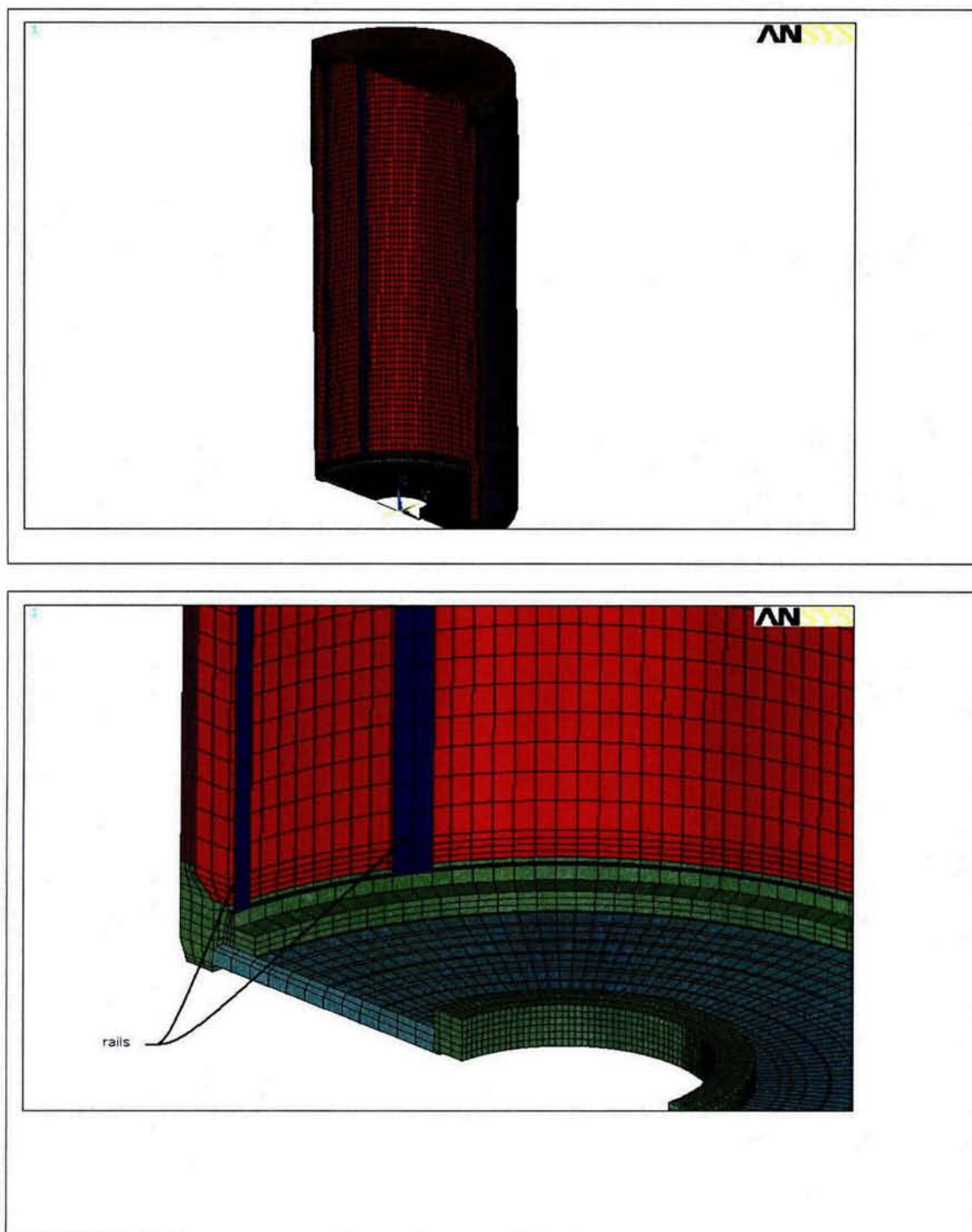


Figure A.3.9.2– 18 Transfer Cask Side Drop Model—Rail Locations for Load Case 2

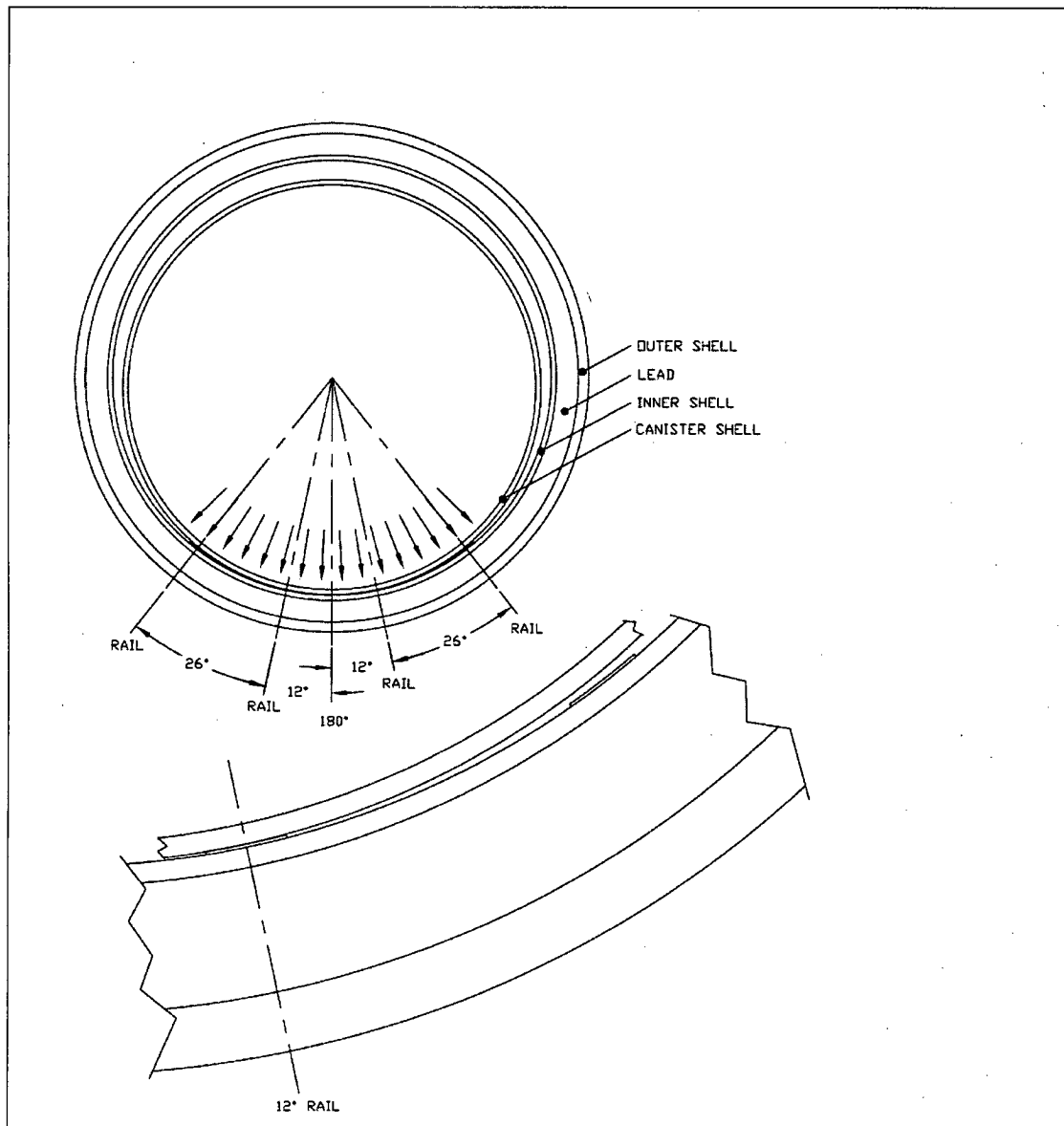


Figure A.3.9.2– 19 Transfer Cask Side Drop—Sketch of Drop Modeling for Load Case 1

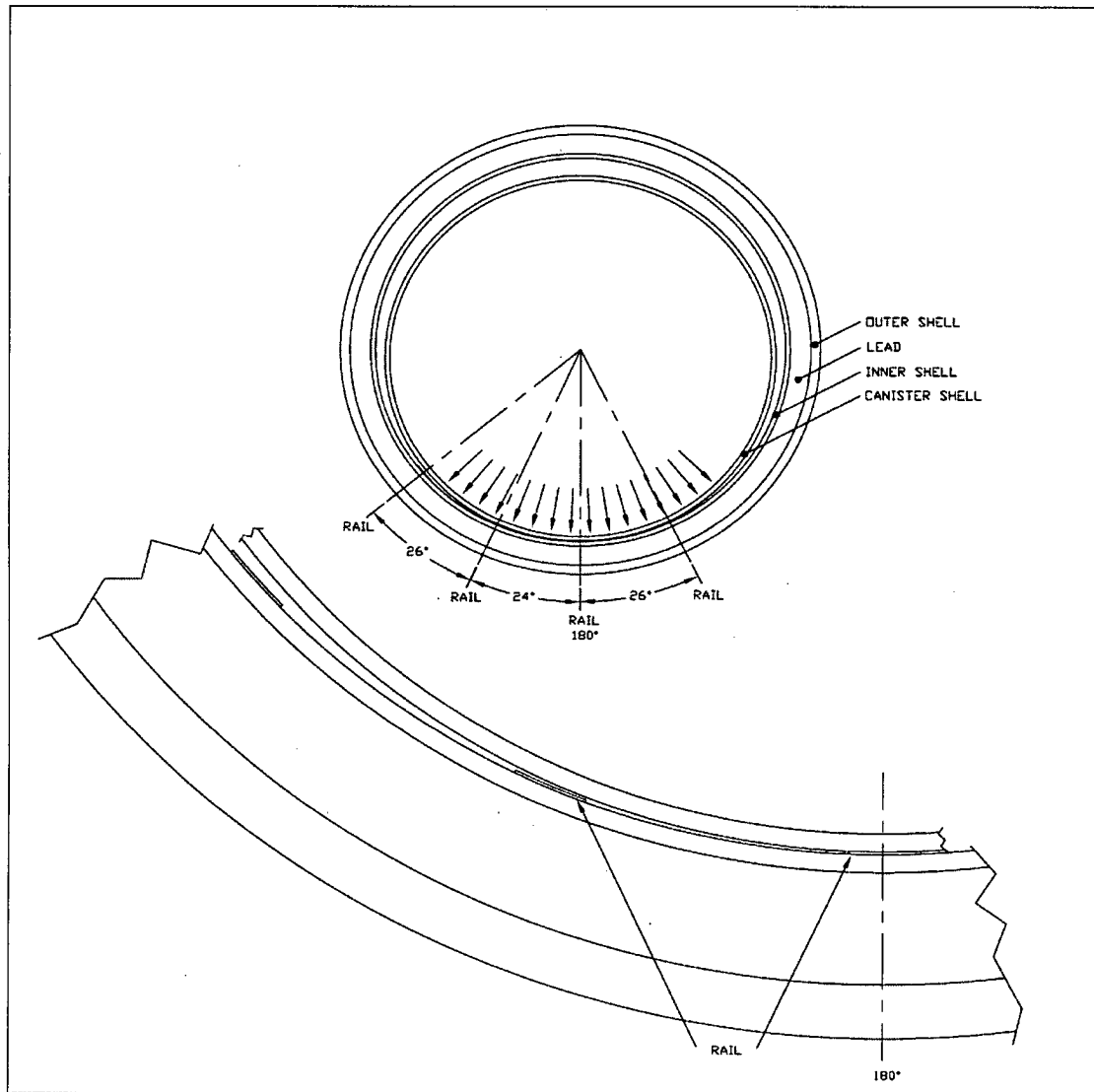


Figure A.3.9.2– 20 Transfer Cask Side Drop—Sketch of Drop Modeling for Load Case 2

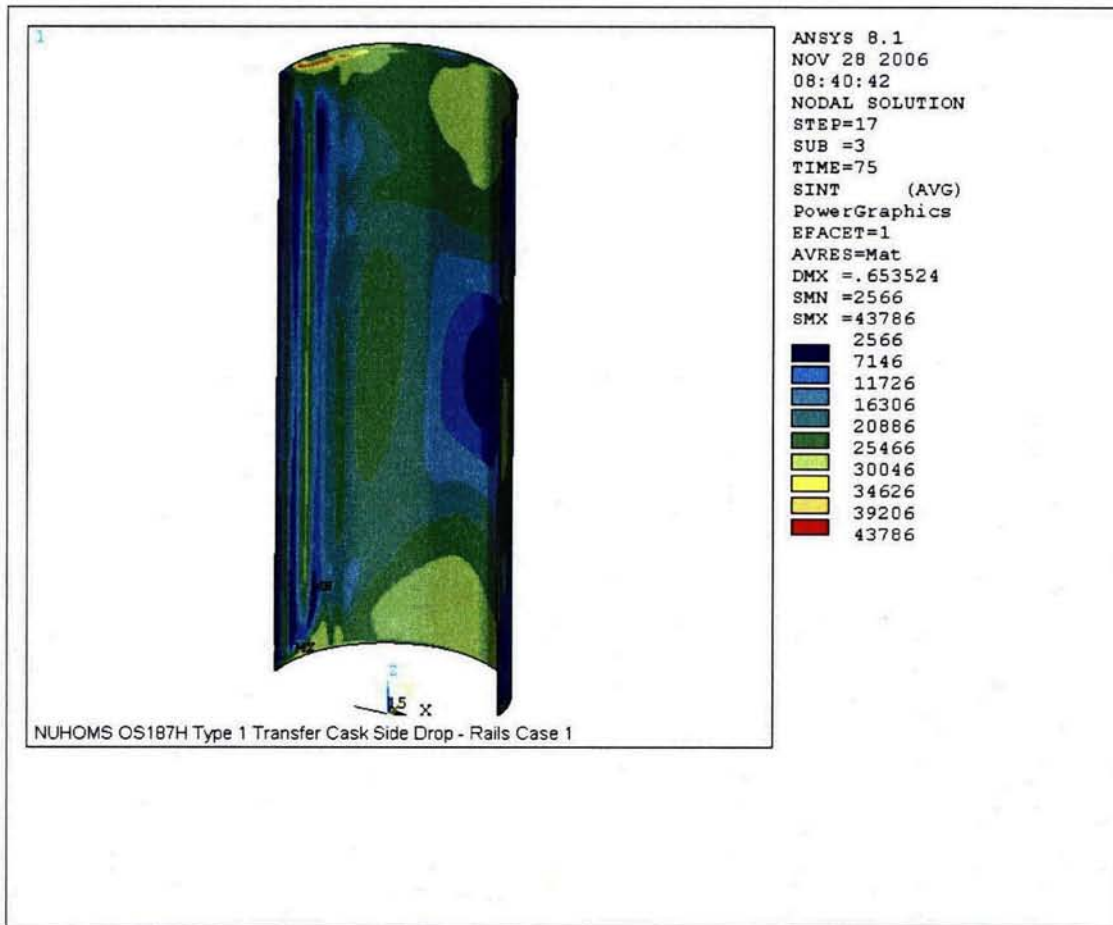


Figure A.3.9.2– 21 Transfer Cask Side Drop Results—Inner Shell Stress Intensity for Load Case 1

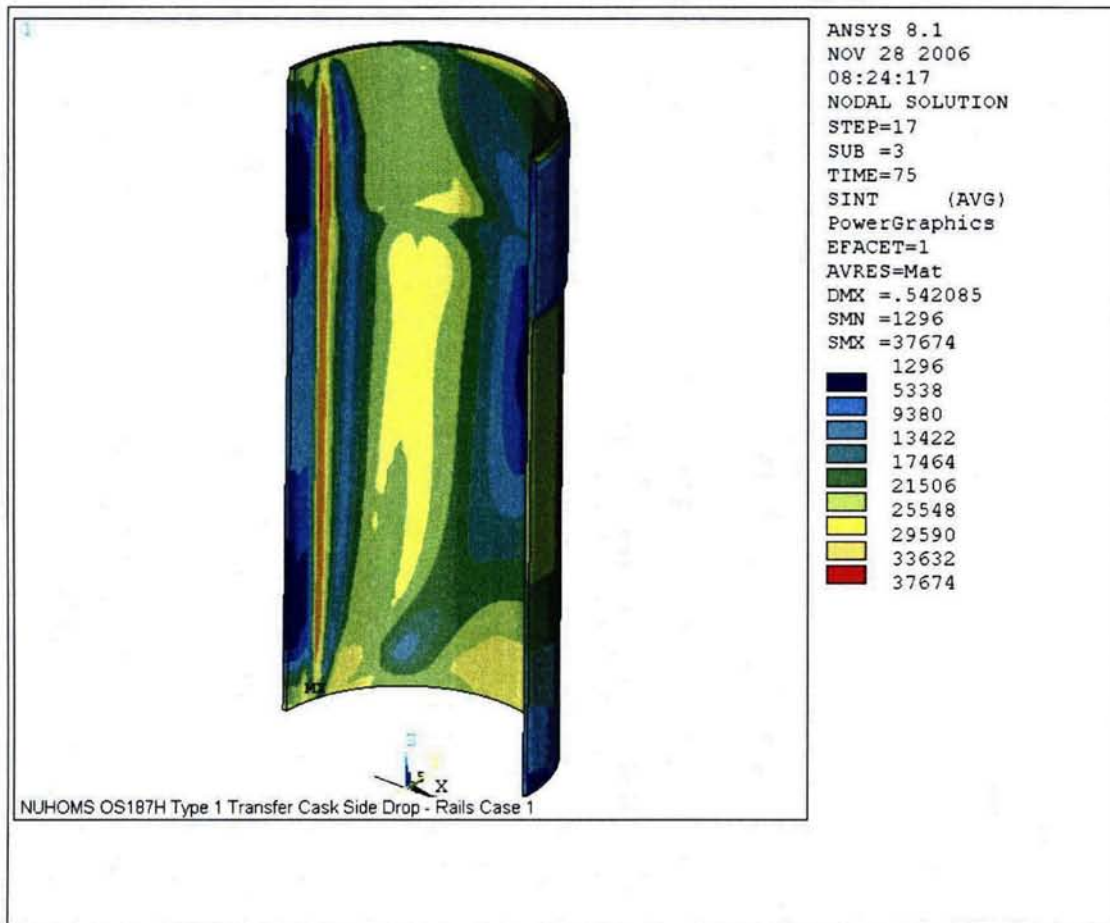


Figure A.3.9.2– 22 Transfer Cask Side Drop Results—Outer Shell Stress Intensity for Load Case 1

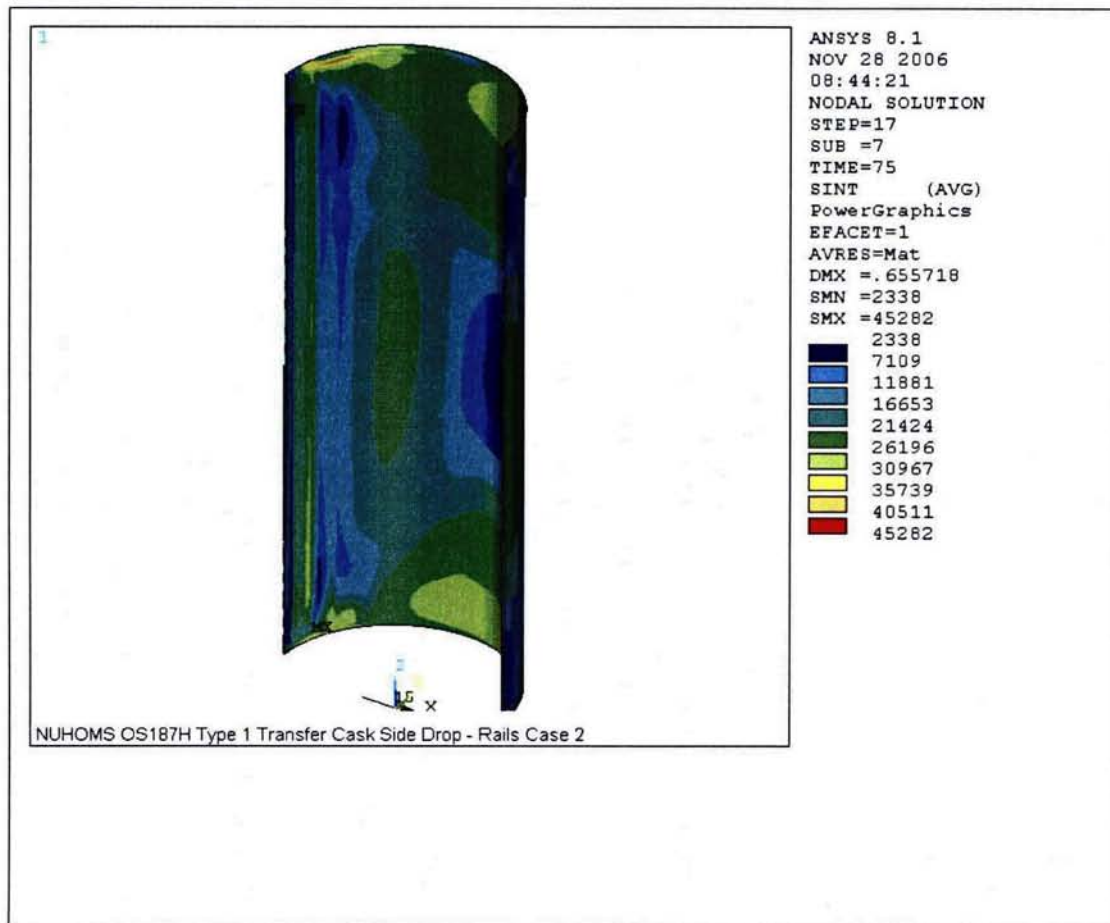


Figure A.3.9.2– 23 Transfer Cask Side Drop Results—Inner Shell Stress Intensity for Load Case 2

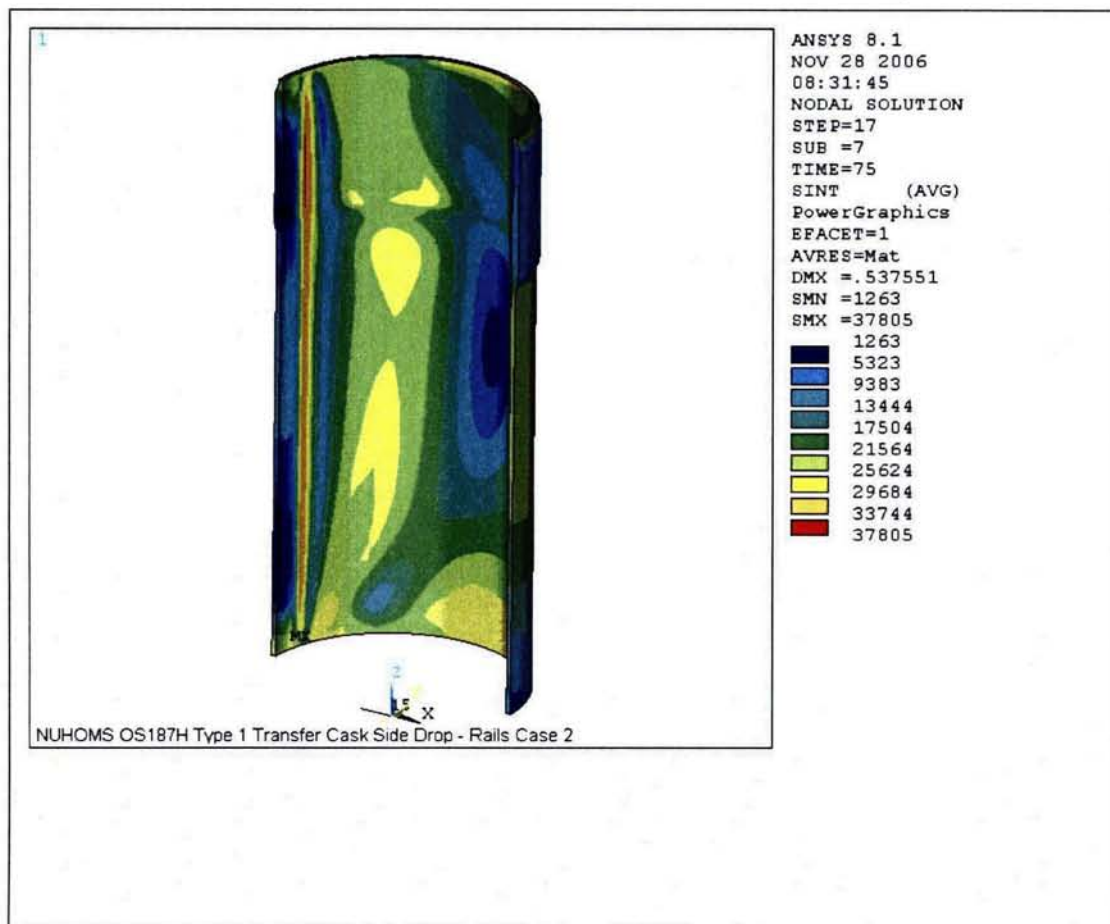


Figure A.3.9.2– 24 Transfer Cask Side Drop Results—Outer Shell Stress Intensity for Load Case 2

Appendix A.3.9.3

OS187H Type 1 Transfer Cask Top Cover and Ram Cover Bolt Analyses

TABLE OF CONTENTS

A.3.9.3	OS187H TYPE 1 TRANSFER CASK TOP COVER AND RAM ACCESS COVER BOLT ANALYSES.....	A.3.9.3-1
A.3.9.3.1	Introduction.....	A.3.9.3-1
A.3.9.3.2	Top Cover Bolt Load Calculations.....	A.3.9.3-3
A.3.9.3.2.1	Top Cover Bolt Preload and Bolt Torque.....	A.3.9.3-3
A.3.9.3.2.2	Top Cover Gasket Seating Load.....	A.3.9.3-4
A.3.9.3.2.3	Pressure Loads.....	A.3.9.3-4
A.3.9.3.2.4	Temperature Loads.....	A.3.9.3-5
A.3.9.3.2.5	Impact Loads.....	A.3.9.3-5
A.3.9.3.3	Top Cover Bolt Load Combinations.....	A.3.9.3-7
A.3.9.3.4	Top Cover Bolt Stress Calculations.....	A.3.9.3-8
A.3.9.3.4.1	Average Tensile Stress.....	A.3.9.3-8
A.3.9.3.4.2	Bending Stress.....	A.3.9.3-9
A.3.9.3.4.3	Shear Stress.....	A.3.9.3-9
A.3.9.3.4.4	Maximum Combined Stress Intensity.....	A.3.9.3-9
A.3.9.3.4.5	Stress Ratios.....	A.3.9.3-10
A.3.9.3.4.6	Bearing Stress (Under Bolt Head).....	A.3.9.3-10
A.3.9.3.5	Top Cover Bolt Analysis Results.....	A.3.9.3-11
A.3.9.3.6	Minimum Engagement Length for Top Cover Bolt and Flange.....	A.3.9.3-12
A.3.9.3.7	Ram Access Cover Bolt Calculations.....	A.3.9.3-14
A.3.9.3.7.1	Ram Access Cover Bolt Preload and Bolt Torque.....	A.3.9.3-14
A.3.9.3.7.2	Ram Access Cover Gasket Seating Load.....	A.3.9.3-14
A.3.9.3.7.3	Pressure Loads.....	A.3.9.3-15
A.3.9.3.7.4	Temperature Loads.....	A.3.9.3-16
A.3.9.3.7.5	Impact Loads.....	A.3.9.3-16
A.3.9.3.8	Ram Access Cover Bolt Load Combinations.....	A.3.9.3-19
A.3.9.3.9	Ram Access Cover Bolt Stress Calculations.....	A.3.9.3-20
A.3.9.3.9.1	Average Tensile Stress.....	A.3.9.3-21
A.3.9.3.9.2	Bending Stress.....	A.3.9.3-22
A.3.9.3.9.3	Shear Stress.....	A.3.9.3-22
A.3.9.3.9.4	Maximum Combined Stress Intensity.....	A.3.9.3-22
A.3.9.3.9.5	Stress Ratios.....	A.3.9.3-22
A.3.9.3.9.6	Bearing Stress (Under Bolt Head).....	A.3.9.3-23
A.3.9.3.10	Ram Access Cover Bolt Analysis Results.....	A.3.9.3-24
A.3.9.3.11	Minimum Engagement Length for Ram Access Cover Bolt.....	A.3.9.3-25

A.3.9.3.12	Brittle Fracture Analysis of Top Cover Bolt.....	A.3.9.3-27
A.3.9.3.13	Conclusions.....	A.3.9.3-30
A.3.9.3.14	References.....	A.3.9.3-31

LIST OF TABLES

Table A.3.9.3– 1	Design Parameters for Top Cover Bolt Analysis.....	A.3.9.3-32
Table A.3.9.3– 2	Design Parameters for Ram Access Cover Bolt Analysis	A.3.9.3-33
Table A.3.9.3– 3	Bolt Data	A.3.9.3-34
Table A.3.9.3– 4	Allowable Stresses in Closure Bolts for Normal Conditions	A.3.9.3-35
Table A.3.9.3– 5	Allowable Stresses in Closure Bolts for Hypothetical Accident Conditions	A.3.9.3-36

LIST OF FIGURES

Figure A.3.9.3– 1	Effect of Tempering Temperature on Notch Toughness	A.3.9.3-37
Figure A.3.9.3– 2	Correlation between Notch Toughness and Yield Strength	A.3.9.3-38
Figure A.3.9.3– 3	Singular Integral Equation and Asymptotic Approximation for Brittle Fracture Evaluation	A.3.9.3-39

A.3.9.3 OS187H TYPE 1 TRANSFER CASK TOP COVER AND RAM ACCESS COVER BOLT ANALYSES

A.3.9.3.1 Introduction

This section documents the evaluation of the top cover bolts and ram access cover bolts of the NUHOMS® OS187H Type 1 transfer cask (TC) under normal and accident conditions. The criteria and methods of evaluation used are the same as those of the OS187H TC documented in Section 3.9.3. The stress analysis is performed in accordance with NUREG/CR-6007 [1].

The NUHOMS® OS187H Type 1 TC top cover closure and ram access cover design, including bolts type and mechanical properties of the bolt material are the same as the OS187H TC. As shown in drawing 10494-72-9003-SAR, the 3.0 inch thick top cover is bolted to the top flange of the TC using twenty four (24) 1½ inch diameter bolts. As shown in drawings 10494-72-9001-SAR and 10494-72-9003-SAR, the 1.0 inch thick ram access cover is bolted to the ram access penetration ring using twelve ½ inch diameter bolts. The bolt material for both applications is SA-540 Gr. B23 Class 1, which has a minimum yield strength of 150 ksi at room temperature [2].

Table A.3.9.3-1 and Table A.3.9.3-2 summarize the design parameters used for the evaluation of the OS187H Type 1 TC top cover bolts and the ram access cover bolts, respectively. These tables are similar to Tables 3.9.3-1 and 3.9.3-2 for the OS187H TC. Based on a comparison between these sets of tables, the table below summarizes the differences that affect the evaluation of the top cover and ram access cover bolts between the two TCs. The evaluations documented in the following sections of this appendix are performed to address the effect of these differences.

Top Lid Closure Parameter	OS187H (See Table 3.9.3-1)	OS187H Type 1 (See Table A.3.9.3-1)
Closure lid diameter (at bolt circle), in.	77.61	76.85
Closure lid diameter (at the seal), in.	74.19	73.61
Closure lid diameter (outer edge), in.	82.20	81.37
Flange thickness, in.	5.575	6.50
Payload weight, lb.	110,000	120,000

Ram Access Cover Parameter	OS187H (See Table 3.9.3-2)	OS187H Type 1 (See Table A. 3.9.3-2)
Ram access cover diameter (at bolt circle), in.	23.50	24.50
Ram access cover diameter (at the seal), in.	21.16	23.16
Ram access cover diameter (outer edge), in.	25.45	26.45
Ram access cover diameter (at inner edge), in.	20.00	22.00
Ram access penetration thickness, in.	4.00	3.00

As with the OS187H TC, the following evaluations are presented in this section:

- Top cover and ram cover bolt torque
- Bolt preload
- Gasket seating load

- Pressure load
- Temperature load
- Impact load
- Thread engagement length evaluation
- Bearing stress
- Load combinations for normal and accident conditions
- Bolt stresses and allowable stresses

A.3.9.3.2 Top Cover Bolt Load Calculations

The design parameters of the top cover are summarized in Table A.3.9.3-1. The top cover bolt data and material allowables are presented in Tables A.3.9.3-3 through A.3.9.3-5. These tables are the same as Tables 3.9.3-3 through 3.9.3-5 and are presented here for completeness of presentation. The temperature of 300 °F is used in the top cover bolt region during normal and accident conditions. The following load cases are considered in the analysis.

- Preload + temperature load (normal condition)
- Pressure load (normal condition)
- Pressure + 80 inch corner drop (accident condition)

Symbols and terminology used in this analysis are taken from NUREG/CR-6007 [1] and are reproduced in Table A.3.9.3-1.

A.3.9.3.2.1 Top Cover Bolt Preload and Bolt Torque

This evaluation is not changed from that presented in Section 3.9.3.2.1 for the OS187H TC and is presented here for purposes of completeness of presentation.

A bolt torque range of 450 to 580 ft. lb. has been selected.

Using the minimum torque,

$$F_a = Q/KD_b = 450 \times 12 / (0.132 \times 1.50) = 27,270 \text{ lb.}, \text{ and}$$

$$\text{Preload stress} = F_a / \text{Stress Area} = 27,270 / 1.406 = 19,400 \text{ psi}$$

Where:

$$\text{Stress Area} = 1.491 \text{ in}^2 \text{ (Table A.3.9.3-3; conservatively, used } 1.406 \text{ in}^2 \text{).}$$

Using the maximum torque,

$$F_a = Q/KD_b = 580 \times 12 / (0.132 \times 1.50) = 35,150 \text{ lb.}, \text{ and}$$

$$\text{Preload stress} = F_a / \text{Stress Area} = 35,150 / 1.406 = 25,000 \text{ psi}$$

Where:

$$\text{Stress Area} = 1.491 \text{ in}^2 \text{ (Table A.3.9.3-3; conservatively, used } 1.406 \text{ in}^2 \text{).}$$

Residual torsional moment for minimum torque of 450 ft. lb. is,

$$M_r = 0.5Q = .5(450 \times 12) = 2,700 \text{ in. lb.}$$

Residual torsional moment for maximum torque of 580 ft. lb. is,

$$M_{tr} = 0.5Q = .5(580 \times 12) = 3,480 \text{ in. lb.}$$

Residual tensile bolt force for maximum torque,

$$F_{ar} = F_a = 35,150 \text{ lb.}$$

A.3.9.3.2.2 Top Cover Gasket Seating Load

Since a self energizing O-ring is used, the gasket seating load is negligible.

A.3.9.3.2.3 Pressure Loads

The methodology of Reference [1], Table 4.3, is used. Axial force per bolt due to internal pressure is

$$F_a = \frac{\pi D_{lg}^2 (P_{li} - P_{lo})}{4N_b}$$

D_{lg} (median lid seal diameter) = 73.61 in. Then,

$$F_a = \frac{\pi(73.61^2)(30 - 0)}{4(24)} = 5,320 \text{ lb./bolt}$$

The fixed edge closure lid force is,

$$F_f = \frac{D_{lb}(P_{li} - P_{lo})}{4} = \frac{76.85(30)}{4} = 576.40 \text{ lb. in.}^{-1}$$

The fixed edge closure lid moment is,

$$M_f = \frac{(P_{li} - P_{lo})D_{lb}^2}{32} = \frac{30(76.85^2)}{32} = 5,537 \text{ in. lb. in.}^{-1}$$

The shear bolt force per bolt is,

$$F_s = \frac{\pi E_l t_l (P_{li} - P_{lo}) D_{lb}^2}{2N_b E_c t_c (1 - N_{ul})} = \frac{\pi(27.0 \times 10^6)(3.0)(30)(76.85)^2}{2(24)(27.0 \times 10^6)(5.06)(1 - 0.3)} = 9,822 \text{ lb./bolt}$$

The top cover shoulder takes this shear force, so that $F_s = 0$.

A.3.9.3.2.4 Temperature Loads

The top cover bolt material is SA-540, Grade B23. The top cover is constructed from SA-240 Type XM-19 or SA-182 Type FXM-19, and the flange is constructed from SA-182 Type F304N. The bolts have a coefficient of thermal expansion of 6.9×10^{-6} in./in.°F⁻¹ at 300 °F, the lid has a coefficient of thermal expansion of 8.8×10^{-6} in./in.°F⁻¹ at 300 °F, and the flange has a coefficient of thermal expansion of 9.2×10^{-6} in./in.°F⁻¹ at 300 °F [2].

Therefore, the tensile load in the bolt due to different thermal expansion is,

$$F_a = 0.25 \pi D_b^2 E_b (a_l T_l - a_b T_b)$$

$$F_a = 0.25(\pi)(1.50^2)(26.7 \times 10^6) \{ (8.8 \times 10^{-6})(230) - (6.9 \times 10^{-6})(230) \} = 20,620 \text{ lb.}$$

Even though the top cover and flange are constructed from different materials, the shear force per bolt, F_s , due to a temperature change of 230 °F is, 0 psi, since the clearance holes in the lid are oversized (1.88 in. diameter) allowing the lid to grow in the radial direction.

$$F_s = 0$$

The temperature difference between the inside and outside of the top cover will always be less than one degree (see Chapter A.4). Consequently, the resulting bending moment is negligible.

$$M_f = 0$$

A.3.9.3.2.5 Impact Loads

Per Reference [1], Table 4.5, the non-prying tensile bolt force per bolt, F_a ,

$$F_a = \frac{1.34 \sin(xi)(DLF)(ai)(W_l + W_c)}{N_b} = \frac{1.34 \sin(xi)(1.1)(ai)(120,000)}{24} = 7,370(ai) \sin(xi) \text{ lb./bolt}$$

Note: $W_l + W_c$ is conservatively assumed to be 120,000 lb. (see Table A.3.9.3-1)

The shear bolt force is,

$$F_s = \frac{\cos(xi)(ai)(W_l)}{N_b} = \frac{5,500(ai) \cos(xi)}{24} = 229.2(ai) \cos(xi) \text{ lb./bolt}$$

The lid shoulder during normal and accident condition drops takes shear force. Therefore,

$$F_s = 0$$

The fixed-edge closure lid force, F_f , is,

$$F_f = \frac{1.34 \sin(xi)(DLF)(ai)(W_l + W_c)}{\pi D_{lh}} = \frac{1.34 \sin(xi)(1.1)(ai)(120,000)}{\pi(76.85)} = 732.6 \sin(xi)(ai) \text{ lb. in.}^{-1}$$

The fixed-edge closure lid moment, M_f , is,

$$M_f = \frac{1.34 \sin(xi)(DLF)(ai)(W_l + W_c)}{8\pi} = \frac{1.34 \sin(xi)(1.1)(ai)(120,000)}{8\pi} = 7,038 \sin(xi)(ai) \text{ in.lb.in}^{-1}$$

The accident condition impact load is taken to be the axial acceleration due to corner drop. As described in Section 3.1.1.4, end and corner drops are not considered credible during transfer operations under 10 CFR Part 72 because the transfer cask is always in the horizontal orientation. The evaluation below is performed in support of a 10 CFR Part 50 evaluation that may be performed by the user if the user cannot demonstrate that these accident drops are not credible. The following corner drop acceleration and impact angle are assumed to bound any possible corner drop accident scenario:

$$ai = 25 \text{ gs, and } xi = 60^\circ$$

Therefore,

$$F_a = 7,370 \times 25 \times \sin(60^\circ) = 159,565 \text{ lb./bolt}$$

$$F_s = 0 \text{ lb./bolt}$$

$$F_f = 732.6 \times 25 \times \sin(60^\circ) = 15,861 \text{ lb./bolt, and}$$

$$M_f = 7,038 \times 25 \times \sin(60^\circ) = 152,373 \text{ lb./bolt}$$

The top cover individual load is summarized in the following table.

Top Cover Bolt Individual Load Summary

Load Case	Applied Load		Non-Prying Tensile Force, F_a (lb.)	Torsional Moment, M_t (in. lb.)	Prying Force, F_f (lb.in. ⁻¹)	Prying Moment, M_f (in. lb. in. ⁻¹)
Preload	Residual	Minimum torque	27,270	2,700	0	0
		Maximum torque	35,150	3,480	0	0
Gasket	Seating load		0	0	0	0
Pressure	50 psig internal		5,320	0	576.4	5,537
Thermal	300 °F		20,620	0	0	0
Impact	Accident condition drop		159,565	0	15,861	152,373

A.3.9.3.3 Top Cover Bolt Load Combinations

A summary of normal and accident condition load combinations ([1], Table 4.9) is presented in the following table.

Top Cover Bolt Normal and Accident Load Combinations

Load Case	Combination Description		Non-Prying Tensile Force, F_a (lb.)	Torsional Moment, M_t (in. lb.)	Prying Force, F_f (lb.in. ⁻¹)	Prying Moment, M_f (in. lb. in. ⁻¹)
1	Preload + temperature (normal condition)	Minimum torque	47,890	2,700	0	0
		Maximum torque	55,770	3,480	0	0
2	Pressure (normal condition)		5,320	0	576.4	5,537
3	Pressure + accident impact (accident condition)		164,885	0	16,437	157,910

A.3.9.3.4 Top Cover Bolt Stress Calculations

Additional Prying Bolt Force

Table *Top Cover Bolt Normal and Accident Load Combinations* above shows that all loading conditions cause outward acting loads only. Outward acting loads generate no additional prying bolt forces, because the gap between the lid and flange at the outer edge prevents the creation of a prying moment.

Bolt Bending Moment

The maximum bending bolt moment, M_{bb} , generated by the applied load is evaluated as follows:

$$M_{bb} = \left(\frac{\pi D_{lb}}{N_b} \right) \left[\frac{K_b}{K_b + K_l} \right] M_f$$

The K_b and K_l are based on geometry and material properties and are defined in Reference [1], Table 2.2. By substituting the values given above,

$$K_b = \left(\frac{N_b}{L_b} \right) \left(\frac{E_b}{D_{lb}} \right) \left(\frac{D_b^4}{64} \right) = \left(\frac{24}{1.5} \right) \left(\frac{26.7 \times 10^6}{76.85} \right) \left(\frac{1.50^4}{64} \right) = 4.397 \times 10^5, \text{ and}$$

$$K_l = \frac{E_l t_l^3}{3 \left[(1 - N_{ul}^2) + (1 - N_{ul})^2 \left(\frac{D_{lb}}{D_{lo}} \right)^2 \right] D_{lb}} = \frac{27.0 \times 10^6 (3.0^3)}{3 \left[(1 - 0.3^2) + (1 - 0.3)^2 \left(\frac{76.85}{81.37} \right)^2 \right] 76.85}$$

$$= 2.347 \times 10^6$$

Therefore,

$$M_{bb} = \left(\frac{\pi 76.85}{24} \right) \left[\frac{4.397 \times 10^5}{4.397 \times 10^5 + 2.347 \times 10^6} \right] M_f = 1.587 M_f$$

For load case 2, $M_f = 5,537$ in. lb. Substituting this value into the equation above gives,

$$M_{bb} = 8,789 \text{ in. lb./bolt}$$

A.3.9.3.4.1 Average Tensile Stress

A summary of the applied loads for the transfer cask lid bolts is provided in Section A.3.9.3.3, in the table *Top Cover Bolt Normal and Accident Load Combinations*.

For the normal condition load cases, the applied bolt preload maintains closure of the transfer cask top cover. The closure force per bolt generated by the minimum lid bolt torque, with or without the additional closure force generated by thermal loads, is greater than the normal condition forces trying to open the top cover.

For accident conditions, the impact loads may instantaneously relax pressure on the top cover seals. However the accident condition loads will not cause lid bolt failure, as shown below, and immediately following the accident impact the top closure seal will be reseated by the bolt preload.

Per Reference [1], Table 5.1,

Normal Condition

$$S_{ba} = 1.2732 \frac{F_a}{D_{ba}^2} = 1.2732 \frac{55,770}{1.378^2} = 37,390 \text{ psi} = 37.4 \text{ ksi}$$

Accident Condition

$$S_{ba} = 1.2732 \frac{F_a}{D_{ba}^2} = 1.2732 \frac{164,885}{1.378^2} = 110,555 \text{ psi} = 110.6 \text{ ksi}$$

A.3.9.3.4.2 Bending Stress

Normal Condition

$$S_{bb} = 10.186 \frac{M_{bb}}{D_{ba}^3} = 10.186 \frac{8,789}{1.378^3} = 34,213 \text{ psi} = 34.2 \text{ ksi}$$

A.3.9.3.4.3 Shear Stress

For both normal and accident conditions, the average shear stress caused by shear bolt force F_s is,

$$S_{bs} = 0$$

For normal and accident conditions the maximum shear stress caused by the torsional moment M_t is,

$$S_{bt} = 5.093 \frac{M_t}{D_{ba}^3} = 5.093 \frac{3,480}{1.378^3} = 6,773 \text{ psi} = 6.8 \text{ ksi}$$

A.3.9.3.4.4 Maximum Combined Stress Intensity

The maximum combined stress intensity is calculated in the following way (Ref. 1, Table 5.1).

$$S_{bi} = \{(S_{ba} + S_{bb})^2 + 4(S_{bs} + S_{bt})^2\}^{0.5}$$

For normal conditions combine tension, shear, bending, and residual torsion.

$$S_{bi} = \{(37,390 + 34,213)^2 + 4(0 + 6,773)^2\}^{0.5} = 72,873 \text{ psi} = 72.9 \text{ ksi}$$

A.3.9.3.4.5 Stress Ratios

In order to meet the stress ratio requirement, the following relationship must hold for both normal and accident conditions.

$$R_t^2 + R_s^2 < 1$$

Where R_t is the ratio of average tensile stress to allowable average tensile stress, and R_s is the ratio of average shear stress to allowable average shear stress.

For normal conditions

$$R_t = 37,390/92,400 = 0.405$$

$$R_s = 6,773/55,400 = 0.122$$

$$R_t^2 + R_s^2 = (0.405)^2 + (0.122)^2 = 0.179 < 1$$

For accident conditions

$$R_t = 110,555/115,500 = 0.957$$

$$R_s = 6,773/69,300 = 0.098$$

$$R_t^2 + R_s^2 = (0.957)^2 + (0.098)^2 = 0.925 < 1$$

A.3.9.3.4.6 Bearing Stress (Under Bolt Head)

A standard 1.50 in. washer is placed under the head of each top cover bolt. The inside and outside diameter of a standard 1.50 in. washer is 1.50 in. and 3.00 in. respectively. The diameter of the bolt clearance hole in the top cover is 1.88 in. Therefore, the total bearing area under the top cover bolts, A_b , is the following.

$$A_b = (\pi/4) [3.00^2 - 1.88^2] = 4.293 \text{ in.}^2$$

According to Reference [1], bearing stress evaluation is required for normal condition loads only. For normal conditions, the maximum bearing stress under the washer, σ_b , is the following.

$$\sigma_b = 55,770 \text{ lb.} / 4.293 \text{ in.}^2 = 12,991 \text{ psi}$$

The normal condition allowable bearing stress on the cover is taken to be the yield stress of the cover material at 300 °F. The cover is manufactured out of SA-240 Type XM-19 or SA-182 Type FXM19, which have a yield stress of 43.3 ksi at 300 °F.

A.3.9.3.5 Top Cover Bolt Analysis Results

A summary of the stresses calculated above is listed in the following table:

Summary of Top Cover Bolt Stresses and Allowables

Stress Type	Normal Condition		Accident Condition	
	Stress	Allowable	Stress	Allowable
Average tensile (ksi)	37.4	92.4	110.6	115.5
Shear (ksi)	6.8	55.4	6.8	69.3
Combined (ksi)	72.9	124.7	Not Required [1]	
Interaction equation $R_t^2 + R_s^2 < 1$	0.179	1	0.925	1
Bearing (ksi) allowable (ksi) (S_v of lid material)	13.0	43.3	Not Required [1]	

A.3.9.3.6 Minimum Engagement Length for Top Cover Bolt and Flange

The top cover bolt and flange minimum engagement length evaluation is not changed from that presented in Section 3.9.3.6 for the OS187H TC and is presented here for purposes of completeness of presentation.

For a 1 1/2" – 8UN – 2A bolt, the material is SA-540 Grade B23 Class 1, with

$$S_u = 165 \text{ ksi and}$$

$$S_y = 150 \text{ ksi (at room temperature)}$$

The helicoil insert is neglected in the thread engagement length computation. It is conservative to neglect the helicoil insert, because it has a much higher tensile strength (200 ksi, [3]) than the flange material. The flange material is constructed from Type 304 stainless steel and has the following material properties.

$$S_u = 75 \text{ ksi and}$$

$$S_y = 30 \text{ ksi (at room temperature)}$$

The minimum engagement length, L_e , for the bolt and flange is ([4], p. 1149),

$$L_e = \frac{2A_t}{3.1416K_{n\max} \left[\frac{1}{2} + .57735n(E_{s\min} - K_{n\max}) \right]}$$

Where,

$$A_t = \text{tensile stress area} = 1.491 \text{ in.}^2,$$

$$n = \text{number of threads per inch} = 8,$$

$$K_{n\max} = \text{maximum minor diameter of internal threads} = 1.390 \text{ in. ([4], p. 1292)}$$

$$E_{s\min} = \text{minimum pitch diameter of external threads} = 1.4093 \text{ in. ([4], p. 1292)}$$

Substituting the values given above,

$$L_e = \frac{2(1.491)}{(3.1416)(1.390) \left[\frac{1}{2} + .57735(8)(1.4093 - 1.390) \right]} = 1.159 \text{ in.}$$

$$J = \frac{A_s \times S_{ue}}{A_n \times S_{ui}} \quad [4]$$

Where, S_{ue} is the tensile strength of external thread material, and S_{ui} is the tensile strength of internal thread material.

$$A_s = \text{shear area of external threads} = 3.1416 n L_e K_{n\max} \{ 1/(2n) + .57735 (E_{s\min} - K_{n\max}) \}$$

$$A_n = \text{shear area of internal threads} = 3.1416 n L_e D_{s \min} \{1/(2n) + .57735(D_{s \min} - E_{n \max})\}$$

For the bolt/Helicoil insert connection:

$$E_{n \max} = \text{maximum pitch diameter of internal threads} = 1.4283 \text{ in. ([4], p.1292)}$$

$$D_{s \min} = \text{minimum major diameter of external threads} = 1.4828 \text{ in. ([4], p. 1292)}$$

Therefore,

$$A_s = 3.1416(8)(1.159)(1.390)\{1/(2 \times 8) + .57735(1.4093 - 1.390)\} = 2.982 \text{ in.}^2$$

$$A_n = 3.1416(8)(1.159)(1.4828)\{1/(2 \times 8) + .57735(1.4828 - 1.4283)\} = 4.059 \text{ in.}^2$$

So,

$$J = \frac{2.982(165.0)}{4.059(75.0)} = 1.616$$

$$Q = L_e J = (1.159)(1.616) = 1.873 \text{ in.}$$

The actual engagement length can be calculated as:

$$4.50 \text{ in. bolt length} - 1.50 \text{ in. cover thickness} - 0.180 \text{ in. washer thickness} = 2.82 \text{ in.} > 1.873 \text{ in.}$$

A.3.9.3.7 Ram Access Cover Bolt Calculations

The design parameters of the ram access cover bolts are summarized in Table A.3.9.3-2. The ram access cover bolt data and material allowables are presented in Tables A.3.9.3-3 through A.3.9.3-5. A temperature of 300 °F is used in the ram access cover bolt region during normal and accident conditions. The following load cases are considered in the analysis.

- Preload + temperature load (normal condition)
- Pressure load (normal condition)
- Pressure + 80 inch corner drop (accident condition)

Symbols and terminology used in this analysis are taken from NUREG/CR-6007 [1] and are reproduced in Table A.3.9.3-2.

A.3.9.3.7.1 Ram Access Cover Bolt Preload and Bolt Torque

A bolt torque range of 35 to 40 ft. lb. has been selected.

Using the minimum torque,

$$F_a = Q/KD_b = 35 \times 12 / (0.132 \times 0.50) = 6,363.6 \text{ lb.}, \text{ and}$$

$$\text{Preload stress} = F_a / \text{Stress Area (Table A.3.9.3-3)} = 6,364 / 0.142 = 44,814 \text{ psi}$$

Using the maximum torque,

$$F_a = Q/KD_b = 40 \times 12 / (0.132 \times 0.50) = 7,273 \text{ lb.}, \text{ and}$$

$$\text{Preload stress} = F_a / \text{Stress Area (Table A.3.9.3-3)} = 7,273 / 0.142 = 51,216 \text{ psi}$$

Residual torsional moment for minimum torque of 35 ft. lb. is,

$$M_{tr} = 0.5Q = .5(35 \times 12) = 210 \text{ in. lb.}$$

Residual torsional moment for maximum torque of 40 ft. lb. is,

$$M_{tr} = 0.5Q = .5(40 \times 12) = 240 \text{ in. lb.}$$

Residual tensile bolt force for maximum torque,

$$F_{ar} = F_a = 7,273 \text{ lb.}$$

A.3.9.3.7.2 Ram Access Cover Gasket Seating Load

Since a self energizing O-ring is used, the gasket seating load is negligible.

A.3.9.3.7.3 Pressure Loads

Axial force per bolt due to internal pressure is (per Reference [1], Table 4.3),

$$F_a = \frac{\pi D_{lg}^2 (P_{li} - P_{lo})}{4 N_b}$$

D_{lg} (median cover seal diameter) = 23.16 in. Then,

$$F_a = \frac{\pi (23.16^2) (30 - 0)}{4(12)} = 1053.2 \text{ lb./bolt}$$

The fixed edge cover force is,

$$F_f = \frac{D_{lb} (P_{li} - P_{lo})}{4} = \frac{24.50(30)}{4} = 183.8 \text{ lb. in.}^{-1}$$

The fixed edge cover moment is,

$$M_f = \frac{(P_{li} - P_{lo}) D_{lb}^2}{32} = \frac{30(24.50^2)}{32} = 562.7 \text{ in. lb. in.}^{-1}$$

The shear bolt force per bolt is,

$$F_s = \frac{\pi E_l t_l (P_{li} - P_{lo}) D_{lb}^2}{2 N_b E_c t_c (1 - N_{ul})} = \frac{\pi (27.0 \times 10^6) (1.0) (30) (24.50)^2}{2(12) (27.0 \times 10^6) (3.0) (1 - 0.3)} = 1122.5 \text{ lb./bolt}$$

The radial growth of the access ring due to an internal pressure of 30 psi, δ_r , is given by the following equation.

$$\delta_r = \frac{Pr^2}{Et_c}$$

Where, P is the applied pressure (30 psi), r is the mean radius of the ram access penetration ring (12.00 in.), E is the material modulus of elasticity (27.0×10^6 psi @ 300° F [2]), and $t_c = 3.0$ in. is the thickness of the ram access penetration (Table A.3.9.3-2).

Therefore,

$$\delta_r = \frac{(30)(12.00)^2}{(27 \times 10^6)(3.00)} = 5.33 \times 10^{-5} \text{ in.}$$

Since the radial growth due to internal pressure is less than the ram access bolt clearance (0.563 in. – 0.5 in. = 0.063 in.), no shear force is generated in the ram access cover bolts. Therefore,

$$F_s = 0$$

A.3.9.3.7.4 Temperature Loads

The cover bolt material is SA-540 Grade B23 Class 1. The ram access penetration and ram access cover are both constructed from SA-240 Type 304. The bolts have a coefficient of thermal expansion of 6.9×10^{-6} in./in. $^{\circ}\text{F}^{-1}$ at 300 $^{\circ}\text{F}$, and the ram access penetration and ram access cover have a coefficient of thermal expansion of 9.2×10^{-6} in./in. $^{\circ}\text{F}^{-1}$ at 300 $^{\circ}\text{F}$. The tensile load in the bolt due to different thermal expansion is,

$$F_a = 0.25 \pi D_b^2 E_b (a_l T_l - a_b T_b)$$

$$F_a = 0.25(\pi)(0.50^2)(26.7 \times 10^6)\{(9.2 \times 10^{-6})(230) - (6.9 \times 10^{-6})(230)\} = 2,773 \text{ lb./bolt}$$

The shear force per bolt, F_s , due to a temperature change of 230 $^{\circ}\text{F}$ is 0 lb, since there is negligible differential thermal expansion between the ram access penetration and ram access cover, which are both constructed from the same material, and since the clearance holes in the cover are oversized (0.563 in. diameter). Therefore,

$$F_s = 0$$

The temperature difference between the inside and outside of the cover will always be less than one degree (see Chapter A4). Consequently, the resulting bending moment is negligible.

$$M_f = 0$$

A.3.9.3.7.5 Impact Loads

The DSC inside the NUHOMS® OS187H Type 1 transfer cask is supported in the axial direction at the bottom of the cask by the bottom end plate. During a free drop event, the inertial load of the transfer cask internals is transferred through the bottom end plate, bottom neutron shield, and neutron shield plate to the impact target. Consequently, only the inertial load of the ram access cover itself generates loads in the bolts.

The non-prying tensile bolt force per bolt, F_a , is (per Reference [1], Table 4.5),

$$F_a = \frac{1.34 \sin(xi)(DLF)(ai)(W_l + W_c)}{N_b} = \frac{1.34 \sin(xi)(1.1)(ai)(200)}{12} = 24.57(ai) \sin(xi) \text{ lb./bolt}$$

Note: $W_l + W_c$ is assumed to be only the weight of the ram access cover, $W_c = 200$ lb. [see table A.3.9.3-2]

The shear bolt force is,

$$F_s = \frac{\cos(xi)(ai)(W_l)}{N_b} = \frac{200(ai) \cos(xi)}{12} = 16.67(ai) \cos(xi) \text{ lb./bolt}$$

The cover shoulder during normal and accident condition drops takes shear force. Therefore,

$$F_s = 0$$

The fixed-edge cover force, F_f , is,

$$F_f = \frac{1.34 \sin(xi)(DLF)(ai)(W_l + W_c)}{\pi D_{lb}} = \frac{1.34 \sin(xi)(1.1)(ai)(200)}{\pi(24.50)} = 3.83 \sin(xi)(ai) \text{ lb. in.}^{-1}$$

The fixed-edge cover moment, M_f , is,

$$M_f = \frac{1.34 \sin(xi)(DLF)(ai)(W_l + W_c)}{8\pi} = \frac{1.34 \sin(xi)(1.1)(ai)(200)}{8\pi} = 11.73 \sin(xi)(ai) \text{ in.lb.in.}^{-1}$$

The accident condition impact load is taken to be the axial acceleration due to corner drop. As described in Section 3.1.1.4, end and corner drops are not considered credible during transfer operations under 10 CFR Part 72 because the transfer cask is always in the horizontal orientation. The evaluation below is performed in support of a 10 CFR Part 50 evaluation that may be performed by the user if the user cannot demonstrate that these accident drops are not credible. The following corner drop acceleration and impact angle are assumed to bound any possible corner drop accident scenario:

$$ai = 25 \text{ gs, and } xi = 60^\circ$$

Therefore,

$$F_a = 24.57 \times 25 \times \sin(60^\circ) = 532.0 \text{ lb./bolt,}$$

$$F_s = 0.0 \text{ lb./bolt,}$$

$$F_f = 3.83 \times 25 \times \sin(60^\circ) = 82.92 \text{ lb./in., and}$$

$$M_f = 11.73 \times 25 \times \sin(60^\circ) = 254.0 \text{ in.lb./in.}$$

The ram cover bolt individual load is summarized in the following table.

Ram Access Cover Bolt Individual Load Summary

Load Case	Applied Load		Non-Prying Tensile Force, F_a (lb.)	Torsional Moment, M_t (in. lb.)	Prying Force, F_f (lb.in.⁻¹)	Prying Moment, M_f (in. lb. in.⁻¹)
Preload	Residual	Minimum torque	6,364	210	0	0
		Maximum torque	7,273	240	0	0
Gasket	Seating load		0	0	0	0
Pressure	30 psig internal		1053.2	0	183.8	562.7
Thermal	300 °F		2,773	0	0	0
Impact	Accident condition drop		532	0	82.92	254.0

A.3.9.3.8 Ram Access Cover Bolt Load Combinations

A summary of normal and accident condition load combinations (Reference [1], Table 4.9) is presented in the following table.

Ram Access Cover Bolt Normal And Accident Load Combinations

Load Case	Combination Description		Non-Prying Tensile Force, F_a (lb.)	Torsional Moment, M_t (in. lb.)	Prying Force, F_f (lb.in. ⁻¹)	Prying Moment, M_f (in. lb. in. ⁻¹)
1	Preload + Temperature (Normal Condition)	Minimum torque	9,134	210	0	0
		Maximum torque	10,043	240	0	0
2	Pressure (Normal Condition)		1053.2	0	183.8	562.7
3	Pressure + Accident Impact (Accident Condition)		1585.2	0	266.7	816.7

A.3.9.3.9 Ram Access Cover Bolt Stress Calculations**Additional Prying Bolt Force (Ref. [1], Table 2.1)**

The additional prying bolt force, F_{ap} , is calculated in the following way.

$$F_{ap} = -\left(\frac{\pi D_{lb}}{N_b}\right) \left[\frac{\frac{2M_f}{(D_{lo}^* - D_{lb})} - C_1(B - F_f) - C_2(B - P)}{C_1 + C_2} \right]$$

where,

$$C_1 = 1,$$

$$C_2 = \left(\frac{8}{3(D_{lo} - D_{lb})^2} \right) \left[\frac{E_f t_f^3}{1 - N_{ul}} + \frac{(D_{lo} - D_{li}) E_{lf} t_{lf}^3}{D_{lb}} \right] \left(\frac{L_b}{N_b D_b^2 E_b} \right)$$

$$= \left(\frac{8}{3(26.45 - 24.50)^2} \right) \left[\frac{27.0 \times 10^6 (1.0)^3}{1 - 0.3} + \frac{(26.45 - 22.00)(27.0 \times 10^6)(3.0)^3}{24.50} \right] \left(\frac{1.00}{(12)(0.50^2)(26.7 \times 10^6)} \right)$$

$$= 1.50,$$

B is the non-prying tensile bolt force, and P is the bolt preload. Since $F_f = 0$, then $F_f < P$, and therefore $B = P$. Parameters B , P , F_f , and M_f are quantities per unit length of bolt circle. The equations above show that it is conservative to use the bolt preload, P , using the minimum bolt torque. For the applied inward force,

$$P = B = \frac{F_a N_b}{\pi D_{lb}} = \frac{(6,364)(12)}{\pi(24.50)} = 992.2 \text{ lb. in.}^{-1},$$

$$M_f = 816.7 \text{ in.lb. in.}^{-1}, \text{ and } F_f = 266.7 \text{ lb. in.}^{-1}.$$

Therefore,

$$F_{ap} = -\left(\frac{\pi(24.50)}{12}\right) \left[\frac{\frac{2(266.7)}{(26.45 - 24.50)} - 1(992.2 - 266.7) - 1.50(992.2 - 992.2)}{1 + 1.50} \right]$$

$$= 1159.6 \text{ lb./bolt}$$

It is observed that the additional tensile bolt force due to prying plus the maximum combined accident condition load is less than the minimum applied bolt preload. Therefore the additional prying bolt force is not critical for the bolt stress evaluation.

Bolt Bending Moment ([1], Table 2.2)

The maximum bending bolt moment, M_{bb} , evaluated for normal conditions only, is evaluated as follows:

$$M_{bb} = \left(\frac{\pi D_{lb}}{N_b} \right) \left[\frac{K_b}{K_b + K_l} \right] M_f$$

K_b and K_l are based on geometry and material properties and are defined in Reference [1], Table 2.2. By substituting the values given above,

$$K_b = \left(\frac{N_b}{L_b} \right) \left(\frac{E_b}{D_{lb}} \right) \left(\frac{D_b^4}{64} \right) = \left(\frac{12}{1.00} \right) \left(\frac{26.7 \times 10^6}{24.50} \right) \left(\frac{0.50^4}{64} \right) = 1.277 \times 10^4, \text{ and}$$

$$K_l = \frac{E_l t_l^3}{3 \left[(1 - N_{ul}^2) + (1 - N_{ul})^2 \left(\frac{D_{lb}}{D_{lo}} \right)^2 \right] D_{lb}} = \frac{27.0 \times 10^6 (1.00^3)}{3 \left[(1 - 0.3^2) + (1 - 0.3)^2 \left(\frac{24.50}{26.45} \right)^2 \right] 24.50}$$

$$= 2.761 \times 10^5$$

Therefore,

$$M_{bb} = \left(\frac{\pi 24.50}{12} \right) \left[\frac{1.277 \times 10^4}{1.277 \times 10^4 + 2.761 \times 10^5} \right] M_f = 0.2836 M_f$$

For load case 2, $M_f = 562.7$ in.lb./in. Substituting this value into the equation above gives,

$$M_{bb} = 159.6 \text{ in. lb./bolt}$$

A.3.9.3.9.1 Average Tensile Stress

A summary of the applied loads for the transfer cask ram access cover bolts is provided in Section A.3.9.3.8, in the table *Ram Access Cover Bolt Normal and Accident Load Combinations*.

For both normal and accident condition load cases, the applied bolt preload maintains closure of the transfer cask ram access cover. The closure force per bolt generated by the minimum ram access cover bolt torque, with or without the additional closure force generated by thermal loads, is greater than all loads trying to open the ram access cover.

Per Reference [1], Table 5.1,

Normal and Accident Condition

$$S_{ba} = 1.2732 \frac{F_a}{D_{ba}^2} = 1.2732 \frac{10,043}{0.425^2} = 70,792 \text{ psi} = 70.8 \text{ ksi}$$

A.3.9.3.9.2 Bending Stress**Normal Condition**

$$S_{bb} = 10.186 \frac{M_{bb}}{D_{ba}^3} = 10.186 \frac{159.6}{0.425^3} = 21,177 \text{ psi} = 21.2 \text{ ksi}$$

A.3.9.3.9.3 Shear Stress

For normal conditions and for accident conditions, the average shear stress caused by shear bolt force F_s is,

$$S_{bs} = 0$$

For normal and accident conditions the maximum shear stress caused by the torsional moment M_t is,

$$S_{bt} = 5.093 \frac{M_t}{D_{ba}^3} = 5.093 \frac{240}{0.425^3} = 15,922 \text{ psi} = 15.9 \text{ ksi}$$

A.3.9.3.9.4 Maximum Combined Stress Intensity

The maximum combined stress intensity is calculated in the following way (Ref. [1], Table 5.1).

$$S_{bi} = [(S_{ba} + S_{bb})^2 + 4(S_{bs} + S_{bt})^2]^{0.5}$$

For normal conditions combine tension, shear, bending, and residual torsion.

$$S_{bi} = [(70,792 + 21,177)^2 + 4(0 + 15,922)^2]^{0.5} = 97,326 \text{ psi} = 97.3 \text{ ksi}$$

A.3.9.3.9.5 Stress Ratios

In order to meet the stress ratio requirement, the following relationship must hold for both normal and accident conditions.

$$R_t^2 + R_s^2 < 1$$

Where R_t is the ratio of average tensile stress to allowable average tensile stress, and R_s is the ratio of average shear stress to allowable average shear stress.

For normal conditions

$$R_t = 70,792/92,400 = 0.766$$

$$R_s = 15,922/55,400 = 0.287$$

$$R_t^2 + R_s^2 = (0.766)^2 + (0.287)^2 = 0.669 < 1$$

For accident conditions

$$R_t = 70,792/115,500 = 0.613$$

$$R_s = 15,922/69,300 = 0.23$$

$$R_t^2 + R_s^2 = (0.613)^2 + (0.23)^2 = 0.429 < 1$$

A.3.9.3.9.6 Bearing Stress (Under Bolt Head)

A 0.5 in. standard washer is placed under the head of each ram access cover bolt. The inside and outside diameter of the washer are 0.531 in. and 1.062 in. respectively. The diameter of the bolt clearance hole in the cover is 0.563 in. Therefore, the total bearing area under the top cover bolts, A_b , is the following.

$$A_b = (\pi/4) [1.062^2 - 0.563^2] = 0.637 \text{ in.}^2$$

According to Reference [1], bearing stress evaluation is required for normal condition loads only. For normal conditions, the maximum bearing stress under the washer, σ_b , is the following.

$$\sigma_b = 10,043 \text{ lb.} / 0.637 \text{ in.}^2 = 15,766 \text{ psi} = 15.8 \text{ ksi}$$

The normal condition allowable bearing stress on the cover is taken to be the yield stress of the cover material at 300 °F. The cover is manufactured out of SA-240 Type 304, which has a yield stress of 22.4 ksi at 300 °F.

A.3.9.3.10 Ram Access Cover Bolt Analysis Results

A summary of the stresses calculated above is given in the following table:

Summary of Stresses and Allowables

Stress Type	Normal Condition		Accident Condition	
	Stress	Allowable	Stress	Allowable
Average tensile (ksi)	70.8	92.4	70.8	115.5
Shear (ksi)	15.9	55.4	15.9	69.3
Combined (ksi)	97.3	124.7	Not Required [1]	
Interaction E.Q. $Rt2 + Rs2 < 1$	0.669	1	0.429	1
Bearing (ksi) allowable (ksi) (Sy of cover material)	15.8	22.4	Not Required [1]	

Note: The preload load case controls for both normal and accident conditions

A.3.9.3.11 Minimum Engagement Length for Ram Access Cover Bolt

The ram access cover bolt minimum engagement length evaluation is not changed from that presented in Section 3.9.3.11 for the OS187H TC and is presented here for purposes of completeness of presentation.

For a 1/2"-13UNC-2A bolt, the material is SA-540 Grade B23 Class 1, with

$$S_u = 165 \text{ ksi, and}$$

$$S_y = 150 \text{ ksi (at room temperature)}$$

The ram access penetration and threaded insert material are both constructed from Type 304 stainless steel and have the following material properties.

$$S_u = 75 \text{ ksi, and}$$

$$S_y = 30 \text{ ksi (at room temperature)}$$

The minimum engagement length, L_e , for the bolt and flange is ([4], p. 119)

$$L_e = \frac{2A_t}{3.1416K_{n\max} \left[\frac{1}{2} + .57735n(E_{s\min} - K_{n\max}) \right]}$$

Where,

$$A_t = \text{tensile stress area} = 0.142 \text{ in.}^2$$

$$n = \text{number of threads per inch} = 13$$

$$K_{n\max} = \text{maximum minor diameter of internal threads} = 0.434 \text{ in. ([4], p. 1283)}$$

$$E_{s\min} = \text{minimum pitch diameter of external threads} = 0.4435 \text{ in. ([4], p. 1283)}$$

Substituting the values given above,

$$L_e = \frac{2(0.142)}{(3.1416)(0.434) \left[\frac{1}{2} + .57735(13)(0.4435 - 0.434) \right]} = 0.365 \text{ in.}$$

$$J = \frac{A_s \times S_{ue}}{A_n \times S_{ui}} [4]$$

Where, S_{ue} is the tensile strength of external thread material, and S_{ui} is the tensile strength of internal thread material.

$$A_s = \text{shear area of external threads} = 3.1416 n L_e K_{n\max} \{ 1/(2n) + .57735 (E_{s\min} - K_{n\max}) \}$$

$$A_n = \text{shear area of internal threads} = 3.1416 n L_e D_{s\min} \{ 1/(2n) + .57735 (D_{s\min} - E_{n\max}) \}$$

For the bolt/Helicoil insert connection:

$E_{n\ max}$ = maximum pitch diameter of internal threads = 0.4565 in. ([4], p. 1283)

$D_{s\ min}$ = minimum major diameter of external threads = 0.4876 in. ([4], p. 1283)

Therefore,

$$A_s = 3.1416(13)(0.365)(0.434)\{1/(2 \times 13) + .57735 (0.4435 - 0.434)\} = 0.2843 \text{ in.}^2$$

$$A_n = 3.1416(13)(0.365)(0.4876)\{1/(2 \times 13) + .57735 (0.4876 - 0.4565)\} = 0.4101 \text{ in.}^2$$

So,

$$J = \frac{0.2843(165.0)}{0.4101(75.0)} = 1.525$$

$$Q = L_e J = (0.365)(1.525) = 0.557 \text{ in.}$$

The actual engagement length can be calculated as:

1.25 in. bolt length – 1.00 in. cover thickness + 0.66 in. cover counter bore – 0.125 in. washer thickness = 0.785 in. > 0.557 in.

A.3.9.3.12 Brittle Fracture Analysis of Top Cover Bolt

The transfer cask and its attachment bolts are designed and fabricated per ASME Subsection NC Code [6]. The fracture toughness requirements for the bolting material are specified in Section NC-2332.3, which indicates that in order to meet the fracture toughness requirements, a Charpy V-notch test shall be performed. The test shall be performed at or below the lowest service metal temperature, and all three specimens shall meet the requirements of [6], Table NC-2332.3-1. The size of the top cover bolt is 1.5" diameter, and based on [6], Table NC-2332.3-1, the required C_v value is 25 mil (lateral expansions).

In addition to the above Charpy V-notch test, a brittle fracture evaluation is performed to demonstrate that brittle fracture is not a concern for the top cover bolts.

The top cover bolts are fabricated from SA-540 Grade B23 Class 1 and have the following material properties.

Material Grade	Yield Strength, ksi (Room Temperature)	Ultimate Tensile Strength, ksi (Room Temperature)
SA-540 Grade B23 Class 1	150	165

In accordance with the ASME Code, Section II, Part A [7], the bar stocks of these materials are quenched and fully tempered (1000 – 1100 °F or higher) to produce a strong and tough microstructure.

ASM Metal Handbook [8], Figure 26 (reproduced here in Figure A.3.9.3-1) shows that a 4340 steel tempered at 1035 °F for 1 ½ hours to produce a yield strength of 158 ksi exhibits a very low Charpy impact transition temperature (< -20 °F) and an upper shelf energy of about 45 ft-lb at –20 °F.

Reference [8], p. 705, Figure 31 (reproduced here in Figure A.3.9.3-2) shows that a medium carbon low alloy steel tempered to a yield strength of 107 ksi (like SA-193, Grade B7) would have an upper shelf energy of about 52 ft-lb and absorb about 48 ft-lb at –20 °F while material at a yield strength of 149 ksi (like SA-540 Grade B23 Class 1) would have an upper shelf energy of 35 ft-lb and absorb about 30 ft-lb at -20 °F.

The following table summarizes the equivalent impact energy of the SA-540 Grade B23 Class 1 at -20 °F and the Charpy values used for the brittle fracture evaluation.

Summary of the Equivalent Impact Energy

Material Grade	Yield Strength (ksi)	Charpy Value, -20 °F (ft-lb)	Charpy Value Used for Brittle Fracture Evaluation (ft-lb)
4340 steel tempered at 1035 °F for 1½ hours (Fig. A.3.9.3-1)	158	45	
Medium-carbon low alloy (Fig. A.3.9.3-2)	149	30	
SA-540 Grade B23 Class 1	150		20*

*By comparison with the similar yield strength materials, lower values are conservatively used for SA-540 Grade B23 Class 1 brittle fracture evaluations.

A brittle fracture evaluation of the top cover bolt is performed based on a service temperature of -20 °F. The work includes the following:

- Methodology
- Stress
- Material fracture toughness
- Fracture toughness criteria
- Allowable flaw calculations
- NDE Inspection Plan

Methodology

The allowable flaw sizes were performed using the Singular Integral Equation and Asymptotic Approximation [9] (see Figure A.3.9.3-3). The total applied stress intensity K_{applied} is calculated based on the following equations.

$$\sigma_{\text{net}} = P/(\pi a^2)$$

$$K_{\text{applied}} = \sigma_{\text{net}} (\pi a)^{1/2} F_1(a/b) \text{ (see Figure A.3.9.3-3 for definitions)}$$

Stress

The maximum tensile stress for the top cover bolts is 110.6 ksi and is calculated in Section A.3.9.3.5. The maximum net tensile stress is calculated based on 0.025" deep 360° circumferential crack.

$$\sigma_{\text{net}} = 110.6 \{1.5/(1.5-2 \times 0.025)\}^2 = 118.36 \text{ ksi}$$

Material Fracture Toughness

The Charpy impact value may be transformed into a fracture toughness value by using the empirical relation developed in Section 4.2 of NUREG/CR-1815 [10] as follows:

$$K_{\text{id}} = \{5E(C_v)\}^{1/2}$$

Where

K_{id} = Dynamic Fracture Toughness, psi-(in)^{1/2}
 E = Modulus of Elasticity, 26.7×10^6 psi
 C_v = Charpy Impact Value, 20 ft-lb

Substituting the values given above,

$$K_{id} = \{5E(C_v)\}^{1/2} = \{5 \times 26.7 \times 10^6 (20)\}^{1/2} = 51,672 \text{ psi-in}^{1/2}$$

Fracture Toughness Criteria

Using the method described in the ASME Code, Section XI, IWB-3613 [11], the limiting fracture toughness values are reduced by a factor of $\sqrt{2}$ for the accident condition and are calculated as follows:

$$K_{\text{allowable}} \leq 51,672/\sqrt{2} = 36.54 \text{ ksi-}\sqrt{\text{in}}$$

Allowable Flaw Size Calculation

Using the above load definitions, fracture toughness values and assumed flaw size (0.025"), the total applied stress intensity K_I (applied) is calculated based on the singular integral equation and asymptotic approximation (see Figure A.3.9.3-3).

$$\begin{aligned} K_{\text{applied}} &= \sigma_{\text{net}} (\pi a)^{1/2} F_I(a/b) \\ 2b &= 1.5 \text{ in.} & b &= 0.75 \text{ in.} \\ 2a &= 1.5 \text{ in.} - 2 \times 0.025 \text{ in.} = 1.45 \text{ in.} & a &= 0.725 \text{ in.} \\ a/b &= 0.725/0.75 = 0.97 & F_I(a/b) &= 0.18 \\ K_{\text{applied}} &= 118.36 (\pi \times 0.725)^{1/2} (0.18) = 32.15 \text{ ksi-}\sqrt{\text{in}} \leq 36.54 \text{ ksi-}\sqrt{\text{in}} \end{aligned}$$

NDE Inspection Plan

The results of the fracture toughness analysis show that the critical flaws in the attachment bolts which would result in unstable crack growth or brittle fracture are larger than those generally observed in the bolt and bar stock.

The allowable flaw size for the attachment bolts is 0.025 in. The attachment bolts are fabricated per ASME Subsection NC code and only visual inspection is required by this code. In order to detect the surface indication, a PT or MT will be performed using NB code paragraph NB-2583.3. The requirement is that any linear nonaxial indications are unacceptable and therefore assuming 0.025" deep 360° circumferential crack for brittle fracture evaluation is conservative.

The liquid penetrant or magnetic particle method will be used in accordance with Section V, Article 6 of the ASME Code [12].

A.3.9.3.13 Conclusions

Top cover and ram access cover bolt stresses meet the acceptance criteria of NUREG/CR-6007 *Stress Analysis of Closure Bolts for Shipping Casks* [1].

The top cover and ram cover bolt, insert, and flange thread engagement length is acceptable.

The calculated stress intensity factor for a maximum flaw size 0.025 in. is less than the allowable stress intensity factor. Hence, there is no potential for top cover bolt brittle fracture failure up to this flaw size.

A.3.9.3.14 References

- [1] Stress Analysis of Closure Bolts for Shipping Casks, NUREG/CR-6007, 1992.
- [2] American Society of Mechanical Engineers, ASME Boiler and Pressure Vessel Code, Section II, Part D, 1998 through 2000 addenda.
- [3] Helicoil Catalog, Heli-Coil 8-Pitch Inserts, Bulletin 913B.
- [4] Machinery Handbook, 21st Ed, Industrial Press, 1979.
- [5] Baumeister, T., Marks, L. S., *Standard Handbook for Mechanical Engineers*, 7th Edition, McGraw-Hill, 1967.
- [6] American Society of Mechanical Engineers, ASME Boiler and Pressure Vessel Code, Section III, Division 1, Subsection NC, 1998, through 2000 addenda.
- [7] American Society of Mechanical Engineers, ASME Boiler and Pressure Vessel Code, Section II, Part A, 1998, through 2000 addenda.
- [8] American Society for Metals (ASM) Metal Handbook (Volume 1), Notch Toughness of Steels Section, 9th Edition, 1978.
- [9] Singular Integral Equation (Bueckner) and Asymptotic Approximation (Benthem).
- [10] NUREG/CR-1815 "Recommendation for Protecting Against Failure by Brittle Fracture in Ferritic Steel Shipping Containers Up to Four Inches Thick" Lawrence Livermore National Laboratory, June 15, 1981.
- [11] American Society of Mechanical Engineers, ASME Boiler and Pressure Vessel Code, Section XI, 1998 through 2000 addenda.
- [12] American Society of Mechanical Engineers, ASME Boiler and Pressure Vessel Code, Section V, Article 6, 1998 through 2000 addenda.

Table A.3.9.3- 1 Design Parameters for Top Cover Bolt Analysis

D_b	Nominal diameter of closure bolt; 1.500 in.
K	Nut factor for empirical relation between the applied torque and achieved preload is 0.132
Q	Applied torque for the preload (in.-lb.)
D_{lb}	Closure lid diameter at bolt circle, 76.85 in.
D_{lg}	Closure lid diameter at the seal = 73.61 in.
E_c	Young's modulus of cask wall material, 27.0×10^6 psi @ 300 °F
E_l	Young's modulus of lid material, 27.0×10^6 psi @ 300 °F
N_b	Total number of closure bolts, 24
N_{ul}	Poisson's ratio of closure lid, 0.3, ([5]. p. 5-6)
P_{ei}	Inside pressure of cask, 30 psig
D_{lo}	Closure lid diameter at outer edge, 81.37 in.
P_{li}	Pressure inside the closure lid, 30 psig
t_c	Thickness of flange, 6.50 in.
t_l	Thickness of lid, 3.0in./1.5 in.
α_b	Thermal coefficient of expansion, bolt material, 6.9×10^{-6} in. in. ⁻¹ °F ⁻¹ at 300 °F
α_c	Thermal coefficient of expansion, cask, 9.2×10^{-6} in. in. ⁻¹ °F ⁻¹ at 300 °F
α_l	Thermal coefficient of expansion, lid, 8.8×10^{-6} in. in. ⁻¹ °F ⁻¹ at 300 °F
E_b	Young's modulus of bolt material, 26.7×10^6 psi at 300 °F
ai	Maximum rigid-body impact acceleration (g) of the cask
DLF	Dynamic load factor to account for any difference between the rigid body acceleration and the acceleration of the contents and closure lid = 1.1
W_c	Weight of contents = 50,720 lb. (fuel) + 29450 lb. (basket) + 28,440 lb. (canister) + 888 lb. (cask spacer) = 109,498 lb.
W_l	Weight of closure lid = 5,360 lb., conservatively use 5,500 lb.
$W_c + W_l$	$109,498 + 5,500 = 114,998$ lb, conservatively use 120,000 lb.
χ_i	Impact angle between the cask axis and target surface
S_{yl}	Yield strength of closure lid material, 43.3 ksi @ 300 °F
S_{ul}	Ultimate strength of closure lid, 94.2 ksi @ 300 °F
S_{yb}	Yield strength of bolt material (see Table A.3.9.3-4)
S_{ub}	Ultimate strength of bolt material (see Table A.3.9.3-5)
P_{lo}	Pressure outside the cover
P_{co}	Pressure outside the cask, 0 psig (worst case scenario)
L_b	Bolt length between the top and bottom surfaces of closure, 1.50 in.

Table A.3.9.3– 2 Design Parameters for Ram Access Cover Bolt Analysis

D_b	Nominal diameter of closure bolt, 0.50 in.
K	Nut factor for empirical relation between the applied torque and achieved preload is 0.132
Q	Applied torque for the preload (in.-lb.)
D_{lb}	Ram access cover diameter at bolt circle, 24.50 in.
D_{lg}	Ram access cover diameter at the seal = 23.16 in.
E_c	Young's modulus of ram access penetration wall material, 27.0×10^6 psi @ 300 °F
E_l	Young's modulus of cover material, 27.0×10^6 psi @ 300 °F
N_b	Total number of closure bolts, 12
N_{ul}	Poisson's ratio of closure ram access cover, 0.3 ([5], pp 5-6)
P_{ci}	Inside pressure of ram access penetration, 30 psig
D_{lo}	Cover diameter at outer edge, 26.45 in.
D_{li}	Cover diameter at inner edge, 22.00 in.
P_{li}	Pressure inside the cover, 30 psig
t_c	Thickness of the ram access penetration, 3.00 in.
t_l	Thickness of cover, 1.0 in.
α_b	Thermal coefficient of expansion, bolt material, 6.9×10^{-6} in. in. ⁻¹ °F ⁻¹ at 300 °F
α_c	Thermal coefficient of expansion, ram access penetration, 9.2×10^{-6} in. in. ⁻¹ °F ⁻¹ at 300 °F
α_l	Thermal coefficient of expansion, ram access cover, 9.2×10^{-6} in. in. ⁻¹ °F ⁻¹ at 300 °F
E_b	Young's modulus of bolt material, 26.7×10^6 psi at 300 °F
ai	Maximum rigid-body impact acceleration (g) of the cask
DLF	Dynamic load factor to account for any difference between the rigid body acceleration and the acceleration of the contents and cover = 1.1
W_c	The inertial load of the transfer cask contents does not affect the cover bolts
W_l	Weight of ram access cover = 157 lb., conservatively use 200 lb.
$W_c + W_l$	$0 + 200 = 200$ lb.
χ_i	Impact angle between the cask axis and target surface
S_{yl}	Yield strength of closure cover material, 22.4 ksi @ 300 °F
S_{ul}	Ultimate strength of closure lid, 66.2 ksi @ 300 °F
S_{yb}	Yield strength of bolt material (see Table A.3.9.3-4)
S_{ub}	Ultimate strength of bolt material (see Table A.3.9.3-5)
P_{lo}	Pressure outside the cover, 0 psig (worst case scenario)
P_{co}	Pressure outside the ram access penetration, 0 psig (worst case scenario)
L_b	Bolt length between the top and bottom surfaces of closure, 1.00 in.

Table A.3.9.3– 3 Bolt Data

Parameter	Top cover bolts (1 1/2"– 8UN – 2A)	Ram closure bolts (1/2"– 13UNC – 2A)
N (no of threads per inch)	8	13
p (pitch)	$1/8 = .125$ in.	$1/13 = .0769$ in.
D_b (nominal diameter)	1.50 in.	0.50 in.
D_{ba} (bolt diameter for stress calculations)	$D_b - .9743p = 1.50 - .9743 (0.125)$ $= 1.378$ in.	$D_b - .9743p = 0.50 - .9743 (0.0769)$ $= 0.425$ in.
Stress area	$\pi/4 (1.378)^2 = 1.491$ in ²	$\pi/4 (0.425)^2 = 0.142$ in ²

Data from [1], Table 5.1

Table A.3.9.3– 4 Allowable Stresses in Closure Bolts for Normal Conditions

(Material: SA-540 Grade B23 Class 1)

Temperature (°F)	Yield Stress ⁽¹⁾ (ksi)	Normal Condition Allowables		
		F_{tb} ^(2,4) (ksi)	F_{vb} ^(3,4) (ksi)	$S.I.$ ⁽⁵⁾ (ksi)
100	150	100.0	60.0	135.0
200	143.4	95.6	57.4	129.1
300	138.6	92.4	55.4	124.7
400	134.4	89.6	53.8	121.0
500	130.2	86.8	52.1	117.2
600	124.2	82.8	49.7	111.8

Notes:

- (1) Yield stress values are from ASME Code, Section II, Table 4 (Ratio: $S_y = 3S_m$) [2]
- (2) Allowable Tensile stress, $F_{tb} = 2/3 S_y$ (Ref. [1], Table 6.1)
- (3) Allowable shear stress, $F_{vb} = 0.4 S_y$ (Ref. [1], Table 6.1)
- (4) Tension and shear stress must be combined using the following interaction equation:

$$\frac{\sigma_{tb}^2}{F_{tb}^2} + \frac{\tau_{vb}^2}{F_{vb}^2} \leq 1.0 \quad [1]$$

Stress intensity from combined tensile, shear and residual torsion loads, $S.I. \leq 0.9 S_y$ (Ref. [1], Table 6.1)

Table A.3.9.3– 5 Allowable Stresses in Closure Bolts for Hypothetical Accident Conditions

(Material: SA-540 Grade B23 Class 1)

Temperature (°F)	Yield Stress ⁽¹⁾ (ksi)	Accident Condition Allowables		
		$0.6 S_y^{(3)}$ (ksi)	$F_{tb}^{(2,4)}$ (ksi)	$F_{vb}^{(3,4)}$ (ksi)
100	150.0	90.0	115.5	69.3
200	143.4	86.0	115.5	69.3
300	138.6	83.2	115.5	69.3
400	134.4	80.6	115.5	69.3
500	130.2	78.1	115.5	69.3
600	124.2	74.5	115.5	69.3

Notes:

- (1) Yield and tensile stress values are from ASME Code, [2], Table 4, Note that S_u is 165.0 ksi at all temperatures of interest.
- (2) Allowable Tensile stress, $F_{tb} = \text{MINIMUM}(0.7 S_u, S_y)$, where $0.7 S_u = 0.7 (165.0) = 115.5$ ksi (Ref. [1], Table 6.3)
- (3) Allowable shear stress, $F_{vb} = \text{MINIMUM}(0.42 S_u, 0.6 S_y)$, where $0.42 S_u = 0.42 (165.0) = 69.3$ ksi (Ref. [1], Table 6.3)
- (4) Tension and shear stresses must be combined using the following interaction equation:

$$\frac{\sigma_{tb}^2}{F_{tb}^2} + \frac{\tau_{vb}^2}{F_{vb}^2} \leq 1.0 \quad [1]$$

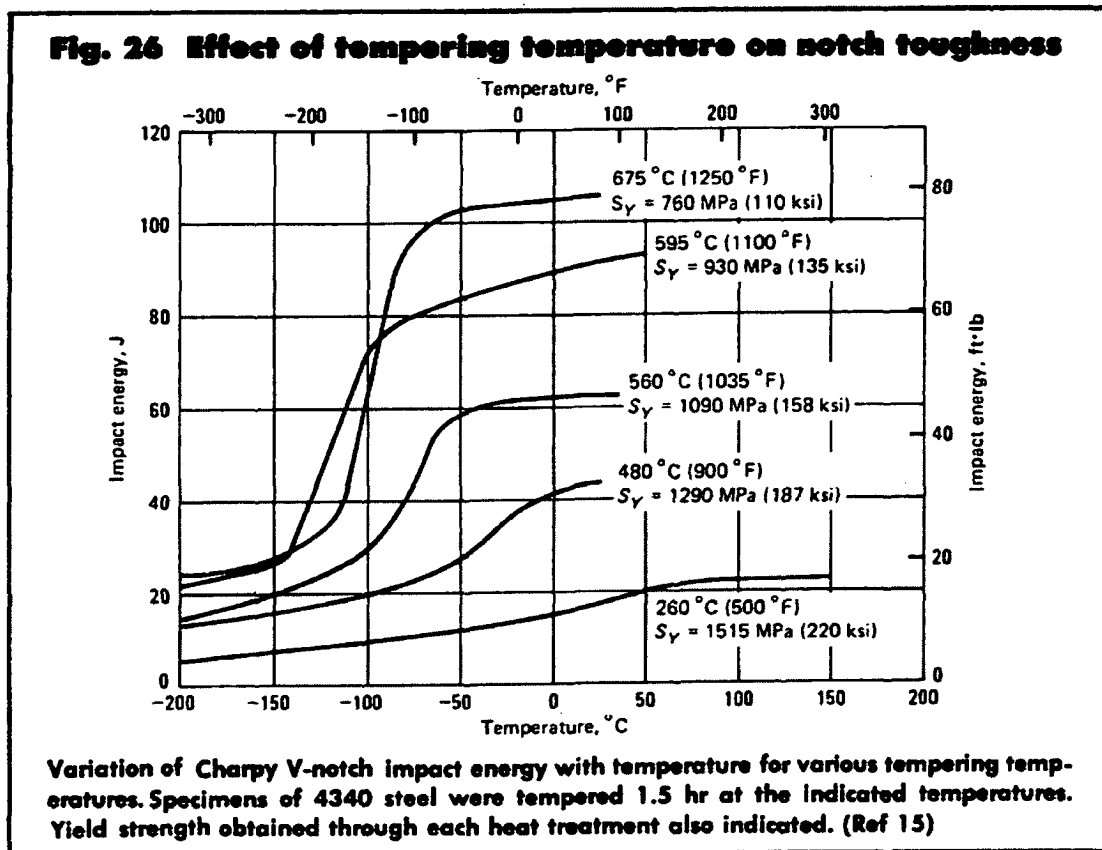


Figure A.3.9.3-1 Effect of Tempering Temperature on Notch Toughness

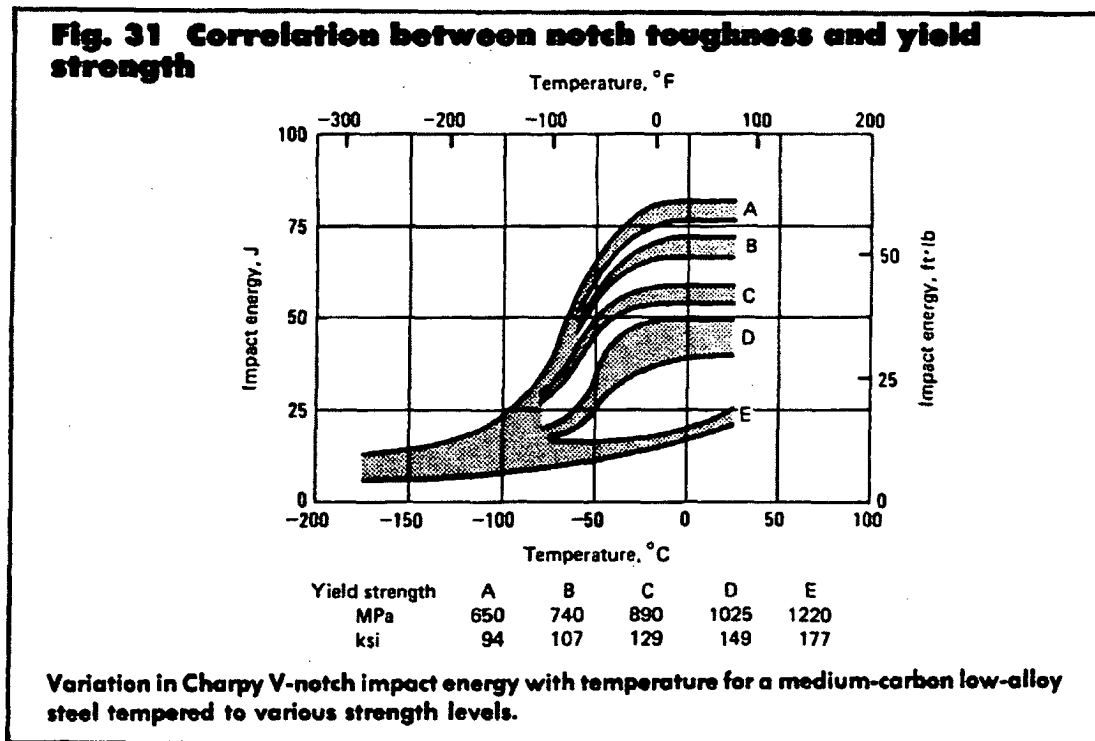


Figure A.3.9.3-2 Correlation between Notch Toughness and Yield Strength

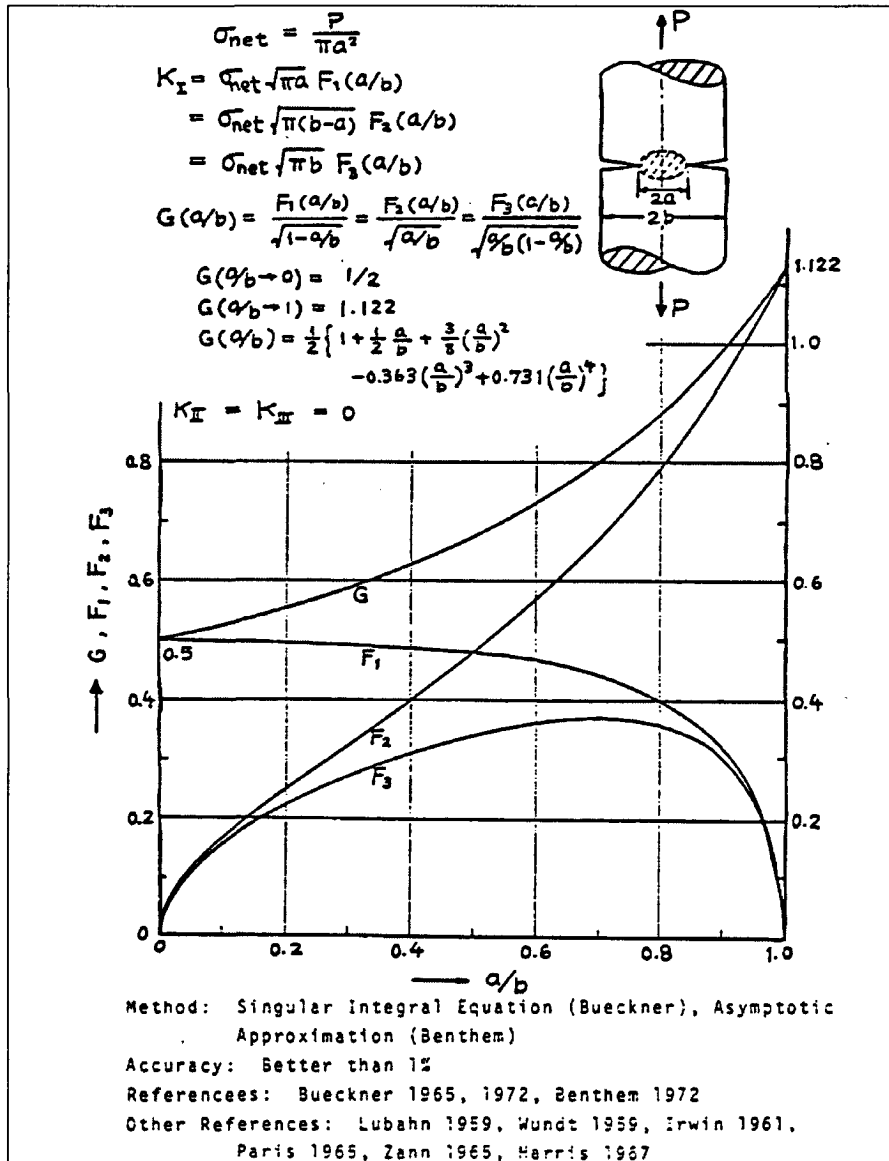


Figure A.3.9.3-3 Singular Integral Equation and Asymptotic Approximation for Brittle Fracture Evaluation

Appendix A.3.9.4

OS187H Type 1 Transfer Cask Lead Slump and Inner Shell Buckling Analysis

In accordance with the HD System Safety Evaluation Report (SER), the top and bottom end accident drops and the corner accident drop are not credible under 10CFR Part 72 because the OS187H Type 1 transfer cask (TC) is always in the horizontal orientation. Therefore, the OS187H Type 1 TC lead slump and shell buckling analysis are not evaluated and, thus, this appendix has been deleted. These analyses may need to be evaluated under 10CFR Part 50 should the user not be able to demonstrate that the top and bottom end and the corner drops are not credible during loading operations, or during transport operations governed under 10CFR Part 71.

Appendix A.3.9.5 OS187H Type 1 Transfer Cask Trunnion Analysis

TABLE OF CONTENTS

A.3.9.5 OS187H TYPE 1 TRANSFER CASK TRUNNION ANALYSIS.....	A.3.9.5-1
A.3.9.5.1 Introduction.....	A.3.9.5-1
A.3.9.5.2 Component Weights.....	A.3.9.5-2
A.3.9.5.3 Material Properties.....	A.3.9.5-3
A.3.9.5.4 Stress Criteria.....	A.3.9.5-4
A.3.9.5.5 Load Cases.....	A.3.9.5-5
A.3.9.5.5.1 Critical Lifts	A.3.9.5-5
A.3.9.5.5.2 Transfer Handling Loads	A.3.9.5-6
A.3.9.5.6 Stress Calculation.....	A.3.9.5-7
A.3.9.5.7 Summary of Computed Stresses.....	A.3.9.5-9
A.3.9.5.8 Conclusions.....	A.3.9.5-10
A.3.9.5.9 References.....	A.3.9.5-11

LIST OF TABLES

Table A.3.9.5- 1 Summary of Computed and Allowable Trunnion Stresses.....	A.3.9.5-12
---	------------

LIST OF FIGURES

Figure A.3.9.5- 1 Upper trunnion, general arrangement.....	A.3.9.5-13
Figure A.3.9.5- 2 Lower trunnion, general arrangement	A.3.9.5-13
Figure A.3.9.5- 3 Loads and stress sections at upper trunnion	A.3.9.5-14
Figure A.3.9.5- 4 Loads and stress sections at lower trunnion	A.3.9.5-14

A.3.9.5 OS187H TYPE 1 TRANSFER CASK TRUNNION ANALYSIS

A.3.9.5.1 Introduction

This appendix presents the evaluation of the NUHOMS® OS187H Type 1 transfer cask (TC) trunnion stresses due to all applied loads during fuel loading and transfer/handling operations at normal (Service Level A) conditions.

The OS187H Type 1 TC has two upper trunnions and two lower trunnions made of monolithic forged stainless steel, SA-182 Type FXM-19 and Type F304N, respectively. Schematic representation of the upper trunnion is shown in Figure A.3.9.5-1, while the lower trunnion is shown in Figure A.3.9.5-2. The design details for both sets of trunnions are provided in Drawing 10494-72-9002-SAR in Section A.1.5.

The two upper trunnions are used to lift the TC containing a canister and an empty basket into a fuel pool prior to loading spent fuel assemblies. After the spent fuel has been loaded into the basket, the TC is lifted to a decontamination area. There, after water has been removed from the TC and the canister, the canister is sealed by welding the canister cover in place. The TC lid is lowered onto the TC and bolted in place. The TC is then placed on a trailer/transfer skid for transfer to an onsite HSM. The TC is vertically lifted above the transfer skid and then lowered until the lower trunnions rest in matching trunnion towers support pockets of the skid. The TC is downended, using the lower trunnion supports as the pivot points, to a horizontal position when the upper trunnions rest on their support pockets. Prior to the downending operation the weight of the TC is carried by the upper trunnions. During the downending, the TC weight is shared by both upper and lower trunnions. After completion of the process, the TC is supported by all four trunnions. After securing the TC onto the skid's trunnion towers, the TC is towed to the ISFSI. At the ISFSI, the TC is aligned to the HSM opening and the DSC is pushed into the HSM. During this operation, the upper trunnions take the reaction force required to push the DSC into the HSM.

Analyzed loads include lifting loads and transfer/handling loads. Acceptance criteria and applicable stress limits for upper and lower trunnions are listed in Section A.3.9.5.4. Stresses caused by handling loads are assessed against the ASME Service Level A criteria [[3]]. Critical lift load stresses for the upper trunnions are evaluated against ANSI N14.6 [[1]] criteria.

The TC shell and trunnions are assumed to be at 300 °F during transfer. This assumption is conservative based on the thermal evaluation performed in Chapter A.4.

A.3.9.5.2 Component Weights

The weight of the OS187H Type 1 TC is 240 kips, including the loaded canister (Section A.3.2.2). However, for conservatism, a weight of 250.00 kips is used in the analysis.

A.3.9.5.3 Material Properties

The following material properties, used in the trunnion stress analysis, are taken from Reference [2], for temperature 300 °F.

Material Property	SA-182, Type FXM-19 (upper trunnions)	SA-182, Type F304N (lower trunnions)
S_m	31.4 ksi	22.5 ksi
S_v	43.3 ksi	25.0 ksi
S_u	94.2 ksi	76.1 ksi

A.3.9.5.4 Stress Criteria

Critical lift load stresses at the upper trunnions are assessed against ANSI N14.6 criteria [[1]]. Upper and lower trunnion stresses caused by transfer and handling loads are assessed against ASME Service Level A criteria [[3]]. Acceptance criteria and applicable stress limits for upper trunnions and lower trunnions are listed in the table below:

	Lift Loads				Handling Loads			
Component	Upper trunnion		Lower trunnion		Upper trunnion		Lower trunnion	
Basis	ANSI N14.6		ASME Level A		ASME Level A		ASME Level A	
Stress classification	Maximum tensile	Combined shear	P_M	$P_M + P_B$	P_M	$P_M + P_B$	P_M	$P_M + P_B$
Criteria	Smaller of $S_y, 0.6S_u$	Smaller of $S_y, 0.6S_u$	S_m	$1.5 S_m$	S_m	$1.5 S_m$	S_m	$1.5 S_m$
Allowable stress	43.3 ksi	43.3 ksi	22.5 ksi	33.8 ksi	31.4 ksi	47.1 ksi	22.5 ksi	33.8 ksi

A.3.9.5.5 Load Cases

The trunnion design is evaluated against the following two load types:

- A. **Lifting loads**—(The OS187H Type 1 TC is in vertical position, lifted from the pool to the decontamination area and then to the trailer). The two upper trunnions are analyzed for this critical lifting load.

The two bottom trunnions are not used for lifting of the TC. However, when the vertical TC is lowered and placed onto the transfer skid, a portion of the TC weight is reacted by the lower trunnions during downending of the TC to its horizontal position.

The lifting loads for upper trunnions and lower trunnions are described in Section A.3.9.5.5.1.

- B. **Transfer handling loads**—(The OS187H Type 1 TC is in a horizontal position on the transfer trailer/skid). All four trunnions rest on the trunnion tower supports. The trunnions are designed to withstand the following transfer handling load combinations, listed below:

1. DW + 1g axial—axial load resisted by lower trunnions only
2. DW + 1g transverse—transverse load resisted by trunnions on one side of TC
3. DW + 1g vertical—vertical load shared by all four trunnions
4. DW + 1/2g axial + 1/2g transverse + 1/2g vertical

In load combination 4, the load components are distributed as defined in load combinations 1 through 3 above.

The distribution of deadweight loads onto upper trunnions and lower trunnions is described in Section A.3.9.5.5.2. In addition to the combinations listed above, the trunnion stresses are also evaluated for the envelope of all four transfer load combinations.

A.3.9.5.5.1 Critical Lifts

ANSI N14.6-1993 [[1]] imposes two requirements on the upper trunnion design. The first is to withstand six times the weight of the lifted TC (6g load) without generating a combined shear stress or maximum tensile stress at any point in excess of the yield strength of the trunnion material, S_y . The second is to withstand ten times the weight of the lifted TC (10g load) without generating a combined shear stress, or maximum tensile stress at any point in excess of the ultimate strength of the trunnion material, S_u .

In the evaluation, the two requirements are reduced to a single criterion for tensile/shear stress limit: the minimum of S_y and $0.6S_u$ ($0.6S_u = 6g / 10g S_u$), applied to the 6g load.

For the lifting load case, the TC weight is increased by a dynamic load factor of 15% to account for dynamic effects that may be experienced during lifting of the TC. The resulting loads are:

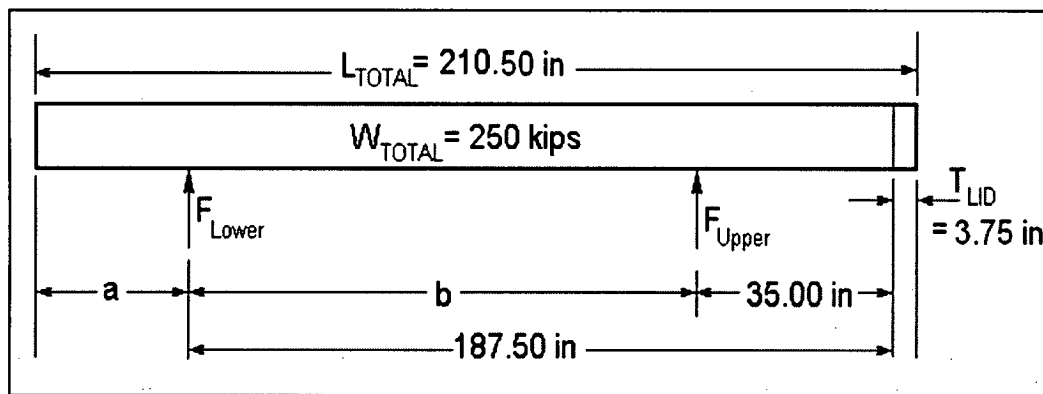
$$F_L (\text{upper trunnion}) = 1.15 \times 6 \times DW/2 = 1.15 \times 6 \times 250.0 / 2 = 862.5 \text{ kips/trunnion}$$

As discussed above, the two bottom trunnions are not used for lifting of the TC. However, the bottom trunnions react a portion of the TC weight during downending of the TC to its horizontal position. For evaluation purposes, it is conservatively assumed that the lower trunnions will react the entire weight of the cask:

$$F_L (\text{lower trunnion}) = 1.15 \times DW / 2 = 1.15 \times 250 / 2 = 143.75 \text{ kips/trunnion}$$

A.3.9.5.5.2 Transfer Handling Loads

The figure below shows the geometry derived from the OS187H Type 1 TC drawings.



These dimensions are used to calculate the reaction forces for the upper and lower trunnions. Dimensions "a" (distance from TC bottom to centerline of lower trunnion) and "b" (distance between upper and lower trunnions) are 19.25 in., and 152.5 in., respectively.

Conservatively assuming a total weight of 250 kips, the support reaction forces at the trunnions can be calculated as $F_{Upper} = 71 \text{ kips}$ for each upper trunnion, and $F_{Lower} = 54 \text{ kips}$ for each lower trunnion.

A.3.9.5.6 Stress Calculation

The geometry and major dimensions used in the stress evaluation of the upper and lower trunnions are shown in Figure A.3.9.5-1 and Figure A.3.9.5-2, respectively. Materials used for each part are listed in Section A.3.9.5.3.

Section properties and moment arms are calculated at the trunnion sections shown in Figure A.3.9.5-3 and Figure A.3.9.5-4 for the upper and lower trunnions, respectively. The following assumptions are used in the specification of loads acting on trunnions:

1. Loads from the skid and lifting yoke are assumed to act at the center of the bearing surface.
2. The lifting load is the total weight of 250 kips times a dynamic load factor of 1.15.
3. All axial and vertical loads on the lower trunnion act through the part of the trunnion that rests on the transfer skid.
4. Transverse (radial) loads are resisted by bearing of the trunnion against the skid support towers. Therefore, the radial load is resisted by Section 1-1 (see table below).

Trunnion moment arms and section properties used in calculations are presented in the table below:

Upper Trunnion									
Section	OD	A	I	S	L _{SKID}	L _{LIFT}	L _{HSM}		
1 - 1	17.15 in	231.0 in ²	4,246 in ⁴	495.2 in ³	7.88 in	11.38 in	13.00 in		
2 - 2	12.00 in	113.1 in ²	1,018 in ⁴	169.7 in ³	1.88 in	5.38 in	7.00 in		
3 - 3	8.00 in	50.27 in ²	201.1 in ⁴	50.28 in ³	n/a	1.63 in	3.25 in		
Lower Trunnion									
Section	OD	A	I	S	L _{SKID}	L _{LIFT}	L _{HSM}		
1 - 1	14.63 in	168.1 in ²	2,249 in ⁴	307.5 in ³	8.75 in	n/a	10.5 in		
2 - 2	12.00 in	113.1 in ²	1,018 in ⁴	169.7 in ³	1.75 in	n/a	3.5 in		

Definitions used in the table above are explained below:

OD	section diameter	
A	section area	$A = \pi \times OD^2 / 4$
I	section moment of inertia	$I = \pi \times OD^4 / 64$
S	section modulus	$S = I \times 2 / OD$

In order to illustrate the calculation method, DW + 1g axial load case, calculated at Section 2-2 of upper trunnion (UT) is detailed below. The load for this case consists of the axial force $F_L = 0$ kips (axial load per upper trunnion) because of the sliding trunnion support, the tangential force $F_T = 71$ kips (deadweight) and the bending moment caused by the tangential force. (Radial load F_R for this case is zero, $F_R = 0$).

The acting moment arm of deadweight is $L_{SKID} = 1.88$ inches, therefore the moment induced by this force is

$$F_T \times L_{SKID} = 71 \times 1.88 = 133.5 \text{ in.-kips}$$

The total shear force acting on section 2-2 is

$$F_v = (F_L^2 + F_T^2)^{0.5} = (0^2 + 71^2)^{0.5} = 71 \text{ kips}$$

The total moment at section 2-2 is

$$M_B = (M_L^2 + M_T^2)^{0.5} = (0^2 + 133.5^2)^{0.5} = 133.5 \text{ in.-kips}$$

The maximum shear stress for a solid circular section is $4/3 \times (\text{Shear Force})/(\text{Section Area})$ (Reference [[4]], page 129). The area of section 2-2 is $A = 113.1 \text{ in}^2$, so the maximum shear stress at section 2-2 is

$$S_v = 4 \times F_v / (A \times 3) = 4 \times 71 / (113.1 \times 3) = 0.837 \text{ ksi}$$

The maximum bending stress is calculated as $S_B = (\text{Total Acting Moment})/(\text{Section Modulus})$. The section modulus of section 2-2 is $S = 169.7 \text{ in}^3$. The resulting bending stress is then

$$S_B = M_B / S = 133.5 / 169.7 = 0.787 \text{ ksi}$$

Maximum normal stress for section 2-2 is calculated as

$$S_R = S_B + F_R / A = 0.787 + 0.0 / 113.1 = 0.787 \text{ ksi}$$

Maximum combined shear stress is calculated as

$$S_v^{\max} = ((S_R/2)^2 + S_v^2)^{0.5} = ((0.787 / 2)^2 + 0.837^2)^{0.5} = 0.925 \text{ ksi}$$

Maximum tensile stress is calculated as

$$S_{\max} = S_B/2 + S_v^{\max} = 0.787 / 2 + 0.925 = 1.319 \text{ ksi}$$

Finally, membrane stress intensity P_M and membrane plus bending stress intensity $P_M + P_B$ are calculated respectively as:

$$P_M = ((F_R/A)^2 + 4 \times S_v^2)^{0.5} = ((0.0 / 113.1)^2 + 4 \times (0.837)^2)^{0.5} = 1.674 \text{ ksi}$$

$$P_M + P_B = 2 \times S_v^{\max} = 2 \times 0.925 = 1.850 \text{ ksi}$$

A.3.9.5.7 Summary of Computed Stresses

The calculated maximum trunnion stresses are summarized in Table A.3.9.5-1 and compared with their corresponding allowable stresses.

A.3.9.5.8 Conclusions

Table A.3.9.5-1 shows that all calculated trunnion stresses are less than their corresponding allowable stresses. Therefore, the NUHOMS® OS187H Type 1 TC trunnions are structurally adequate to withstand loads during lifting and transfer operations.

A.3.9.5.9 References

- [1] "Special Lifting Devices for Shipping Containers Weighing 10,000 Pounds or More," ANSI N14.6, 1993.
- [2] American Society of Mechanical Engineers, ASME Boiler and Pressure Vessel Code, Section II, Part D, 1998, through 2000 addenda.
- [3] American Society of Mechanical Engineers, ASME Boiler and Pressure Vessel Code, Section III, Division 1, Subsection NC, 1998, through 2000 addenda.
- [4] Warren C. Young, Richard G. Budynas, "Roark's Formulas for Stress and Strain," Seventh Edition, 2002, McGraw-Hill.

Table A.3.9.5– 1 Summary of Computed and Allowable Trunnion Stresses

Upper Trunnions					
Load type	Load combination	Maximum Stress [ksi]		Allowable (ksi)	Stress ratio
		Type	Magnitude		
Lifting loads	Critical lift	Combined shear	26.81	43.3	0.62
		Max tensile	40.79	43.3	0.94
Handling loads	DW+1g axial	PM	1.67	31.4	0.05
		PM+PB	1.85	47.1	0.04
	DW+1g transverse	PM	1.67	31.4	0.05
		PM+PB	1.93	47.1	0.04
	DW+1g vertical	PM	3.35	31.4	0.11
		PM+PB	3.70	47.1	0.08
	1/2g axial + 1/2g transverse + 1/2g vertical + DW	PM	2.51	31.4	0.08
		PM+PB	2.78	47.1	0.06
Lower Trunnions					
Load type	Load combination	Maximum stress [ksi]		Allowable (ksi)	Stress ratio
		Type	Magnitude		
Lifting loads	Critical lift	PM	3.39	22.5	0.15
		PM+PB	4.69	33.8	0.14
Handling loads	DW+1g axial	PM	3.21	22.5	0.14
		PM+PB	4.44	33.8	0.13
	DW+1g transverse	PM	1.27	22.5	0.06
		PM+PB	2.34	33.8	0.07
	DW+1g vertical	PM	2.55	22.5	0.11
		PM+PB	3.52	33.8	0.10
	1/2g axial + 1/2g transverse + 1/2g vertical + DW	PM	2.41	22.5	0.11
		PM+PB	3.62	33.8	0.11

**Figure Withheld
under 10 CFR 2.390**

Figure A.3.9.5– 1 Upper trunnion, general arrangement

**Figure Withheld
under 10 CFR 2.390**

Figure A.3.9.5– 2 Lower trunnion, general arrangement

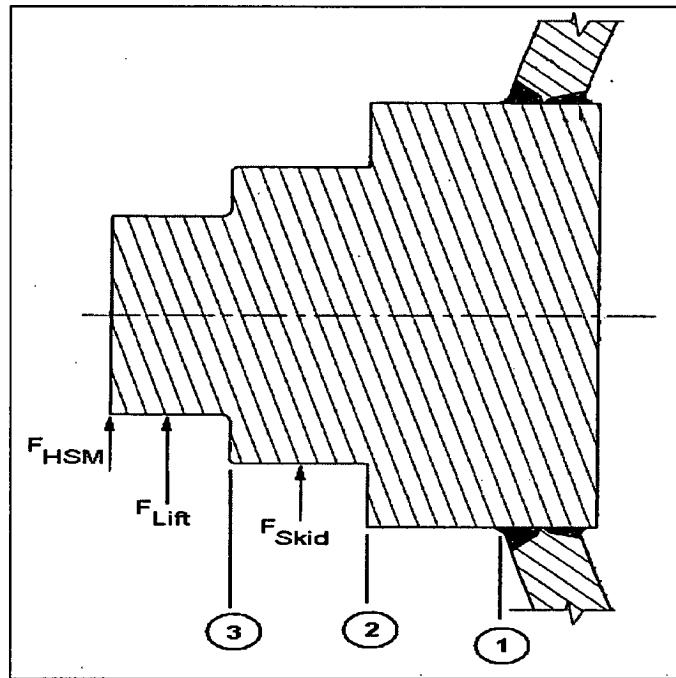


Figure A.3.9.5- 3 Loads and stress sections at upper trunnion

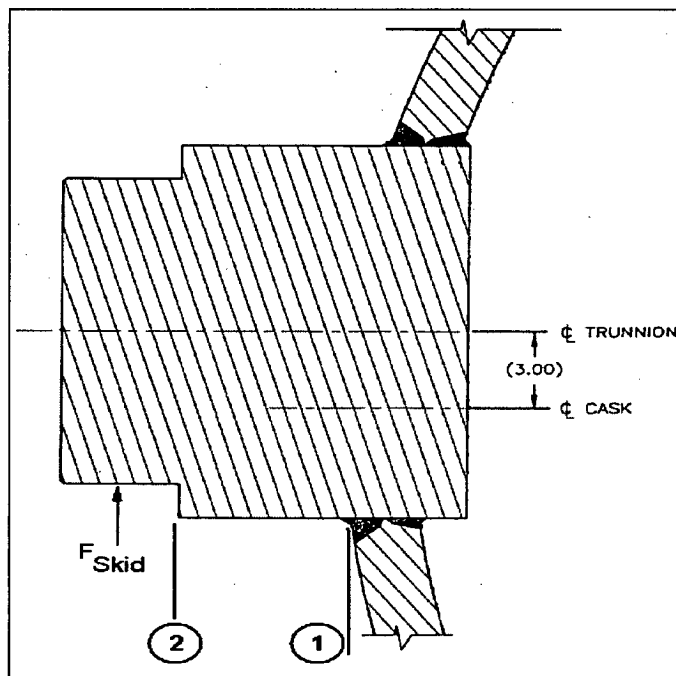


Figure A.3.9.5- 4 Loads and stress sections at lower trunnion

Appendix A.3.9.6
OS187H TYPE 1 Transfer Cask Shield Panel Structural Analysis

TABLE OF CONTENTS

A.3.9.6 OS187H TYPE 1 TRANSFER CASK SHIELD PANEL STRUCTURAL ANALYSIS A.3.9.6-1

A.3.9.6.1 Introduction..... A.3.9.6-1

A.3.9.6.2 Material Properties..... A.3.9.6-2

A.3.9.6.3 Component Weights..... A.3.9.6-3

A.3.9.6.4 Stress Criteria..... A.3.9.6-4

A.3.9.6.5 Load Cases..... A.3.9.6-5

A.3.9.6.6 Stress Calculations..... A.3.9.6-6

 A.3.9.6.6.1 3 g Lifting Load Case A.3.9.6-6

 A.3.9.6.6.2 Transfer Load Condition..... A.3.9.6-6

 A.3.9.6.6.3 Thermal Analyses A.3.9.6-7

 A.3.9.6.6.4 Thermal Stress Analyses..... A.3.9.6-7

 A.3.9.6.6.5 Weld Stresses..... A.3.9.6-7

A.3.9.6.7 Conclusions..... A.3.9.6-8

A.3.9.6.8 References..... A.3.9.6-9

LIST OF TABLES

Table A.3.9.6– 1 Summary of Calculated and Allowable Neutron Shield Shell Stresses.....	A.3.9.6-10
Table A.3.9.6– 2 Summary of Weld Stresses (3 g Lifting)	A.3.9.6-10
Table A.3.9.6– 3 Summary of Weld Stresses (Transfer Load).....	A.3.9.6-11

LIST OF FIGURES

Figure A.3.9.6– 1 Neutron Shield Shell Finite Element Model.....	A.3.9.6-12
Figure A.3.9.6– 2 Neutron Shield Shell Finite Element Model, Top Plate Region.....	A.3.9.6-13
Figure A.3.9.6– 3 Neutron Shield Shell Finite Element Model, Bottom Plate Region	A.3.9.6-14
Figure A.3.9.6– 4 Neutron Shield Shell Finite Element Model, 3 g Lifting Loads.....	A.3.9.6-15
Figure A.3.9.6– 5 3 g Lifting Stress Intensity Distribution	A.3.9.6-16
Figure A.3.9.6– 6 Neutron Shield Shell Finite Element Model, Transfer Loads	A.3.9.6-17
Figure A.3.9.6– 7 Transfer Loads Stress Intensity Distribution	A.3.9.6-18
Figure A.3.9.6– 8 Cold Ambient Environment Temperature Distribution.....	A.3.9.6-19
Figure A.3.9.6– 9 Hot Ambient Environment Temperature Distribution.....	A.3.9.6-20
Figure A.3.9.6– 10 Transfer Loads plus Cold Ambient Condition Stress Intensity Distribution	A.3.9.6-21
Figure A.3.9.6– 11 Transfer Loads plus Hot Ambient Condition Stress Intensity Distribution	A.3.9.6-22

A.3.9.6 OS187H TYPE 1 TRANSFER CASK SHIELD PANEL STRUCTURAL ANALYSIS

A.3.9.6.1 Introduction

The purpose of this appendix is to present the evaluation of the stresses in the NUHOMS® OS187H Type 1 transfer cask (TC) neutron shield shell assembly due to all applied loads during fuel loading and transfer operations.

A finite element model of the neutron shield shell assembly was built for the structural analysis. The model includes the outer neutron shield panel, the top and bottom support ring plates, the shield panel stiffener plates, and the structural shell. These components were modeled with the ANSYS 2D Structural Solid PLANE42 elements with axisymmetric option. Double nodes were created at all weld locations. These nodes were coupled in x and y directions to simulate the weld effect. Figures A.3.9.6-1, A.3.9.6-2 and A.3.9.6-3 show the overall finite element model and its details. The same finite element model is used for all loading conditions.

A.3.9.6.2 Material Properties

The TC neutron shield shell is assumed to be at a 300 °F uniform temperature during transfer operations. This assumption is based on the thermal evaluations performed in Chapter 4. Material allowables are conservatively taken at 350 °F.

All shell components are constructed from stainless steel SA-240, Grade 304. The following mechanical and thermal material properties taken from Reference 1 are used in the analysis:

Material	Temp. °F	S _u (ksi)	S _y (ksi)	S _m (ksi)	E (10 ⁶ psi)	α (10 ⁻⁶) (in/in/°F)	Conductivity (Btu/hr-in-°F)	Density (lb/in ³)
SA-240 Stainless Steel 304	70	75.0	30.0	20.0	28.3	8.5	0.7217	0.29
	200	71.0	25.0	20.0	27.6	8.9	0.775	0.29
	300	66.2	22.4	20.0	27.0	9.2	0.8167	0.29
	400	64.0	20.7	18.7	26.5	9.5	0.8667	0.29

A.3.9.6.3 Component Weights

The weight of the NUHOMS® OS187H Type 1 TC neutron shield shell, including the cylindrical shell, the top and bottom support rings, and the 16 central support rings is 5,134 lb. The weight of the neutron shield shell water is 8,671 lb (the transfer component weights are tabulated in Section A.3.2). However, for conservatism, a bounding weight of 8,900 lb. is used for the weight of water in this analysis.

For the TC in the vertical orientation, the inertial force due to water weight is applied as pressure in the following way.

The weight of the neutron shield water, W is 8,900 lb. The maximum hydrostatic pressure at the bottom of the neutron shield shell, W_h , is,

$$W_h = 62.4 \text{ lb/ft}^3 \times 190.1 \text{ in} / 12^3 = 6.86 \text{ psi}$$

This hydrostatic pressure is uniformly applied to the entire internal region of the neutron shield.

In addition to the water weight pressure, an additional internal uniform pressure of 45 psig is used in all load cases.

A.3.9.6.4 Stress Criteria

All load cases are analyzed and results evaluated to the requirements of ASME Code, Subsection NC [2] as normal condition (Level A) load cases. According to Reference 2, the maximum allowable membrane (P_m) and membrane plus bending ($P_m + P_b$) stress intensities for normal conditions are S_m and $1.5 S_m$, respectively. Also, average pure shear is limited to $0.6 S_m$. The maximum primary plus secondary stress is limited to $3.0 S_m$.

The components of the neutron shield shell assembly are constructed from SA-240, Type 304 stainless steel. Therefore, the maximum allowable membrane and membrane plus bending stress intensities (conservatively taken at 350 °F) are as follows:

Stress Category	Stress Criteria	Maximum Allowable Stress
P_m	S_m	19.35 ksi
$P_m + P_b$	$1.5 S_m$	29.03 ksi
$P_m + P_b + Q$	$3.0 S_m$	58.05 ksi
Pure Shear	$0.6 S_m$	11.61 ksi

A.3.9.6.5 Load Cases

The following load cases are considered. When transferring the loaded cask to the ISFSI, the transfer loads are 1 g axial, 1 g transverse, and 1 g vertical. For conservatism, a bounding 2 g axial + 2 g transverse + 2 g vertical is used for stress calculations.

Load Case	Applied Load
3 g Lifting (cask vertical)	45 psi pressure + hydrostatic pressure + 3 g longitudinal
Transfer loads (cask horizontal)	45 psi pressure + water pressure + 2 g longitudinal + 2 g vertical + 2 g transverse + dead weight 45 psi pressure + water pressure + 2 g longitudinal + 2 g vertical + 2 g transverse + cold thermal + dead weight 45 psi pressure + water pressure + 2 g longitudinal + 2 g vertical + 2 g transverse + hot thermal + dead weight

A.3.9.6.6 Stress Calculations

A.3.9.6.6.1 3 g Lifting Load Case

The pressure at the bottom plate due to the 3 g lifting load for water = $3 \times 6.86 = 20.58$ psi (use 21 psi).

The ANSYS elastic stress run is made by applying a 45 psi internal pressure and a 21 psi hydrostatic pressure. The loading applied to the model is shown in Figure A.3.9.6-4. A 3 g vertical acceleration is applied to account for the inertia loads. As shown in Figure A.3.9.6-4, an internal pressure of 66.0 psi (45 psi + 21 psi) is uniformly applied to the entire internal region of the neutron shield.

The resulting stress intensity distribution in the various shell components is shown in Figure A.3.9.6-5. It is seen that the maximum nodal stress intensity in the shell model is 28,058 psi. This maximum stress occurs near the weld between the center support ring and the neutron shield panel. In the stress evaluation, nodal stresses corresponding to the centerline nodes (through the component's plate thicknesses) are considered membrane stresses. Conservatively, membrane plus bending stresses are taken as the maximum stress at any node in the various structural components. These stresses are presented in Table A.3.9.6-1.

A.3.9.6.6.2 Transfer Load Condition

During transfer operations, the cask is in the horizontal position and the neutron shield shell is subjected to 45 psi internal pressure, transfer handling loads (2 g vertical + 2 g lateral + 2 g axial) and dead weight.

The vertical and lateral loads are combined in the following way.

$$g_{\text{transverse}} = (3.0^2 + 2.0^2)^{1/2} = 3.61 \text{ g}$$

The stress due to the 3.61 g inertia load conservatively assumes that the weight of the shell structure (5,134 lb.) and water (8,900 lb.) are uniformly distributed only over the 190.1 inch length and a 60° arc. Therefore, the equivalent pressure applied to the outer shell is,

$$p_{vl} = [(5,134 + 8,900) \times 3.61] / [2 \pi (45.87)(190.1) \times (60^\circ/360^\circ)] = 5.55 \text{ psi}$$

Again, the 5.55 psi load on the 60° sector is conservatively assumed to act on the full 360°. This pressure is added to 45 psi pressure and applied to the shield shell.

For 2 g axial acceleration, the pressure due to the water inertial load on the top plate is,

$$p_a = 8,900 \times 2.0 / [\pi \times (45.87^2 - 40.935^2)] = 13.23 \text{ psi}$$

Therefore, a pressure of 58.23 psi (45 + 13.23) is applied to the top plate. Also, there is a 45 psi pressure applied to the bottom plate.

An ANSYS elastic stress run is made by applying the above calculated pressures to the finite element model. The loading is shown in Figure A.3.9.6-6. The resulting stress intensity distribution is shown in Figure A.3.9.6-7. It is seen that the maximum nodal stress intensity in the shell model is 21,458 psi. This maximum stress occurs in the outer shell near the bottom plate weld. Nodal stresses at the middle thickness (considered P_m) and the maximum stresses (considered $P_m + P_b$) are summarized and evaluated in Table A.3.9.6-1.

A.3.9.6.6.3 Thermal Analyses

The thermal analysis of the neutron shield shell assembly model is conducted for both cold and hot environmental conditions. Steady-state ANSYS thermal analyses of the model are conducted to obtain the nodal temperature distribution in the structural model by mapping the temperatures from the thermal heat transfer analysis model as the boundary conditions for both cold and hot conditions. The mapped temperature distribution bounds that resulting from the Chapter 4 thermal analysis. Two-dimensional thermal elements (PLANE55) are used in the analyses. Temperature dependent thermal material properties are also used in the analysis.

The resulting temperature distributions for cold and hot ambient cases are shown in Figures A.3.9.6-8 and A.3.9.6-9, respectively.

A.3.9.6.6.4 Thermal Stress Analyses

Elastic stress analyses of the neutron shield shell structure are conducted in order to evaluate the transfer plus thermal loads. The transfer condition loading as shown in Figure A.3.9.6-6 and the nodal temperature distribution from the above thermal analyses results are combined and applied to the stress model to obtain the transfer plus thermal stresses in the model.

The nodal stress intensity distribution is shown in Figure A.3.9.6-10 for the cold condition analysis case and in Figure A.3.9.6-11 for the 115 °F hot ambient condition case. The critical stress intensities (considered $P_m + P_b + Q$ stresses) are summarized in Table A.3.9.6-1.

It is seen from Figure A.3.9.6-10 and Figure A.3.9.6-11 that the maximum thermal stress intensities are generated in the cold ambient case. The maximum nodal stress intensity in the neutron shield shell assembly model is 26,805 psi. This maximum stress occurs in the outer shell near the bottom support ring plate weld. Cold and hot nodal stresses maximum stresses are summarized and evaluated in Table A.3.9.6-1.

A.3.9.6.6.5 Weld Stresses

Per Section A.3.9.6.4, the pure shear allowable stress in the fillet and plug welds is 0.6 times the base material allowable membrane stress. The analysis utilizes an axisymmetric model for which loads and force results are applied on a 360-degree basis, the weld stress is based on the total area of the weld around the circumference of the structure. The weld stresses are summarized in Table A.3.9.6-2 for the 3 g lifting load case and Table A.3.9.6-3 for the transfer load cases.

A.3.9.6.7 Conclusions

Based on the results of the analyses, it is concluded that the outer shell structure is structurally adequate for the specified lifting and transfer loads.

A.3.9.6.8 References

- [1] American Society of Mechanical Engineers, ASME Boiler and Pressure Vessel Code, Section II, Part D, 1998, including 2000 addenda.
- [2] American Society of Mechanical Engineers, ASME Boiler and Pressure Vessel Code, Section III, Division 1, Subsection NC, 1998, including 2000 addenda.

Table A.3.9.6– 1 Summary of Calculated and Allowable Neutron Shield Shell Stresses

Load Case	Stress Category	Maximum Stress (ksi)	Allowable Stress (ksi)
3 g lifting	P_m	17.73	19.35
	$P_m + P_b$	28.06	29.02
Transfer load	P_m	13.64	19.35
	$P_m + P_b$	21.46	29.02
	$P_m + P_b + Q$ (Cold)	26.81	58.05
	$P_m + P_b + Q$ (Hot)	24.78	58.05

Table A.3.9.6– 2 Summary of Weld Stresses (3 g Lifting)

Stress	Weld Locations				
	Top and Bottom Support Rings, Structural Shell	Central Support Rings, Structural Shell	Central Support Rings, T Section	Neutron Shield Shell Plug Welds	Neutron Shield Shell, Top and Bottom Rings
Max. shear (S) [kips]	41.85	32.92	19.74	2.6	97.6
Max. tension (T)[kips]	265.76	74.89	68.07	72.36	17.3
Weld area (A) [in ²]	56.8	11.4	7.58	4.5	38.3
Tensile stress (S1=T/A) [ksi]	4.68	6.57	8.98	16.08	0.45
Shear stress (S2=S/A) [ksi]	0.74	2.89	2.60	0.58	2.55
Max. stress intensity (S=(S1 ² +4S2 ²) ^{1/2}) [ksi]	4.91	8.75	10.38	16.12	5.12
Pure shear allowable stress 0.6 S _m (Sa1) [ksi]	11.61	11.61	11.61	11.61	11.61
Weld allowable stress (Sa2) S _m [ksi]	19.35	19.35	19.35	19.35	19.35
Shear stress ratio (S2/Sa1)	0.06	0.25	0.22	0.05	0.22
Stress ratio (S/Sa2)	0.25	0.45	0.54	0.83	0.26

Table A.3.9.6- 3 Summary of Weld Stresses (Transfer Load)

Stress	Weld Location				
	Top and Bottom Support Rings, Structural Shell	Central Support Rings, Structural Shell	Central Support Rings, T Section	Neutron Shield Shell Plug Welds	Neutron Shield Shell, Top and Bottom Rings
Max. shear (S) [kips]	36.92	32.95	1.36	2.71	92.68
Max. tension (T)[kips]	239.56	77.86	73.19	80.69	17.38
Weld area (A) [in ²]	56.8	11.4	7.58	4.5	38.3
Tensile stress (S1=T/A) [ksi]	4.22	6.83	9.66	17.93	0.45
Shear stress (S2=S/A) [ksi]	0.65	2.89	0.18	0.60	2.42
Max. stress intensity ($S=(S1^2+4S2^2)^{1/2}$) [ksi]	4.41	8.95	9.66	17.97	4.86
Pure shear allowable stress $0.6S_m$ (Sa1) [ksi]	11.61	11.61	11.61	11.61	11.61
Weld allowable stress (Sa2) S_m [ksi]	19.35	19.35	19.35	19.35	19.35
Shear stress ratio (S2/Sa1)	0.06	0.25	0.02	0.05	0.21
Stress ratio (S/Sa2)	0.23	0.46	0.50	0.93	0.25

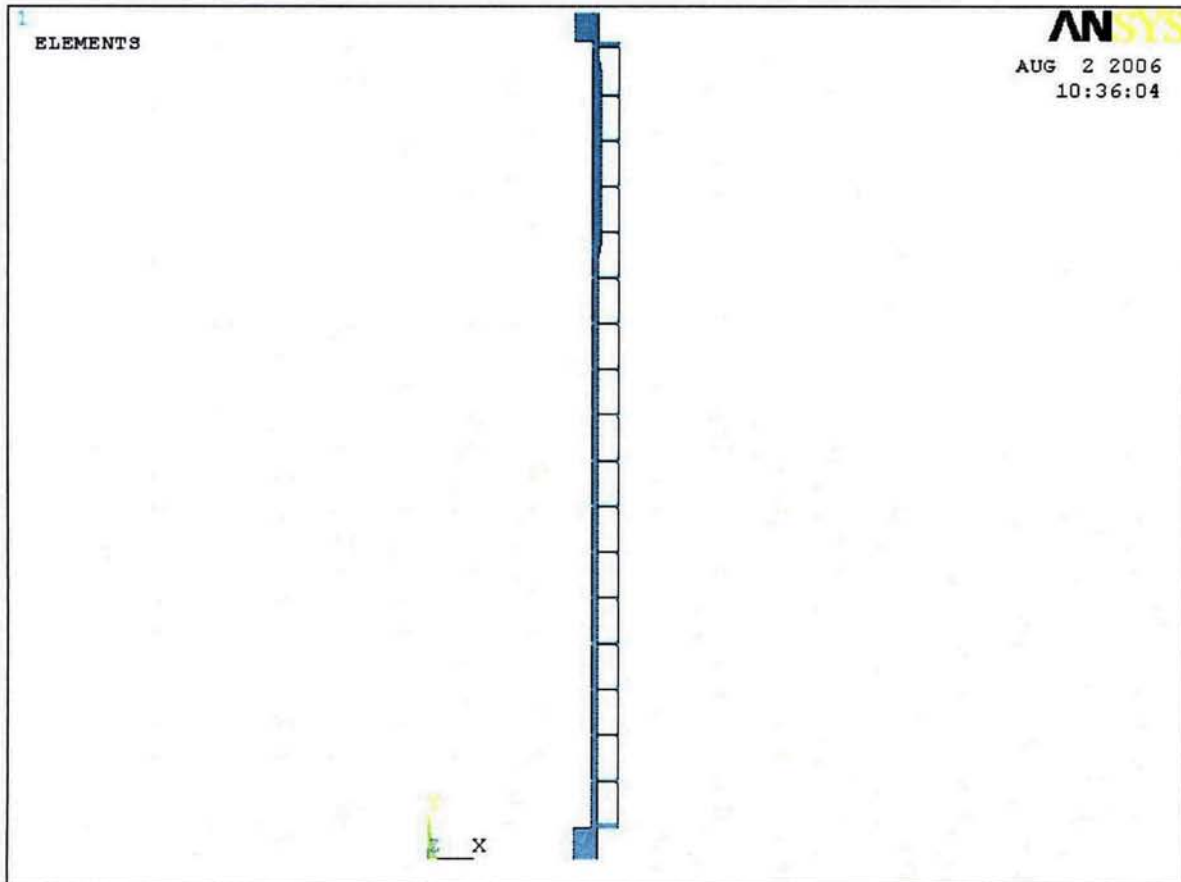


Figure A.3.9.6– 1 Neutron Shield Shell Finite Element Model

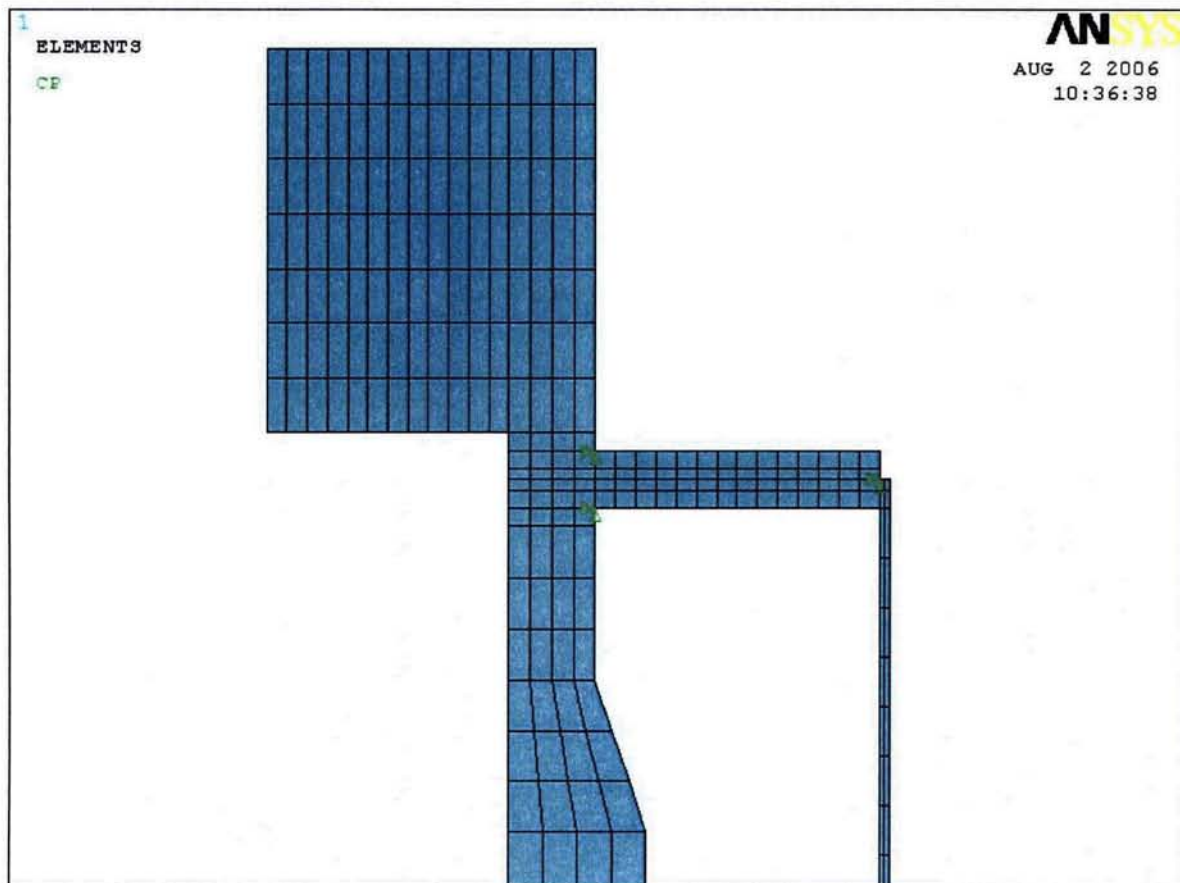


Figure A.3.9.6– 2 Neutron Shield Shell Finite Element Model, Top Plate Region

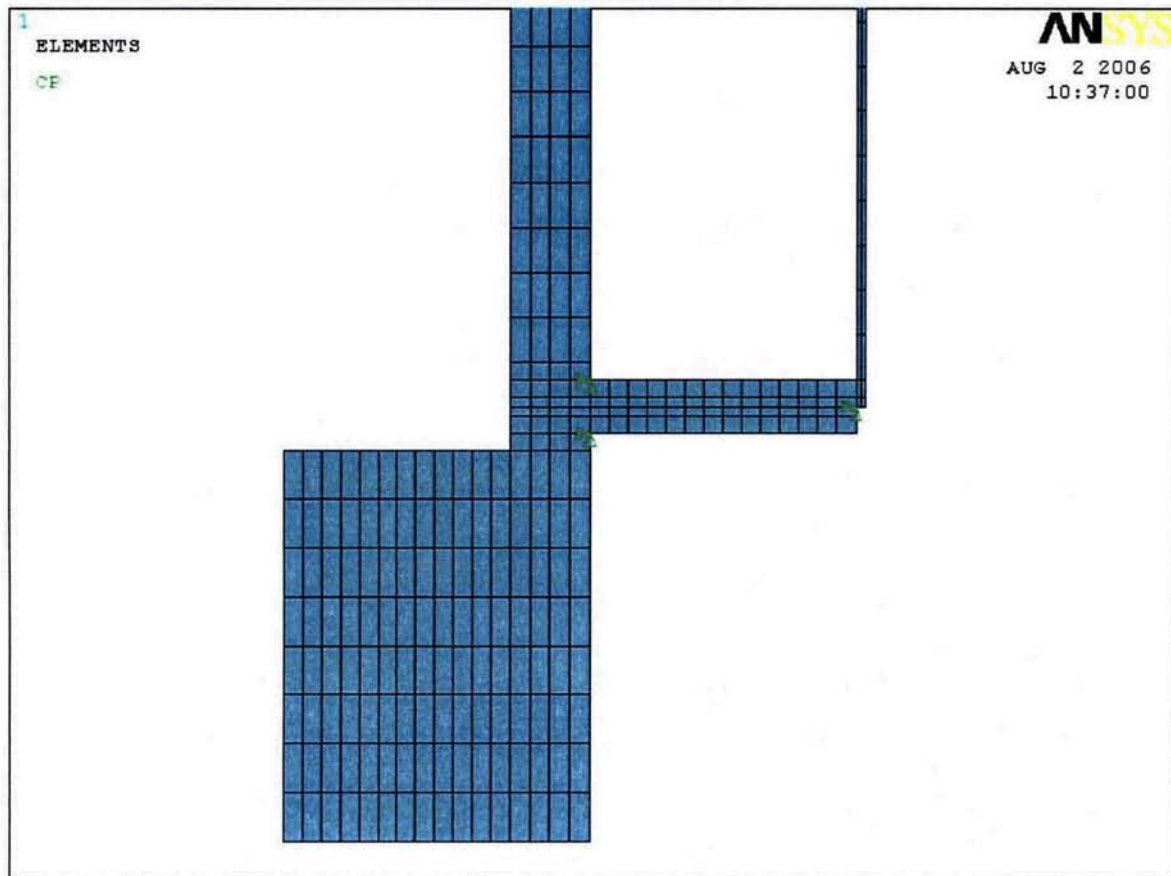


Figure A.3.9.6– 3 Neutron Shield Shell Finite Element Model, Bottom Plate Region

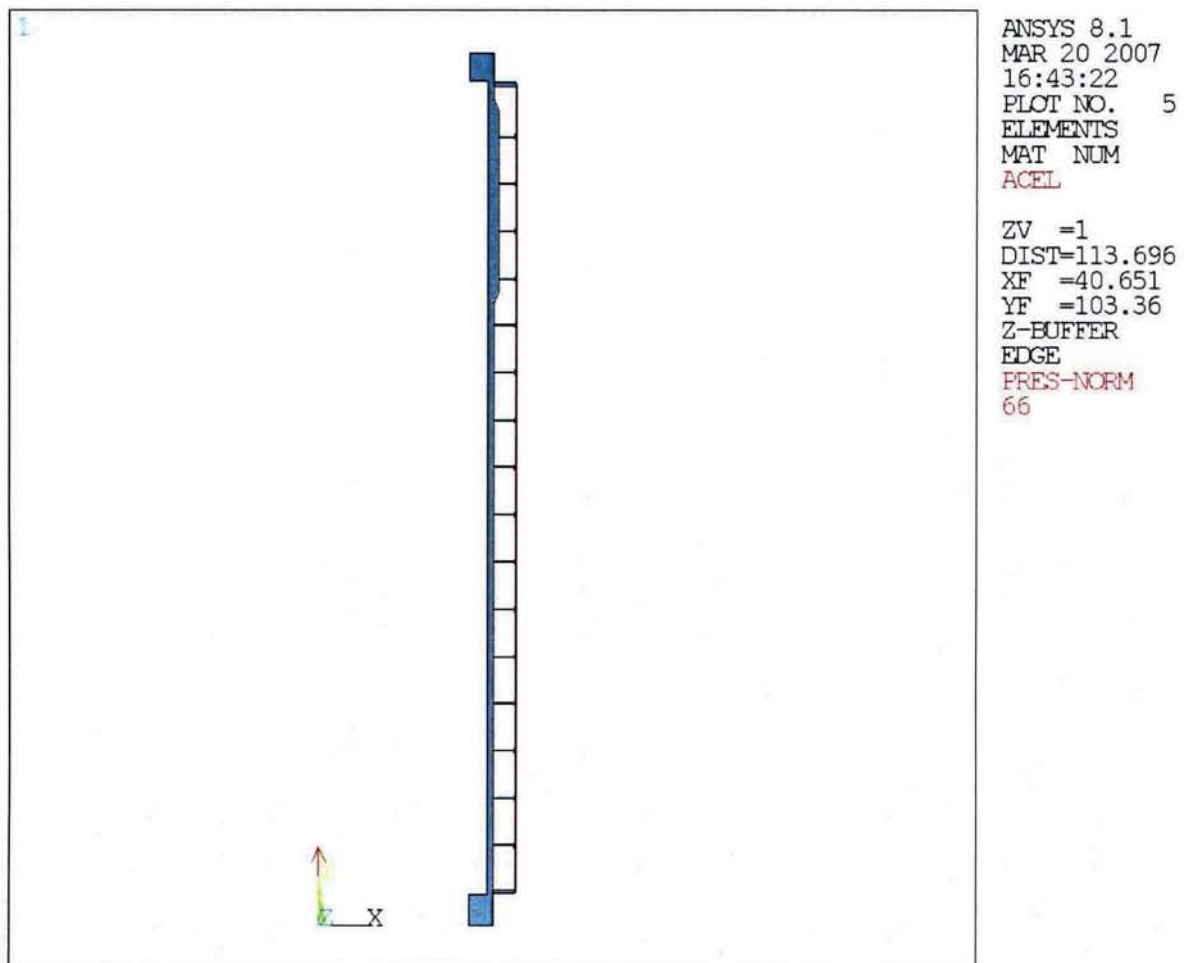


Figure A.3.9.6– 4 Neutron Shield Shell Finite Element Model, 3 g Lifting Loads

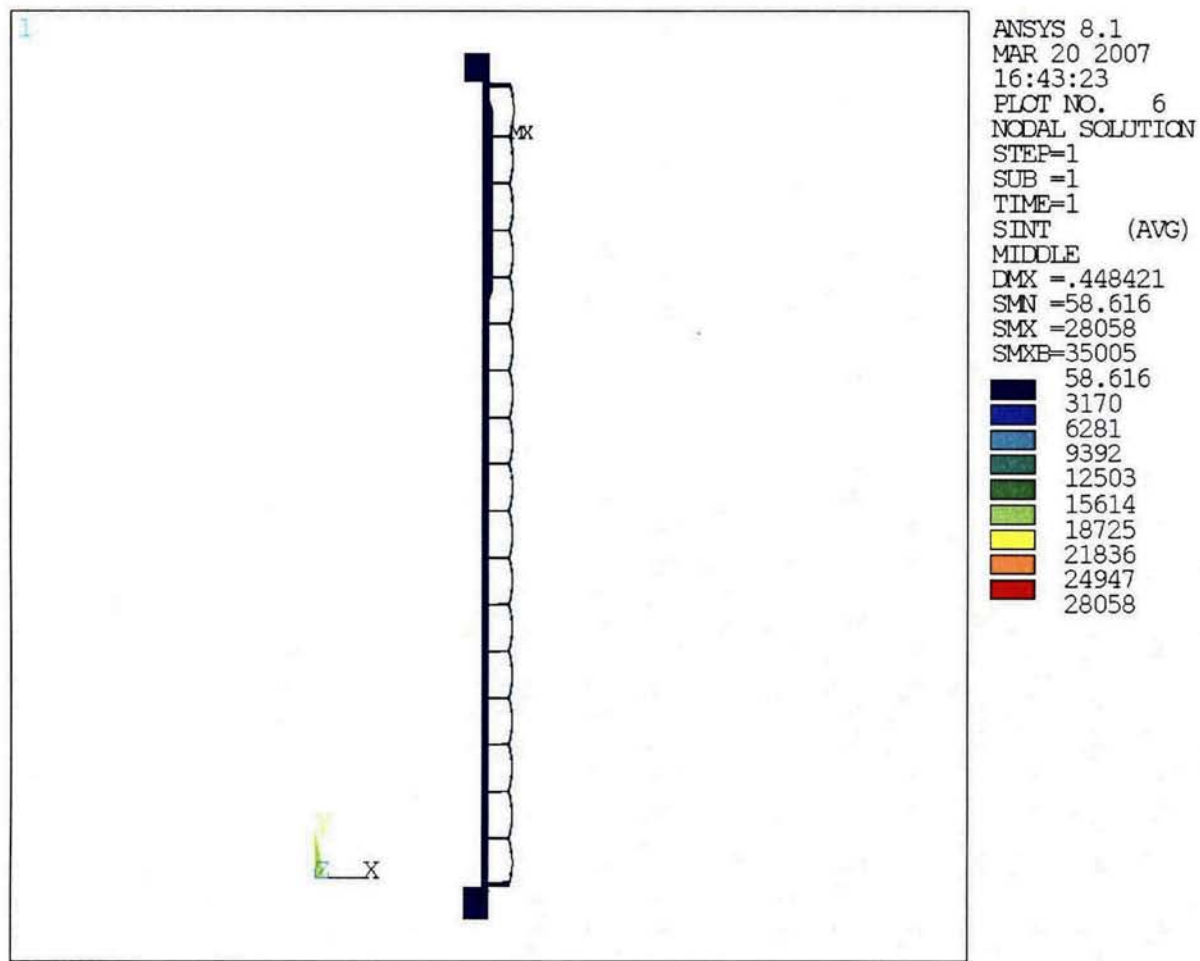


Figure A.3.9.6– 5 3 g Lifting Stress Intensity Distribution

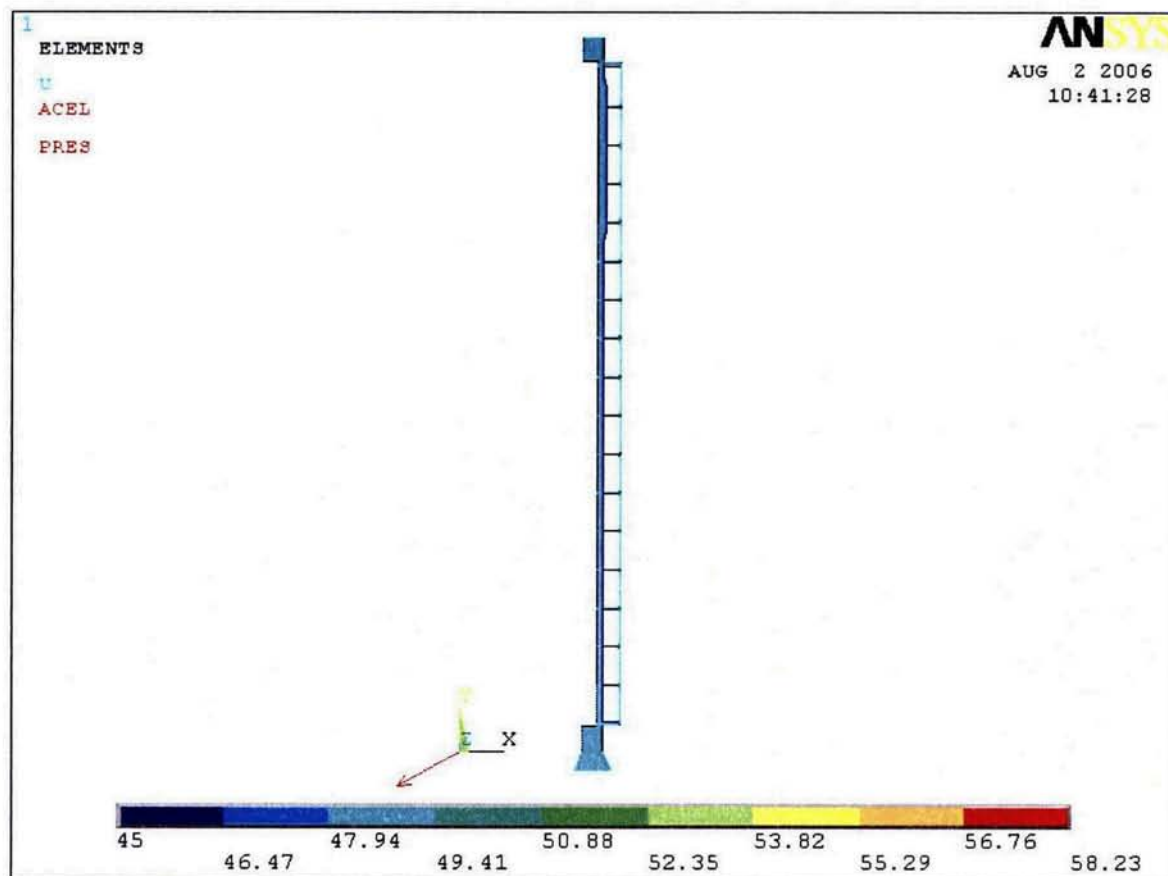


Figure A.3.9.6– 6 Neutron Shield Shell Finite Element Model, Transfer Loads

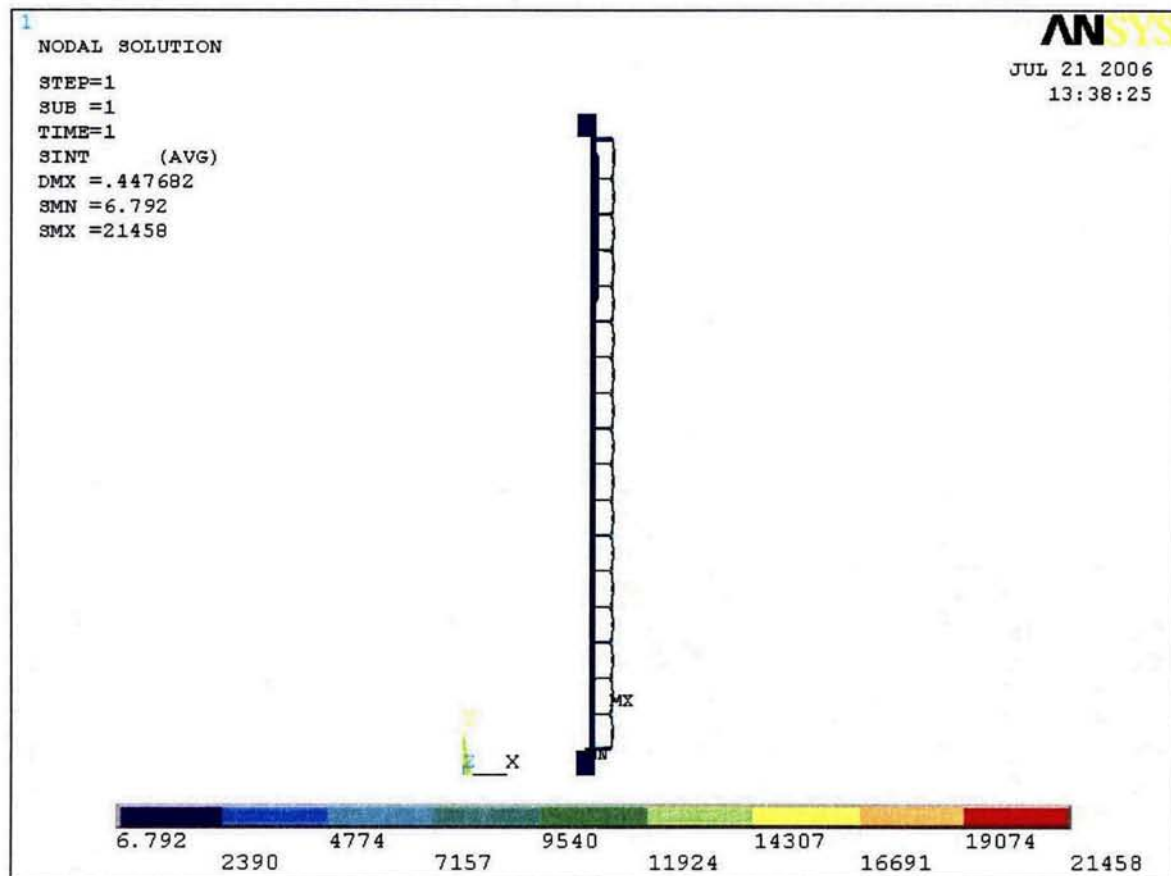


Figure A.3.9.6– 7 Transfer Loads Stress Intensity Distribution

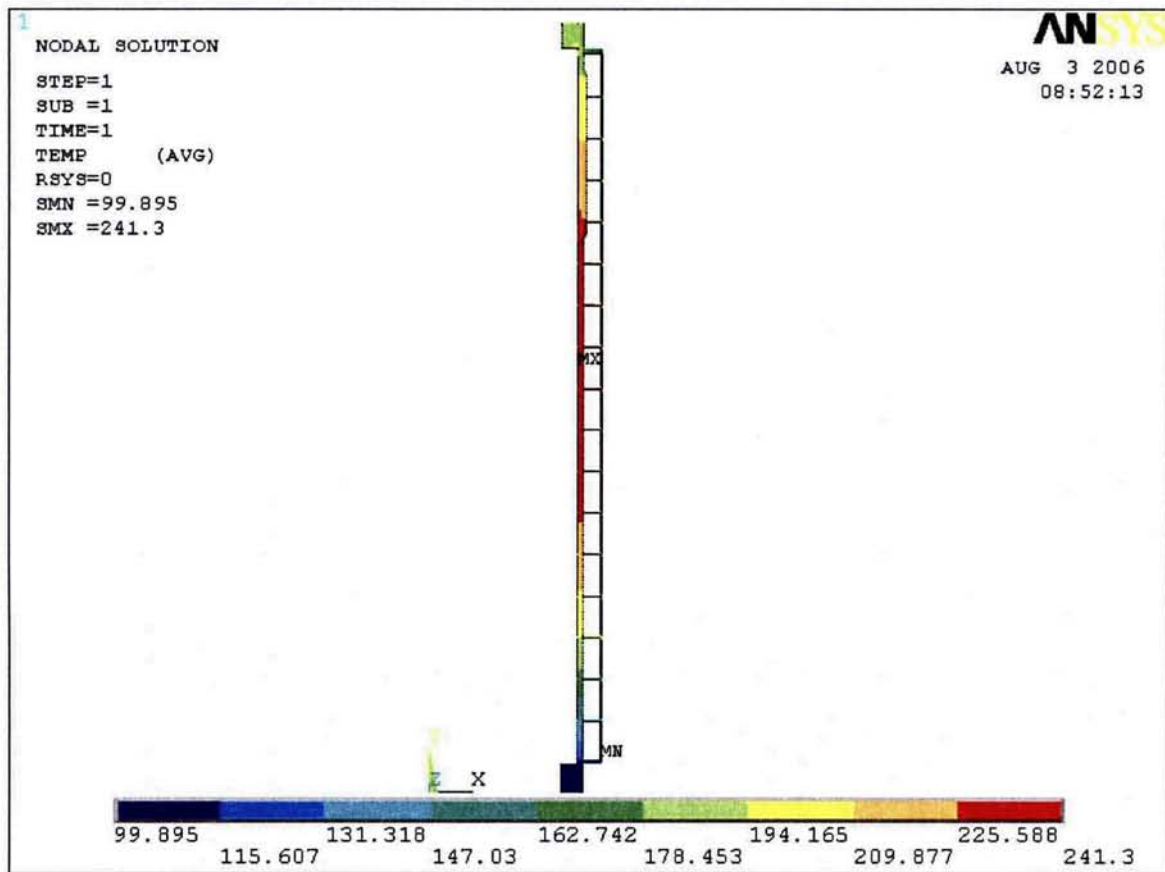


Figure A.3.9.6– 8 Cold Ambient Environment Temperature Distribution

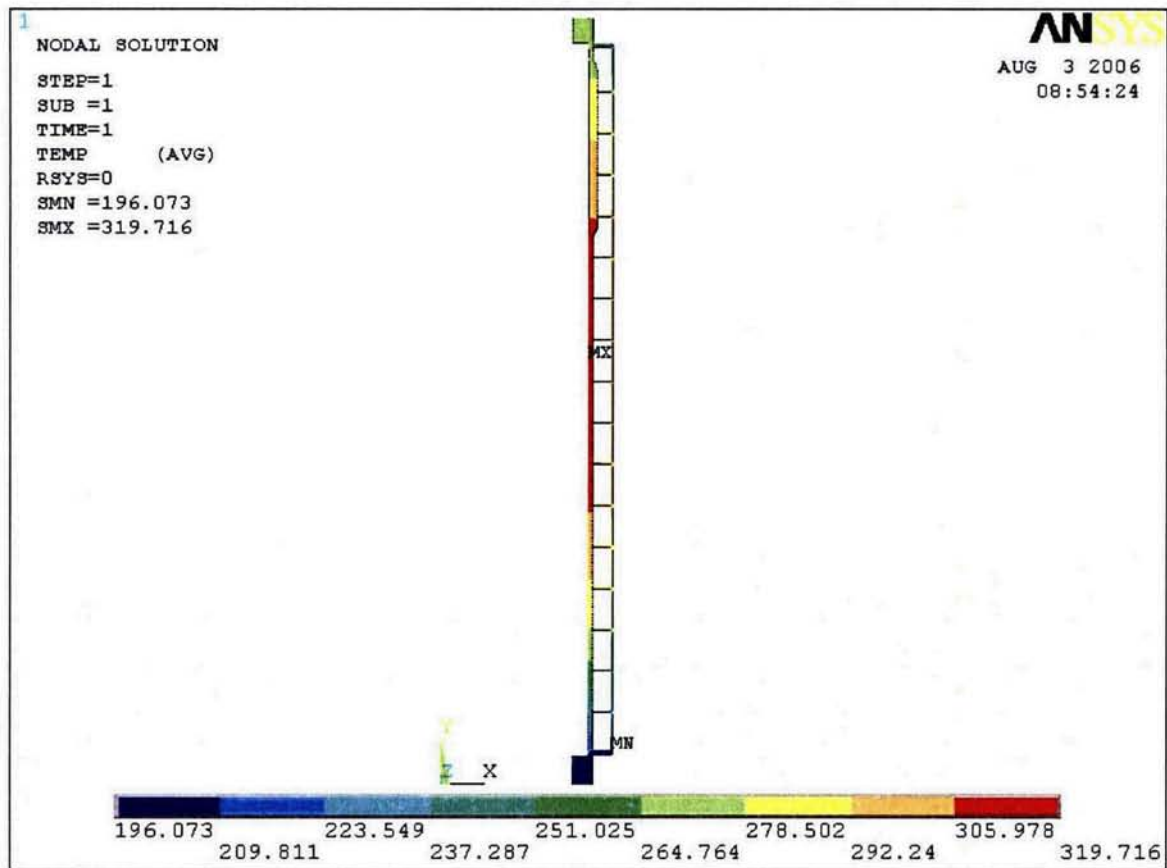


Figure A.3.9.6- 9 Hot Ambient Environment Temperature Distribution

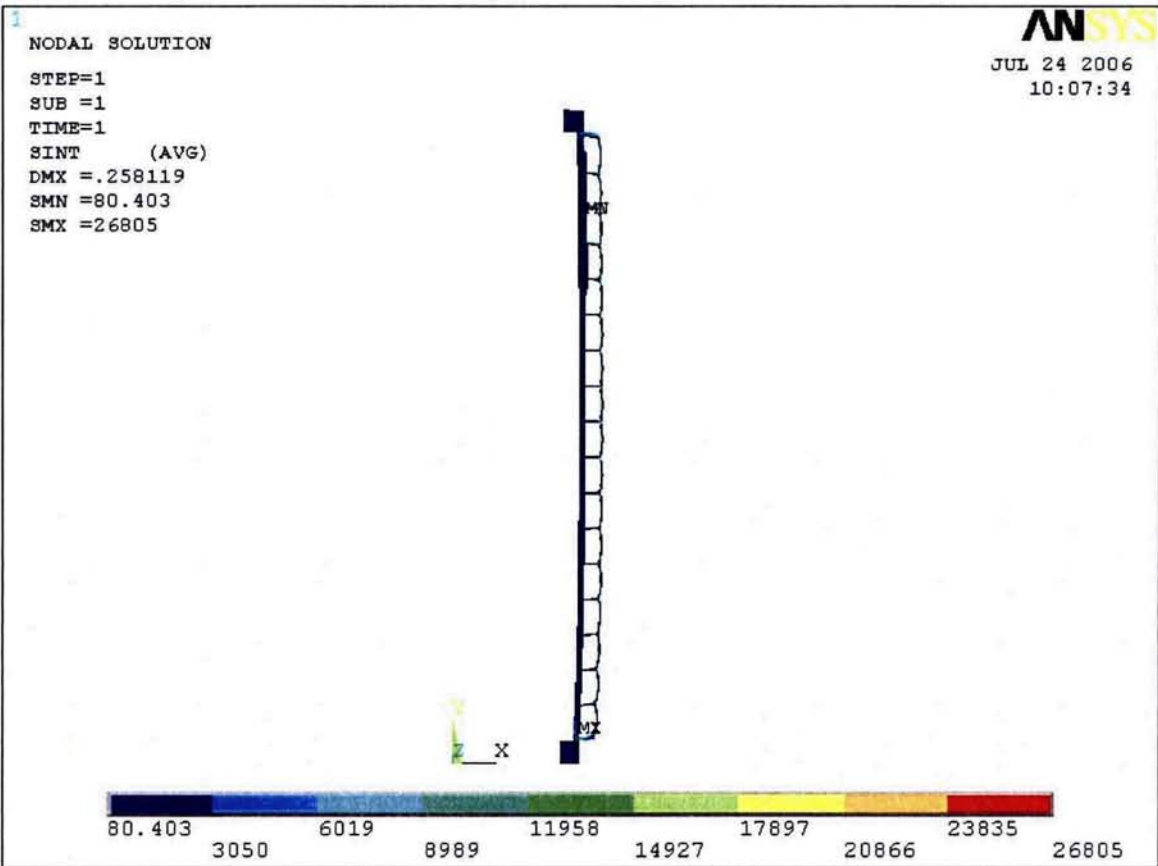


Figure A.3.9.6– 10 Transfer Loads plus Cold Ambient Condition Stress Intensity Distribution

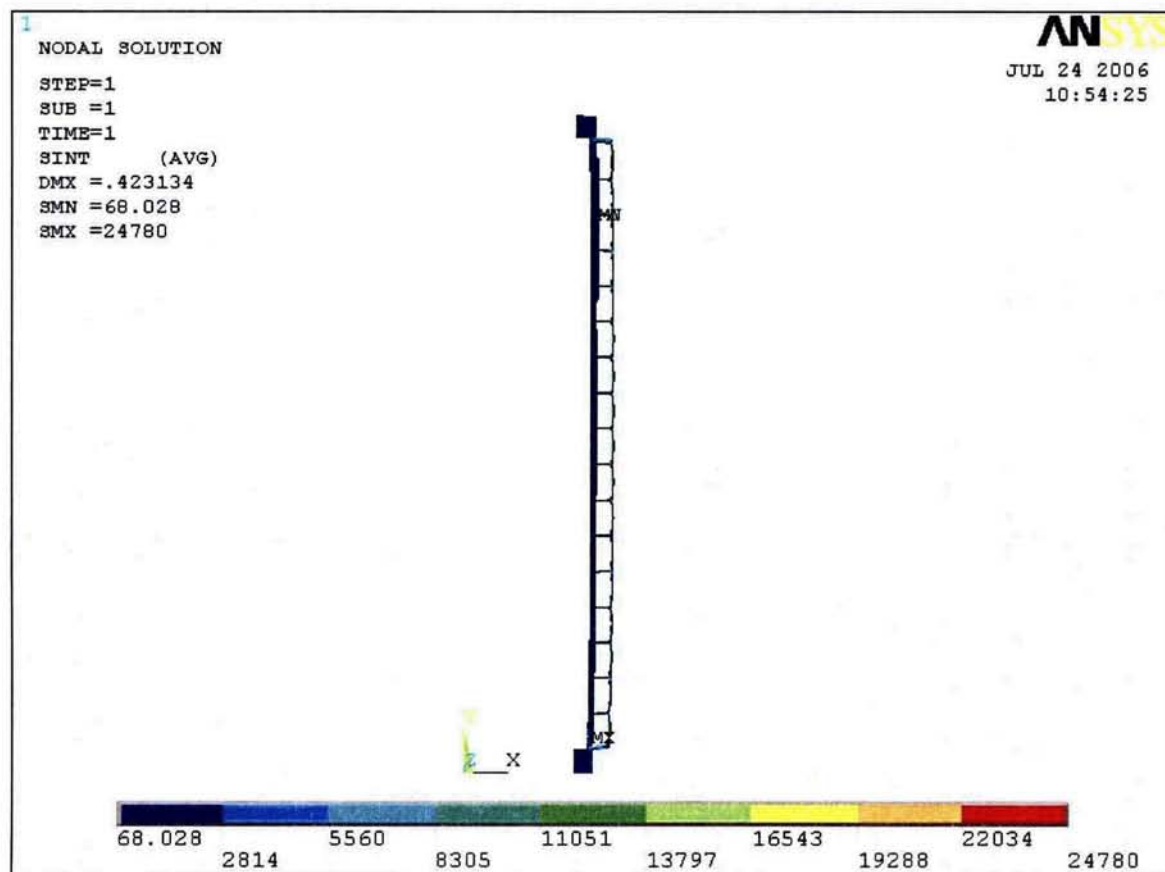


Figure A.3.9.6– 11 Transfer Loads plus Hot Ambient Condition Stress Intensity Distribution

Appendix A.3.9.7

OS187H Type 1 Transfer Cask Impact Analysis

Appendix 3.9.7 describes the evaluations originally performed to substantiate the 75g accident drop decelerations used for the structural evaluation of the NUHOMS® HD System components. During the licensing of the 32PTH System and as part of the RAI process, TN performed an accident drop analysis of the OS187H TC using the LS-DYNA computer code. This LS-DYNA evaluation is documented in Appendix 3.9.10 and forms the basis for the acceleration values used for evaluation of the NUHOMS® HD System components. The justification for applicability of the Appendix 3.9.7 to the 32PTH Type 1 DSC and OS187H Type 1 TC is provided in Appendix A.3.9.10. Therefore, Appendix A.3.9.7 is deleted.

Appendix A.3.9.8

Damaged Fuel Cladding Structural Evaluation

No change. The damaged fuel cladding evaluations documented in Appendix 3.9.8 are applicable without change to the 32PTH Type 1 DSC.

Appendix A.3.9.9 HSM-H Structural Analysis

The structural evaluation of the HSM-H documented in Appendix 3.9.9 remains applicable when the HSM-H is loaded with a 32PTH Type 1 DSC. The HSM-H evaluation in Appendix 3.9.9 is based on a DSC weight of 110 kips which bounds the weight of the loaded 32PTH Type 1 DSC of 108.61 kips. Also, as documented in Chapter 4, the HSM-H design is based on temperature distributions resulting from thermal analysis using a bounding heat load of 40.8 kW which is higher than the 32PTH Type 1 maximum heat load of 34.8 kW. As documented in Chapter A.4, the longer 32PTH Type 1 DSC is not expected to significantly change the HSM-H temperature distributions documented in Chapter 4 for the HSM-H loaded with a 32PTH DSC.

Two minor design modifications are made to the HSM-H to accommodate the 32PTH Type 1 DSC. These consist of a small ($\frac{1}{2}$ ") increase in the length of the support rail structure, and, to accommodate the rail length increase, an alternate design of the DSC stop plate at the rear of the rail support structure is implemented (the 1" thick stiffened canister stop plate assembly is replaced with a single 2" thick plate welded to the top flange of the support rail structure). These design modifications are shown in drawings 10494-72-100-SAR and 10494-72-107-SAR. These modifications do not affect the overall structural qualification of the HSM-H as documented in Appendix 3.9.9. The increased length provides additional bearing area for the support rail structure on its concrete support on the rear wall of the module and, thus, has no effect on the structural qualification of the rail support structure. The alternate DSC stop plate is evaluated using the same loads and allowables as the original stop plate design and is shown to meet the same stress allowable criteria. The maximum bending and shear stresses are on the order of 13.0 ksi and 2.5 ksi, respectively, versus allowable stresses of 18.9 ksi and 12.5 ksi, respectively. The weld between the stop plate and the top flange of the rail is conservatively specified as a full penetration weld.

Therefore, the HSM-H as evaluated in Appendix 3.9.9 with the minor design modifications described above is qualified to store a 32PTH Type 1 DSC.

Appendix A.3.9.10 OS187H Type 1 Transfer Cask Dynamic Impact Analysis

The analysis to determine the rigid body accelerations for the NUHOMS® OS187H transfer cask (TC) documented in Appendix 3.9.10 is applicable to the OS187H Type 1 TC. This is based on the overall similarity of the two transfer cask designs. Both the OS187H and the OS187H Type 1 TCs have similar geometric and mass configuration and are fabricated using the same materials of construction. The OS187H Type 1 has the same diameter, its overall length is approximately 14" longer (210.5" versus 197.07", about a 7% difference) and its maximum weight, including payload, is about 10 kips heavier (239 kips versus 229 kips, about a 4% difference).

Overall, the magnitude of the noted differences is not significant enough to alter appreciably the resulting rigid body accelerations determined from the LS-DYNA analysis documented in Appendix 3.9.10. This is confirmed by energy balance considerations, whereby the increased potential energy resulting from the increased weight of the OS187H Type 1 TC is equated to the strain energy of the TC. Based on these energy balance considerations, it is estimated that the OS187H Type 1 TC drop accelerations would be on the order of 2% to 2.5% higher than the OS187H TC accelerations.

Therefore, the maximum accelerations obtained for the various components of the OS187H TC by the LS-DYNA analysis are conservatively increased by 2.5%. The table below summarizes the OS187H TC and the OS187H Type 1 TC maximum accelerations. These accelerations are well below the acceleration of 75 g used in the accident drop evaluations, and therefore, have no effect on the structural evaluations of the NUHOMS® HD 32PTH Type 1 and OS187H Type 1 components, documented in Chapter A.3, and Appendices A.3.9.1 and A.3.9.2.

Transfer Cask Section	OS187H TC (LS-DYNA) Maximum Accelerations	OS187H Type 1 TC (Estimated) Maximum Accelerations
Lid section	62.9 g	64.5 g
Top trunnion section	55.8 g	57.2 g
Middle section	57.3 g	58.7 g
Bottom trunnion section	46.9 g	48.1 g
Bottom plate section	44.0 g	45.1 g

Appendix A.3.9.11
NUHOMS® 32PTH Type 1 DSC Dynamic Amplification Factor Analysis

TABLE OF CONTENTS

A.3.9.11 NUHOMS® 32PTH TYPE 1 DSC DYNAMIC AMPLIFICATION FACTOR ANALYSISA.3.9.11-1

A.3.9.11.1 Introduction.....A.3.9.11-1

A.3.9.11.2 Side Drop Modal Analysis.....A.3.9.11-2

A.3.9.11.3 Dynamic Load Factor Calculations.....A.3.9.11-3

A.3.9.11.4 Summary of g-Loads for 32PTH Type 1 DSC Impact AnalysesA.3.9.11-4

A.3.9.11.5 References.....A.3.9.11-5

A.3.9.11 NUHOMS® 32PTH TYPE 1 DSC DYNAMIC AMPLIFICATION FACTOR ANALYSIS

A.3.9.11.1 Introduction

This appendix computes the dynamic amplification factor (DAF) to be applied to the response accelerations obtained from the drop accident dynamic analysis of the OS187H Type 1 transfer cask (TC) when applying those accelerations as input to an equivalent static analysis of the 32PTH Type 1 DSC of the same postulated drop accident event.

The DAF is computed for the loaded 32PTH Type 1 DSC in the horizontal orientation. Vertical and corner drop accidents are not credible events since the TC is always in the horizontal configuration.

A.3.9.11.2 Side Drop Modal Analysis*A. Canister Shell*

The fundamental natural frequency of the 32PTH Type 1 DSC shell corresponding to an ovaling (radial-axial) mode is determined assuming the cylindrical shell is simply supported without axial constraint. The natural frequency of the cylindrical shell ovaling mode is given by the following [1, p. 305, Table 12-2, Frame 5]:

$$f_{ij} = \frac{\lambda_{ij}}{2\pi R} \left(\frac{E}{\mu(1-\nu^2)} \right)^{1/2}$$

$$\lambda_{ij} = \frac{\left\{ (1-\nu^2)(j\pi R/L)^4 + (h^2/12R^2) \left[i^2 + (j\pi R/L)^2 \right]^4 \right\}^{1/2}}{(j\pi R/L)^2 + i^2}$$

Where L is taken to be the length between the top and bottom shield plugs, which is roughly 171.63 in, $E = 25.8 \times 10^6$ psi (for SA-240 Type 304 stainless steel at 500 °F [2]), R is the average shell radius, 34.625 in., ν is Poisson's ratio, which is 0.305 for stainless steel [3, page 5-6], $\mu = 0.29/386.4 = 0.000751$ lbm. in⁻³, and thickness $h = 0.5$ in.

For the fundamental mode, $i = 2$ and $j = 1$.

$$\lambda_{ij} = \frac{\left\{ (1-.305^2)(\pi \times 34.625/171.63)^4 + (0.5^2/12 \times 34.625^2) \left[2^2 + (\pi 34.625/171.63)^2 \right]^4 \right\}^{1/2}}{(\pi 34.625/171.63)^2 + 2^2}$$

$$= 0.0888$$

$$f_{21} = \frac{0.0888}{2\pi \times 34.625} \left(\frac{25.8 \times 10^6}{0.000751(1-0.305^2)} \right)^{1/2} = 79.4 \text{ Hz}$$

B. Basket with Fuel Assemblies

The basket for the 32PTH Type 1 DSC is identical to the 32PTH DSC, except that the length of the basket is longer in the 32PTH Type 1 DSC and the fuel tubes at the top of the basket are also connected with crossbars and fusion welds. The length of the 32PTH DSC basket is 162 inches and the length of the 32PTH Type 1 DSC is 169 inches. The weight of the fuel remains the same. As discussed in Appendix A.3.9.1, the axial length of the finite element model of the 32PTH basket assembly is based on a 15 inch segment which corresponds to the pitch of the cross bars where the compartment tubes are welded together. This basket model and analysis results are also applicable to the 32PTH Type 1 basket. Thus, the DAF for the 32PTH DSC basket assembly computed in Appendix 3.9.11 are also applicable to the 32PTH Type 1 basket assembly.

A.3.9.11.3 Dynamic Load Factor Calculations

The natural frequency of the 32PTH Type 1 canister (79.4 Hz) is lower than the 32PTH canister (86.0 Hz) in the horizontal orientation. It is concluded from the results in Section 3.9.11.5 and the amplification factor results for a half sine wave [4, Figure 2.15] that frequencies lower than 86 Hz will result in a lower DAF than 1.03. Thus the DAF calculated for the 32PTH canister side drop bounds the DAF for the 32PTH Type 1 canister.

Since the natural frequencies of the NUHOMS® 32PTH Type 1 basket are the same as the NUHOMS® 32PTH basket, the DAF for the NUHOMS® 32PTH Type 1 will also be the same as the DAF for the NUHOMS® 32PTH basket, which is 1.18.

A.3.9.11.4 Summary of g-Loads for 32PTH Type 1 DSC Impact Analyses

Appendix A.3.9.10 summarizes the maximum g-loads computed for the OS187H Type 1 transfer cask during an 80 inch side drop. A DAF of 1.18 is used to compute g-loads for canister and basket impact loads for side drops. These impact loads are computed in the following table:

Drop Orientation	Acceleration Direction	Maximum Transfer cask g-Load	Maximum DSC g-Load	g-Load Used for Canister and Basket Analyses
Side drop	Transverse	58.73 g ⁽¹⁾	58.73 g x 1.18 = 69.30 g	75 g

Note:

(1) A total of five sections ranging from the lid down to the bottom plate are reported in A.3.9.10. However, only the middle three sections (top trunnion, middle, and bottom trunnion sections) will transmit loads to the canister and basket. Therefore, only the maximum g load in these sections is used to compute the g load seen by the canister and basket.

A.3.9.11.5 References

- [1] Blevins, Formulas for Natural Frequency and Mode Shape, Krieger Publishing Company, 1995.
- [2] American Society of Mechanical Engineers, ASME Boiler and Pressure Vessel Code, Section II, Part D, 1998 through 2000 addenda.
- [3] Baumeister & Marks, Standard Handbook for Mechanical Engineers, 7th Edition.
- [4] Methods for Impact Analysis of Shipping Containers, NUREG/CR-3966, UCID-20639, LLNL, 1987.

Chapter A.4
Thermal Evaluation

TABLE OF CONTENTS

A.4 THERMAL EVALUATION..... A.4-1

A.4.1 Discussion..... A.4-1

A.4.1.1 Air Flow Evaluation for 32PTH Type 1 DSC in HSM-H A.4-1

A.4.1.2 Thermal Evaluation of 32PTH Type 1 DSC in HSM-H..... A.4-2

A.4.1.3 Thermal Evaluation of 32PTH Type 1 DSC in OS187H Type 1 TC A.4-2

A.4.1.4 Maximum 32PTH Type 1 DSC Internal Pressure for Storage and
Transfer Conditions A.4-3

LIST OF TABLES

Table A.4-1 Airflow Calculation Results for HSM-H Loaded with 32PTH Type
1 DSC..... A.4-1

Table A.4-2 Applied Decay Heat Load and Heat Generation Rate within 32PTH
DSC and 32PTH Type 1 DSC in HSM-H A.4-2

A.4 THERMAL EVALUATION

A.4.1 Discussion

The NUHOMS® 32PTH Type 1 DSC is designed to passively reject decay heat during storage and transfer for normal, off-normal, and accident conditions while maintaining temperatures and pressures within specified limits. There are changes to the thermal evaluation as discussed in Chapter 4 of the SAR.

In general, the thermal evaluations and results documented in Chapter 4 for the 32PTH DSC inside the HSM-H and OS187H TC are bounding for the 32PTH Type 1 DSC inside the HSM-H and the OS187H Type 1 TC.

As shown in Table A.1-1, the main differences between the 32PTH DSC and the 32PTH Type 1 DSC consist of a longer overall DSC length and a corresponding longer internal cavity length to accommodate an increased basket length. The effect of these differences is addressed below and shown to have a negligible effect on the overall thermal performance of the 32PTH Type 1 DSC as compared to the 32PTH DSC.

The longer length of the 32PTH Type 1 DSC affects the HSM-H air flow calculation, and the longer cavity length affects the decay heat flux and heat generation rate of the 32PTH Type 1 DSC.

A.4.1.1 Air Flow Evaluation for 32PTH Type 1 DSC in HSM-H

The mass flow rates, exit and average air temperatures, and total loss coefficients for the 32PTH Type 1 DSC in the HSM-H are calculated for the bounding off-normal conditions using the same methodology used for the 32PTH DSC described in Chapter 4. Table A.4-1 shows the results of the air flow calculations in comparison to those from the 32PTH DSC.

Table A.4-1 Airflow Calculation Results for HSM-H Loaded with 32PTH Type 1 DSC

Parameter	32PTH Type 1 DSC	32PTH DSC	32PTH Type 1 DSC	32PTH DSC
Ambient temperature, T_{amb} , (°F)	-20	-20	115*	115*
Exit air temperature, T_{Exit} , (°F)	46.1	46.2	191.8	191.9
Average air temperature, T_{aver} , (°F)	13.0	13.1	148.4	148.4
Total loss coefficient, ΣK , (ft ⁻⁴)	0.0984	0.0988	0.1012	0.1016
Mass flow rate, (lbm/s)	2.076	2.073	1.577	1.574

*24-hour average of 105 °F used

As seen from Table A.4-1, the differences in the air flow calculation results for HSM-H loaded with 32PTH Type 1 DSC or 32PTH DSC are insignificant. The exit air temperatures for 32PTH Type 1 DSC are bounded by those of the 32PTH DSC due to the longer DSC length which results in a lower decay heat flux at the DSC surface and a larger heat transfer surface. The reduced air temperature difference from the exit to the inlet of the HSM-H results in increasing air mass flow rate through the HSM-H cavity. Thus, the air flow calculation results used for the

thermal evaluation of the 32PTH DSC in the HSM-H can be conservatively used for thermal evaluation of the 32PTH Type 1 DSC in the HSM-H.

A.4.1.2 Thermal Evaluation of 32PTH Type 1 DSC in HSM-H

The main design differences between the 32PTH DSC and the 32PTH Type 1 DSC listed in Table A.1-1 only affect applied decay heat load used for normal and off-normal conditions and heat generation rate within the DSC used for blocked vent accident conditions. Table A.4-2 summarizes the applied decay heat load and heat generation rate for 32PTH DSC and 32PTH Type 1 DSC in the HSM-H.

Table A.4-2 Applied Decay Heat Load and Heat Generation Rate within 32PTH DSC and 32PTH Type 1 DSC in HSM-H

Parameter	32PTH Type 1 DSC	32PTH DSC
Total decay heat load, Q	118748 Btu/hr (34.8kW)	
DSC inner diameter, D_i , (in.)	68.75	
DSC cavity length, L , (in.)	171.63	164.5
Decay heat flux = $Q/(\pi D_i L)$, (Btu/hr-in. ²)	3.2034	3.3422
Heat generation rate = $Q/(\pi D_i^2 L/4)$, (Btu/hr-in. ³)	0.1864	0.1945

As seen from Table A.4-2, both the decay heat flux and the heat generation rate for the 32PTH Type 1 DSC are bounded by those used for 32PTH DSC in HSM-H. The 32PTH Type 1 DSC is longer, which provides larger heat transfer surface for DSC outer shell than 32PTH DSC. The added length of the 32PTH Type 1 DSC basket increases the heat rejection capacity of the basket. Therefore, the temperatures of 32PTH Type 1 DSC in HSM-H for storage conditions are bounded by those calculated for 32PTH DSC.

Due to the longer length of the 32PTH Type 1 DSC, the HSM-H is exposed to a lower heat flux/heat generation rate than the 32PTH DSC. Thus, the temperature distribution in the HSM-H concrete structure and steel support structure will correspondingly decrease with the lower heat flux/heat generation rate. Therefore, the temperatures in the HSM-H loaded with a 32PTH DSC as calculated in Chapter 4 are bounding.

A.4.1.3 Thermal Evaluation of 32PTH Type 1 DSC in OS187H Type 1 TC

Since the 32PTH Type 1 DSC cavity and OS187H Type 1 TC cavity are longer than that of 32PTH DSC and OS187H TC, the total decay heat load (34.8kW) would be distributed over a larger radial inner surface of the DSC cavity than the one considered in the Chapter 4 thermal analysis for transfer conditions. This means the applied heat fluxes and heat generation rates considered in Chapter 4 bound those for the 32PTH Type 1 DSC and OS187H Type 1 TC. Furthermore, the longer DSC/TC length provide large heat transfer surface for heat rejection from the DSC to the ambient. The maximum DSC/TC component temperatures decrease with a lower heat flux/heat generation rate and a larger DSC/TC heat transfer surface, and therefore the results of the 32PTH DSC in OS187H thermal analysis bound those for the 32PTH Type 1 DSC and OS187H Type 1 TC.

A.4.1.4 Maximum 32PTH Type 1 DSC Internal Pressure for Storage and Transfer Conditions

The 32PTH Type 1 DSC has a longer cavity length in comparison to 32PTH DSC, which provides an additional 4.3% of cavity volume. The overall 32PTH Type 1 DSC cavity gas volume with the increased basket length is still higher than that of 32PTH DSC. Furthermore, the authorized fuel assembly types and decay heat loads are the same for 32PTH Type 1 DSC, and, therefore, the volumes of fission and fill gas calculated for 32PTH DSC are unchanged. As discussed in Sections A.4.1.2 and A.4.1.3, the average cavity gas temperatures for 32PTH Type 1 DSC for both storage and transfer conditions are bounded by the 32PTH DSC. Therefore, the maximum internal pressures within the 32PTH Type 1 DSC are bounded by those for 32PTH DSC design and the pressure design criteria are satisfied for the 32PTH Type 1 DSC.

Chapter A.5 Shielding Evaluation

TABLE OF CONTENTS

A.5	SHIELDING EVALUATION.....	A.5-1
------------	----------------------------------	--------------

LIST OF TABLES

Table A.5-1	Material Composition of NS-3 Neutron Shielding Resin.....	A.5-3
Table A.5-2	Type 1 Transfer Cask Top and Bottom Dose Rate Summary During Transfer Operations	A.5-3

A.5 SHIELDING EVALUATION

The NUHOMS® 32PTH Type 1 DSC and the OS187H Type 1 transfer cask (TC) are designed to be equivalent to the NUHOMS® 32PTH DSC and OS187H TC from a shielding standpoint for all conditions of loading, storage and transfer. In general, the shielding evaluation documented in Chapter 5 for the 32PTH DSC and OS187H TC is applicable and bounding for the 32PTH Type 1 DSC and OS187H Type 1 TC.

The effect on shielding due to the small changes in the geometry and material design of the 32PTH Type 1 DSC and OS187H Type 1 TC is evaluated herein. The 32PTH Type 1 DSC and OS187H Type 1 TC are designed to be longer than the 32PTH DSC and OS187H TC. Since there is no change in the authorized fuel contents of the NUHOMS® HD System, all the source terms and fuel qualification tables determined in Chapter 5 remain unchanged. The computational model of the DSC inside the HSM-H for long term storage described in Chapter 5 is insensitive to the length of the DSC. Therefore, the shielding evaluations for the 32PTH DSC inside the HSM-H documented in Section 5.4.8.1 are applicable to the 32PTH Type 1 DSC. The differences between the 32PTH and 32PTH Type 1 DSCs inside the OS187H TC and the OS187H Type 1 TCs, respectively, that are relevant to the calculation of dose rates during loading and transfer are evaluated and discussed below:

- The OS187H Type 1 TC inner liner thickness is increased from 0.500" to 0.625". This change results in a reduction in radial dose rates and is an improvement in the shielding design.
- The OS187H Type 1 TC lead shielding thickness is reduced from 3.60" to 3.56". The shielding calculations documented in Chapter 5 utilize a lead shield thickness of 3.56" and therefore, the results from Chapter 5 radial dose rate calculations are applicable for the Type 1 DSC and Type 1 TC.
- Type 1 TC water (radial) neutron shield is extended to mate with the upper trunnion. This design change is an improvement and results in a reduction in the neutron dose rates below the upper trunnion as there are no pocket-to-neutron shield gaps.
- Type 1 TC trunnions utilize a monolithic forging (solid steel) with removal of the solid neutron shield resin inside the trunnions. This is an improvement in design since it results in a significant reduction in the gamma dose rates around the trunnions. The slight increase in the neutron dose rates due to the removal of the solid neutron shield resin inside the trunnions is more than compensated by the increase in the gamma shielding due to the stainless steel. Note that the dose rates around the transfer cask are mostly due to contribution from gamma sources.
- The solid neutron shielding material (resin) at the top and bottom of the OS187H Type 1 TC is changed from TN Proprietary Polyester Resin to NS-3. The material composition of the resin material is shown in Table 5-17. The material composition of the NS-3 material is shown in Table A.5-1. The shielding characteristics of these materials are similar and do not result in a substantial change in the dose rate magnitude and distribution at the top and bottom of the transfer cask.

A shielding evaluation with the MCNP computer code (described in Chapter 5, Section 5.4) is performed to determine the effect of the change of the solid neutron shield material for the OS187H Type 1 TC. The MCNP model for this evaluation is identical to that described in Chapter 5, Section 5.3.1.3 for the transfer configuration (shown in Figures 5-5 through 5-7) except for the use of NS-3 as the solid neutron shield material at the axial ends of the TC. The results of this evaluation are shown in Table A.5-2. A comparison of the dose rates at the top and bottom ends of the Type 1 TC with those shown in Table 5-4 and Table 5-5 for the OS187H TC indicates that the differences in dose rates from use of NS-3 vary from being up to 33% higher at the top end to being statistically insignificant at the bottom end. The dose rate increase at the top end of the OS187H Type 1 TC due to the use of NS-3 as the solid neutron shielding material is relatively insignificant in comparison to the dose rates at the side and bottom of the TC. More specifically, the average dose rates at the top end during the transfer operations (approximately 30 mrem/hr at the surface) are significantly lower than the average dose rates at the bottom end (approximately 180 mrem/hr at the surface) or the TC side (approximately 330 mrem/hr at the surface, Table 5-3).

Further, the average dose rates at the top end of the TC during transfer operations (approximately 30 mrem/hr at the top surface) are significantly lower than those during welding operations (approximately 200 mrem/hr at the top surface, Table 5-4) or during decontamination operations (approximately 700 mrem/hr at the top surface, Table 5-4). Therefore, even a 33% increase in the top end dose rates during transfer operations is a statistically insignificant increase in comparison to all of the loading and transfer operations involving the OS187H Type 1 TC.

- The 32PTH Type 1 DSC top shielding design includes a two-piece assembly, consisting of separate top shield plug and the inner top cover plate. This configuration is equivalent to the single piece top shield plug/inner top cover plate assembly modeled in the Chapter 5 shielding calculations for all operations following decontamination. During decontamination, the 32PTH Type 1 DSC top shielding configuration consists of the shield plug only which results in a reduction of the amount of steel at the top of the DSC (during decontamination operations) by 2". The shielding models for decontamination are described in Chapter 5, Section 5.3.1.2. Due to the two-piece top shield plug and inner top cover plate assembly design, it is not necessary to decontaminate the top surface of the shield plug (as opposed to the single piece design where it is required). Therefore, top dose rates during this stage of operation do not significantly impact total occupational exposure and are not calculated. The radial dose results for these operations from Chapter 5, Section 5.4.8 are applicable for both the 32PTH Type 1 DSC and OS187H Type 1 TC.

In summary, the shielding evaluation documented in Chapter 5 for the 32PTH DSC and OS187H TC is applicable and bounding for the 32PTH Type 1 DSC and OS187H Type 1 TC for all conditions of loading, storage and transfer, except for the TC top end dose rate calculation with NS3 which is documented herein. However, it has been shown that the increase in dose rates due to the change in the neutron shielding material has a relatively insignificant impact in comparison to the dose rates around the TC during loading and transfer operations.

Table A.5-1 Material Composition of NS-3 Neutron Shielding Resin

Element	Weight %
Hydrogen	4.85
Carbon	9.35
Calcium	5.61
Oxygen	57.05
Silicon	3.36
Aluminum	17.89
Iron	0.56
Trace ⁽¹⁾	1.33
Density (g/cm3)	1.76

Note:

(1) Trace elements were modeled as oxygen in the shielding analysis

Table A.5-2 Type 1 Transfer Cask Top and Bottom Dose Rate Summary During Transfer Operations

Location	Dose Rate mrem/hr	On Outside Surface		1.5 Feet from Surface		Three Feet from Surface	
		Gamma	Neutron	Gamma	Neutron	Gamma	Neutron
Top end	Maximum	19.8	34.4	9.55	21.2	5.07	12.6
	Minimum	6.16	12.1	5.16	7.49	3.69	6.20
	Average ⁽¹⁾ surface	10.9	18.6	6.37	11.5	4.10	8.08

Location	Dose Rate mrem/hr	On Outside Surface		One Foot from Surface		Three Feet from Surface	
		Gamma	Neutron	Gamma	Neutron	Gamma	Neutron
Bottom end	Maximum	460	1318	119	289	57.1	113
	Minimum	13.7	47.2	18.6	41.1	16.9	39.2
	Average ⁽¹⁾ surface	48.4	133	36.2	86.9	26.8	58.3

Note:

(1) Surface weighted average of ring detectors used as tally surfaces

Chapter A.6

Criticality Evaluation

The NUHOMS® 32PTH Type 1 DSC and the OS187H Type 1 transfer cask (TC) are designed to be identical to the NUHOMS® 32PTH DSC and OS187H TC from a criticality standpoint for all conditions of loading, storage and transfer. In general, the criticality analysis documented in Chapter 6 for the 32PTH DSC in the OS187H TC is applicable and bounding for the 32PTH Type 1 DSC in the OS187H Type 1 TC.

The effect on criticality due to the small changes in the geometry of the Type 1 DSC and Type 1 TC is determined by investigating the effect due to the geometry modeling employed in the criticality calculations documented in Chapter 6. These considerations are listed below:

- The height of the individual egg-crate sections in the active fuel region of the basket of the 32PTH Type 1 DSC does not change. The increase in overall height of the 32PTH Type 1 DSC is due to an increase in the number of egg-crate sections. Though the height of the top egg-crate section of the Type 1 DSC is different from that of the 32PTH DSC, the top section of the Type 1 DSC contains more neutron poison than that of the 32PTH DSC. Therefore, the criticality analysis model in Chapter 6, that considers an infinite axial array of egg-crate sections, is applicable, conservatively, to the Type 1 DSC. Note that the gap between the top of the neutron poison sheets and the bottom of the top shield plug is decreased for the 32PTH Type 1 DSC.
- The difference between the basket length and the DSC cavity length for the Type 1 DSC is greater than that of the 32PTH DSC by approximately 0.15 inches. However, this difference is well within the conservatism employed in the damaged fuel criticality calculations documented in Section 6.4.2.4 (shifting of fuel assemblies beyond fixed the poison sheet height) of Chapter 6.

In summary, the criticality analysis documented in Chapter 6 for the 32PTH DSC in the OS187H TC is applicable and bounding for the 32PTH Type 1 DSC in the OS187H Type 1 TC for all conditions of loading, storage, and transfer.

Chapter A.7 Confinement

TABLE OF CONTENTS

A.7	CONFINEMENT	A.7-1
A.7.1	Confinement Boundary	A.7-1
A.7.2	Requirements for Normal Conditions of Storage	A.7-2
A.7.3	Confinement Requirements for Hypothetical Accident Conditions	A.7-3
A.7.4	Supplemental Data.....	A.7-4
A.7.4.1	Confinement Monitoring Capability.....	A.7-4
A.7.5	References.....	A.7-5

LIST OF FIGURES

Figure A.7– 1	32PTH Type 1 DSC Confinement Boundaries and Welds for Three-Part Top End Configuration	A.7-6
---------------	---	-------

A.7 CONFINEMENT

A.7.1 Confinement Boundary

No change. Section 7.1 applies in its entirety to the 32PTH Type 1 DSC. The 32PTH DSC confinement boundary described in Section 7.1 and shown in Figure 7-1 is applicable without change to the 32PTH Type 1 DSC design when the optional two-part top end closure assembly is used. In addition, as described in Chapter A.1, the 32PTH Type 1 DSC also features a three-part top end closure assembly, consisting of separate top shield plug, inner top cover and outer top cover plates. This three-part closure design is the same as that used in other NUHOMS® canister designs [1] and includes a vent and siphon block which is welded to the shell during fabrication.

The confinement boundary for the three-part closure consists of the DSC cylindrical shell, the inner top cover plate, the siphon and vent block, the inner bottom cover plate, and the associated welds. At the top, the inner top cover plate, the siphon and vent block, and the DSC shell are welded to each other using partial penetration welds, which are subject to multi-level PT examination. The vent and siphon block contains two ports which are used for draining, vacuum drying, and backfilling. These ports are closed with welded cover plates which are also subject to multi-level PT. Along the shell and at the bottom end of the DSC, the confinement boundary is the same as for the 32PTH DSC.

The confinement boundary for the three-part top end closure configuration is shown in Figure A.7-1.

A.7.2 Requirements for Normal Conditions of Storage

No change.

A.7.3 Confinement Requirements for Hypothetical Accident Conditions

No change.

A.7.4 Supplemental Data

A.7.4.1 Confinement Monitoring Capability

No change.

A.7.5 References

- [1] Updated Final Safety Analysis Report, Standardized NUHOMS® Horizontal Modular Storage System for Irradiated Nuclear Fuel, Revision 9, February 2006, USNRC Docket No. 72-1004.

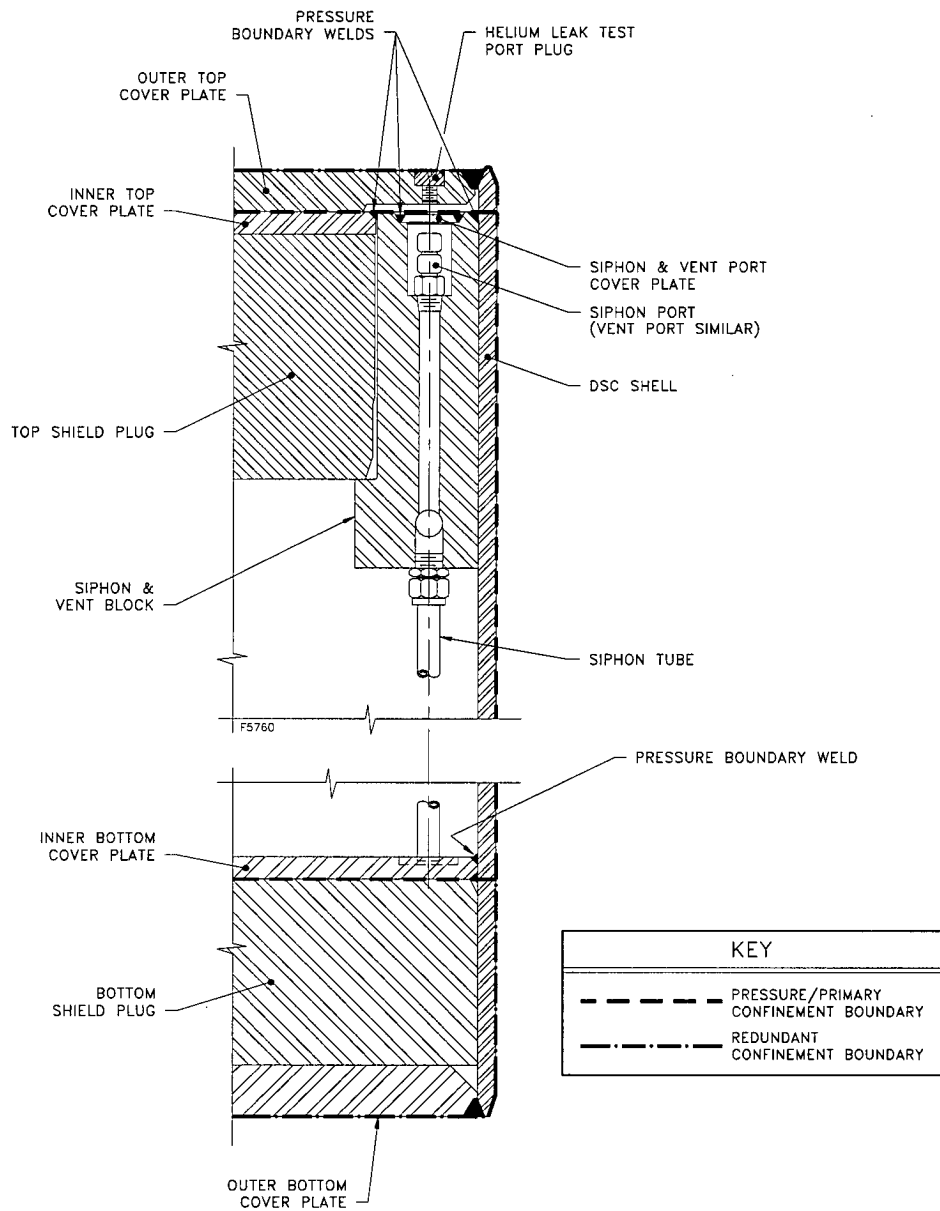


Figure A.7– 1 32PTH Type 1 DSC Confinement Boundaries and Welds for Three-Part Top End Configuration

Chapter A.8 Operation Procedures

TABLE OF CONTENTS

A.8	OPERATING PROCEDURES.....	A.8-1
A.8.1	Procedures for Loading the DSC and Transfer to the HSM-H.....	A.8-2
A.8.1.1	Narrative Description.....	A.8-2
A.8.2	Procedures for Unloading the DSC.....	A.8-8
A.8.2.1	DSC Retrieval from the HSM-H.....	A.8-8
A.8.2.2	Removal of Fuel from the DSC	A.8-8
A.8.3	Supplemental Information	A.8-11
A.8.4	References.....	A.8-12

A.8 OPERATING PROCEDURES

Chapter 8 applies in its entirety and without change to the 32PTH Type 1 DSC when the optional two-part top end closure assembly (which is similar to the 32PTH DSC) is used. In addition, as described in Chapter A.1, the 32PTH Type 1 DSC also features a three-part top end closure assembly, consisting of separate top shield plug, inner top cover and outer top covers. The modifications to the operating procedures described in this chapter apply to the three-part closure design and are based on the similar three-part closure used in other NUHOMS® canister designs [3].

A.8.1 Procedures for Loading the DSC and Transfer to the HSM-H

A.8.1.1 Narrative Description

The following steps describe the recommended modifications to the generic operating procedures described in Sections 8.1 and 8.2, and are applicable when the standard three-part top end closure assembly is implemented in the 32PTH Type 1 DSC. For purposes of completeness of presentation, the entire sequence of operational steps is presented whenever a modification has been introduced in any particular operation. When no changes are made to a section, "No Change" is indicated and a reference is listed to the applicable section in Chapter 8.

A.8.1.1.1 Transfer Cask and DSC Preparation

1. Verify by plant records or other means that candidate fuel assemblies meet the physical, thermal and radiological criteria specified in the Technical Specifications.
2. Clean or decontaminate the transfer cask as necessary to meet licensee pool and ALARA requirements, and to minimize transfer of contamination from the cask cavity to the DSC exterior.
3. Examine the transfer cask cavity for any physical damage. Insert cask spacer at the bottom of the transfer cask, if required.
4. Verify specified lubrication of the transfer cask rails.
5. Examine the DSC for any physical damage and for cleanliness. Verify that bottom fuel spacers or damaged fuel bottom end caps, if required, are present in all fuel compartments. Remove damaged fuel top end caps if they are in place. Record the DSC serial number which is located on the grappling ring. Verify the basket type by identifying the last character in the serial number.
6. Not used.
7. Lift the DSC by the internal lifting lugs and lower it into the cask cavity. Rotate the DSC to match the transfer cask alignment marks.
8. Not used.
9. Fill the transfer cask/DSC annulus with clean water.
10. Seal the top of the annulus, using for example an inflatable seal.
11. A tank filled with clean water, and kept above the pool surface may be connected to the top vent port of the transfer cask via a hose to provide a positive pressure in the annulus. This is an optional arrangement, which provides additional assurance that contaminated water from the fuel pool will not enter the annulus. Do not pressurize this tank, nor raise it sufficiently high to float the DSC. For the 32PTH Type 1 DSC with a 69.75 inch OD, and an empty weight of 45,000 lb, a differential pressure of

approximately 11.7 psi, equivalent to 27.1 ft of pure water, would be sufficient to lift the DSC.

12. If the DSC top shield plug and top cover plates were trial fitted, they must be removed prior to filling the DSC with water. The vent port quick connect fitting in the inner top cover may be removed to facilitate hydrogen monitoring later. The drain port fitting may be either left in place or removed—water may be pumped from the DSC either with or without the fitting.
13. The licensee shall develop procedures to verify that the boron content of the water added to the DSC conforms to the Technical Specifications. Fill the DSC with water from the fuel pool or an equivalent source meeting the minimum boron concentration required by the Technical Specifications. Optionally, this may be done at the time of immersing the cask in the pool. If the pool water is allowed to flow over the transfer cask lip and into the DSC, provision must be made to protect the annulus seal from being dislodged by the water running over it.
- 14a. Optionally, secure a sheet of suitable material to the bottom of the cask to minimize the potential for ground-in contamination. This step may be done at any convenient time prior to immersion.
- 14b. Drain or fill the transfer cask liquid neutron shield, as required by licensee ALARA requirements and crane weight limits. This step may be done at any convenient time prior to immersion.
15. Prior to the cask being lifted into the fuel pool, the water level in the pool should be adjusted as necessary to accommodate the transfer cask and DSC volume. If the water placed in the DSC cavity was obtained from the fuel pool, a level adjustment may not be necessary.

A.8.1.1.2 DSC Fuel Loading

1. Verify proper engagement of the lifting yoke with the transfer cask lifting trunnions.
2. Lift the transfer cask/DSC and position them over the cask loading area of the spent fuel pool.
3. Lower the cask into the fuel pool until the bottom of the cask is at the height of the fuel pool surface. As the cask is lowered into the pool, spray the exterior surface of the cask with clean water to minimize surface adhesion of contamination.
4. Place the cask in the location of the fuel pool designated as the cask loading area.
5. Disengage the lifting yoke from the transfer cask lifting trunnions and move the yoke clear of the cask. Spray the lifting yoke with clean water if it is raised out of the fuel pool.

6. Load pre-selected spent fuel assemblies into the DSC basket compartments. The licensee shall develop procedures to verify that the boron content of the water conforms to the Technical Specifications, and that fuel identifications are verified and documented. Damaged fuel must be loaded only in designated compartments fitted with a damaged fuel bottom end cap.
7. After all the fuel assemblies have been placed into the DSC and their identities verified, install damaged fuel top end caps into designated compartments containing damaged fuel.
8. Lower the top shield plug into the DSC.
9. Visually verify that the top shield plug is properly seated in the DSC. Reseat if necessary.
10. Position the lifting yoke and verify that it is properly engaged with the transfer cask trunnions.
11. Lift the transfer cask to the pool surface and spray the exposed portion of the cask with clean water.
12. Drain any water from above the top shield plug back to the spent fuel pool. Up to 1300 gallons of water may be removed from the DSC prior to lifting the transfer cask clear of the pool surface. Up to 15 psig of nitrogen or helium may be used to assist the removal of water. The DSC shall be backfilled with nitrogen or helium after drainage of bulk water.
13. Lift the cask from the fuel pool, continuing to spray the cask with clean water.
14. Move the cask with loaded DSC to the area designated for DSC draining and closure operations. The set-down area should be level, or if slightly sloped, the transfer cask and DSC should be placed with the slope down toward the DSC drain/siphon tube.

A.8.1.1.3 DSC Closing, Drying, and Backfilling

1. Fill the transfer cask liquid neutron shield if it was drained for weight reduction during preceding operations.
2. Decontaminate the transfer cask exterior.
3. Disengage the rigging from the top shield plug, and remove the eyebolts. Disengage the lifting yoke from the trunnions.
4. Disconnect the annulus overpressure tank if one was used, decontaminate the exposed surfaces of the DSC shell perimeter, remove any remaining water from the top of the annulus seal, and remove the seal.

5. Open the cask cavity drain port and allow water from the annulus to drain out until the water level is approximately twelve inches below the top of the DSC shell. Take swipes around the outer surface of the DSC shell to verify conformance with Technical Specification limits.
6. Cover the transfer cask/DSC annulus to prevent debris and weld splatter from entering the annulus.
7. If water was not drained from the DSC earlier, connect a pump to the DSC drain port and remove up to 1,300 gallons of water. Use nitrogen or helium to assist the removal of water. This lowers the water sufficiently to allow welding of the inner top cover, while keeping a sufficient volume of water in the DSC to cool the spent fuel (Pay special attention to step 14 below). Up to 15 psig of nitrogen, or helium gas may be applied at the vent port to assist the water pump down.

CAUTION: Radiation dose rates are expected to be high at the vent and siphon port locations. Use proper ALARA practices (e.g., use of temporary shielding, appropriate positioning of personnel, etc.) to minimize personnel exposure.

8. Install the automated welding machine onto the inner top cover and place the inner top cover with the automatic welding machine onto the DSC. Optionally, the inner top cover and the automatic welding machine can be placed separately. Verify proper fit up of the inner top cover with the DSC shell.
9. Hydrogen monitoring is required prior to commencing and continuously during the welding of the inner top cover. Insert a hydrogen monitor intake line through the vent port such that it terminates just below the top shield plug. Temperature monitoring of the TC cavity/annulus water is also required, see step 14.
10. Verify that the hydrogen concentration does not exceed 2.4% [1]. If this limit is exceeded, stop all welding operations and purge the DSC cavity with helium (or other inert gas) via the vent port to reduce hydrogen concentration safely below the 2.4% limit.
11. Complete the inner top cover welding and perform the non-destructive examinations as required by the Technical Specifications. The weld must be made in at least two layers.
12. Remove the automated welding machine.
13. Pump remaining water from the DSC. Remove as much free standing water as possible to shorten vacuum drying time. Up to 15 psig of nitrogen, or helium gas may be applied at the vent port to assist the water pump down.
14. There are three methods described in Chapter 4 to assure that the fuel temperature limit is not exceeded during vacuum drying. Each method is associated with a time limit for vacuum drying, starting from the time that pumping of liquid water from the DSC is complete as required by the Technical Specifications for vacuum drying. As required by the technique chosen, either

- a) install annulus water circulation equipment, or
- b) drain annulus water if temperature exceeds 180 °F

For either (a) or (b), the DSC may be evacuated to 100 mbar or lower, and backfilled with helium to atmospheric pressure prior to start of vacuum drying. All helium used in backfilling operations shall be at least 99.99% pure (this may be done as part of step 15).

NOTE: Proceed cautiously when evacuating the dry shielded canister (DSC) to avoid freezing consequences.

15. Connect a vacuum pump/helium backfill manifold to the vent port or to both the vent and drain ports. The quick connect fittings may be removed and replaced with stainless steel pipe nipple/vacuum hose adapters to improve vacuum conductance. Make provision to prevent icing, for example by avoiding traps (low sections) in the vacuum line. Provide appropriate measures as required to control any airborne radionuclides in the vacuum pump exhaust. Purge air from the helium backfill manifold.

Optionally, leak test the manifold and the connections to the DSC. The DSC may be pressurized to no more than 15 psig for leak testing.

CAUTION: Radiation dose rates are expected to be high at the vent and siphon port locations. Use proper ALARA practices (e.g., use of temporary shielding, appropriate positioning of personnel, etc.) to minimize personnel exposure.

16. Evacuate the DSC to the pressure required by the Technical Specification for vacuum drying, and isolate the vacuum pump. The isolation valve should be as near to the DSC as practicable, with a pressure gauge on the DSC side of the valve. Prior to performing the vacuum hold for 30 minutes as required by the Technical Specification, the vacuum pump must be turned off; or if the pump is **not** turned off, provide a tee and valve (or other means) to open the line to atmosphere between the pump and the DSC isolation valve.
17. Maintain the water condition in the transfer cask/DSC annulus as required by the technique chosen (step 14).
18. If the Technical Specification is satisfied, i.e., if the pressure remains below the specified limit for the required duration with the pump isolated, continue to the next step. If not, repeat steps 16 and 17.
- 19a. Purge air from the backfill manifold, open the isolation valve, and backfill the DSC cavity with helium to 16.5 to 18 psig and hold for 10 minutes.
- 19b. Reduce the DSC cavity pressure to atmospheric pressure, or slightly over.
20. If the quick connect fittings were removed for vacuum drying, remove the vacuum line adapters from the ports, and re-install the quick connect fittings using suitable pipe

thread sealant.

CAUTION: Radiation dose rates are expected to be high at the vent and siphon port locations. Use proper ALARA practices (e.g., use of temporary shielding, appropriate positioning of personnel, etc.) to minimize personnel exposure.

21. Evacuate the DSC through the vent port quick connect fitting to a pressure of 100 mbar or less.
22. Backfill the DSC with helium to the pressure specified in the Technical Specifications, and disconnect the vacuum/backfill manifold from the DSC.
23. Repeat steps 21 and 22 if the DSC interior is exposed to nitrogen during any succeeding operations.
- 24a. Weld the covers over the vent and drain ports, performing non-destructive examination as required by the Technical Specifications. The welds shall have at least two layers.
- 24b. Install a temporary test head fixture (or any other alternative means). Perform a leak test of the inner top cover to the DSC shell welds and siphon/vent cover welds in accordance with the Technical Specification limits. Verify that the personnel performing the leak test are qualified in accordance with SNT-TC-1A.
25. Place the outer top cover plate onto the DSC and verify correct rotational alignment of the cover and the DSC shell. Install the automated welding machine onto the outer top cover plate. As an option, the welding machine may be mounted onto the cover plate and then placed together on the DSC.
26. Complete the outer top cover welding and perform the non-destructive examinations as required by the Technical Specifications. The weld must be made in at least two layers.
27. Remove everything except the DSC from the transfer cask cavity: welding machine, protective covering from the transfer cask / DSC annulus, annulus temperature monitoring or water circulation equipment, temporary shielding, etc.
28. Install the transfer cask lid and bolt it.
29. Evacuate the transfer cask cavity to below 100 mbar, and backfill the transfer cask annulus with helium in accordance with the Technical Specifications pressure tolerance and time limit.

A.8.1.1.4 Transfer Cask Downending and Transport to ISFSI

No change. See Section 8.1.1.4.

A.8.1.1.5 DSC Transfer to the HSM-H

No change. See Section 8.1.1.5.

A.8.1.1.6 Monitoring Operations

No change. See Section 8.1.1.6.

A.8.2 Procedures for Unloading the DSC

The following section outlines the procedures for retrieving the DSC from the HSM-H and for removing the fuel assemblies from the DSC.

A.8.2.1 DSC Retrieval from the HSM-H

No change. See Section 8.2.1.

A.8.2.2 Removal of Fuel from the DSC

If it is necessary to remove fuel from the DSC, it can be removed in a dry transfer facility or the initial fuel loading sequence can be reversed and the plant's spent fuel pool utilized.

Procedures for wet unloading of the DSC are presented here. Dry unloading procedures are essentially identical up to the removal of the DSC vent and drain port covers.

1. Tow the trailer with the loaded cask to the cask handling area inside the plant's fuel handling building. Drain the transfer cask liquid neutron shield as required by licensee ALARA requirements and crane weight limits.
2. Position and ready the trailer for access by the crane.
3. Engage the lifting yoke with the trunnions of the transfer cask.
4. Verify that the yoke lifting hooks are properly aligned and engaged onto the transfer cask trunnions.
5. Lift the transfer cask approximately one inch off the trunnion supports. Verify that the yoke lifting hooks are properly positioned on the trunnions.
6. Move the crane in a horizontal motion while simultaneously raising the crane hook vertically and lift the transfer cask off the trailer. Move the transfer cask to the cask decontamination area.
7. Lower the transfer cask into the cask staging area in the vertical position.
8. Unbolt the transfer cask lid and remove it.
9. Install temporary shielding to reduce personnel exposure as required. Fill the transfer cask/DSC annulus with clean water and seal the top of the annulus, using, for example, an inflatable seal.
10. Locate the drain and vent port using the indications on the outer top cover plate. Place a portable drill press on the top of the DSC. Align the drill over the drain port.
11. Cut or drill a hole through the top cover plate to expose the drain port on the inner top cover. Remove the drain port cover plate with an annular hole cutter. Repeat for the vent port.

CAUTION: Radiation dose rates are expected to be high at the vent and siphon port locations. Use proper ALARA practices (e.g., use of temporary shielding, appropriate positioning of personnel, etc.) to minimize personnel exposure.

12. Obtain a sample of the DSC atmosphere. Confirm acceptable hydrogen concentration and check for presence of fission gas indicative of degraded fuel cladding.
13. If degraded fuel is suspected, additional measures appropriate for the specific conditions are to be planned, reviewed, and implemented to minimize exposures to workers and radiological releases to the environment.
14. Verify that the boron content of the fill water conforms to the Technical Specifications. Fill the DSC with water from the fuel pool or equivalent source through the drain port with the vent port open. The vented cavity gas may include steam, water, and radioactive material, and should be routed accordingly. Monitor the vent pressure and regulate the water fill rate to ensure that the pressure does not exceed 15 psig.
15. Provide for continuous hydrogen monitoring of the DSC cavity atmosphere during all subsequent cutting operations to ensure that hydrogen concentration does not exceed 2.4%. Purge with helium (or any other inert gas) as necessary to maintain the hydrogen concentration below this limit.
16. Provide suitable protection for the transfer cask during cutting operations.
17. Using a suitable method, such as mechanical cutting, remove the weld of the outer top cover plate to the DSC shell.
18. Remove the outer top cover plate.
19. Remove the weld of the inner top cover to the shell in the same manner as the outer cover plate. Remove the inner top cover. Do not remove the top shield plug at this time unless the removal is being done remotely in a dry transfer system.
20. Remove any remaining excess material on the inside shell surface by grinding.
21. Clean the transfer cask surface of dirt and any debris which may be on the transfer cask surface as a result of the weld removal operation.
22. Engage the yoke onto the trunnions, install eyebolts or other lifting attachment(s) into the top shield plug, and connect the rigging cables to the eyebolts/lifting attachment(s).
23. Verify that the lifting hooks of the yoke are properly positioned on the trunnions.
24. Lift the transfer cask just far enough to allow the weight of the transfer cask to be distributed onto the yoke lifting hooks. Verify that the lifting hooks are properly positioned on the trunnions.

25. Optionally install suitable protective material onto the bottom of the transfer cask to minimize cask contamination. Move the transfer cask to the spent fuel pool.
26. Prior to lowering the transfer cask into the pool, adjust the pool water level, if necessary, to accommodate the volume of water which will be displaced by the transfer cask during the operation.
27. Position the transfer cask over the cask loading area in the spent fuel pool.
28. Lower the transfer cask into the pool. As the transfer cask is being lowered, the exterior surface of the transfer cask should be sprayed with clean water.
29. Disengage the lifting yoke from the transfer cask and lift the top shield plug from the DSC.
30. Remove any failed fuel top end caps.
31. Remove the fuel from the DSC.

A.8.3 Supplemental Information

No change. See Section 8.3.

A.8.4 References

- [1] U.S. Nuclear Regulatory Commission, Office of the Nuclear Material Safety and Safeguards, "Safety Evaluation of VECTRA Technologies' Response to Nuclear Regulatory Commission Bulletin 96-04 for NUHOMS®-24P and NUHOMS® 7P Dry Spent Fuel Storage System," November 1997 (Dockets 72-1004, 72-3, 72-4, 72-8, and 72-14).
- [2] NUREG-0612, "Control of Heavy Loads at Nuclear Power Plants," USNRC, July 1980.
- [3] Transnuclear Inc., UFSAR, Standardized NUHOMS® Horizontal Modular Storage Systems for Irradiated Nuclear Fuel, Revision 9, Docket 72-1004.

Chapter A.9

Acceptance Tests and Maintenance Program

No change. Chapter 9 applies in its entirety to this Appendix A. The pressure and leak tests of the DSC confinement boundary as described in Section 9.1.2 are equally applicable to the 32PTH Type 1 DSC with a three-part top end closure assembly, consisting of separate top shield plug, inner top cover and outer top cover plates, as described in Chapter A.1. This three-part closure design is the same as that is used in other NUHOMS® canister designs.

Chapter A.10
Radiation Protection

TABLE OF CONTENTS

A.10 RADIATION PROTECTION A.10-1

A.10.1 Ensuring That Occupational Radiation Exposures Are As Low As Reasonably Achievable (ALARA)..... A.10-1

A.10.2 Radiation Protection Design Features A.10-2

A.10.3 Estimated Onsite Collective Dose Assessment A.10-3

A.10 RADIATION PROTECTION

A.10.1 Ensuring That Occupational Radiation Exposures Are As Low As Reasonably Achievable (ALARA)

No change.

A.10.2 Radiation Protection Design Features

The estimates of off-site dose rates in and around an ISFSI containing arrays (two generic arrays – 2x10 back-to-back array and 2-1x10 front-to-front array) of loaded HSM-Hs (each HSM-H containing a 32PTH DSC fully loaded with design basis fuel) during long term storage are presented in Section 10.2 of Chapter 10. As described in Chapter A.5, the authorized fuel content has not changed, the top and bottom canister shielding thicknesses are not changed, and therefore there is no change in the dose rates in and around the HSM-H loaded with a 32PTH Type 1 DSC. Therefore, the off-site dose estimates presented in Chapter 10 are applicable to the 32PTH Type 1 DSC.

A.10.3 Estimated Onsite Collective Dose Assessment

The estimates of occupational dose during the loading of a 32PTH DSC fully loaded with design basis fuel for long term storage in an HSM-H using an OS187H TC during transfer are presented in Section 10.3 of Chapter 10. As described in Chapter A.5, the differences in the design of the 32PTH Type 1 DSC and the OS187H Type 1 TC do not result in a substantial change in the dose rates in and around the TC during loading and transfer operations. Some of the design changes result in a reduction in these near field dose rates. For the top end design option with separate shield plug and inner cover plate, the occupational exposure during decontamination operations is expected to be lower because the DSC top shield plug is not required to be decontaminated. Overall, the occupational exposure estimates presented in Chapter 10 are applicable and bounding to the Type 1 DSC and Type 1 TC.

Chapter A.11 Accident Analysis

TABLE OF CONTENTS

A.11	ACCIDENT ANALYSIS	A.11-1
A.11.1	Introduction.....	A.11-1
A.11.2	Off-Normal Operation.....	A.11-2
A.11.3	Postulated Accident	A.11-3
A.11.3.1	Cask Drop	A.11-3
A.11.3.2	Earthquake	A.11-3
A.11.3.3	Tornado Wind and Tornado Missiles Effect on HSM-H.....	A.11-3
A.11.3.4	Tornado Wind and Tornado Missiles Effect on Transfer Cask	A.11-3
A.11.3.5	Flood	A.11-9
A.11.3.6	Blockage of HSM-H Air Inlet and Outlet Openings	A.11-9
A.11.3.7	Lightning.....	A.11-9
A.11.3.8	Fire/Explosion.....	A.11-9
A.11.4	References.....	A.11-10

A.11 ACCIDENT ANALYSIS

A.11.1 Introduction

No change.

A.11.2 Off-Normal Operation

No change.

A.11.3 Postulated Accident

No change.

A.11.3.1 Cask Drop

No change.

A.11.3.2 Earthquake

No change.

A.11.3.3 Tornado Wind and Tornado Missiles Effect on HSM-H

No change.

A.11.3.4 Tornado Wind and Tornado Missiles Effect on Transfer Cask

This section summarizes the evaluation of the OS187H Type 1 transfer cask (TC) for tornado wind speed and tornado missile spectrum specified in Chapter 2, Section 2.2.1. This evaluation is similar to the evaluation for the OS187H presented in Section 11.3.4 and is performed to reconcile the changes in geometry parameters between the two TCs as documented in the table below. Subsections which are not affected by the changes in TC geometry are not repeated and are indicated as "No change."

Parameter	OS187H TC	OS187H Type 1
Length of structural shell, in.	193.2	206.7
OD of structural shell, in.	82.70	81.87
OD of neutron shield, in.	92.20	92.11
Thickness of lead shielding, in.	3.60	3.56
Thickness of inner liner, in.	0.50	0.625

The maximum DBT tornado wind speed of 360 mph produces a design pressure of 304 psi. The 4,000 pound automobile and 276 pound eight inch diameter shell missiles were also considered. The other types of missiles are enveloped by the eight inch shell missile.

This analysis is performed for the cask secured in the horizontal position on the support skid. The following criteria are used to evaluate the adequacy of the transfer cask for the loads described above.

- Penetration resistance
- Impact stress analysis

Stability analysis is not required since the cask is already evaluated for a design basis cask drop accident.

A.11.3.4.1 Penetration Resistance

No change.

A.11.3.4.2 Impact Stress Analysis*Tornado Wind Load*

Chapter 2, Section 2.2.1.1 specifies a maximum tornado wind speed at 360 mph. The corresponding velocity pressure, q_z , can be calculated by Eq. 6-1 of [12].

$$q_z = 0.00256 K_z K_{zt} V^2 I \text{ (lb/ft}^2\text{)}$$

Where,

$$\begin{aligned} K_z &= \text{velocity pressure exposure coefficient} \\ &= 1.03 \text{ (height above ground} < 15 \text{ ft in Exposure D, Table 6-3 of [12])} \\ K_{zt} &= \text{topographic factor} \\ &= 1 \\ V &= \text{basic wind speed} \\ &= 360 \text{ mph} \\ I &= \text{importance factor} \\ &= 1.15 \text{ (Category IV, Table 6-2 of [12])} \\ q_z &= 0.00256 \times 1.03 \times 1 \times 1.15 = 393 \text{ lb/ft}^2 \end{aligned}$$

(a) Transverse wind pressure acting on cask shell surface

The projected area of the transfer cask normal to the wind is equal to the OD (92.11 inch) of the neutron shield multiplied by the length of the cask. The total wind force is then equal to the wind pressure multiplied by this projected area. This total wind force is equivalent to a line force, p , acting at the elevation of the cask centerline and along the entire cask length. This wind force will be assumed to be solely resisted only by the cask outer structural shell, which has a length of 206.7" with an OD of 81.87" and a thickness of 1.5".

$$\begin{aligned} p &= q_z \times (\text{OD of neutron shield}) \\ &= 393 \text{ lb/ft}^2 \times (92.11 / 12) \text{ ft} \\ &= 3016.6 \text{ lb/ft} \\ &= 251.4 \text{ lb/in} \end{aligned}$$

Case 9c in Table 31 of [13] provides stress formula for a thin-walled cylindrical vessel supported at both ends and subjected to a uniform load over the entire length of its top element as follows.

$$B = [12(1-\nu^2)]^{1/8} = 1.348, \nu = 0.3$$

Maximum hoop membrane stress,

$$\begin{aligned} \sigma_2 &= -0.492 B p R^{3/4} L^{-1/2} t^{-5/4} \\ &= -0.492 \times (1.348) \times 251.4 \times (81.87/2)^{3/4} \times (206.7)^{-1/2} \times (1.5)^{-5/4} \end{aligned}$$

$$= -113.1 \text{ psi}$$

Maximum hoop bending stress,

$$\begin{aligned}\sigma_2' &= -1.217 B^{-1} p R^{1/4} L^{1/2} t^{-7/4} \\ &= -1.217 \times (1.348)^{-1} \times 251.4 \times (81.87/2)^{1/4} \times (206.7)^{1/2} \times (1.5)^{-7/4} \\ &= -4059.8 \text{ psi}\end{aligned}$$

Maximum hoop membrane plus bending stress,

$$(\sigma_2)_{\text{Total}} = \sigma_2 + \sigma_2' = -113.1 \text{ psi} - 4059.8 \text{ psi} = -4172.9 \text{ psi}$$

Maximum axial membrane stress,

$$\begin{aligned}\sigma_1 &= \text{axial membrane stress} \\ &= -0.1188 B^3 p R^{1/4} L^{1/2} t^{-7/4} \\ &= -0.1188 \times (1.348)^3 \times 251.4 \times (81.87/2)^{1/4} \times 206.7^{1/2} \times (1.5)^{-7/4} \\ &= -1308.5 \text{ psi}\end{aligned}$$

Maximum axial bending stress,

$$\sigma_1' \approx \nu \times \sigma_2' = 0.3 \times (-4059.8 \text{ psi}) = -1217.9 \text{ psi}$$

Maximum axial membrane plus bending stress,

$$(\sigma_1)_{\text{Total}} = \sigma_1 + \sigma_1' = -1308.5 \text{ psi} + (-1217.9 \text{ psi}) = -2526.4 \text{ psi}$$

Maximum membrane plus bending stress intensity = $0 - (-4172.9) = 4172.9 \text{ psi}$

The ASME code allowable stress for the general membrane stress intensity will be conservatively used for evaluation of the above calculated maximum membrane plus bending stress intensity. The Service Level D allowable stress for the membrane stress intensity is the lesser of $2.4S_m$ and $0.7S_u$. For SA-240 Gr. 304 cask structural shell material, $S_m = 20,000 \text{ psi}$ at 300°F and $S_u = 66,200 \text{ psi}$. Thus the allowable stress is $0.7S_u = 46,340 \text{ psi}$.

Therefore the maximum calculated membrane plus bending stress intensity, under tornado wind load, in the cask shell is acceptable.

(b) Axial wind pressure acting on the top end cover of the transfer cask

Case 10b in Table 24 of [13] provides a formula for calculating the resultant moment on the 1.5" recessed flange thickness of the fixed cask top end plate under the wind pressure.

Maximum bending moment,

$$\begin{aligned}M_{ra} &= -q_z a^2 / 8 \\ &= -393 \text{ lb/ft}^2 \times (1 \text{ ft}^2 / 144 \text{ in}^2) \times (81.87/2 \text{ in})^2 / 8\end{aligned}$$

$$= -571.6 \text{ in-lb/in}$$

Maximum bending stress,

$$\begin{aligned}\sigma &= 6M_{ra} / t^2 \\ &= 6 \times (571.6 \text{ in-lb/in}) / (1.5 \text{ in})^2 \\ &= 1524.4 \text{ psi} < 46,340 \text{ psi OK}\end{aligned}$$

(c) Axial wind pressure acting on the bottom end cover of the transfer cask

Case 2f in Table 24 of [13] provides a formula for calculating the resultant moment on the 2" thick fixed bottom end plate of the cask under the wind pressure.

$$\begin{aligned}b &= 14" = \text{radius of the cask bottom ram penetration ring} \\ a &= 81.87" / 2 = 40.935" = \text{outer radius of bottom end plate} \\ b/a &= .3420 \Rightarrow K_{Mra} = -0.0889 \text{ (by interpolation)}\end{aligned}$$

Maximum bending moment,

$$M_{ra} = K_{Mra} q_z a^2 = -0.0889 \times 393/144 \times 40.935^2 = -406.6 \text{ in-lb/in}$$

Maximum bending stress,

$$\sigma = 6M_{ra} / t^2 = 6 \times (406.6 \text{ in-lb/in}) / (2 \text{ in})^2 = 609.9 \text{ psi} < 46,340 \text{ psi OK}$$

Massive Automobile Missile

The impact forces applied to the cask as it is struck by the automobile missile is determined as follows:

The massive automobile missile is assumed to crush 3 feet under a constant force during the impact. The loss of kinetic energy is assumed to be dissipated by crushing of the missile. The frontal contact area of the automobile is specified to be 20 sq. ft.

$$\begin{aligned}F_a \times 3\text{ft} &= \frac{1}{2} [m_a v_o^2] \\ P_a &= F_a / 20 \text{ ft}^2\end{aligned}$$

where:

$$\begin{aligned}m_a &= \text{mass of missile} = 4,000 \text{ lb} \\ v_o &= \text{missile initial velocity} = 195 \text{ ft/sec} \\ F_a &= \text{impact force on cask by missile automobile} \\ p_a &= \text{impact pressure on cask by missile automobile}\end{aligned}$$

$$\begin{aligned}F_a &= \frac{1}{2} \times \{4,000 \text{ lbm} \times [(195 \times 12) \text{ in/sec}]^2\} / (3 \times 12) \text{ in} \\ &= 3.042 \times 10^8 \text{ lbm-in/sec}^2 \\ &= 3.042 \times 10^8 \text{ lbm-in/sec}^2 \times [1 \text{ lb}_f / (386.4 \text{ lb}_m\text{-in/sec}^2)] \\ &= 787,267 \text{ lb}_f\end{aligned}$$

$$P_a = 787,267 \text{ lb}_f / [20 \times (12)^2 \text{ in}^2]$$

$$= 273.4 \text{ psi}$$

The automobile missile deforms and is crushed during the impact. The shear stress in the cask wall is conservatively calculated below. It is assumed that the impact force is concentrated on a small curved section of the cask wall having dimensions $w \times L$. It is also assumed that only two side edges of the impact section are tending to shear. Edges above and below the impact section are assumed to bend, not shear. It is also assumed that the concentrated impact section is 3 ft wide, half of the automotive width. The impact area is then 36" wide by 80" high (equal to 20 ft² area).

$$\text{Shear area} = 2 \times (20 \text{ ft}^2 / 3 \text{ ft}) \times \text{the thickness of the cask outer structural shell}$$

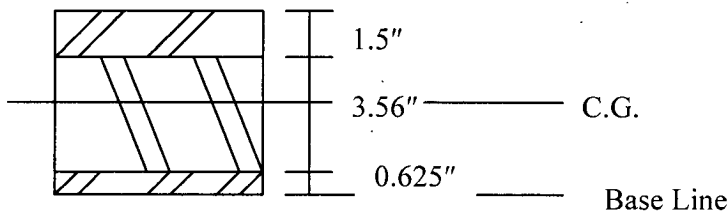
$$= 2 \times 80" \times 1.5" = 240 \text{ in}^2$$

$$\text{The shear stress, } \tau = \text{force/area} = 787,267 \text{ lb} / 240 \text{ in}^2 = 3,280 \text{ psi}$$

The level D allowable shear stress for the cask shell is $0.42 S_u = 0.42 \times 66,200 = 26,480 \text{ psi}$. The shear stress is well below the allowable shear stress.

Assuming that the impact on the side of the cask is reacted by a 36"×80" section of the cask shell, Case 1c from Table 26 of [13] is used to calculate the resulted stresses in the shell. This case represents a flat plate with simply supported edges under a uniform load over a central rectangular area. It is conservative for this case to represent the automotive crushing onto a curved section of the cask.

The transfer cask shell is made of a three-layer composite. It consists of a 1.5" outer structural shell, a 3.56" lead gamma shield, and a 0.625" inner liner (see sketch below). This sandwiched composite plate may be represented by an equivalent one-piece plate which has a thickness producing the same moment of inertia as that of the composite. The thickness of its equivalent one-piece plate is calculated as follows.



For unit length of the composite plate,
neglecting the strength of the 3.6" thick lead,
the distance from base line to C.G.

$$= [(1.5" \times 1") \times (1.5"/2 + 3.56" + 0.625") + (0.625" \times 1") \times (0.625"/2)] \div$$

$$[(1.5" \times 1") + (0.625" \times 1")]$$

$$= 7.6" \div 2.125$$

$$= 3.58"$$

The combined moment of inertia of the composite structural plates, I_{comb}

$$I_{\text{comb}} = (1 \times 1.5^3 / 12) + (1.5 \times 1) \times (1.5/2 + 3.56 + 0.625 - 3.58)^2 + (1 \times 0.625^3 / 12) + (0.625 \times 1) \times (3.58 - 0.625/2)^2 \\ = 9.73 \text{ in}^4$$

The thickness of the equivalent one-piece plate, t_{eq}

$$I_{\text{comb}} = 9.73 \text{ in}^4 = (1 \times t_{\text{eq}}^3) / 12 \Rightarrow t_{\text{eq}} = 4.89''$$

An automobile missile crushing into the horizontal cylindrical canister with an impact area of 36" wide by 80" high is conservatively analyzed by a case that the same impact is applied to a rectangular plate of dimensions at the cask length by the cask OD. All edges of the rectangular plate are assumed simply supported. Case 1c in Table 26 of [13] provides maximum stress calculation of this rectangular plate as follows.

$$\text{Max } \sigma = (\beta W) / t^2$$

$$W = F_a = 787,267 \text{ lb, calculated in Section 11.3.4.2} \\ t = t_{\text{eq}} = 4.89''$$

$$a_1 = 36'', b_1 = 80'' \\ a = 206.7'' \text{ (cask length)} \\ b = 81.87'' \text{ (cask OD)} \\ a_1 / b = 0.4397 \\ b_1 / b = 0.977 \\ a / b = 2.525$$

Use $(b_1 / b) = 0.8$, and $(a_1 / b) = 0.4$ for the table given under the Case 1c in Table 26 of [13];

From this table,

$$\beta = 0.68 \text{ for } (a / b) = 1.4, \text{ and } \beta = 0.76 \text{ for } (a / b) = 2$$

By extrapolation, $\beta = 0.83$ for $(a / b) = 2.525$

$$\therefore \text{Max } \sigma = (0.83 \times 787,267 \text{ lb}) / (4.89^2) = 27,326 \text{ psi}$$

The ASME code allowable stress for the general membrane stress intensity will be conservatively used for evaluation of the above calculated maximum membrane plus bending stress intensity. The Service Level D allowable stress for the membrane stress intensity is the lesser of $2.4S_m$ and $0.7S_u$. For SA-240 Gr. 304 cask structural shell material, $S_m = 20,000$ psi at 300°F and $S_u = 66,200$ psi. Thus the allowable stress is $0.7S_u = 46,340$ psi. Therefore the maximum membrane plus bending stress of 27,326 psi is acceptable.

A.11.3.4.3 Accident Dose Calculation

Based on the above analyses, the 32PTH Type 1 DSC confinement boundary will not be breached as a result of the missile impacts. Accordingly, no 32PTH Type 1 DSC damage or release of radioactivity is postulated.

The missile impact scenario may result in the loss of cask neutron shielding and local deformation/damage of the gamma shielding. The effect of loss of the neutron shielding due to a missile impact is bounded by that resulting from a cask drop scenario. The radiation dose due to local deformation/damage of the gamma shielding is negligible.

A.11.3.4.4 Corrective Action

The transfer cask will be inspected for damage. These operations will take place in the plant fuel building decontamination area and spent fuel pool after recovery of the transfer cask.

Following recovery of the transfer cask and unloading of the DSC, the transfer cask will be inspected, repaired and tested as appropriate prior to reuse.

For recovery of the cask and contents, it may be necessary to develop a special sling/lifting apparatus to move the transfer cask from the site to the fuel pool. This may require several weeks of planning to ensure all steps are correctly organized. During this time, lead blankets may be added to the transfer cask to minimize on-site exposure to site operations personnel. The transfer cask would be roped off to ensure the safety of the site personnel.

A.11.3.5 Flood

No change.

A.11.3.6 Blockage of HSM-H Air Inlet and Outlet Openings

No change.

A.11.3.7 Lightning

No change.

A.11.3.8 Fire/Explosion

No change.

A.11.4 References

No change.

Chapter A.12

Operating Controls and Limits

No change.

Chapter A.13

Quality Assurance

No change.

Chapter A.14 Decommissioning

No change.